

Copyright
by
Andrew Michael Camelio
2014

The Dissertation Committee for Andrew Michael Camelio Certifies that this is the approved version of the following dissertation:

**Studies Toward the Synthesis of Celastrol
and
The Late-Stage Hydroxylation of Arenes Mediated by 4,5-
Dichlorophthaloyl Peroxide**

Committee:

Dionicio R. Siegel, Supervisor

Guangbin Dong

Eric V. Anslyn

Adrian Keatinge-Clay

John DiGiovanni

**Studies Toward the Synthesis of Celastrol
and
The Late-Stage Hydroxylation of Arenes Mediated by 4,5-
Dichlorophthaloyl Peroxide**

by

Andrew Michael Camelio, B.S.

Dissertation

Presented to the Faculty of the Graduate School of
The University of Texas at Austin
in Partial Fulfillment
of the Requirements
for the Degree of

Doctor of Philosophy

The University of Texas at Austin

May, 2014

Dedication

For Grandpa

Acknowledgements

I would like to extend my deepest gratitude to Professor Dionicio Siegel. Nearly five years ago you granted me the opportunity to join your lab and since then you have helped me become the scientist that I am today. Despite some turbulent times, you have always supported me. I am eternally thankful for your guidance and perpetual support; especially this past fall when you helped me obtain a job at Dow Chemical, an opportunity potentially unattainable without you. From TLC to properly cooling reactions, you have taught me several techniques at the bench that I will still use many years from now. More importantly, you have taught me how to conduct hypothesis driven science, interpret experimental results and develop new strategies to ultimately solve complex problems. I am proud to be a part of your group and work with you each day. Of the many techniques and lessons that you have taught me, there are three that will always resonate: the harder you work, the luckier you get; the busier you are, the more efficient you become; and in order to know what you like to do, you have to know what you don't like to do (a lesson passed down during the Shiso isolation project).

I also extend thanks to Professor Guangbin Dong, Professor Eric Anslyn, Professor Adrian Keatinge-Clay, and Professor John DiGiovanni for their unflinching support, helpful discussions, and taking the time to serve on my doctoral committee. Also, I would like to thank Professor Christine Schmidt for granting me the ability to work in her lab during our collaboration and learn several new techniques. I am eternally indebted to Professor Ben Shoulders, Steve Sorey, Angela Spangenberg, and Dr. Vince Lynch for all of their help and enormous generosity with their time spent aiding me in solving numerous structures.

To the members of the lab, past and present: I am truly blessed to have worked with you all each day. You have made this experience bearable and created a scientific atmosphere that is genuinely fun and exciting, but also intellectually stimulating. Special thanks to my dear friend Tom Barton for all of the constructive and insightful conversations, the several laboratory techniques that you taught me, and the great times that we had together working side by side in Welch and NHB. You always looked after me like a big brother. I appreciate the support for without you a lot my synthetic successes would not be possible. Particular thanks to Bram Axelrod and Aurpon Mitra for being such great friends as well as co-workers. I appreciate all of the intellectual conversations that we shared and the laboratory techniques that you both have taught me. During some of my lowest times you both helped me in ways that cannot be described. Special thanks to Anders, Katie, Matt, Trevor, and Andrew for always making the lab a place that is a relaxed, fun atmosphere where we can work together to produce great science. I learn valuable lessons from each one of you every day, and I am blessed to have worked in an environment where we support each other like a family during the roller coaster of emotions that this experience can be. Particular thanks to Changxia Yuan for passing down certain techniques that can make all of the difference between a successful reaction and one that fails. You have always made lab an interesting place filled with entertainment. Without the indefatigable support of our group, this thesis would not have been possible. I also would like to extend thanks to the several undergraduates that I have had the pleasure to work with and train over these past five years. Travis, Nicole, Gina, Rachel, Alex, Karin, Valyn, and Ramsey, you are all very bright and I cherish our experiences together. I hope that I was able to teach you as much as you all have taught me.

Special thanks to Yong Liang and Professor Ken Houk for their computational expertise and providing several insights regarding the phthaloyl peroxide hydroxylation project.

Additional thanks to Ryan, Vanessa, Emma, Jason, Chris, Joe, Scott, Nicole, and Melissa for sharing in the difficulties and celebrating the successes during our time together. I appreciate all of your love and support.

The support from my family has been invaluable. Mom, Dad, Diane, Holli, Dan, my grandparents, aunts, uncles, and cousins – I am forever grateful for your love and support. You have always been there for me. The lessons that you have all instilled in me have made me the man that I am today. My successes are just as much yours. I love you all!

Lastly, I am so blessed to have such a beautiful, wonderful woman in my life who has supported and cared for me during some of my lowest times here at UT. Alia, you have helped me to traverse the obstacles and the appreciation that I have for you is beyond what words can describe.

Studies Toward the Synthesis of Celastrol
And
The Late-Stage Hydroxylation of Arenes Mediated by 4,5-
Dichlorophthaloyl Peroxide

Andrew Michael Camelio, Ph.D.

The University of Texas at Austin, 2014

Supervisor: Dionicio R. Siegel

The natural product celastrol (**1**) possesses a wide array of promising biological activities related to diseases characterized by protein misfolding including those associated with neuronal degradation, inflammation, and cancer. Relevant to cancer, celastrol functions as a non-ATP-competitive inhibitor of heat shock protein-90, providing a potential lead for the development of new inhibitors with improved pharmacology. A laboratory preparation of the small molecule was undertaken to provide access to the unnatural enantiomer of celastrol. The lack of understanding of the chemistry and biology of the growing class of celastroids is attributed to the incompatibility of biologically inspired polyene cyclization strategies to assemble friedelin triterpenoids. As a result of these problems residing at the interface of chemistry and biology, a purely synthesis-based strategy for polyene cyclizations to rapidly construct the pentacyclic core of the friedelin and celastroid natural products has been developed. This efficient strategy is gram scalable culminating in the first total synthesis of wilforic acid (**127**) and an advanced intermediate capable of delivering celastrol (**1**) as well as numerous celastroid natural products.

Phenols possess broad utility serving as key materials in all facets of chemical industries, especially the pharmaceutical industry. The ideal synthesis of a phenolic compound entails the direct oxidation of an aryl C-H bond remains to be a difficult synthetic challenge. Following our initial report describing the hydroxylation of arenes using phthaloyl peroxide, new peroxide derivatives were investigated to probe their reactivity in an effort to hydroxylate aromatics which were previously unreactive. Electronically poor to moderately rich arenes were successfully hydroxylated with a broad functional group tolerance using 4,5-dichlorophthaloyl peroxide. This protocol has been applied toward the rapid synthesis of phenolic analogs and metabolites of current pharmaceuticals as well as biocides. Mechanistic studies using kinetic isotope effect, competition, and benzylic oxidation experiments indicate that a novel diradical reverse-rebound mechanism is the likely pathway. Further examination of the transition-state using linear free energy relationships with σ vs. σ^+ values established a linear trend with a low negative *rho* value (- 3.92) corresponding best using σ values supporting a diradical reverse-rebound addition.

Table of Contents

List of Tables	xi
List of Schemes	xiii
List of Figures	xv
Abbreviations	xvi
Chapter 1 - Significance of Celastrol and Evolution of the Polyene Cascade	1
Isolation, Characterization, Biological Activity	3
Biosynthesis	6
The Evolution of Cationic Polyolefin Cyclizations and Polyprenoid Synthesis	10
Conclusion	35
Chapter 2 - Studies Toward the Synthesis of Celastrol	36
Retrosynthetic Analysis	36
Forward Synthesis	38
Conclusion	88
Experimental Section	90
Chapter 3 - Aryl Hydroxylation Mediated by 4,5-Dichlorophthaloyl Peroxide	281
Synthetic Protocols to Access Phenols	283
Phthaloyl Peroxide Mediated Hydroxylation	288
Development of an Arene Hydroxylation Protocol using 4,5- Dichlorophthaloyl Peroxide	294
Conclusion	322
Experimental Section	323
References	507

List of Tables

Table 2.1:	Survey of olefination conditions to provide tetrasubstituted alkene 140	39
Table 2.2:	Alkylation of different enolates using bromide 123 ultimately providing diketone 171	56
Table 2.3:	Differentiation of symmetrical ketone 171 via HWE olefination.....	57
Table 2.4:	Selected examples of the cationic cyclization of cyclohexenone 174	65
Table 2.5:	Polyene cyclization of the allylic alcohol 190	68
Table 2.6:	Slow addition protocol for the polyolefin cascade of allylic alcohol 190	70
Table 2.7:	Selected attempts to access methyl enol ether 196 or alcohols 198 and 200	78
Table 2.8:	Alkylation of ester 201 and attempted formation of ketene acetals 205	82
Table 2.9:	Synthesis of acid 128 through the dianionic alkylation of 199	85
Table 2.10:	Crystal data and structure refinement for 175	136
Table 2.11:	Atomic coordinates ($\times 10^4$) and equivalent isotropic displacement parameters ($\text{\AA}^2 \times 10^3$) for 1. $U(\text{eq})$ is defined as one third of the trace of the orthogonalized U^{ij} tensor.....	137
Table 2.12:	Bond lengths [\AA] and angles [$^\circ$] for 175	139
Table 2.13:	Anisotropic displacement parameters ($\text{\AA}^2 \times 10^3$) for 1. The anisotropic displacement factor exponent takes the form: $-2\pi^2 [h^2 a^{*2} U^{11} + \dots + 2 h k$ $a^* b^* U^{12}]$	143
Table 2.14:	Hydrogen coordinates ($\times 10^4$) and isotropic displacement parameters ($\text{\AA}^2 \times$ 10^3) for 175	145
Table 2.15:	Torsion angles [$^\circ$] for 175	147
Table 3.1:	Scope of arenes hydroxylated by phthaloyl peroxide.....	289
Table 3.2:	Reactivity comparison between peroxides 211 and 296 using <i>p</i> - anisaldehyde.....	301

Table 3.3:	Hydroxylation of arenes mediated by 4,5-dichlorophthaloyl peroxide	308
Table 3.4:	Hydroxylation of drugs to provide phenolic derivatives and metabolites using phthaloyl and 4,5-dichlorophthaloyl peroxide	311
Table 3.5:	Incompatible functional groups and arenes that are not oxidized using 4,5-dichlorophthaloyl peroxide.....	313
Table 3.6:	Oxidation of halobenzenes and <i>p</i> -trimethylsilyl toluene using 4,5- dichlorophthaloyl peroxide	314
Table 3.7:	Phthalic peroxide mediated benzylic oxidation experiments using mesitylene	319
Table 3.8:	Competition experiments using mesitylene and dimethoxy methylvanillate comparing the rates of reactivity between 4,5- dichlorophthaloyl peroxide and phthaloyl peroxide in different solvents and temperatures	321

List of Schemes

Scheme 1.1: Proposed biosynthesis of celastrol	8
Scheme 1.2: Biosynthesis of the protosterol cation (14) from 2,3-(S)-oxidosqualene.....	10
Scheme 1.3: Early examples of ene-cascade cyclizations in terpenoid synthesis	12
Scheme 1.4: Enzymatic and non-enzymatic cyclization pathways for 2,3-(S)- oxidosqualene	14
Scheme 1.5: Ireland and Johnson's collaborative total synthesis of (±)-germanicol.....	16
Scheme 1.6: Corey's total syntheses of oleanolic acid, erythrodiol, and β-amyrin	18
Scheme 1.7: Johnson's total synthesis of sopharadiol	20
Scheme 1.8: Corey's formal synthesis of (+)-germanicol.....	23
Scheme 1.9: Corey's total synthesis of (+)-lupeol	25
Scheme 1.10: Natural products accessed via cationic rearrangements of (+)-lupeol.....	27
Scheme 1.11: Rearrangement of friedelin in the reverse direction promoted by acid	28
Scheme 1.12: Ireland's total synthesis of (±)-alnusenone	30
Scheme 1.13: Ireland's total synthesis of friedelin	32
Scheme 1.14: Ireland's polyene cyclization approaches toward (±)-alnusenone	34
Scheme 2.1: Synthesis of the ketone fragment.....	38
Scheme 2.2: Synthesis of the aryl fragment	42
Scheme 2.3: Attempted Grignard formation and fragment coupling	43
Scheme 2.4: Synthesis of aryl dioxolane 151	45
Scheme 2.5: Synthesis of iodo-enoate fragment.....	47
Scheme 2.6: Synthesis of triene fragment	49
Scheme 2.7: Failed B-Alkyl Suzuki-Miyaura to couple fragments	50
Scheme 2.8: Wacker oxidation strategy to access diketone 171	53

Scheme 2.9: Wacker oxidation of triene 178 using the Sigman protocol	53
Scheme 2.10: Synthesis of trienonate 183	59
Scheme 2.11: Synthesis of the polyene enone 174	61
Scheme 2.12: Attempted allylic oxidations of pentacycle 191 or benzyl ketone 194	72
Scheme 2.13: Synthesis of ketone 175	73
Scheme 2.14: Synthesis of the saturated acid 199 and ester 201	80
Scheme 2.15: Synthesis of wilforic acid (127), enone 210 , and final strategy	87
Scheme 2.16: Overall synthesis of wilforic acid (127) and enone 210	89
Scheme 3.1: CYP450 mediated hydroxylation of arenes.....	284
Scheme 3.2: Early peroxide mediated hydroxylation of arenes.....	285
Scheme 3.3: Transition metal catalyzed and Friedel-Crafts/Baeyer Villiger syntheses	
of phenols.....	287
Scheme 3.4: CPCM-(U)B3LYP/6-31+G(d) computed free energy surfaces for aryl and benzylic functionalization of mesitylene using phthaloyl peroxide.....	291
Scheme 3.5: CPCM-(U)B3LYP/6-31+G(d) computed free energy surfaces for aryl and benzylic functionalization of mesitylene using benzoyl peroxide	293
Scheme 3.6: Syntheses of different phthalic peroxides.....	300
Scheme 3.7: Decomposition pathway of 4,5-dichlorophthaloyl peroxide in HFIP	302
Scheme 3.8: Thermal stability of 4,5-dichlorophthaloyl peroxide and phthaloyl peroxide.....	303
Scheme 3.9: Reaction between hexamethylbenzene and 4,5-dichlorophthaloyl peroxide.....	317

List of Figures

Figure 1.1: Celastrol, pristimerin, tingenone, and the <i>p</i> -bromobenzoate of pristimerin	4
Figure 1.2: Stereospecific formation of celastrol/protein adducts through conjugate addition of nucleophiles into the quinone methide	6
Figure 2.1: Key disconnections of celastrol and the linear precursors for the polyene cyclization	37
Figure 2.2: New bond disconnections to construct the desired tetrasubstituted olefin ...	41
Figure 2.3: New strategy for the synthesis of the polyene 174	52
Figure 2.4: New retrosynthetic analysis through a bifurcated strategy from the alkene 191	71
Figure 2.5: View of cyclized ketone 175 . Displacement ellipsoids are scaled to the 50% probability level	74
Figure 2.6: Retrosynthesis to access wilforic acid (127) and celastrol (1) from the ketone 175	76
Figure 3.1: Arene reactivity difference between 4,5-dichloro- and phthaloyl peroxide via diradical addition	296
Figure 3.2: 4,5- and 3,6-dichlorophthaloyl peroxide oxidation of 1,3,5-trichlorobenzene	297
Figure 3.3: TGA data for 4,5-dichlorophthaloyl peroxide	305
Figure 3.4: Linear free energy σ plot for the 4,5-dichlorophthaloyl peroxide mediated arene oxidation, computational analysis for the EAS and diradical addition pathways, and KIE experiments depicting the major mechanistic pathway	316

Abbreviations

2D-NMR	two dimensional nuclear magnetic resonance
9-BBN	9-borabicyclononane
Å	angstrom
Ac ₂ O	acetic anhydride
AcOH	acetic acid
ADH	asymmetric dihydroxylation
ALS	amyotrophic lateral sclerosis
atm	atmosphere
ATP	adenosine triphosphate
BF ₃ -OEt ₂	boron trifluoride diethyl etherate
BHT	butylated hydroxytoluene
BQ	1,4-benzoquinone
Bu	butyl
Cdc37	cell division cycle control protein-37
¹³ C-NMR	carbon nuclear magnetic resonance
CI	chemical ionization
<i>cis</i>	<i>L.</i> on the same side
cm ⁻¹	inverse centimeters
CO	carbon monoxide
COSY	correlation spectroscopy
CYP450	cytochrome P450
D	dextrorotatory
DABCO	1,4-diazobicyclooctane

DBU	1,8-diazobicycloundecene
DCE	1,2-dichloroethane
DCPP	4,5-dichlorophthaloyl peroxide
DDQ	2,3-dichloro-5,6-dicyano-1,4-benzoquinone
DEPT	distortionless enhancement polarization transfer
DFT	density functional theory
DIBAL	diisobutylaluminum hydride
DMA	dimethylacetamide
DMAP	<i>N,N</i> -dimethylamino pyridine
DME	dimethoxyethane
DMF	dimethylformamide
DMM	dimethoxymethane
DMP	Dess-Martin Periodinane
DMSO	dimethylsulfoxide
dppf	1,1'-bis(diphenylphosphino)ferrocene
d.r.	diastereomeric ratio
<i>E</i>	<i>Ger.</i> , entgegen
EAS	electrophilic aromatic substitution
ee	enantiomeric excess
Enz-H ⁺	proton in the active site of an enzyme
eq.	equivalent
equiv	equivalent
ESI	electrospray ionization
Et	ethyl

EtOAc	ethyl acetate
FDA	Federal Drug Administration
FG	functional group
FMO	Frontier molecular orbital theory
g	gram
¹ H-NMR	proton nuclear magnetic resonance
HFIP	1,1,1,3,3,3,-hexafluoro-2-propanol
HMPA	hexamethylphosphoramide
HMBC	heteronuclear multi-bond correlation
HOMO	highest occupied molecular orbital
hr	hour
HRMS	high resolution mass spectrometry
HSF-1	heat shock transcription factor-1
HSQC	heteronuclear single quantum correlation
HSP90	heat shock protein-90
HSR	heat shock response
HWE	Horner-Wadsworth-Emmons
Hz	hertz
IKK β	inhibitor of nuclear factor kappa- β -kinase
imid.	imidazole
INADEQUATE	incredible natural-abundance double-quantum transfer experiment
<i>i</i> -Pr	isopropyl
IR	infrared spectroscopy
<i>J</i>	coupling constant

KIE	kinetic isotope effect
KiHMDS	potassium hexamethyldisilazide
LDA	lithium diisopropyl amide
LiHMDS	lithium hexamethyldisilazide
M	molar
<i>m</i> -CPBA	<i>meta</i> -chloroperoxybenzoic acid
Me	methyl
Me ₂ CO	acetone
MeCN	acetonitrile
MeLi	methyllithium
mg	milligram
MHz	megahertz
mL	milliliter
mmol	millimole
mol	mole
MsCl	methanesulfonyl chloride
MS	mass spectrometry
N	normal
NaHMDS	sodium hexamethyldisilazide
NBS	<i>N</i> -bromosuccinimide
<i>n</i> -BuLi	normal butyllithium
NIH	National Institutes of Health
nM	nanomolar
nm	nanometer
NMR	nuclear magnetic resonance

NOE	nuclear Overhauser effect
OAc	acetate
OBz	benzoate
p23	prostaglandin E synthase-23
<i>p</i>	<i>para</i>
PAH	polyaromatic hydrocarbons
PPO	phthaloyl peroxide
<i>p</i> -TsOH	<i>para</i> -toluenesulfonic acid monohydrate
PDC	pyridinium dichromate
Pd-C	palladium on carbon
Ph	phenyl
PhH	benzene
PhMe	toluene
Pin	pinacol
PPA	polyphosphoric acid
ppm	parts per million
pyr.	pyridine
R _f	retention factor
<i>s</i> -BuLi	<i>sec</i> -butyllithium
SET	single electron transfer
Sia ₂ BH	diisosiarylborohydride
SM	starting material
SOMO	singly occupied molecular orbital
<i>t</i> -Am	<i>tert</i> -amyl
<i>t</i> -Bu	<i>tert</i> -butyl

TBAF	tetrabutylammonium fluoride
TBHP	<i>tert</i> -butyl hydrogen peroxide
TBSCl	<i>tert</i> -butyldimethylsilyl chloride
TBSOTf	<i>tert</i> -butyldimethyltrifluoromethane sulfonate
TEG	triethylene glycol
NTf	trifluoromethane sulfonimide
OTf	trifluoromethane sulfonate
TFA	trifluoroacetic acid
TFAA	trifluoroacetic anhydride
TFE	2,2,2-trifluoroethanol
TfOH	trifluoromethane sulfonic acid
Tf ₂ O	trifluoromethane sulfonic anhydride
TGA	thermogravimetric analysis
THF	tetrahydrofuran
THP	tetrahydropyran
TIPS	triisopropylsilyl
TIPSOTf	triisopropylsilyl trifluoromethane sulfonate
TLC	thin-layer chromatography
TMEDA	tetramethylethylenediamine
TMS	trimethylsilyl
TMSOTf	trimethylsilyl trifluoromethane sulfone
<i>trans</i>	<i>L.</i> , across
μM	micromolar
<i>Z</i>	<i>Ger.</i> , zusammen

Chapter 1 – Significance of Celastrol and Evolution of the Polyene Cyclization

Molecular chaperones play an integral role in maintaining proteostasis, in particular, protein folding and conformation.¹ Chaperone malfunction triggers several diseases which includes cancers as well as those associated with neurodegeneration such as Huntington's, Parkinson's, Alzheimer's, and amyotrophic lateral sclerosis (ALS).^{2,3} Quintessential to the proper folding of various proteins is the heat-shock transcription factor-1 (HSF-1). Activation of HSF-1 by external stresses, either physiological or environmental, induces the rapid manufacture of heat shock proteins (HSPs) which serve as molecular chaperones procuring a surveillance role in maintaining protein homeostasis.⁴⁻¹¹ Suppression of neurodegenerative diseases, lysosomal storage diseases (Gaucher and Tay-Sachs), and cancers (i.e. pancreatic, breast, leukemia, and hepatic) has been observed through the upregulation of molecular chaperones including HSP90. Modulation of the heat shock response (HSR) and HSPs through the use of small molecules and natural products has gained enormous pharmacological focus due to the potential therapeutic modalities in human diseases.^{1,2,12-19}

The small molecule celastrol (**1**), which belongs to the friedelin family of natural products, possesses a potent, broad array of promising biological activities in the diseases triggered by malfunctioning chaperones.² One of the protein targets of celastrol is HSP90, but unlike other small molecules that target this protein, celastrol acts as a non-ATP-competitive inhibitor. This provides a different avenue for the development of new inhibitors with improved pharmacology.^{17,20} Celastrol also induces neuronal and tissue

regeneration by invoking an immunosuppressant response during refractory periods.²¹ *In vitro* analyses has found that the various biological effects are caused through covalent modification via conjugate addition of biological nucleophiles, such as cysteine residues, into the quinone methide.^{2,22-26} Since other molecules that possess quinone methides do not interact with HSP90 or provoke HSR, celastrol possesses special structural features that facilitate the induction of HSR and cause the reaction with certain proteins. These features are unknown, and the true mechanism by which celastrol interacts with its targets in their native environment also remains elusive.²

The development of a scalable concise synthetic approach could help solve these issues. A platform that constructs celastrol, its unnatural enantiomer, a variety of celastroid natural products as well as their antipodes, and structural derivatives inaccessible through semi-synthesis provides a new biological tool to investigate the mechanisms of action of this natural product. Developing a synthetic platform is, however, not easily accomplished as the molecule's complex topology is comprised of several all-carbon quarternary stereocenters including angular methyls. Despite the evolution of triterpenoid synthesis and the cationic polyene cascades used to access a variety of pentacyclic triterpenes, there remain difficult synthetic problems in regards to constructing the friedelin family of natural products. Therefore, the laboratory synthesis of celastrol and its enantiomer could provide an important tool to investigate its biological mode of action affording valuable information regarding HSP90 while simultaneously solving longstanding synthetic problems.

Isolation, Characterization, Biological Activity

For centuries extracts of the *Tryptergium wilfordii* Hook F. vine (Thunder of God or lei gong teng) have provided remedies used in Chinese traditional medicine for various ailments including edema, fever, chills, joint pain, inflammation, and rheumatoid arthritis.^{2,27} In 1930 cultivation of the vines' roots was requested to be forbidden in the Chekiang province. Resistant local farmers argued that they were unable to successfully harvest their crops without using the powdered roots as an insecticidal agent. These disputes inspired entomologists to extract the natural products from the vine; culminating in 1936 when Chou and Mei published their findings concluding that the major constituent of the orange extract is β -carotene. This was proven to be incorrect in 1939 by the work of Gisvold, but the actual structure remained elusive for 36 years. Over this time period, structural characterization of celastrol and the methyl ester pristimerin (**2**) indicated the presence of the distinct quinone methide chromophore (425 nm and 255 nm). IR spectroscopy showed the presence of a chelated hydroxyl (3380 cm^{-1}), ester carbonyl (1740 cm^{-1}), and the quinone methide (1607 cm^{-1}). The extract also proved to be chiral as the observed optical rotation of pristimerin is $[\alpha]_D -168^\circ$. The limited NMR studies of celastrol and pristimerin had shown six methyls represented as singlets, two coupled olefinic protons, and unresolved aliphatic protons suggesting a natural product belonging to the friedelin family.²⁷ Then in a landmark publication in 1972 Ham and Whiting extracted pristimerin (**2**), performed a conjugate reduction with NaBH_4 , and subsequently esterified the catechol to afford the *p*-bromobenzoate (**3**). After several recrystallization attempts, they discovered that rapidly cooling a hot benzene/ethanol solution of **3** produced crystals suitable for X-ray diffraction which unambiguously

confirmed the structure of **3** and as a result celastrol (**1**) as well as pristimerin (**2**).²⁸ The absolute configuration revealed the sterically encumbered friedelanyl triterpenoid core possessing the *trans*-angular disposed methyls residing in the C-D ring juncture, three other all-carbon quaternary stereocenters, and the discrete quinone methide functionality which ultimately provides the red-orange color of celastrol. The isolation and purification process to extract celastrol has been extensively examined and perfected so that starting from 15 kg of raw dry roots, 798 mg of celastrol (**1**) is isolated in 99.5% purity.²⁹

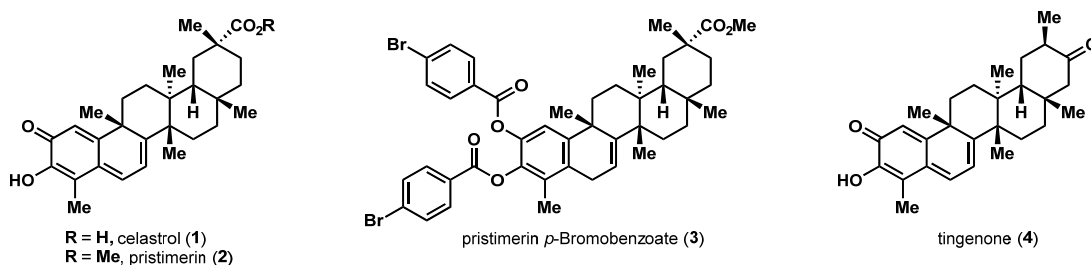


Figure 1.1. Celastrol, pristimerin, tingenone, and the *p*-bromobenzoate of pristimerin.

Celastrol exhibits a broad array of potent biological activities. Diseases associated with cancers, neurodegeneration, and inflammation can be reversed, either *in vitro* or *in vivo*.²⁻²⁷ A major protein target of celastrol is HSP90, but it can also act as an antioxidant provoking an autoimmune response which induces neural and tissue regeneration during dormant periods at potencies as low as 50 nM in tadpoles.²¹ Other members of the celastroid family of natural products (i.e. tingenone (**4**)) also exhibit cytotoxicity towards skin, stomach, uterine, and lymphoepithelioma cancers in clinical trials with minimal side effects.^{27,30,31} The therapeutic effects of the whole extracts from *Trypterygium wilfordii* are also being examined in over 20 clinical trials ranging from

HIV, Lupus, Crohn's disease, kidney disease, and rheumatoid arthritis which are at various stages of completion.³²

Despite the spectrum of biological activity, the mode of action of celastrol and the related natural products remains elusive.² Recently, *in vitro* analysis has shown that biological nucleophiles, such as cysteine residues, add conjugately in a 1,6-Michael-like fashion into the quinone-methide (Figure 1.2).²⁴ Silverman and co-workers showed that this addition is stereospecific with β -facial selectivity, potentially leading to specificity.²³ Covalent modification of biological targets has also been studied in the context of celastrol and tingenone interacting with DNA as well as modifying cysteine residues of protein targets.^{22,23,33,34} Researchers have discovered that the signaling pathways and proteins affected by celastrol include HSP90, Cdc37, p23, NF- κ B, and IKK β .² In regards to HSP90, unlike other small molecule quinone and quinone methide modulators, celastrol does not act as an ATP-competitive inhibitor. Binding to the C-terminus, not the N-terminus like other modulators, causes a conformational change which inhibits the docking of Cdc37. This enhances client protein degradation inducing cellular apoptosis.²⁰ Despite their potency, no ATP-competitive inhibitor of HSP90 has been FDA approved because of low selectivity which leads to undesirable side effects. Therefore, celastrol represents a new class of inhibitors as therapeutic targets, especially in a variety of cancers including pancreatic cancer due to the high expression of HSP90 in tumor cells.¹⁷

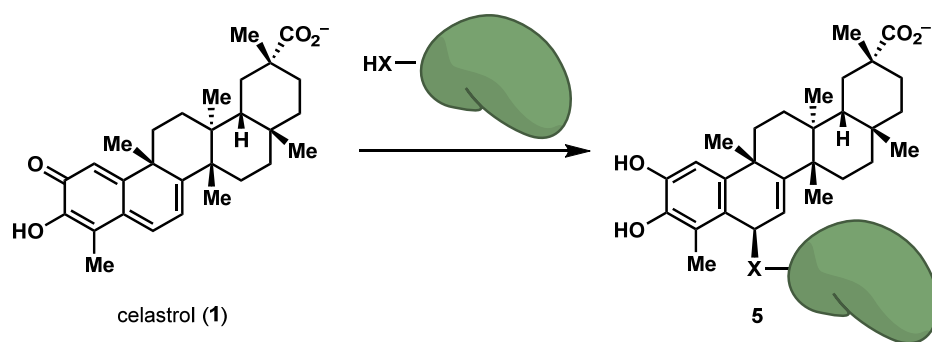


Figure 1.2. Stereospecific formation of celastrol/protein adducts through conjugate addition reactions of nucleophiles into the quinone methide.²³

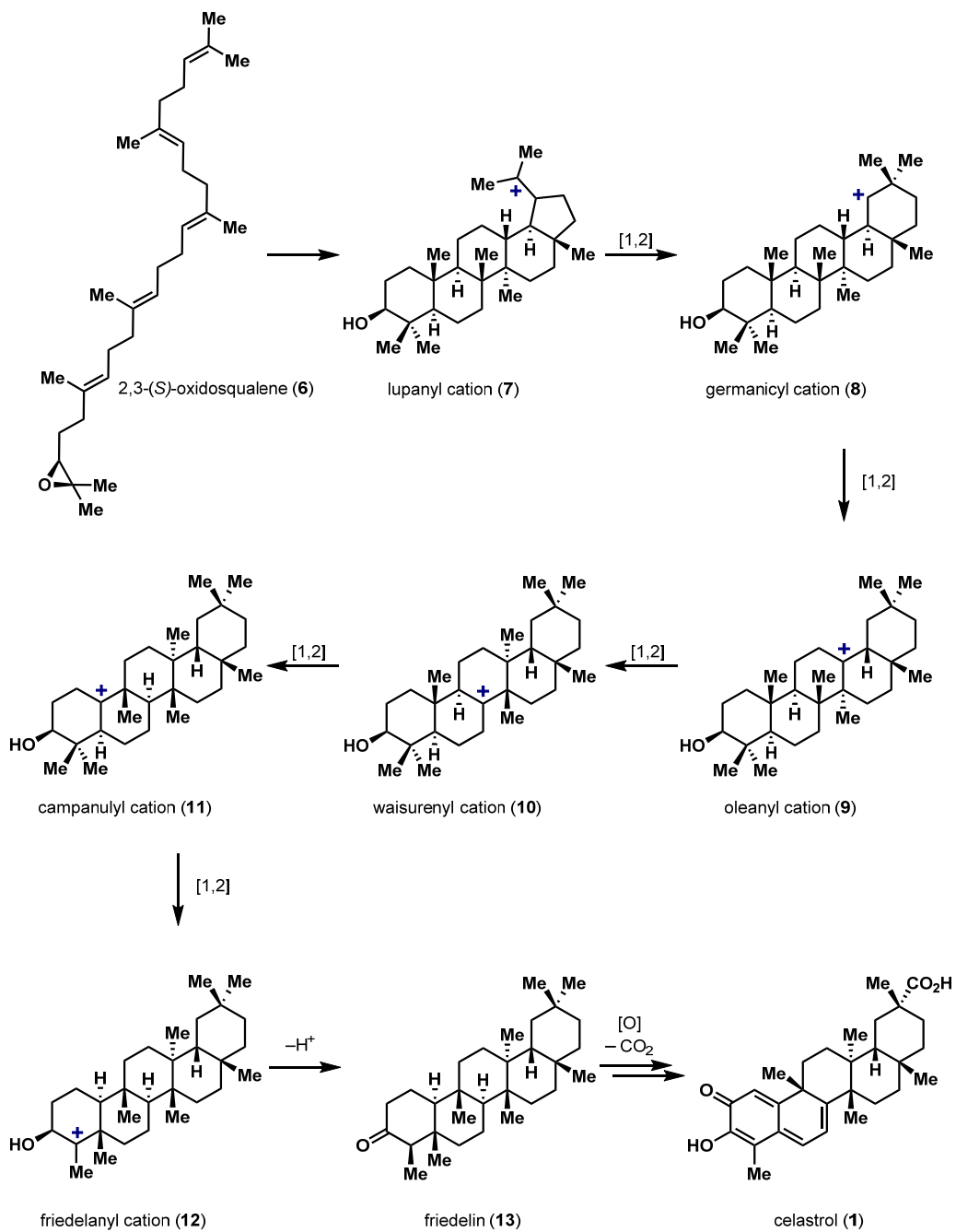
There are inherent structural features that celastrol possesses besides the quinone methide functionality which facilitate the small molecule's interaction with its protein targets. These features are still unknown and therefore many questions regarding the biological mode of action, native protein targets, how celastrol affects these numerous targets, the relationship between the varied biological effects, and if the small molecule is a specific alkylating agent remain unanswered.² Synthetic access to the enantiomer would provide a tool to further study the small molecule's mode of action through determining if the effects are promoted by specific covalent modification. This in turn reveals the important structural features for future potential therapeutics which are non-ATP competitive inhibitors of HSP90 as well as provide a strategic direction for the synthesis of celastroid analogs.

Biosynthesis

Celastrol is a triterpenoid belonging to the D:A-friedo-nor-oleananes, a subgroup of the friedelin family of natural products.²⁷ The celastroids bear structurally similar

characteristics, but differ mainly in oxygenation states in the A, B, and E rings. Friedelins are characterized by the fused pentacyclic framework, and more distinctly, the vicinal *trans*-angular methyl groups positioned in the C-D ring juncture. Severe 1,3-diaxial strain occurs between both methyls and their adjacent sterically condensed environment. For this reason, as well as the number of stereocenters and all-carbon quaternary centers, there is a lack of synthetic routes to the perpetually growing class of celastroid natural products which has limited the understanding of their chemistry and biology. The absence of a synthesis can in part be attributed to the incompatibility of biologically inspired polyene cyclization strategies to assemble the celastroid or friedelin natural products.³⁵ The implementation of these reactions for the syntheses of polycyclic triterpenoids is highly desirable as they provide rapid access to relatively large molecules with multiple stereogenic centers in a single transformation.^{36,37} Due to the vast number of friedelin natural products that are co-isolated with celastrol it has been postulated that celastrol is biosynthetically derived from friedelin.²⁷ Unfortunately, the polyene cyclization leading to friedelin is exceedingly challenging to reproduce in the laboratory due to a set of complex, energetically unfavorable methyl and hydride shifts (Scheme 1.1).³⁵

Scheme 1.1. Proposed biosynthesis of celastrol.^{27,35}

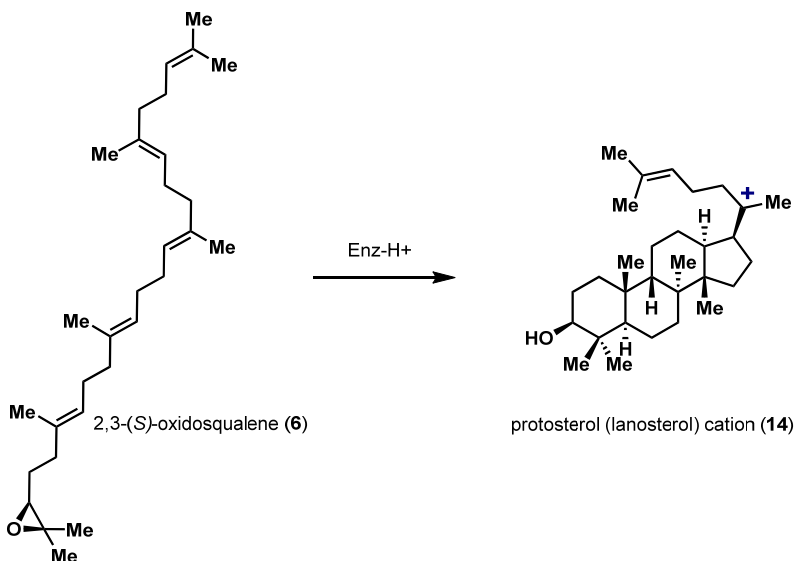


The biosynthesis of celastrol commences in the friedelin cyclase enzyme which converts 2,3-(*S*)-oxidosqualene (**6**) into the lupanyl cation (**7**). The epoxide is initially ionized by a proton transfer from an aspartic acid residue in the active site. The lupanyl cation then undergoes a series of [1,2] hydride and methyl shifts in a suprafacial manner to arrive at the friedelanyl cation (**12**) (Scheme 1.1). Next, an oxidative hydride migration affords friedelin, which is oxidized in the A, B, and E rings to generate celastrol. The energetics of the suprafacial [1,2]-shifts proceeding from the lupanyl cation (**7**) have been examined by E. J. Corey. The friedelanyl cation is the highest energy species as determined by B3LYP 6-31 G* DFT and *ab initio* Hartree-Fock (6-31* or 3-21(*) levels) calculations. This calls into question if the friedelin-based natural products are derived from other pentacyclic triterpenes. The formation of the friedelanyl cation is thermodynamically unfavored by ~20 kcal/mol. Corey and co-workers propose that the same cyclase enzyme which induces the cyclization of 2,3-(*S*)-oxidosqualene also promotes the subsequent rearrangements driving the reaction forward. Friedelin cyclase uses the exothermicity of the cyclization to perform a nonstop sequence of cyclization and multistep [1,2] rearrangements. The energy gained in the formation of the pentacyclic framework from 2,3-(*S*)-oxidosqualene (~30 kcal/mol) compensates for the high-energy friedelanyl cation (**12**). They also propose that the other natural products (i.e. lupeanes, oleananes, and ursanes) are not generated in the friedelin cyclase due to the lack of correctly positioned proton acceptors in the catalytic site which would facilitate elimination or diversion to the other cations.³⁵

The Evolution of Cationic Polyolefin Cyclizations and Polyprenoid Synthesis

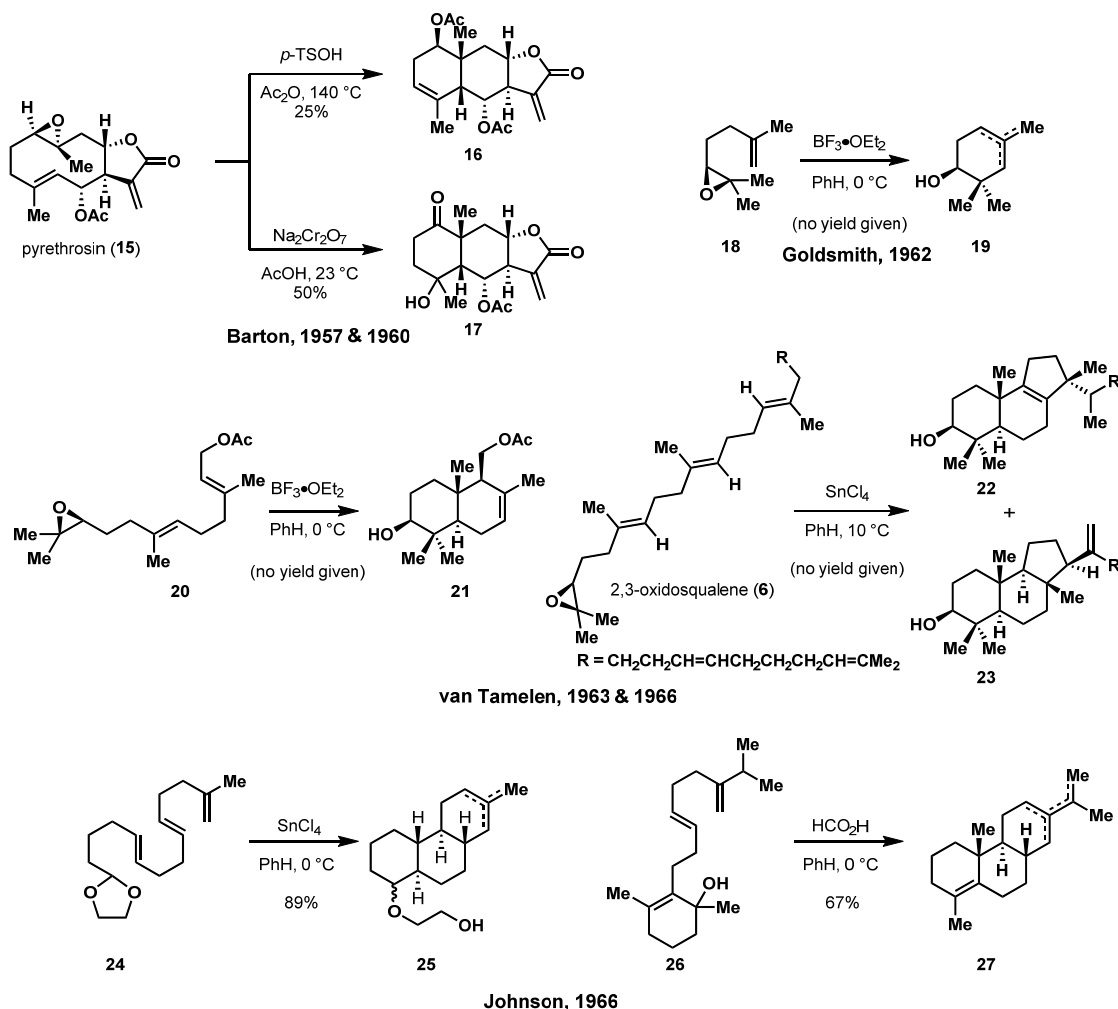
Extensive investigation in the biosynthesis of lanosterol and cholesterol ultimately led to the finding that 2,3-(S)-oxidosqualene (**6**) was cyclized upon acid activation to generate the lanosterol cation (**14**) through a cationic polyolefin cyclization or polyene cascade (Scheme 1.2). Stork and Eschenmoser postulated that upon activation of the epoxide in the active site, the tethered alkenes engage in a concerted manner producing a highly delocalized cation in the transition state. This results in the formation of several carbon-carbon bonds in a single diastereoselective operation to afford the protosterol cation **14**. The landmark insight of these findings is that the reaction is stereospecific. The configuration of the alkene, either *cis* or *trans*, leads to different cyclized products.^{38,39}

Scheme 1.2. Biosynthesis of the protosterol cation (**14**) from 2,3-(S)-oxidosqualene.



Early pioneers in steroid synthesis examined the synthetic plausibility of this theory to rapidly construct a variety of terpenoids in a biomimetic fashion starting from the readily accessible linear precursors. During the course of elucidating the structure of the sesquiterpenoid pyrethrosin (**15**) Barton discovered that under mild acidic conditions the activated epoxide underwent a transannular ene-cyclization to rapidly generate the fused tricyclic lactones **16** and **17** (Scheme 1.3).^{40,41} The viability of this strategy towards steroid synthesis was then investigated by Goldsmith, van Tamelen, and Johnson through the syntheses of various mono-, di-, and tri-terpenoids. They examined several initiators (i.e. epoxides, acetals, and allylic alcohols), the optimal acid promoters (i.e. $\text{BF}_3\text{-OEt}_2$, SnCl_4 , and HCO_2H), and solvents (i.e. PhH or CH_2Cl_2).⁴²⁻⁴⁶ These original accounts are exceedingly important because they set the precedent for utilizing these types of cation initiated polyolefin cyclizations in a non-enzymatic environment. The experiments also provide significant information regarding the use of $\text{BF}_3\text{-OEt}_2$ and solvent comparisons between methylene chloride and benzene. $\text{BF}_3\text{-OEt}_2$ proved to be a poor Lewis acid for these cyclizations because it prompted the formation of byproducts such as rearranged ketones, fluorohydrins, and fluorination adducts of the subsequent carbonium ions formed after the initial cyclization.

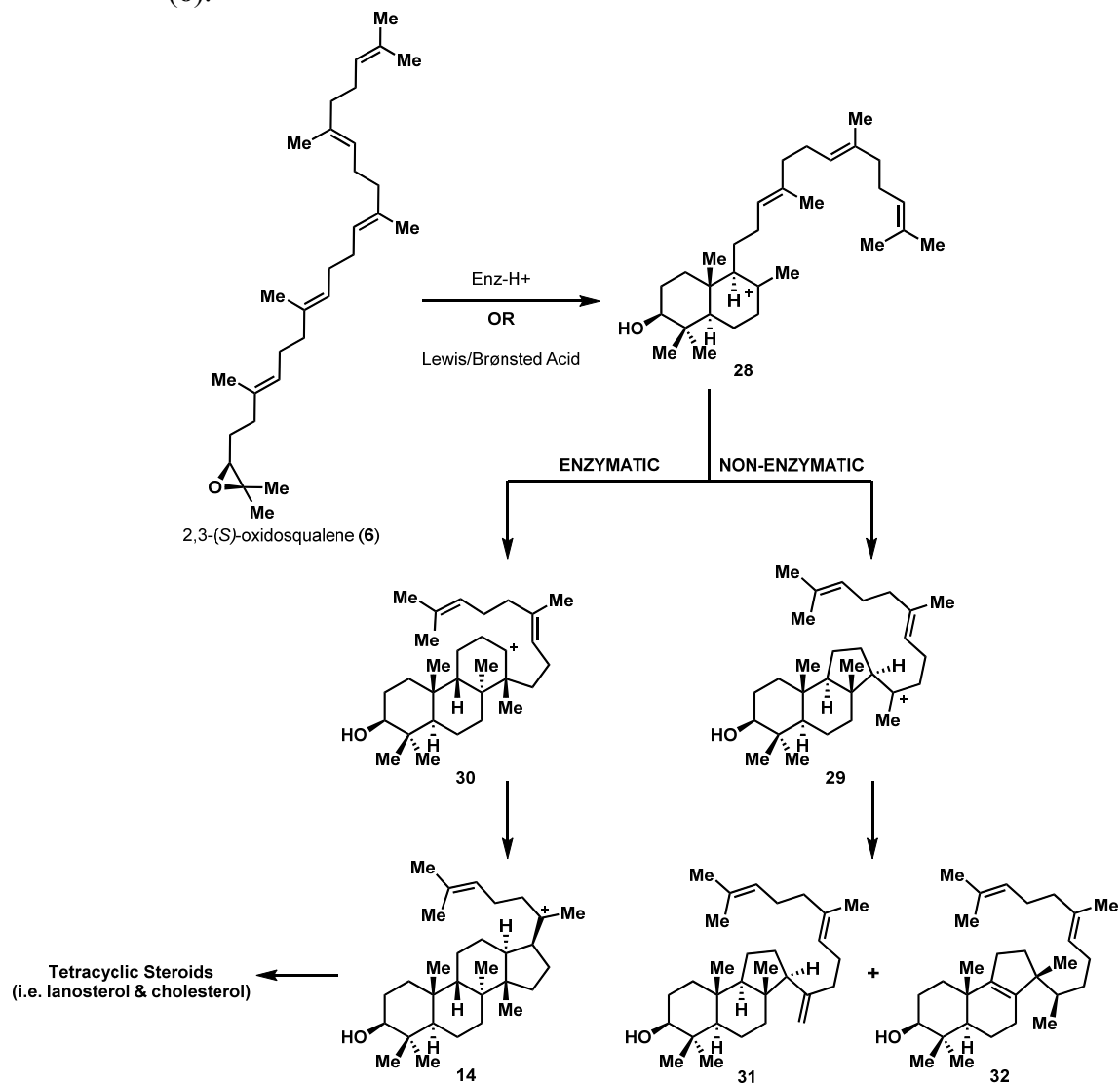
Scheme 1.3. Early examples of ene-cascade cyclizations in terpenoid synthesis.



Using polyene cascade strategies to access natural pentacyclic triterpenoids is capricious in the laboratory setting as compared to the controlled enzymatic environment. The challenges reside in the construction of the polyprenoid precursors and successfully performing the cationic cyclizations to provide advanced intermediates in appreciable yields and adequate scalability. The pentacycles possess strain energy due to the steric

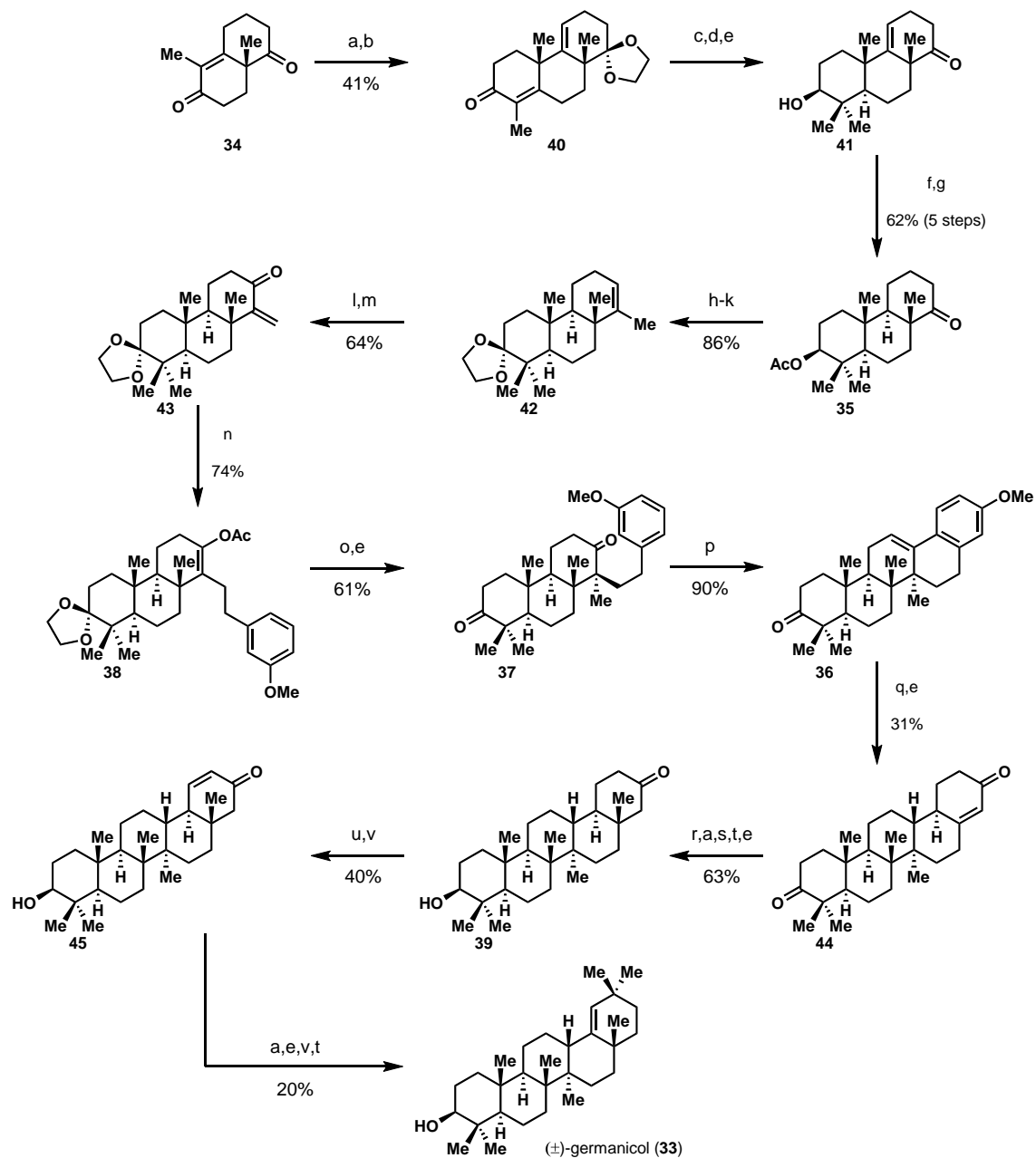
constraints of the angular methyls and the distortion of the cyclic backbone which make these cyclizations a daunting task (See Scheme 1.1). Early studies by van Tamelen on the cyclization of oxidosqualene (**6**) proved vital illustrating that upon activation **6** folds preferentially to form a 5-member ring over the desired 6-member ring after the initial cyclization to provide the *trans*-decalin adduct **28** (Scheme 1.4).⁴⁶ The second annulation generates the carbonium intermediate **29** which possesses a more stable tertiary carbocation as compared to the 6-membered tricyclic adduct **30** which possesses the less stable secondary carbocation. The cation **29** can then undergo elimination or a combination of [1,2] methyl and hydride shifts with a subsequent elimination to afford the trienes **31** and **32**.

Scheme 1.4. Enzymatic and non-enzymatic cyclizing pathways for 2,3-(S)-oxidosqualene (6).



This finding prompted the joint efforts of the Ireland and Johnson laboratories to conduct the total synthesis of (\pm)-germanicol (**33**) in a non-biomimetic linear strategy (Scheme 1.5).⁴⁷ Commencing from diketone **34**, the tricyclic acetate **35** was synthesized in 7 steps with an overall yield of 25% using a Robinson annulation approach. Compound **35** was elaborated through a low yielding 11 step sequence culminating with the ene-cyclization generating pentacycle **36** from arene **37**. Another highlight of this sequence is the conjugate Grignard addition and trapping of the insipient enolate to construct the tetrasubstituted enol acetate **38**. This was used to deliver the angular methyl in a diastereoselective fashion using an *in situ* acetate cleavage/alkylation protocol to afford **37**. The total synthesis of racemic germanicol (**33**) was then concluded in a 13 step sequence highlighted by the installation of the last angular methyl in the D-E ring juncture through a novel hydrocyanation/reduction protocol developed by Nagata to arrive at ketone **39**.^{48,49} The 31 step synthesis afforded racemic germanicol with an overall yield of 0.001% starting from the enone **34**. This underscores the power of the cyclase enzyme and the disparity between the biosynthetic, single step operation versus the multi-step conventional synthesis required to construct these complex terpenoids.

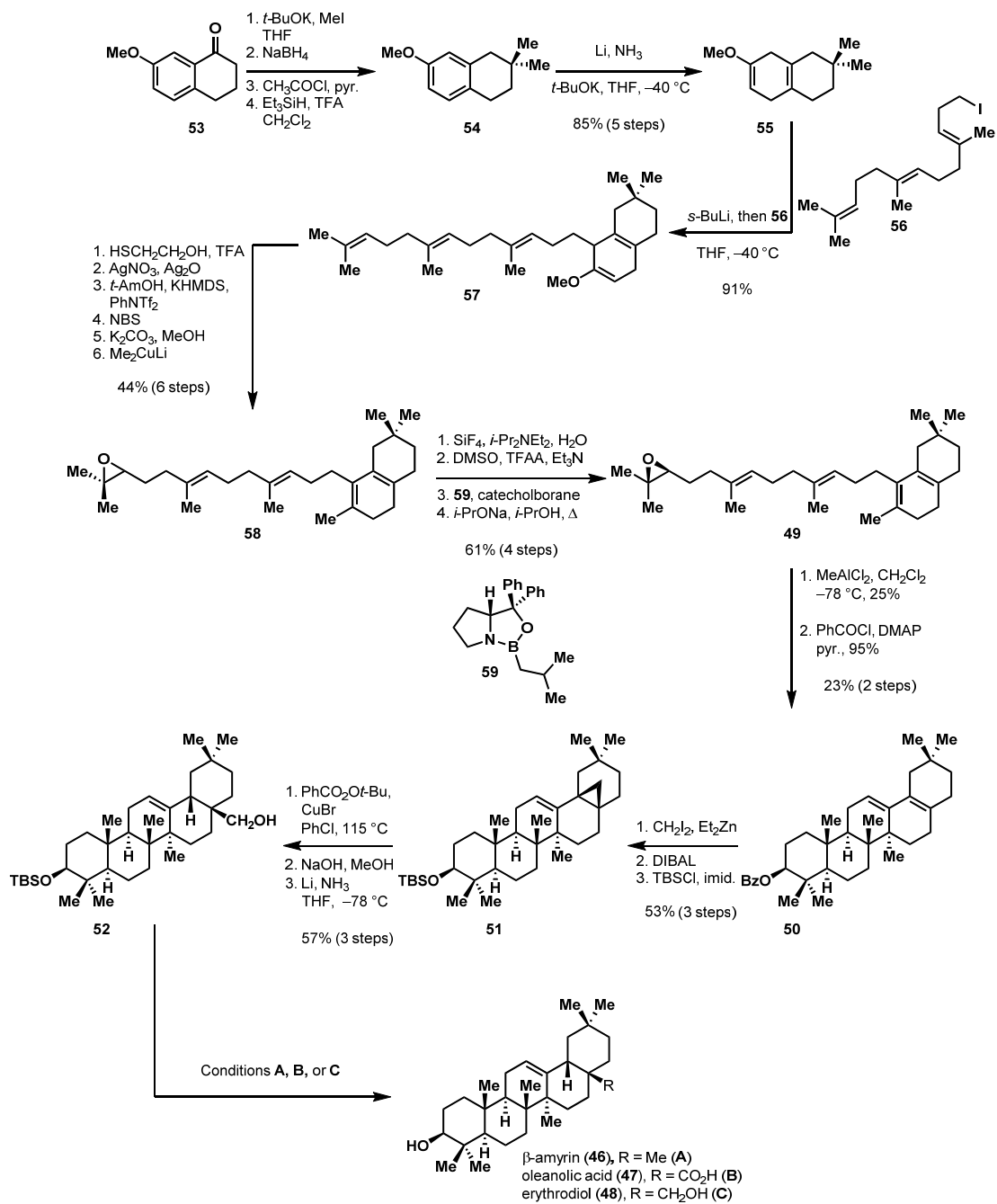
Scheme 1.5. Ireland and Johnson's collaborative total synthesis of (±)-germanicol.⁴⁷



(a) $(\text{CH}_2\text{OH})_2$, H^+ (b) $\text{C}_2\text{H}_5\text{COCH}=\text{CH}_2$, NaOMe , MeOH (c) Li , NH_3 , $t\text{-BuOH}$, MeI (d) $\text{LiAl}(\text{O}t\text{-Bu})_3\text{H}$ (e) H_3O^+ (f) Ac_2O , pyr. (g) H_2 , Pd-C , AcOH (h) MeLi , DME (i) $8\text{ N H}_2\text{CrO}_4$, Me_2CO (j) SOCl_2 , pyr. (k) $p\text{-TOSOH}$, PhH , $(\text{CH}_2\text{OH})_2$ (l) O_2 , $h\nu$, sensitizer, pyr. LiAlH_4 (m) CrO_3 , pyr. (n) $m\text{-MeOC}_6\text{H}_4\text{CH}_2\text{MgCl}$, Ac_2O (o) MeLi , DME , MeI (p) PPA (q) Li , NH_3 , EtOH (r) AlEt_3 , HCN , THF (s) $(i\text{-Bu})_2\text{AlH}$, PhH (t) N_2H_4 , OH^- , TEG (u) Br_2 , AcOH (v) CaCO_3 , DMA (v) $\text{KO}t\text{-Bu}$, $t\text{-BuOH}$, MeI

Ireland and Johnson's synthesis of germanicol represents a landmark in terpenoid synthesis. This single ring annelation strategy as well as van Tamelen's tactic to construct the A,B,C rings through an epoxide activated cascade proved optimal to access these highly complex pentacyclic targets.⁵⁰ Overriding the inherent selectivity with the polyolefin cyclization to deliver these natural products in a more efficient, higher yielding fashion remained an elusive problem for some time. Corey, in 1993, provided a unique solution in the total syntheses of β -amyrin (**46**), oleanolic acid (**47**), and erythrodiol (**48**) from polyene **49** in a strategy reminiscent of the biosynthesis of these natural products. Corey and Lee used a highly stabilized tertiary allylic carbocation to force the desired 6-member ring formation under very mild conditions (MeAlCl₂ in CH₂Cl₂ at -78 °C) to access the pentacycle **50** in a modest yield of 25% (Scheme 1.6).⁵¹ The low yield is superseded by the ability to construct the polyene **49** rapidly on multigram scale as well as the number of stereocenters and angular methyls installed in a single operation. This synthesis also highlights the utility of a stereoselective cyclopropanation strategy to install the angular methyl from intermediate **51**. This was a strategy originally developed by Wenkert and then exploited by Ireland in the total synthesis of (\pm)-shionone.^{52,53} The cyclopropane was then opened using a Kharasch free radical chain oxygenation. Then, a dissolving metal reduction delivered a proton with the desired β -facial selectivity due to an internal proton transfer from the free hydroxyl to a π -radical anion to form the alcohol **52**. From this intermediate, varying the set of reaction conditions completed the total syntheses of oleanolic acid, erythrodiol, and β -amyrin in 24, 24, and 27 steps respectively with a 0.01% overall yield.

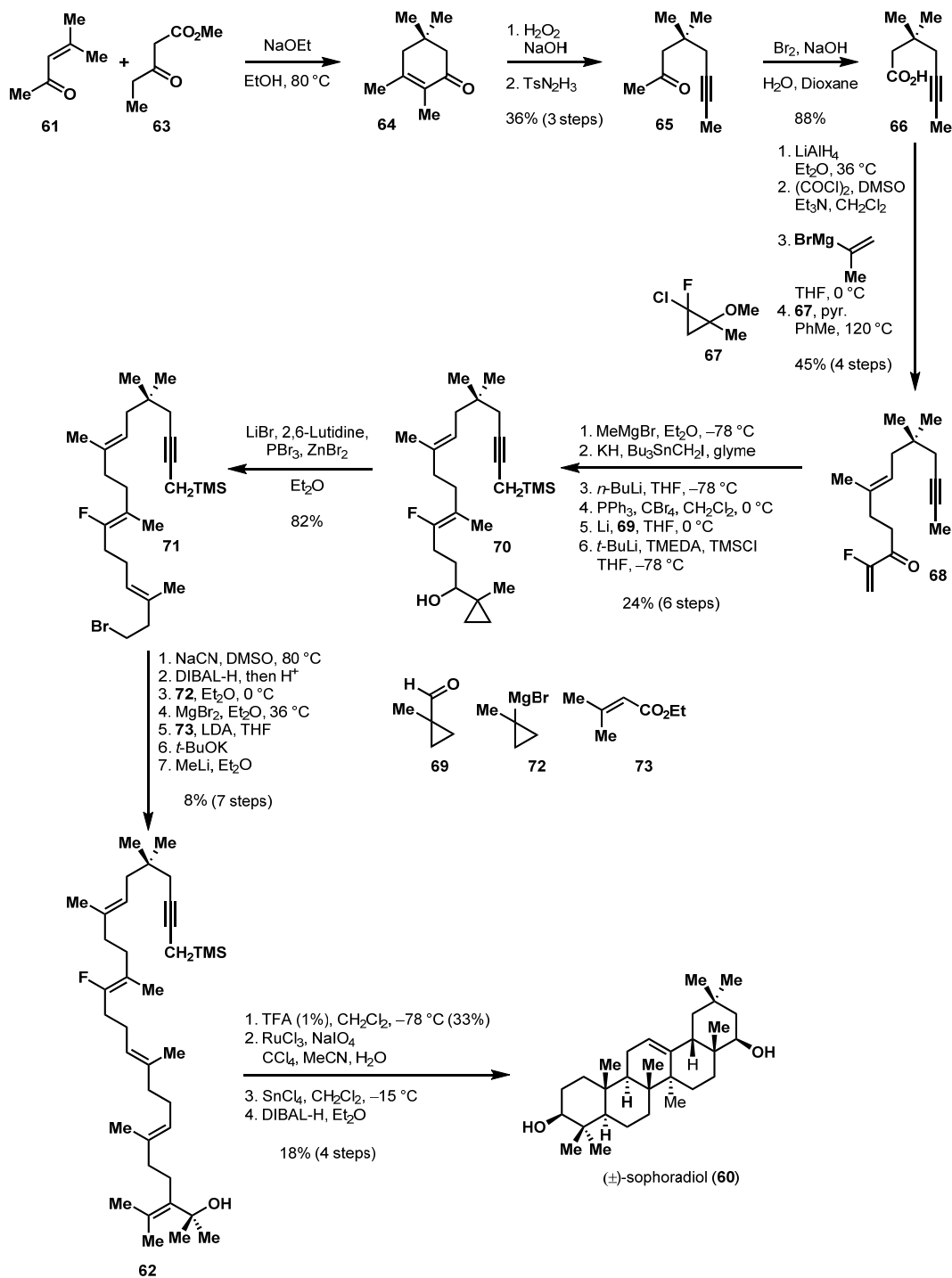
Scheme 1.6. Corey's total syntheses of oleanolic acid, erythrodiol, and β -amyrin.⁵⁰



- A.** (1) *n*-BuLi, CIPO(NMe₂)₂, THF/HMPA (2) Li, EtNH₂, THF, *t*-BuOH (3) TBAF, THF; 69% (3 steps)
B. (1) PDC (2) NaClO₂, NaH₂PO₄, 2-methyl-2-butene, *t*-BuOH (3) TBAF, THF; 76% (3 steps)
C. TBAF, THF; 95%

Still a biomimetic approach could cut down the number of synthetic steps to deliver a more economic, ideal strategy. However, due to the intrinsic nature of following a Markovnikov pathway outside of enzymatic control, the cyclization of squalene-type precursors to form pentacyclic triterpenoids remained an elusive problem until 1994. Johnson and co-workers developed the first non-enzymatic, biomimetic pentacyclization using fluorine as an auxiliary to stabilize carbocations. The formal synthesis of (\pm)- β -amyirin (**46**) and the total synthesis of (\pm)-sophoradiol (**60**) utilizing a polyolefin cascade showcases the first example of constructing these complex natural products in a single diastereoselective operation from completely acyclic precursors (Scheme 1.7).^{54,55} Commencing from mesityl oxide (**61**), **62** was constructed in a scalable 22 step sequence highlighted by the utilization of an Ireland-Claisen rearrangement and three separate cyclopropane-mediated rearrangements to ultimately deliver the polyene **62** with excellent selectivity. Under mild conditions the tertiary allylic carbinol was ionized with TFA in CH₂Cl₂ at -78 °C to initiate the polyolefin cascade to generate the pentacycle in 33% yield. After a ruthenium-mediated oxidation, stannic chloride facilitated the elimination of the fluoride to provide the desired alkene. Lastly, a stereoselective double reduction provided the natural product sophoradiol (**60**) in 26 steps with an overall yield of 0.004%. Johnson's biomimetic strategy represents a large advancement in terpenoid synthesis; showcasing the plausibility of accessing these pentacyclic targets in a single diastereoselective operation from completely acyclic precursors utilizing a functional group stabilized cation to promote the desired Markovnikov cyclization pathway.

Scheme 1.7. Johnson's total synthesis of sophoradiol.

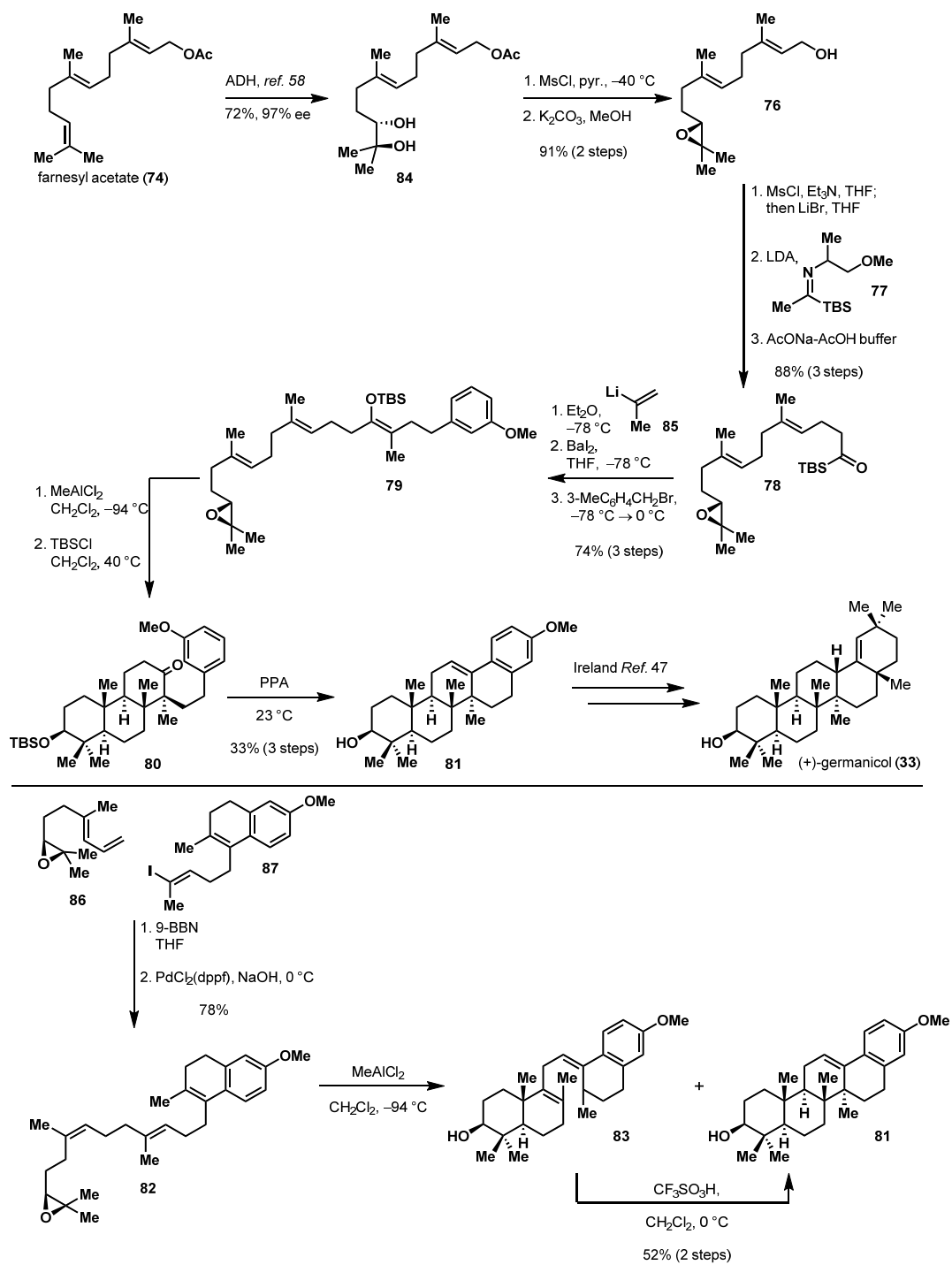


The major drawbacks of Johnson's strategy are the length (22 steps) and complexity of the synthesis of the polyene **62**. This warranted further development of shorter, more efficient approaches to construct these precursors and ultimately the natural products in appreciable yields. Recently, in two elegant syntheses Corey solved these problems by constructing the polyolefin precursor in only nine steps. Starting from farnesyl acetate (**74**), a rapid enantioselective formal synthesis of (+)-germanicol (**33**) and the total synthesis of (+)-lupeol (**75**) were conducted utilizing biomimetic polyolefin cascades (Scheme 1.8).^{56,57} An asymmetric dihydroxylation provided the chiral epoxide **76** in a three step sequence.⁵⁸ Alkylation of the silyl imine **77** followed by hydrolysis delivered the acyl silane **78**. The desired oxirane **79** was then assembled in a three step, single flask operation. Beginning with the addition of 2-propenyllithium followed by a [1,2]-Brook rearrangement facilitated by BaI₂, the corresponding allyl lithium species was alkylated by 3-methoxybenzyl bromide to provide the polyene. Enol ether **79** was then cyclized using MeAlCl₂ to afford the ketone **80**, which after silylation underwent a smooth annulation promoted by polyphosphoric acid to generate the pentacycle **81**.⁵⁶ This advanced intermediate could be used to finish the total synthesis of (+)-germanicol (**33**) using the known procedures originally developed by Ireland.⁴⁷

The epoxy triene **82** was synthesized in an alternative strategy employing a Suzuki-Miyaura cross-coupling, and then cyclized using MeAlCl₂ at -94 °C to produce the pentacycle **81**. Similar to the total synthesis of (+)-oleanolic acid (**47**), a benzyl-tetrasubstituted olefin was utilized to direct the desired cyclization. This reaction produced a 7:3 mixture of the diene **83** and the desired pentacycle **81** which was subsequently treated with triflic acid (5 equiv.) to convert the diene into **81**. The formation of **83** under the reaction conditions warranted further investigation. After

significant probing, they discovered that the polyene **82** undergoes a rare intramolecular 1,5-migration of a *proton* to form a highly stabilized benzylic cation which elimination produced the byproduct **83**.⁵⁶

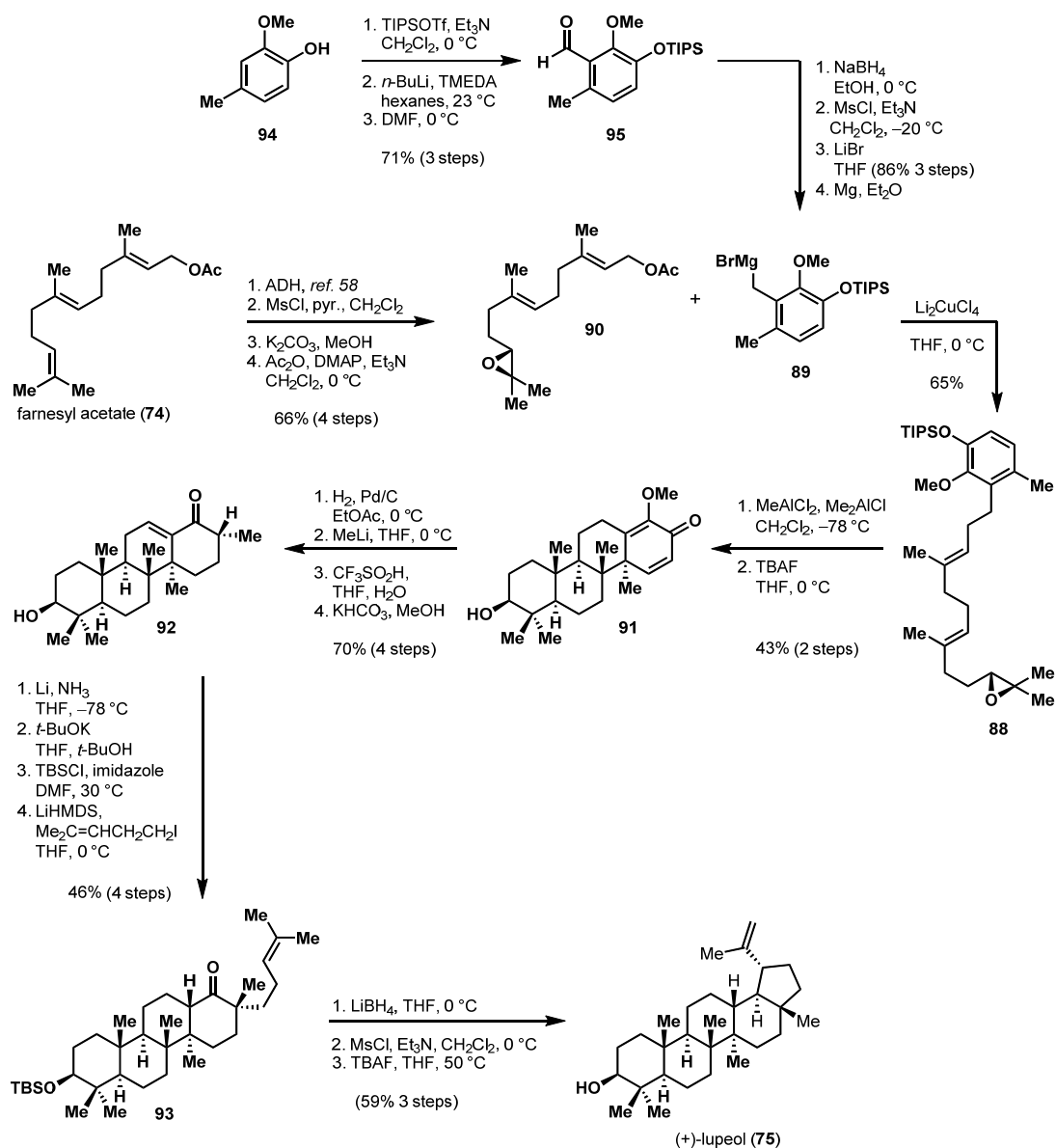
Scheme 1.8. Corey's formal synthesis of (+)-germanicol.⁵⁶



The efficiency of the biosynthesis of the natural triterpenoid lupeol (**75**) is truly remarkable. Chemical emulation of these biosynthetic transformations has been a major synthetic challenge existing since Stork and Eschenmoser first postulated lupeol's native synthesis.^{38,39} Recently, the evolution of the synthetic success and overall efficiency of not only the polyene cascade, but also the polyolefin precursors culminated in the enantioselective total synthesis of (+)-lupeol.⁵⁷ Corey and Surendra devised a seven step synthesis of the epoxy-triene **88**, the shortest to date. The natural product is accessed in a scalable 20 step synthesis (Scheme 1.9).

Polyene **88** was assembled using a copper-mediated coupling of Grignard **89** and the epoxy-acetate **90**. Grignard **89** was generated in a 6 step sequence, whereas acetate **90** was constructed in 4 steps. Polyene cyclization of the activated epoxide, followed by desilylation yielded tetracyclic dienone **91** in 43% yield. Reduction, addition of methyl lithium, isomerization mediated by trifluoromethane sulfonic acid, and subsequent epimerization furnished the enone **92** in good yield over four steps. A dissolving metal reduction using the Birch protocol followed by a second epimerization and a TBS protection yielded the silyl ether. Alkylation of the insipient enolate generated the ketone **93**, which after reduction, the activated alcohol was cyclized and deprotected to complete the total synthesis of lupeol.⁵⁷

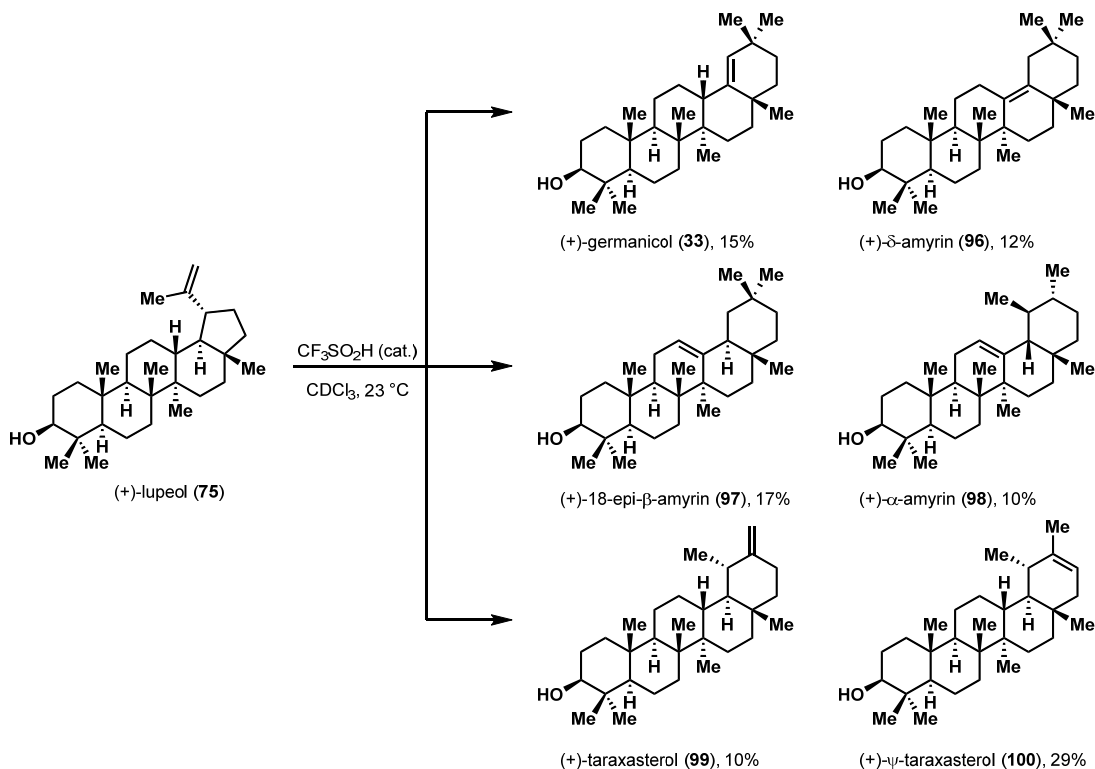
Scheme 1.9. Corey's total synthesis of (+)-lupeol.⁵⁷



With adequate material in hand, chemically emulating the biosynthesis of various triterpenoids from lupeol through cationic rearrangements was investigated. This reaction is postulated to occur in the active site of various cyclase enzymes due to the

exact positioning of a proton accepting group which channels the synthesis of various pentacyclic triterpenes.³⁵ At equilibrium, carbocation formation was promoted by catalytic trifluoromethane sulfonic acid at 23 °C in deuterated chloroform. Observed by ¹H-NMR, lupeol rearranged to six different pentacyclic natural products: (+)-germanicol (**33**), (+)- δ -amyrin (**96**), (+)-18-epi- β -amyrin (**97**), (+)- α -amyrin (**98**), (+)-taraxasterol (**99**), and (+)- ψ -taraxasterol (**100**) (Scheme 1.10).⁵⁷ This illustrates the capacity at which lupeol can be diverted to various natural triterpenoids. However, further backbone rearrangement to reveal friedelin was not observed due to the high energy associated with the strain of the conformation primarily caused by the steric encumbrance of the angular methyls. Enzymatically this rearrangement can occur as previously discussed, but outside of enzymatic control this has not been observed indicating that alternative strategies must be developed in order to construct these triterpenoids.

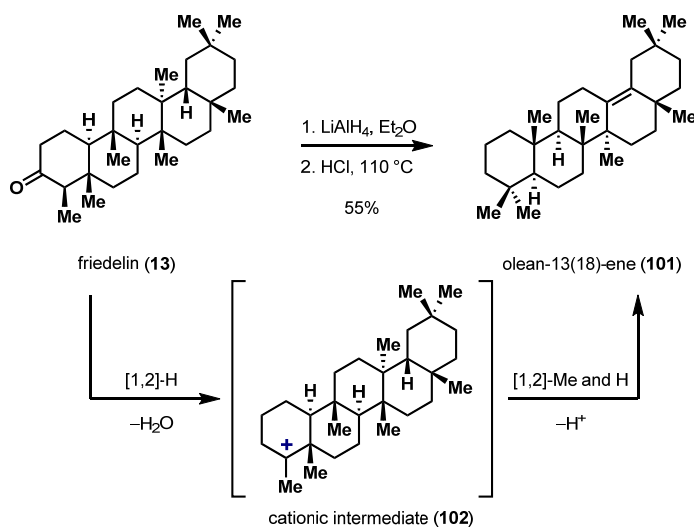
Scheme 1.10. Natural products accessed via cationic rearrangements of (+)-lupeol.⁵⁷



The lack of synthetic routes to the growing class of friedelin natural products, including celastroids, has limited the understanding of their chemistry and biology. Unlike other terpenoids, the absence of a synthesis is attributed to the incompatibility of biologically inspired polyene cyclization strategies to efficiently assemble the pentacyclic core. Implementation of these reactions is highly desirable as it provides rapid access to relatively large molecules possessing a complex topology including several stereogenic centers and the angular methyls in a single transformation. The biological polyene cyclization leading to friedelin (**13**), however, is exceedingly challenging to reproduce chemically due to a set of complex energetically unfavorable methyl and hydride shifts

(see Scheme 1.1).³⁵ In a non-enzymatically controlled environment the friedelin-based cationic intermediate **12** undergoes remarkable reversion to the more stable oleanyl cation (**9**).^{59,60} In structural elucidation studies of friedelin, (**13**) Corey and Ursprung reduced the natural product with LiAlH_4 and heated the alcohol in acid which induced a deep-seated rearrangement. The shifts proceeded in the reverse direction of the biosynthesis to provide olean-13(18)-ene (**101**) in a single operation showcasing the instability of the carbocyclic core under cation promoting conditions (Scheme 1.11).

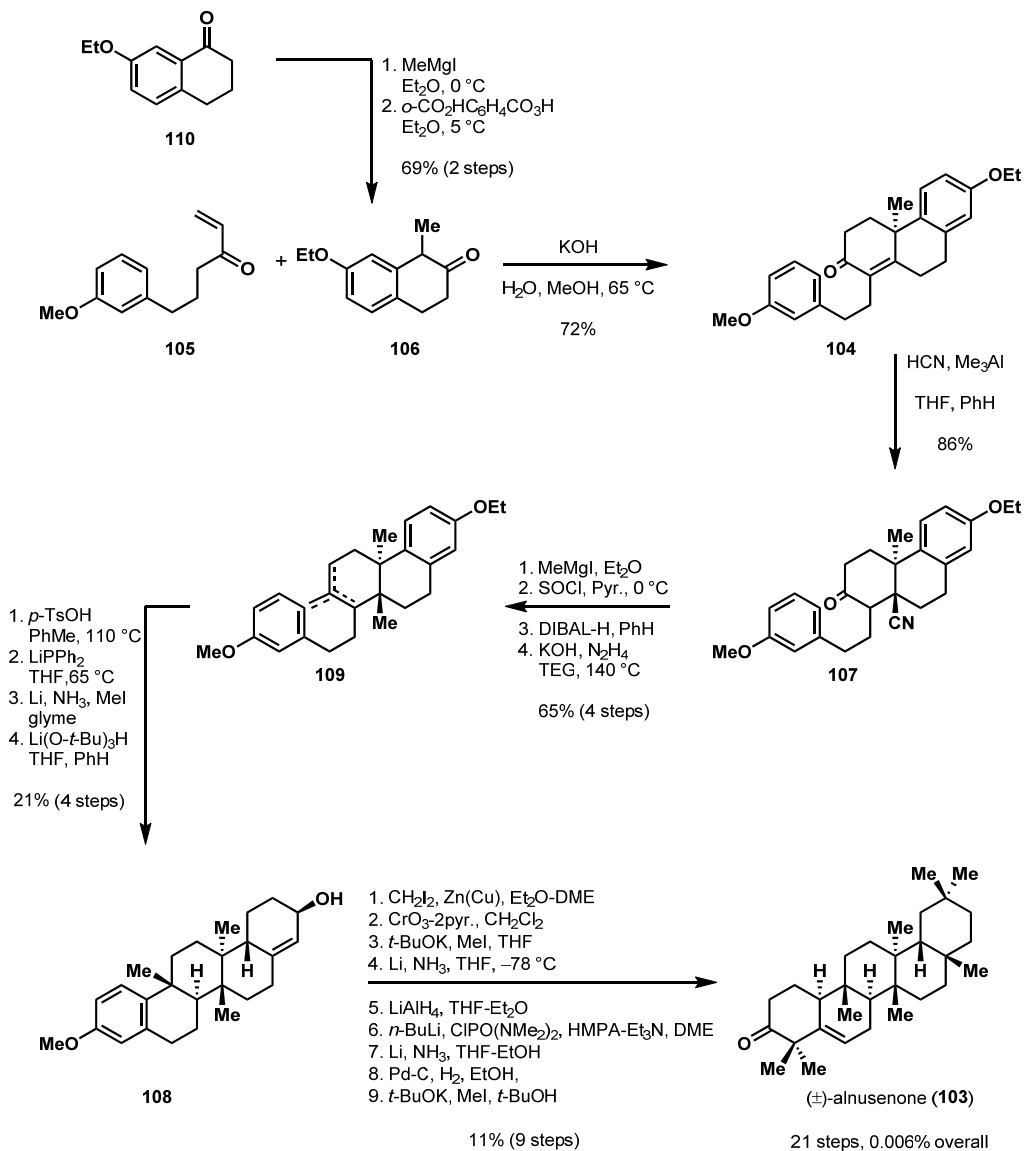
Scheme 1.11. Rearrangement of friedelin in the reverse direction promoted by acid.^{59,60}



Ireland's total syntheses of (\pm)-alnutenone (**103**) and (\pm)-friedelin (**13**) fully delineate the synthetic challenges that this class of triterpenoids possess.⁵⁹⁻⁶¹ Alnutenone was constructed in 21 linear steps beginning with a Robinson annulation to generate the tricyclic **104** from the enone **105** and ethoxytetralone **106** (Scheme 1.12). After intense investigation, a modified Nagata hydrocyanation protocol was developed to afford the

nitrile **107**. This served as a functional handle to install the *trans*-vicinal angular methyls at the C-D ring juncture. Acid mediated annulation, selective methyl ether cleavage, chemoselective Birch reduction, and then a diastereoselective reduction generated the alcohol **108**. The alcohol directed the cyclopropanation which was employed to install the last angular methyl positioned in the E-ring. After oxidation manipulations and a double alkylation of the thermodynamic enolate, the total synthesis of alnusenone was completed in an overall 0.006% yield.^{59,60}

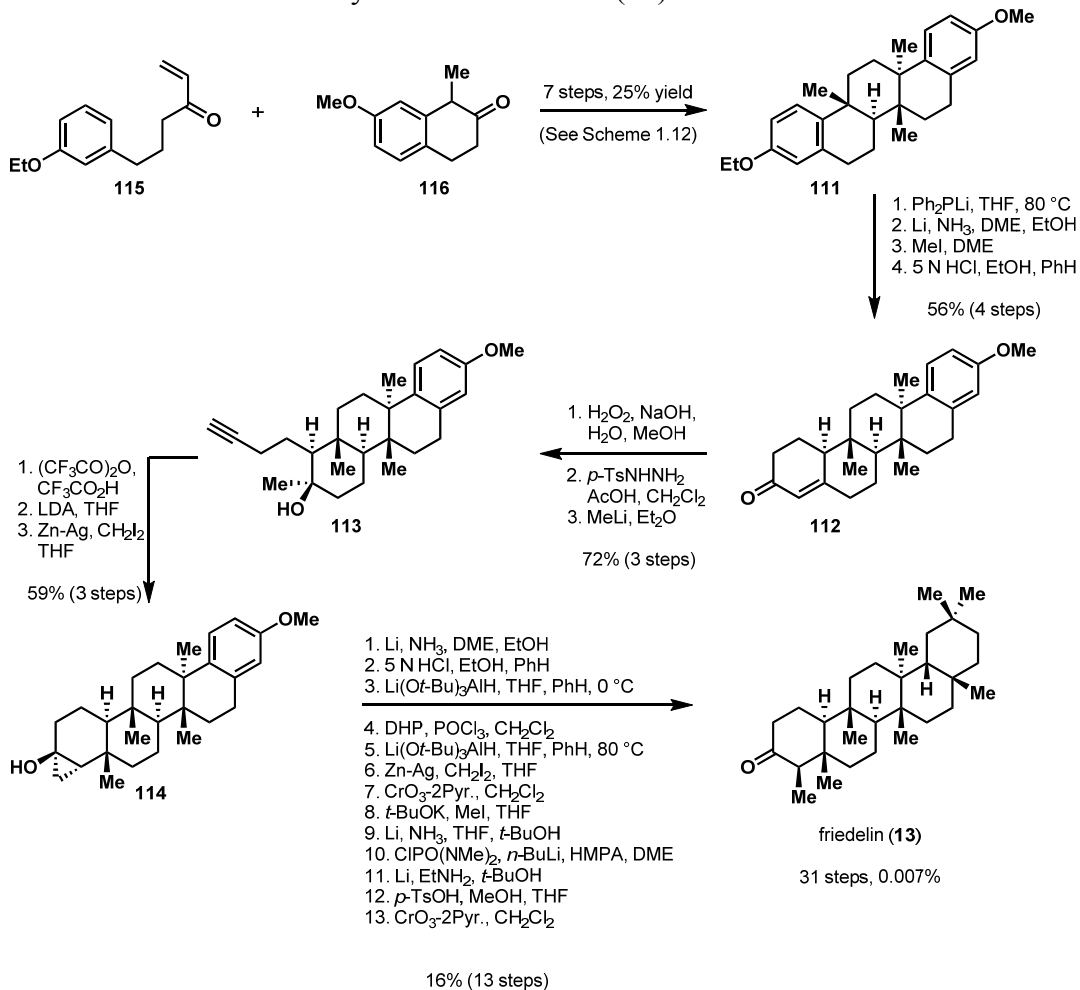
Scheme 1.12. Ireland's total synthesis of (±)-alnusene (**103**).^{59,60}



The total synthesis of (±)-friedelin (**13**) was completed in a similar fashion where the pentacyclic diether **111** was accessed in an analogous seven step sequence beginning

with the Robinson annulation depicted in Scheme 1.12 (Scheme 1.13).⁶¹ The only difference was the methyl and ethyl groups were swapped to functionalize the A ring prior to the E ring thereby circumventing backbone rearrangement which proved to be an insurmountable issue. Selective deprotection and Birch reduction followed by re-etherification and hydrolysis generated the enone **112** which underwent epoxidation and then Eschenmoser fragmentation. Addition of methyl lithium to the insipient ketone provided the alkynol **113** in seven steps from **111**. Cationic annulation promoted by trifluoroacetic acid followed by cyclopropanation afforded the desired alcohol **114**. This installed the angular methyl in the A-B ring juncture where cuprate addition strategies generated the undesired *cis*-fused decalin.⁶² The synthesis was concluded through a 13 step sequence involving several oxidation manipulations to provide (±)-friedelin (**13**) in 31 steps with an overall yield of 0.007%.⁶¹

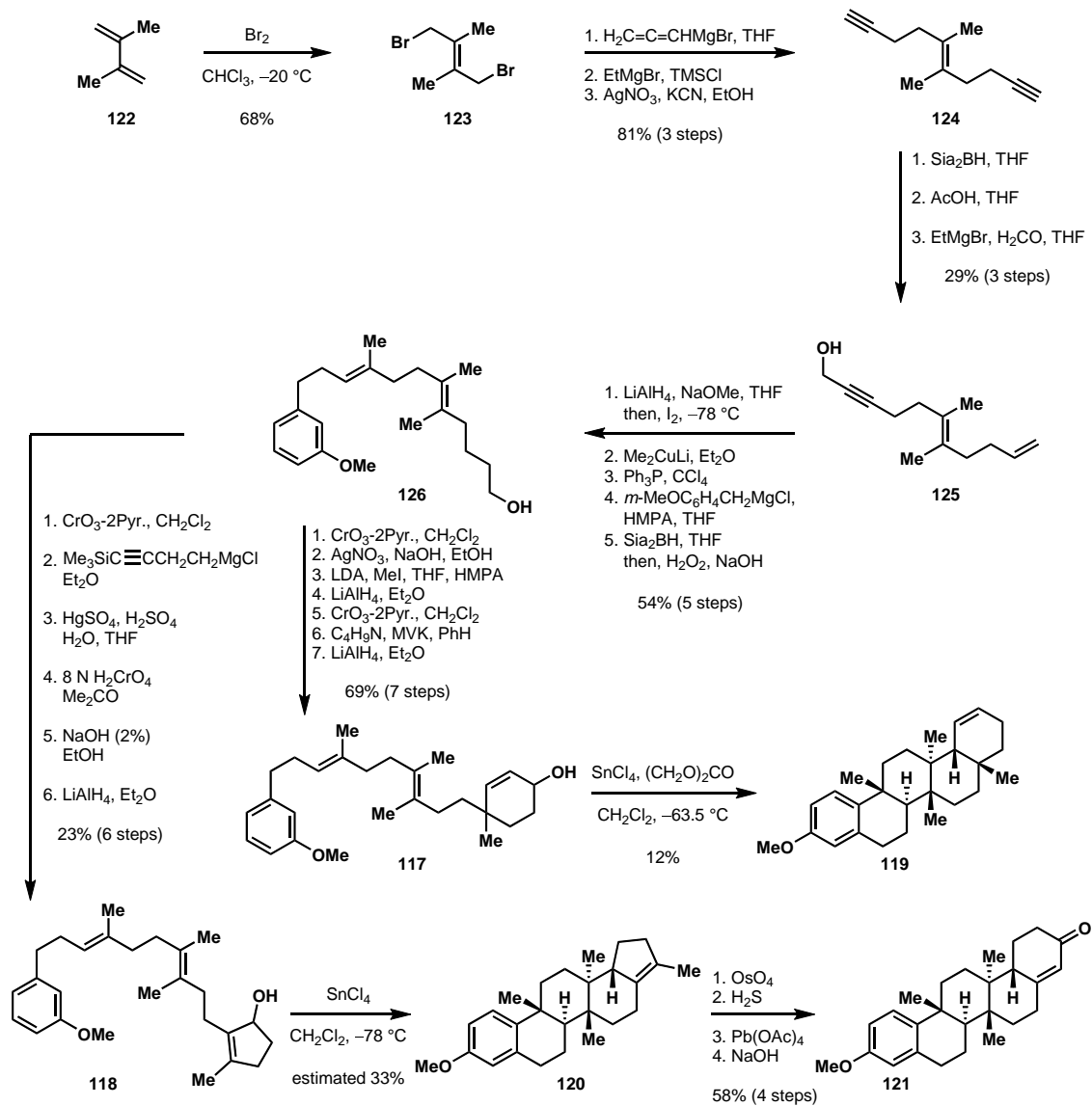
Scheme 1.13. Ireland's total synthesis of friedelin (**13**).⁶¹



In addition to the annulation strategies presented in schemes 1.12 and 1.13, a series of attempts were made to implement polyene cyclizations to provide a faster, more efficient synthesis of (\pm)-alnusone (**103**).⁶³⁻⁶⁵ These cyclizations proceeded in the opposite direction of the biosynthesis, where the E-ring bore the initial cation. The polyolefin cascades were initiated through ionizing the allylic alcohols of the cyclohexenol **117** or the cyclopentenol **118**. These transformations provided the pentacyclic adducts in low yield, either 12% in the case of the cyclohexenol or an estimated 33% for the cyclopentenol (Scheme 1.14). The low yields in the cyclization

forming the pentacycle **119** prevented this advanced intermediate from being converted to alnusenone (**103**) or any of the synthetic intermediates in the previous synthetic route. Conversion of the cyclopentene **120** to cyclohexenone **121** permitted a formal synthesis of (\pm)-alnusenone (**103**), although this approach did not improve upon the group's existing route due to lower yields and scalability. Both approaches utilized tetrasubstituted olefins to engage the initial cation to form the *trans*-fused C-D decalin core thereby installing the angular methyls in a single transformation. This approach was inferior, however, to the linear annulation strategies since the syntheses of the polyenes **117** and **118** were not higher yielding, as scalable, or more efficient.

Scheme 1.14. Ireland's polyene cyclization approaches toward (\pm)-alnuseneone.⁶³⁻⁶⁵



Conclusion

Since the initial postulate regarding (+)-lupeol's biosynthesis, intense research has been conducted to provide strategies that chemically emulate the biosyntheses of various natural tetracyclic and pentacyclic triterpenoids. The polyene cyclization has evolved into a new successful, efficient strategy to access these natural products substantiated by the recent work of Corey and Surendra.^{56,57} However, there has not been significant progress utilizing this strategy to access the friedelin natural products thereby alternative approaches have been required to synthesize this class of terpenes. These strategies are longer, inefficient syntheses that implement a high number of oxidation manipulation steps.⁵⁹⁻⁶¹ This warrants in-depth investigation to develop a more efficient, scalable route to provide access to these small molecules in a manner which maximizes C-C bond formation, and installs the angular methyls as well as the all-carbon quaternary centers in a stereoselective fashion while minimizing protecting group and oxidation steps. The polyene cascade provides this solution, but minimal success has been observed utilizing this strategy.⁶³⁻⁶⁵ Developing a novel polyolefin cyclization employing new initiators as well as milder Lewis or Brønsted acid promoters could change these outcomes ultimately providing a successful protocol to rapidly access this class of natural products. This would allow the synthesis of celastrol (**1**), its enantiomer, and other celastroids in appreciable amounts. On the biological front, access to these small molecules would provide tools to investigate their modes of action thereby providing answers to important biological questions and directing the future development of this growing class of compounds.

Chapter 2 – Studies Toward the Synthesis of Celastrol

Retrosynthetic Analysis

The optimal synthetic strategy to construct (±)-celastrol (**1**) was planned with the goal of installing the reactive quinone methide functionality in the last step through oxidation of (±)-wilforic acid (**127**), which in turn could be derived from the permethylated pentacycle **128** (Figure 2.1). Introduction of the fully substituted carbon center at C-20 from a ketone simplified the molecule providing the pentacycle **129** as a subtarget accessed through the polyene cyclization of an achiral cyclohexadienone (**130**). The polyolefin cascade rapidly constructs the friedelin core installing each angular methyl and six contiguous stereocenters in a single diastereoselective operation. Strategic use of a chiral Lewis or Brønsted acid could impart stereoinduction to provide access to either enantiomer of celastrol (**1**) making this strategy highly desirable. The electron rich tetrasubstituted arene provides a trap for the cyclization, and due to substitution it is forced to react at a single position. The cyclization precursor was envisioned to be assembled in a convergent manner using three separate fragments: the arene, the tetrasubstituted olefin fragment, and the dienone. The crux of the strategy relied on a precedented olefination protocol to provide the tetrasubstituted alkene **131**.⁶⁵ The dienone was to be synthesized through a Birch reduction/alkylation sequence using benzoic acid (**132**) followed by a Wolff-Kishner reduction and a site-selective allylic oxidation.^{59,66-72} Olefin **131** was foreseen to be derived from the ketone **133** which is accessed through the copper-mediated coupling of arene **134** to acetate **135**.⁵⁷ The arene was to be derived from the cheap, commercially available vanillin (**136**), while **135** could

be synthesized from geraniol acetate (**137**) through a simple selective oxidation approach.^{73,74}

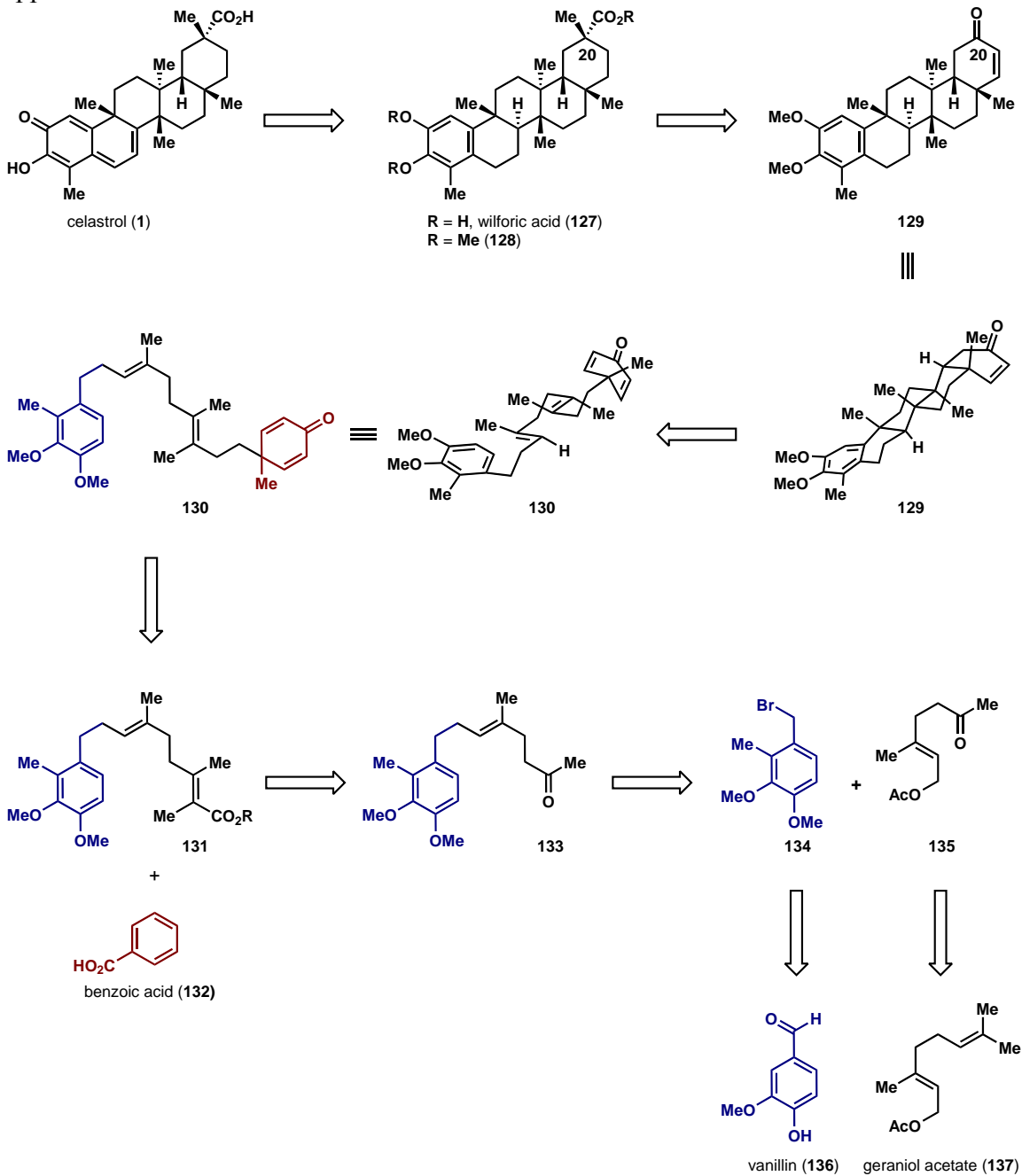
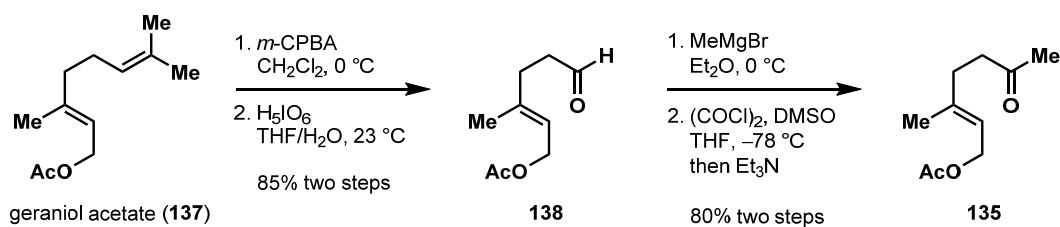


Figure 2.1. Key disconnections of celastrol and the linear precursors for the polyene cyclization.

Forward Synthesis

Starting from geraniol acetate, selective oxidation of the exterior olefin by treatment with *m*-CPBA in methylene chloride at 0 °C provided the epoxide; which underwent smooth oxidative cleavage with periodic acid in THF/water to provide the aldehyde **138** in good yield over two steps (Scheme 2.1).⁷³ This provided the aldehyde cleanly with no purification required. Ozonolysis also generated the aldehyde in a single step, but suffered from long reaction times and poor scalability. Addition of a 3 M solution of methylmagnesium bromide in diethyl ether at 0 °C provided the alcohol which was then subjected to a Swern oxidation in THF at -78 °C to provide the desired ketone **135** in four scalable steps.⁷⁴

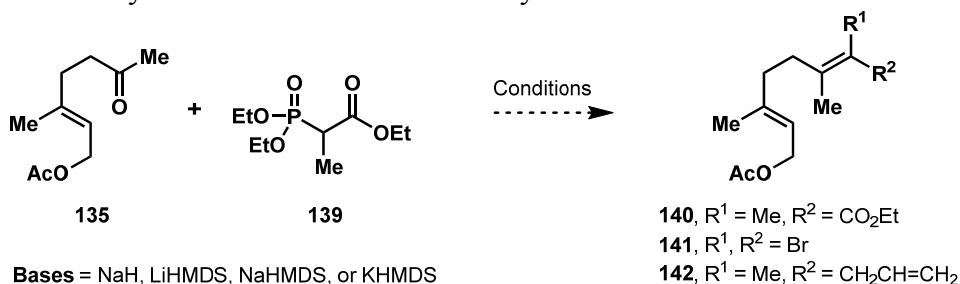
Scheme 2.1. Synthesis of the ketone fragment.^{73,74}



The main synthetic challenge was selectively installing the tetrasubstituted alkene in appreciable yield. Bestmann demonstrated that Horner-Wadsworth-Emmons (HWE) olefinations were a viable approach to access tetrasubstituted olefins.⁶⁵ To test the plausibility of this transformation, **135** was submitted to a number of conditions. Initially, the HWE olefination between **135** and the phosphonate **139** was examined to access the desired alkene **140**. The ketone, however, was recalcitrant toward olefination

using HWE, Wittig, Julia, or even Corey-Fuchs protocols.^{65,75-78} The use of different bases, counter ions, additives, solvents, and temperatures did not affect any appreciable conversion of the starting ketone; only unreacted starting material was returned (Table 2.1). The Corey-Fuchs reaction would have provided the tetrasubstituted dibromo-olefin **141** which would have served as a functional handle for selective cross-coupling reactions. Literature precedence in the total syntheses of FR182877 by Evans and kedarcidin by Myers illustrated that 1,1-dibromo-alkenes can be differentiated using cross-couplings mitigated by palladium catalysis.^{79,80}

Table 2.1. Survey of olefination conditions to synthesize the tetrasubstituted alkene **140**.



Solvent	Additives	Temperature (°C)	SM Conversion	Product E/Z Ratio
THF	-----	23 → 65	-----	-----
PhMe	-----	110	trace	1:1
xylene	-----	140	< 5%	1:1
diglyme	-----	165	< 5%	1:1
MeCN	LiCl / DBU	77	trace	-----
MeCN	LiCl / <i>i</i> -Pr ₂ NEt	77	trace	-----
CH ₂ Cl ₂	PPh ₃ , CBr ₄ , Et ₃ N	0 → 40	trace	-----
CH ₂ Cl ₂	PPh ₃ , CBr ₄ , Zn	0 → 40	trace	-----
THF	PhSO ₂ Et	0 → 65	trace	-----
THF	PhSO ₂ CH ₂ CH=CH ₂	0 → 65	trace	-----

An alternative approach to the polyene utilizing a B-alkyl Suzuki-Miyaura cross coupling was devised to construct the tetrasubstituted olefin from the iodo-enoate **143** and the alkyl boronate **144** (Figure 2.2).^{81,82} Subjecting the aldehyde **145** to a Seyferth-Gilbert homologation followed by lithiation and trapping with ethyl chloroformate affords the ynoate.^{83,84} Addition of Gilman's reagent and trapping the insipient copper allenolate with iodine would provide the enoate **143** using a landmark protocol developed by Corey and Katzenellenbogen.^{85,86} The boronate **144** could be generated from benzoic acid through a sequence utilizing a Birch reduction/alkylation, selective reductions as well as oxidations, and then a selective hydroboration.^{66-71,87-89}

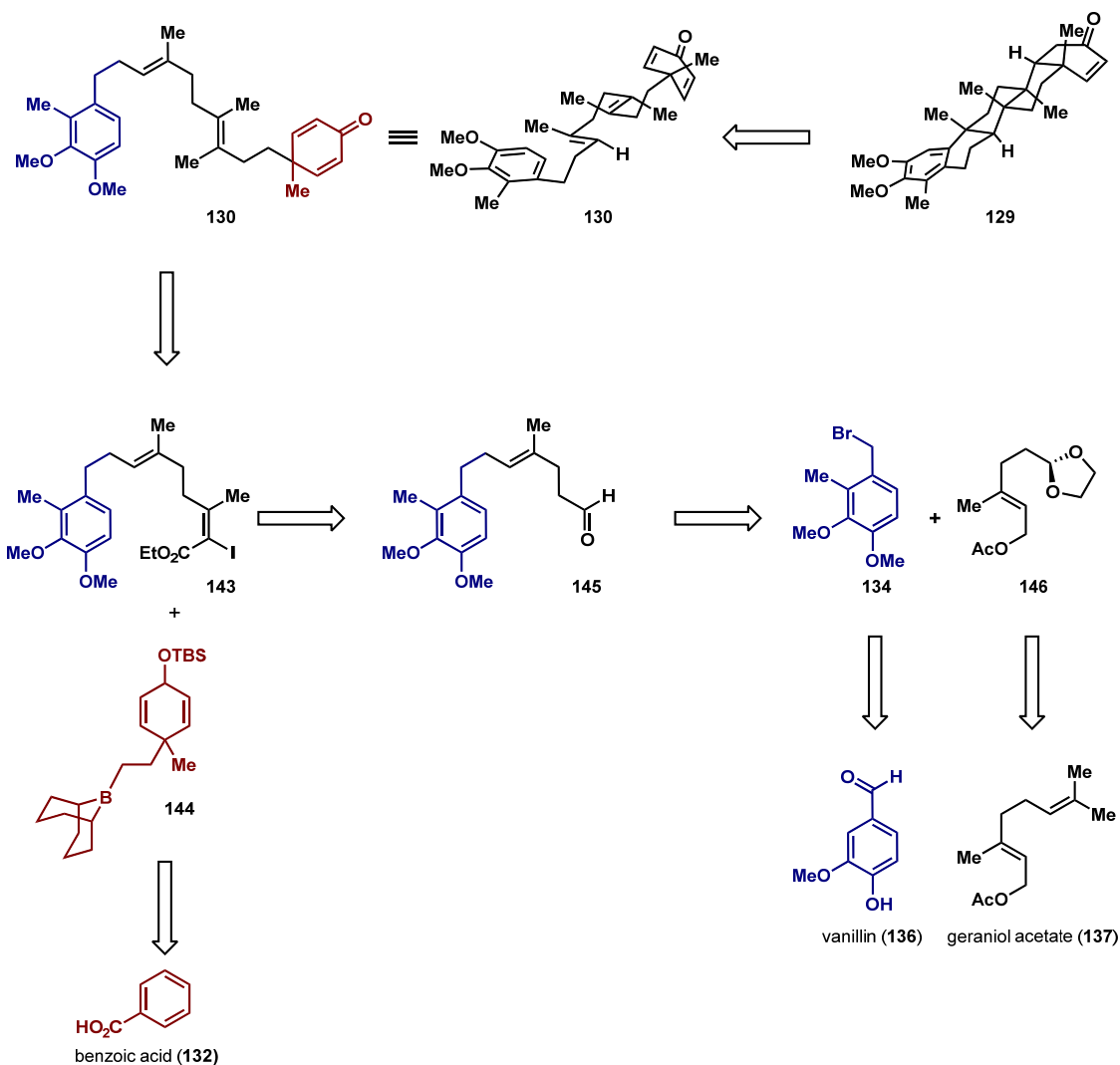
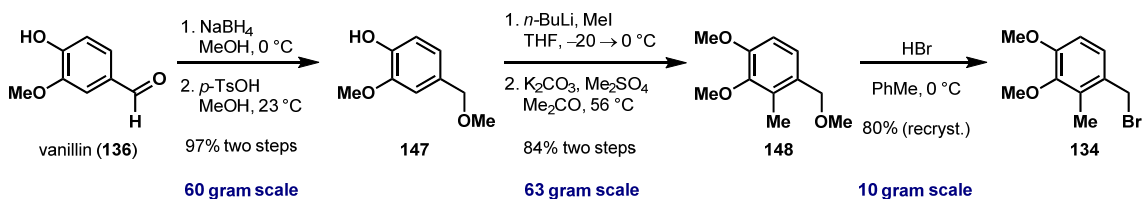


Figure 2.2. New bond disconnections to construct the desired tetrasubstituted olefin.

Accessing the key diene **143** required the synthesis of the aryl fragment which was conducted in a highly scalable, five step sequence (Scheme 2.2). Reduction of vanillin with NaBH_4 in methanol at $0\text{ }^\circ\text{C}$ furnished the diol. Selective protection using catalytic *p*-toluenesulfonic acid in methanol provided the ether **147** in 97% yield over two steps on 60 gram scale. The ether was then subjected to a directed *ortho*-metallation

protocol using *n*-butyllithium in THF at $-20\text{ }^{\circ}\text{C}$. After 2.5 hours iodomethane was added to the resultant red-orange colored solution alkylating the dianion to install the tolyl methyl. The crude phenol was then etherified using dimethyl sulfate and potassium carbonate in acetone heated to reflux to generate the arene **148** in an 84% yield over two steps on 63 gram scale.⁷² Unfortunately, the dianion could not be alkylated and etherified in a single operation thus requiring the two separate steps. Bromide **134** was then accessed through a reaction using concentrated hydrobromic acid in toluene at $0\text{ }^{\circ}\text{C}$. The biphasic mixture was stirred vigorously for two hours, and after an aqueous work-up the crude brown solid was recrystallized from hexane to afford **134** as a white crystalline solid in 80% yield.

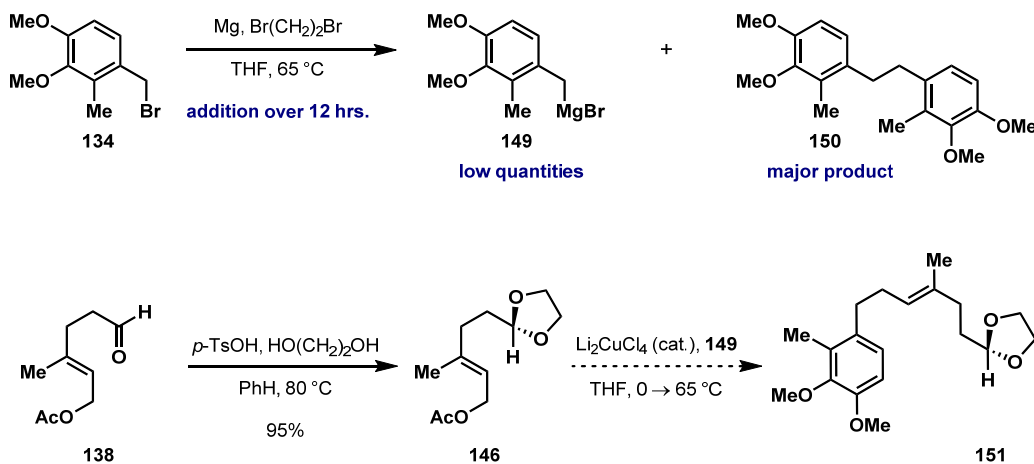
Scheme 2.2. Synthesis of the aryl fragment.



The aryl fragment was ready to be installed through a copper mediated coupling of the Grignard **149** and the allylic acetate.⁵⁷ This warranted protection of the aldehyde therefore the dioxolane **146** was synthesized in 95% yield using catalytic *p*-toluenesulfonic acid and ethylene glycol in benzene heated to reflux (Scheme 2.3). Unfortunately, the coupling of the two fragments failed due to the inability to form the Grignard. After surveying a variety of conditions to generate the Grignard (**149**), only minimal quantities could be generated due to extensive Wurtz coupling which formed the

dimer **150**. This occurred despite the slow addition of the bromide as a solution in THF over 12 hours to activated magnesium.⁹⁰ After titration, the freshly prepared green colored solution of the Grignard **149** was subjected to acetate **146** in the presence of Kochi's catalyst in THF at a range of temperatures.⁵⁷ This reaction did not render the desired coupled adduct **151**, however, only the benzyl dimer and the unreacted acetate **146** were isolated warranting a new coupling strategy.

Scheme 2.3. Attempted Grignard formation and fragment coupling.



With problematic Grignard formation, tin was installed to provide a functional handle to couple the fragments avoiding significant Wurtz coupling. Stannane **152** was synthesized in the variable yields of 40-70% by alkylating lithium tri-*n*-butylstannane in THF with the benzyl bromide (Scheme 2.4). The stannyl lithium reagent was initially generated by stirring a heterogeneous mixture of lithium metal and tri-*n*-butylstannyl chloride in THF at 0 °C.⁹¹ However, use of this green mixture afforded **152** in variable yields (40-70%) due to Wurtz coupling. After experimentation, I discovered that freshly

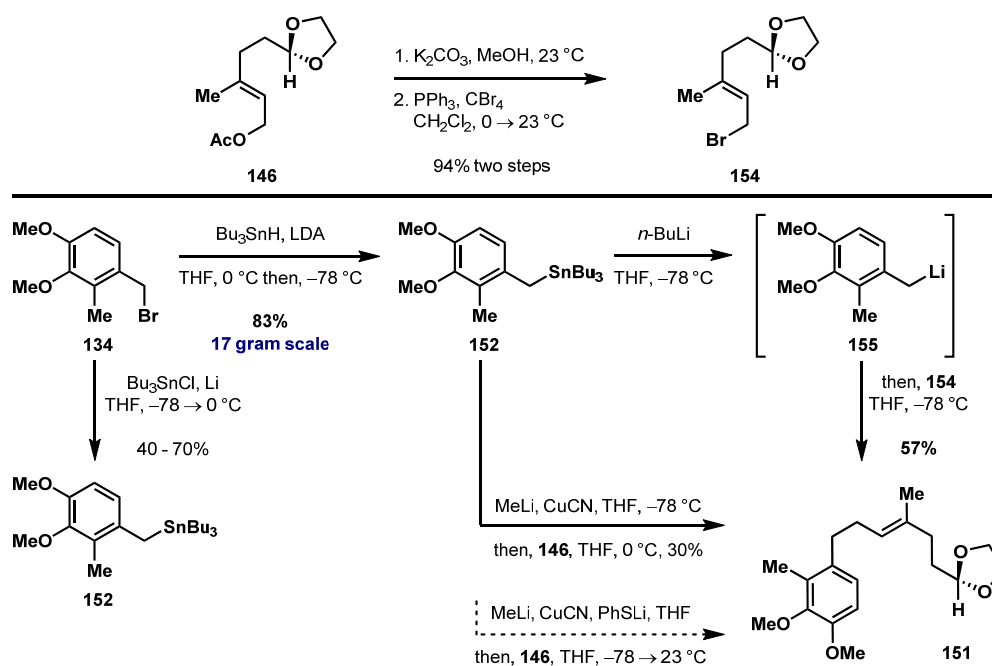
preparing the lithium tri-*n*-butylstannane proved optimal. Deprotonating tri-*n*-butyltin hydride with freshly prepared LDA at 0 °C in THF and then slowly adding a 0.2 M solution of the bromide **134** in THF at -78 °C over three hours afforded the desired product in 83% yield.⁹²

Using palladium or zinc catalysis the dioxolane **151** was inaccessible through a Stille coupling approach. However, treating two equivalents of the stannane with the freshly prepared higher order cuprate Me₂CuCNLi₂ in THF at -78 °C followed by warming the golden-yellow solution to 0 °C afforded the desired benzyl cuprate. Slowly adding the allylic acetate to the cuprate successfully coupled the fragments together to provide the arene **151** in 30% yield. The yields of this reaction varied, and using excess stannane was not ideal. Attempts to improve the reaction by using one equivalent of the benzyl tin reagent or a thio-cuprate unfortunately failed to provide the coupled product. It is important to note that this is a modification of the established protocol developed by Lipshutz, representing an extension of his work in the coupling of allylic acetates and alkyl halides to allylic stannanes.⁹³⁻⁹⁵

Despite successful coupling, the low variable yields and the required use of excess stannane proved inadequate to generate sufficient material. So, a new coupling strategy was devised employing a hard alkylation of the lithiated arene which was generated through a tin-lithium exchange. Treating the benzyl stannane with *n*-butyllithium in deoxygenated THF at -78 °C provided an orange colored solution containing the benzyl lithium species. The bromide **154** was then added to this solution to afford the desired coupled product in 57% yield. It is imperative that deoxygenated THF was used and the bromide was added slowly over the course of 1 hour or else significant Wurtz coupling was observed. Bromide **154** was prepared in two steps by

treating the acetate with a mixture of potassium carbonate in methanol and then subjecting the allylic alcohol to an Appel reaction to generate the bromide using carbon tetrabromide and triphenylphosphine in methylene chloride. The byproduct, triphenylphosphine oxide, complicated the purification because the crude bromide rapidly decomposed on silica gel, basic alumina, and during distillation. However, triturating the mixture with cold pentane delivered the bromide after filtration as a pale yellow oil in >95% purity and 94% yield.

Scheme 2.4. Synthesis of aryl dioxolane **151**.

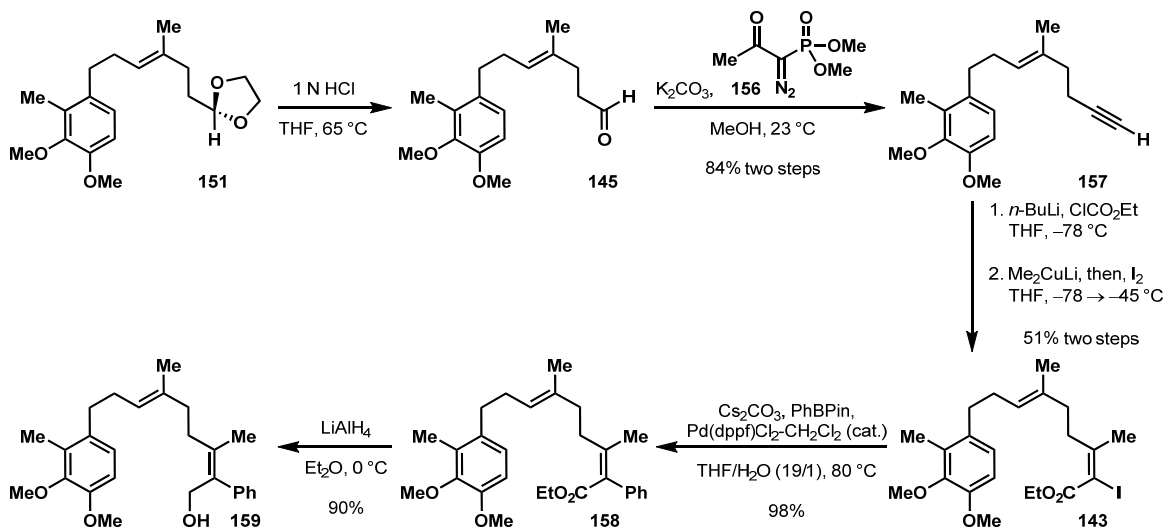


The dioxolane was hydrolyzed using a solution of 1 N HCl and THF heated to 65 °C to deliver the aldehyde **145** (Scheme 2.5). Treatment with the Bestmann-Ohira reagent (**156**) and potassium carbonate in methanol generated the terminal acetylene **157**

through a Seyferth-Gilbert homologation.^{83,84} The alkyne was then metalated using *n*-butyllithium in THF at $-78\text{ }^{\circ}\text{C}$, and the resultant lithium acetylide was trapped with ethyl chloroformate to afford the ynoate in 83% yield. Conjugate addition using freshly prepared Gilman's reagent in THF at $-78\text{ }^{\circ}\text{C}$ generated the copper allenolate which was iodinated to provide the tetrasubstituted iodo-enoate **143** in 61% yield using the protocol developed by Corey and Katzenellenbogen.^{85,86} The observed side products were over addition of Me_2CuLi and those associated with adducts of halo-ene cyclizations. It was imperative that this reaction be conducted at temperatures lower than $-45\text{ }^{\circ}\text{C}$ as isomerization of the copper allenolate would occur to provide the undesired *cis*-vinyl iodide.⁸⁵ Unfortunately, the copper allenolate could not be alkylated using alkyl halides thereby eliminating the potential to assemble the polyene in a single operation.

The capability of **143** to participate in a Suzuki-Miyaura cross-coupling was then examined. Subjection to catalytic palladium(dppf) dichloride and cesium carbonate in a THF/water mixture heated to $80\text{ }^{\circ}\text{C}$, the iodide could be coupled to the pinacolate ester of phenyl boronic acid in near quantitative yield to afford the styrene **158**.^{96,97,82} At this point the ester was reduced with lithium aluminum hydride in ether to access the allylic alcohol **159** in 90% yield with the desired *trans*-alkene confirmed by NOE spectroscopy.

Scheme 2.5. Synthesis of iodo-enoate fragment.

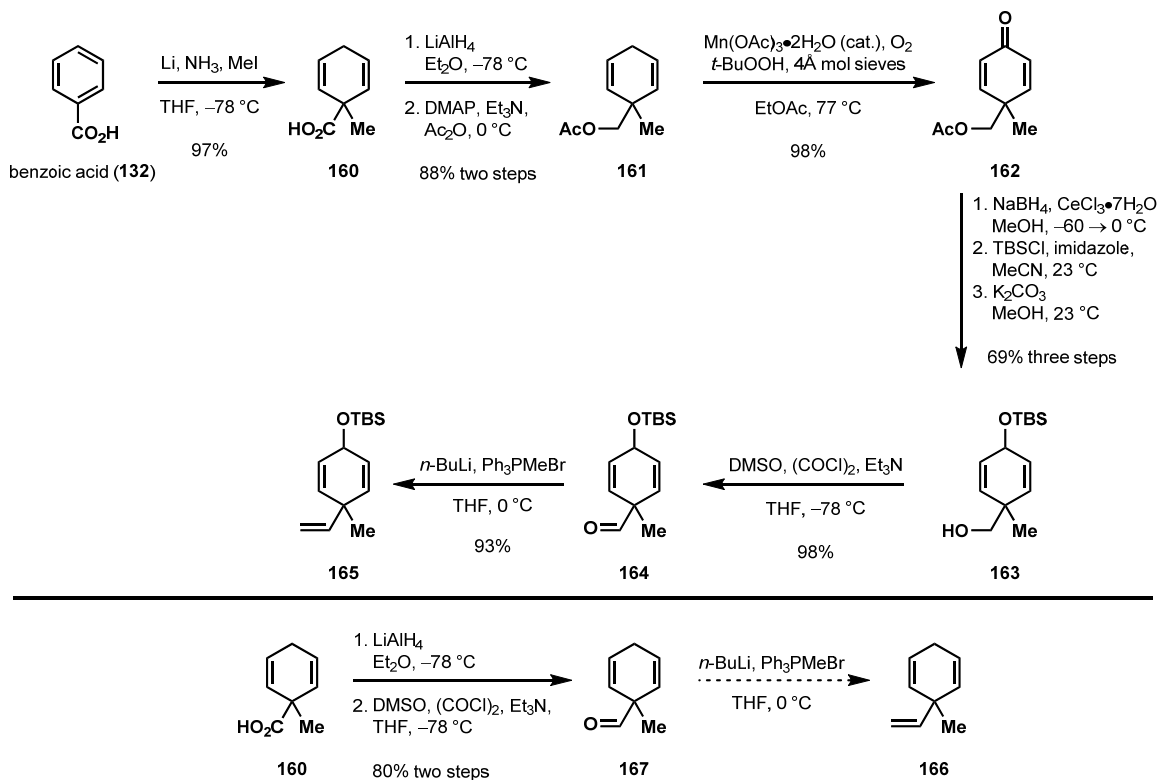


With access to **143** and proof of its excellent potential as a partner in cross-couplings, attention was directed towards constructing the alkyl boronate fragment **144** and examining its reactivity in B-alkyl Suzuki reactions. Birch reduction of benzoic acid using lithium metal in THF and liquid ammonia at $-78\text{ }^\circ\text{C}$ and then addition of iodomethane to the dark blue mixture to alkylate the resultant dianionic enolate afforded the cyclohexadiene **160** in 97% yield.⁶⁶⁻⁷⁰ The acid was reduced with lithium aluminum hydride in ether at $-78\text{ }^\circ\text{C}$ to render the alcohol which was then immediately protected without purification as the acetate using DMAP, triethylamine, and acetic anhydride to provide the acetate **161** in 88% over two steps. It was imperative to conduct the reduction at $-78\text{ }^\circ\text{C}$ due to the facile nature of isomerization to the conjugated diene. Also, the acetate was a vital protecting group because of its easy deprotection in later stages where other protecting groups facilitated decomposition during their removal.

Employing the protocol developed by Shing and co-workers, allylic oxidation mediated by manganese triacetate and *tert*-butylhydrogen peroxide in ethyl acetate heated to reflux under an aerobic atmosphere afforded the dienone **162** in near quantitative yield.⁷¹ This material was extremely sensitive to acidic and basic conditions primarily decomposing through a 1,4-phenolic rearrangement pathway. It was therefore subjected to a Luche reduction using sodium borohydride and cerium trichloride heptahydrate in methanol at -60 °C to deliver the alcohol.⁸⁹ The temperature of this reaction was critical because significant 1,4-reduction was observed without proper cooling of the reaction. The allylic alcohol was then protected as the silyl ether with *tert*-butyldimethyl chlorosilane and imidazole in acetonitrile which was subjected to methanolysis to generate the alcohol **163** in 69% yield over three steps.

The use of Dess-Martin periodinane to oxidize the alcohol was problematic because the aldehyde rapidly decomposed under these conditions despite buffering the reaction. However, a modified Swern oxidation successfully generated the aldehyde **164** in near quantitative yield.⁷⁴ Lastly, Wittig olefination of the aldehyde with the freshly prepared methyl triphenylphosphorane ylide in THF at 0 °C delivered the triene **165** in 93% yield.⁷⁷ Despite undesired oxidation and protecting group manipulation steps, this route worked successfully on multigram scale to provide the triene. Attempts to minimize these unwanted steps were unsuccessful because of the volatility of triene **166**. Wittig olefination of the aldehyde **167** did work, but **166** could not be purified. The triene forms a positive azeotrope with THF and distillation caused decomposition to a black tar substance even in the presence of BHT. Hydroborating the crude material directly also did not work thereby prompting the lengthy oxidation strategy.

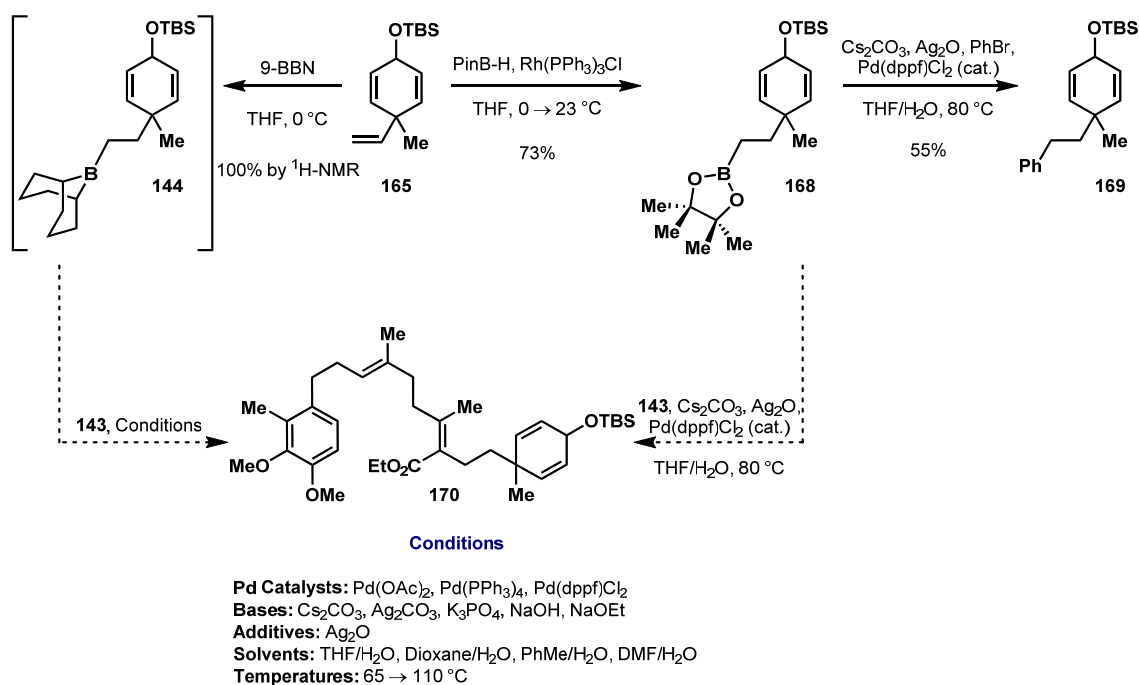
Scheme 2.6. Synthesis of triene fragment.



Employing the protocol developed by Evans, the triene **165** was selectively hydroborated using Wilkinson's catalyst and pinacolborane in deoxygenated THF to provide the desired alkylboronic ester **168** in 73% yield (Scheme 2.7). This moiety was initially reluctant to couple to simple aryl halides through a B-alkyl Suzuki coupling, but eventually I discovered that using a mixture of stoichiometric silver (I) oxide, catalytic palladium(dppf) dichloride, and cesium carbonate in hot THF/water, the alkyl boronic ester couples to simple aryl halides such as bromobenzene in modest yield. The silver (I) oxide is critical as no coupling occurs in its absence; only unreacted starting material is returned. Unfortunately, treating the mixture of boronate **168** and iodide **143** to these

same conditions caused decomposition of the starting materials with no observation of the coupled product. At this stage, due to the difficulty of coupling the pinacolate to even simple substrates, boronate **144** was envisioned to be a better coupling partner due to the enhanced reactivity of these entities in cross-couplings.^{81,82} Boronate **144** was accessed by selectively hydroborating the triene **165** with crystalline 9-BBN in THF at 0 °C. After examination of the key coupling reaction, however, the two fragments did not couple using this strategy thereby warranting a different approach to the polyene.

Scheme 2.7. Failed B-alkyl Suzuki-Miyaura to couple fragments.



Constructing the tetrasubstituted alkene remained elusive, so installing the olefin at the beginning became the focus. Originally, I sought to construct the alkene using a

protocol developed by Maercker entailing the stereoselective reduction of an internal alkyne which generates a vicinal dimetallated olefin. Alkylation of the dianion with iodomethane would then deliver the desired alkene.¹⁰⁰⁻¹⁰³ Unfortunately, this procedure failed. It was foreseen that the desired olefin could be synthesized in the initial step through a bromination of 2,3-dimethyl butadiene to afford the bromide **123**.^{104,53} This provides a synthon to access the symmetrical diketone **171** which installs the functionality required to obtain the alcohol **172**. Coupling this moiety to the aryl fragment through a tin-lithium exchange mediated alkylation sequence would deliver the triene **173**. A selective oxidation and annulation installs the cyclohexenone fragment ultimately to afford the desired polyene **174**. This new strategy maximizes C-C bond formation and eliminates undesired oxidation and protecting group manipulation steps.

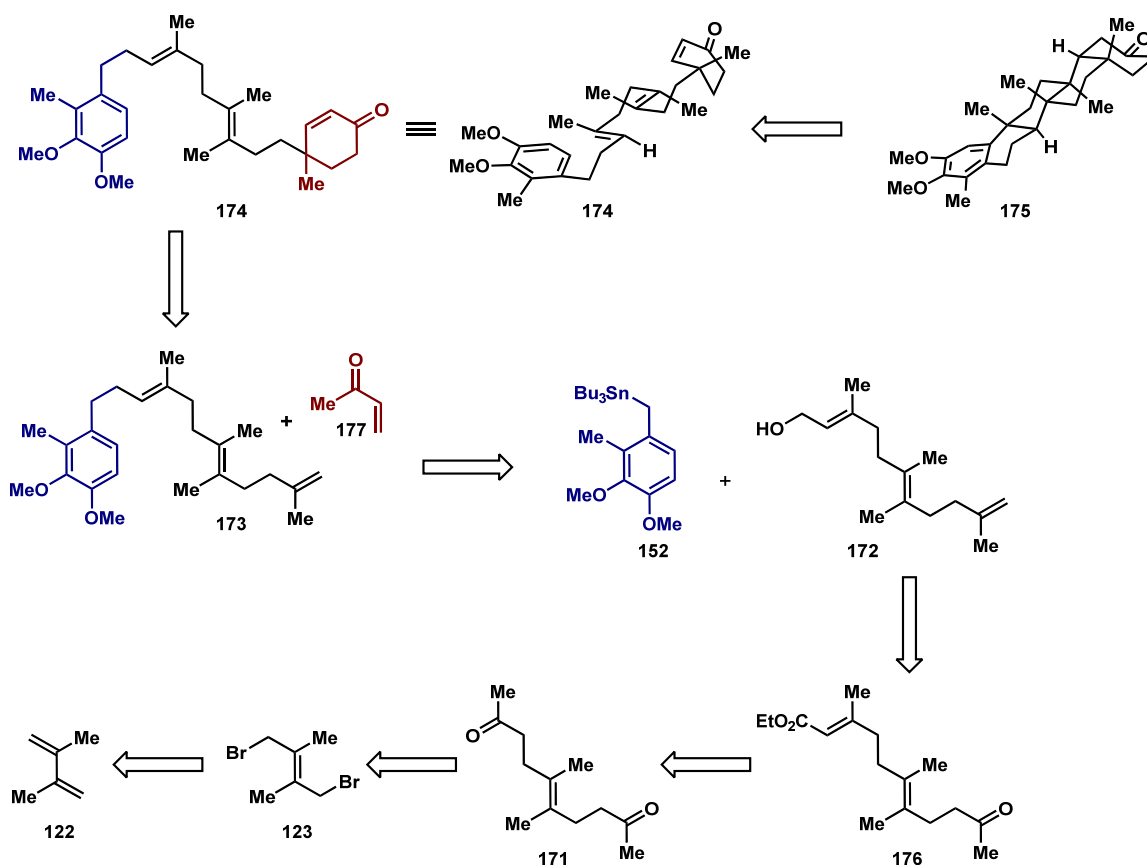
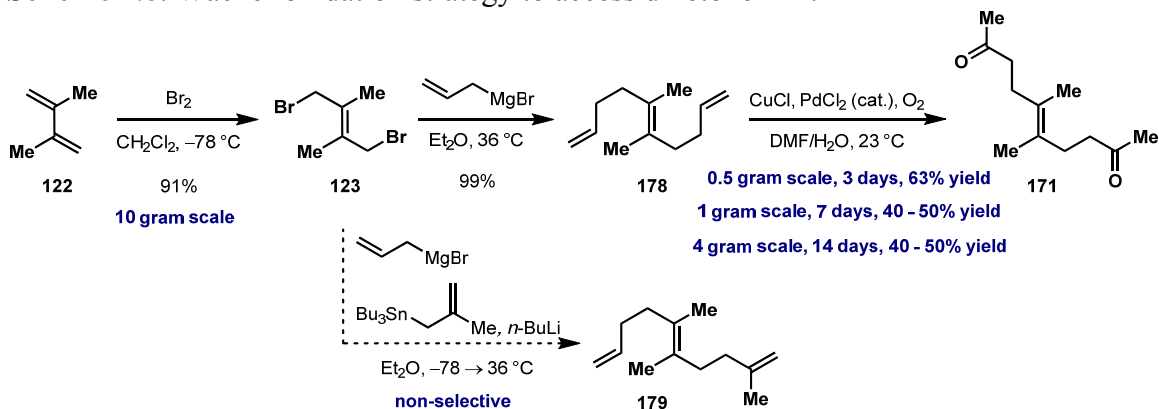


Figure 2.3. New strategy for the synthesis of the polyene **174**.

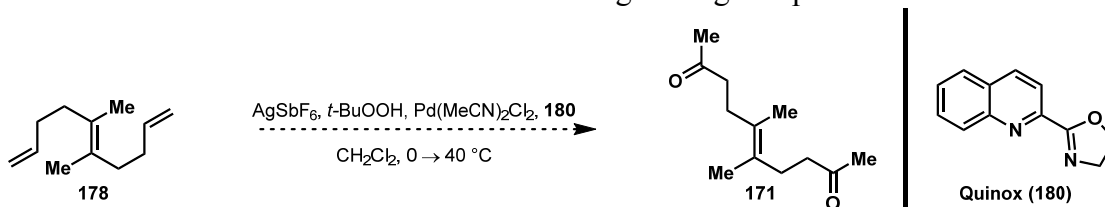
Slow addition of one equivalent of bromine to 2,3-dimethyl butadiene in methylene chloride at $-78\text{ }^{\circ}\text{C}$ afforded the dibromide **123** as a crystalline, lacrimating solid.¹⁰⁴ Desymmetrization proved unsuccessful using one equivalent of allylmagnesium bromide and methylallyl lithium (Scheme 2.8). However, allylation of the bromide with two equivalents of allylmagnesium bromide in ether heated to reflux provided the triene **178** in quantitative yield. Double Wacker oxidation using the Tsuji protocol produced the diketone, albeit in modest yields with moderate scalability.¹⁰⁵

Scheme 2.8. Wacker oxidation strategy to access diketone **171**.



The long reaction times and low yields on appreciable scales warranted investigation into a more efficient process. The Wacker protocol developed by Sigman and co-workers was then employed using the quinox ligand **180**, catalytic palladium, TBHP, and silver hexafluoroantimonate in methylene chloride (Scheme 2.9).^{106,107} These conditions induced rapid decomposition only to afford the desired diketone in low yields.

Scheme 2.9. Wacker oxidation of triene **178** using the Sigman protocol.



Heavy focus was now placed on alkylating enolates with the dibromide to install the desired carbonyl functionality. This was not a trivial task due to the formation of undesired cyclopropanated products (Table 2.2). Using the enolate of dimethylacetamide, however, the formation of these undesired adducts was minimized.

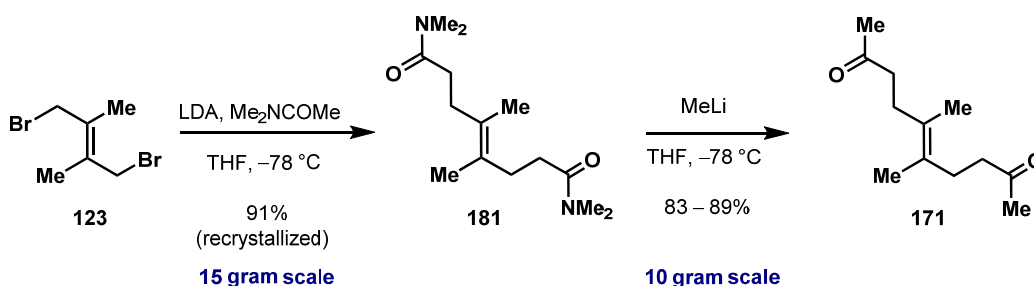
The steric bulk and the difficult nature of deprotonating the α -carbon of amides compared to esters, malonates, and β -keto esters facilitated the alkylation to generate the diamide **181** in high yield forestalling intramolecular cyclopropanation. Slow addition of dimethylacetamide to a freshly prepared solution of LDA in THF at $-78\text{ }^{\circ}\text{C}$ followed by the slow dropwise addition of bromide **123** as a solution in THF generated the diamide as a white crystalline solid in 91% yield after recrystallization. This reaction was successfully repeated on 15 gram scale to provide appreciable quantities of **181**.

Subjecting the amide to methylmagnesium bromide either alone or in combination with anhydrous cerium trichloride as well as $\text{BF}_3\text{-OEt}_2$ at various temperatures returned the unreacted starting material. Using methyl lithium at different temperatures in THF was unselective, but combined with freshly dried zinc bromide in ether at $-10\text{ }^{\circ}\text{C}$ afforded the desired ketone, albeit in variable yields with moderate scalability.^{108,109} However, after examining the solubility of the diamide in ethereal solvents I discovered that prolonged cooling in THF at $-78\text{ }^{\circ}\text{C}$ produced a white heterogeneous mixture, and slow addition of methyl lithium to the mixture facilitated the synthesis of the diketone selectively in high yields reliably on multigram scales. The selective delivery of one equivalent of an alkyl lithium or a lithium acetylide into amides to generate ketones in a single operation has also been observed by Trost.^{110,111} At $-78\text{ }^{\circ}\text{C}$ the tetrahedral intermediate, formed after the initial nucleophilic addition, is persistent which causes a selective addition to occur as long as the temperature remains at $-78\text{ }^{\circ}\text{C}$. This was confirmed by Trost and Phan when they attempted to add a lithium acetylide into an amide.¹¹⁰ Upon neutralization of the reaction media with water the starting amide was returned. However, when $\text{BF}_3\text{-OEt}_2$ was added at $-78\text{ }^{\circ}\text{C}$ the propargyl ketone was afforded in high yield after neutralization. Alkyl lithium reagents, however, do not

require the use of Lewis acids prior to neutralization. This predicated the minimal selectivity originally observed at reaction temperatures warmer than $-78\text{ }^{\circ}\text{C}$ when using methyl lithium. However, upon properly cooling the reaction mixture to $-78\text{ }^{\circ}\text{C}$ through equilibration over one hour and maintaining this temperature through a controlled dropwise addition of methyl lithium, the diketone could be synthesized in high yield. Recrystallization from hexane produced a white crystalline solid which X-ray diffraction unambiguously confirmed as the diketone **171** (see Experimental Section).

Table 2.2. Alkylation of different enolates using bromide **123** ultimately providing diketone **171**.

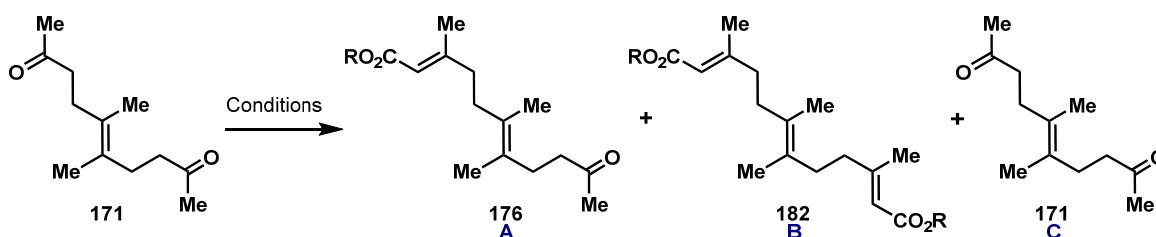
Base	Reagent	Temperature (°C)	Isolated Yield of Product (%)
NaH	EtO ₂ CCH ₂ COMe	0 → 23	trace, R = CH ₂ CO ₂ Et
LiHMDS	EtO ₂ CCH ₂ COMe	0 → 23	trace, R = CH ₂ CO ₂ Et
LDA	MeCO ₂ Me	-78	34, R = OMe
LDA	MeCO ₂ Et	-78	35, R = OEt
LDA	MeCON(OMe)Me	-78	0, R = N(OMe)Me
LDA	MeCONMe ₂	-78	85, R = NMe ₂



A Horner-Wadsworth-Emmons olefination was employed to desymmetrize the ketone (Table 2.3).¹¹² After varying the phosphonates, bases, solvents, and temperatures I discovered the ideal conditions, in regards to yield and E/Z selectivity, were triethyl acetophosphonate and sodium bis(trimethylsilyl) amide in warm toluene. The enoate **176** was provided in a 60% isolated yield with a 6:1 E/Z selectivity using this protocol. The remaining material consisted of the undesired dienolate **182** isolated in 26% yield and recovered starting material isolated in 14%. This yield varies from the expected statistical outcome possibly due to the slow elimination of the insipient alkoxy

phosphonate after the initial nucleophilic addition. This produces an intermediate which is reluctant to form the high energy dianion generated through a second addition of the remaining acetophosphonate.

Table 2.3. Differentiation of symmetrical ketone **171** via HWE olefination.

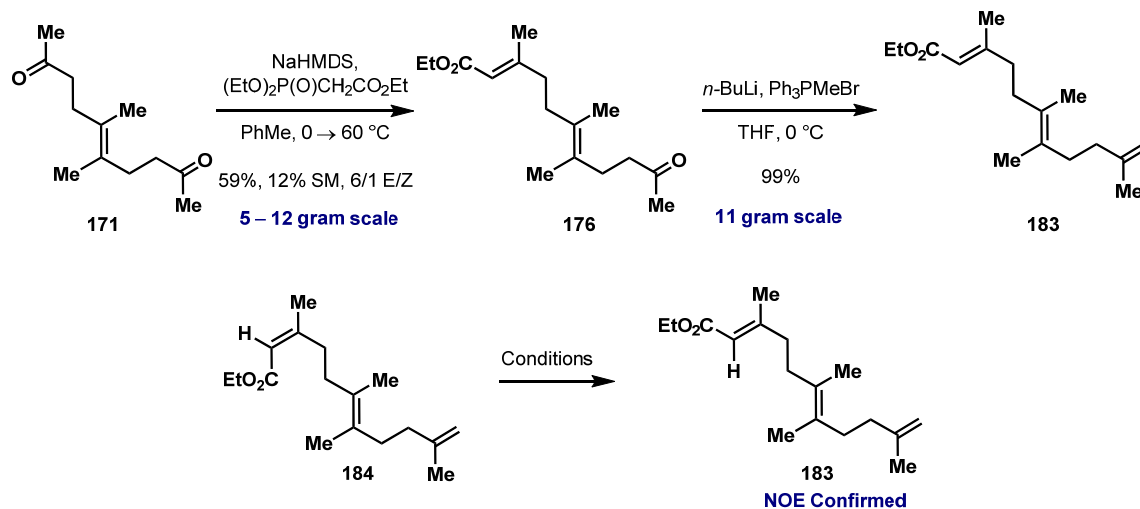


Solvent	Phosphonate	Base	Temp. (°C)	% Yield (A / B / C)	E : Z Ratio
THF	<i>t</i> -BuO ₂ CCH ₂ PO(OMe) ₂	LiHMDS	0 → 23	24 / 40 / 36	4 : 1
THF	<i>t</i> -BuO ₂ CCH ₂ PO(OMe) ₂	NaHMDS	0 → 23	33 / 30 / 36	3 : 1
THF	<i>t</i> -BuO ₂ CCH ₂ PO(OEt) ₂	NaHMDS	0 → 23	37 / 30 / 33	6 : 1
THF	EtO ₂ CCH ₂ PO(OEt) ₂	NaHMDS	0 → 23	60 / 18 / 21	4 : 1
PhMe	EtO ₂ CCH ₂ PO(OEt) ₂	NaHMDS	0 → 23	37 / 20 / 43	6 : 1
PhMe	EtO ₂ CCH ₂ PO(OEt) ₂	NaHMDS	0 → 60	60 / 26 / 14	6 : 1

The fidelity of this transformation was preserved on multigram scale with minimal loss in yield, but at this stage the olefin isomers were inseparable. Subjecting the ketone **176** to a Wittig olefination using the freshly prepared methyl triphenylphosphorane ylide in THF at 0 °C, the triene **183** was generated in quantitative yield (Scheme 2.10). After examination of different solvent conditions, the E/Z isomers could be separated chromatographically using benzene as the eluent, and the correct

isomer was confirmed through NOE spectroscopy (see Experimental Section). In order to maximize material pushed to the forefront, the isomerization of the *cis*-isomer **184** was investigated. Usually iodine or transition metal catalysis is employed to isomerize these types of olefins, but these conditions are detrimental. So, different nucleophiles which add in a conjugate fashion to facilitate formation of the thermodynamic *trans*-isomer were examined. However, phosphine, thiol, and nitrogen nucleophiles were recalcitrant to reacting with this moiety. Focus was then placed on using bases to promote extended enolization. Subjecting the *cis*-enoate **184** to freshly prepared sodium ethoxide in ethanol at 23 °C generated the desired product in 51% isolated yield. The remaining recovered material was the *cis*-isomer.

Scheme 2.10. Synthesis of trienoate **183**.



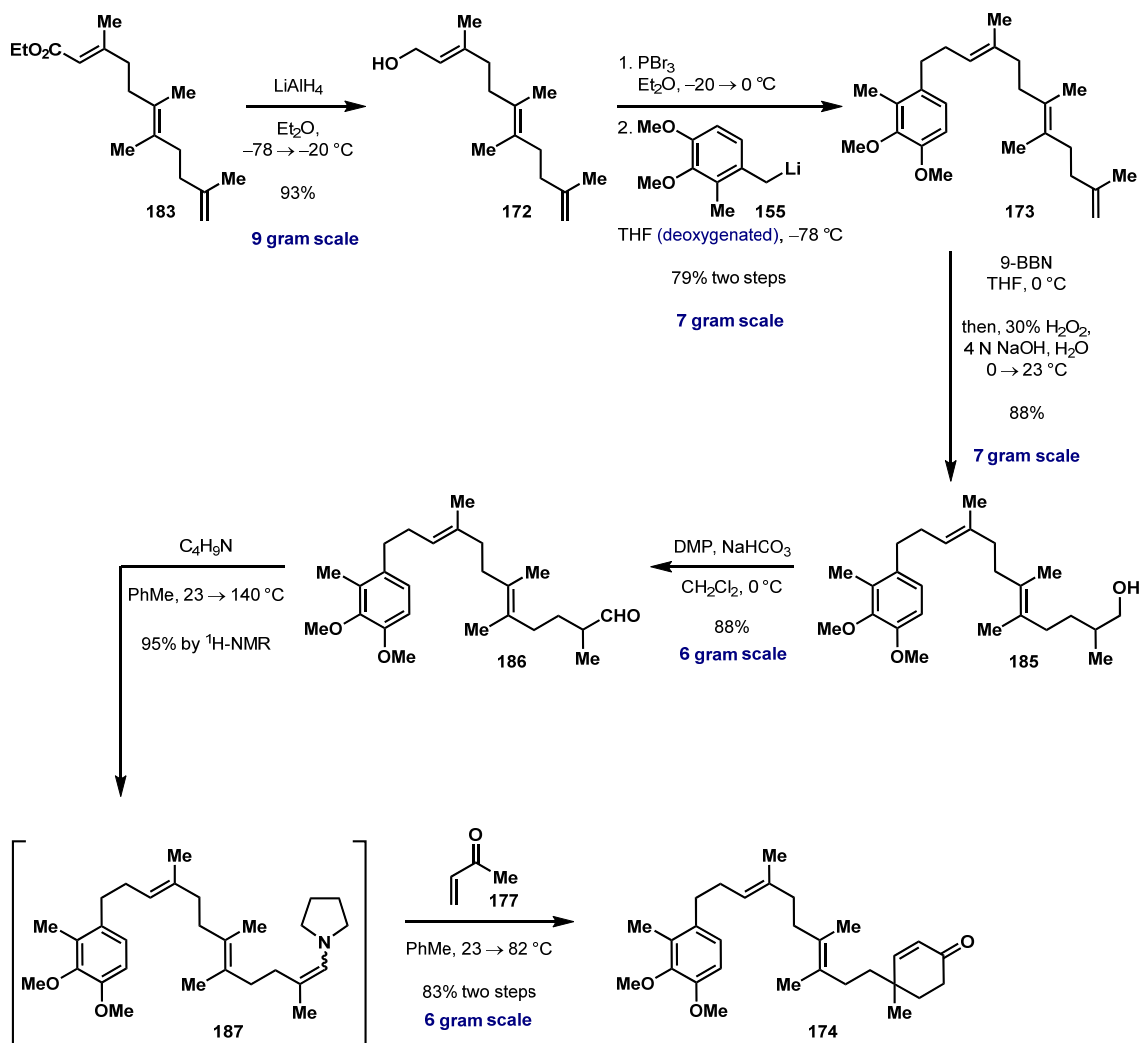
Solvent	Reagent	Temperature (°C)	Result (<i>trans/cis</i> %)
EtOH/CHCl ₃	DABCO	0 → 80	No isomerization
EtOH/CHCl ₃	PPh ₃	0 → 80	No isomerization
EtOH/CHCl ₃	PhSH/NaH	0 → 80	No isomerization
EtOH/CHCl ₃	L-cysteine	0 → 80	No isomerization
EtOH/CHCl ₃	L-cysteine•HCl	0 → 80	No isomerization
EtOH	NaOEt	0	<5% <i>trans</i> , 95% <i>cis</i>
EtOH	NaOEt	23	51% <i>trans</i> , 48% <i>cis</i>
EtOH	NaOEt	23 → 80	Decomposition

Addition of lithium aluminum hydride to an ethereal solution of the ester, and allowing the pale yellow homogeneous solution to warm gradually from -78 to -20 °C over five hours provided the alcohol **172** in 93% yield (Scheme 2.11). Careful analysis of the reaction progress by TLC proved necessary because significant 1,4-reduction was observed when the temperature rose above -10 °C. Halogenation of the alcohol using phosphorus tribromide in ether provided the allylic bromide.¹¹² After aqueous work-up,

the crude bromide was used directly in the alkylation step without purification. Addition of *n*-butyllithium to a solution of the benzyl stannane **152** in deoxygenated THF at -78 °C generated a red-orange solution of the benzyl lithium species **155**. This was then alkylated by the bromide to couple the two fragments together, generating the aryl triene **173** in 79% yield starting from the alcohol. Selective hydroboration of the 1,1-disubstituted olefin with crystalline 9-BBN dimer in THF at 0 °C proceeded smoothly.⁸⁸ NMR analysis of an aliquot from the crude reaction solution determined complete conversion after four hours upon which a solution of 4 N NaOH with 30% H₂O₂ in water was added. The biphasic mixture was stirred vigorously for 60 hours to produce the desired alcohol **185** in 88% yield. Oxidation using Dess-Martin periodinane with solid sodium bicarbonate in methylene chloride at 0 °C afforded the aldehyde **186** in 88% yield.¹¹³ Treatment with pyrrolidine in toluene and heating the solution to 140 °C for 24 hours generated the enamine **187**. After concentrating the reaction solution, analysis of the crude orange viscous oil by ¹H-NMR in C₆D₆ revealed the enamine was approximately 95% pure with 4% of the starting aldehyde remaining. Treatment with two equivalents of methyl vinyl ketone in toluene at 82 °C afforded the resultant annulated β-pyrrolidine adduct which was hydrolyzed with an acetic acid/sodium acetate buffer to deliver the desired enone **174** in 83% yield from the starting aldehyde.^{64,115}

Commencing from 2,3-dimethyl butadiene, the polyene **174** was synthesized in 11 steps in an overall 21% yield. It is a highly scalable strategy capable of reliably providing the enone in quantities greater than five grams representing one of the most efficient, highest yielding syntheses of a polyene precursor to date.

Scheme 2.11. Synthesis of the polyene enone **174**.



Significant examination of the polyolefin cyclization ensued (Table 2.4). As a new type of initiator, this transformation is highly desirable not only to rapidly construct the carbocyclic core in a diastereoselective fashion, but also to deliver the pentacycle at the correct oxidation state. Heating the enone to various temperatures in methylene chloride, dichloroethane or even chlorobenzene under pressure promoted no reactivity.

The use of $\text{BF}_3\text{-OEt}_2$ or titanium tetrachloride at a range of temperatures only promoted decomposition of the starting material with no observation of the cyclized product. Titanium *iso*-propoxide induced no conversion of starting material despite heating the reaction mixture to reflux in methylene chloride.

Treating the enone with *tert*-butyldimethylsilyl trifluoromethane sulfonate in a dilute solution of methylene chloride at 0 °C afforded **what was initially believed** to be the cyclized product **175** in an isolated 5% yield. No increase in yield was attained despite conducting the reaction at lower temperatures in a more dilute solution. Throughout the course of the reaction the silyl enol ether was never observed dictating that it was either being hydrolyzed or trifluoromethane sulfonic acid was actually promoting the cyclization. To confirm the latter, two control experiments were conducted. First, the enone was treated with the silyl triflate in the presence of freshly distilled Hunig's base. No cyclization was observed, only unreacted starting material was returned. Second, the enone was treated with catalytic and stoichiometric quantities of trifluoromethane sulfonic acid. Stoichiometric amounts of the acid prompted swift decomposition of the polyene, but the cyclized adduct was attained in 5% yield by treating the enone with 10 mol% of the acid. The remainder of the material consisted of products which were beyond structural assignment.

The use of milder Brønsted acids such as pyridinium *p*-toluenesulfonate, diphenyl phosphoric acid, or *p*-toluenesulfonic acid did not induce any reaction. Switching to concentrated hydrochloric acid in methylene chloride at 23 °C generated the product in a 35% yield as a 2:1 mixture of diastereomers. This result was somewhat surprising as in theory the cyclization should occur in a stereospecific manner. The diastereomers are formed as the aryl ring engages the trisubstituted olefin, which was determined by

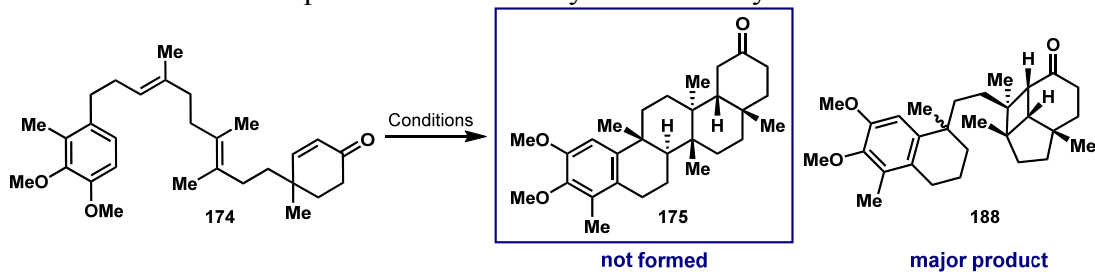
subjecting the isomerically impure starting material (6:1, trisubstituted alkene) to the identical reaction conditions. The product was isolated in the exact same yield and d.r. as when isomerically pure material was used. This was also unambiguously confirmed by 2D-NMR spectroscopy.

The lower yields and diastereoselectivity warranted further probing of milder Lewis acids to improve the yield. Despite literature precedence on promoting ene-type reactions with enones, aluminum reagents showed modest improvements in yield or diastereoselectivity.¹¹⁵ Sen and co-workers showcased the use of anhydrous ferric chloride as well as its hexahydrate to promote polyene cyclizations with epoxides which prompted exploration of these reagents in the cyclization of enone **174**.¹¹⁶ Treating a highly dilute solution of the enone in deoxygenated methylene chloride with 1.5 equivalents of anhydrous ferric chloride promoted the cyclization to afford the product in an isolated 77% yield on 20 milligram scale.

At this stage only ¹H-NMR analysis in a variety of deuterated solvents as well as IR spectroscopy and mass spectrometry were used to assign the structure because the mixture of diastereomers severely complicated the ¹³C-NMR spectra. Therefore, the tentative structural assignment remained invalidated. After an exhaustive investigation, I discovered that using an isochratic solution of dioxane in hexane the diastereomers could be separated by silica gel chromatography. X-ray diffraction could not be used to confirm the structure because the ketone was an amorphous foam. Reducing the ketone and protecting the alcohol as the tosylate, conversion to the tosyl hydrazone, or protecting the catechol as either the *m*-dinitro or *p*-bromo benzoates only produced foams unworthy of X-ray diffraction. However, the fidelity of the cyclization translated excellently above the milligram scale. On one gram scale, the cyclized adduct was provided in 65% yield

as a 3:1 mixture of diastereomers. The scalability of the reaction provided a surplus of material and the ability to separate the diastereomers allowed the structure to be elucidated by 2D-NMR: COSY, DEPT, NOESY, HSQC, HMBC, and ¹³C-INADEQUATE. The results of these experiments clearly indicated that the cyclohexanone **188** was the actual product of these cyclizations, not the desired pentacycle **175**. This molecule was produced through a cationic [2+2] pathway to generate the 4,5,6-tricycle which then undergoes a second annulation between the arene and the trisubstituted olefin, ultimately generating the diastereomers of the reaction.¹¹⁷⁻¹¹⁹ This heartbreaking result nearly thwarted future endeavors.

Table 2.4. Selected examples of the cationic cyclization of cyclohexenone **174**.



Reagent	Mol %	Solvent	Concentration (mM)	Temperature (°C)	Result (% Yield, D.R.)
-----	-----	CH ₂ Cl ₂ , DCE, or PhCl	100	40 → 165	No Reaction
PPTS	110	CH ₂ Cl ₂	2	0 → 40	No Reaction
(PhO) ₂ PO ₂ H	110	CH ₂ Cl ₂	2	0 → 40	No Reaction
TsOH – H ₂ O	110	CH ₂ Cl ₂	2	0 → 40	No Reaction
HCl	110	CH ₂ Cl ₂	2	0 → 23	188 (35%, 2:1)
TfOH	150	CH ₂ Cl ₂	3	-78 → 0	Decomposition
TfOH	10	CH ₂ Cl ₂	3	-78 → 0	188 (5%, 2:1)
Tf ₂ O	110	CH ₂ Cl ₂	1	-78 → 0	No Reaction
Tf ₂ O	110	CH ₂ Cl ₂	1	0 → 23	Decomposition
Tf ₂ O / K ₂ CO ₃	110 / 300	CH ₂ Cl ₂	1	-78 → 23	Decomposition
TBSOTf	150	CH ₂ Cl ₂	3	-78 → 0	188 (5%, 2:1)
TBSOTf / <i>i</i> -Pr ₂ NEt	150	CH ₂ Cl ₂	3	-78 → 0	No Reaction
BF ₃ -OEt ₂	150	CH ₂ Cl ₂	3	-78 → 23	Decomposition
TiCl ₄	150	CH ₂ Cl ₂	3	-78 → 23	Decomposition
Ti(O- <i>i</i> -Pr) ₄	150	CH ₂ Cl ₂	3	-78 → 40	No Reaction
Me ₂ AlCl	150	CH ₂ Cl ₂	3	0 → 23	Decomposition
AlMe ₃	150	CH ₂ Cl ₂	3	0 → 23	Decomposition
EtAlCl ₂	150	CH ₂ Cl ₂	3	0 → 23	188 (14%, 4:1)
EtAlCl ₂	150	CH ₂ Cl ₂	2	0 → 23	188 (34%, 4:1)
EtAlCl ₂	150	PhH	2	5 → 23	188 (<5%)
EtAlCl ₂	150	PhMe	2	-78 → 23	188 (<5%)
FeCl₃	110	CH₂Cl₂	2	0	188 (60%, 3:1)
FeCl₃	150	CH₂Cl₂	1	0	188 (77%, 3:1)
FeCl ₃	10	CH ₂ Cl ₂	2	0	trace conversion of 174
FeCl ₃ (H ₂ O) ₆	110	CH ₂ Cl ₂	2	0	188 (55%, 3:1)

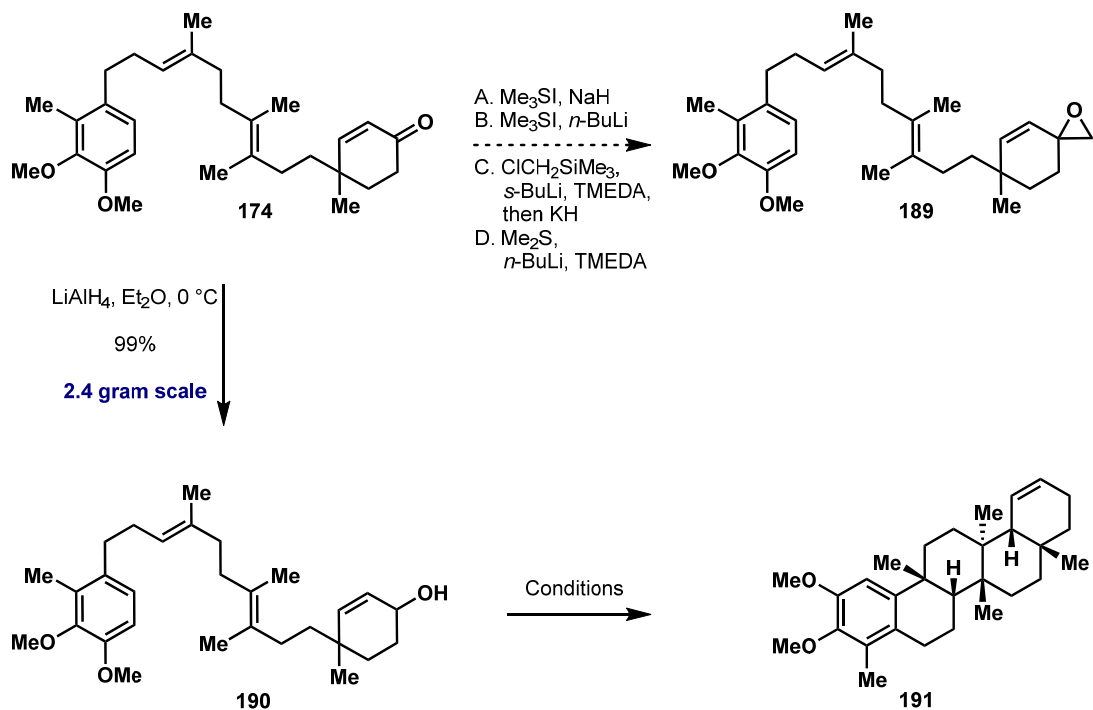
Inability to emulate the friedelin biosynthesis combined with the synthetic difficulties observed by Ireland and co-workers inspired the examination of new initiators for cationic polyolefin cyclizations which provide products at the desired oxidation state. The result of the cationic [2+2] prompted the use of an allylic epoxide as the initiator. However, this strategy was unsuccessful because the linear enone **174** could not be converted into the epoxide **189** (Table 2.5). Steric encumbrance of the 4,4-disubstituted cyclohexenone prevents proper orbital alignment for addition of various nucleophiles thereby promoting enolization of the readily accessible α -protons as the sole pathway. Due to the presence of multiple alkenes I did not foresee selective epoxidation to occur through another manifold so this strategy was abandoned.

Ireland's work on polyene cascades using allylic alcohols coupled with the observations I had made attempting this reaction on the enone **174** led me to hypothesize that this transformation using the allylic alcohol would be viable. The use of strong protic acids as well as Lewis acids that strongly promote discrete cation formation (i.e. boron, aluminum, and tin) proved deleterious to the polyene causing degradation of the alkenes. However, iron induced the cyclization, albeit through the wrong pathway, in mild manner which did not decompose the olefins. High dilution also proved to be critical. Ireland's protocol used a concentration of 25 mM in methylene chloride. The enone **174** underwent massive degradation at this concentration, but this decomposition was not observed at 1 mM inspiring deeper experimentation.

Enone **174** was reduced using lithium aluminum hydride in ether at 0 °C to provide the allylic alcohol **190** in quantitative yield (Table 2.5). Under the identical conditions used by Ireland, the alcohol was treated with 1.5 equivalents of stannic chloride in a 25 mM solution of methylene chloride at -78 °C to afford the desired

pentacyclic product **191** in a 15% isolated yield. Diluting the reaction concentration to 1 mM generated the cyclized product in 26% yield. Switching to ferric chloride and increasing the temperature to 0 °C, the pentacycle **191** was obtained in 33% yield. Increasing the amount of ferric chloride and allowing the temperature to warm from -78 to -30 °C provided the product in 38% yield, and finally, diluting the reaction to 500 μ M with careful monitoring by TLC as the reaction warmed to -30 °C the pentacycle was afforded in a hard earned yield of 51%. The remainder of the material consisted of interrupted cyclized adducts as well as a small amount of polymerized products. It is important to note that the reaction occurred stereospecifically to provide a single diastereomer as initially postulated. When the isomerically impure material (6:1 at the trisubstituted olefin) was subjected to the reaction conditions, the pentacycle was generated as a diastereomeric mixture matching that of the starting material.

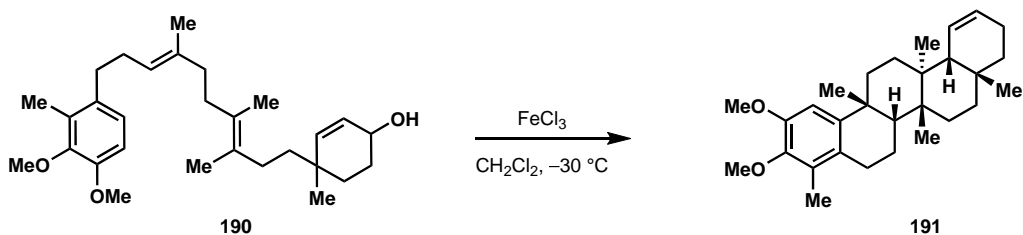
Table 2.5. Polyene cyclization of the allylic alcohol **190**.



Reagent	Mol %	Solvent	Concentration	Temperature ($^\circ\text{C}$)	Isolated Yield (%)
SnCl_4	120	CH_2Cl_2	25 mM	$-78 \rightarrow 0$	15
SnCl_4	120	CH_2Cl_2	1 mM	$-78 \rightarrow 0$	26
FeCl_3	120	CH_2Cl_2	1 mM	0	33
FeCl_3	150	CH_2Cl_2	1 mM	$-78 \rightarrow -30$	38
FeCl_3	150	CH_2Cl_2	500 μM	$-78 \rightarrow -30$	51

Fortunately, the polyene cyclization proceeded smoothly on scales up to 1 gram with minimal loss in yield (Scheme 2.12). In regard to my knowledge of the literature this is the largest scale a polyolefin cascade has been conducted to generate either a tetracyclic or pentacyclic triterpenoid. Reactions larger than 1 gram scale were not

conducted due to the lack of a flask large enough to accommodate the amount of solvent needed for the reaction at the optimal concentration. For instance, on 1 gram scale **4.7 L of methylene chloride** is needed in order to produce the pentacycle **191** in a 38% yield. This warranted further improvement in order to decrease the amount of solvent required to perform the cyclization successfully on larger scale in good yield while still maintaining the effective molarity of the substrate. Utilizing the concept of effective molarity, a protocol employing the syringe pump addition of a dilute solution of the substrate in a slow dropwise manner to a dilute solution of FeCl₃ in methylene chloride was investigated. While maintaining the reaction temperature at -30 °C the concentration of the substrate, addition rate, and concentration of ferric chloride were variables that were systematically examined, and they all proved to be critical. After optimization, the cyclization proceeded well on 100 mg scale to afford the cyclized product in 51% yield (Table 2.6). This proof of concept warranted further probing of the protocol's scalability. On 1 gram scale the starting alcohol was added as a dilute solution in methylene chloride over 6 hrs using a syringe pump to a solution of ferric chloride maintained at -30 °C, however, this only produced the pentacycle **191** in 26% yield. Although successful the yield is much lower on gram scale as compared to the original method to conduct the cyclization using very high dilution and a gradual warming of the temperature from -78 °C. It is important to note that using this strategy only **1.2 L of methylene chloride** was required to perform the cyclization which represents a 4-fold decrease in the amount of solvent used for this reaction.

Table 2.6. Slow addition protocol for the polyolefin cascade of allylic alcohol **190**.

Scale	Substrate Solution	Addition Rate	FeCl_3 Solution	Concentration	Isolated Yield (%)
100 mg	2.5 mL	0.8 mL / hr	225 mL	1 mM	48
100 mg	2.5 mL	2.5 mL / hr	225 mL	1 mM	43
100 mg	2.5 mL	2.5 mL / hr	110 mL	2 mM	41
100 mg	5 mL	10 mL / hr	110 mL	2 mM	47
100 mg	5 mL	5 mL / hr	55 mL	4 mM	42
100 mg	5 mL	10 mL / hr	55 mL	4 mM	35
100 mg	10 mL	20 mL / hr	110 mL	2 mM	51
100 mg	20 mL	40 mL / hr	110 mL	2 mM	48
300 mg	30 mL	20 mL / hr	330 mL	2 mM	42
1 gram	100 mL	20 mL / hr	1.1 L	2 mM	26

With adequate access to the pentacycle **191**, a bifurcated retrosynthetic analysis to install the remaining carbons and stereocenter was devised (Figure 2.4). Hydroboration of the alkene followed by oxidation would generate a carbonyl at C-20 which could provide the desired quaternary center (path A). However, the installation of a ketone at C-21 through an allylic oxidation could also provide a functional handle to install the remaining carbons. The latter was ideal as reduction and alkylation of an enolate was foreseen to generate the quaternary center at C-20 more selectively and in higher yield. The resultant molecule would be stable to a Wolff-Kishner reduction due to the saturated

hydrocarbon backbone and literature precedence in regard to these moieties in these reductions.

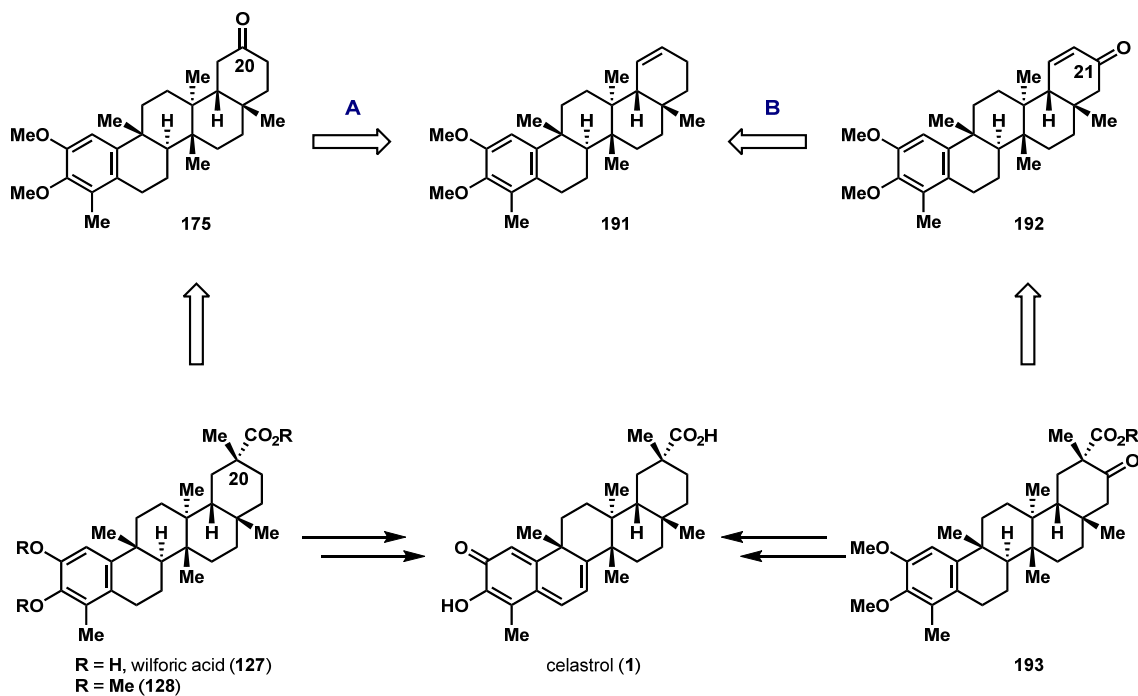
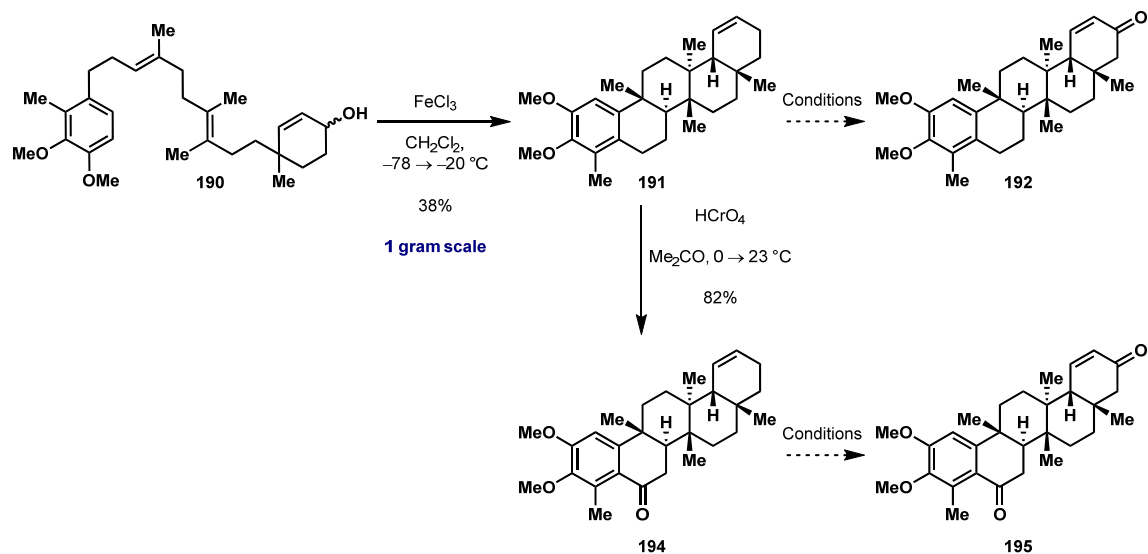


Figure 2.4. New retrosynthetic analysis through a bifurcated strategy from the alkene **191**.

Subjecting this material to a myriad of conditions to facilitate allylic oxidation failed because of selective benzylic oxidation. Treating **191** with 1.1 equivalents of Jones reagent in acetone at 0 °C and allowing the mixture to gradually warm generated the benzyl ketone **194** in 82% yield. Unfortunately, treating **191** with other oxidants or re-subjecting **194** to oxidizing conditions did not deliver the desired α,β -unsaturated ketones **192** or **195**. Only returned starting benzyl ketone or decomposed material was obtained.

Attempts to protect the benzyl ketone as a ketal or thio-ketal failed, and due to the observed adverse reactivity this strategy was abandoned.

Scheme 2.12. Attempted allylic oxidations of pentacycle **191** or benzyl ketone **194**.

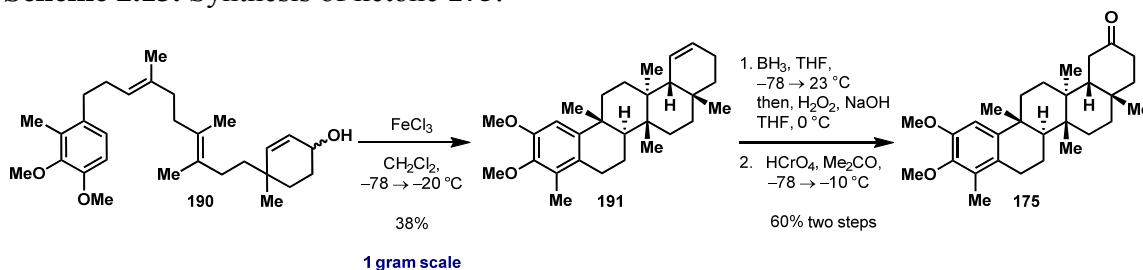


Starting Material	Reagent	Additive	Solvent	Temperature ($^\circ\text{C}$)	Result
191	HCrO_4	-----	Me_2CO	$0 \rightarrow 23$	Benzylic Oxidation
191 and 194	HCrO_4	-----	Me_2CO	$23 \rightarrow 56$	Decomposition
191	$\text{Mn}(\text{OAc})_3 \cdot 2\text{H}_2\text{O}$	TBHP	EtOAc	77	Benzylic Oxidation
194	$\text{Mn}(\text{OAc})_3 \cdot 2\text{H}_2\text{O}$	TBHP	EtOAc	77	Decomposition
191	CrO_3	3,5-dimethyl pyrazole	CH_2Cl_2	$-20 \rightarrow 0$	Benzylic Oxidation
191 and 194	CrO_3	3,5-dimethyl pyrazole	CH_2Cl_2	$-20 \rightarrow 23$	Decomposition
191	SeO_2	H_2O	1,4-Dioxane	$23 \rightarrow 101$	Diene
191	SeO_2	HCO_2H	1,4-Dioxane	$23 \rightarrow 101$	Decomposition

Hydroboration of the pentacycle **191** proceeded with moderate selectivity using borane in THF while allowing the reaction to gradually warm to 23°C from -78°C . Steric compression of the E-ring prevented the use of larger hydroborating agents such as

9-BBN, which after heating to reflux in THF over 24 hours only returned unreacted starting material. After oxidative work-up the crude alcohol was oxidized with Jones reagent in acetone to afford the desired ketone **175** as a white solid in 60% yield over two steps (Scheme 2.13). The temperature of the reaction was critical due to competing benzylic oxidation, but this pathway was minimized by allowing the reaction to warm gradually from $-78\text{ }^{\circ}\text{C}$ to $-10\text{ }^{\circ}\text{C}$ with careful monitoring of the reaction's progress by TLC.

Scheme 2.13. Synthesis of ketone **175**.



Initially, the structure of the ketone was assigned using 2D-NMR (COSY, NOESY, HSQC, HMBC, and DEPT, see Experimental Section) as well as through subsequent reactions and full characterization of those products (see Scheme 2.14). Later, I fortuitously discovered that dissolving the white solid in hot methanol and patiently allowing the clear colorless solution to cool to $23\text{ }^{\circ}\text{C}$, a crystalline solid slowly formed. These colorless crystals were suitable for X-ray diffraction which unambiguously confirmed the structure as the ketone **175** (Figure 2.5). Analysis of the crystal structure clearly shows the sterical arrangement of the carbocyclic core and the twisting of the B, C, and D rings out of traditional chair conformity, preventing clashes between the angular methyls. Also observed is the half-chair conformation in which the

E-ring resides thereby forestalling the backside angular methyl at the C-D ring juncture from colliding with C-19 and C-21, their hydrogens, as well as C-20. This dictates that nucleophilic addition should occur diastereoselectively from the top face and electrophiles appended in a similar fashion.

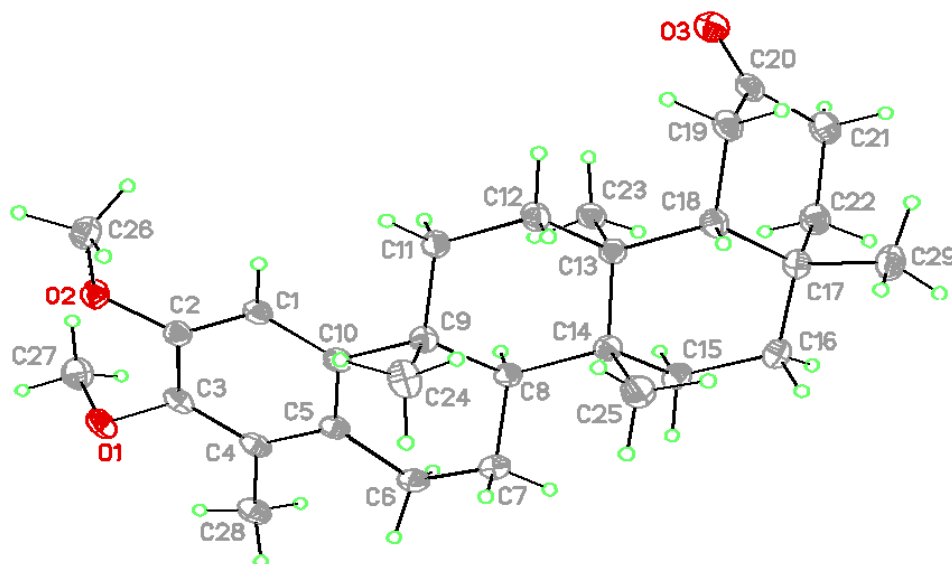


Figure 2.5. View of cyclized ketone **175**. Displacement ellipsoids are scaled to the 50% probability level.

At this stage the remainder of the synthesis entailed installation of the carbonyl and the methyl poised at C-20 as well as oxidation of wilforic acid (**127**) to afford celastrol (**1**) (Figure 2.6). Stereochemical analysis of the crystal structure delineated that the last methyl would be difficult to install because of sterics. A retrosynthetic analysis was conceived based on the literature precedence regarding installing methyls in crowded

environments using cyclopropanation strategies.^{47,51,53,59-61,120} A substrate guided cyclopropanation of methyl enol ether **196** provides **197**, which an acid mediated ring opening and oxidation sequence affords the acid **128**. Deprotection of the methyl ethers then generates wilforic acid. This strategy introduces the remaining carbons in a stereoselective fashion from **197**, which is accessed through a Wittig olefination of ketone **175**. If sterics precluded this transformation then a Peterson olefination of the methoxymethyl trimethylsilyl alcohol **198** could also provide access to the enol ether. Literature precedent established by Magnus and co-workers to access methyl enol ethers from sterically demanding ketones not amenable to Wittig olefinations further corroborated the viability of this approach.¹²¹⁻¹²³ Alternatively, the ketone **175** could be used in a carbonylation sequence to access **199** which provides a synthon to install the remaining methyl through an enolate alkylation strategy delivering **128**.

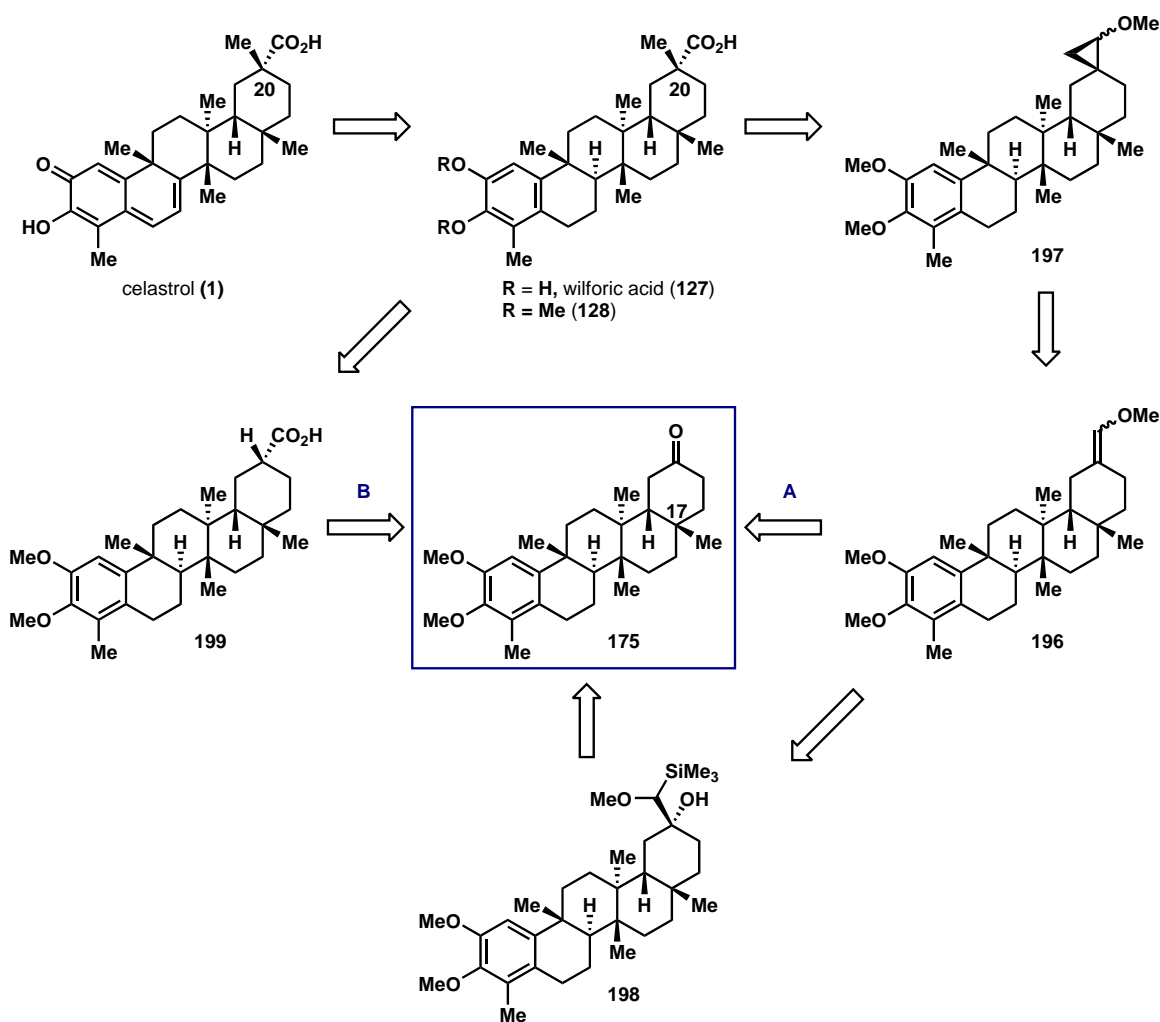
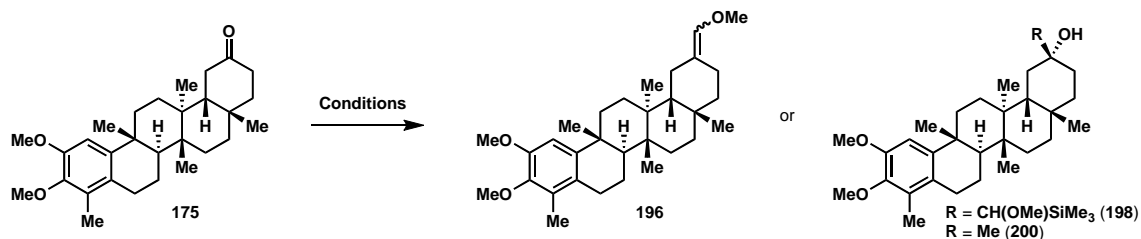


Figure 2.6. Retrosynthesis to access wilforic acid (**127**) and celastrol (**1**) from ketone **175**.

The ability of ketone **175** to undergo nucleophilic addition was examined with a variety of nucleophiles. The methyl positioned at C-17 posed a significant problem as it blocked the necessary trajectory for nucleophilic addition. To further complicate this issue, the ketone is flanked by two α -carbons bearing protons susceptible to enolization. Large reagents such as the ylides methoxymethyl triphenylphosphorane and methyl

triphenylphosphorane did not react with the ketone in a productive manner despite using various equilibrating or non-equilibrating bases as well as different solvents and reaction temperatures. This also proved to be the case for the anions of methoxymethyl trimethylsilane, chloromethyl trimethylsilane, trimethyl sulfonium iodide, and trimethyl sulfoxonium iodide.¹²¹⁻¹²⁴ However, treating the ketone with methyl lithium at 23 °C generated the carbinol **200** in 72% yield as a single diastereomer, with the remaining material consisting of the starting ketone **175**. This enlightening result illustrates that small nucleophiles react diastereoselectively as initially postulated showcasing the potential of the enolate alkylation strategy.

Table 2.7. Selected attempts to access methyl enol ether **196** or alcohols **198** and **200**.

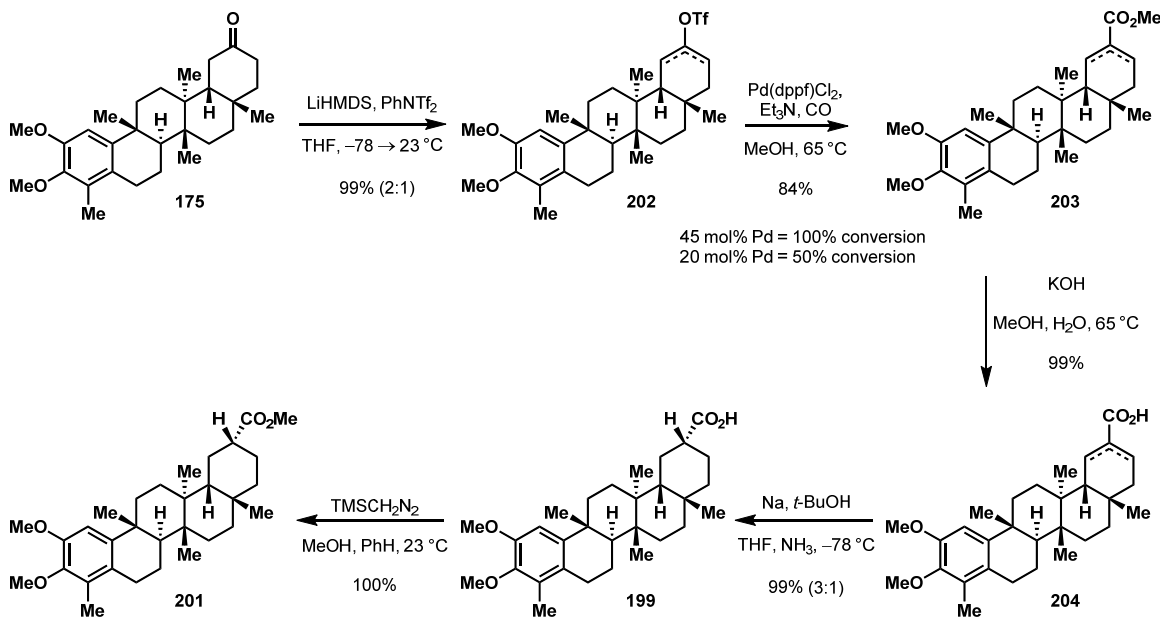


Reagent	Base	Solvent	Temperature (°C)	Result
Ph ₃ PCH ₂ OMeCl	LiHMDS	THF	23	No Reaction
Ph ₃ PCH ₂ OMeCl	PhLi	THF/Bu ₂ O	23	trace
Ph ₃ PCH ₂ OMeCl	NaHMDS	THF	23	No Reaction
Ph ₃ PCH ₂ OMeCl	<i>t</i> -BuOK	THF/ <i>t</i> -BuOH	23	No Reaction
Ph ₃ PCH ₂ OMeCl	KOC(Me) ₂ CH ₂ Me	PhMe	0 → 23	No Reaction
Ph ₃ PCH ₂ OMeCl	KOC(Me) ₂ CH ₂ Me	PhMe	23	trace
Ph ₃ PMeBr	KOC(Me) ₂ CH ₂ Me	PhMe	23 → 110	trace
MeOCH ₂ SiMe ₃	<i>s</i> -BuLi	THF	-78 → 0	trace
MeOCH ₂ SiMe ₃	<i>s</i> -BuLi	THF	0	Decomposition
ClCH ₂ SiMe ₃	<i>s</i> -BuLi	THF/TMEDA	-55 → 0	trace
MeLi	-----	THF	23	72% Product (200), 28% SM
MeMgBr	-----	THF	23	trace
Me ₃ Si	<i>n</i> -BuLi	THF	23	No Reaction
Me ₃ Si	NaH	DMSO/THF	23	No Reaction
Me ₃ SOI	NaH	DMSO/THF	23 → 60	trace
Me ₃ SOI	<i>n</i> -BuLi	THF	23 → 60	trace

To examine the enolate alkylation strategy the syntheses of acid **199** and ester **201** were required. After the azeotropic removal of water with toluene, the ketone was deprotonated with a 1 M solution of LiHMDS in THF at -78 °C. After 1 hour the resultant enolate was trapped with N-phenyl-bis(trifluoromethanesulfonylimide) to afford the enol triflate **202** in 99% yield as a 2:1 mixture of olefinic isomers (Scheme 2.14). The isomeric mixture was carried forward because the olefin would ultimately be

reduced. The carbonylation proceeded smoothly using palladium(dppf) dichloride and triethylamine in methanol heated to reflux under an atmosphere of carbon monoxide to provide the α,β -unsaturated ester **203** in an 84% yield. To facilitate maximum conversion of the starting material, 45 mol% of palladium(dppf) dichloride was needed. This is because only approximately 50% conversion was observed when lower amounts of the catalyst were used whereas other palladium catalysts rendered minimal success. Unfortunately, sterics made this material resistant to reduction using hydrogenation with platinum, palladium on carbon, or Pearlman's catalyst. Nickel boride, Stryker's reagent, and Lipshutz's modified Stryker's reagent likewise did not afford the reduced product, only unreacted starting material was returned.¹²⁵⁻¹²⁷ A dissolving metal reduction in liquid ammonia reduced the enoate **203**, but amidation of the ester was observed. So, the ester was saponified, and as a solution in THF the acid **204** was added to a dark blue solution of sodium in liquid ammonia at $-78\text{ }^{\circ}\text{C}$ which generated the reduced product **199** as a 3:1 mixture of diastereomers in 98% yield over two steps. Presuming the dianionic enolate alkylation would be difficult, the acid was treated with trimethylsilyl diazomethane in a 1:1 mixture of methanol/benzene at $23\text{ }^{\circ}\text{C}$ to afford the ester **201** as a white amorphous solid in quantitative yield.¹²⁸

Scheme 2.14. Synthesis of the saturated acid **199** and ester **201**.

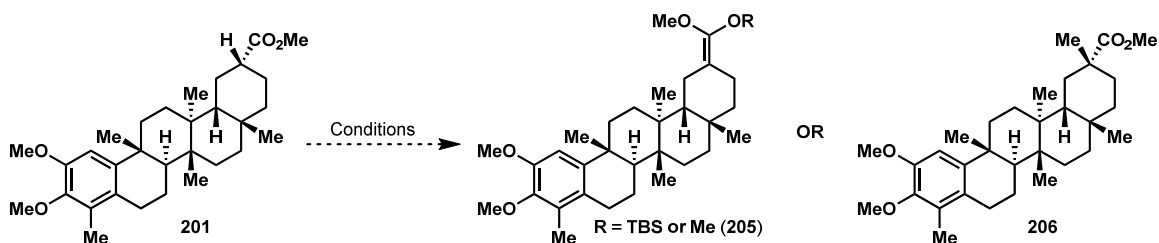


The original plan centered on converting the ester to its silyl or methyl ketene acetal (**205**) followed by cyclopropanation. Acid mediated hydrolysis would reveal the alkylated ester **206** or acid **128** as a single diastereomer. Initially, the ester proved reluctant to silyl ketene acetal formation using soft as well as hard enolization techniques (Table 2.8). LDA was too bulky of a base to promote full enolization, however, treating the ester with *tert*-butyldimethylsilyl trifluoromethane sulfonate in THF at 23 °C for one minute and then adding a freshly prepared solution of LDA in THF generated the desired silyl ketene acetal in ~75% yield. The other 25% of the material was the minor diastereomer of unreacted starting material which did not react with LDA as proven by treating this compound with freshly prepared LDA in THF at 23 °C for one hour, and

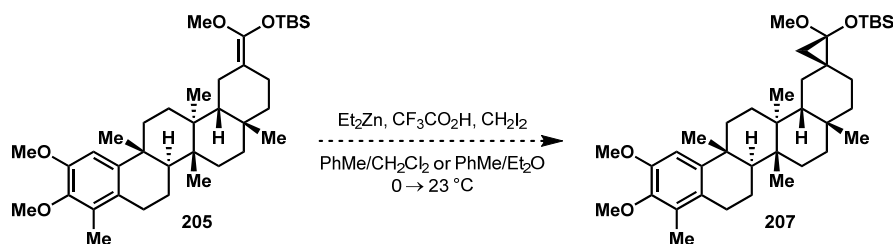
then neutralizing this reaction at different temperatures. After an aqueous work-up, ¹H-NMR analysis showed pure starting material, revealing no enolization had occurred.

The silyl ketene acetal **205** was unfortunately resistant to cyclopropanation. Focus was then placed on generating the dimethyl variant as I hypothesized that this compound might be a more competent participant in the subsequent cyclopropanation. Despite using dimethyl sulfate, which prefers O-alkylation over C-alkylation, as well as using distilled HMPA as a co-solvent, the ketene acetal was not observed and only a trace amount of the alkylated adduct **206** was produced.¹²⁹ Subjecting the ester to a freshly prepared solution of lithium diethyl amide in THF at 23 °C for five minutes followed by the addition of iodomethane generated the alkylated product as a single diastereomer in 25% yield. The low yield is attributed to amidation of the starting ester. To circumvent this issue the reaction was cooled to -78 °C and then treated with freshly prepared lithium diethyl amide in order to promote enolization. The mixture was gradually warmed to 23 °C and iodomethane was added to the golden brown solution, however, this afforded the amidated product in a greater yield of approximately 90%.

Table 2.8. Alkylation of ester **201** and attempted formation of ketene acetals **205** and ester **206**.



Base	Reagent	Solvent	Temperature (°C)	Result
LDA	TMSOTf	THF	-78 → 23	No Product
LDA	TBSOTf	THF	-78 → 23	No Product
Et ₃ N	TMSOTf	CH ₂ Cl ₂	-78 → 40	No Reaction
LDA	TBSOTf	THF	23	Silyl Ketene Acetal 205 (~75%)
LDA	Me ₂ SO ₄	THF	23	Trace Alkylation, No Ketene Acetal
LDA	Me ₂ SO ₄	THF/HMPA	23	Trace Alkylation, No Ketene Acetal
Et ₂ NLi	MeI	THF	23	25% Alkylation, ~75% Amidation
Et ₂ NLi	MeI	THF	-78 → 23	10% Alkylation, ~90% Amidation



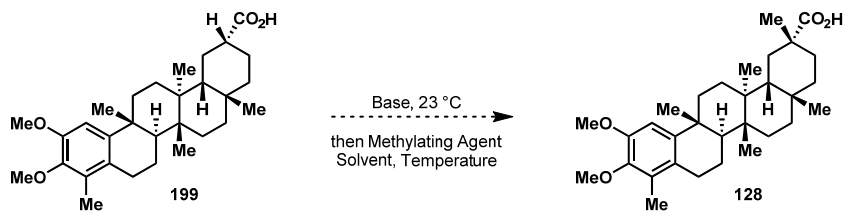
Compelled by the successful diastereoselective alkylation of the ester, heavy focus was centered on synthesizing the acid **128**. After azeotropic removal of water with toluene, the solid acid **199** was dissolved in THF, and this clear colorless solution was treated with an excess of freshly prepared LDA at 23 °C for 1 hour to provide a dark golden yellow solution of the dianionic enolate. Addition of iodomethane induced an exothermic reaction alkylating the enolate to afford **128** in 25% yield (Table 2.9). The

residual material consisted of ~25% of the undesired diastereomer of **128** and ~50% of the starting material as an approximate 1:1.5 mixture of diastereomers. The recovery of starting material was surprising as 20 equivalents of LDA were used. Based on work conducted by Tamm, Seebach, and Meyers on the behavior of lithium enolates in solution, excess amide base should promote full alkylation.^{129,130} Even more surprising was that the alkylation proceeded with no observed diastereoselectivity.

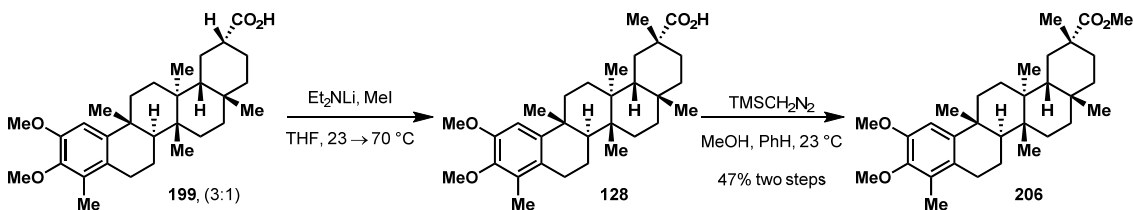
In order to solve the first issue, freshly prepared lithium diethyl amide was used to promote the full enolization of **199**. Despite using lithium diethyl amide in combination with *n*-butyllithium to deprotonate the two equivalents of diethyl amine generated in producing the dianion, enolized starting material was always recovered. The use of distilled HMPA as a co-solvent to break lithium aggregates or using stronger methylating agents only promoted O-alkylation to afford the ester **201**.¹²⁹ Neither the product **128** nor dimethyl ketene acetal **205** were observed. To insure **205** was not being hydrolyzed, a basic work-up as well as freshly base-washed glassware were used and the crude material was then analyzed by ¹H-NMR using C₆D₆. In an effort to enhance the diastereoselectivity, the alkylation step was conducted at -78 °C and allowed to warm gradually to 23 °C. This however only afforded trace amounts of the desired product. Interestingly, when the reaction mixture was placed in a 23 °C water bath and the dianion was treated with iodomethane, only a trace amount of the desired product was observed; enolized starting material was returned in both cases. The exothermicity of the alkylation when the reaction was initially conducted at 23 °C without the water bath proved to be a highly critical observation. So, the starting acid was treated with an excess of a freshly prepared solution of lithium diethyl amide in THF at 23 °C for 30 minutes, and the resulting dark golden yellow solution was placed in an oil bath heated to 70 °C for 30

minutes. Iodomethane was then added, producing a heterogeneous mixture which was kept at 70 °C for 30 minutes which afforded the alkylated product in high yields, but with minimal diastereoselectivity. The alkylated acid was then dissolved in a 1:1 mixture of methanol/benzene and treated with a 2 M solution of trimethylsilyl diazomethane in ether. The ester was then purified by silica gel chromatography to afford the alkylated adduct **206** in an isolated yield of 47% over the two steps. The undesired diastereomer was also isolated in 36% yield. The esterification was conducted to aid the isolation and chromatographical separation of the diastereomers. The structure of the major product **206** was assigned using 2D-NMR spectroscopy (see Experimental Section).

Table 2.9. Synthesis of acid **128** through the dianionic alkylation of **199**.



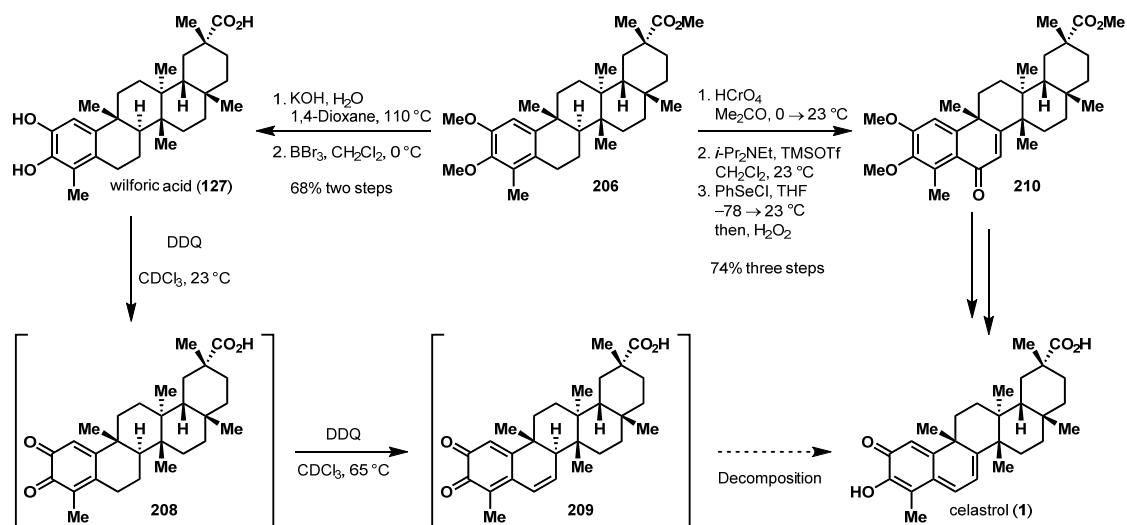
Base	Methylating Agent	Solvent	Temperature (°C)	Result (% Yield, D.R.)
LDA	MeI	THF	23	128 (50%, 1:1), 199 (50%, 1:1.5)
LDA	MeI	THF/HMPA	23	Non-Alkylated Ester 201 (80%, 1:1.5)
LDA	Me ₂ SO ₄	THF	23	Non-Alkylated Ester 201 , No Ketene Acetal
LDA	Me ₂ SO ₄	THF/HMPA	23	Non-Alkylated Ester 201 , No Ketene Acetal
Et ₂ NLi, then <i>n</i> -BuLi	MeI	THF	23	128 (50%, 1:1), 199 (48%, 1:1)
Et ₂ NLi, then <i>n</i> -BuLi	MeI	THF	23 °C water bath	Trace Alkylation, Enolized SM (199)
Et ₂ NLi, then <i>n</i> -BuLi	MeI	THF	-78 → 23	Trace Alkylation, Enolized SM (199)
Et ₂ NLi	MeI	THF	70	128 (83%, 1.3:1), SM (16%)



The ester **206** was saponified using potassium hydroxide in dioxane/water heated to reflux (Scheme 2.15). Treating the acid **128** with boron tribromide in methylene chloride at 0 °C for five minutes afforded wilforic acid (**127**) as a white amorphous solid in 68% yield over two steps after recrystallization. ¹H-NMR analysis of this material in deuterated pyridine matched the reported chemical shifts for wilforic acid (see Experimental Section) representing the first total synthesis of wilforic acid.¹³¹ The catechol was then oxidized instantaneously in CDCl₃ with two equivalents of DDQ to provide the *ortho*-quinone **208** as observed by ¹H-NMR. After placing the NMR tube in

an oil bath heated to 65 °C for two hours the unsaturated quinone **209** was produced from the oxidation of **208**. Unfortunately, prolonged heating or the use of acids did not promote tautomerization to afford celastrol (**1**), only decomposition of the material was observed. Alternatively, ester **206** was oxidized to the benzyl ketone using Jones reagent which was then further oxidized to the enone **210** in a 74% yield over three steps using a selenoxide elimination. This is where the project currently lies. The final strategy is to reduce the enone to the benzyl alcohol using a Luche reduction, and the activated alcohol is foreseen to rapidly eliminate *in situ* during the deprotection of the methyl ethers to ultimately provide celastrol in a single step.

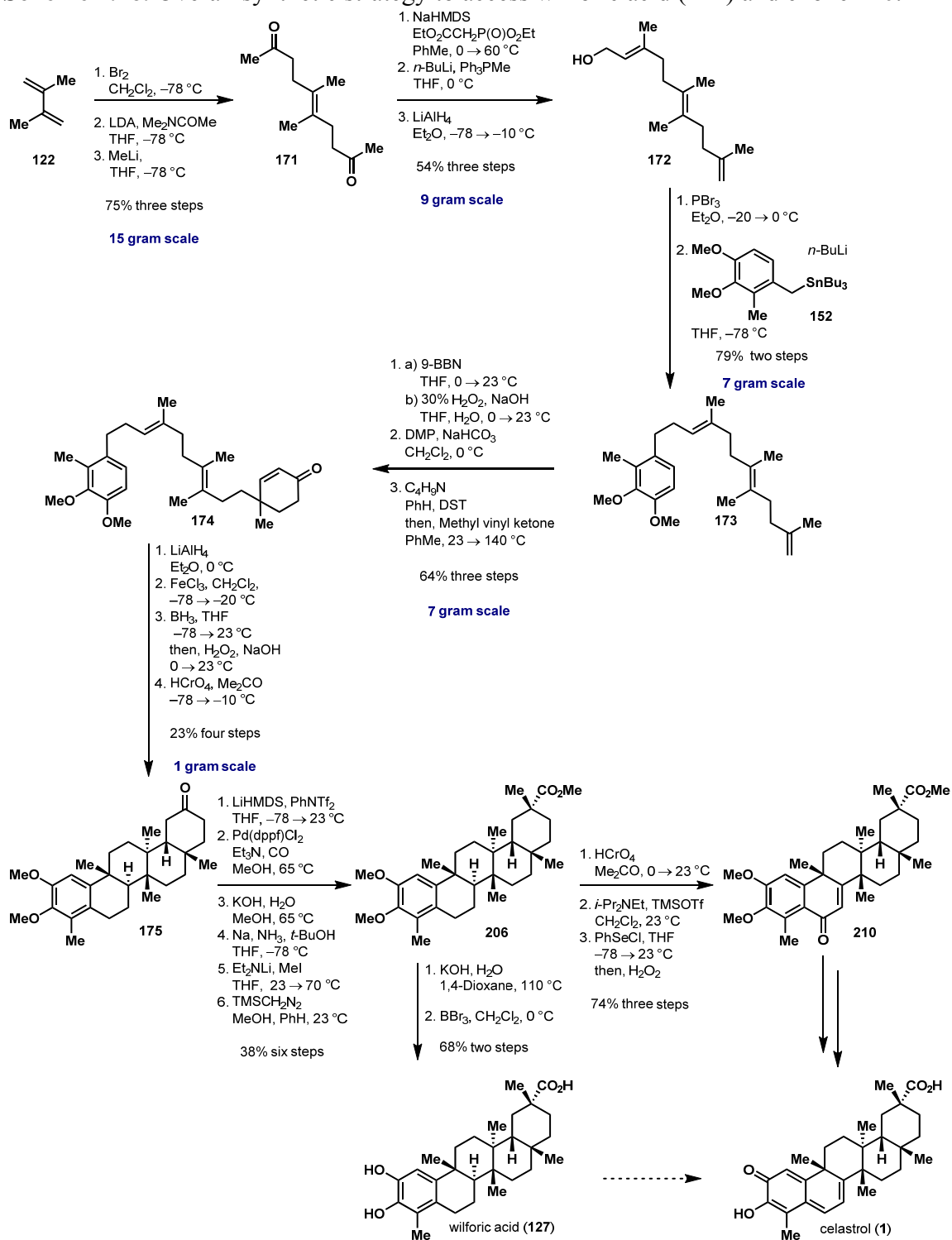
Scheme 2.15. Synthesis of wilforic acid (**127**), enone **210**, and the final strategy.



Conclusion

The total synthesis of celastrol (**1**) remains a work in progress. The arduous process of developing a strategy to access the natural product ultimately culminated in one of the fastest, highest yielding syntheses of a polyene to date. More importantly, a polyene cyclization that constructs the friedelin pentacyclic core in a diastereoselective fashion on one gram scale was developed providing rapid access to these complex frameworks. This is the highest scale a polyolefin cascade has been conducted to access a tetracyclic or pentacyclic terpenoid to date. Commencing from 2,3-dimethyl butadiene, the polyene **174** is accessed routinely in 5 gram quantities in 11 steps with an overall 21% yield (Scheme 2.16). Using ferric chloride and a slow addition protocol, the pentacycle **191** is generated in a single operation on 1 gram scale in a 38% yield improving the strategy originally exploited by Ireland. The alkene is then used to install the remaining functionality with the proper stereoselectivity highlighted by a carbonylation and a dianionic enolate alkylation. This strategy successfully completed the first total synthesis of wilforic acid (**127**); which unfortunately could not be oxidized to celastrol (**1**). A new strategy to synthesize celastrol from enone **210** that invokes an *in situ* deprotection and elimination is under development.

Scheme 2.16. Overall synthetic strategy to access wilforic acid (**127**) and enone **210**.



Experimental Section

Studies Toward the Synthesis of Celastrol

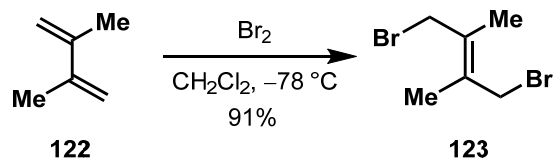
Table of Contents

1. General Information	91
2. Experimental Procedures for the Synthesis of Wilforic Acid and 210	92
3. Experimental Procedures for the Synthesis of Benzyl Stannane 152	129
4. Crystallographic Information for Pentacyclic Ketone 175	134
5. Experimental Procedures for the Synthesis of Iodo-enoate 143	150
6. Experimental Procedures for the Synthesis of Triene 165	162
7. Catalog of Spectra	171

1. General Information

All reactions were performed in flame-dried round-bottomed or modified Schlenk flasks fitted with rubber septa under a positive pressure of argon, unless otherwise noted. Air- and moisture-sensitive liquids and solutions were transferred via syringe or stainless steel cannula. Solvents (methylene chloride, ether, tetrahydrofuran, benzene, and toluene) were purified using a Pure-Solv MD-5 Solvent Purification System (Innovative Technology). Where necessary, solvents were deoxygenated by sparging with nitrogen for at least 1 hour unless otherwise noted. All other reagents were used directly from the supplier without further purification unless otherwise noted. Organic solutions were concentrated by rotary evaporation at ~25 mbar in a water bath heated to 40 °C unless otherwise noted. The molarity of n-butyllithium and methyllithium were determined by titration against diphenylacetic acid. Analytical thin-layer chromatography (TLC) was carried out using 0.2 mm commercial glass-coated silica gel plates (silica gel 60, F254, EMD chemical). Thin layer chromatography plates were visualized by exposure to ultraviolet light and/or exposure to an acidic solution of ceric ammonium molybdate or a basic solution of potassium permanganate followed by heating on a hot plate. Infrared spectra were recorded on a Nicolet 380 FTIR using neat thin film technique. High-resolution mass spectra (HRMS) were obtained on a Karatos MS9 and reported as m/z (relative intensity). Accurate masses are reported for the molecular ion $[M+Na]^+$, $[M+H]^+$, $[M-H]^-$, $[M-AcOH]^-$, $[M]$, or $[M+2H]^{2+}$. Nuclear magnetic resonance spectra (1H -NMR and ^{13}C -NMR) were recorded with a Varian Gemini (400 MHz, 1H at 400 MHz, ^{13}C at 100 MHz, 500 MHz, 1H at 500 MHz, ^{13}C at 125 MHz, or 600 MHz, 1H at 600 MHz, ^{13}C at 150 MHz). For $CDCl_3$ and C_6D_6 solution, chemical shifts are reported as parts per million (ppm) referenced to residual protium or carbon of the solvent; $CHCl_3$ δ 7.26 ppm, $CDCl_3$ δ 77.0 ppm, C_6D_5H δ 7.15 ppm, C_6D_6 δ 128.0 δ ppm, C_5D_4HN δ 7.19 ppm, C_5D_5N δ 135.9 ppm, and CD_2HCN δ 1.93 ppm. Coupling constants are reported in Hertz (Hz). Data for 1H -NMR spectra are reported as follows: chemical shift (ppm, referenced to protium; (bs = broad singlet, s = singlet, br d = broad doublet, d = doublet, t = triplet, q = quartet, dd = doublet of doublets, td = triplet of doublets, ddd = doublet of doublet of doublets, m = multiplet, integration, and coupling constants (Hz)).

2. Synthesis of Wilforic Acid (127) and the Enone 210

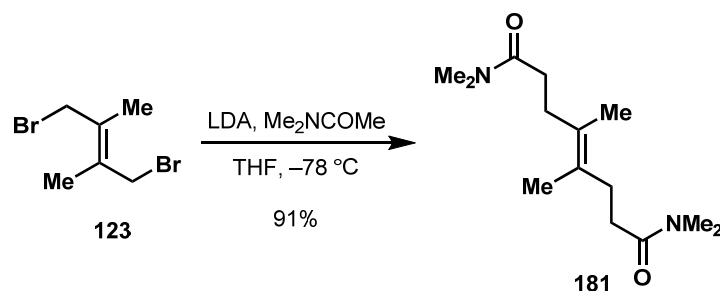


A solution of 2,3-dimethylbutadiene (10.1 g, 13.9 mL, 124 mmol, 1.00 eq.) in CH₂Cl₂ (88 mL) was placed in a bath cooled to -78 °C and allowed to stir vigorously (600 rpm) for 30 minutes. A solution of bromine (19.8 g, 6.3 mL, 124 mmol, 1.00 eq.) in CH₂Cl₂ (36 mL) was added dropwise via addition funnel over 4 hours. The heterogeneous and pale yellow colored mixture was allowed to stir for 2 hours after the complete addition of bromine at -78 °C upon which the golden yellow mixture was removed from the cooling bath and concentrated via rotary evaporation. (**Note:** The product readily sublimates and is a lachrymator. The pressure of the rotary evaporator was reduced to no lower than 100 mbar and the flask was submerged into an ice water bath). After complete evacuation of CH₂Cl₂, the golden yellow solution was allowed to stand at 23 °C in the dark upon which the colorless solid crystallized out of solution. Cooling in a freezer chilled to -20 °C aids full recovery of the crystalline solid. Removal of the mother liquor afforded the dibromide **123** as a colorless crystalline solid (27.5 g, 113 mmol, 91% yield). The spectral data matches that of the reported compound (Farkas, F.; Wellauer, T.; Esser, T.; and Sequin, U. *Helvetica Chimica Acta* **1991**, 74, 1511).

¹H-NMR (400 MHz, CDCl₃): δ 4.00 (s, 4H), 1.88 (s, 6H)

¹³C-NMR (100MHz, CDCl₃): δ 131.90, 35.00, 17.20

M.P.: 45 – 46 °C



A solution of diisopropylamine (12.9 g, 17.8 mL, 127 mmol, 2.05 eq.) in THF (300 mL) was placed in a bath cooled to $-78\text{ }^{\circ}\text{C}$ for 30 minutes. *n*-Butyllithium (55.7 mL, 2.28 M in hexanes, 127 mmol, 2.05 eq.) was added dropwise over 5 minutes. After 5 minutes the colorless solution was placed in an ice water bath cooled to $0\text{ }^{\circ}\text{C}$ for 20 minutes, and placed back into the bath cooled to $-78\text{ }^{\circ}\text{C}$ for 30 minutes. A solution of *N,N*-dimethylacetamide (11.1 g, 11.8 mL, 127 mmol, 2.05 eq.) in THF (100 mL) was placed in a bath cooled to $-78\text{ }^{\circ}\text{C}$ for 30 minutes and then added to the pale yellow solution of freshly prepared LDA by cannula over 1 hr. The residual *N,N*-dimethylacetamide in the reaction vessel was dissolved THF (10 mL) and transferred via cannula to the solution of LDA. This was repeated once more and the pale yellow solution was stirred for 30 minutes to provide a freshly prepared solution of lithium dimethyl acetamide.

A pale yellow solution of the dibromide **123** (15.0 g, 62.0 mmol, 1.00 eq.) in THF (270 mL) was placed in a bath cooled to $-78\text{ }^{\circ}\text{C}$ for 30 minutes and then added to the solution of lithium dimethyl acetamide dropwise under nitrogen via cannula over 90 minutes. Residual dibromide was dissolved in THF (10 mL) and transferred via cannula to the reaction solution. This process was repeated once more. After 20 minutes the excess enolate was quenched with brine (200 mL), the reaction vessel was quickly removed from the cooling bath, and the white mixture was allowed to stir vigorously (1000 rpm) at $23\text{ }^{\circ}\text{C}$ for 1 hr. EtOAc (500 mL) was added to the biphasic mixture which was poured into a separatory funnel, partitioned, and the residual organics were extracted from the aqueous layer using EtOAc (4 x 100 mL). (**Note:** The product is soluble in water, so brine (50 mL) is added during each extraction). The combined organic extracts were washed with brine (2 x 50 mL), dried over solid Na₂SO₄, decanted, and concentrated. Recrystallization of the yellow solid from hexane-ethyl ether (3:2, 50 mL) afforded the diamide **181** as colorless crystalline solid (14.4 g, 56.5 mmol, 91%).

$R_f = 0.35$ (5% MeOH in CH₂Cl₂)

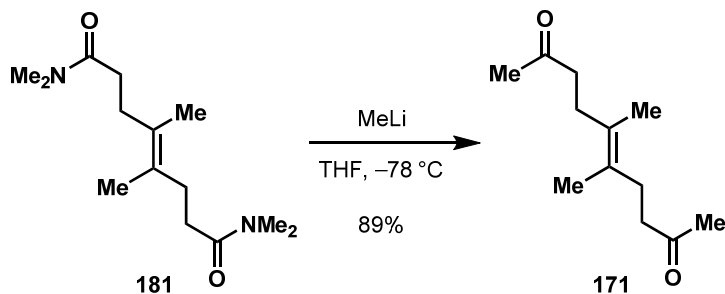
¹H-NMR (400 MHz, CDCl₃): δ 3.00 (s, 6H), 2.94 (s, 6H), 2.33 (s, 8H), 1.67 (s, 6H)

¹³C-NMR (100 MHz, CDCl₃): δ 173.06, 128.36, 37.48, 35.55, 31.98, 30.44, 18.11

IR (neat film, cm⁻¹): 3479, 2929, 1637, 1398

HRMS (EC-CI): calcd. for $C_{14}H_{27}N_2O_2$ $[M+H]^+$ 255.2073, found 255.2074.

M.P.: 69 – 71 °C.



A solution of diamide **181** (8.5 g, 33.4 mmol, 1.00 eq.) in deoxygenated THF (334 mL) was placed into a bath cooled to $-78\text{ }^\circ\text{C}$ for 1 hour upon which the clear colorless solution became a white heterogeneous mixture. While stirring vigorously (700 rpm) methyl lithium (50.0 mL, 73.5 mmol, 1.47 M in ethyl ether, 2.20 eq.) was added dropwise over 15 minutes. 5 minutes after the complete addition of methyl lithium the heterogeneous mixture had changed to a yellow homogeneous solution. After 15 minutes the yellow solution had changed to a white heterogeneous mixture upon which excess methyl lithium was quenched with an aqueous phosphate buffer (100 mL, pH = 7, 0.2 M). The reaction vessel was removed from the cooling bath and allowed to warm to $23\text{ }^\circ\text{C}$ over 30 minutes. The biphasic mixture was poured into a separatory funnel, partitioned, and the organics were extracted from the aqueous layer with ethyl ether (3 x 50 mL). Combined organics were washed with brine (1 x 50 mL), dried over solid Na_2SO_4 , decanted, and concentrated under vacuum. The resulting yellow solid was purified by silica gel chromatography; 10 → 30% EtOAc in hexane to afford **171** as a white crystalline solid (5.9 g, 29.9 mmol, 89%). Crystals suitable for X-ray diffraction were grown from hexane by slow cold evaporation under a stream of nitrogen.

$R_f = 0.43$ (30% EtOAc in hexane)

$^1\text{H-NMR}$ (400 MHz, CDCl_3): δ 2.49 (dd, 4H, $J = 7.2, 8.6$ Hz), 2.26 (dd, 4H, $J = 7.2, 8.6$ Hz), 2.14 (s, 6H), 1.62 (s, 6H)

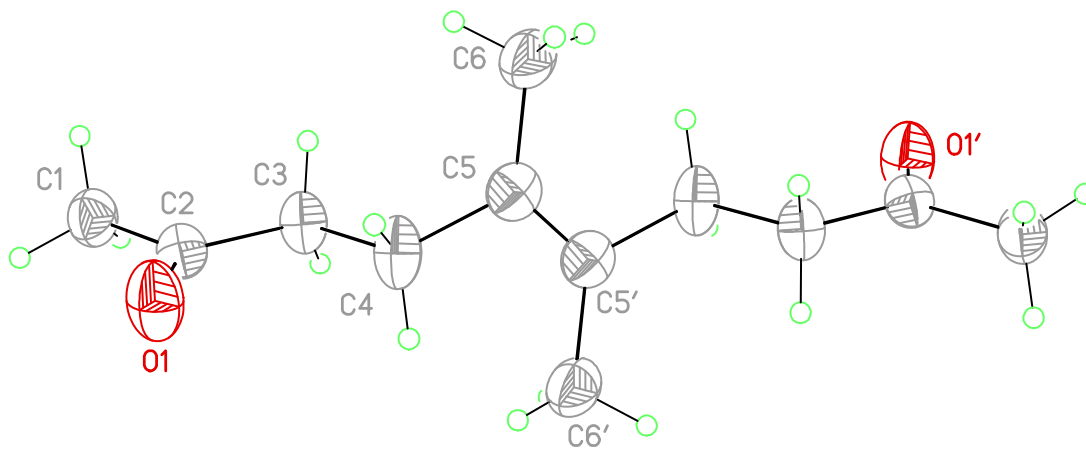
$^{13}\text{C-NMR}$ (100 MHz, CDCl_3): δ 208.96, 127.92, 42.19, 30.04, 28.94, 17.93

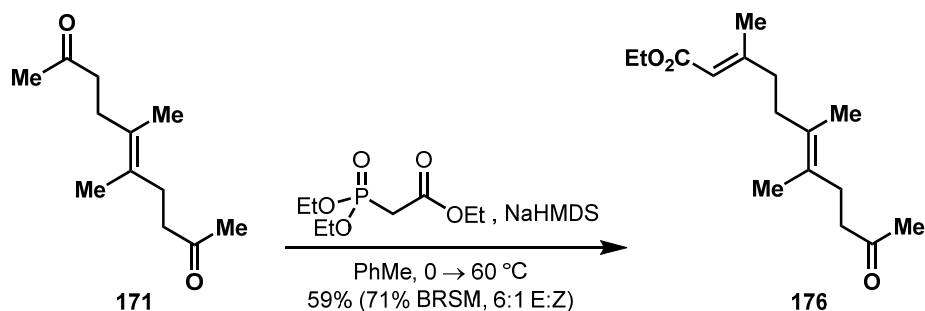
IR (neat film, cm^{-1}) 2360, 2340, 1708, 1364

HRMS (EC-CI): calcd. for $C_{12}H_{21}O_2$ $[M+H]^+$ 197.1542, found 197.1544.

M.P.: 55 – 57 °C

Crystal Structure of Diketone 171:





A solution of triethylacetophosphonate (5.6 g, 5.0 mL, 25 mmol, 1.35 eq.) in toluene (90 mL) was cooled to 0 °C in an ice bath. After stirring for 20 minutes NaHMDS (12.5 mL, 2.0 M in THF, 25 mmol, 1.35 eq.) was added dropwise over 3 minutes. After 30 minutes a solution of the diketone **171** (3.63 g, 18.5 mmol, 1.0 eq.) in toluene (74 mL) was cooled to 0 °C in an ice bath, stirred for 20 minutes, and to this clear solution was transferred the phosphonate via cannula over 15 minutes. Remaining phosphonate in the vessel was dissolved in toluene (7.0 mL) and transferred via cannula to the reaction solution. This process was repeated twice more. The golden-yellow solution was allowed to gradually warm to 23 °C over 60 minutes, stirred vigorously (1000 rpm) for 60 minutes at 23 °C, and the golden yellow solution was placed in an oil bath heated to 60 °C. After 22 hours the heterogeneous golden-orange mixture was removed from the oil bath and excess phosphonate was quenched with an aqueous phosphate buffer (10 mL, pH = 7, 0.2 M). The biphasic mixture was stirred vigorously (1000 rpm) for 10 minutes followed by which solid Na₂SO₄ was added and stirred for 10 minutes. The solid Na₂SO₄ was suction filtered over a pad of solid Na₂SO₄ and the golden-yellow filtrate solution was concentrated under vacuum. The resulting brown oil was purified by silica gel chromatography; hexane \rightarrow 20% Et₂O in hexane to afford the enoate **176** as a clear yellow oil as a 6:1 mixture of *trans* : *cis* isomers (2.9 g, 10.9 mmol, 59%). Further elution with 20% EtOAc in hexane affords the starting diketone **171** (0.4 g, 2.2 mmol, 12%).

Mixture of Isomers: (*) denotes *cis* isomer

R_f = 0.21 (15% EtOAc in hexane)

¹H-NMR (400 MHz, CDCl₃): δ 5.63 (s, 1H), 4.13 (q, 2H, *J* = 2.4 Hz), 4.12* (q, 2H, *J* = 2.4 Hz), 2.44 (dd, 2H, *J* = 7.5, 8.6 Hz), 2.27 (dd, 2H, *J* = 7.2, 8.6 Hz), 2.16* (d, 3H, *J* = 1.4 Hz), 2.14 (s, 2H), 2.13 (s, 4H), 1.88* (d, 3H, *J* = 1.4 Hz), 1.68* (s, 3H), 1.66* (s, 3H), 1.63 (s, 3H), 1.60 (s, 3H), 1.26 (t, 3H, *J* = 7.0 Hz), 1.25 (t, 3H, *J* = 7.0 Hz)

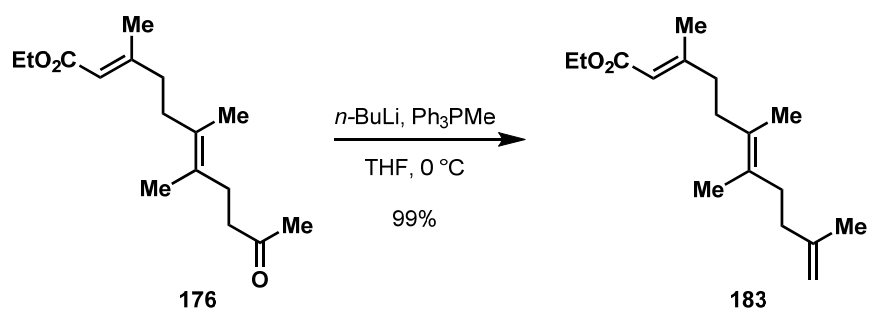
¹H-NMR (400 MHz, C₆D₆): δ 5.77 (s, 1H), 5.71* (s, 1H), 4.02 (q, 2H, *J* = 7.0 Hz), 3.90* (q, 2H, *J* = 7.1 Hz), 2.22* (s, 2H), 2.20* (s, 3H), 2.18 (s, 3H), 2.01 (dd, 2H, *J* = 7.2, 8.6

Hz), 1.96 – 1.84 (m, 4H), 1.69* (s, 3H), 1.64* (s, 3H), 1.63 (s, 3H), 1.51* (s, 3H), 1.43 (s, 3H), 1.39 (s, 3H), 0.98 (t, 3H, $J = 6.9$ Hz)

$^{13}\text{C-NMR}$ (100 MHz, CDCl_3): δ 208.95, 166.90 (166.37*), (160.23*) 159.60, (129.01*) 128.29, 127.98 (127.59*), (116.30*) 115.78, 59.59, 42.28, 39.45, (33.49*) 33.07, (32.13*) 30.06, (29.05*) 28.97, (25.56*), 19.05, 18.17 (18.13*), 17.98, 14.51

IR (neat film, cm^{-1}): 2980, 2930, 1717, 1647, 1446, 1366, 1224, 1145

HRMS (EC-Cl): calcd. for $\text{C}_{16}\text{H}_{27}\text{O}_3$ $[\text{M}+\text{H}]^+$ 267.1960, found 267.1961.



A white suspension of methyl triphenylphosphonium bromide (18.1 g, 50.7 mmol, 1.25 eq.) in THF (205 mL) was placed in an ice water bath cooled to 0 °C and stirred vigorously (600 rpm) for 20 minutes. *n*-butyllithium (22.3 mL, 2.07 M in hexane, 46.2 mmol, 1.14 eq.) was added dropwise over 5 minutes and the resulting orange heterogeneous mixture was stirred for 30 minutes. The cooling bath was removed and the mixture was stirred for 10 minutes at 23 °C, and placed back into the ice water bath. After 10 minutes a solution of **176** (10.8 g, 40.5 mmol, 1.00 eq.) in THF (170 mL) was added dropwise via cannula over 15 minutes. Residual enoate **176** was dissolved THF (10 mL) and transferred via cannula to the now pale yellow reaction mixture. This process was repeated twice more. After 45 minutes excess ylide was quenched with an aqueous phosphate buffer (3 mL, pH = 7, 0.2 M) followed by the addition of pentane (100 mL). The biphasic mixture was stirred vigorously (600 rpm) for 10 minutes followed by which solid Na₂SO₄ was added. Vigorous stirring was continued for 10 minutes, and the solid Na₂SO₄, residual methyl triphenylphosphonium bromide, and triphenylphosphonium oxide were suction filtered over a pad of celite using pentane as the eluent. The resulting yellow solution was concentrated under vacuum to approximately 20 mL. Residual triphenylphosphonium oxide was triturated with pentane (100 mL). The resulting yellow mixture was suction filtered over a pad of celite using pentane and concentrated. The crude yellow oil was purified by silica gel chromatography; hexane → 2% EtOAc in hexane to afford the triene **183** as a clear yellow oil as a mixture of *trans* : *cis* isomers (10.7 g, 40.1 mmol, 99%). The isomers were then separated by silica gel chromatography; benzene.

***Trans* Isomer 183:**

R_f = 0.49 (15% EtOAc in hexane) and 0.45 (benzene):

¹H-NMR (400 MHz, CDCl₃): δ 5.66 (s, 1H), 4.69 (s, 1H), 4.67 (s, 1H), 4.15 (q, 2H, *J* = 7.2 Hz), 2.18 (d, 3H, *J* = 1.1 Hz), 2.16 (s, 4H), 2.14 – 2.11 (m, 2H), 2.04 – 2.00 (m, 2H), 1.74 (s, 3H), 1.64 (s, 6H), 1.27 (t, 3H, *J* = 7.2 Hz)

¹H-NMR (400 MHz, C₆D₆): δ 5.79 (s, 1H), 4.77 (s, 2H), 4.01 (q, 2H, *J* = 7.2 Hz), 2.20 (d, 3H, *J* = 1.0 Hz), 2.11 – 2.07 (m, 2H), 2.01 (m, 4H), 1.93 – 1.89 (m, 2H), 1.64 (s, 3H), 1.48 (s, 6H), 0.98 (t, 3H, *J* = 7.2 Hz)

¹³C-NMR (100 MHz, CDCl₃): δ 167.08, 160.30, 146.36, 129.44, 127.37, 115.74, 109.83, 59.65, 39.67, 36.44, 33.44, 33.19, 22.74, 19.13, 18.24, 18.18, 14.55

IR (neat film, cm⁻¹): 2979, 2934, 2867, 1717, 1649, 1446, 1373, 1223, 1144

HRMS (EC-CI): calcd. for C₁₇H₂₈O₂ [M+H]⁺ 264.2089, found 264.2089.

***Cis* Isomer 184:**

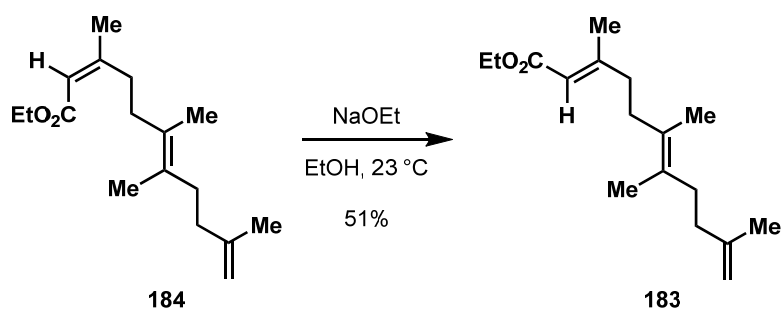
R_f = 0.49 (15% EtOAc in hexane) and 0.51 (benzene)

¹H-NMR (400 MHz, CDCl₃): δ 5.64 (s, 1H), 4.69 (s, 1H), 4.68 (s, 1H), 4.14 (q, 2H, *J* = 7.2 Hz), 2.64 (dd, 2H, *J* = 7.9, 8.6 Hz), 2.16 (m, 4H), 2.04 – 2.00 (m, 2H), 1.90 (s, 3H), 1.74 (s, 3H), 1.70 (s, 3H), 1.69 (s, 3H), 1.27 (t, 3H, *J* = 7.2 Hz)

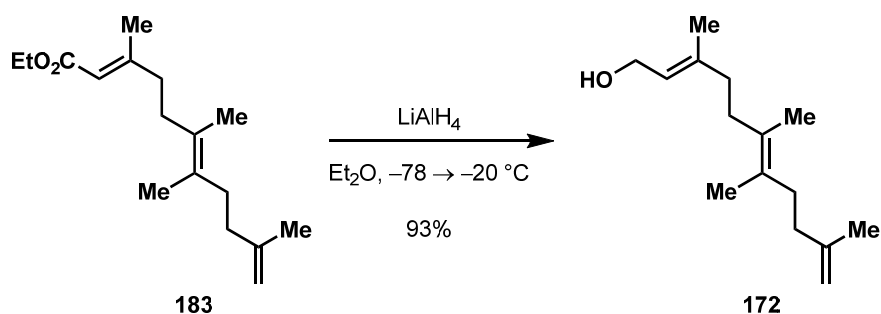
¹H-NMR (400 MHz, C₆D₆): δ 5.72 (s, 1H), 4.78 (s, 1H), 4.77 (s, 1H), 4.00 (q, 2H, *J* = 7.2 Hz), 2.77 (dd, 2H, *J* = 7.9, 8.6 Hz), 2.23 (d, 1H, *J* = 8.2 Hz), 2.21 (d, 1H, *J* = 8.2 Hz), 2.18 – 2.13 (m, 2H), 2.05 – 2.00 (m, 2H), 1.74 (s, 3H), 1.73 (s, 3H), 1.64 (s, 3H), 1.53 (d, 3H, *J* = 1.4 Hz), 0.96 (t, 3H, *J* = 7.2 Hz)

IR (neat film, cm⁻¹) 2979, 2934, 2867, 1717, 1649, 1446, 1373, 1223, 1144

HRMS (EC-CI): calcd. for C₁₇H₂₈O₂ [M+H]⁺ 264.2089, found 264.2089.



To a clear colorless solution of freshly prepared sodium ethoxide (prepared from sodium metal (1.65 g, 72.2 mmol, 10.0 eq.) and anhydrous ethanol (52 mL)) was added the *cis*-isomer **184** (1.91 g, 7.22 mmol, 1.0 eq.) as a solution in ethanol (20 mL) via cannula. After 24 hours the solution had changed to a golden orange color and excess sodium ethoxide was quenched with an aqueous phosphate buffer (100 mL, pH = 7, 0.2 M). The ethanol was removed via rotary evaporation, and the resultant yellow mixture was diluted with ethyl ether (100 mL) and water (50 mL), poured into a separatory funnel, partitioned, and the organics were washed with water (1 x 50 mL). Residual organics were back extracted from the aqueous layer with ethyl ether (2 x 50 mL), washed with brine (1 x 25 mL), dried over sodium sulfate, decanted, concentrated and the resulting golden yellow oil was purified via silica gel chromatography; benzene to afford triene **183** (0.97 g, 3.68 mmol, 51%) as a clear golden yellow oil and the starting *cis*-isomer **184** (0.92 g, 3.47 mmol, 48%) as a clear golden yellow oil.



A yellow solution of the triene **183** (9.18 g, 34.7 mmol, 1.00 eq.) in ethyl ether (346 mL) was cooled to $-78\text{ }^\circ\text{C}$ and allowed to stir for 60 minutes. Lithium Aluminum Hydride (17.3 mL, 4 M in ethyl ether, 69.4 mmol, 2.00 eq.) was added dropwise over 5 minutes. The yellow solution was allowed to warm to $-20\text{ }^\circ\text{C}$ over 5 hours upon which the slightly white heterogeneous mixture was diluted with 300 mL of ethyl ether and excess lithium aluminum hydride was quenched by the sequential dropwise addition of water (5 mL), aqueous 15% NaOH solution (5 mL), and water (10 mL). The mixture was placed in an ice water bath cooled to $0\text{ }^\circ\text{C}$, stirred for 5 minutes, and an aqueous phosphate buffer (10 mL, pH = 7, 0.2 M) was added to the white heterogeneous mixture. The mixture was stirred vigorously (900 rpm) for 15 minutes and the cold bath was removed. Solid Na_2SO_4 was added and the heterogeneous mixture was stirred vigorously (1000 rpm) for 5 minutes, suction filtered over a pad of solid Na_2SO_4 , and concentrated to reveal the alcohol **172** as a clear colorless oil (7.16 g, 32.2 mmol, 93%) which is submitted into the next reaction without further purification. An analytical sample was attained by purification via silica gel chromatography; 10% dioxane in hexane.

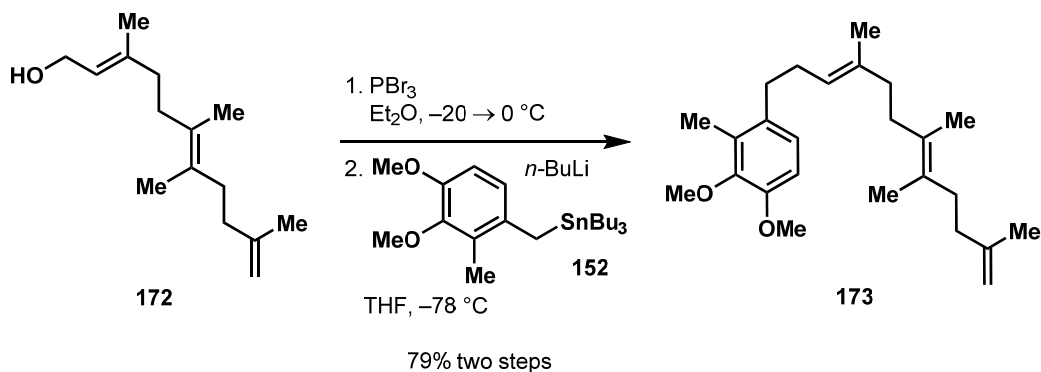
$R_f = 0.56$ (25% dioxane in hexane)

$^1\text{H-NMR}$ (400 MHz, CDCl_3): δ 5.41 (dt, 1H, $J = 7.2, 6.6$ Hz), 4.68 (s, 1H), 4.67 (s, 1H), 4.14 (d, 2H, $J = 6.6$ Hz), 2.14 – 2.09 (m, 4H), 2.05 – 1.99 (m, 4H), 1.73 (s, 3H), 1.69 (s, 3H), 1.64 (s, 6H)

$^{13}\text{C-NMR}$ (100 MHz, CDCl_3): δ 146.3, 140.2, 128.4, 128.0, 123.1, 109.5, 59.4, 38.0, 36.3, 33.3, 33.2, 22.5, 18.01, 17.98, 16.37

IR (neat film, cm^{-1}): 3325, 2930, 2863, 1652, 1648, 1456, 1373, 1002, 885

HRMS (EC-CI): calcd. for $\text{C}_{15}\text{H}_{28}\text{O}$ $[\text{M}+2\text{H}]^{2+}$ 224.2140, found 224.2140.



A solution of the alcohol **172** (6.95 g, 31.3 mmol, 1.00 eq.) in ethyl ether (104 mL) was placed in a bath cooled to $-20\text{ }^{\circ}\text{C}$ and stirred for 20 minutes. PBr_3 (1.65 mL, 16.4 mmol, 0.51 eq.) was added dropwise over 2 minutes and the resulting pale yellow solution was stirred for 2 hours gradually warming to $0\text{ }^{\circ}\text{C}$. The solution was diluted with hexane (100 mL) and then the HBr was slowly neutralized with a saturated aqueous mixture of NaHCO_3 (20 mL). The biphasic mixture was poured into a separatory funnel and partitioned. (NOTE: The separatory funnel was swirled, not shaken, to avoid emulsion. If emulsion occurs, wash with copious amounts of water). The organic layer was washed with water (3 x 50 mL), and the residual organics were extracted from the aqueous layer using hexane (2 x 50 mL). The combined organics were washed with brine (2 x 30 mL), dried over solid Na_2SO_4 , decanted, and concentrated under vacuum. The resulting clear pale yellow oil (8.90 g, 31.2 mmol, 100%) was used directly in the next reaction without further purification.

A solution of stannane **152** (13.0 g, 28.6 mmol, 1.20 eq.) in deoxygenated THF (177 mL) was placed in a bath cooled to $-78\text{ }^{\circ}\text{C}$ and stirred for 1 hour. *n*-Butyllithium (14.6 mL, 1.96 M in hexane, 28.6 mmol, 1.20 eq.) was added dropwise over 15 minutes and the color of the resulting solution changed to golden orange. After stirring for 30 minutes, a solution of the triene allylic bromide (6.8 g, 23.9 mmol, 1.00 eq.) in deoxygenated THF (40 mL) was added dropwise over 1 hour to the golden orange solution. Residual bromide was dissolved in deoxygenated THF (10 mL) and transferred to the now golden yellow reaction solution. This process was repeated once more. After stirring for 1 hour the excess benzyl anion was quenched with water (200 mL) and allowed to warm to room temperature while stirring for 30 minutes. The biphasic solution was poured into a separatory funnel containing water (200 mL) and hexane (300 mL). (NOTE: If emulsion occurs, add copious amounts of water and swirl the mixture, do not shake). The organics were washed with water (2 x 100 mL). Residual organics were extracted from the aqueous layer using hexane (2 x 100 mL), washed with brine (1 x 100 mL), dried over solid Na_2SO_4 , decanted, and concentrated under vacuum. The resulting clear colorless oil was purified by silica gel chromatography; hexane (1 L) and then 2% benzene in toluene. Impure product is purified again by silica gel

chromatography; 2% benzene in toluene to afford the triene **173** as a clear colorless oil (7.0 g, 19.0 mmol, 79%).

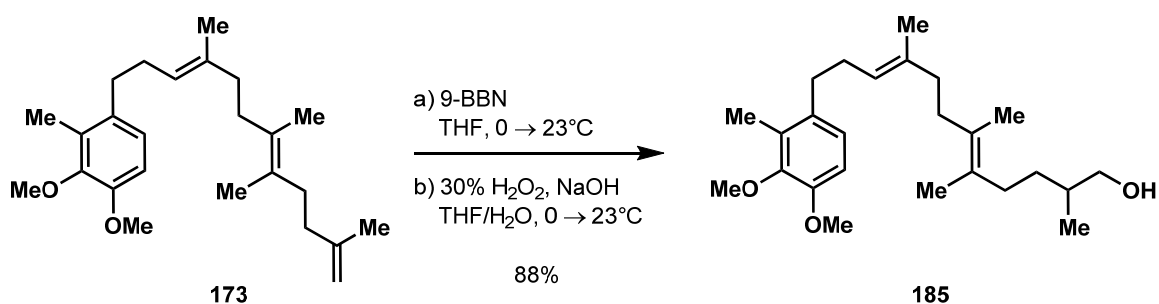
R_f = 0.36 (2% benzene in toluene)

$^1\text{H-NMR}$ (400 MHz, CDCl_3): δ 6.85 (d, 1H, J = 8.2 Hz), 6.70 (d, 1H, J = 8.2), 5.20 (dd, 1H, J = 7.2, 6.5 Hz), 4.69 (s, 1H), 4.68 (s, 1H), 3.84 (s, 3H), 3.79 (s, 3H), 2.55 (dd, 2H, J = 7.5, 5.8 Hz), 2.24 (s, 3H), 2.24 – 2.18 (m, 2H), 2.15 – 2.07 (m, 4H), 2.05 – 1.97 (m, 4H), 1.75 (s, 3H), 1.65 (s, 6H), 1.59 (s, 3H)

$^{13}\text{C-NMR}$ (100 MHz, CDCl_3): δ 151.02, 147.47, 146.62, 136.24, 134.13, 130.47, 128.62, 128.34, 124.29, 123.80, 109.76, 109.52, 60.42, 55.92, 38.41, 36.57, 33.89, 33.52, 33.50, 29.33, 22.83, 18.31, 18.25, 16.32, 11.97

IR (neat film, cm^{-1}): 1490, 1453, 1271, 1086

HRMS (EC-Cl): calcd. for $\text{C}_{25}\text{H}_{38}\text{O}_2$ [M] 370.2872, found 370.2871.



A solution of the triene **173** (7.0 g, 18.9 mmol, 1.00 eq.) in THF (73 mL) was placed in an ice water bath cooled to 0 $^{\circ}$ C and stirred vigorously (500 rpm) for 20 minutes. Crystalline 9-BBN dimer (2.4 g, 9.8 mmol, 0.52 eq.) was added under a stream of nitrogen and the heterogeneous mixture was stirred (500 rpm) for 4 hours upon which the cooling bath had warmed to 23 $^{\circ}$ C. The clear solution was placed in an ice bath cooled to 0 $^{\circ}$ C and stirred for 20 minutes. Excess 9-BBN was quenched with water (31 mL) followed by the addition of an aqueous solution of H₂O₂ (30% w/v in water, 9.7 mL, 94.0 mmol, 5.00 eq.) and NaOH (4 N, 23.6 mL, 94.0 mmol, 5.00 eq.). The biphasic mixture was stirred vigorously (800 rpm) and allowed to gradually warm to 23 $^{\circ}$ C. After 60 hours, excess H₂O₂ was quenched with a saturated aqueous mixture of Na₂S₂O₃ (100 mL). After stirring for 10 minutes excess hydroxide was quenched with an aqueous phosphate buffer (50 mL, pH = 7, 0.2 M). The biphasic mixture was poured into a separatory funnel, partitioned, and residual organics were extracted from the aqueous layer using ethyl acetate (4 x 50 mL). The combined organics were washed with brine (1 x 100 mL), dried over Na₂SO₄, decanted, and concentrated under vacuum. The resulting clear colorless oil was purified by silica gel chromatography; 1 \rightarrow 12% EtOAc in hexane to afford the alcohol **185** as a clear colorless oil (6.48 g, 16.6 mmol, 88%) and the starting triene **173** as a clear colorless oil (0.70 g, 1.9 mmol, 10%).

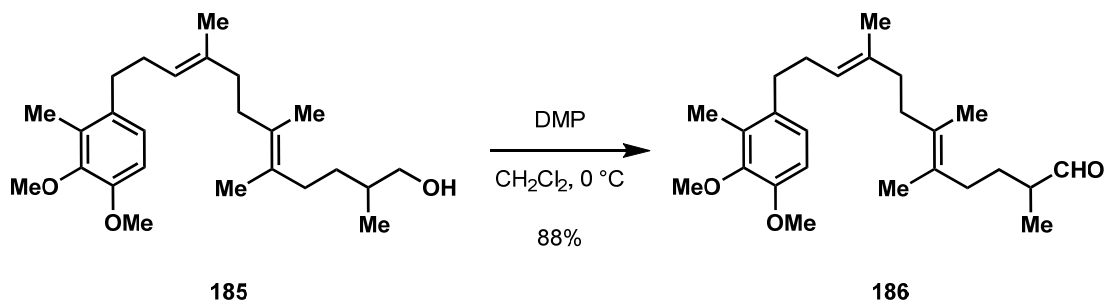
R_f = 0.50 (50% EtOAc in hexane):

¹H-NMR (400 MHz, CDCl₃): δ 6.85 (d, 1H, J = 8.2 Hz), 6.70 (d, 1H, J = 8.2), 5.20 (dd, 1H, J = 7.2, 6.8 Hz), 3.83 (s, 3H), 3.78 (s, 3H), 3.52 (dd, 1H, J = 5.8 Hz), 3.43 (dd, 1H, J = 6.5, 6.8 Hz), 2.55 (dd, 2H, J = 7.5, 5.8 Hz), 2.24 (s, 3H), 2.24 – 2.18 (m, 2H), 2.10 – 1.94 (m, 6H), 1.64 (s, 6H), 1.59 (s, 3H), 1.51 (m, 2H), 1.31 (bs, 1H), 1.19 – 1.09 (m, 1H), 0.95 (d, 3H, J = 6.5 Hz)

¹³C-NMR (100 MHz, CDCl₃): δ 150.78, 147.29, 136.00, 133.91, 130.21, 128.38, 128.10, 124.04, 123.55, 109.38, 68.35, 60.16, 55.71, 38.15, 35.88, 36.65, 33.23, 32.04, 31.55, 29.07, 18.06, 17.96, 16.60, 16.05, 11.70

IR (neat film, cm⁻¹): 3391, 1490, 1453, 1270, 1085

HRMS (EC-CI): calcd. for C₂₅H₄₀O₃ [M] 388.2977, found 388.2978.



A solution of the alcohol (6.48 g, 16.8 mmol, 1.00 eq.) in methylene chloride (162 mL) was placed in an ice bath cooled to 0 °C. After 20 minutes, solid NaHCO₃ (5.45 g, 64.9 mmol, 4.00 eq.), Dess-Martin periodinane (14.1 g, 33.6 mmol, 2.00 eq.), and water (2 drops) were added sequentially and the mixture was stirred vigorously (700 rpm). After 80 minutes residual acetic acid was neutralized with a saturated aqueous mixture of NaHCO₃ (100 mL) and excess Dess-Martin periodinane was quenched with a saturated aqueous mixture of Na₂S₂O₃ (200 mL). The biphasic mixture was removed from the cooling bath, stirred vigorously (1000 rpm) for 60 minutes at 23 °C, poured into a separatory funnel, and partitioned. The organic layer was washed with a saturated mixture of Na₂S₂O₃ and NaHCO₃ (2 x 50 mL, 1:1). Residual organics were extracted from the aqueous layer using methylene chloride (3 x 50 mL). The combined organics were washed with brine (1 x 25 mL), dried over solid Na₂SO₄, filtered, and concentrated under vacuum. The resulting clear pale yellow oil was purified by silica gel chromatography; hexane → 5% EtOAc in hexane to afford the aldehyde **186** as a clear colorless oil (5.73 g, 14.8 mmol, 88%).

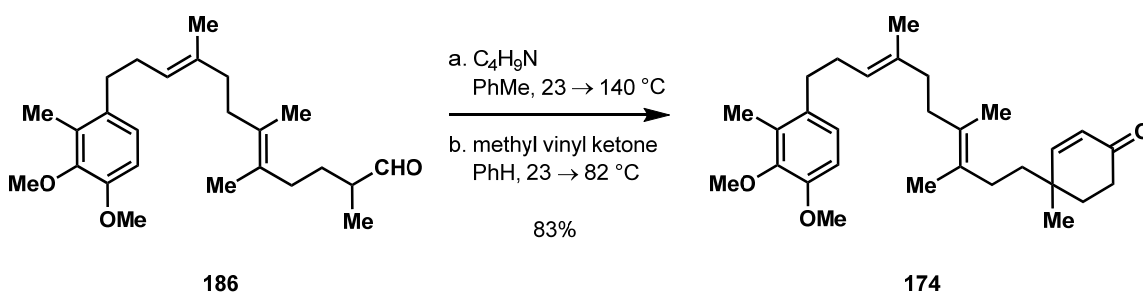
R_f = 0.65 (50% EtOAc in hexane):

¹H-NMR (400 MHz, CDCl₃): δ 9.62 (d, 1H, *J* = 2.1 Hz), 6.85 (d, 1H, *J* = 8.2 Hz), 6.70 (d, 1H, *J* = 8.2), 5.20 (dd, 1H, *J* = 7.2, 6.8 Hz), 3.84 (s, 3H), 3.78 (s, 3H), 2.55 (dd, 2H, *J* = 7.9, 5.8 Hz), 2.31 (ddd, 1H, *J* = 1.7 Hz), 2.23 (s, 3H), 2.24 – 2.18 (m, 2H), 2.10 – 1.96 (m, 6H), 1.78 (m, 1H), 1.64 (s, 6H), 1.59 (s, 3H), 1.40 (m, 1H), 1.11 (d, 3H, *J* = 7.2 Hz)

¹³C-NMR (100 MHz, CDCl₃): δ 205.26, 151.02, 147.47, 136.10, 134.05, 130.42, 129.49, 127.56, 124.29, 123.88, 109.54, 60.38, 55.89, 46.37, 38.30, 33.86, 33.47, 32.12, 29.32, 29.17, 18.42, 18.14, 16.28, 13.72, 11.96

IR (neat film, cm⁻¹): 1724, 1490, 1454, 1271, 1085

HRMS (EC-CI): calcd. for C₂₅H₃₈O₃ [M] 386.2821, found 386.2822.



To a solution of the aldehyde **186** (5.73 g, 14.8 mmol, 1.00 eq.) in toluene (100 mL) in a reaction vessel equipped with a Dean-Stark trap was added pyrrolidine (15.2 mL, 185.0 mmol, 12.50 eq.). The yellow solution was stirred for 8 hours at 23 °C and then placed in an oil bath heated to 140 °C for 24 hours. The golden-yellow solution was removed from the oil bath, cooled to 23 °C, and concentrated under vacuum to remove excess pyrrolidine. The viscous orange oil was dissolved in toluene (100 mL) and then methyl vinyl ketone (2.4 mL, 29.6 mmol, 2.00 eq.) was added. The orange solution was stirred at 23 °C for 24 hours and then placed in an oil bath heated to 82 °C. After 48 hours, a solution of sodium acetate (4.0 g) and acetic acid (6.1 mL) in water (6.1 mL) was added to the dark red solution. The biphasic mixture was placed in an oil bath heated to 82 °C and stirred vigorously (700 rpm) for 6 hours. The reaction vessel was removed from the oil bath, cooled to 23 °C, and diluted with an aqueous phosphate buffer (50 mL, pH = 4, 0.2 M) and ethyl acetate (50 mL). The biphasic mixture was poured into a separatory funnel and partitioned. The organic layer was washed with an aqueous phosphate buffer (50 mL, pH = 4, 0.2 M) and then residual organics were extracted from the aqueous layer using ethyl acetate (3 x 50 mL). The combined organics were washed with brine (1 x 100 mL), dried over solid Na₂SO₄, decanted, and concentrated under vacuum. The resulting viscous red-brown oil was purified by silica gel chromatography; hexane → 10% EtOAc in hexane to afford the cyclohexenone **174** as a viscous clear amber oil (5.41 g, 12.3 mmol, 83%).

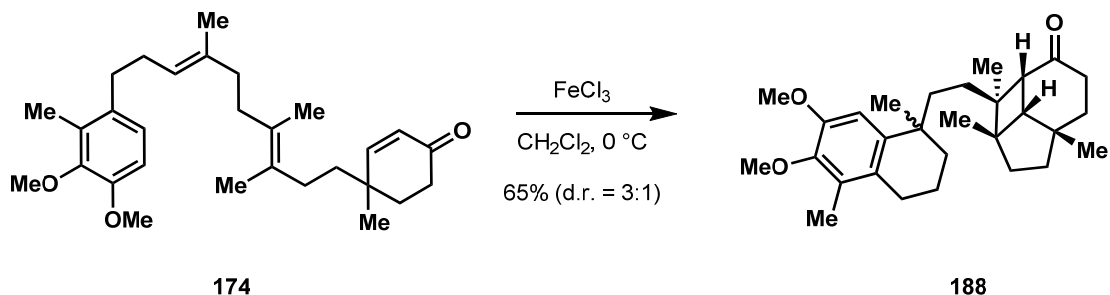
R_f = 0.37 (30% EtOAc in hexane)

¹H-NMR (400 MHz, CDCl₃): δ 6.85 (d, 1H, *J* = 8.2 Hz), 6.70 (d, 1H, *J* = 7.9 Hz), 6.69 (d, 1H, *J* = 11.6 Hz), 5.90 (d, 1H, *J* = 10.3 Hz), 5.19 (t, 1H, *J* = 6.8 Hz), 3.83 (s, 3H), 3.78 (s, 3H), 2.55 (dd, 2H, *J* = 7.5, 5.8 Hz), 2.47 (dd, 1H, *J* = 2.4, 3.4 Hz), 2.45 (d, 1H, *J* = 6.2 Hz), 2.23 (s, 3H), 2.24 – 2.17 (m, 2H), 2.10 – 1.96 (m, 8H), 1.80 – 1.76 (m, 1H), 1.633 (s, 3H), 1.628 (s, 3H), 1.58 (s, 3H), 1.47 (m, 1H), 1.16 (s, 3H)

¹³C-NMR (100 MHz, CDCl₃): δ 199.97, 159.51, 151.02, 147.47, 136.11, 134.07, 130.44, 128.84, 127.95, 127.60, 124.27, 123.87, 109.53, 60.42, 55.92, 39.29, 38.32, 35.88, 34.40, 33.83, 33.56, 33.47, 29.55, 29.33, 24.96, 18.37, 18.25, 16.31, 11.97

IR (neat film, cm^{-1}): 1683, 1490, 1454, 1271, 1084

HRMS (ESI): calcd. for $\text{C}_{29}\text{H}_{42}\text{O}_3$ $[\text{M}+\text{Na}]^+$ 461.3026, found 461.3027.



Anhydrous ferric chloride (1.12 g, 6.90 mmol, 3.00 eq.) was crushed under vacuum by stirring the solid vigorously (600 rpm) for 30 minutes. Deoxygenated CH_2Cl_2 (550 mL) was added and the suspension was vigorously stirred (600 rpm) at 23 °C for 20 minutes. Stirring was stopped and the residual powder was allowed to settle on the bottom of the reaction vessel and the yellow-green liquid was decanted by cannulation under nitrogen to a separate flask. The solubility of ferric chloride in deoxygenated CH_2Cl_2 was measured to be 1.1 mg / mL.

A solution of the enone **174** (1.00 g, 2.28 mmol, 1.00 eq.) in deoxygenated CH_2Cl_2 (2.3 L) was placed in an ice water bath cooled to 0 °C and stirred for 1 hour. The solution of FeCl_3 in CH_2Cl_2 was added dropwise over 70 minutes. The resulting yellow-orange solution was allowed to stir for 8 hours at 0 °C and then diluted with an aqueous phosphate buffer (400 mL, pH = 4, 0.2 M). The biphasic mixture was stirred vigorously (1000 rpm) for 60 minutes, poured into a separatory funnel, and the organic layer was removed. Residual organics were extracted from the aqueous layer using methylene chloride (3 x 100 mL). The combined organics were washed with brine, dried over solid Na_2SO_4 , decanted, and concentrated. The resulting brown oil was purified by silica gel chromatography; hexane \rightarrow 2% acetone in hexane to afford the ketone **188** as a colorless viscous foam (0.65 g, 1.50 mmol, 65%, d.r. = 3:1). The diastereomers were separated by silica gel chromatography several times; 3% 1,4-dioxane in hexane.

Major Diastereomer:

R_f = 0.43 (30% EtOAc in hexane) and 0.58 (10% 1,4-dioxane in hexane)

$^1\text{H-NMR}$ (400 MHz, CDCl_3): δ 6.70 (s, 1H), 3.77 (s, 3H), 3.75 (s, 3H), 2.59 – 2.41 (m, 2H), 2.32 (dd, 2H, J = 9.2, 9.6 Hz), 2.23 (dt, 2H, J = 4.5, 4.8 Hz), 2.13 (s, 3H), 2.03 (d, 1H, J = 10.2 Hz), 1.89 – 1.70 (m, 8H), 1.53 – 1.35 (m, 5H), 1.26 (s, 3H), 1.06 (s, 3H), 1.02 (s, 3H), 0.83 (s, 3H)

¹³C-NMR (100 MHz, CDCl₃): δ 213.86, 150.24, 144.83, 140.17, 129.51, 128.77, 107.95, 60.25, 55.65, 52.74, 50.84, 49.05, 44.50, 39.76, 37.72, 37.16, 36.47, 36.24, 36.03, 35.89, 34.63, 32.07, 30.97, 29.70, 27.59, 23.20, 19.44, 16.65, 11.90

IR (neat film, cm⁻¹): 1692, 1489, 1456, 1089

HRMS (EC-CI): calcd. for C₂₉H₄₂O₃ [M] 438.3134, found 438.3130.

Minor Diastereomer:

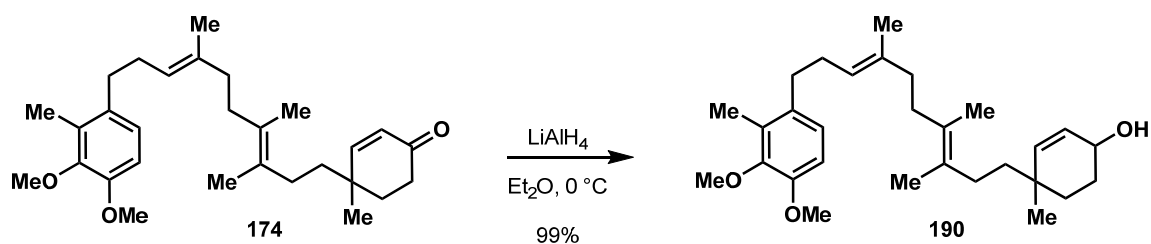
R_f = 0.43 (30% EtOAc in hexane) and 0.52 (10% 1,4-dioxane in hexane)

¹H-NMR (400 MHz, CDCl₃): δ 6.68 (s, 1H), 3.81 (s, 3H), 3.74 (s, 3H), 2.53 (dt, 1H, *J* = 5.5, 5.9 Hz), 2.48 – 2.44 (m, 1H), 2.41 (d, 1H, *J* = 10.4 Hz), 2.36 – 2.19 (m, 3H), 2.12 – 2.10 (m, 1H), 2.11 (s, 3H), 1.88 – 1.65 (m, 8H), 1.56 – 1.40 (m, 5H), 1.23 (s, 3H), 1.09 (s, 3H), 1.03 (s, 3H), 0.82 (s, 3H)

¹³C-NMR (100 MHz, CDCl₃): δ 213.82, 150.27, 144.86, 140.66, 129.43, 128.21, 108.24, 60.27, 55.73, 52.97, 50.92, 49.02, 44.45, 39.77, 37.57, 36.68, 36.53, 36.28, 36.06, 35.81, 34.61, 32.11, 30.21, 29.77, 27.43, 23.45, 19.36, 16.87, 11.88

IR (neat film, cm⁻¹): 1694, 1489, 1456, 1088

HRMS (EC-CI): calcd. for C₂₉H₄₂O₃ [M] 438.3134, found 438.3130.



A yellow solution of the enone **174** (2.35 g, 5.36 mmol, 1.00 eq.) in ethyl ether (54 mL) was placed in an ice bath cooled to 0 °C and stirred for 20 minutes. LiAlH₄ (1.4 mL, 4 M in ethyl ether, 5.62 mmol, 1.05 eq.) was added dropwise over 2 minutes. After 5 minutes the clear colorless solution was diluted with ethyl ether (30 mL) and excess lithium aluminum hydride was quenched by the sequential dropwise addition of water (0.5 mL), aqueous NaOH (15%, 0.5 mL), and water (1.5 mL). After stirring for 5 minutes an aqueous phosphate buffer (1.5 mL, pH = 7, 0.2 M) was added to the white heterogeneous mixture and stirred vigorously (900 rpm) for 15 minutes. The cold bath was removed and the mixture was allowed to warm to 23 °C. Solid Na₂SO₄ was added and the heterogeneous mixture was stirred vigorously for 10 minutes, suction filtered over a pad of Na₂SO₄, and concentrated to reveal the alcohol **190** as a clear colorless oil (2.35 g, 5.33 mmol, 99%, d.r. = 1.4 : 1).

Major Diastereomer:

$R_f = 0.24$ (50% Et₂O in hexane)

¹H-NMR (400 MHz, CDCl₃): δ 6.85 (d, 1H, *J* = 8.2 Hz), 6.70 (d, 1H, *J* = 8.2), 5.63 (dd, 1H, *J* = 2.3, 9.8 Hz), 5.52 (d, 1H, *J* = 10.2 Hz), 5.19 (t, 1H, *J* = 7.0 Hz), 4.14 (m, 1H), 3.83 (s, 3H), 3.78 (s, 3H), 2.55 (m, 1H), 2.23 (s, 3H), 2.21 (m, 1H), 2.09 – 1.84 (m, 8H), 1.64 (s, 3H), 1.62 (s, 3H), 1.58 (s, 3H), 1.74 – 1.24 (m, 5H), 1.02 (s, 3H)

¹³C-NMR (100 MHz, CDCl₃): δ 150.76, 139.98, 139.15, 135.96, 133.87, 128.64, 128.49, 127.85, 127.56, 124.05, 123.56, 109.30, 66.58, 60.18, 55.68, 40.37, 38.13, 34.70, 33.58, 33.25, 31.34, 29.27, 29.17, 29.10, 26.47, 18.13, 17.95, 16.08, 11.72

IR (neat film, cm⁻¹): 3370, 2931, 1490, 1454, 1270, 1084

HRMS (EC-CI): calcd. for C₂₉H₄₄O₃ [M] 440.3290, found 440.3288.

Minor Diastereomer:

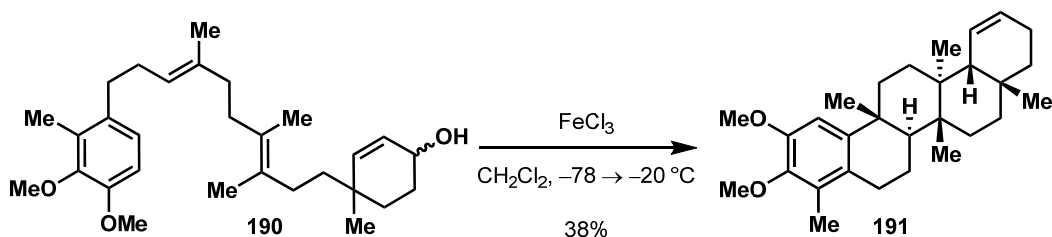
$R_f = 0.24$ (50% Et₂O in hexane)

¹H-NMR (400 MHz, CDCl₃): δ 6.85 (d, 1H, *J* = 8.2 Hz), 6.70 (d, 1H, *J* = 8.2), 5.67 (dd, 1H, *J* = 3.6, 10.2 Hz), 5.57 (d, 1H, *J* = 10.2 Hz), 5.19 (t, 1H, *J* = 7.0 Hz), 4.14 (m, 1H), 3.83 (s, 3H), 3.78 (s, 3H), 2.55 (m, 1H), 2.23 (s, 3H), 2.21 (m, 1H), 2.09 – 1.84 (m, 8H), 1.64 (s, 3H), 1.62 (s, 3H), 1.58 (s, 3H), 1.74 – 1.24 (m, 5H), 0.96 (s, 3H)

¹³C-NMR (100 MHz, CDCl₃): δ 147.22, 139.98, 139.15, 135.98, 130.20, 128.64, 128.47, 127.87, 127.56, 124.06, 123.56, 109.30, 65.32, 60.18, 55.68, 40.22, 38.13, 34.58, 33.58, 33.25, 30.39, 29.40, 29.10, 28.17, 26.00, 18.15, 16.08, 15.28, 11.72.

IR (neat film, cm⁻¹): 3370, 2931, 1490, 1454, 1270, 1084

HRMS (EC-CI): calcd. for C₂₉H₄₄O₃ [M] 440.3290, found 440.3288.



Ferric chloride (1.10 g, 6.81 mmol, 3.00 eq.) was added into a flame-dried round-bottomed flask in a glove box, removed, and crushed under vacuum by stirring the solid vigorously for 30 minutes. Freshly deoxygenated CH_2Cl_2 (550 mL) was added and the suspension was vigorously stirred (600 rpm) at 23 °C for 30 minutes. Stirring was stopped and the residual powder was allowed to congregate on the bottom of the reaction vessel. The yellow liquid was decanted by cannulation under nitrogen to a separate flame-dried flask.

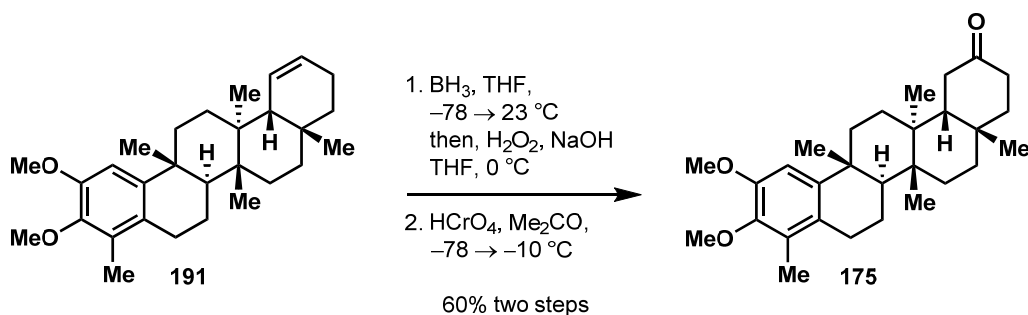
A solution of the alcohol **190** (1.00 g, 2.27 mmol, 1.00 eq.) in freshly deoxygenated CH_2Cl_2 (4.15 L) was placed in a bath cooled to -78 °C and stirred (500 rpm) for 1 hr. The solution of FeCl_3 in CH_2Cl_2 was added via cannula under nitrogen over 20 minutes. The golden yellow solution was stirred (500 rpm) for 6 hrs while gradually warming to -20 °C affording a purple-red solution. The excess FeCl_3 was quenched with an aqueous phosphate buffer (300 mL, pH = 7, 0.2 M), and the biphasic mixture was immediately removed from the cold bath, stirred vigorously (1000 rpm) for 60 minutes, poured into a separatory funnel, and the organic layer was removed. Residual organics were extracted from the aqueous layer using methylene chloride (2 x 100 mL), combined, dried over solid Na_2SO_4 , decanted, and concentrated. The resulting golden yellow amorphous oil was purified by silica gel chromatography; benzene to afford the pentacycle **191** as a white solid which was ~65% pure determined by GC (300 °C) and $^1\text{H-NMR}$ (0.57 g, 0.86 mmol, 38%). Further purification using trituration, recrystallization, silica gel chromatography, or preparative TLC did not afford a more pure product. The impure compound was carried onto the next step without full structural characterization.

R_f = 0.64 (5% EtOAc in benzene)

$^1\text{H-NMR}$ (400 MHz, CDCl_3): δ 6.69 (s, 1H), 5.70 (m, 2H), 3.83 (s, 3H), 3.75 (s, 3H), 2.72 (dd, 1H, J = 4.8, 13.0 Hz), 2.54 (q, 1H, J = 8.5 Hz), 2.11 (s, 3H), 2.00 – 1.52 (m, 12H), 1.44 – 1.28 (m, 4H), 1.26 (s, 3H), 1.03 (s, 3H), 0.95 (s, 3H), 0.92 (s, 3H)

HRMS (ESI): calc'd. for $\text{C}_{29}\text{H}_{42}\text{O}_2\text{Na}$ $[\text{M}+\text{Na}]^+$ 445.3077, found 445.3082.

M.P.: 49 – 53 °C



A solution of the impure pentacycle **191** (0.25 g, 0.58 mmol, 1.00 eq.) in THF (5.8 mL) was placed in a bath cooled to $-78 \text{ }^\circ\text{C}$ and stirred for 1 hour. A solution of borane in THF (1 M, 5.22 mL, 5.22 mmol, 9.00 eq.) was added to the pale yellow solution and stirred for 12 hrs. warming gradually to $23 \text{ }^\circ\text{C}$. The clear solution was placed in an ice water bath cooled to $0 \text{ }^\circ\text{C}$ for 10 minutes and an aqueous solution of H_2O_2 (30% w/v, 7.0 mL) and NaOH (4 N, 7.0 mL) was added. The biphasic mixture was stirred for 8 hrs and excess peroxide was quenched with a saturated aqueous mixture of $\text{Na}_2\text{S}_2\text{O}_3$ (10 mL). An aqueous phosphate buffer (10 mL, pH = 7, 0.2 M) and EtOAc (10 mL) were added, the mixture was poured into a separatory funnel, partitioned, residual organics were extracted from the aqueous layer with EtOAc (2 x 15 mL), combined, washed with brine (1 x 10 mL), dried over solid Na_2SO_4 , decanted, and concentrated. The crude alcohol was then submitted into the next reaction without purification or characterization.

A solution of the crude alcohol (0.26 g) in acetone (28.9 mL) was placed in a bath cooled to $-78 \text{ }^\circ\text{C}$ and stirred for 30 minutes. Jones reagent (1.53 M, 0.40 mL, 0.61 mmol, 1.05 eq.) was added and the red-brown solution was allowed to warm gradually to $-10 \text{ }^\circ\text{C}$ over 2 hrs. Excess chromic acid was quenched with 2-propanol (10 mL) and the green mixture was diluted with ethyl ether (30 mL) and an aqueous phosphate buffer (10 mL, pH = 7, 0.2 M). The biphasic mixture was poured into a separatory funnel, partitioned, and the organic layer was washed with a saturated aqueous mixture of NaHCO_3 (2 x 10 mL). The residual organics were extracted from the aqueous layer with ethyl ether (3 x 20 mL), combined, washed with brine (1 x 10 mL), dried over solid Na_2SO_4 , decanted, and concentrated. The crude green mixture was purified by silica gel chromatography; 5% EtOAc in hexane to afford the pentacyclic ketone **175** as a white solid (0.152 g, 0.35 mmol, 60%).

$R_f = 0.71$ (40% EtOAc in hexane)

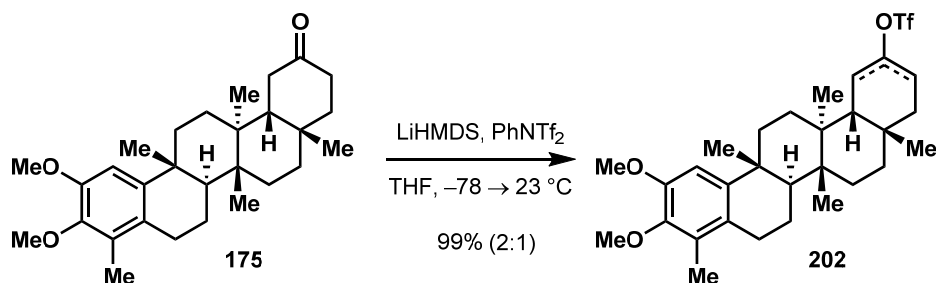
$^1\text{H-NMR}$ (400 MHz, CDCl_3): δ 6.66 (s, 1H), 3.83 (s, 3H), 3.75 (s, 3H), 2.72 (dd, 1H, $J = 6.5, 17.6 \text{ Hz}$), 2.56 (dd, 1H, $J = 7.3, 17.6 \text{ Hz}$), 2.53 – 2.27 (m, 5H), 2.10 (s, 3H), 2.04 – 2.00 (m, 2H), 1.92 (ddd, 1H, $J = 4.4, 13.7 \text{ Hz}$), 1.85 (m, 2H), 1.73 – 1.33 (m, 8H), 1.28 (s, 3H), 1.23 (s, 3H), 1.00 (s, 3H), 0.88 (s, 3H)

¹³C-NMR (100 MHz, CDCl₃): δ 213.80, 150.44, 146.86, 144.93, 129.45, 126.33, 105.83, 60.29, 55.86, 47.98, 43.58, 40.10, 39.55, 37.72, 37.68, 37.56, 37.17, 35.06, 33.78, 31.50, 31.22, 29.42, 28.11, 27.88, 27.84, 18.13, 16.29, 15.02, 11.73

IR (neat film, cm⁻¹): 2935, 1709, 1487, 1091

HRMS (EC-Cl): calcd. for C₂₉H₄₂O₃ [M] 438.3134, found 438.3129.

M.P.: 58 – 62 °C



The ketone was dried by the azeotropic removal of water using toluene (3 x 3 mL) prior to use. A solution of the ketone **175** (114 mg, 0.26 mmol, 1.00 eq.) in THF (3.7 mL) was placed in a bath cooled to $-78\text{ }^{\circ}\text{C}$ and stirred for 1 hr. A solution of LiHMDS (1 M, 1.00 mL, 1.04 mmol, 4.00 eq.) was added and the pale yellow solution was stirred for 1 hr. A solution of *N*-phenyl-bis(trifluoromethanesulfonimide) (371 mg, 1.04 mmol, 4.00 eq.) in THF (1.5 mL) was added to the enolate in a dropwise manner by cannula under nitrogen. The golden yellow solution was stirred for 20 minutes, the cold bath was removed, and the solution was allowed to gradually warm to $23\text{ }^{\circ}\text{C}$ over 1 hr. An aqueous phosphate buffer (5 mL, pH = 10, 0.2 M) was added to neutralize excess LiHMDS and the biphasic mixture was poured into a separatory funnel containing Et_2O (10 mL). The organic layer was washed with a saturated aqueous mixture of NaHCO_3 (2 x 10 mL). Residual organics were extracted from the aqueous layer using Et_2O (2 x 10 mL), combined, dried over solid Na_2SO_4 , decanted, and concentrated. The crude pale orange solid was purified by silica gel chromatography; 2% Et_2O in hexane to provide the enol triflate **202** as a white solid (0.146 g, 0.26 mmol, 99%, 2:1 mixture of olefin isomers).

Mixture of Isomers: (*) denotes minor isomer

$R_f = 0.51$ (15% Et_2O in hexane)

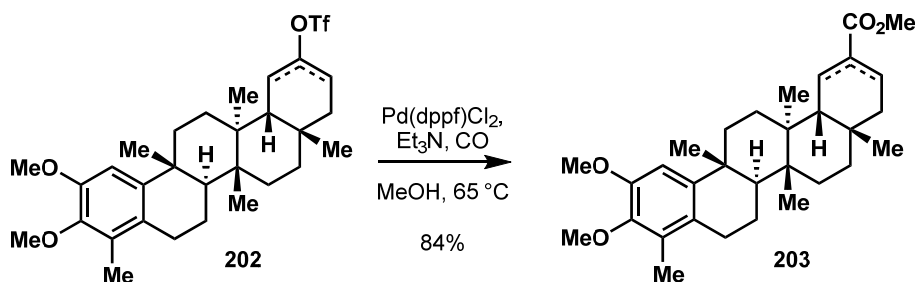
$^1\text{H-NMR}$ (400 MHz, CDCl_3): δ 6.67 (s, 1H), 5.77* (m, 1H), 5.64 (m, 1H), 3.82 (s, 3H), 3.75 (s, 3H), 2.72 (dd, 1H, $J = 6.5, 17.6$ Hz), 2.66 – 2.20 (m, 8H), 2.10 (s, 3H), 2.05 – 1.40 (m, 8H), 1.25* (s, 3H), 1.23 (s, 3H), 1.05 (s, 3H), 1.03* (s, 3H), 1.01 (s, 3H), 1.00* (s, 3H), 0.93* (s, 3H), 0.92 (s, 3H)

$^{13}\text{C-NMR}$ (100 MHz, CDCl_3): δ 150.43 (150.44*), 148.98 (148.89*), 146.94 (146.69*), 144.91 (144.87*), 129.45 (129.48*), 126.28 (126.32*), 119.09 (120.13*), 116.73, 105.70 (105.79*), 60.30, 55.78, (47.25*), (43.94*), 43.73, 43.39, (40.34*), 39.94, 39.84, (39.10*), (37.39*), 37.35, 37.11, 34.38 (34.52*), 34.08 (33.87*), 32.54, (31.12*), 30.55 (29.68*), 29.60 (29.45*), 28.31 (28.26*), 27.92, 27.82, 27.76, 24.44 (24.67*), 18.05 (18.21*), 16.91, 15.14 (15.09*), 13.83, 11.76

IR (neat film, cm^{-1}): 2924, 1413, 1207, 1143

HRMS (EC-Cl): calcd. for $\text{C}_{30}\text{H}_{41}\text{O}_5\text{F}_3\text{S}$ $[\text{M}+\text{H}]^+$ 570.2627, found 570.2622.

M.P.: 54 – 56 °C



A mixture of the enol triflate **202** (109.0 mg, 0.19 mmol, 1.00 eq.) and $\text{Pd}(\text{dppf})\text{Cl}_2\text{-CH}_2\text{Cl}_2$ (31.5 mg, 0.04 mmol, 0.20 eq.) was evacuated and then refilled with nitrogen. To the dry red mixture was added triethylamine (0.54 mL, 3.83 mmol, 20.0 eq.) and methanol (3 mL). The reaction vessel was stoppered with a plastic PTFE cap under a positive flow of carbon monoxide. The vessel was placed under an atmosphere of carbon monoxide (balloon), the dark red solution was placed in an oil bath heated to 65 and stirred (500 rpm) for 12 hrs. The black mixture was removed from the oil bath, cooled to 23 °C, and a second loading of $\text{Pd}(\text{dppf})\text{Cl}_2\text{-CH}_2\text{Cl}_2$ (38.8 mg, 0.05 mmol, 0.25 eq.) was added. The black mixture was purged, placed under an atmosphere of carbon monoxide (balloon), and placed into the oil bath heated to 65 °C. After 24 hrs. the black mixture was removed from the oil bath, concentrated, and residual methanol was azeotropically removed with chloroform (3 x 3 mL). The black solid was dissolved in chloroform and hexane (2 mL, 3:1), loaded directly onto silica gel, and purified by silica gel chromatography; hexane \rightarrow 10% EtOAc in hexane to afford the enoate **203** as a white solid (77.4 mg, 0.16 mmol, 84%).

Mixture of Isomers: (*) denotes minor isomer

$R_f = 0.48$ (35% Et_2O in hexane)

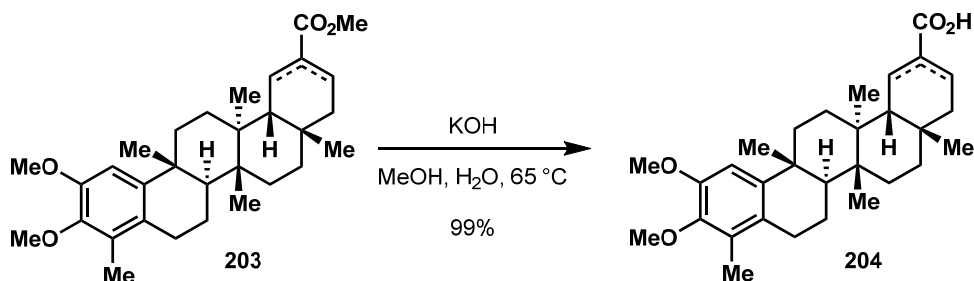
$^1\text{H-NMR}$ (400 MHz, CDCl_3): δ 7.06* (d, 1H, $J = 4.5$ Hz), 6.89 (m, 1H), 6.67 (s, 1H), 3.82 (s, 3H), 3.75 (s, 3H), 3.73 (s, 3H), 2.72 – 2.68 (m, 1H), 2.58 – 2.48 (m, 2H), 2.40 – 2.34* (m, 1H), 2.30 – 2.20 (m, 1H), 2.10 (s, 3H), 2.02 – 1.35 (m, 17H), 1.27* (s, 3H), 1.23 (s, 3H), 1.05* (s, 3H), 1.03 (s, 3H), 0.96 (s, 3H), 0.90* (s, 3H), 0.88* (s, 3H), 0.80 (s, 3H)

¹³C-NMR (100 MHz, CDCl₃): δ (167.97*) 167.86, (150.47*) 150.38, 147.19 (146.85*), (144.87*) 144.80, 140.97, 138.70, (129.54*), (129.47*), (129.41*) 129.39, (126.42*) 126.37, (105.82*) 105.75, 60.30, 55.79, 51.51, (48.10*), (43.91*) 43.40, 41.78, (40.75*) 40.04, 39.92, (39.35*) 38.74, (37.40*) 37.14, (35.24*) 34.97, 34.13 (33.96*), (33.47*) 33.02, (31.58*) 31.38, 30.27 (29.57*), 29.52 (29.50*), 28.41 (28.37*), (27.96*) 27.88, (22.66*), (21.45*) 20.91, (18.21*) 18.01, (17.64*), 15.30 (15.29*), (15.26*) 13.89, 11.75

IR (neat film, cm⁻¹): 3368, 2925, 1712, 1251, 1091

HRMS (EC-CI): calcd. for C₃₁H₄₄O₄ [M+H]⁺, 480.3240 found. 480.3241

M.P.: 83 – 87 °C



To a white mixture of the ester **203** (97.0 mg, 0.20 mmol, 1.00 eq.) in methanol (4.5 mL) and water (1.5 mL) was added KOH (227 mg, 4.04 mmol, 20.0 eq.). The reaction vessel was equipped with a plastic PTFE cap under a purging flow of nitrogen and placed in an oil bath heated to 65 °C. After stirring (500 rpm) for 2 hrs. the clear colorless solution was removed from the oil bath, allowed to cool to 23 °C, acidified to pH = 2 using 1 N HCl, diluted with EtOAc (5 mL), poured into a separatory funnel containing an aqueous phosphate buffer (10 mL, pH = 2, 0.2 M), and partitioned. The organic layer was washed with water (1 x 10 mL). The residual organics were extracted from the aqueous layer with EtOAc (2 x 10 mL), combined, dried over solid Na₂SO₄, decanted, and concentrated to afford the acid **204** as a white solid (92.2 mg, 0.20 mmol, 99%, 2:1). The product was carried onto the next step without further purification.

Mixture of Isomers: (*) denotes minor isomer

R_f = 0.31 (50% EtOAc in hexane)

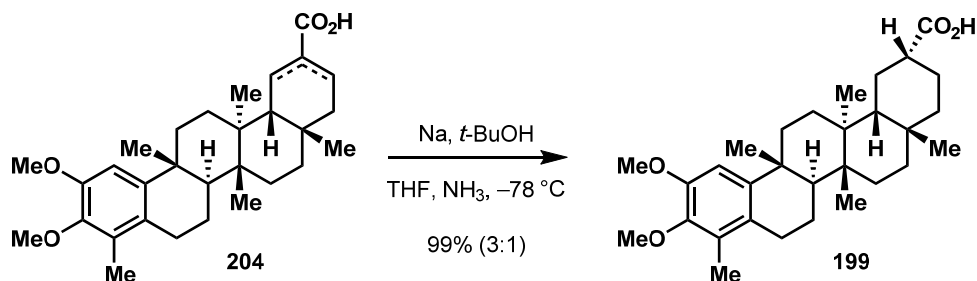
¹H-NMR (400 MHz, CDCl₃): δ 7.22* (s, 1H), 7.06 (s, 1H), 6.67 (s, 1H), 3.82 (s, 3H), 3.75 (s, 3H), 2.71 (dd, 1H, *J* = 5.0, 16.1 Hz), 2.54 (m, 2H), 2.41 – 2.10 (m, 2H), 2.10 (s, 3H), 2.06 – 1.91 (m, 4H), 1.88 – 1.57 (m, 7H), 1.48 – 1.31 (m, 3H), 1.27* (s, 3H), 1.23 (s, 3H), 1.06* (s, 3H), 1.03 (s, 3H), 0.98 (s, 3H), 0.92* (s, 3H), 0.89* (s, 3H), 0.81 (s, 3H)

¹³C-NMR (100 MHz, CDCl₃): δ (172.80*) 172.71, (150.41*) 150.38, 147.18 (146.83*), (144.86*) 144.80, (143.85*) 141.53, (129.49*) 129.43, (129.08*) 128.91, (126.42*) 126.39, (105.84*) 105.77, 60.33, 55.81, (48.34*), (43.89*) 43.39, 41.70 (40.91*), 40.06, 39.92 (39.39*), (39.97*), (37.41*) 37.15, (35.18*) 34.94, 34.11 (33.94*), (33.41*), 33.06, (31.40*), 30.26, (29.71*), (29.61*) 29.54, 29.48, 28.41, (27.96*), 27.88, (21.07*) 20.49, (18.22*) 18.01, 17.74, 15.31 (15.28*), 13.94, 11.77

IR (neat film, cm⁻¹): 2946, 2636, 2527, 2250, 1683, 1486, 1278, 1092, 910, 732

HRMS (EC-CI): calcd. for C₃₀H₄₂O₄ [M+H]⁺, 466.3083 found. 466.3075

M.P.: 159 – 162 °C



To a solution of liquid ammonia (5 mL) in a bath cooled to $-78\text{ }^\circ\text{C}$ was added sodium metal (46.0 mg, 2.00 mmol, 10.0 eq.) under a positive flow of nitrogen. The blue heterogeneous mixture was stirred (800 rpm) for 10 minutes upon which a solution of the acid **204** (92.2 mg, 0.20 mmol, 1.00 eq.) in THF (6 mL) was added over 1 minute via cannula under nitrogen. The blue heterogeneous mixture was stirred for 30 minutes and then *t*-BuOH (1.9 mL) was added to quench the excess sodium metal, sodium amide, and the enolate. After 30 minutes the mixture was slowly acidified to $\text{pH} = 2$ using concentrated HCl and then diluted with EtOAc (20 mL). The biphasic solution was removed from the cold bath, warmed to $23\text{ }^\circ\text{C}$, poured into a separatory funnel containing an aqueous phosphate buffer (10 mL, $\text{pH} = 2$, 0.2 M), and partitioned. The organics were extracted from the aqueous layer with EtOAc (2 x 20 mL), combined, washed with brine, dried over solid Na_2SO_4 , decanted, and concentrated. The crude off-white solid was purified by silica gel chromatography; 2% EtOAc and 2% AcOH in hexane to afford the acid **199** as a white solid (91.7 mg, 0.20 mmol, 99%, d.r. = 3:1).

Mixture of Isomers: (*) denotes minor isomer

$R_f = 0.66$ (40% EtOAc and 2% AcOH in hexane)

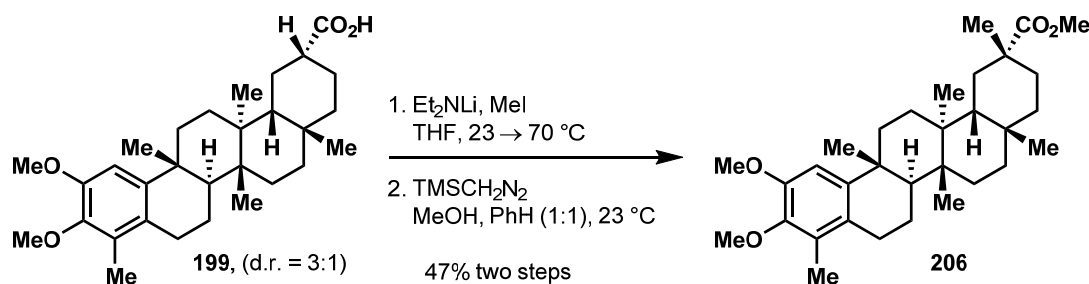
$^1\text{H-NMR}$ (400 MHz, CDCl_3): δ 6.69 (s, 1H), 3.84 (s, 3H), 3.76 (s, 3H), 2.75 – 2.65 (m, 2H), 2.57 – 2.50 (m, 1H), 2.11 (s, 3H), 2.02 (d, 1H, $J = 7.2$ Hz), 1.90 – 1.46 (m, 16H), 1.38 – 1.32 (m, 2H), 1.26* (s, 3H), 1.23* (s, 3H), 1.19 (s, 6H), 1.11* (s, 3H), 1.10* (s, 3H), 1.07 (s, 3H), 0.98 (s, 3H)

$^{13}\text{C-NMR}$ (100 MHz, CDCl_3): δ 183.59, 150.41, 146.52, 144.84, 129.54, 126.61 (126.52*), 106.10, 60.33, 55.85, 46.24, 44.94, 43.26, (40.10*), (39.68*), 39.40, 38.30, 37.42, 37.26, 36.43, 35.47, 34.27, 33.07, 32.17 (31.51*), 30.62, 30.27 (29.71*), 28.57 (28.07*), (27.83*), 26.50, 24.30, 21.10, (20.19*) 20.13, 16.96, (15.07*), 11.78

IR (neat film, cm^{-1}): 2932, 2871, 1699, 1486, 910, 734

HRMS (EC-CI): calcd. for $\text{C}_{30}\text{H}_{44}\text{O}_4$ [M], 468.3240 found. 468.3239

M.P.: 179 – 183 $^\circ\text{C}$



A solution of diethylamine (0.25 mL, 2.42 mmol, 1.00 eq.) in THF (4.7 mL) was placed in a bath cooled to -78 $^\circ\text{C}$ and stirred (500 rpm) for 20 minutes. *n*-Butyllithium (1.26 mL, 2.42 mmol, 1.92 M in hexane, 1.00 eq.) was added, the pale yellow solution was stirred for 30 minutes at -78 $^\circ\text{C}$, the cold bath was removed, and allowed to warm gradually to 23 $^\circ\text{C}$ over 20 minutes to provide a freshly prepared solution of lithium diethylamide (0.4 M).

Acid **199** was azeotroped with toluene (3 x 3 mL) and dried *in vacuo* prior to use. To a solution of the acid **199** (28.0 mg, 0.06 mmol, 1.00 eq.) in THF (1 mL) at 23 $^\circ\text{C}$ in a vessel equipped with a Claisen adapter and reflux condenser was added a freshly prepared solution of lithium diethylamide (3.00 mL, 1.19 mmol, 20.0 eq., 0.4 M in THF). The resultant golden yellow solution was stirred for 30 minutes and then placed in an oil bath heated to 70 $^\circ\text{C}$. After 30 minutes iodomethane (0.17 mL, 2.68 mmol, 45.0 eq.) was added to the golden yellow solution. The now pale yellow mixture was stirred for 30 minutes, removed from the oil bath, cooled to 23 $^\circ\text{C}$, and the mixture was acidified to a pH = 2 with an aqueous phosphate buffer (10 mL, pH = 2, 0.2 M). The biphasic mixture was diluted with EtOAc (10 mL), poured into a separatory funnel, partitioned, and the organic layer washed with an aqueous phosphate buffer (1 x 10 mL, pH = 2, 0.2 M). Residual organics were extracted from the aqueous layer with EtOAc (2 x 10 mL), combined, dried over solid Na_2SO_4 , decanted, concentrated, and the crude golden yellow mixture was purified using silica gel chromatography; toluene (50 mL) and then 2% EtOAc and 2% AcOH in hexane (150 mL) to afford a mixture of the starting acid **199** and the methylated acid **128** (R_f = 0.75 (40% EtOAc and 2% AcOH in hexane)) as a white solid.

This mixture was azeotroped with toluene (3 x 3 mL), dried *in vacuo*, and subjected to the identical reaction conditions above. After aqueous work-up, the concentrated crude golden yellow mixture was purified by silica gel chromatography; toluene (50 mL) and then 2% EtOAc and 2% AcOH in hexane (150 mL) to afford the alkylated acid as a white solid which was dissolved in a solution of methanol-benzene (2 mL, 1 : 1). A solution of trimethylsilyl diazomethane (0.20 mL, 0.40 mmol, 6.67 eq., 2 M in Et_2O) was added. After 5 minutes the golden yellow solution was concentrated and purified by silica gel chromatography; 1% acetone in hexane to afford the ester **206** as a white amorphous foam (14.1 mg, 0.03 mmol, 47%).

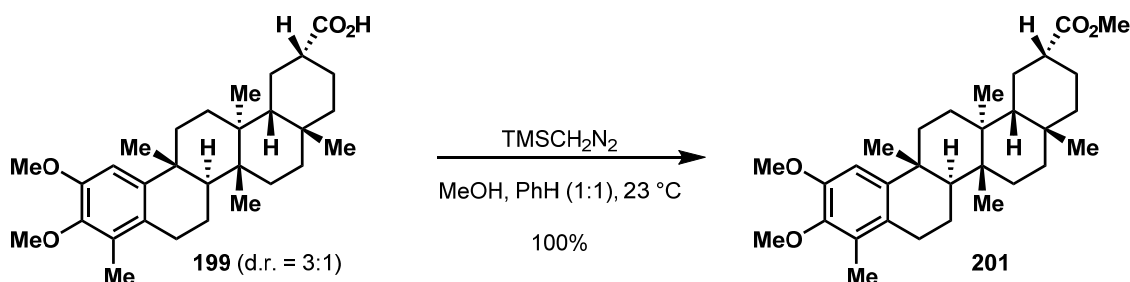
R_f = 0.54 (10% acetone in hexane)

¹H-NMR (400 MHz, CDCl₃): δ 6.68 (s, 1H), 3.84 (s, 3H), 3.75 (s, 3H), 3.60 (s, 3H), 2.72 (dd, 1H, *J* = 5.1, 17.1 Hz), 2.55 – 2.48 (m, 1H), 2.42 – 2.34 (m, 1H), 2.19 – 2.13 (m, 1H), 2.10 (s, 3H), 2.04 – 1.98 (m, 3H), 1.82 – 1.30 (m, 13H), 1.20 (s, 3H), 1.19 (s, 3H), 1.10 (s, 3H), 0.95 (s, 3H), 0.80 (s, 3H)

¹³C-NMR (100 MHz, CDCl₃): δ 179.25, 150.35, 146.87, 144.81, 129.52, 126.61, 105.84, 60.31, 55.83, 51.52, 44.46, 43.98, 40.56, 39.47, 38.90, 37.24, 36.51, 36.24, 34.02, 32.01, 31.83, 30.60, 30.25, 30.17, 29.70, 28.90, 28.31, 27.33, 18.45, 17.35, 15.89, 11.75

IR (neat film, cm⁻¹): 2978, 2869, 1732, 1487, 1464, 1093

HRMS (EC-CI): calc'd. for C₃₂H₄₈O₄ [M], 496.3553 found. 496.3551



To a solution of the acid **199** (10.0 mg, 21.4 μmol , 1.00 eq.) in methanol and benzene (1 mL, 1:1) was added trimethylsilyl diazomethane (11.5 μL , 22.4 μmol , 1.05 eq., 2 M in Et_2O) at 23 $^\circ\text{C}$. After 5 minutes the benzene and methanol were evaporated from the golden yellow solution by a continuous flow of nitrogen and the resultant pale yellow residue was fully concentrated *in vacuo* to afford the ester **201** as a white amorphous foam (10.3 mg, 21.4 μmol , 100%).

Mixture of Isomers: (*) denotes minor isomer

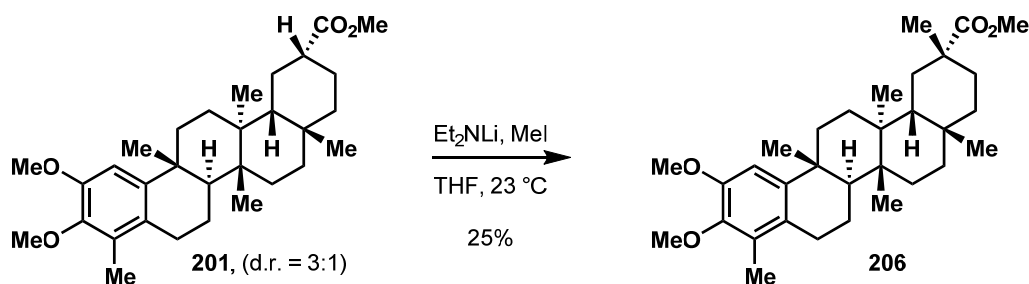
$R_f = 0.55$ (20% EtOAc in hexane)

$^1\text{H-NMR}$ (400 MHz, C_6D_6): δ 6.73* (s, 1H), 6.72 (s, 1H), 3.72 (s, 3H), 3.71* (s, 3H), 3.54* (s, 3H), 3.49 (s, 3H), 3.40 (s, 3H), 3.39* (s, 3H), 2.62 – 2.52 (m, 2H), 2.48 – 2.34 (m, 1H), 2.14 (s, 3H), 2.13* (s, 3H), 2.10 – 2.05 (m, 1H), 1.98 – 1.57 (m, 10H), 1.50 – 1.24 (m, 7H), 1.21* (s, 3H), 1.20 (s, 3H), 1.00 (s, 3H), 0.99* (s, 3H), 0.92 (s, 3H), 0.89* (s, 3H), 0.80* (s, 3H), 0.77 (s, 3H)

$^{13}\text{C-NMR}$ (100 MHz, C_6D_6): δ 176.62, 151.02, 146.12, 145.81, 129.29, 126.48, 106.75 (106.28*), 59.61, 55.35, 50.82 (50.68*), 46.30, 44.76, 43.35, (39.93*), (39.47*), 39.15, 38.11, (37.27*), 37.22, (37.04*), 36.48 (36.38*), 35.47, 34.33 (33.96*), 32.74, 32.05 (31.24*), 30.37, (30.12*) 30.04, 28.56 (28.03*), (27.66*) 26.39, (24.63*) 24.53, (23.68*) 21.29, 19.87 (19.75*), 18.47 (18.40*), 16.58 (14.85*), 11.69

IR (neat film, cm^{-1}): 2944, 1734, 1487, 1093

HRMS (EC-CI): calcd. for $\text{C}_{31}\text{H}_{46}\text{O}_4$ [M], 482.3396 found. 482.3391



A solution of diethylamine (0.25 mL, 2.42 mmol, 1.00 eq.) in THF (4.7 mL) was placed in a bath cooled to -78 °C and stirred (500 rpm) for 20 minutes. *n*-Butyllithium (1.26 mL, 2.42 mmol, 1.92 M in hexane, 1.00 eq.) was added, the pale yellow solution was stirred for 30 minutes at -78 °C, the cold bath was removed, and allowed to warm gradually to 23 °C over 20 minutes to provide a freshly prepared solution of lithium diethylamide (0.4 M).

Ester **201** was azeotroped with toluene (3 x 3 mL) and dried *in vacuo* prior to use. To a solution of the ester **201** (10.3 mg, 21.4 μmol , 1.00 eq.) in THF (1 mL) at 23 °C was added a freshly prepared solution of lithium diethylamide (27 μL , 107 μmol , 5.00 eq., 0.4 M in THF). The resultant golden yellow-brown solution was stirred for 5 minutes and then iodomethane (16 μL , 256 μmol , 12.0 eq.) was added to the golden brown solution. The now pale yellow mixture was stirred for 30 minutes and diluted with an aqueous phosphate buffer (5 mL, pH = 7, 0.2 M). The biphasic mixture was diluted with EtOAc (10 mL), poured into a separatory funnel, partitioned, and the organic layer washed with an aqueous phosphate buffer (2 x 10 mL, pH = 7, 0.2 M). Residual organics were extracted from the aqueous layer with EtOAc (2 x 10 mL), combined, dried over solid Na_2SO_4 , decanted, concentrated, and the crude golden brown mixture was purified using silica gel chromatography; 1% acetone in hexane to afford the mixture of the ester **206** as a white amorphous film (2.7 mg, 5.4 μmol , 25%)

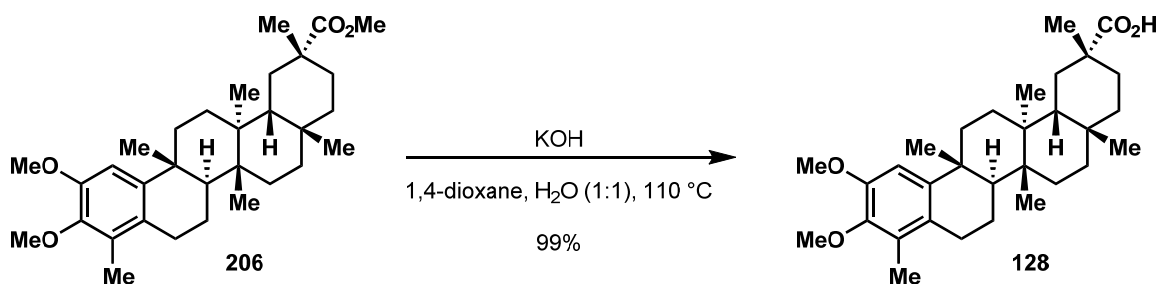
$R_f = 0.54$ (10% acetone in hexane)

$^1\text{H-NMR}$ (400 MHz, CDCl_3): δ 6.68 (s, 1H), 3.84 (s, 3H), 3.75 (s, 3H), 3.60 (s, 3H), 2.72 (dd, 1H, $J = 5.1, 17.1$ Hz), 2.55 – 2.48 (m, 1H), 2.42 – 2.34 (m, 1H), 2.19 – 2.13 (m, 1H), 2.10 (s, 3H), 2.04 – 1.98 (m, 3H), 1.82 – 1.30 (m, 13H), 1.20 (s, 3H), 1.19 (s, 3H), 1.10 (s, 3H), 0.95 (s, 3H), 0.80 (s, 3H)

$^{13}\text{C-NMR}$ (100 MHz, CDCl_3): δ 179.25, 150.35, 146.87, 144.81, 129.52, 126.61, 105.84, 60.31, 55.83, 51.52, 44.46, 43.98, 40.56, 39.47, 38.90, 37.24, 36.51, 36.24, 34.02, 32.01, 31.83, 30.60, 30.25, 30.17, 29.70, 28.90, 28.31, 27.33, 18.45, 17.35, 15.89, 11.75

IR (neat film, cm^{-1}): 2978, 2869, 1732, 1487, 1464, 1093

HRMS (EC-CI): calc'd. for $\text{C}_{32}\text{H}_{48}\text{O}_4$ [M], 496.3553 found. 496.3551



To a solution of the ester **206** (4.0 mg, 8.05 μmol , 1.00 eq.) in 1,4-dioxane and water (3 mL, 1:1) was added KOH (9.0 mg, 161 μmol , 20.0 eq.) under a positive flow of nitrogen and the reaction vessel was equipped with a plastic PTFE cap. The clear colorless solution was placed in an oil bath heated to 110 $^\circ\text{C}$ for 4 hrs., removed from the oil bath, and allowed to cool to 23 $^\circ\text{C}$. The clear pale yellow solution was acidified to pH = 2 with an aqueous phosphate buffer (5 mL, pH = 2, 0.2 M) affording a white mixture which was diluted with EtOAc (10 mL), poured into a separatory funnel, and partitioned. The organic layer was washed with an aqueous phosphate buffer (1 x 5 mL, pH = 2, 0.2 M). The residual organics were extracted from the aqueous layer with EtOAc (2 x 10 mL), combined, dried over solid Na_2SO_4 , decanted, and concentrated to afford the acid **128** as a crude white amorphous foam which was carried onto the next reaction without further purification (3.9 mg, 7.97 μmol , 99%).

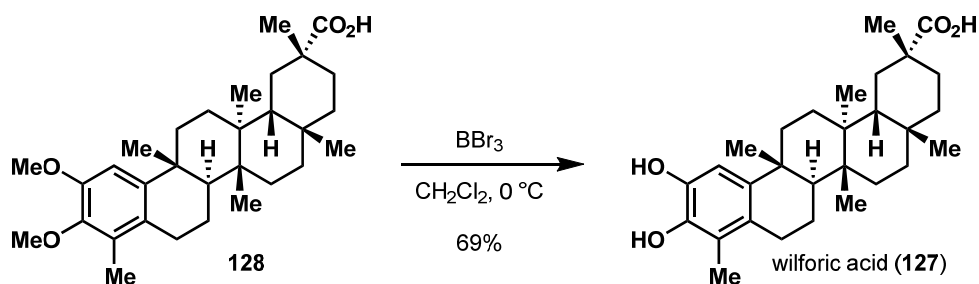
R_f = 0.75 (40% EtOAc and 2% AcOH in hexane)

$^1\text{H-NMR}$ (500 MHz, CDCl_3): δ 6.68 (s, 1H), 3.83 (s, 3H), 3.77 (s, 3H), 2.72 (dd, 1H, J = 6.1, 17.1 Hz), 2.56 – 2.48 (m, 1H), 2.37 – 2.33 (m, 1H), 2.10 (s, 3H), 1.98 (br d, 2H, J = 12.9 Hz), 1.83 – 1.61 (m, 8H), 1.46 – 1.36 (m, 5H), 1.28 – 1.22 (m, 2H), 1.22 (s, 6H), 1.16 (s, 3H), 1.11 (s, 3H), 0.96 (s, 3H),

$^{13}\text{C-NMR}$ (125 MHz, CDCl_3): δ 184.42, 150.36, 146.87, 144.81, 129.47, 126.55, 105.85, 60.29, 55.81, 44.21, 39.41, 39.00, 37.24, 36.57, 36.19, 34.05, 31.82, 31.50, 30.45, 30.29, 30.15, 29.69, 29.65, 29.58, 29.16, 28.28, 27.27, 18.47, 17.81, 16.29, 11.76

IR (neat film, cm^{-1}): 2929, 2870, 1697, 1487, 1463, 1270, 1093, 734

HRMS (EC-CI): calc'd. for $\text{C}_{31}\text{H}_{46}\text{O}_4$ [M], 482.3396 found. 482.3406

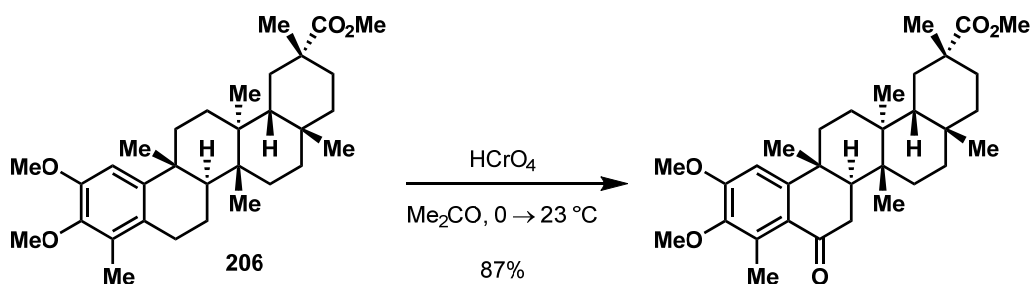


A solution of the crude acid **128** (3.9 mg, 7.97 μmol , 1.00 eq.) in methylene chloride (1 mL) was placed in an ice water bath cooled to 0 $^\circ\text{C}$. After stirring for 20 minutes neat BBr_3 (3.0 μL , 24.0 μmol , 3.00 eq.) was added. The golden yellow-orange solution was stirred for 5 minutes, acidified with 1 N HCl (3 mL), and the cold bath was removed. The orange mixture was diluted with EtOAc (10 mL) and an aqueous phosphate buffer (5 mL, pH = 2, 0.2 M), stirred vigorously for 2 minutes, poured into a separatory funnel containing EtOAc (10 mL), and the organics were washed with an aqueous phosphate buffer (2 x 10 mL, pH = 2, 0.2 M). Residual organics were extracted from the aqueous layer with EtOAc (3 x 10 mL), washed with brine (1 x 10 mL), dried over solid Na_2SO_4 , decanted, and concentrated. (**NOTE:** Throughout the work-up the catechol **127** remained under a positive flow of nitrogen to prevent oxidative degradation). The crude golden yellow mixture was dissolved in methylene chloride (0.5 mL), placed in an ice water bath cooled to 0 $^\circ\text{C}$, and hexane (10 mL) was added to triturate the white solid product. After stirring for 2 minutes the mixture was concentrated by rotary evaporation to ~3 mL (100 mBar, no water bath) and hexane (10 mL) was added. The mixture was concentrated by rotary evaporation to ~3 mL (100 mBar, no water bath). This was repeated once more upon which hexane (5 mL) was added to the white mixture, and the suspension was placed in an ice water bath cooled to 0 $^\circ\text{C}$ for 20 minutes. The cold yellow liquid was decanted by syringe. The white solid was washed with hexane (2 x 3 mL) which was decanted by syringe to afford wilforic acid (**127**) as a white solid (2.5 mg, 5.50 μmol , 69%). The spectral data matches that of the reported compound (Li, K.; Duan, H.; Kawazoe, K.; and Takashi, Y. *Phytochemistry* **1997**, 45, 791.).¹³¹

¹H-NMR Shifts of Wilforic Acid in C₅D₅N:

Isolated	Synthesized	Deviation
7.07 (s, 1H)	7.07 (s, 1H)	0.00
2.78 (dd, 1H)	2.78 (dd, 1H)	0.00
2.66 (dd, 1H)	2.66 (dd, 1H)	0.00
2.59 (m, 1H)	2.57 (m, 1H)	- 0.02
2.52 (m, 1H)	2.52 (m, 1H)	0.00
2.39 (s, 3H)	2.38 (s, 3H)	- 0.01
2.31 (ddd, 1H)	2.30 (ddd, 1H)	- 0.01
1.98 (br d, 1H)	1.99 (br d, 1H)	+ 0.01
1.44 (s, 3H)	1.42 (s, 3H)	- 0.02
1.29 (s, 3H)	1.26 (s, 3H)	- 0.03
1.19 (s, 3H)	1.17 (s, 3H)	- 0.02
1.16 (s, 3H)	1.13 (s, 3H)	- 0.03
1.01 (s, 3H)	0.94 (s, 3H)	- 0.07

¹H-NMR (400 MHz, CD₃CN): δ 6.59 (s, 1H), 3.37 (bs, 2H), 2.67 (dd, 1H, $J = 5.9, 6.8$ Hz), 2.52 – 2.42 (m, 3H), 2.36 – 2.28 (m, 4H), 2.00 (s, 3H), 1.76 – 1.24 (m, 13H), 1.17 (s, 3H), 1.13 (s, 3H), 1.09 (s, 3H), 0.94 (s, 3H), 0.89 (s, 3H)



A clear colorless solution of the ester **206** (10.0 mg, 19.6 μmol , 1.00 eq.) in acetone (1.5 mL) was placed in an ice water bath cooled to 0 $^\circ\text{C}$ for 20 minutes. Jones reagent (27.0 μL , 41.1 μmol , 2.10 eq., 1.53 M) was added and after 2 minutes the red-brown mixture was removed from the cold bath. After 5 minutes the brown mixture was diluted with isopropanol (1 mL) to quench excess Jones reagent. The green mixture was diluted with Et₂O (10 mL) and an aqueous phosphate buffer (5 mL, pH = 7, 0.2 M), poured into a separatory funnel, partitioned, and the organic layer was washed with water (2 x 10 mL). Residual organics were extracted from the aqueous layer with Et₂O (2 x 10 mL), combined, dried over solid Na₂SO₄, decanted, and concentrated. The crude green mixture was purified by silica gel chromatography; hexane \rightarrow 10% EtOAc in hexane to afford the benzyl ketone as a white amorphous foam (8.7 mg, 17.0 μmol , 87%).

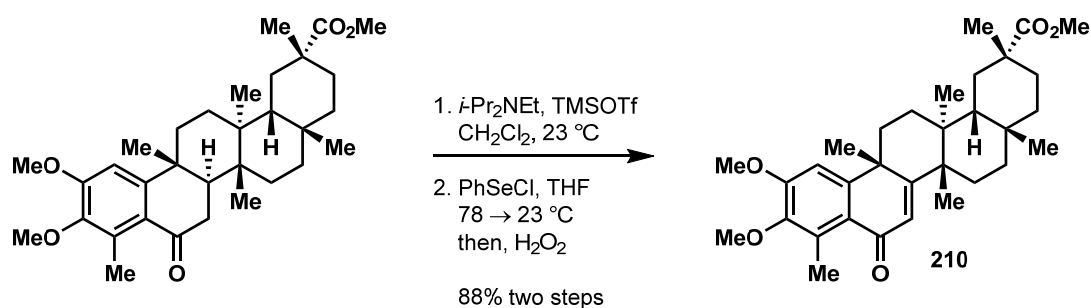
R_f = 0.51 (30% EtOAc in hexane)

¹H-NMR (400 MHz, CDCl₃): δ 6.69 (s, 1H), 3.93 (s, 3H), 3.74 (s, 3H), 3.61 (s, 3H), 2.53 (d, 2H, J = 7.4 Hz), 2.51 (s, 3H), 2.42 – 2.38 (m, 1H), 2.30 (d, 1H, J = 7.4 Hz), 2.24 (dd, 1H, J = 5.9, 12.9 Hz), 2.16 (br d, 1H, J = 14.4 Hz), 2.05 – 1.93 (m, 4H), 1.72 – 1.28 (m, 8H), 1.19 (s, 3H), 1.16 (s, 3H), 1.09 (s, 3H), 1.02 (s, 3H), 0.81 (s, 3H)

¹³C-NMR (100 MHz, CDCl₃): δ 200.42, 179.35, 155.94, 155.52, 134.77, 128.22, 124.48, 103.79, 60.24, 55.59, 51.62, 44.63, 42.38, 40.59, 39.41, 38.74, 37.66, 37.43, 36.15, 36.03, 33.24, 32.40, 31.71, 30.64, 30.26, 29.82, 29.76, 28.35, 25.53, 16.92, 15.35, 13.94

IR (neat film, cm⁻¹): 2924, 2852, 1734, 1669, 1585, 1484, 1287, 1099, 1020

HRMS (EC-CI): calc'd. for C₃₂H₄₆O₅ [M], 510.3345 found. 510.3346



To a solution of the ketone (8.7 mg, 17.0 μmol , 1.00 eq.) in methylene chloride (1 mL) was added freshly distilled Hunig's base (12.0 μL , 68.0 μmol , 4.00 eq.) and trimethylsilyl trifluoromethane sulfonate (16.0 μL , 85.0 μmol , 5.00 eq.) sequentially. After 1 hr. the clear golden yellow solution was concentrated *in vacuo* to afford the crude silyl enol ether as a golden yellow solid mixture.

A solution of the crude silyl enol ether in THF (1 mL) was placed in a bath cooled to -78 °C for 30 minutes upon which a solution of PhSeCl (16.3 mg, 85.0 μmol , 5.00 eq.) in THF (1 mL) was added over 1 minute under nitrogen via cannula. After 30 minutes the yellow solution was removed from the cooling bath and allowed to gradually warm to 23 °C. After 1 hr the yellow solution was placed in an ice water bath for 20 minutes and then an aqueous solution of H_2O_2 (5.0 μL , 170.0 μmol , 10.0 eq., 30% w/v) was added. The pale yellow solution was stirred for 10 minutes, the cooling bath was removed, and after 10 minutes a saturated aqueous mixture of $\text{Na}_2\text{S}_2\text{O}_3$ (3 mL) was added followed by an aqueous phosphate buffer (3 mL, pH = 7, 0.2 M) and EtOAc (10 mL). The biphasic mixture was poured into a separatory funnel, partitioned, and the organic layer was washed with water (2 x 5 mL). The residual organics were extracted from the aqueous layer with EtOAc (2 x 10 mL), dried over solid Na_2SO_4 , decanted, and concentrated. The crude yellow solid was purified by silica gel chromatography; hexane \rightarrow 10% EtOAc in hexane to afford the enone **210** as a pale yellow amorphous foam (7.6 mg, 14.9 μmol , 88%).

R_f = 0.65 (35% EtOAc in hexane)

$^1\text{H-NMR}$ (400 MHz, CDCl_3): δ 6.82 (s, 1H), 6.23 (s, 1H), 3.91 (s, 3H), 3.75 (s, 3H), 3.52 (s, 3H), 2.63 (s, 3H), 2.42 (bd d, 1H, J = 15.7 Hz), 2.26 – 2.23 (m, 1H), 2.17 (br d, 1H, J = 14.4 Hz), 2.05 (dd, 1H, J = 4.1, 14.1 Hz), 2.01 (dd, 1H, J = 4.1, 8.0 Hz), 1.97 (dd, 1H, J = 5.0, 13.6 Hz), 1.86 (ddd, 1H, J = 6.2, 14.1 Hz), 1.82 (m, 1H), 1.72 – 1.56 (m, 4H), 1.54 (s, 3H), 1.49 (dd, 1H, J = 5.0, 16.0 Hz), 1.40 – 1.34 (m, 2H), 1.28 (s, 3H), 1.16 (s, 3H), 1.08 (s, 3H), 0.57 (s, 3H)

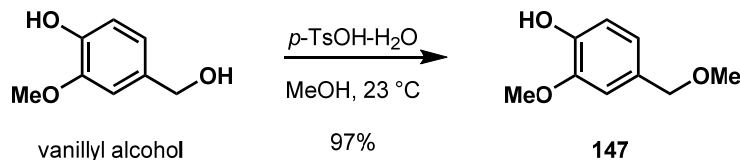
$^{13}\text{C-NMR}$ (100 MHz, CDCl_3): δ 187.25, 178.97, 170.83, 155.63, 154.01, 145.93, 133.69, 126.29, 123.29, 105.41, 60.33, 55.61, 51.55, 44.68, 44.28, 40.49, 40.43, 38.94, 37.61,

36.68, 34.84, 34.23, 32.85, 31.60, 30.93, 30.53, 29.88, 29.76, 29.69, 28.53, 20.87, 18.35, 13.98

IR (neat film, cm^{-1}): 2924, 1734, 1653, 1457, 1294, 1093

HRMS (EC-CI): calc'd. for $\text{C}_{32}\text{H}_{45}\text{O}_5$ $[\text{M}+\text{H}]^+$, 509.3267 found. 510.3252

3. Preparation of the Benzyl Stannane 152



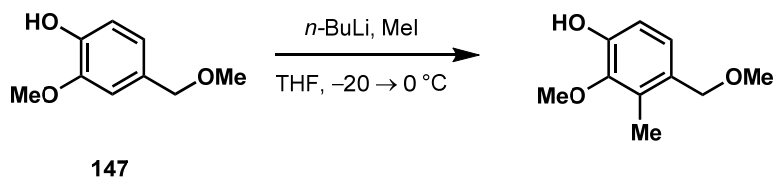
To a solution of vanillyl alcohol (56.0 g, 363 mmol, 1.00 eq.) in methanol (560 mL) at 23 °C was added *p*-toluenesulfonic acid monohydrate (3.5 g, 18.2 mmol, 0.05 eq.). After 6 hours the golden-yellow solution was diluted with an aqueous phosphate buffer (200 mL, pH = 4, 0.2 M) and brine (200 mL). Excess methanol was removed by rotary evaporation and the mixture was further diluted with EtOAc (400 mL). The biphasic mixture was poured into a separatory funnel, partitioned, and the organic layer was washed with water (1 x 100 mL). Residual organics were extracted from the aqueous layer using EtOAc (3 x 150 mL), combined, washed with brine (1 x 100 mL), dried over solid Na₂SO₄, filtered, and concentrated. The resulting golden-brown oil was dissolved in EtOAc (100 mL) and purified by elution through a short plug of silica gel using ethyl acetate (1.5 L) to afford the dimethyl ether **147** as a light yellow oil (59.3 g, 352 mmol, 97%). The spectral data matches that of the reported compound (Cook, S.P. and Danishefsky, S.J. *Organic Letters* **2006**, 8, 5693).

¹H-NMR (400 MHz, CDCl₃): δ 6.86 (m, 3H), 5.76 (s, 1H), 4.38 (s, 2H), 3.88 (s, 3H), 3.37 (s, 3H)

¹³C-NMR (100 MHz, CDCl₃): δ 146.2, 144.8, 129.6, 120.3, 113.6, 110.0, 74.3, 57.3, 55.4;

IR (film, cm⁻¹): 3390, 2935, 1606, 1515, 1464, 1431, 1368, 1276, 1241, 1188, 1154, 1089.

HRMS (FAB): calcd. for C₉H₁₂O₃ [M]⁺ 168.0786, found 168.0789



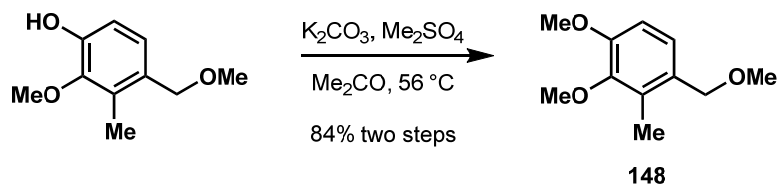
The phenol **147** (62.3 g, 0.37 mol, 1.00 eq.) was azeotroped with toluene (3 x 50 mL) and dissolved in THF (570 mL). The clear solution was placed in a bath cooled to $-20\text{ }^{\circ}\text{C}$. After 30 minutes *n*-butyllithium (529 mL, 2.17 M in hexanes, 1.15 mol, 3.10 eq.) was added dropwise over 2.5 hours. The dark golden-yellow solution was placed in an ice bath cooled to $0\text{ }^{\circ}\text{C}$ for 2.5 hours. The dark red-orange mixture was placed in a bath cooled to $-20\text{ }^{\circ}\text{C}$ for 30 minutes upon which iodomethane (92.0 mL, 1.48 mol, 4.00 eq.) was added dropwise over 30 minutes while stirring vigorously (800 rpm). The pale yellow solution was placed in a bath cooled to $0\text{ }^{\circ}\text{C}$ for 30 minutes and then acidified to a pH = 7 with 1 N HCl (500 mL). The biphasic mixture was diluted with EtOAc (200 mL), poured into a separatory funnel and partitioned. Residual organics were extracted from the aqueous layer using ethyl acetate (4 x 200 mL). The combined organics were washed with brine (1 x 200 mL), dried over solid Na_2SO_4 , decanted, and concentrated to afford the product as a crude brown oil (67.4 g) which was used directly in the next reaction without purification. The spectral data matches that of the reported compound (Cook, S.P. and Danishefsky, S.J. *Organic Letters* **2006**, 8, 5693).

$^1\text{H-NMR}$ (400 MHz, CDCl_3): δ 6.96 (d, 1H, $J = 8.2\text{ Hz}$), 6.77 (d, 1H, $J = 8.2\text{ Hz}$), 5.72 (bs, 1H), 4.36 (s, 2H), 3.77 (s, 3H), 3.37 (s, 3H), 2.29 (s, 3H)

$^{13}\text{C-NMR}$ (100 MHz, CDCl_3) : δ 148.2, 145.2, 130.0, 128.5, 125.6, 111.8, 72.8, 60.4, 57.5, 11.2

IR (film, cm^{-1}): 3367, 2928, 1603, 1491, 1460, 1290, 1177, 1070.

HRMS (FAB): calcd. For $\text{C}_{10}\text{H}_{14}\text{O}_3$ [M] 182.0943, found 182.0947.



To a solution of the crude brown oil (67.4 g, 370 mmol, 1.00 eq) in acetone (1.2 L) was added potassium carbonate (102 g, 740 mmol, 2.00 eq.) and dimethyl sulfate (56.0 mL, 444 mmol, 1.49 eq) sequentially. The mixture was placed in an oil bath heated to 56 °C and stirred vigorously (800 rpm) for 48 hours. The heterogeneous mixture was removed from the oil bath, filtered over a pad of celite using acetone, and concentrated. The resulting brown oil was purified by silica gel chromatography; toluene → 4% EtOAc in toluene to afford the trimethyl ether **148** as a clear pale yellow oil (64.0 g, 294 mmol, 84% two steps).

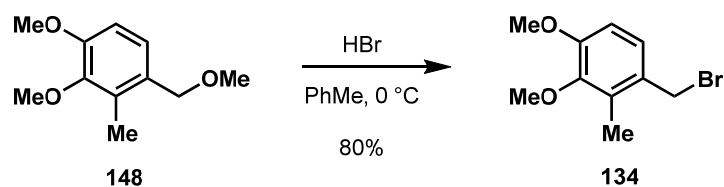
R_f = 0.43 (30% EtOAc in hexane)

$^1\text{H-NMR}$ (400 MHz, CDCl_3): δ 7.00 (d, 1H, J = 8.2 Hz), 6.72 (d, 1H, J = 8.2 Hz), 4.37 (s, 2H), 3.84 (s, 3H), 3.78 (s, 3H), 3.37 (s, 3H), 2.27 (s, 3H)

$^{13}\text{C-NMR}$ (100MHz, CDCl_3): δ 152.7, 147.6, 131.5, 129.6, 125.1, 109.1, 73.4, 60.4, 58.2, 55.9, 11.5

IR (neat film, cm^{-1}): 2932, 2821, 1604, 1492, 1456, 1380, 1271, 1223, 1083, 1007, 805

HRMS (EC-Cl): calcd. for $\text{C}_{11}\text{H}_{16}\text{O}_3$ [M] 196.1099, found 196.1097.



A solution of the trimethyl ether **148** (9.8 g, 50.0 mmol, 1.00 eq.) in toluene (125 mL) was placed in an ice water bath cooled to 0 °C, stirred vigorously (1000 rpm) for 20 minutes, and then concentrated HBr (48% w/v, 29.4 mL, 260 mmol, 5.20 eq.) was added. The brown biphasic mixture was stirred for 2 hours upon which the excess acid was slowly quenched with a saturated aqueous mixture of NaHCO₃ (100 mL). The biphasic mixture was poured into a separatory funnel, partitioned, and residual organics were extracted from the aqueous layer using toluene (3 x 50 mL). The combined organics were washed with brine (1 x 50 mL), dried over solid Na₂SO₄, decanted, and concentrated. Recrystallization of the brown solid from hexane (30 mL) provided the bromide **134** as white needles (9.8 g, 40.0 mmol, 80%).

¹H-NMR (400 MHz, CDCl₃): δ 7.06 (d, 1H, *J* = 8.2 Hz), 6.72 (d, 1H, *J* = 8.2 Hz), 4.52 (s, 2H), 3.85 (s, 3H), 3.79 (s, 3H), 2.33 (s, 3H)

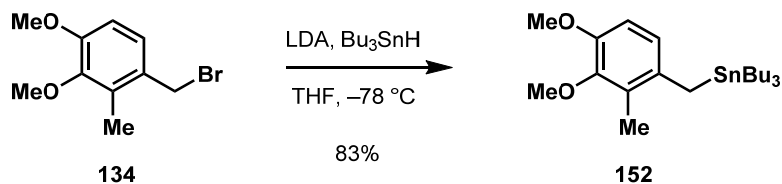
¹³C-NMR (100 MHz, CDCl₃): δ 153.49, 147.82, 132.00, 129.12, 126.07, 109.67, 60.54, 55.89, 33.66, 11.67

IR (neat film, cm⁻¹): 1602, 1456, 1441, 1313, 1276, 1083, 1000, 807, 684, 661

HRMS (EC-CI): calcd. for C₁₀H₁₄O₂Br(79) [M+H]⁺ 245.0177, found 245.0179

HRMS (EC-CI): calcd. for C₁₀H₁₄O₂Br(81) [M+H]⁺ 247.0157, found 245.0154

M.P.: 66 – 68 °C.



A solution of diisopropylamine (10.4 mL, 74.1 mmol, 1.10 eq.) in THF (340 mL) was placed in a bath cooled to $-78\text{ }^\circ\text{C}$ for 30 minutes. *n*-Butyllithium (37.8 mL, 74.1 mmol, 1.10 eq., 1.96 M in hexane) was added dropwise over 15 minutes. The clear colorless solution was stirred for 5 minutes, placed in an ice water cooling bath, and stirred for 30 minutes. Tri-*n*-butyltin hydride (19.9 mL, 74.1 mmol, 1.10 eq.) was added dropwise over 10 minutes to the clear pale yellow solution of LDA and stirred for 20 minutes. The olive green solution was placed in a bath cooled to $-78\text{ }^\circ\text{C}$ for 30 minutes upon which a solution of the bromide **134** (16.5 g, 67.4 mmol, 1.00 eq.) in THF (310 mL) was added under nitrogen via cannula to the olive green solution over 3 hrs. Residual bromide **152** in the vessel was dissolved in THF (10 mL) and transferred via cannula to the now pale yellow colored reaction solution. This process was repeated twice more. After 1 hr. the pale yellow solution was placed in an ice bath cooled to $0\text{ }^\circ\text{C}$, stirred for 10 minutes, and excess tri-*n*-butylstannyl lithium was quenched with an aqueous phosphate buffer (100 mL, pH = 7, 0.2 M). The biphasic mixture was poured into a separatory funnel, partitioned, and residual organics were extracted from the aqueous layer with ethyl ether (3 x 50 mL). The combined organics were washed with brine (1 x 100 mL), dried over solid Na_2SO_4 , decanted, and concentrated. The crude pale yellow oil was purified using silica gel chromatography; hexane (1.5 L) and then toluene to provide the stannane **152** as a clear colorless oil (25.4 g, 55.9 mmol, 83%).

$R_f = 0.69$ (30% EtOAc in hexane)

$^1\text{H-NMR}$ (400 MHz, CDCl_3): δ 6.68 (d, 1H, $J = 8.2$ Hz), 6.63 (d, 1H, $J = 8.2$ Hz), 3.81 (s, 3H), 3.75 (s, 3H), 2.22 (s, 2H), 2.12 (s, 3H), 1.43 – 1.35 (m, 6H), 1.27 – 1.21 (q, 6H, $J = 7.3$ Hz), 0.85 (t, 9H, $J = 7.3$ Hz), 0.77 (dd, 6H, $J = 8.2, 6.5$ Hz)

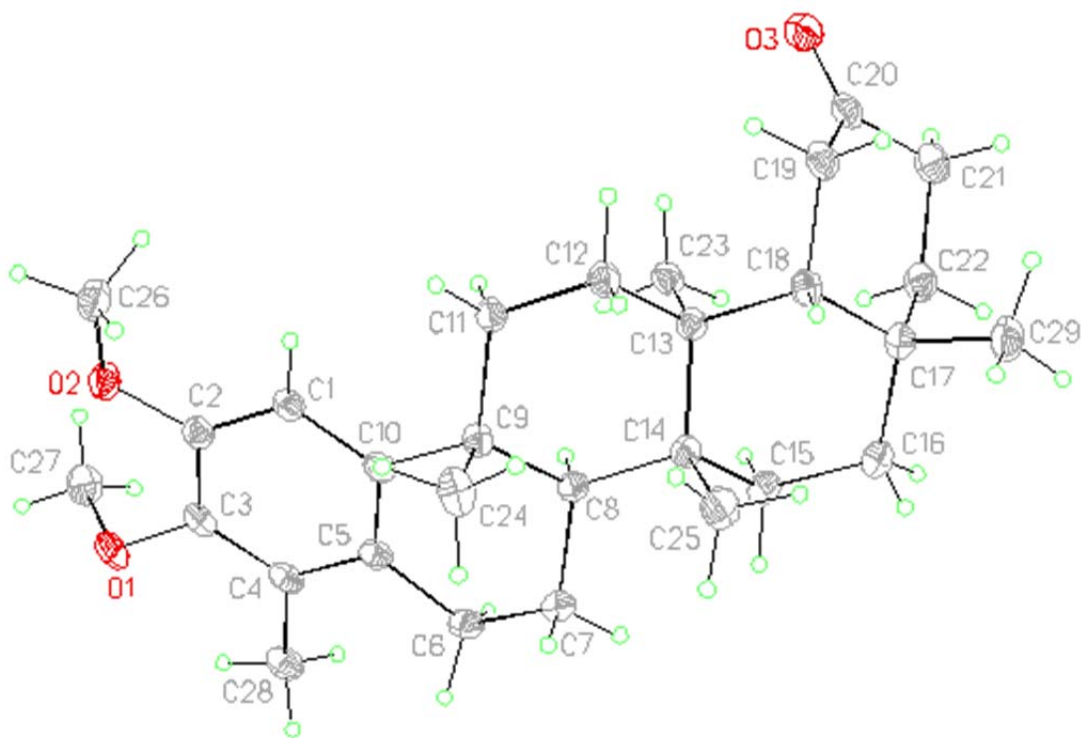
$^{13}\text{C-NMR}$ (100 MHz, CDCl_3): δ 149.11, 147.66, 135.57, 127.93, 122.57, 110.15, 60.40, 56.11, 29.25, 27.60, 15.80, 13.91, 12.75, 9.90

IR (neat film, cm^{-1}): 2955, 2925, 1486, 1465, 1456, 1272, 1086, 1223, 1083, 1007, 805

HRMS (EC-CI): calcd. for $\text{C}_{22}\text{H}_{40}\text{O}_2\text{Sn}$ [M] 456.2050, found 456.2057.

4. Crystallographic Information for Pentacyclic Ketone 175

Crystal Structure of ketone 175. View of 175 showing the atom labeling scheme. Displacement ellipsoids are scaled to the 50% probability level.



The crystals grew as large colorless prisms by slow evaporation from methanol. The data crystal was cut from a larger crystal and had approximate dimensions; 0.25 x 0.16 x 0.12 mm. The data were collected on a Rigaku AFC12 diffractometer with a Saturn 724+ CCD using a graphite monochromator with MoK α radiation ($\lambda = 0.71073\text{\AA}$). A total of 1832 frames of data were collected using ω -scans with a scan range of 0.5° and a counting time of 36 seconds per frame. The data were collected at 100 K using a Rigaku XStream low temperature device. Details of crystal data, data

collection and structure refinement are listed in Table 1. Data reduction were performed using the Rigaku Americas Corporation's Crystal Clear version 1.40.¹ The structure was solved by direct methods using SIR97² and refined by full-matrix least-squares on F^2 with anisotropic displacement parameters for the non-H atoms using SHELXL-97.³ Structure analysis was aided by use of the programs PLATON98⁴ and WinGX.⁵ The hydrogen atoms on carbon were calculated in ideal positions with isotropic displacement parameters set to 1.2xUeq of the attached atom (1.5xUeq for methyl hydrogen atoms).

The function, $\sum w(|F_o|^2 - |F_c|^2)^2$, was minimized, where $w = 1/[(\sigma(F_o))^2 + (0.0503*P)^2 + (0.8402*P)]$ and $P = (|F_o|^2 + 2|F_c|^2)/3$. $R_w(F^2)$ refined to 0.107, with $R(F)$ equal to 0.0409 and a goodness of fit, S , = 1.04. Definitions used for calculating $R(F)$, $R_w(F^2)$ and the goodness of fit, S , are given below.⁶ The data were checked for secondary extinction effects but no correction was necessary. Neutral atom scattering factors and values used to calculate the linear absorption coefficient are from the International Tables for X-ray Crystallography (1992).⁷ All figures were generated using SHELXTL/PC.⁸ Tables of positional and thermal parameters, bond lengths and angles, torsion angles and figures are found elsewhere.

Table 2.10. Crystal data and structure refinement for **175**.

Empirical formula	C ₂₉ H ₄₂ O ₃	
Formula weight	438.62	
Temperature	100(2) K	
Wavelength	0.71073 Å	
Crystal system	monoclinic	
Space group	P 21/n	
Unit cell dimensions	a = 15.2493(6) Å	α = 90°.
	b = 7.6076(3) Å	β = 98.2440(10)°.
	c = 20.7445(8) Å	γ = 90°.
Volume	2381.71(16) Å ³	
Z	4	
Density (calculated)	1.223 Mg/m ³	
Absorption coefficient	0.077 mm ⁻¹	
F(000)	960	
Crystal size	0.250 x 0.160 x 0.120 mm ³	
Theta range for data collection	2.999 to 27.485°.	
Index ranges	-19 ≤ h ≤ 19, -9 ≤ k ≤ 9, -26 ≤ l ≤ 26	
Reflections collected	41833	
Independent reflections	5445 [R(int) = 0.0534]	
Completeness to theta = 25.242°	99.9 %	
Absorption correction	Semi-empirical from equivalents	
Max. and min. transmission	1.00 and 0.810	
Refinement method	Full-matrix least-squares on F ²	
Data / restraints / parameters	5445 / 0 / 296	
Goodness-of-fit on F ²	1.040	
Final R indices [I > 2σ(I)]	R1 = 0.0409, wR2 = 0.1029	
R indices (all data)	R1 = 0.0482, wR2 = 0.1070	
Extinction coefficient	n/a	
Largest diff. peak and hole	0.298 and -0.172 e.Å ⁻³	

Table 2.11. Atomic coordinates ($\times 10^4$) and equivalent isotropic displacement parameters ($\text{\AA}^2 \times 10^3$) for 1. U(eq) is defined as one third of the trace of the orthogonalized U^{ij} tensor.

	x	y	z	U(eq)
C1	2648(1)	5262(2)	3690(1)	17(1)
C2	3181(1)	6309(2)	3364(1)	17(1)
C3	4104(1)	6050(2)	3467(1)	18(1)
C4	4477(1)	4749(2)	3890(1)	18(1)
C5	3924(1)	3632(1)	4199(1)	16(1)
C6	4350(1)	2158(2)	4623(1)	19(1)
C7	3696(1)	831(2)	4832(1)	20(1)
C8	2878(1)	1785(1)	5009(1)	15(1)
C9	2368(1)	2642(2)	4380(1)	16(1)
C10	3007(1)	3902(1)	4103(1)	16(1)
C11	1547(1)	3625(2)	4552(1)	20(1)
C12	996(1)	2535(2)	4968(1)	21(1)
C13	1530(1)	1885(1)	5612(1)	16(1)
C14	2312(1)	707(1)	5438(1)	16(1)
C15	2871(1)	180(2)	6088(1)	21(1)
C16	2342(1)	-936(2)	6514(1)	24(1)
C17	1415(1)	-246(2)	6615(1)	20(1)
C18	935(1)	743(2)	6000(1)	17(1)
C19	110(1)	1726(2)	6173(1)	20(1)
C20	243(1)	2810(2)	6785(1)	20(1)
C21	705(1)	1873(2)	7374(1)	24(1)
C22	1539(1)	902(2)	7236(1)	23(1)
C23	1855(1)	3546(2)	6007(1)	19(1)
C24	2051(1)	1364(2)	3811(1)	24(1)

Table 2.11, continued.

C25	1990(1)	-1021(2)	5086(1)	24(1)
C26	1933(1)	7580(2)	2713(1)	24(1)
C27	4740(1)	8805(2)	3293(1)	26(1)
C28	5472(1)	4503(2)	4004(1)	22(1)
C29	853(1)	-1860(2)	6745(1)	27(1)
O1	4633(1)	7001(1)	3105(1)	23(1)
O2	2868(1)	7565(1)	2916(1)	21(1)
O3	-50(1)	4295(1)	6806(1)	29(1)

Table 2.12. Bond lengths [Å] and angles [°] for **175**.

C1-C2	1.3824(15)	C13-C18	1.5604(15)
C1-C10	1.4037(15)	C13-C14	1.5745(15)
C1-H1	0.95	C14-C15	1.5407(15)
C2-O2	1.3704(13)	C14-C25	1.5497(15)
C2-C3	1.4061(15)	C15-C16	1.5338(16)
C3-O1	1.3828(13)	C15-H15A	0.99
C3-C4	1.3896(16)	C15-H15B	0.99
C4-C5	1.4142(15)	C16-C17	1.5509(16)
C4-C28	1.5134(15)	C16-H16A	0.99
C5-C10	1.3985(15)	C16-H16B	0.99
C5-C6	1.5138(15)	C17-C29	1.5434(16)
C6-C7	1.5249(16)	C17-C22	1.5452(16)
C6-H6A	0.99	C17-C18	1.5681(15)
C6-H6B	0.99	C18-C19	1.5491(16)
C7-C8	1.5326(15)	C18-H18	1.00
C7-H7A	0.99	C19-C20	1.5038(16)
C7-H7B	0.99	C19-H19A	0.99
C8-C14	1.5595(15)	C19-H19B	0.99
C8-C9	1.5632(15)	C20-O3	1.2179(15)
C8-H8	1.00	C20-C21	1.5001(17)
C9-C10	1.5362(15)	C21-C22	1.5340(17)
C9-C11	1.5436(15)	C21-H21A	0.99
C9-C24	1.5507(15)	C21-H21B	0.99
C11-C12	1.5319(15)	C22-H22A	0.99
C11-H11A	0.99	C22-H22B	0.99
C11-H11B	0.99	C23-H23A	0.98
C12-C13	1.5430(15)	C23-H23B	0.98
C12-H12A	0.99	C23-H23C	0.98
C12-H12B	0.99	C24-H24A	0.98
C13-C23	1.5485(15)	C24-H24B	0.98

Table 2.12, continued.

C24-H24C	0.98	C27-H27A	0.98
C25-H25A	0.98	C27-H27B	0.98
C25-H25B	0.98	C27-H27C	0.98
C25-H25C	0.98	C28-H28A	0.98
C26-O2	1.4277(14)	C28-H28B	0.98
C26-H26A	0.98	C28-H28C	0.98
C26-H26B	0.98	C29-H29A	0.98
C26-H26C	0.98	C29-H29B	0.98
C27-O1	1.4301(15)	C29-H29C	0.98
C2-C1-C10	121.18(10)	C6-C7-H7A	109.6
C2-C1-H1	119.4	C8-C7-H7A	109.6
C10-C1-H1	119.4	C6-C7-H7B	109.6
O2-C2-C1	124.15(10)	C8-C7-H7B	109.6
O2-C2-C3	116.37(10)	H7A-C7-H7B	108.2
C1-C2-C3	119.42(10)	C7-C8-C14	115.08(9)
O1-C3-C4	119.83(10)	C7-C8-C9	108.81(9)
O1-C3-C2	119.54(10)	C14-C8-C9	116.49(9)
C4-C3-C2	120.42(10)	C7-C8-H8	105.1
C3-C4-C5	119.77(10)	C14-C8-H8	105.1
C3-C4-C28	119.87(10)	C9-C8-H8	105.1
C5-C4-C28	120.34(10)	C10-C9-C11	111.29(9)
C10-C5-C4	119.82(10)	C10-C9-C24	104.63(9)
C10-C5-C6	121.91(10)	C11-C9-C24	107.79(9)
C4-C5-C6	118.27(10)	C10-C9-C8	107.77(8)
C5-C6-C7	114.32(9)	C11-C9-C8	109.38(9)
C5-C6-H6A	108.7	C24-C9-C8	115.94(9)
C7-C6-H6A	108.7	C5-C10-C1	119.29(10)
C5-C6-H6B	108.7	C5-C10-C9	122.04(10)
C7-C6-H6B	108.7	C1-C10-C9	118.37(9)
H6A-C6-H6B	107.6	C12-C11-C9	113.38(9)
C6-C7-C8	110.05(9)	C12-C11-H11A	108.9

Table 2.12, continued

C9-C11-H11A	108.9	C17-C16-H16B	108.0
C12-C11-H11B	108.9	H16A-C16-H16B	107.3
C9-C11-H11B	108.9	C29-C17-C22	107.94(9)
H11A-C11-H11B	107.7	C29-C17-C16	107.16(10)
C11-C12-C13	113.38(9)	C22-C17-C16	107.39(10)
C11-C12-H12A	108.9	C29-C17-C18	108.56(9)
C13-C12-H12A	108.9	C22-C17-C18	113.18(9)
C11-C12-H12B	108.9	C16-C17-C18	112.36(9)
C13-C12-H12B	108.9	C19-C18-C13	113.68(9)
H12A-C12-H12B	107.7	C19-C18-C17	110.10(9)
C12-C13-C23	106.62(9)	C13-C18-C17	116.69(9)
C12-C13-C18	110.58(9)	C19-C18-H18	105.1
C23-C13-C18	110.29(9)	C13-C18-H18	105.1
C12-C13-C14	107.92(9)	C17-C18-H18	105.1
C23-C13-C14	112.96(9)	C20-C19-C18	116.40(9)
C18-C13-C14	108.45(9)	C20-C19-H19A	108.2
C15-C14-C25	106.88(9)	C18-C19-H19A	108.2
C15-C14-C8	110.77(9)	C20-C19-H19B	108.2
C25-C14-C8	109.90(9)	C18-C19-H19B	108.2
C15-C14-C13	106.85(9)	H19A-C19-H19B	107.3
C25-C14-C13	113.09(9)	O3-C20-C21	122.92(11)
C8-C14-C13	109.30(9)	O3-C20-C19	122.21(11)
C16-C15-C14	112.17(10)	C21-C20-C19	114.73(10)
C16-C15-H15A	109.2	C20-C21-C22	112.44(10)
C14-C15-H15A	109.2	C20-C21-H21A	109.1
C16-C15-H15B	109.2	C22-C21-H21A	109.1
C14-C15-H15B	109.2	C20-C21-H21B	109.1
H15A-C15-H15B	107.9	C22-C21-H21B	109.1
C15-C16-C17	117.05(9)	H21A-C21-H21B	107.8
C15-C16-H16A	108.0	C21-C22-C17	114.98(10)
C17-C16-H16A	108.0	C21-C22-H22A	108.5
C15-C16-H16B	108.0	C17-C22-H22A	108.5

Table 2.12, continued.

C21-C22-H22B	108.5	H26A-C26-H26B	109.5
C17-C22-H22B	108.5	O2-C26-H26C	109.5
H22A-C22-H22B	107.5	H26A-C26-H26C	109.5
C13-C23-H23A	109.5	H26B-C26-H26C	109.5
C13-C23-H23B	109.5	O1-C27-H27A	109.5
H23A-C23-H23B	109.5	O1-C27-H27B	109.5
C13-C23-H23C	109.5	H27A-C27-H27B	109.5
H23A-C23-H23C	109.5	O1-C27-H27C	109.5
H23B-C23-H23C	109.5	H27A-C27-H27C	109.5
C9-C24-H24A	109.5	H27B-C27-H27C	109.5
C9-C24-H24B	109.5	C4-C28-H28A	109.5
H24A-C24-H24B	109.5	C4-C28-H28B	109.5
C9-C24-H24C	109.5	H28A-C28-H28B	109.5
H24A-C24-H24C	109.5	C4-C28-H28C	109.5
H24B-C24-H24C	109.5	H28A-C28-H28C	109.5
C14-C25-H25A	109.5	H28B-C28-H28C	109.5
C14-C25-H25B	109.5	C17-C29-H29A	109.5
H25A-C25-H25B	109.5	C17-C29-H29B	109.5
C14-C25-H25C	109.5	H29A-C29-H29B	109.5
H25A-C25-H25C	109.5	C17-C29-H29C	109.5
H25B-C25-H25C	109.5	H29A-C29-H29C	109.5
O2-C26-H26A	109.5	H29B-C29-H29C	109.5
O2-C26-H26B	109.5	C3-O1-C27	113.96(9)
		C2-O2-C26	116.20(9)

Table 2.13. Anisotropic displacement parameters ($\text{\AA}^2 \times 10^3$) for 1. The anisotropic displacement factor exponent takes the form: $-2\pi^2 [h^2 a^{*2} U^{11} + \dots + 2 h k a^* b^* U^{12}]$

	U ¹¹	U ²²	U ³³	U ²³	U ¹³	U ¹²
C1	14(1)	20(1)	17(1)	0(1)	4(1)	0(1)
C2	20(1)	17(1)	15(1)	-1(1)	4(1)	0(1)
C3	18(1)	20(1)	18(1)	-4(1)	8(1)	-4(1)
C4	15(1)	22(1)	17(1)	-6(1)	4(1)	-2(1)
C5	16(1)	18(1)	16(1)	-4(1)	3(1)	0(1)
C6	15(1)	22(1)	21(1)	-1(1)	3(1)	3(1)
C7	19(1)	19(1)	22(1)	0(1)	4(1)	4(1)
C8	15(1)	15(1)	16(1)	0(1)	2(1)	1(1)
C9	14(1)	18(1)	16(1)	1(1)	1(1)	-2(1)
C10	15(1)	17(1)	15(1)	-3(1)	3(1)	-1(1)
C11	14(1)	25(1)	20(1)	7(1)	3(1)	2(1)
C12	14(1)	28(1)	20(1)	7(1)	2(1)	0(1)
C13	15(1)	16(1)	16(1)	1(1)	2(1)	-1(1)
C14	17(1)	15(1)	17(1)	0(1)	2(1)	0(1)
C15	20(1)	22(1)	21(1)	4(1)	2(1)	4(1)
C16	26(1)	22(1)	24(1)	8(1)	5(1)	5(1)
C17	22(1)	18(1)	19(1)	3(1)	4(1)	-1(1)
C18	17(1)	18(1)	17(1)	0(1)	2(1)	-4(1)
C19	16(1)	25(1)	19(1)	3(1)	3(1)	-4(1)
C20	16(1)	22(1)	24(1)	1(1)	8(1)	-4(1)
C21	26(1)	28(1)	17(1)	-1(1)	4(1)	-3(1)
C22	24(1)	27(1)	16(1)	3(1)	1(1)	-1(1)
C23	19(1)	17(1)	23(1)	-1(1)	7(1)	-2(1)
C24	26(1)	28(1)	18(1)	-1(1)	2(1)	-10(1)
C25	29(1)	18(1)	26(1)	-3(1)	7(1)	-4(1)
C26	20(1)	27(1)	23(1)	8(1)	1(1)	-1(1)

Table 2.13, continued.

C27	26(1)	25(1)	29(1)	2(1)	6(1)	-7(1)
C28	16(1)	29(1)	23(1)	-4(1)	5(1)	-1(1)
C29	33(1)	20(1)	29(1)	5(1)	9(1)	-4(1)
O1	22(1)	26(1)	22(1)	-1(1)	11(1)	-6(1)
O2	19(1)	24(1)	22(1)	7(1)	4(1)	-2(1)
O3	31(1)	26(1)	33(1)	1(1)	13(1)	2(1)

Table 2.14. Hydrogen coordinates ($\times 10^4$) and isotropic displacement parameters ($\text{\AA}^2 \times 10^3$) for **175**.

	x	y	z	U(eq)
H1	2027	5467	3634	20
H6A	4697	2675	5018	23
H6B	4770	1528	4382	23
H7A	3984	159	5213	24
H7B	3515	-8	4473	24
H8	3118	2796	5288	18
H11A	1744	4715	4790	24
H11B	1167	3968	4144	24
H12A	748	1505	4712	25
H12B	492	3256	5069	25
H15A	3395	-493	5997	25
H15B	3085	1256	6330	25
H16A	2703	-1067	6947	29
H16B	2267	-2124	6318	29
H18	694	-207	5692	20
H19A	-112	2510	5804	24
H19B	-358	848	6212	24
H21A	291	1018	7527	29
H21B	871	2738	7727	29
H22A	1751	143	7614	27
H22B	2008	1780	7197	27
H23A	2268	4198	5776	29
H23B	2156	3197	6437	29
H23C	1347	4295	6058	29
H24A	1849	2041	3416	36
H24B	1562	645	3924	36

Table 2.14, continued.

H24C	2543	599	3735	36
H25A	2497	-1637	4949	36
H25B	1558	-747	4702	36
H25C	1713	-1772	5383	36
H26A	1734	6397	2575	35
H26B	1791	8399	2349	35
H26C	1633	7956	3077	35
H27A	4156	9351	3283	39
H27B	5071	9421	2990	39
H27C	5066	8879	3735	39
H28A	5755	5452	3789	34
H28B	5623	3369	3825	34
H28C	5684	4530	4473	34
H29A	1177	-2568	7096	40
H29B	732	-2571	6349	40
H29C	291	-1465	6875	40

Table 2.15. Torsion angles [°] for **175**.

C10-C1-C2-O2	174.68(10)	C24-C9-C10-C5	-95.42(12)
C10-C1-C2-C3	-2.43(16)	C8-C9-C10-C5	28.53(14)
O2-C2-C3-O1	-2.30(15)	C11-C9-C10-C1	-37.93(13)
C1-C2-C3-O1	175.03(10)	C24-C9-C10-C1	78.21(12)
O2-C2-C3-C4	-177.01(10)	C8-C9-C10-C1	-157.85(9)
C1-C2-C3-C4	0.31(16)	C10-C9-C11-C12	-166.91(9)
O1-C3-C4-C5	-172.15(10)	C24-C9-C11-C12	78.90(12)
C2-C3-C4-C5	2.55(16)	C8-C9-C11-C12	-47.96(12)
O1-C3-C4-C28	6.26(16)	C9-C11-C12-C13	57.12(13)
C2-C3-C4-C28	-179.04(10)	C11-C12-C13-C23	61.70(12)
C3-C4-C5-C10	-3.34(16)	C11-C12-C13-C18	-178.39(9)
C28-C4-C5-C10	178.26(10)	C11-C12-C13-C14	-59.93(12)
C3-C4-C5-C6	176.21(10)	C7-C8-C14-C15	59.42(12)
C28-C4-C5-C6	-2.19(15)	C9-C8-C14-C15	-171.47(9)
C10-C5-C6-C7	10.20(15)	C7-C8-C14-C25	-58.46(12)
C4-C5-C6-C7	-169.35(10)	C9-C8-C14-C25	70.66(12)
C5-C6-C7-C8	-40.62(13)	C7-C8-C14-C13	176.88(9)
C6-C7-C8-C14	-160.82(9)	C9-C8-C14-C13	-54.00(12)
C6-C7-C8-C9	66.37(11)	C12-C13-C14-C15	176.24(9)
C7-C8-C9-C10	-58.27(11)	C23-C13-C14-C15	58.63(11)
C14-C8-C9-C10	169.67(9)	C18-C13-C14-C15	-63.94(11)
C7-C8-C9-C11	-179.38(9)	C12-C13-C14-C25	-66.45(11)
C14-C8-C9-C11	48.55(12)	C23-C13-C14-C25	175.94(9)
C7-C8-C9-C24	58.53(12)	C18-C13-C14-C25	53.38(12)
C14-C8-C9-C24	-73.53(12)	C12-C13-C14-C8	56.33(11)
C4-C5-C10-C1	1.28(16)	C23-C13-C14-C8	-61.28(11)
C6-C5-C10-C1	-178.26(10)	C18-C13-C14-C8	176.15(8)
C4-C5-C10-C9	174.84(10)	C25-C14-C15-C16	-58.41(12)
C6-C5-C10-C9	-4.70(16)	C8-C14-C15-C16	-178.11(9)
C2-C1-C10-C5	1.62(16)	C13-C14-C15-C16	62.93(12)
C2-C1-C10-C9	-172.18(10)	C14-C15-C16-C17	-48.94(14)
C11-C9-C10-C5	148.44(10)	C15-C16-C17-C29	152.96(11)

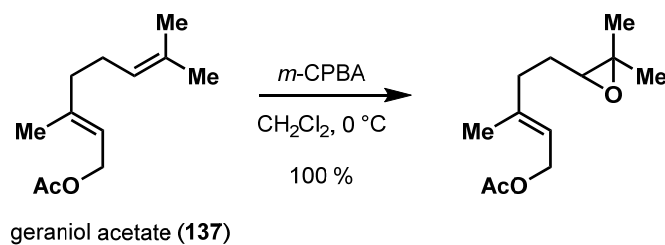
Table 2.15, continued.

C15-C16-C17-C22	-91.29(12)	C16-C17-C18-C13	-36.88(13)
C15-C16-C17-C18	33.80(14)	C13-C18-C19-C20	-85.46(12)
C12-C13-C18-C19	-58.99(12)	C17-C18-C19-C20	47.60(13)
C23-C13-C18-C19	58.69(12)	C18-C19-C20-O3	134.71(11)
C14-C13-C18-C19	-177.14(9)	C18-C19-C20-C21	-49.38(13)
C12-C13-C18-C17	171.19(9)	O3-C20-C21-C22	-136.65(12)
C23-C13-C18-C17	-71.14(12)	C19-C20-C21-C22	47.47(14)
C14-C13-C18-C17	53.04(12)	C20-C21-C22-C17	-48.16(14)
C29-C17-C18-C19	73.28(11)	C29-C17-C22-C21	-71.28(13)
C22-C17-C18-C19	-46.53(12)	C16-C17-C22-C21	173.48(10)
C16-C17-C18-C19	-168.38(9)	C18-C17-C22-C21	48.89(13)
C29-C17-C18-C13	-155.22(10)	C4-C3-O1-C27	-111.35(12)
C22-C17-C18-C13	84.97(12)	C2-C3-O1-C27	73.90(13)
		C1-C2-O2-C26	-9.63(16)
		C3-C2-O2-C26	167.55(10)

References

- 1) CrystalClear 1.40 (2008). Rigaku Americas Corporation, The Woodlands, TX.
- 2) SIR97. (1999). A program for crystal structure solution. Altomare A., Burla M.C., Camalli M., Cascarano G.L., Giacovazzo C. , Guagliardi A., Moliterni A.G.G., Polidori G., Spagna R. J. Appl. Cryst. 32, 115-119.
- 3) Sheldrick, G. M. (2008). SHELXL-2013. Program for the Refinement of Crystal Structures. Acta Cryst., A64, 112-122.
- 4) Spek, A. L. (1998). PLATON, A Multipurpose Crystallographic Tool. Utrecht University, The Netherlands.
- 5) WinGX 1.64. (1999). An Integrated System of Windows Programs for the Solution, Refinement and Analysis of Single Crystal X-ray Diffraction Data. Farrugia, L. J. J. Appl. Cryst. 32. 837-838.
- 6) $R_w(F^2) = \{\sum w(|F_o|^2 - |F_c|^2)^2 / \sum w(|F_o|^4)\}^{1/2}$ where w is the weight given each reflection.
 $R(F) = \sum(|F_o| - |F_c|) / \sum |F_o|$ for reflections with $F_o > 4(\sigma(F_o))$.
 $S = [\sum w(|F_o|^2 - |F_c|^2)^2 / (n - p)]^{1/2}$, where n is the number of reflections and p is the number of refined parameters.
- 7) International Tables for X-ray Crystallography (1992). Vol. C, Tables 4.2.6.8 and 6.1.1.4, A. J. C. Wilson, editor, Boston: Kluwer Academic Press.
- 8) Sheldrick, G. M. (1994). SHELXTL/PC (Version 5.03). Siemens Analytical X-ray Instruments, Inc., Madison, Wisconsin, USA.

5. Experimental Procedures for the Synthesis of the Iodo-enoate 143



A solution of geranyl acetate (5.20 g, 5.7 mL, 26.3 mmol, 1.00 eq.) in methylene chloride (176 mL) was placed in an ice water bath cooled to 0 °C for 20 minutes. *m*-CPBA (6.49 g, 26.3 mmol, 70% w/w, 1.00 eq.) was added in three separate portions over 15 minutes. After 45 minutes a saturated aqueous mixture of NaHCO₃ (25 mL) and a saturated aqueous mixture of Na₂S₂O₃ (25 mL) were added sequentially to the white heterogeneous reaction mixture. The biphasic mixture was poured into a separatory funnel, partitioned, and the organic layer was washed with a saturated aqueous mixture of Na₂S₂O₃ (1 x 20 mL) and a saturated aqueous mixture of NaHCO₃ (2 x 20 mL). Residual organics were extracted from the aqueous with methylene chloride (3 x 20 mL), dried over solid Na₂SO₄, decanted, and concentrated to afford the crude epoxide as a clear colorless oil (5.58 g) which was carried onto the next reaction without further purification.

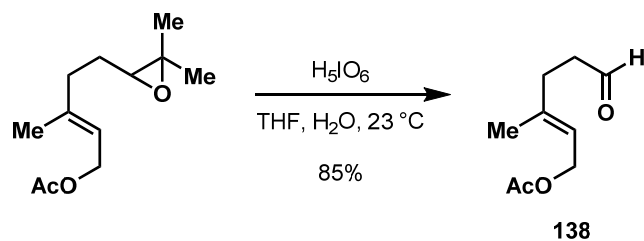
R_f = 0.30 (10% EtOAc in hexane)

¹H-NMR (400 MHz, CDCl₃): δ 5.40 – 5.36 (m, 1H), 4.59 (d, 2H, *J* = 7.2 Hz), 2.70 (t, 1H, *J* = 6.1 Hz), 2.26 – 2.10 (m, 2H), 2.05 (s, 3H), 1.72 (s, 3H), 1.70 – 1.63 (m, 2H), 1.30 (s, 3H), 1.29 (s, 3H)

¹³C-NMR (100 MHz, CDCl₃): δ 170.81, 141.04, 118.87, 63.72, 61.06, 58.18, 36.07, 26.94, 24.70, 20.86, 18.62, 16.32

IR (neat film, cm⁻¹): 1739, 1378, 1233, 1025

HRMS (EC-CI): calc'd. for C₁₀H₁₇O [M-AcOH]⁻, 153.1279 found. 153.1278



A biphasic solution of the crude epoxide (5.58 g, 26.3 mmol, 1.00 eq.) in THF-water (130 mL, 1:1) was placed in an ice water bath cooled to 0 °C for 20 minutes. Periodic acid (6.59 g, 28.9 mmol, 1.10 eq.) was added in four separate portions over 20 minutes. After 1 hr the excess acid was neutralized with a saturated aqueous mixture of NaHCO₃ (25 mL). The colorless biphasic solution was diluted with ethyl ether (50 mL), poured into a separatory funnel, and partitioned. The residual organics were extracted from the aqueous layer with ethyl ether (4 x 25 mL), dried over solid Na₂SO₄, decanted, and concentrated. The crude pale yellow oil was purified by silica gel chromatography; 15% EtOAc in hexane to afford the aldehyde **138** as a clear colorless oil (3.81 g, 22.4 mmol, 85%).

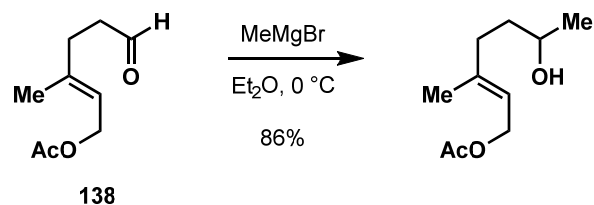
R_f = 0.37 (20% EtOAc in hexane)

¹H-NMR (400 MHz, CDCl₃): δ 9.78 (t, 1H, *J* = 1.7 Hz), 5.36 (tq, 1H, *J* = 1.4 Hz), 4.57 (d, 2H, *J* = 7.2 Hz), 2.59 – 2.54 (m, 2H), 2.38 (t, 2H, *J* = 7.5 Hz), 2.05 (s, 3H), 1.72 (s, 3H)

¹³C-NMR (100 MHz, CDCl₃): δ 201.91, 171.23, 140.20, 119.50, 61.29, 41.91, 31.62, 21.21, 16.80

IR (neat film, cm⁻¹): 1733, 1384, 1025

HRMS (EC-Cl): calc'd. for C₇H₁₀O [M-AcOH]⁻, 110.0732 found. 110.0732



A solution of the aldehyde (76.0 mg, 0.45 mmol, 1.00 eq.) in ethyl ether (4.5 mL) was placed in an ice water bath cooled to 0 °C for 30 minutes. Methyl magnesiumbromide (0.21 mL, 0.63 mmol, 1.40 eq., 3 M in ethyl ether) was added via syringe. After 15 minutes an aqueous phosphate buffer (5 mL, pH = 7, 0.2 M) was added to the white heterogenous mixture to neutralize the excess Grignard and alkoxide. The biphasic mixture was poured into a separatory funnel, and partitioned. The residual organics were extracted from the aqueous layer with ethyl ether (3 x 10 mL), combined, dried over solid Na₂SO₄, decanted, and concentrated. The crude pale yellow oil was purified by silica gel chromatography; 15% EtOAc in hexane to afford the alcohol (71.4 mg, 0.38 mmol, 86%) as a clear colorless oil.

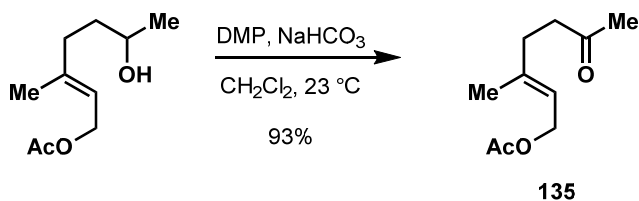
R_f = 0.19 (30% EtOAc in hexane)

¹H-NMR (400 MHz, CDCl₃): δ 5.37 (dt, 1H, *J* = 1.0, 7.1 Hz), 4.58 (d, 2H, *J* = 7.1 Hz), 3.79 (q, 1H, *J* = 6.1 Hz), 2.21 – 2.06 (m, 2H), 2.05 (s, 3H), 1.71 (s, 3H), 1.62 – 1.54 (m, 2H), 1.39 (bs, 1H), 1.20 (d, 3H, *J* = 6.1 Hz)

¹³C-NMR (100 MHz, CDCl₃): δ 171.07, 142.06, 110.30, 67.60, 61.21, 36.86, 35.66, 23.41, 20.93, 16.33

IR (neat film, cm⁻¹): 3411, 2966, 2930, 1739, 1235

HRMS (EC-CI): calc'd. for C₁₀H₁₉O₃ [M+H]⁺, 187.1334 found. 187.1331



To a mixture of the alcohol (0.30 g, 1.61 mmol, 1.00 eq.) and solid NaHCO₃ (0.54 g, 6.44 mmol, 4.00 eq.) in methylene chloride (16.0 mL) was added Dess-Martin periodinane (0.82 g, 1.93 mmol, 1.20 eq.). After two hours a saturated aqueous mixture of NaHCO₃ (20 mL) and a saturated aqueous mixture of Na₂S₂O₃ (20 mL) were added to the white heterogeneous reaction mixture to quench the residual acetic acid and Dess-Martin periodinane. The biphasic mixture was stirred vigorously (1000 rpm) for 30 minutes, poured into a separatory funnel, and partitioned. The organic layer was washed with a saturated aqueous mixture of Na₂S₂O₃ (2 x 20 mL) and a saturated aqueous mixture of NaHCO₃ (1 x 20 mL). The residual organics were extracted from the aqueous layer with methylene chloride (2 x 20 mL), dried over solid Na₂SO₄, decanted, and concentrated. The crude pale yellow mixture was purified by silica gel chromatography; 15% EtOAc in hexane to provide the ketone **135** as a clear colorless oil (0.28 g, 1.50 mmol, 93%).

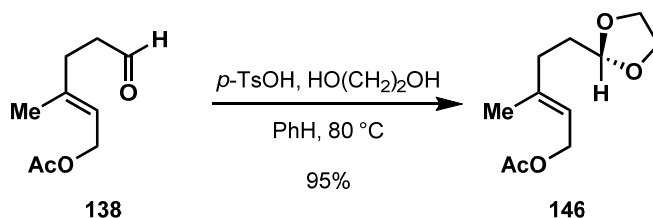
R_f = 0.51 (30% EtOAc in hexane)

¹H-NMR (400 MHz, CDCl₃): δ 5.33 (dt, 1H, *J* = 1.3 Hz), 4.57 (d, 2H, *J* = 6.8 Hz), 2.57 (t, 2H, *J* = 7.2 Hz), 2.31 (t, 2H, *J* = 7.2 Hz), 2.16 (s, 3H), 2.05 (s, 3H), 1.70 (s, 3H)

¹³C-NMR (100 MHz, CDCl₃): δ 207.95, 170.98, 140.64, 118.73, 61.11, 41.62, 33.00, 29.91, 20.97, 16.54

IR (neat film, cm⁻¹): 1738, 1718, 1367, 1234, 1024

HRMS (EC-CI): calc'd. for C₈H₁₃O [M-AcOH]⁻, 125.0966 found. 125.0963



A solution of the aldehyde **138** (3.47 g, 20.4 mmol, 1.00 eq.), ethylene glycol (12.7 g, 11.4 mL, 204 mmol, 10.0 eq.), and p -toluenesulfonic acid monohydrate (0.09 g, 0.41 mmol, 0.02 eq.) in benzene (68 mL) was placed in an oil bath heated to $80\text{ }^\circ\text{C}$. After 24 hrs the pale yellow solution was removed from oil bath, cooled to $23\text{ }^\circ\text{C}$, and an aqueous phosphate buffer (20 mL, pH = 7, 0.2 M) was added. The biphasic solution was poured into a separatory funnel, partitioned, and the organic layer was washed with water (2 x 20 mL). Residual organics were extracted from the aqueous layer with EtOAc (3 x 25 mL), dried over solid Na_2SO_4 , decanted, and concentrated. The crude yellow oil was purified by silica gel chromatography; 10% EtOAc in hexane to afford the dioxolane **146** as a clear colorless oil (4.15 g, 19.4 mmol, 95%).

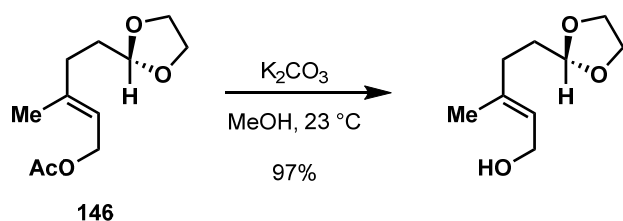
$R_f = 0.53$ (30% EtOAc in hexane)

$^1\text{H-NMR}$ (400 MHz, CDCl_3): δ 5.37 (tq, 1H, $J = 1.4, 6.8$ Hz), 4.86 (t, 1H, 4.8 Hz), 4.58 (d, 2H, $J = 6.8$ Hz), 3.97 – 3.83 (m, 4H), 2.16 (m, 2H), 2.05 (s, 3H), 1.79 (m, 2H), 1.71 (s, 3H)

$^{13}\text{C-NMR}$ (100 MHz, CDCl_3): δ 170.93, 141.31, 118.33, 103.91, 64.77, 61.51, 33.46, 31.83, 20.91, 16.35

IR (neat film, cm^{-1}): 2955, 2885, 1738, 1234, 1141, 1027

HRMS (EC-CI): calc'd. for $\text{C}_9\text{H}_{15}\text{O}_2$ $[\text{M}-\text{AcOH}]^-$, 155.1072 found. 155.1068



To a solution of the acetate **146** (2.53 g, 11.81 mmol, 1.00 eq.) in methanol (40 mL) was added solid K_2CO_3 (3.25 g, 23.62 mmol, 2.00 eq.). After 15 minutes an aqueous phosphate buffer (20 mL, pH = 7, 0.2 M) and EtOAc (50 mL) was added to the white heterogenous mixture. The biphasic solution was poured into a separatory funnel, partitioned, and the organic layer was washed with water (2 x 30 mL). The residual organics were extracted from the aqueous layer with EtOAc (3 x 20 mL), combined, dried over solid Na_2SO_4 , decanted, and concentrated. The crude colorless oil was purified by silica gel chromatography; 25% EtOAc in hexane to provide the alcohol product as a clear colorless oil (1.97 g, 11.44 mmol, 97%).

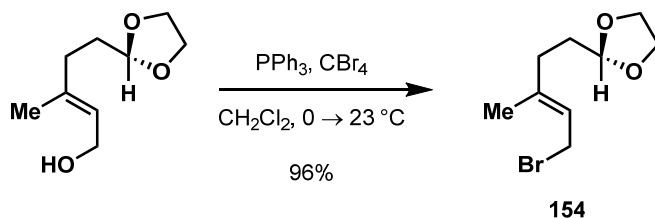
R_f = 0.42 (60% EtOAc in hexane)

1H -NMR (400 MHz, $CDCl_3$): δ 5.45 (dt, 1H, J = 1.0, 6.8 Hz), 4.86 (t, 1H, J = 4.8 Hz), 4.15 (d, 2H, J = 6.8 Hz), 3.99 – 3.84 (m, 4H), 2.15 (dd, 2H, J = 7.6, 8.5 Hz), 1.79 (m, 2H), 1.69 (s, 3H), 1.20 (bs, 1H)

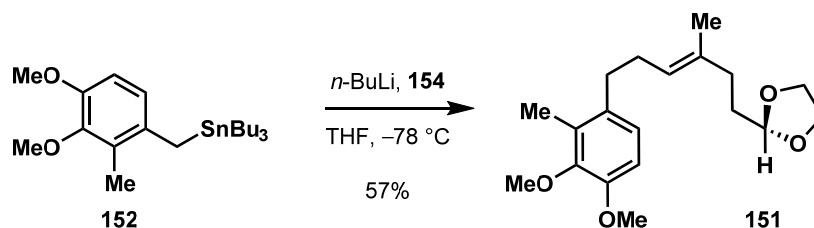
^{13}C -NMR (100 MHz, $CDCl_3$): δ 130.10, 123.72, 104.07, 64.76, 58.92, 33.57, 31.90, 16.17

IR (neat film, cm^{-1}): 3401, 2955, 2920, 1403, 1140, 1030

HRMS (EC-CI): calc'd. for $C_9H_{15}O_3$ $[M+H]^+$, 171.1021 found. 171.1022



A solution of CBr_4 (4.17 g, 12.58 mmol, 1.10 eq.) in methylene chloride (10 mL) was placed in an ice water bath cooled to $0 \text{ }^\circ\text{C}$ for 20 minutes and then solid Ph_3P (3.30 g, 12.58 mmol, 1.10 eq.) was added under a positive flow of nitrogen. After 10 minutes a solution of the alcohol (1.97 g, 11.44 mmol, 1.00 eq.) was added via syringe to the golden yellow reaction solution. After 2 hrs the golden yellow solution was removed from the cold bath and allowed to stir for 30 minutes at $23 \text{ }^\circ\text{C}$ upon which pentane (50 mL) was added. The heterogeneous mixture was suction filtered through a pad of celite and concentrated to $\sim 10 \text{ mL}$. Pentane (50 mL) was added and the mixture was placed in an ice water bath cooled to $0 \text{ }^\circ\text{C}$ for 10 minutes, suction filtered cold through a pad of celite, and concentrated to $\sim 10 \text{ mL}$. This process was repeated once more to afford the bromide **154** as a pale yellow oil (2.58 g, 10.98 mmol, 96%). The bromide was carried onto the next reaction without characterization.



A solution of the benzyl stannane **152** (100.0 mg, 0.22 mmol, 1.00 eq.) in freshly deoxygenated THF (1.1 mL) was placed in a bath cooled to $-78\text{ }^\circ\text{C}$. After 30 minutes n -butyllithium (0.11 mL, 0.24 mmol, 1.10 eq., 2.20 M in hexane) was added dropwise by syringe over 1 minute. After 1 hr the bromide **154** (72.3 mg, 0.31 mmol, 1.40 eq.) was added neat to the red-orange solution. After 1 hr the cold bath was removed and the golden yellow solution was warmed gradually to $23\text{ }^\circ\text{C}$. After 20 minutes the excess tolyl anion was neutralized with an aqueous phosphate buffer (10 mL, pH = 7, 0.2 M), the biphasic solution was poured into a separatory funnel, and partitioned. The residual organics were extracted from the aqueous layer with ethyl ether (3 x 10 mL), dried over solid Na_2SO_4 , decanted, and concentrated. The crude pale yellow oil was purified by silica gel chromatography; hexane \rightarrow 15% 1,4-dioxane in hexane to afford the arene **151** as a clear colorless oil (40.0 mg, 0.13 mmol, 57%).

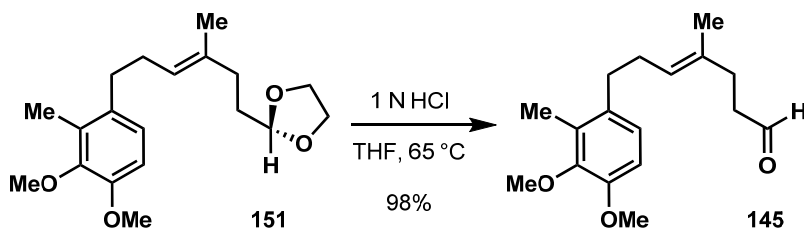
$R_f = 0.55$ (20% 1,4-dioxane in hexane)

$^1\text{H-NMR}$ (400 MHz, CDCl_3): δ 6.83 (d, 1H, $J = 8.2$ Hz), 6.69 (d, 1H, $J = 8.2$ Hz), 5.24 (m, 1H), 4.84 (t, 1H, $J = 4.8$ Hz), 3.99 – 3.84 (m, 4H), 3.83 (s, 3H), 3.77 (s, 3H), 2.55 (t, 2H, $J = 8.5$ Hz), 2.23 (s, 3H), 2.20 – 2.08 (m, 4H), 1.78 – 1.73 (m, 2H), 1.57 (s, 3H),

$^{13}\text{C-NMR}$ (100 MHz, CDCl_3): δ 151.01, 147.45, 135.07, 133.97, 130.44, 124.32, 109.51, 104.56, 65.09, 60.40, 55.89, 34.11, 33.38, 32.63, 29.19, 16.20, 11.95

IR (neat film, cm^{-1}): 2930, 1490, 1453, 1270, 1084

HRMS (EC-CI): calc'd. for $\text{C}_{19}\text{H}_{28}\text{O}_4$ [M], 320.1988 found. 320.1985



A biphasic solution of the dioxolane **151** (1.09 g, 3.39 mmol, 1.00 eq.) in THF (17 mL) and 1 N HCl (17 mL) was placed in an oil bath heated to 65 °C. After 12 hrs the pale yellow biphasic solution was removed from the oil bath, neutralized to pH = 7 using an aqueous phosphate buffer (50 mL, pH = 7, 0.2 M), poured into a separatory funnel containing ethyl ether (30 mL), and partitioned. Residual organics were extracted from the aqueous layer with ethyl ether (4 x 10 mL), washed with brine (1 x 20 mL), dried over solid Na₂SO₄, decanted, and concentrated. The crude pale yellow oil was purified by silica gel chromatography; 10% EtOAc in hexane to afford the aldehyde **145** as a clear colorless oil (0.92 g, 3.33 mmol, 98%).

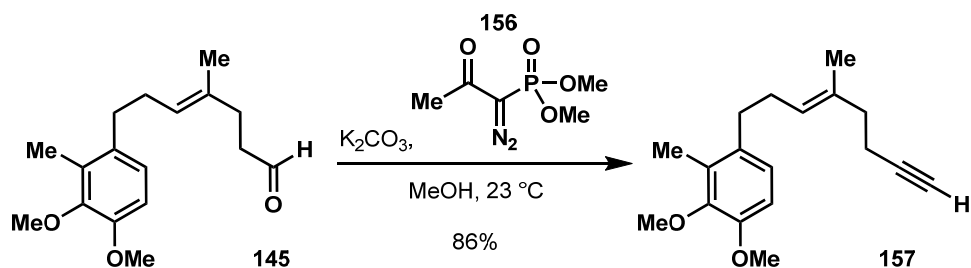
R_f = 0.55 (20% 1,4-dioxane in hexane)

¹H-NMR (400 MHz, CDCl₃): δ 9.75 (t, 1H, *J* = 1.7 Hz), 6.82 (d, 1H, *J* = 8.6 Hz), 6.69 (d, 1H, *J* = 8.6 Hz), 5.25 – 5.20 (m, 1H), 3.84 (s, 3H), 3.78 (s, 3H), 2.58 – 2.49 (m, 5H), 2.40 – 2.35 (m, 1H), 2.32 (t, 2H, *J* = 7.5 Hz), 2.28 (s, 3H), 1.56 (s, 3H)

¹³C-NMR (100 MHz, CDCl₃): δ 202.85, 151.08, 147.50, 133.88, 133.73, 130.42, 124.34, 109.52, 60.42, 55.92, 42.33, 33.27, 32.03, 29.12, 16.26, 11.96

IR (neat film, cm⁻¹): 2933, 2835, 1723, 1489, 1455, 1418, 1270, 1224, 1083, 1005, 804

HRMS (EC-CI): calc'd. for C₁₇H₂₄O₃ [M], 276.1725 found. 276.1725



A mixture of the aldehyde **145** (0.93 g, 3.33 mmol, 1.00 eq.) and K_2CO_3 (1.62 g, 11.73 mmol, 3.50 eq.) in methanol (16.8 mL) was placed in an ice water bath cooled to 0 °C for 20 minutes and then the Bestman-Ohira reagent **156** (1.61 g, 8.38 mmol, 2.50 eq.) was added neat. The yellow heterogeneous mixture was rapidly stirred (800 rpm) for 12 hrs warming gradually to 23 °C, diluted with an aqueous phosphate buffer (20 mL, pH = 7, 0.2 M) and EtOAc (20 mL), poured into a separatory funnel, and partitioned. The organic layer was washed with water (1 x 20 mL). Residual organics were extracted from the aqueous layer with EtOAc (3 x 10 mL), washed with brine (1 x 10 mL), dried over solid Na_2SO_4 , decanted, and concentrated. The crude pale yellow oil was purified by silica gel chromatography; benzene to afford the enyne **157** as a clear colorless oil (0.78 g, 2.88 mmol, 86%).

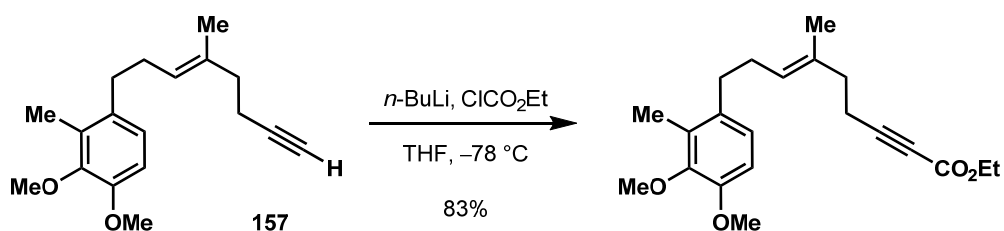
$R_f = 0.43$ (benzene)

$^1\text{H-NMR}$ (400 MHz, CDCl_3): δ 6.85 (d, 1H, $J = 8.2$ Hz), 6.70 (d, 1H, $J = 8.2$ Hz), 5.26 (t, 1H, $J = 7.2$ Hz), 3.84 (s, 3H), 3.77 (s, 3H), 2.60 – 2.54 (m, 2H), 2.30 – 2.23 (m, 2H), 2.23 (s, 3H), 2.23 – 2.18 (m, 4H), 1.96 (t, 1H, $J = 2.8$ Hz), 1.57 (s, 3H)

$^{13}\text{C-NMR}$ (100 MHz, CDCl_3): δ 150.81, 147.24, 133.87, 133.65, 130.21, 125.04, 124.11, 109.28, 84.38, 68.39, 60.16, 55.68, 38.40, 33.11, 28.92, 17.55, 15.73, 11.73

IR (neat film, cm^{-1}): 2929, 1492, 1270, 1085

HRMS (EC-CI): calc'd. for $\text{C}_{18}\text{H}_{24}\text{O}_2$ [M], 272.1776 found. 272.1777



A clear colorless solution of the enyne **157** (0.44 g, 1.62 mmol, 1.00 eq.) in THF (16.2 mL) was placed in a bath cooled to $-78\text{ }^\circ\text{C}$ for 30 minutes. *n*-Butyllithium (1.00 mL, 2.26 mmol, 1.40 eq., 2.2 M in hexane) was added via syringe. After 1 hr ethyl chloroformate (0.35 g, 0.31 mL, 3.23 mmol, 2.00 eq.) was added neat to the clear colorless solution. After 30 minutes the solution was diluted with an aqueous phosphate buffer (10 mL, pH = 7, 0.2 M) and the mixture was removed from the cold bath, diluted with ethyl ether (20 mL), poured into a separatory funnel, and partitioned. Residual organics were extracted from the aqueous layer with ethyl ether (3 x 10 mL), dried over solid Na_2SO_4 , decanted, and concentrated. The crude clear colorless oil was purified by silica gel chromatography; benzene to afford the ynoate product as a clear colorless oil (0.46 g, 1.34 mmol, 83%).

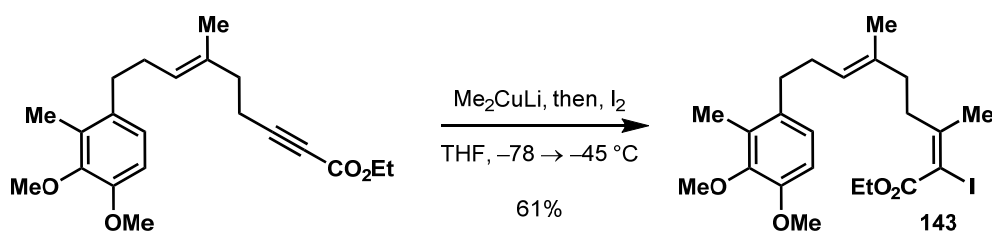
$R_f = 0.33$ (benzene)

$^1\text{H-NMR}$ (400 MHz, CDCl_3): δ 6.84 (d, 1H, $J = 8.6$ Hz), 6.70 (d, 1H, $J = 8.6$ Hz), 5.27 (t, 1H, $J = 6.8$ Hz), 4.21 (q, 2H, $J = 7.2$ Hz), 3.84 (s, 3H), 3.77 (s, 3H), 2.57 (t, 2H, $J = 8.2$ Hz), 2.41 (t, 7.9 Hz), 2.29 – 2.19 (m, 4H), 2.23 (s, 3H), 1.56 (s, 3H), 1.30 (t, 3H, $J = 7.1$ Hz)

$^{13}\text{C-NMR}$ (100 MHz, CDCl_3): δ 153.82, 150.83, 147.24, 133.52, 133.11, 130.15, 125.68, 124.13, 109.29, 88.99, 73.47, 61.75, 60.15, 55.66, 37.30, 33.03, 28.91, 17.82, 15.67, 14.04, 11.70

IR (neat film, cm^{-1}): 2933, 2234, 1711, 1492, 1250, 1082

HRMS (EC-CI): calc'd. for $\text{C}_{21}\text{H}_{28}\text{O}_4$ [M], 344.1988 found. 344.1985



A suspension of CuI (34.0 mg, 0.18 mmol, 2.05 eq.) in THF (0.46 mL) under nitrogen was placed in an ice water bath cooled to 0 °C. After 20 minutes methyl lithium (0.32 mL, 0.35 mmol, 4.00 eq., 1.10 M in Et₂O) was added. After 10 minutes the clear colorless solution was placed in a bath cooled to -78 °C. After 10 minutes a solution of the ynoate (30.0 mg, 0.09 mmol, 1.00 eq.) in THF (0.15 mL) was added by syringe in a dropwise fashion. After 1 hr a solution of iodine (66.3 mg, 0.26 mmol, 3.00 eq.) in THF (0.15 mL) was added under nitrogen via cannula in a dropwise fashion to the clear golden yellow solution. The purple solution was warmed to -45 °C and after 1 hr a saturated aqueous mixture of NH₄Cl (5 mL) was added. The blue mixture was removed from the cooling bath, diluted with Et₂O (5 mL), poured into a separatory funnel, partitioned, and the organic layer was washed with a saturated aqueous mixture of NH₄Cl (2 x 10 mL). Residual organics were extracted with Et₂O (2 x 10 mL), dried over solid Na₂SO₄, decanted, and concentrated. The crude brown amorphous oil was purified by silica gel chromatography; 2% benzene in toluene to afford the iodo-enoate **143** as a clear colorless oil (25.9 mg, 0.05 mmol, 61%).

R_f = 0.72 (10% Et₂O in benzene)

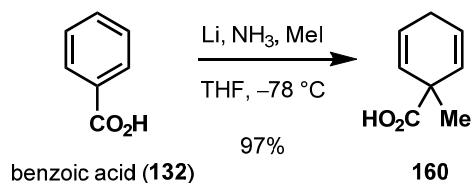
¹H-NMR (400 MHz, CDCl₃): δ 6.84 (d, 1H, *J* = 8.6 Hz), 6.70 (d, 1H, *J* = 8.6 Hz), 5.21 (t, 1H, *J* = 6.5 Hz), 4.24 (q, 2H, *J* = 7.2 Hz), 3.83 (s, 3H), 3.77 (s, 3H), 2.57 – 2.53 (m, 3H), 2.23 (s, 3H), 2.23 – 2.12 (m, 5H), 2.06 (s, 3H), 1.56 (s, 3H), 1.31 (t, 3H, *J* = 7.2 Hz)

¹³C-NMR (100 MHz, CDCl₃): δ 165.89, 154.30, 151.05, 147.50, 134.71, 134.63, 130.45, 124.61, 109.54, 85.68, 62.11, 60.39, 55.90, 38.33, 35.80, 33.43, 29.93, 29.68, 29.19, 16.07, 14.30, 11.96

IR (neat film, cm⁻¹): 2919, 1706, 1489, 1270, 1237, 1085

HRMS (EC-CI): calc'd. for C₂₂H₃₁O₄I [M], 486.1267 found. 486.1263

6. Experimental Procedures for Synthesis of Triene 165



A solution of benzoic acid (5.23 g, 42.8 mmol, 1.00 eq.) in THF (210 mL) was placed in a bath cooled to $-78\text{ }^\circ\text{C}$ and liquid ammonia (500 mL) was condensed. Lithium wire (0.95 g, 137 mmol, 3.20 eq.) was added as small chunks over 1 minute. After two hours iodomethane (30.4 g, 13.3 mL, 214 mmol, 5.00 eq.) was added to the blue mixture. The resultant white heterogeneous mixture was removed from the cold bath and the ammonia was evaporated using a positive flow of nitrogen. The mixture was placed in an ice water bath cooled to $0\text{ }^\circ\text{C}$ and water (150 mL) was added. The white mixture was acidified to $\text{pH} = 3$ using 1 N HCl, diluted with ethyl ether (100 mL), poured into a separatory funnel, and partitioned. Residual organics were extracted from the aqueous layer with ethyl ether (3 x 50 mL), washed with brine (1 x 50 mL), dried over solid Na_2SO_4 , decanted, and concentrated. The pale yellow oil was then purified by distillation under vacuum to afford the acid **160** as a clear pale amber oil (5.74 g, 41.5 mmol, 97%, b.p. = $85 - 92\text{ }^\circ\text{C}$ at 0.1 mmHg).

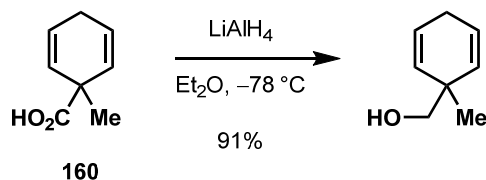
$R_f = 0.46$ (5% MeOH in CH_2Cl_2)

$^1\text{H-NMR}$ (400 MHz, CDCl_3): δ 10.75 (bs, 1H), 5.85 (dt, 2H, $J = 3.1, 10.2$ Hz), 5.77 (dt, 2H, $J = 1.7, 10.2$ Hz), 2.66 (m, 2H), 1.36 (s, 3H)

$^{13}\text{C-NMR}$ (100 MHz, CDCl_3): δ 181.67, 128.08, 124.90, 43.65, 27.22, 25.85

IR (neat film, cm^{-1}): 3035 - 2817, 1699, 1415, 1294, 1260, 1126, 942, 702

HRMS (EC-CI): calc'd. for $\text{C}_8\text{H}_{11}\text{O}_2$ $[\text{M}+\text{H}]^+$, 139.0759 found. 139.0759



A solution of the acid **160** (5.92 g, 42.8 mmol, 1.00 eq.) in ethyl ether (214 mL) was placed in a bath cooled to $-78\text{ }^\circ\text{C}$ for 30 minutes. Lithium aluminum hydride (24.0 mL, 96.0 mmol, 2.24 eq., 4.0 M in ethyl ether) was added dropwise by syringe over 5 minutes. After 10 minutes the colorless solution was diluted with ethyl ether (200 mL), placed in an ice water bath cooled to $0\text{ }^\circ\text{C}$, and residual LiAlH_4 was quenched by the cautious, slow sequential addition of water (5 mL), NaOH (5 mL, 15% in water), and water (15 mL). After 5 minutes an aqueous phosphate buffer (10 mL, $\text{pH} = 7$, 0.2 M) was added. After 2 minutes solid Na_2SO_4 was added and the solid mixture was stirred vigorously (1000 rpm). After 20 minutes the white mixture was suction filtered through a pad of solid Na_2SO_4 and concentrated to afford the pure alcohol as a clear colorless oil (4.84 g, 38.95 mmol, 91%). **NOTE:** The product is slightly volatile under reduced pressure.

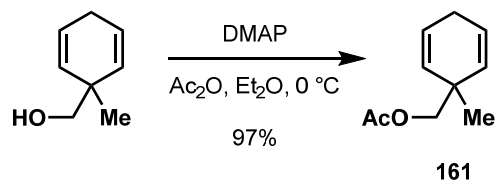
$R_f = 0.36$ (50% Et_2O in hexane)

$^1\text{H-NMR}$ (400 MHz, CDCl_3): δ 5.87 (dt, 2H, $J = 3.4, 10.6$ Hz), 5.43 (dt, 2H, $J = 2.1, 10.6$ Hz), 3.29 (d, 2H, $J = 5.4$ Hz), 2.63 (m, 2H), 1.60 (t, 1H, $J = 5.4$ Hz), 0.98 (s, 3H)

$^{13}\text{C-NMR}$ (100 MHz, CDCl_3): δ 131.34, 126.24, 71.08, 39.25, 26.65, 25.01

IR (neat film, cm^{-1}): 3363, 3015, 2958, 2924, 2865, 2818, 1421, 1376, 1040, 711

HRMS (EC-CI): calc'd. for $\text{C}_8\text{H}_{13}\text{O}$ $[\text{M}+\text{H}]^+$, 125.0966 found. 125.0967



A solution of the alcohol (4.84 g, 39.0 mmol, 1.00 eq.) and *N,N*-dimethylamino pyridine (10.47 g, 86.0 mmol, 2.21 eq.) in ethyl ether (430 mL) was placed in an ice water bath cooled to 0 °C for 30 minutes upon which acetic anhydride (12.0 mL, 129 mmol, 4.46 eq.) was added by syringe over 2 minutes. After 20 minutes the golden yellow solution was removed from the cold bath, warmed gradually to 23 °C over 20 minutes, and an aqueous phosphate buffer (100 mL, pH = 4, 0.2 M) was added. The biphasic solution was poured into a separatory funnel, partitioned, and the organic layer was washed with an aqueous phosphate buffer (2 x 50 mL, pH = 4, 0.2 M). Residual organics were extracted from the aqueous with ethyl ether (2 x 25 mL), combined, and washed with a saturated aqueous mixture of NaHCO₃ (2 x 50 mL). Residual organics were extracted from the aqueous NaHCO₃ layer with ethyl ether (1 x 25 mL), washed with brine (1 x 100 mL), dried over solid Na₂SO₄, decanted, and concentrated to afford the acetate **161** as a pure clear colorless oil (6.28 g, 37.8 mmol, 97%).

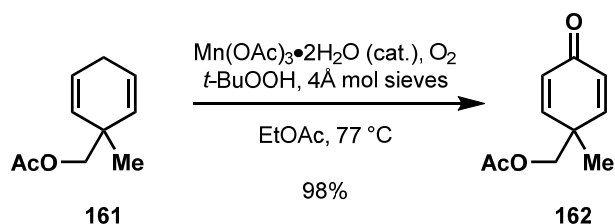
R_f = 0.67 (50% Et₂O in hexane)

¹H-NMR (400 MHz, CDCl₃): δ 5.75 (dt, 2H, *J* = 3.1, 10.2 Hz), 5.48 (dt, 2H, *J* = 2.1, 10.2 Hz), 3.85 (s, 2H), 2.60 (m, 2H), 2.02 (s, 3H), 1.04 (s, 3H)

¹³C-NMR (100 MHz, CDCl₃): δ 171.27, 130.93, 124.98, 71.74, 36.90, 26.55, 25.46, 21.12

IR (neat film, cm⁻¹): 3018, 2964, 2872, 1743, 1382, 1235, 1038

HRMS (EC-CI): calc'd. for C₈H₁₁ [M-AcOH]⁻, 107.0861 found. 107.0858



To a mixture of the acetate **161** (2.00 g, 12.03 mmol, 1.00 eq.), activated crushed mol sieves (1.0 g), and *t*-BuOOH (7.75 g, 8.3 mL, 60.2 mmol, 5.00 eq., 70% w/v) in EtOAc (80 mL) was added manganese triacetate dihydrate (0.32 g, 1.20 mmol, 0.10 eq.). The reaction vessel was equipped with a plastic PTFE cap and placed under an atmosphere of oxygen (balloon). The brown mixture was placed in an oil bath heated to 77 °C and stirred vigorously (800 rpm). After 12 hrs. the brown mixture was removed from the oil bath, cooled to 23 °C, suction filtered, concentrated, and purified by silica gel chromatography; 10% EtOAc in hexane → 30% EtOAc in hexane to afford the dienone **162** as a clear yellow oil (2.12 g, 11.8 mmol, 98%).

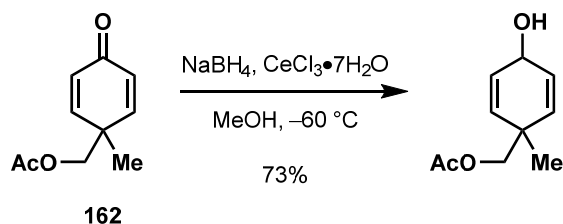
$R_f = 0.41$ (40% EtOAc in hexane)

$^1\text{H-NMR}$ (400 MHz, CDCl_3): δ 6.78 (d, 2H, $J = 10.5$ Hz), 6.26 (d, 2H, $J = 10.5$ Hz), 4.08 (s, 2H), 1.97 (s, 3H), 1.23 (s, 3H)

$^{13}\text{C-NMR}$ (100 MHz, CDCl_3): δ 185.69, 170.52, 151.94, 129.80, 68.31, 41.92, 21.70, 20.65

IR (neat film, cm^{-1}): 1743, 1668, 1628, 1403, 1378, 1248, 1042, 862

HRMS (ESI): calc'd. for $\text{C}_{10}\text{H}_{12}\text{O}_3\text{Na}$ $[\text{M}+\text{Na}]^+$, 203.0679 found. 203.6810



A solution of the dienone **162** (99.0 mg, 0.55 mmol, 1.00 eq.) in methanol (5.5 mL) was placed in a bath cooled to $-60\text{ }^{\circ}\text{C}$ for 30 minutes. Cerium trichloride heptahydrate (614 mg, 1.65 mmol, 3.00 eq.) was added and the mixture was stirred vigorously (800 rpm) for 30 minutes upon which the reaction mixture had become a clear pale yellow homogeneous solution and then solid NaBH_4 (22.9 mg, 0.60 mmol, 1.10 eq.) was added. After 30 minutes excess NaBH_4 and the alkoxide were quenched with an aqueous phosphate buffer (10 mL, pH = 7, 0.2 M). The mixture was removed from the cold bath, diluted with EtOAc (20 mL), poured into a separatory funnel, partitioned, and the organic layer was washed with an aqueous phosphate buffer (2 x 10 mL). Residual organics were extracted from the aqueous layer with EtOAc (3 x 15 mL), washed with brine (1 x 10 mL), dried over solid Na_2SO_4 , decanted, and concentrated. The crude pale yellow oil was purified by silica gel chromatography; 20% EtOAc in hexane to afford the alcohol as a clear pale yellow oil (73.0 mg, 0.40 mmol, 73%, d.r. = 1.5:1). **Note:** The crude alcohol can be carried on to the next step without purification.

Mixture of Isomers: (*) denotes minor isomer

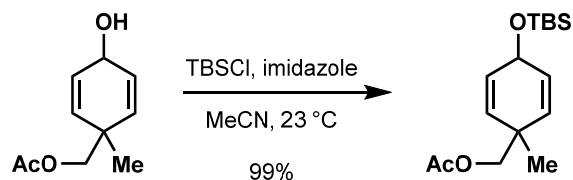
$R_f = 0.39$ (40% EtOAc in hexane)

$^1\text{H-NMR}$ (400 MHz, CDCl_3): δ 5.94 (m, 2H), 5.71 (t, 2H, $J = 10.2$ Hz), 5.49 (br d, 1H, $J = 12.6$ Hz), 3.92* (s, 2H), 3.87 (s, 2H), 2.05* (s, 3H), 2.02 (s, 3H), 1.58 (bs, 1H), 1.12* (s, 3H), 1.07 (s, 3H)

$^{13}\text{C-NMR}$ (100 MHz, CDCl_3): δ 170.94 (170.90*), 133.67, 133.20, 128.46, 128.14, (70.59*) 70.04, (62.22*) 62.06, (37.68*) 37.55, 24.27, 23.68, (20.90*) 20.85

IR (neat film, cm^{-1}): 3399, 2966, 1741, 1254, 1037

HRMS (ESI): calc'd. for $\text{C}_{10}\text{H}_{14}\text{O}_3\text{Na}$ $[\text{M}+\text{Na}]^+$, 205.0835 found. 205.0840



A solution of the alcohol (60.0 mg, 0.33 mmol, 1.00 eq.) in acetonitrile (3.3 mL) was placed in an ice water bath cooled to 0 °C for 10 minutes upon which a mixture of TBSCl (54.6 mg, 0.36 mmol, 1.10 eq.) and imidazole (29.0 mg, 0.43 mmol, 1.30 eq.) was added together. After 2 minutes the white mixture was removed from the cold bath and allowed to stir (500 rpm) at 23 °C. After 2 hrs the heterogeneous mixture was diluted with an aqueous phosphate buffer (10 mL, pH = 7, 0.2 M) and EtOAc (10 mL), poured into a separatory funnel, partitioned, and the organic layer was washed with an aqueous phosphate buffer (1 x 10 mL, pH = 7, 0.2 M). Residual organics were extracted with EtOAc (2 x 10 mL), dried over solid Na₂SO₄, decanted, and concentrated. The crude pale yellow mixture was purified by silica gel chromatography; 2% EtOAc in hexane to afford the silyl ether product as a clear pale yellow oil (97.0 mg, 0.33 mmol, 99%).

Mixture of Isomers: (*) denotes minor isomer

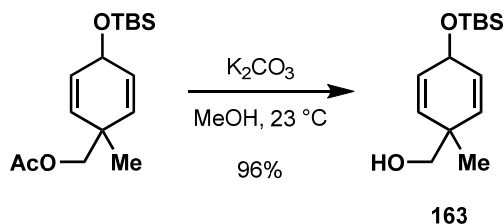
R_f = 0.75 (10% EtOAc in hexane)

¹H-NMR (400 MHz, CDCl₃): δ 5.80 (ddd, 2H, *J* = 2.8, 10.2 Hz), 5.66* (dd, 2H, *J* = 1.7, 10.2 Hz), 5.61 (dd, 2H, *J* = 2.1, 10.2 Hz), 4.61 (m, 1H), 3.93* (s, 2H), 3.85 (s, 2H), 2.04* (s, 3H), 2.02 (s, 3H), 1.13 (s, 3H), 1.03* (s, 3H), 0.91 (s, 9H), 0.90* (s, 9H), 0.11* (s, 6H), 0.98 (s, 3H), 0.97 (s, 3H)

¹³C-NMR (100 MHz, CDCl₃): δ (171.07*) 170.88, 132.23, 131.87, 129.43, 128.79, 70.92 (70.04*), 63.20 (63.07*), (37.56*) 37.43, 25.93 (25.90*), 25.65, 24.42, 23.33, 20.94 (20.86*), (18.35*) 18.24

IR (neat film, cm⁻¹): 2957, 2930, 2857, 1747, 1253, 1056, 873, 837

HRMS (ESI): calc'd. for C₁₆H₂₈O₃SiNa [M+Na]⁺, 319.1700 found. 319.1750



To a solution of the silyl ether (1.07 g, 3.61 mmol, 1.00 eq.) in methanol (36 mL) was added K_2CO_3 (0.55 g, 3.97 mmol, 1.10 eq.) and the mixture was rapidly stirred (800 rpm) at 23 °C. After 1 hr. the heterogeneous mixture was diluted with an aqueous phosphate buffer (20 mL, pH = 7, 0.2 M) and EtOAc (20 mL), poured into a separatory funnel, partitioned, and the organic layer was washed with water (2 x 10 mL). Residual organics were extracted from the aqueous layer with EtOAc (2 x 20 mL), dried over solid Na_2SO_4 , decanted, and concentrated. The crude yellow oil was purified by silica gel chromatography; 5% EtOAc in hexane to afford the alcohol **163** as a clear pale yellow oil (0.88 g, 3.46 mmol, 96%).

Mixture of Isomers: (*) denotes minor isomer

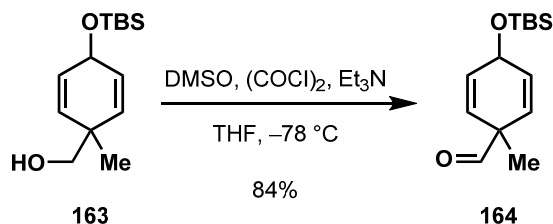
R_f = 0.33 (10% EtOAc in hexane)

1H -NMR (400 MHz, $CDCl_3$): δ 5.89 (m, 2H), 5.65* (dd, 2H, J = 1.2, 10.0 Hz), 5.61 (dd, 2H, J = 2.0, 10.1 Hz), 4.65 (m, 1H), 4.60* (m, 1H), 3.38 (s, 2H), 3.34* (s, 2H), 1.80 (bs, 1H), 1.07 (s, 3H), 1.01* (s, 3H), 0.91 (s, 9H), 0.89* (s, 9H), 0.11 (s, 6H), 0.10* (s, 6H)

^{13}C -NMR (100 MHz, $CDCl_3$): δ 133.79, 132.30, 130.31, 129.71, (70.30*) 69.03, 63.12 (62.58*), 40.04 (39.88*), 25.96 (25.90*), (23.88*) 22.92, 18.37 (18.24*), -4.34 (-4.43*)

IR (neat film, cm^{-1}): 3401, 2956, 2929, 2857, 1256, 1056, 872, 836, 776

HRMS (EC-Cl): calc'd. for $C_{14}H_{27}O_2Si$ $[M+H]^+$, 255.1780 found. 255.1780



A solution of oxalyl chloride (1.76 g, 1.2 mL, 13.8 mmol, 4.00 eq.) in THF (5 mL) was placed in a bath cooled to $-78\text{ }^\circ\text{C}$ for 30 minutes upon which dimethyl sulfoxide (2.16 g, 2.0 mL, 27.7 mmol, 8.00 eq.) was added dropwise by syringe over 2 minutes. After 10 minutes a solution of the alcohol **163** (0.88 g, 3.46 mmol, 1.00 eq.) in THF (12 mL) was added by syringe over 5 minutes to the slightly heterogeneous mixture. After 1 hr triethylamine (7.00 g, 9.7 mL, 69.2 mmol, 20.0 eq.) was added by syringe to the pale yellow mixture. After 1 hr the yellow solution was removed from the cold bath and allowed to stir (500 rpm) at $23\text{ }^\circ\text{C}$. After 1 hr the golden yellow solution was diluted with an aqueous phosphate buffer (20 mL, pH = 7, 0.2 M) and ethyl ether (20 mL), poured into a separatory funnel, partitioned, and the organic layer was washed with water (2 x 10 mL). Residual organics were extracted from the aqueous layer with ethyl ether (3 x 15 mL), washed with brine (1 x 10 mL), dried over solid Na_2SO_4 , decanted, and concentrated. The crude pale yellow oil was purified by silica gel chromatography; hexane \rightarrow 2% EtOAc in hexane to afford the aldehyde **164** as a pale yellow oil (0.73 g, 2.91 mmol, 84%).

Mixture of Isomers: (*) denotes minor isomer

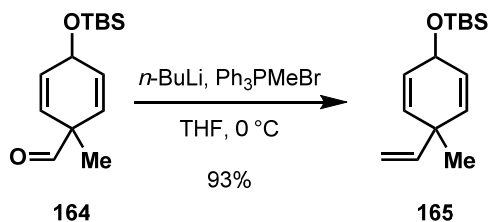
$R_f = 0.53$ (5% EtOAc in hexane)

$^1\text{H-NMR}$ (400 MHz, CDCl_3): δ 9.26* (s, 1H), 9.01 (s, 1H), 6.01 (m, 2H), 5.65* (d, 2H, $J = 9.9$ Hz), 5.52 (dd, 2H, $J = 2.0, 10.2$ Hz), 4.72 – 4.70 (m, 1H), 4.69 – 4.67* (m, 1H), 1.30 (s, 3H), 1.19* (s, 3H), 0.92 (s, 9H), 0.91* (s, 9H), 0.13 (s, 6H), 0.12* (s, 6H)

$^{13}\text{C-NMR}$ (100 MHz, CDCl_3): δ (198.81*), 197.19, 131.64, 131.33, 128.30, 126.27, (62.57*) 62.54, 51.64 (50.55*), 25.87, (20.97*) 19.33, 18.31 (18.24*), (-4.33*) -4.47

IR (neat film, cm^{-1}): 2966, 2929, 2857, 1728, 1069, 868, 836, 776

HRMS (EC-CI): calcd. for $\text{C}_{14}\text{H}_{25}\text{O}_2\text{Si}$ $[\text{M}+\text{H}]^+$, 253.1624 found. 253.1624



A mixture of Ph_3PMeBr (1.36 g, 3.81 mmol, 1.00 eq.) in THF (15 mL) was placed in a bath cooled to $-78\text{ }^\circ\text{C}$ for 20 minutes upon which *n*-butyllithium (1.97 mL, 3.36 mmol, 1.10 eq., 1.70 M in hexane) was added. After 20 minutes the orange heterogeneous mixture was removed from the cold bath and allowed to warm to $23\text{ }^\circ\text{C}$. After 20 minutes the orange mixture was placed in an ice water bath cooled to $0\text{ }^\circ\text{C}$ for 30 minutes upon which a solution of the aldehyde **164** (0.77 g, 3.05 mmol, 1.00 eq.) in THF (15 mL) was added dropwise by syringe over 2 minutes. After 1 hr the pale yellow mixture was removed from the cold bath. After 30 minutes at $23\text{ }^\circ\text{C}$ an aqueous phosphate buffer (20 mL, pH = 7, 0.2 M) was added to the pale yellow mixture to quench the excess ylide. The mixture was diluted with ethyl ether (20 mL), poured into a separatory funnel, and partitioned. Residual organics were extracted from the aqueous with ethyl ether (2 x 20 mL), dried over solid Na_2SO_4 , suction filtered over a pad of celite, and concentrated. The crude pale yellow mixture was purified by silica gel chromatography; hexane \rightarrow 2% EtOAc in hexane to afford the triene **165** as a pale yellow oil (0.71 g, 2.83 mmol, 93%).

Mixture of Isomers: (*) denotes minor isomer

$R_f = 0.84$ (5% EtOAc in hexane)

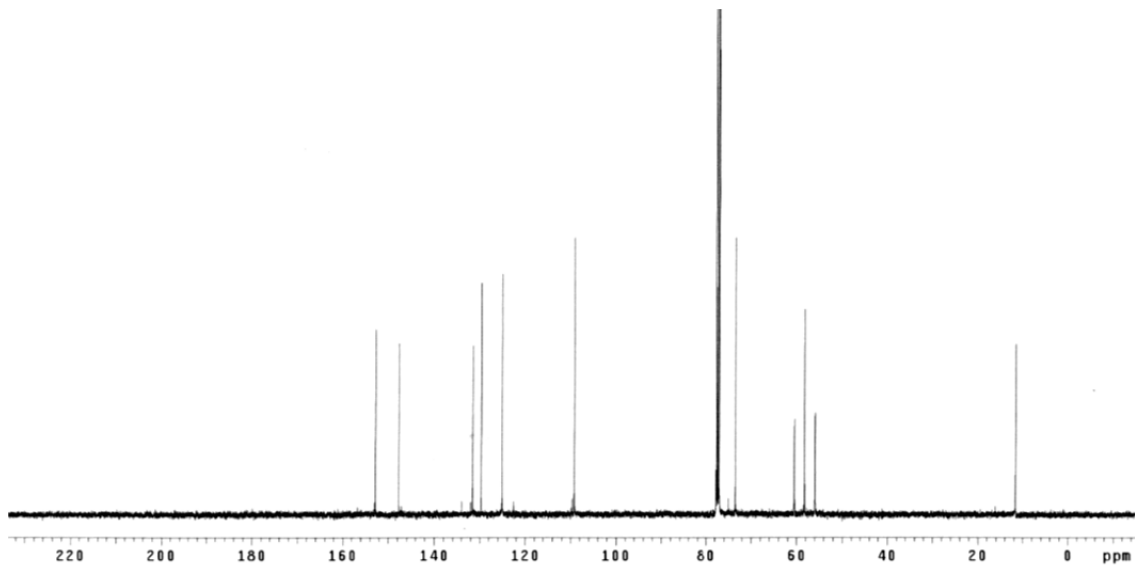
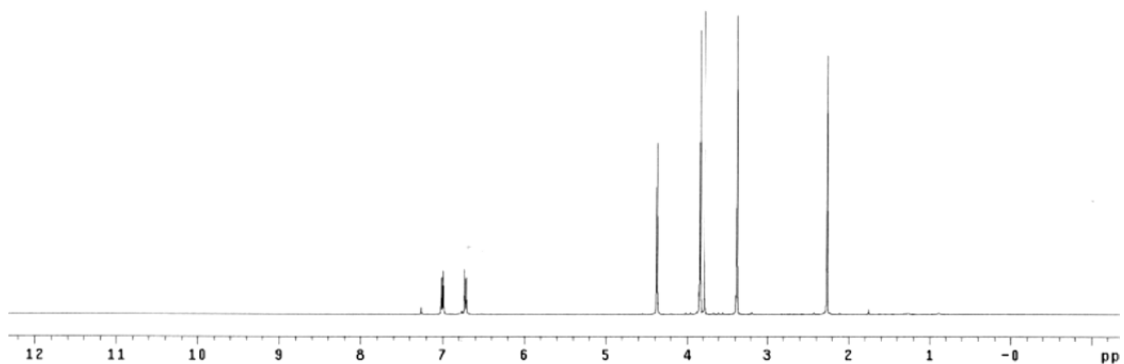
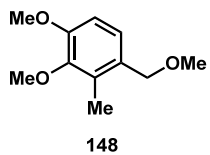
$^1\text{H-NMR}$ (400 MHz, CDCl_3): δ 5.83 – 5.62 (m, 5H), 5.06 – 4.91 (m, 2H), 4.63 – 4.61 (m, 1H), 1.20 (s, 3H), 1.12* (s, 3H), 0.92 (s, 9H), 0.91* (s, 9H), 0.11 (s, 6H), 0.10* (s, 6H)

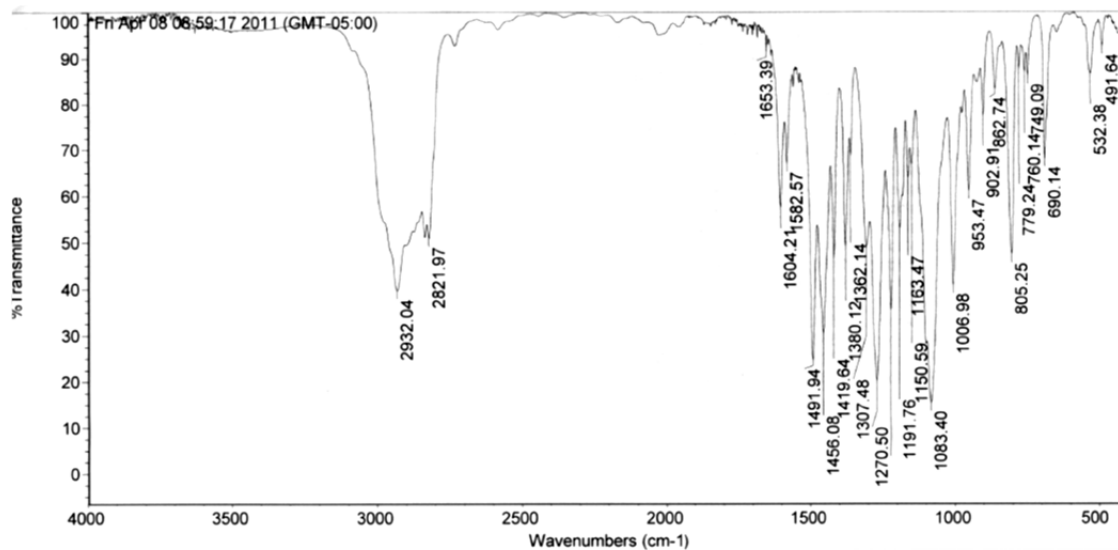
$^{13}\text{C-NMR}$ (100 MHz, CDCl_3): δ 144.73 (144.09*), (134.21*) 133.76, 126.90 (126.69*), (112.44*) 111.75, 63.22 (63.05*), 40.07 (39.53*), 26.95, 25.99, 18.37 (18.36*), (-4.23*) -4.33

IR (neat film, cm^{-1}): 2958, 2928, 2857, 1253, 1063, 873, 836, 775

HRMS (EC-CI): calc'd. for $\text{C}_{15}\text{H}_{27}\text{OSi}$ $[\text{M}+\text{H}]^+$, 251.1831 found. 251.1823

7. Catalog of Spectra





Fri Apr 08 09:01:42 2011 (GMT-05:00)

IND PEAKS:

Spectrum: *Fri Apr 08 08:59:17 2011 (GMT-05:00)

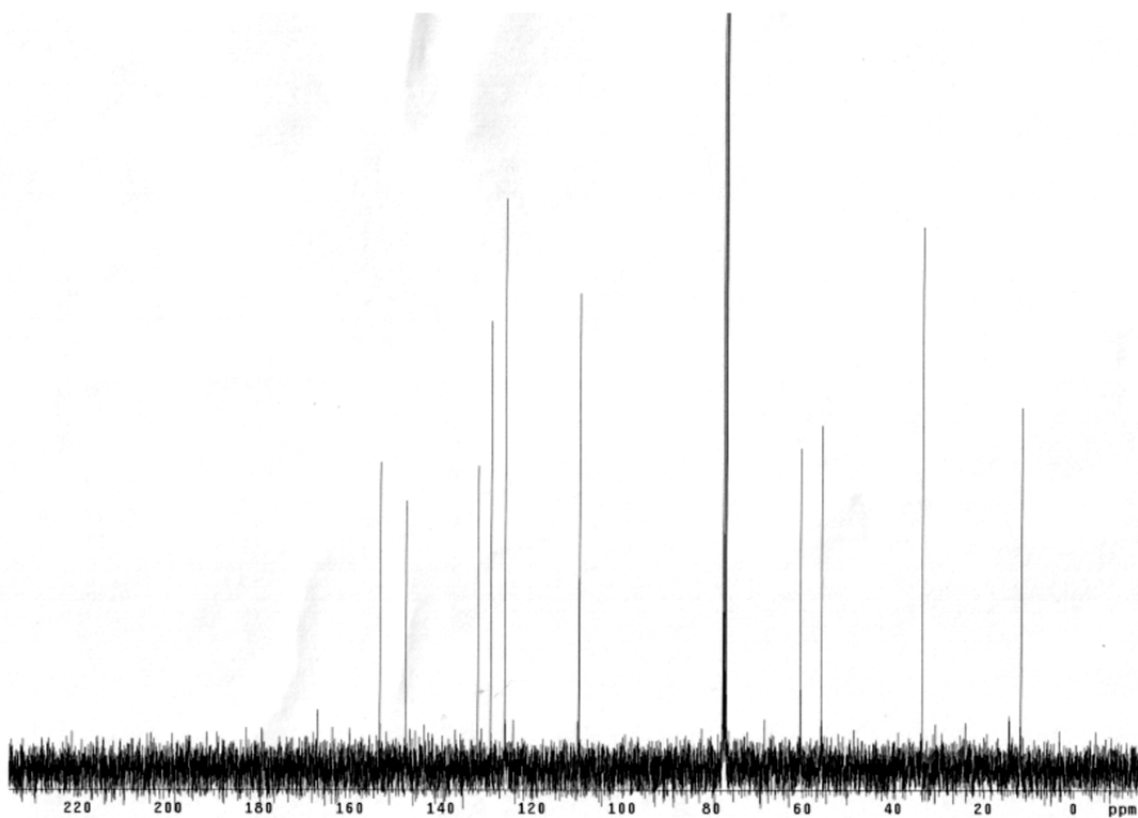
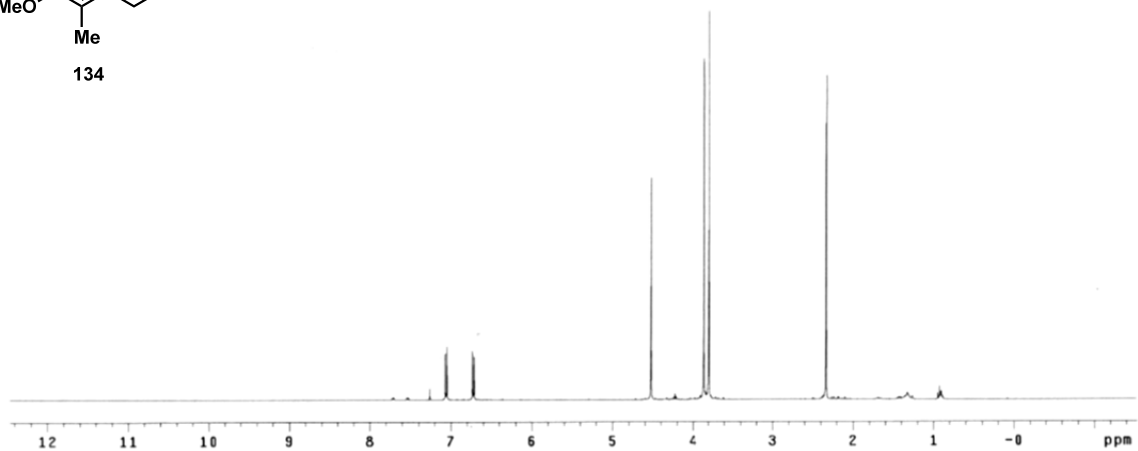
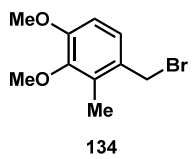
Region: 4000.00 400.00

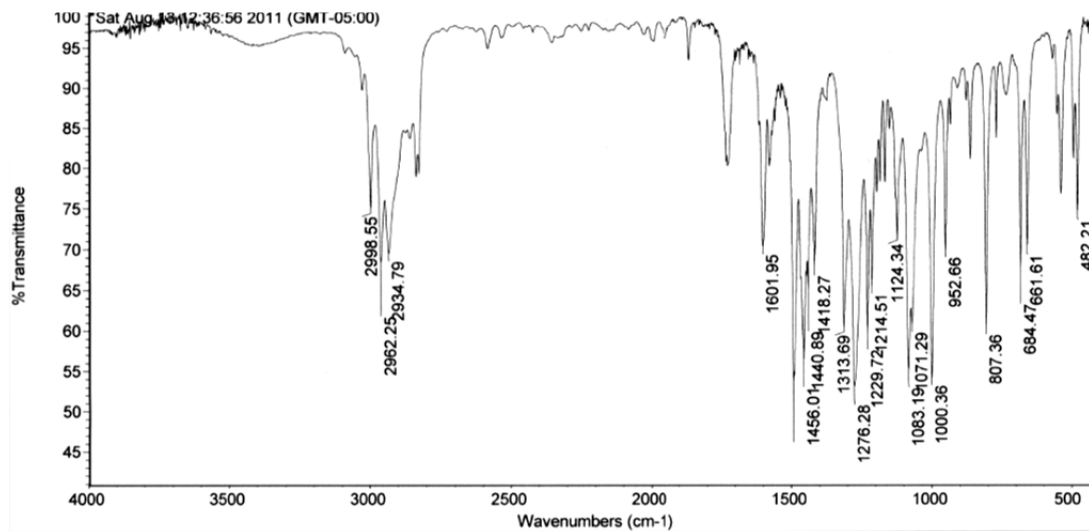
Absolute threshold: 94.127

Sensitivity: 50

Peak list:

Position:	Intensity:
491.64	92.845
532.38	86.788
690.14	68.079
749.09	86.347
760.14	87.167
779.24	87.809
805.25	47.490
862.74	83.450





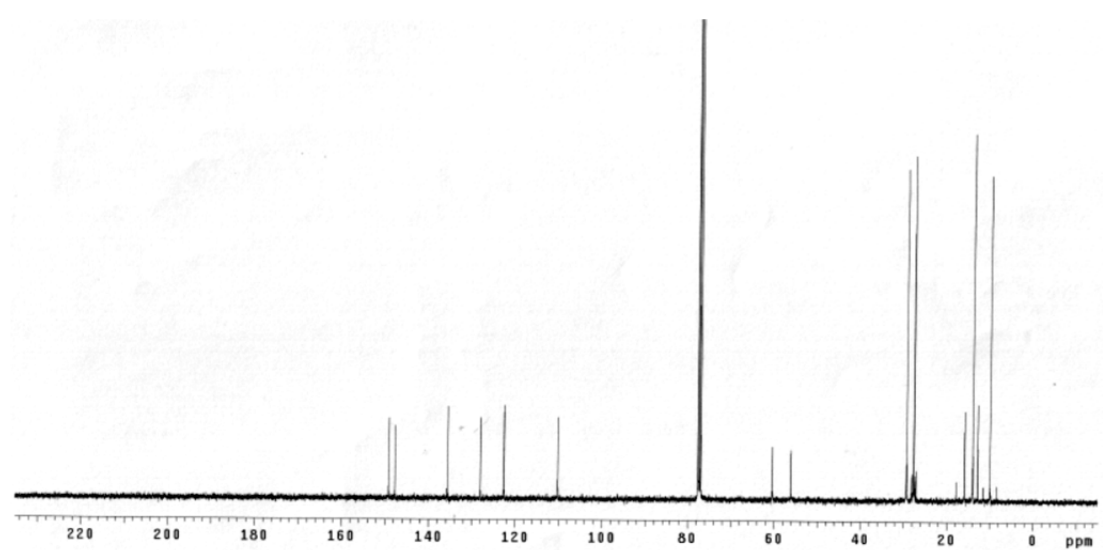
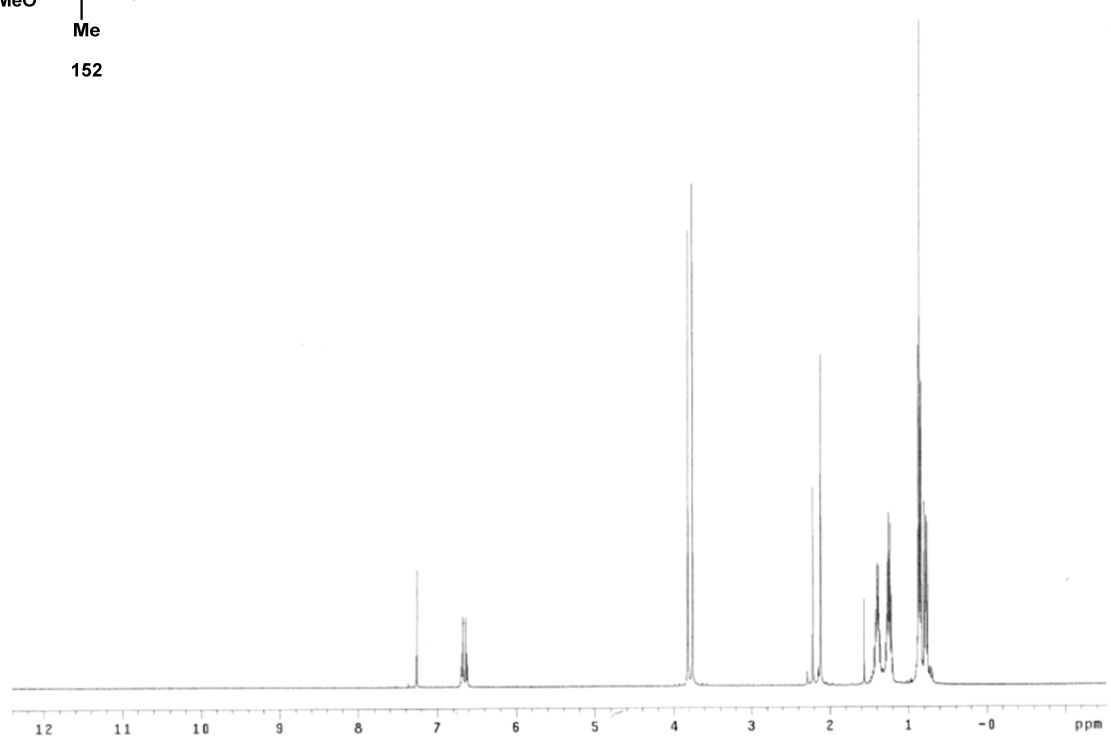
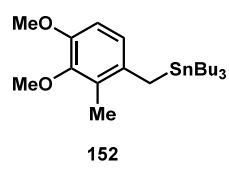
Sat Aug 13 12:43:52 2011 (GMT-05:00)

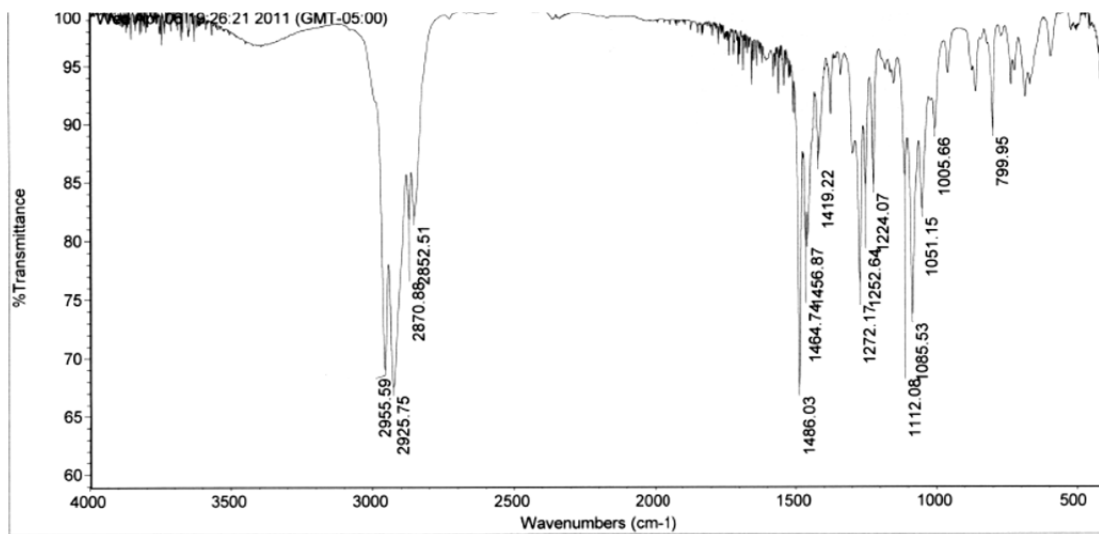
FIND PEAKS:

Spectrum: *Sat Aug 13 12:36:56 2011 (GMT-05:00)
 Region: 4000.00 400.00
 Absolute threshold: 75.362
 Sensitivity: 50

Peak list:

Position:	Intensity:
482.21	74.631
661.61	70.333
684.47	67.741
807.36	60.487
952.66	70.047
1000.36	54.115
1071.29	60.863
1083.19	55.201





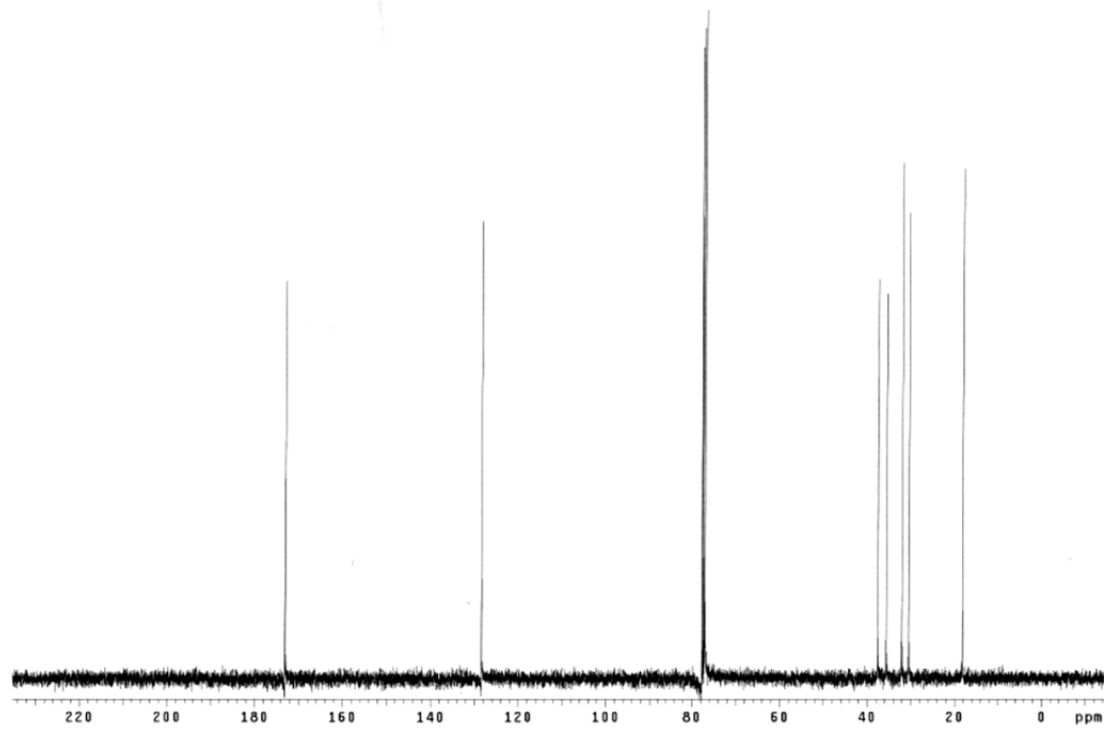
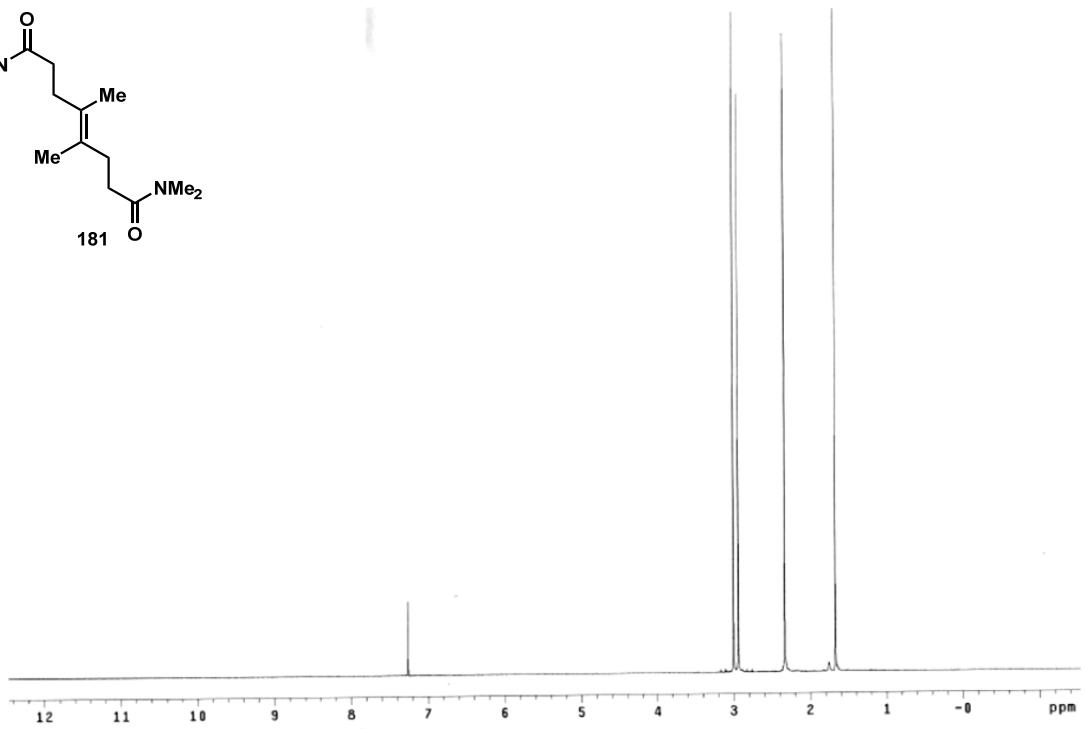
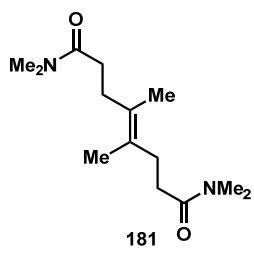
Wed Apr 06 19:32:53 2011 (GMT-05:00)

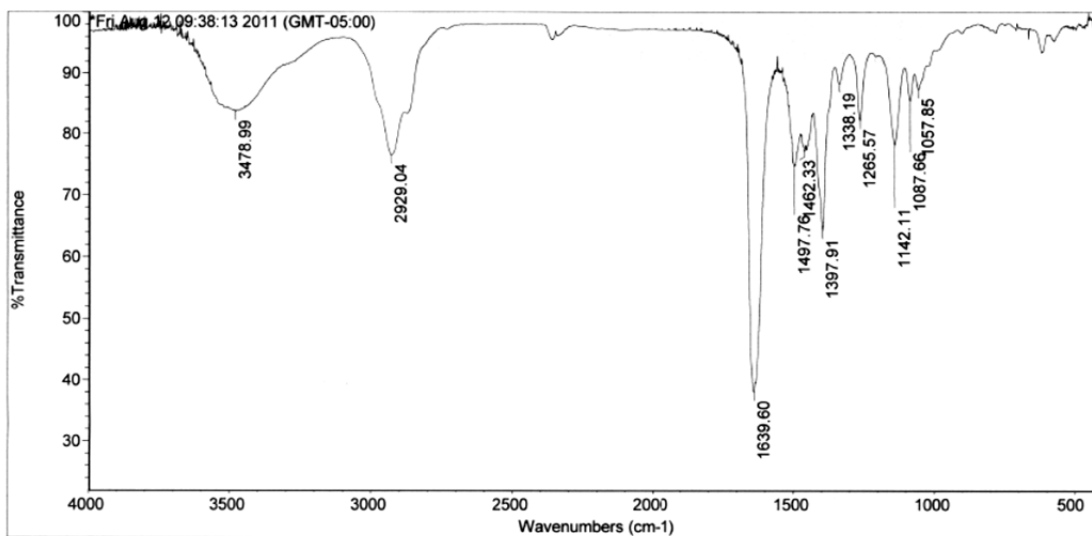
FIND PEAKS:

Spectrum: *Wed Apr 06 19:26:21 2011 (GMT-05:00)
 Region: 4000.00 400.00
 Absolute threshold: 89.660
 Sensitivity: 50

Peak list:

Position	Intensity
799.95	89.441
1005.66	89.464
1051.15	82.644
1085.53	73.635
1112.08	85.469
1224.07	84.627
1252.64	84.606
1272.17	76.282





Fri Aug 12 09:40:48 2011 (GMT-05:00)

FIND PEAKS:

Spectrum: *Fri Aug 12 09:38:13 2011 (GMT-05:00)

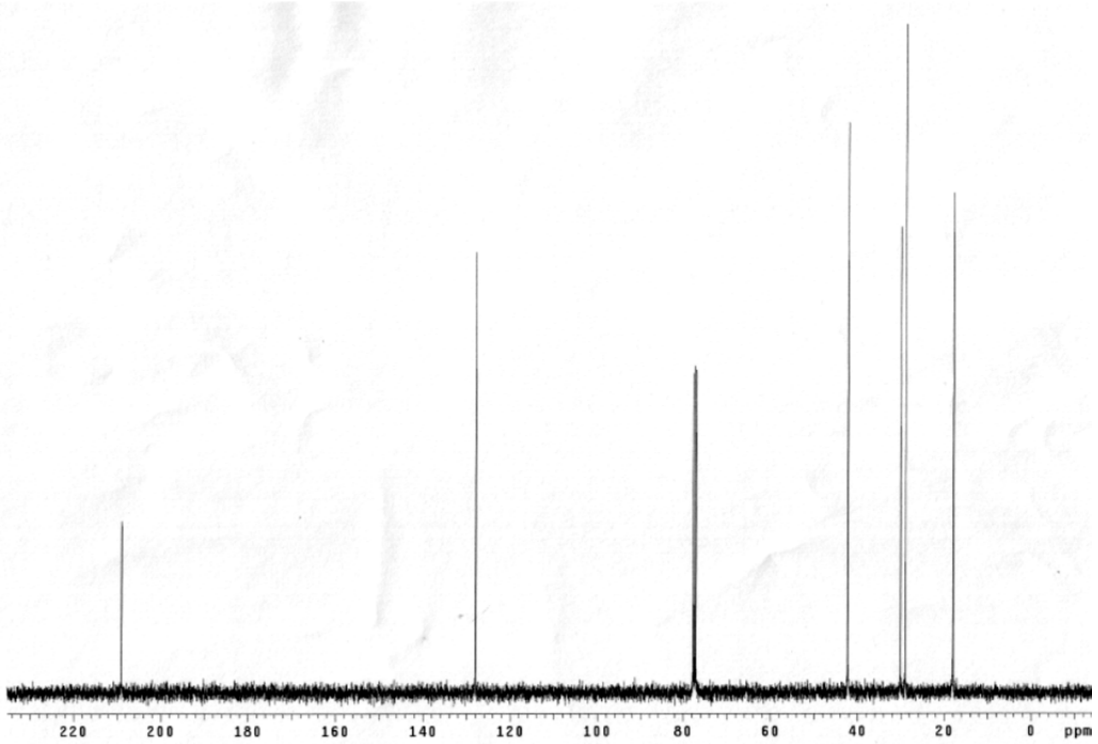
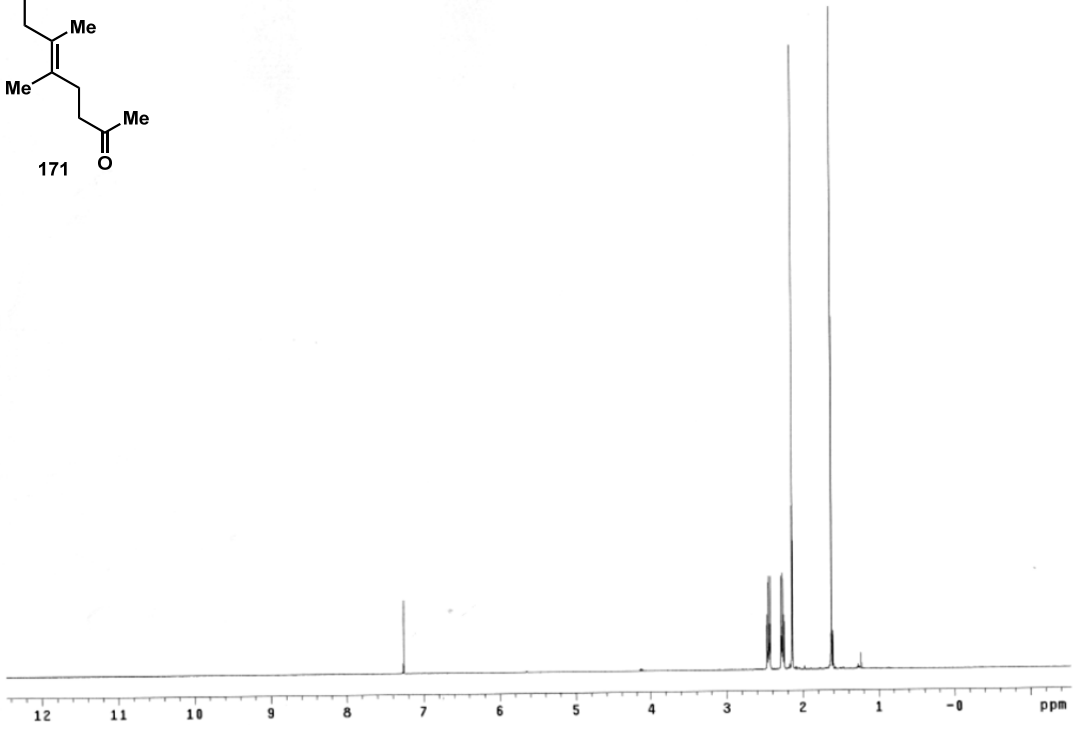
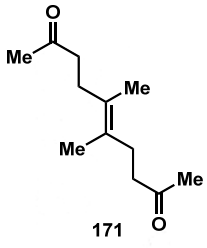
Region: 4000.00 400.00

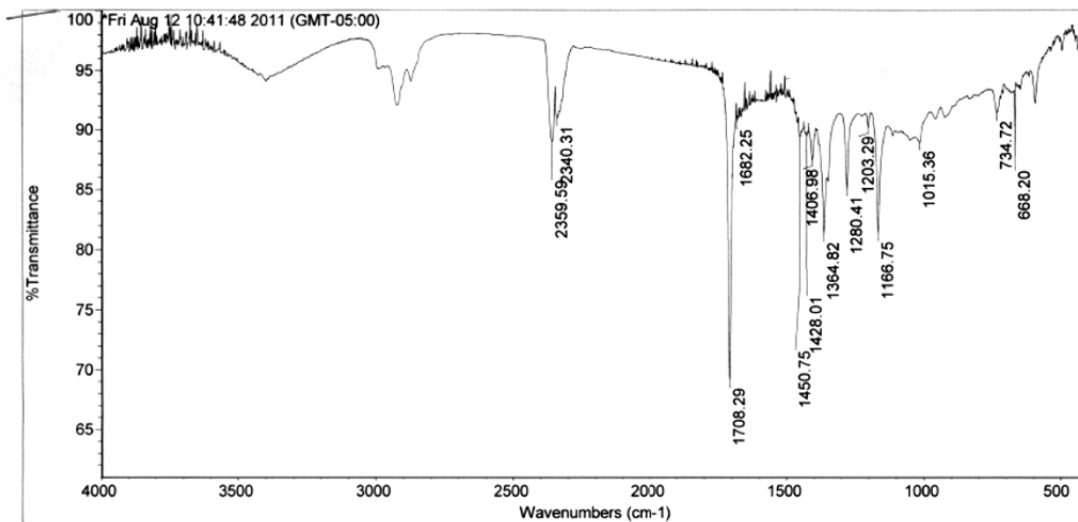
Absolute threshold: 92.267

Sensitivity: 50

Peak list:

Position: 1057.85	Intensity: 87.345
Position: 1087.66	Intensity: 85.477
Position: 1142.11	Intensity: 78.215
Position: 1265.57	Intensity: 82.225
Position: 1338.19	Intensity: 88.261
Position: 1397.91	Intensity: 64.214
Position: 1462.33	Intensity: 77.139
Position: 1497.76	Intensity: 74.602





Fri Aug 12 10:45:43 2011 (GMT-05:00)

FIND PEAKS:

Spectrum: *Fri Aug 12 10:41:48 2011 (GMT-05:00)

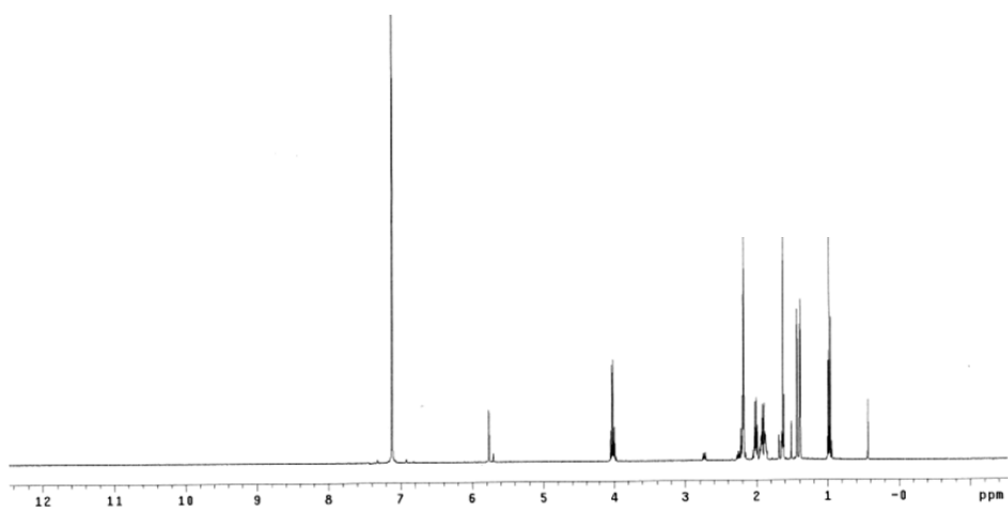
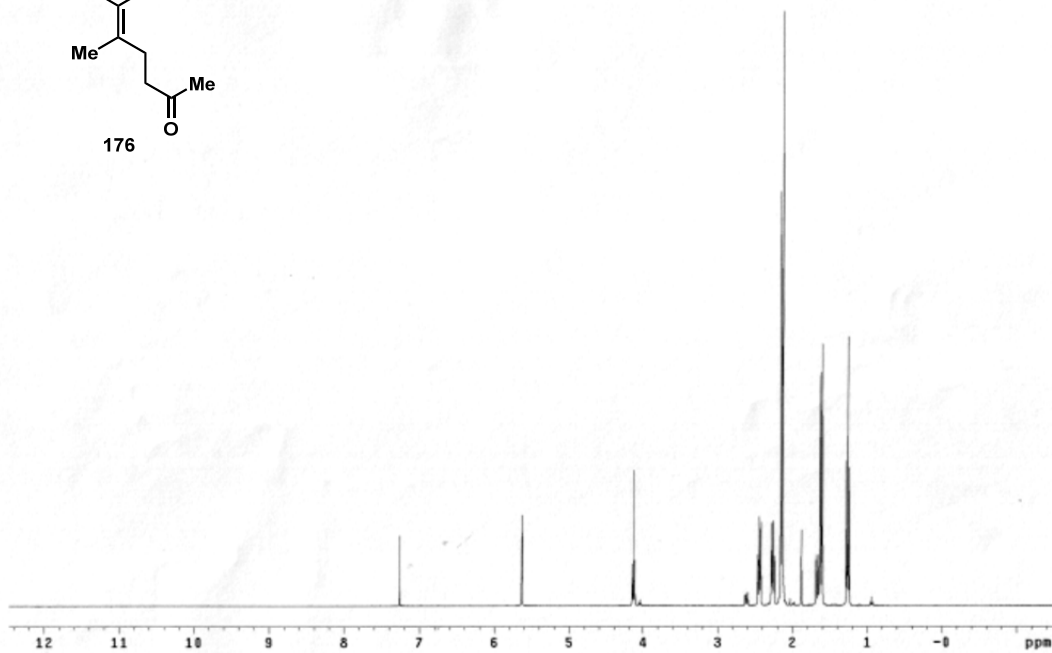
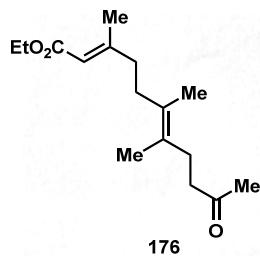
Region: 4000.00 400.00

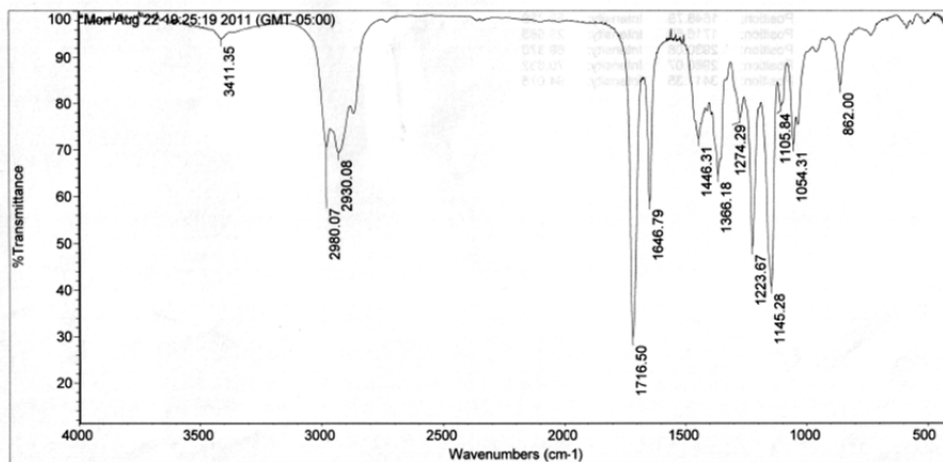
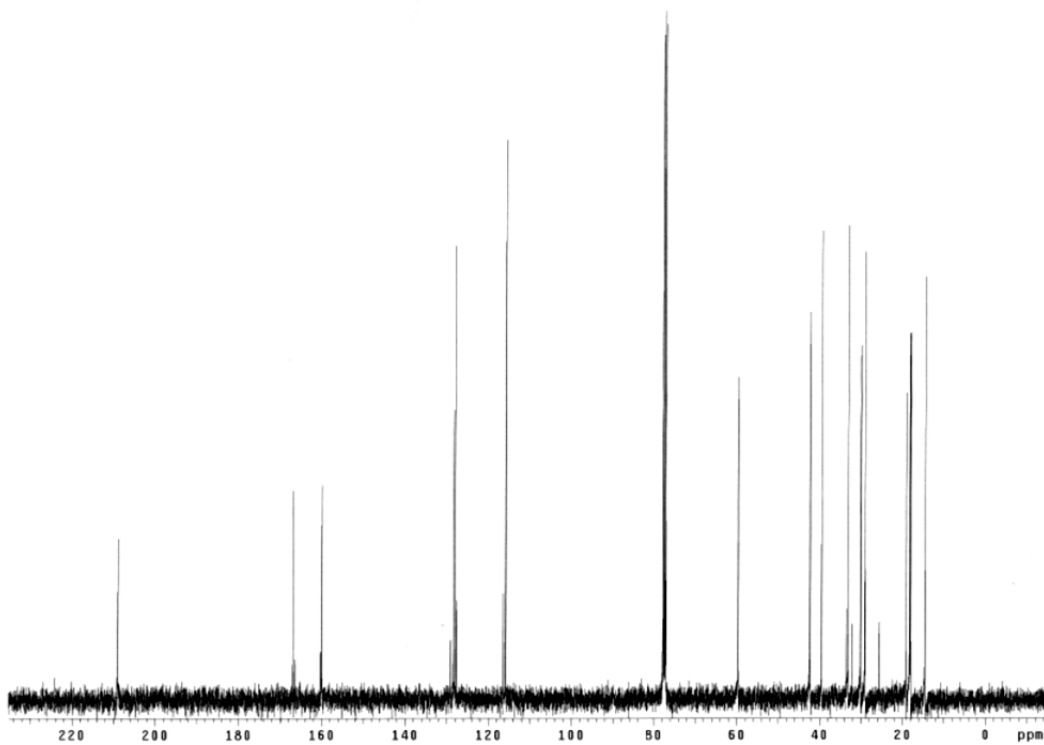
Absolute threshold: 91.536

Sensitivity: 50

Peak list:

Position	Intensity
688.20	87.249
734.72	91.428
1015.36	88.904
1166.75	81.348
1203.29	90.144
1280.41	85.077
1364.82	81.263
1406.98	87.349



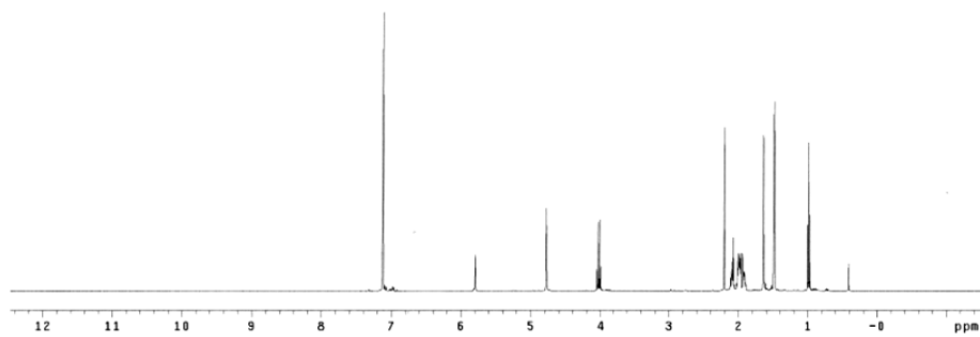
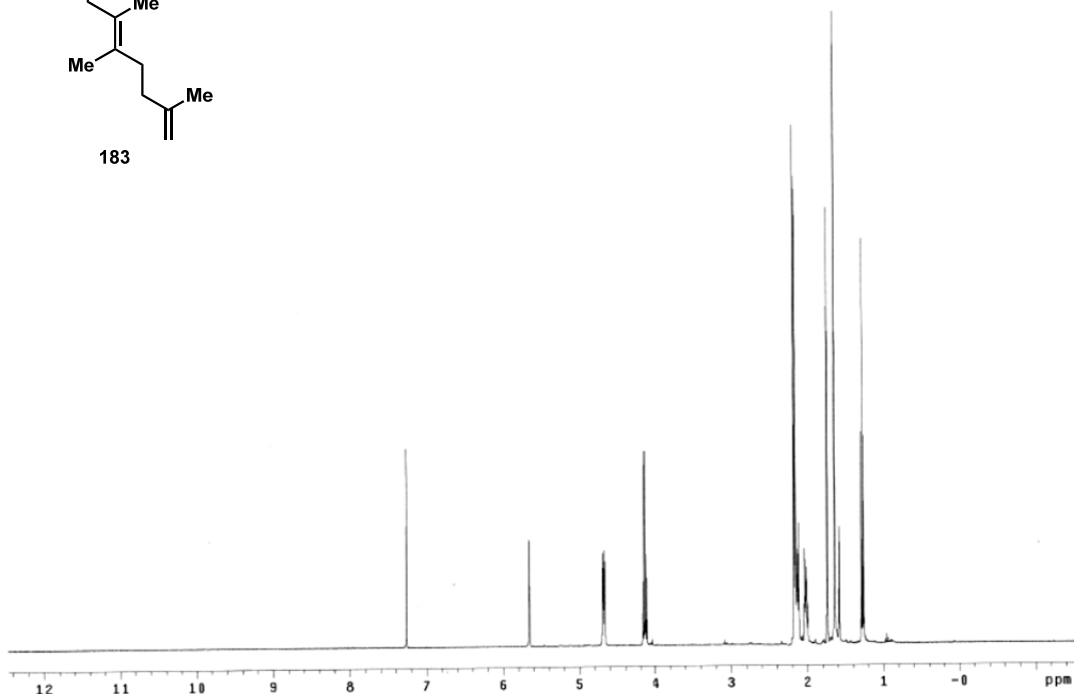
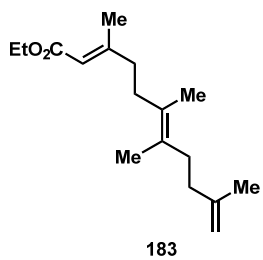


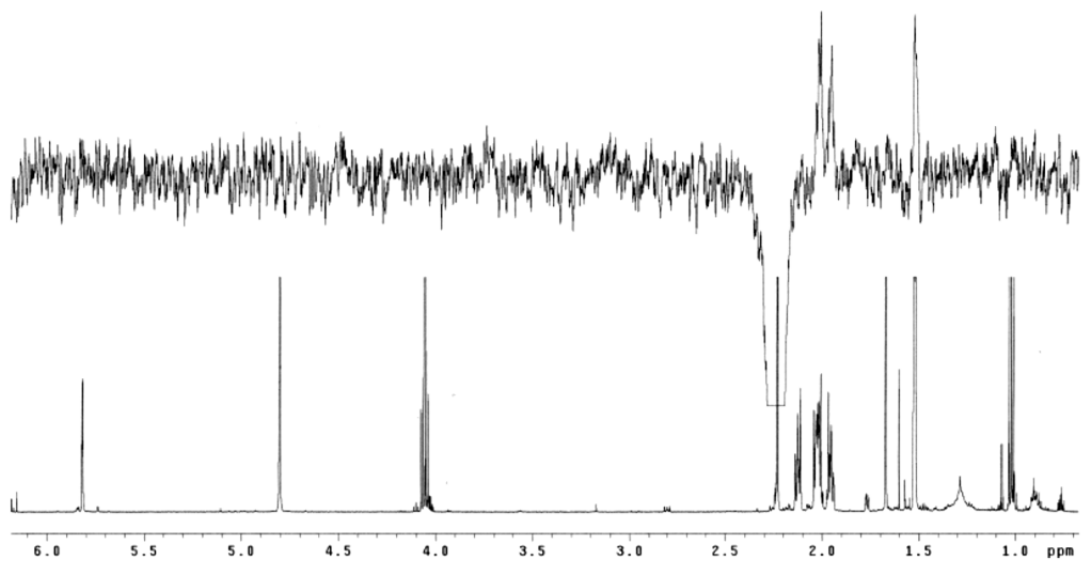
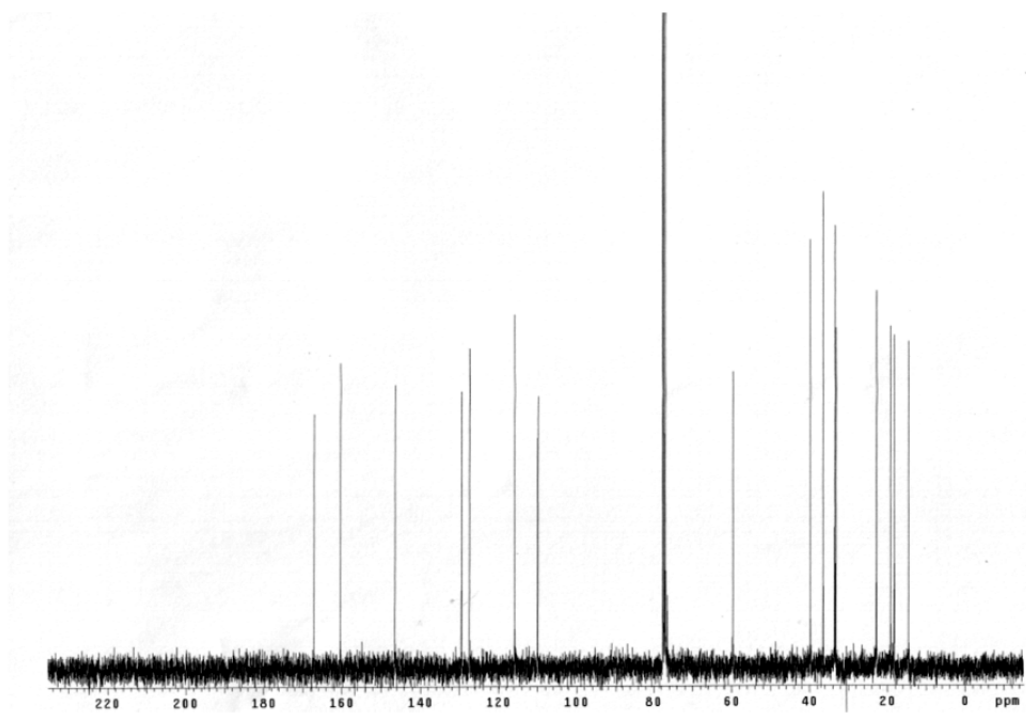
Mon Aug 22 19:28:01 2011 (GMT-05:00)

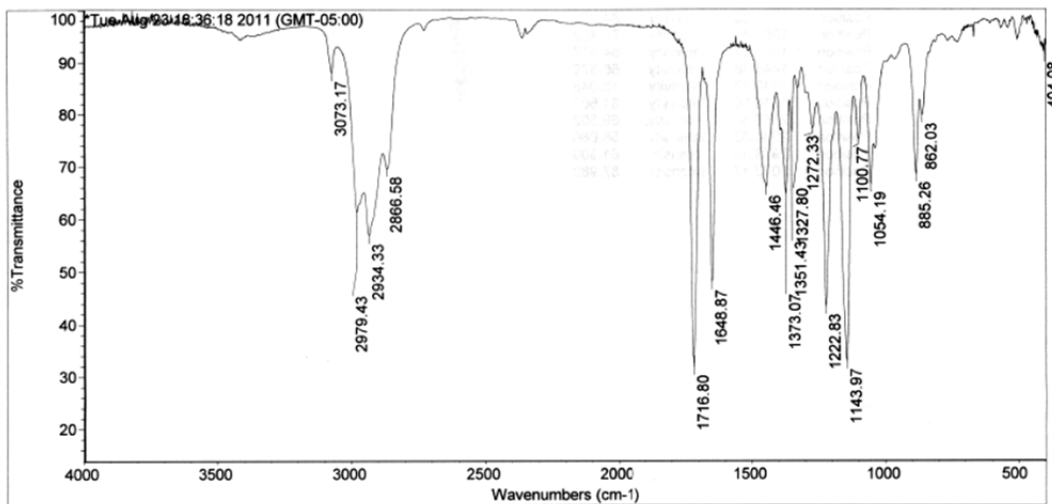
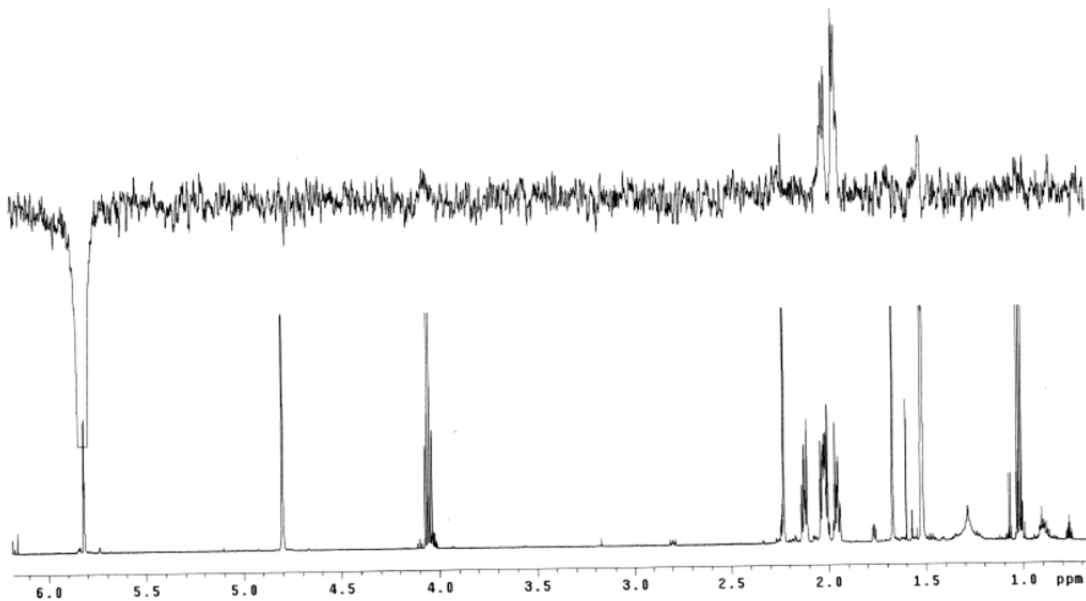
FIND PEAKS:

Spectrum: *Mon Aug 22 19:25:19 2011 (GMT-05:00)
 Region: 4000.00 400.00
 Absolute threshold: 94.146
 Sensitivity: 50

Position:	Intensity:
862.00	83.939
1054.31	71.139
1105.84	79.445
1145.28	40.744
1223.67	49.168
1274.29	76.862
1366.18	64.563
1446.31	72.290







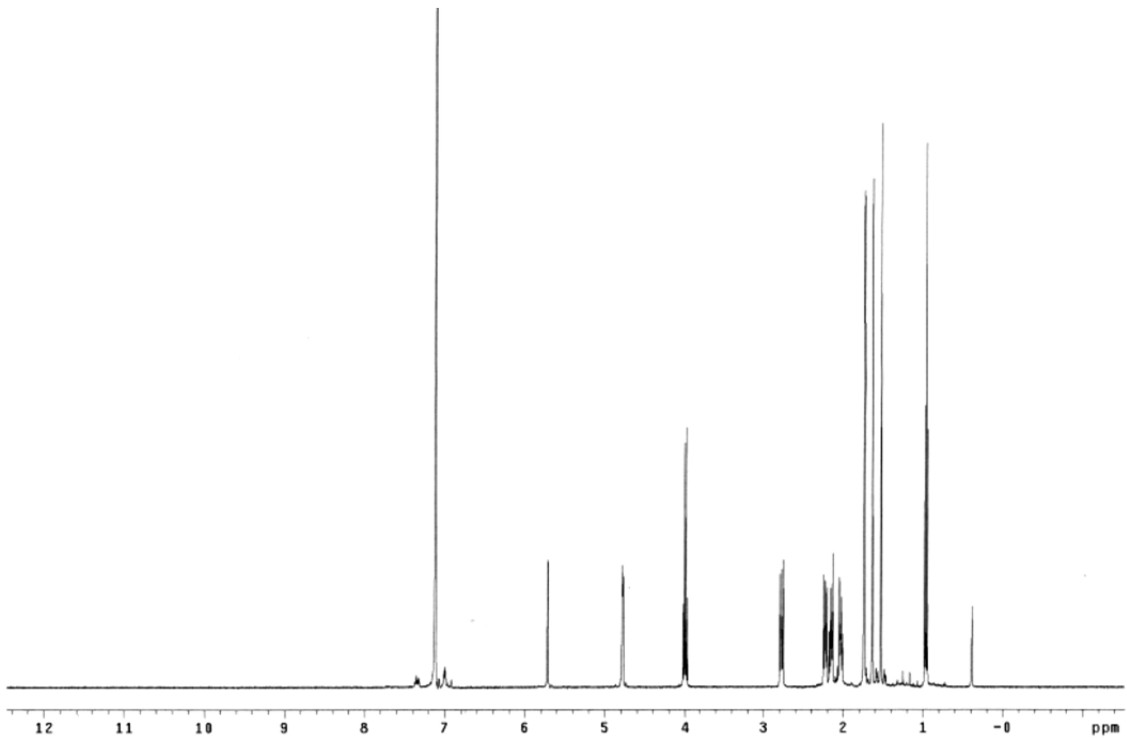
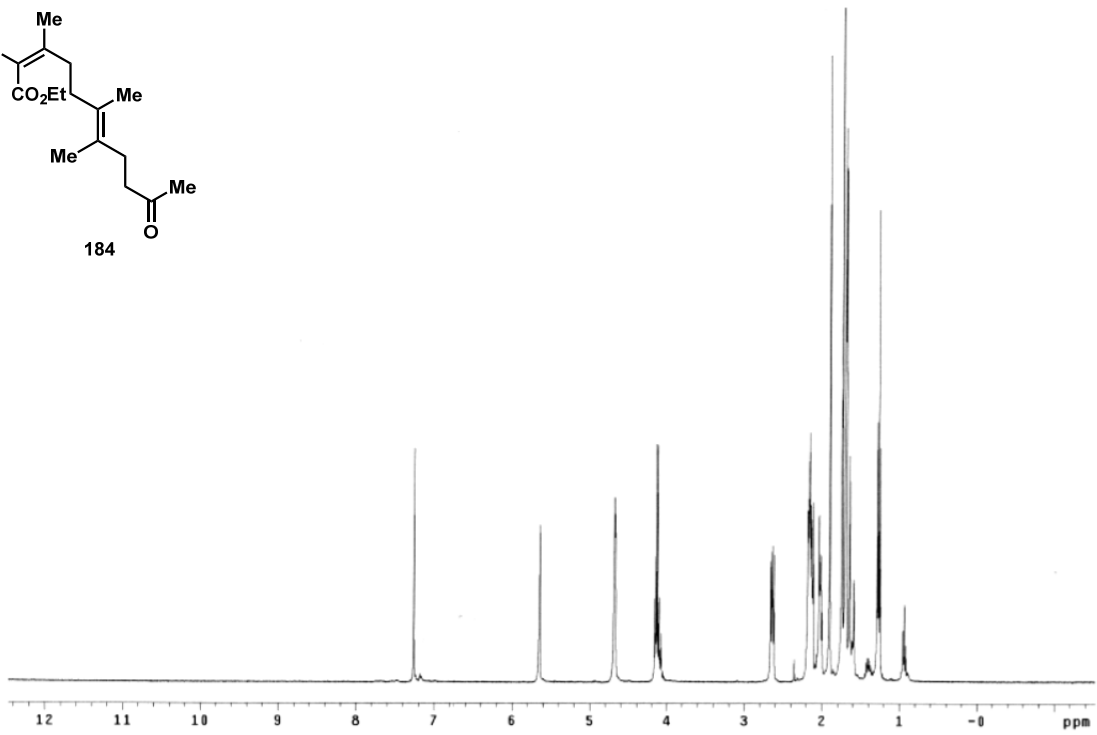
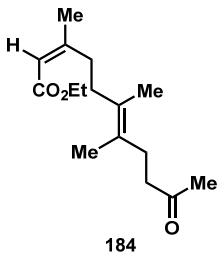
Tue Aug 23 18:38:45 2011 (GMT-05:00)

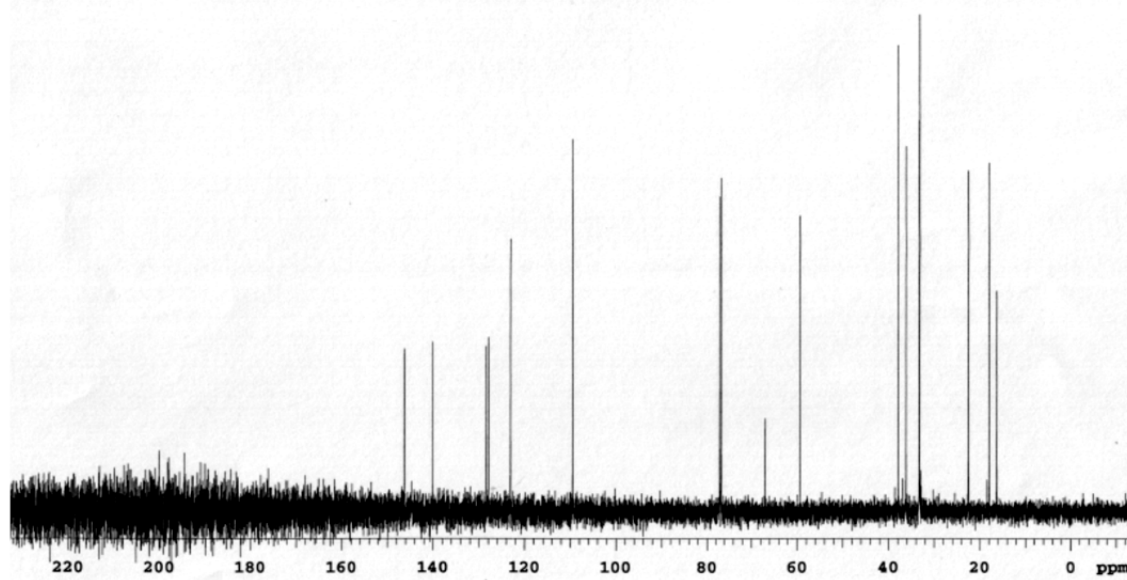
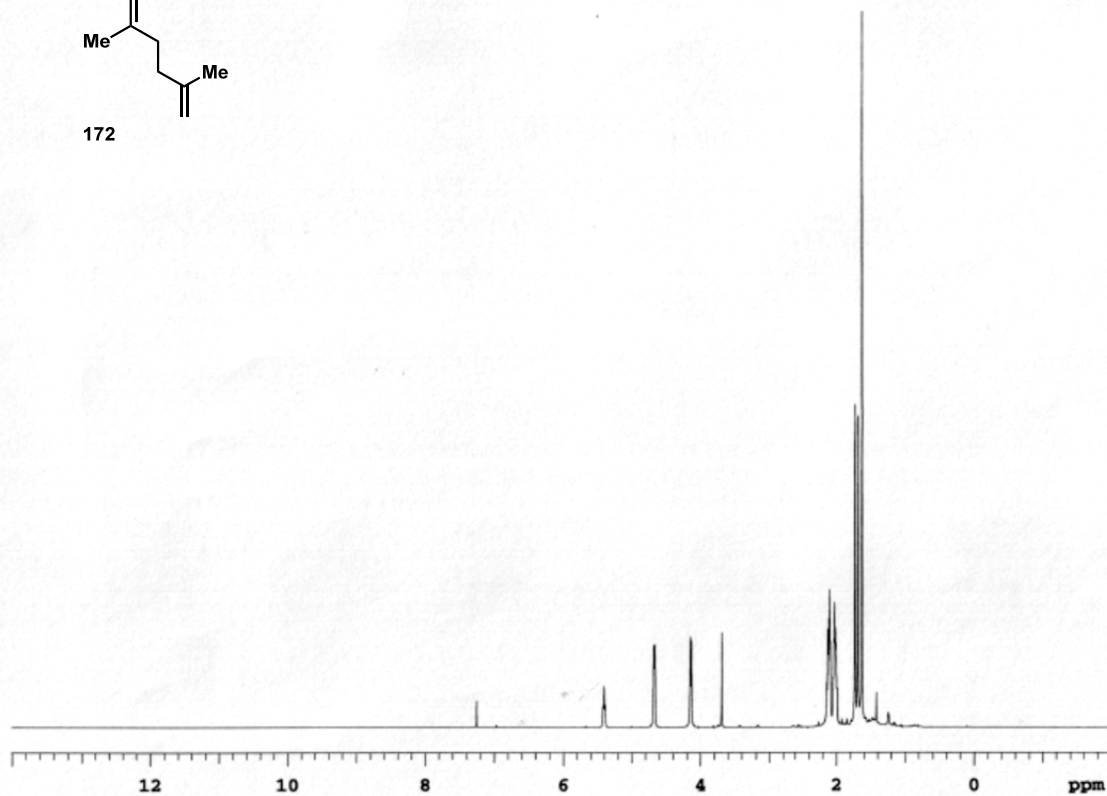
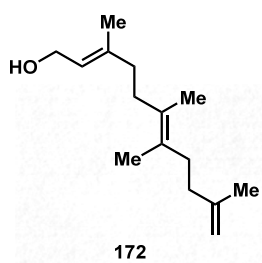
FIND PEAKS:

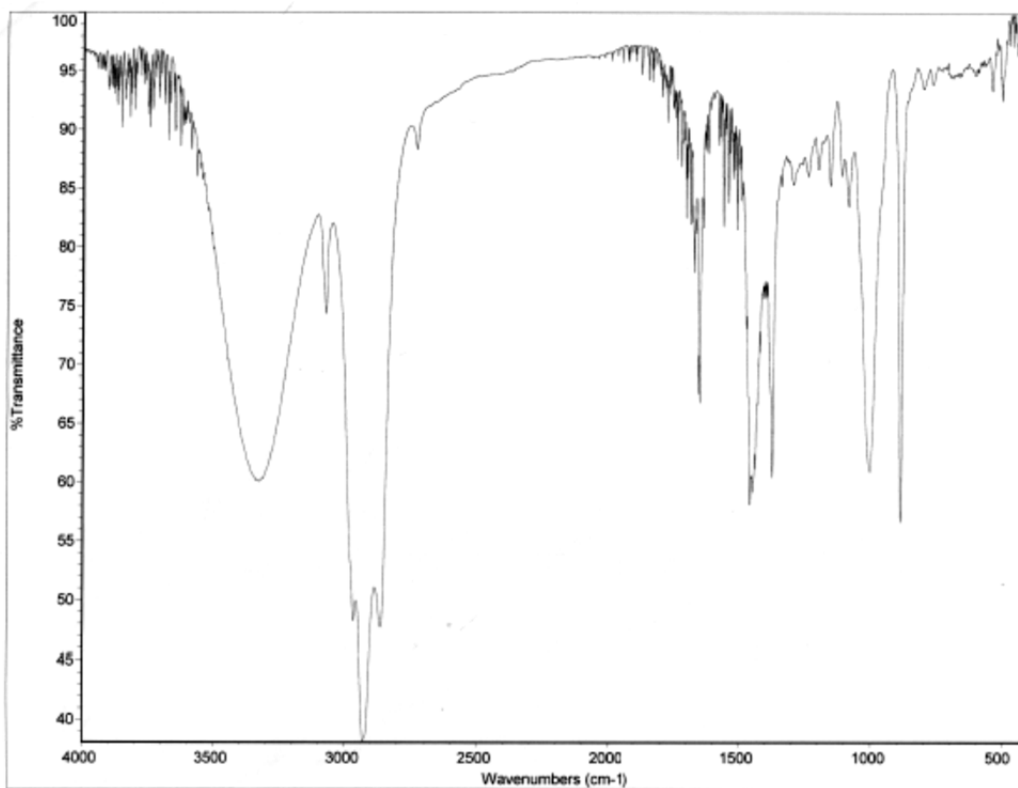
Spectrum: *Tue Aug 23 18:36:18 2011 (GMT-05:00)
 Region: 4000.00 400.00
 Absolute threshold: 92.825
 Sensitivity: 50

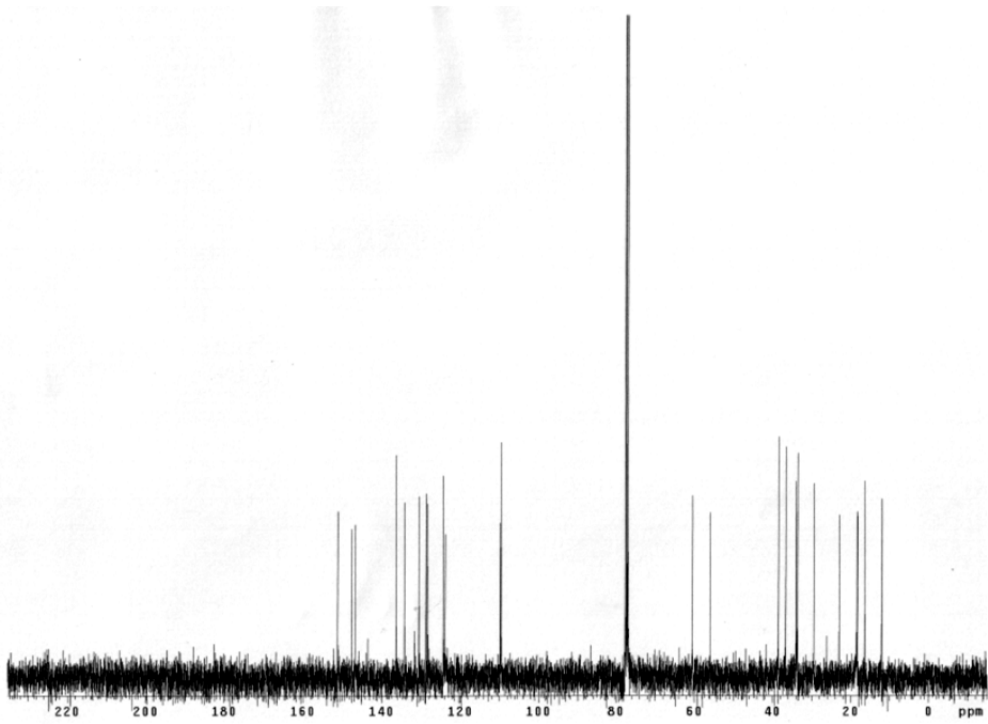
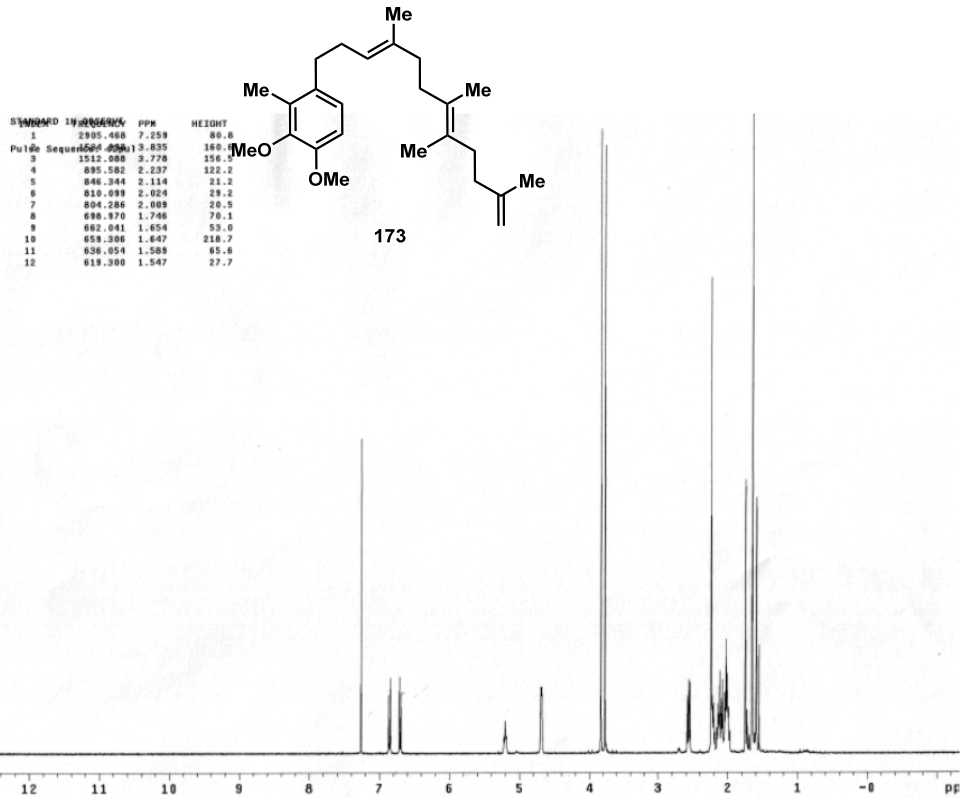
Peak list:

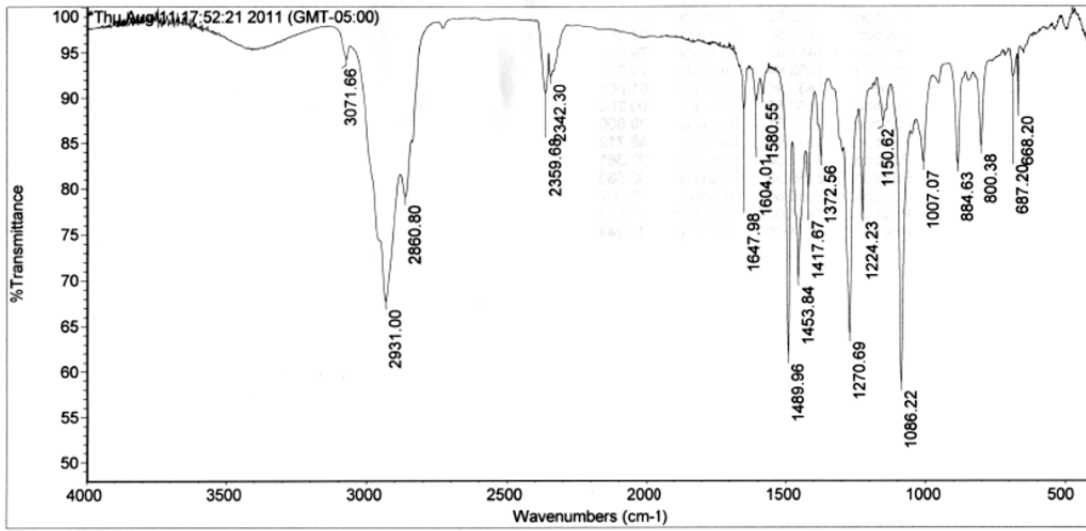
Position	Intensity
404.08	91.470
862.03	79.738
885.26	68.475
1054.19	66.543
1100.77	75.087
1143.97	32.920
1222.83	43.352
1272.33	77.254











Thu Aug 11 17:57:34 2011 (GMT-05:00)

FIND PEAKS:

Spectrum: *Thu Aug 11 17:52:21 2011 (GMT-05:00)

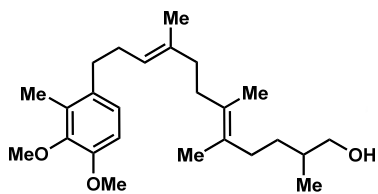
Region: 4000.00 400.00

Absolute threshold: 94.763

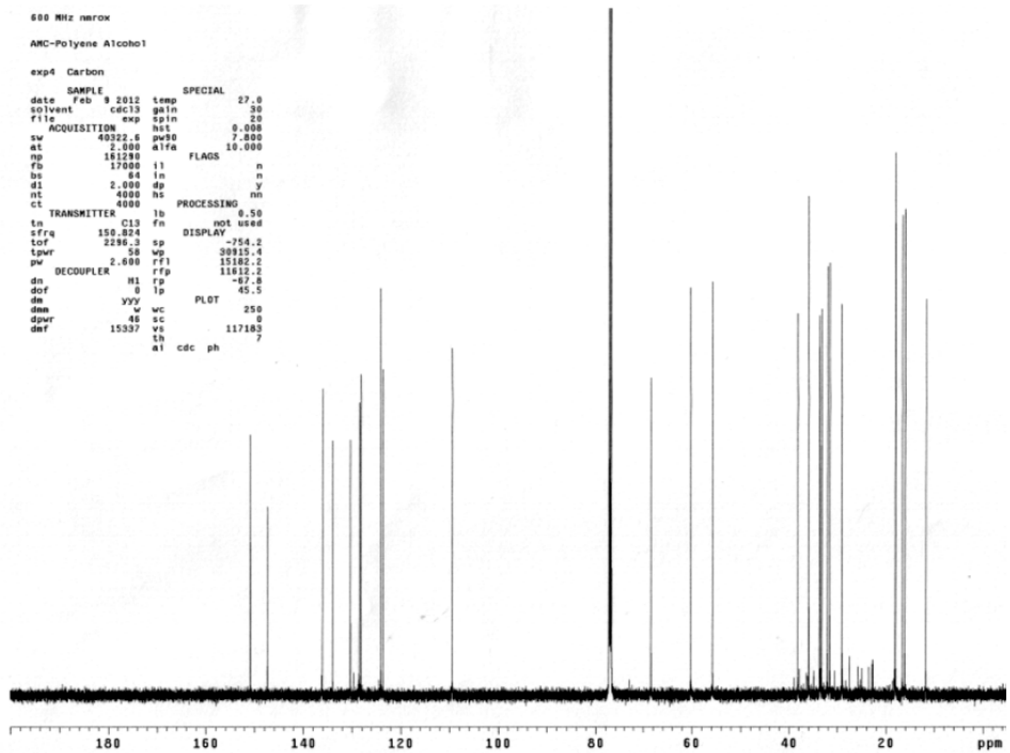
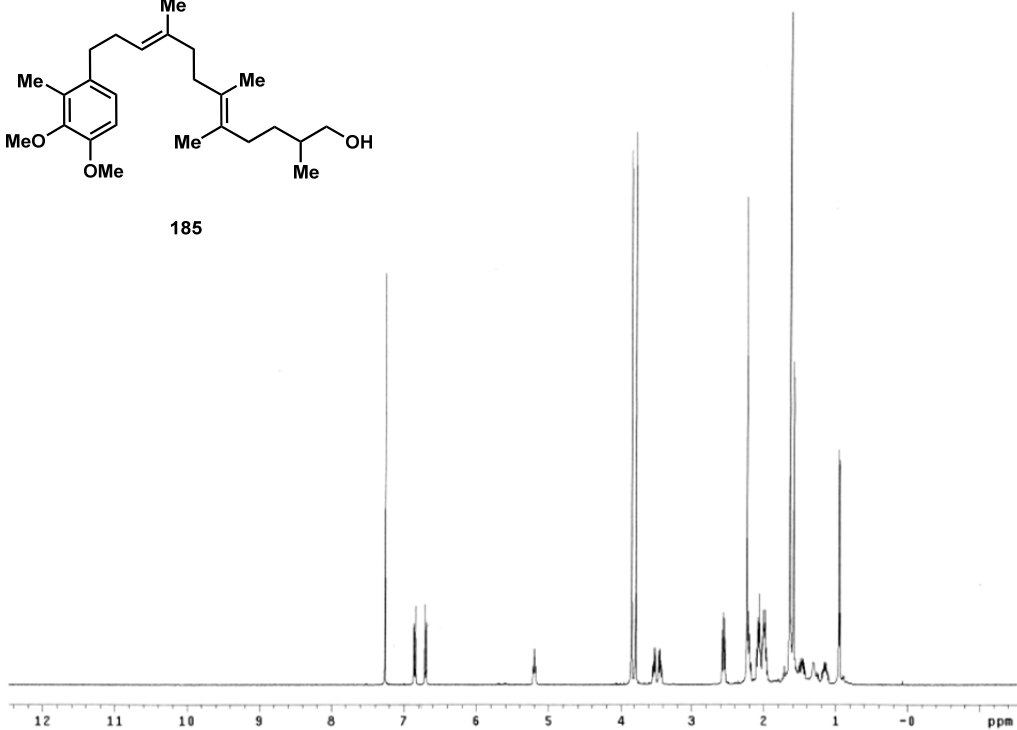
Sensitivity: 50

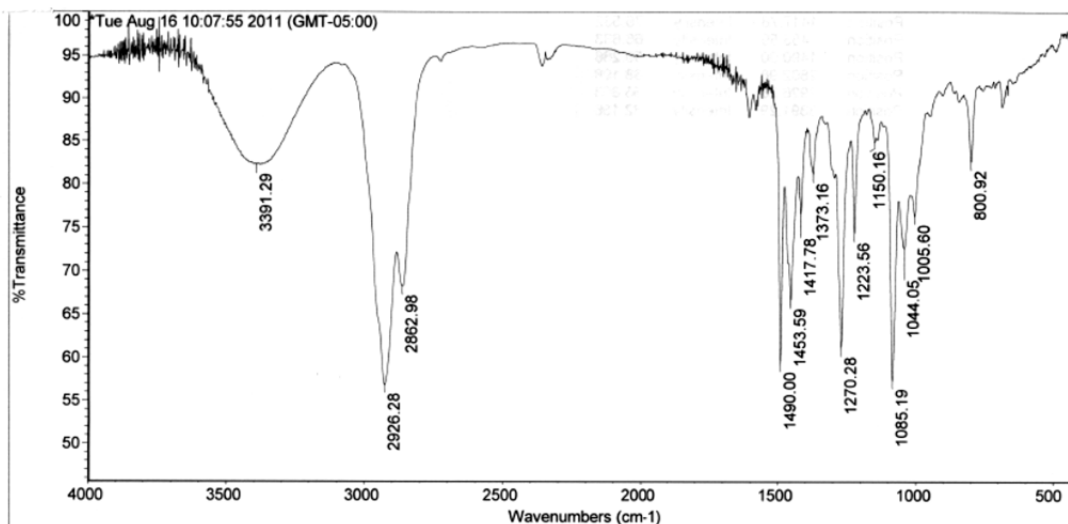
Peak list:

Position	Intensity
668.20	88.789
687.20	92.369
800.38	84.656
884.63	82.641
1007.07	82.815
1086.22	58.662
1150.62	87.394
1224.23	77.202



185





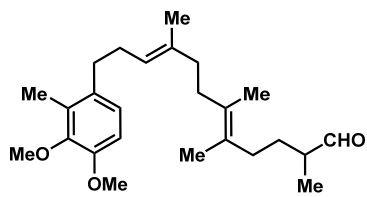
Tue Aug 16 10:16:14 2011 (GMT-05:00)

FIND PEAKS:

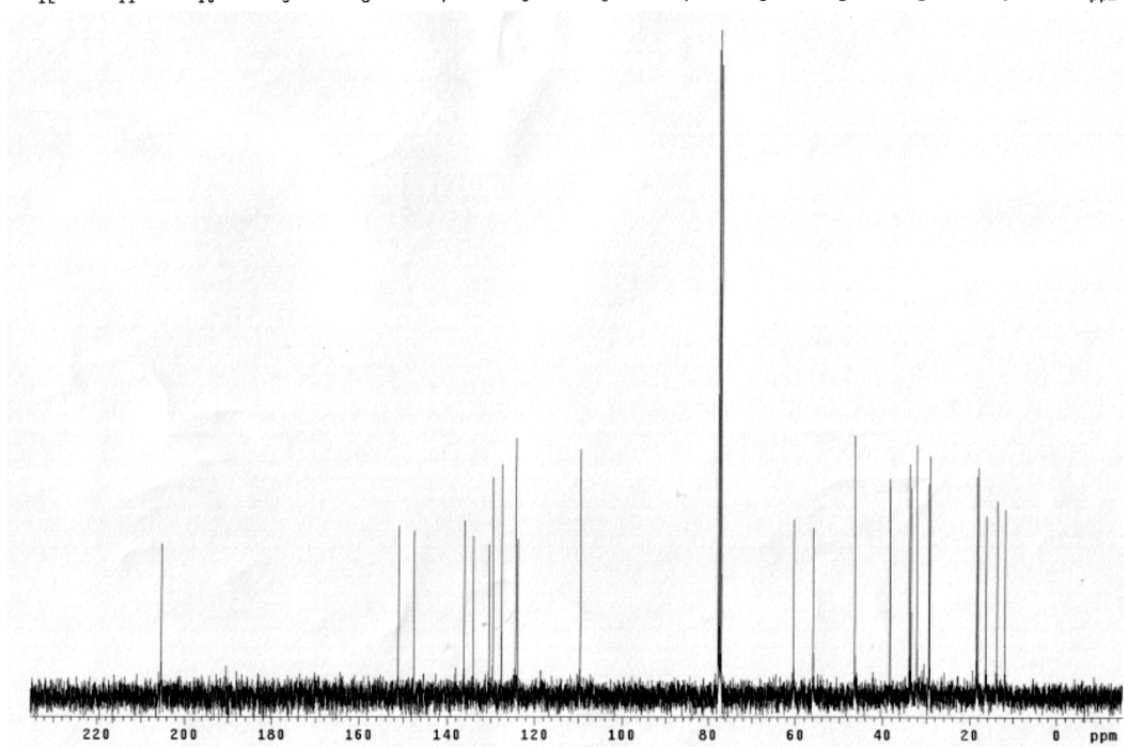
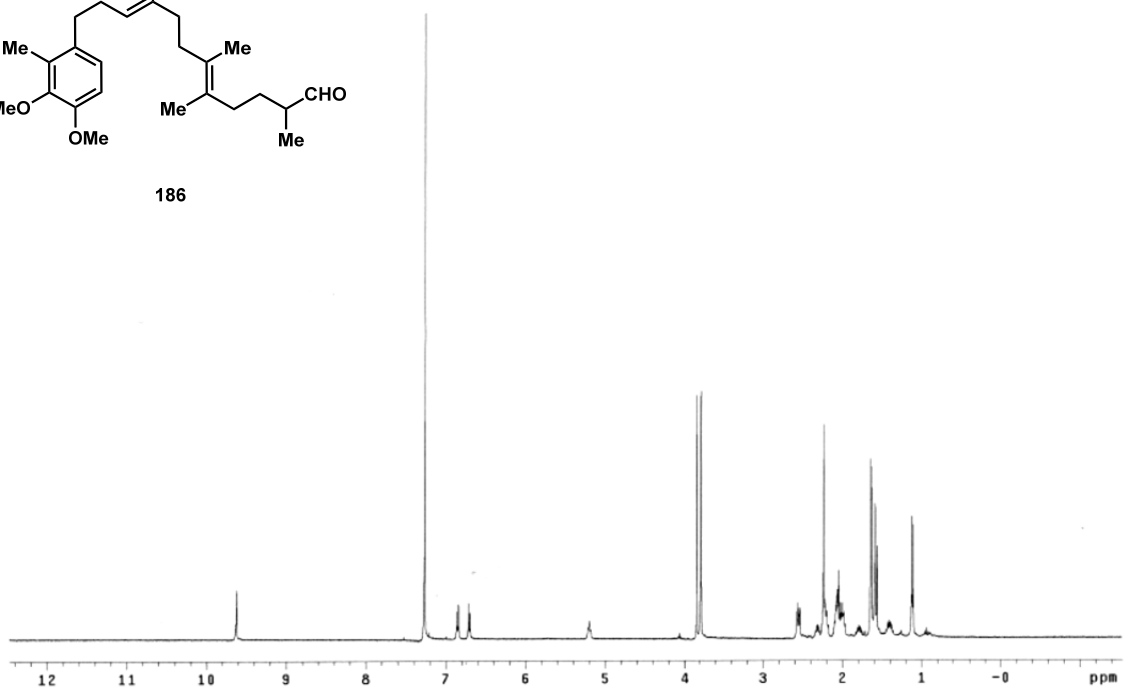
Spectrum: *Tue Aug 16 10:07:55 2011 (GMT-05:00)
 Region: 4000.00 400.00
 Absolute threshold: 85.023
 Sensitivity: 50

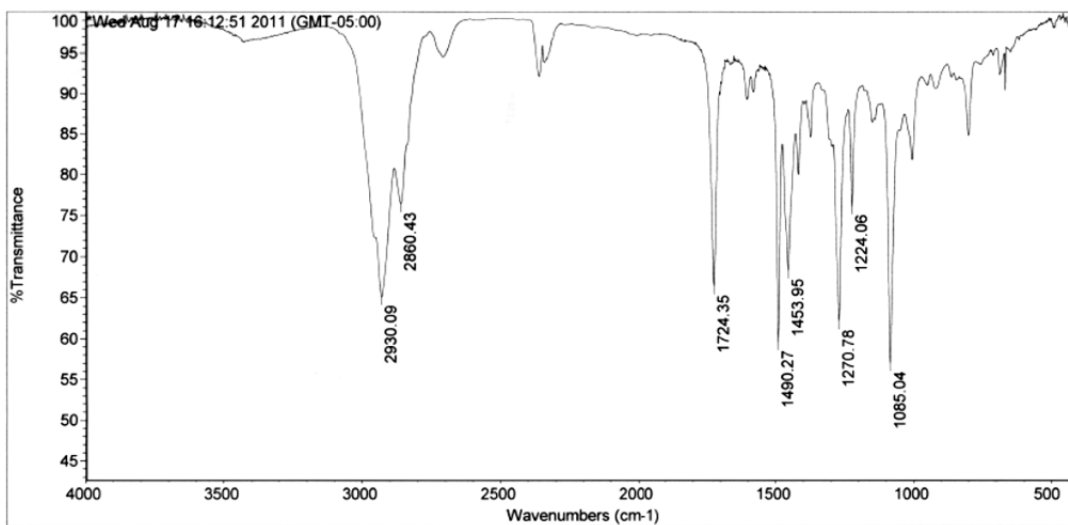
Peak list:

Position	Intensity
800.92	82.569
1005.60	76.289
1044.05	72.614
1085.19	57.244
1150.16	84.823
1223.56	74.238
1270.28	61.054
1373.16	81.150



186





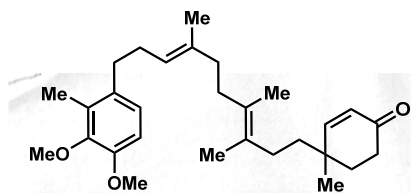
Wed Aug 17 16:15:06 2011 (GMT-05:00)

FIND PEAKS:

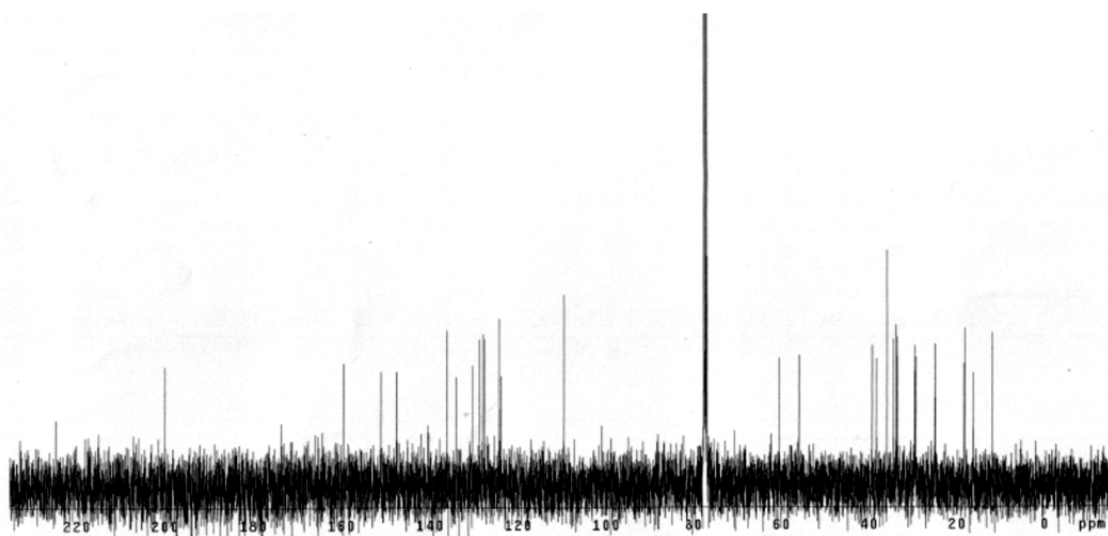
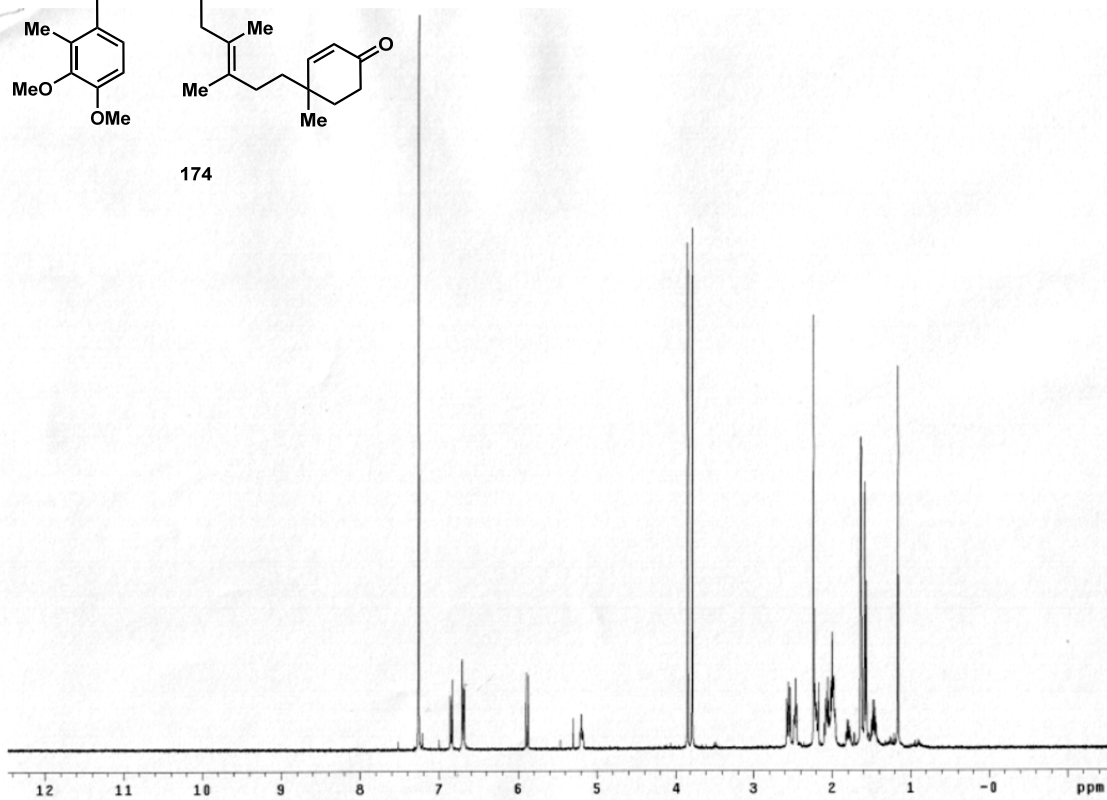
Spectrum: *Wed Aug 17 16:12:51 2011 (GMT-05:00)
 Region: 4000.00 400.00
 Absolute threshold: 78.477
 Sensitivity: 50

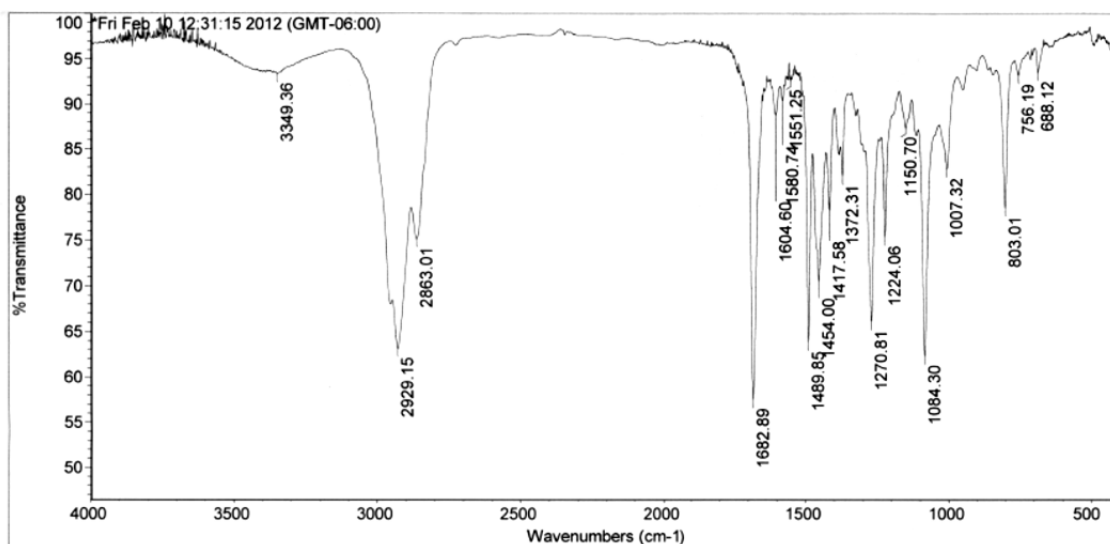
Peak list:

Position:	1085.04	Intensity:	56.939
Position:	1224.06	Intensity:	76.009
Position:	1270.78	Intensity:	62.123
Position:	1453.95	Intensity:	68.346
Position:	1490.27	Intensity:	59.436
Position:	1724.35	Intensity:	66.350
Position:	2860.43	Intensity:	76.412
Position:	2930.09	Intensity:	65.065



174





Fri Feb 10 12:33:26 2012 (GMT-06:00)

FIND PEAKS:

Spectrum: *Fri Feb 10 12:31:15 2012 (GMT-06:00)

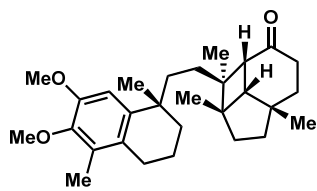
Region: 4000.00 400.00

Absolute threshold: 94.445

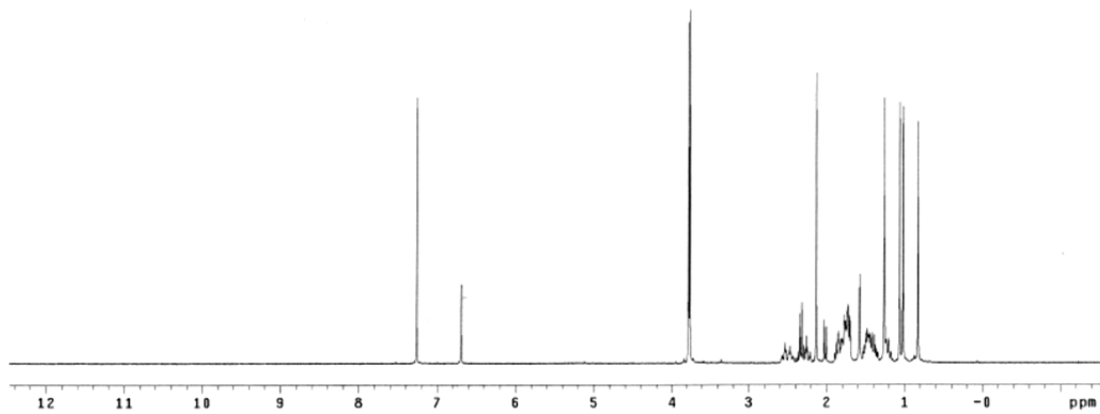
Sensitivity: 50

Peak list:

Position:	688.12	Intensity:	93.513
Position:	756.19	Intensity:	93.218
Position:	803.01	Intensity:	78.503
Position:	1007.32	Intensity:	82.770
Position:	1084.30	Intensity:	62.223
Position:	1150.70	Intensity:	87.323
Position:	1224.06	Intensity:	75.312
Position:	1270.81	Intensity:	66.045



188 (Major)

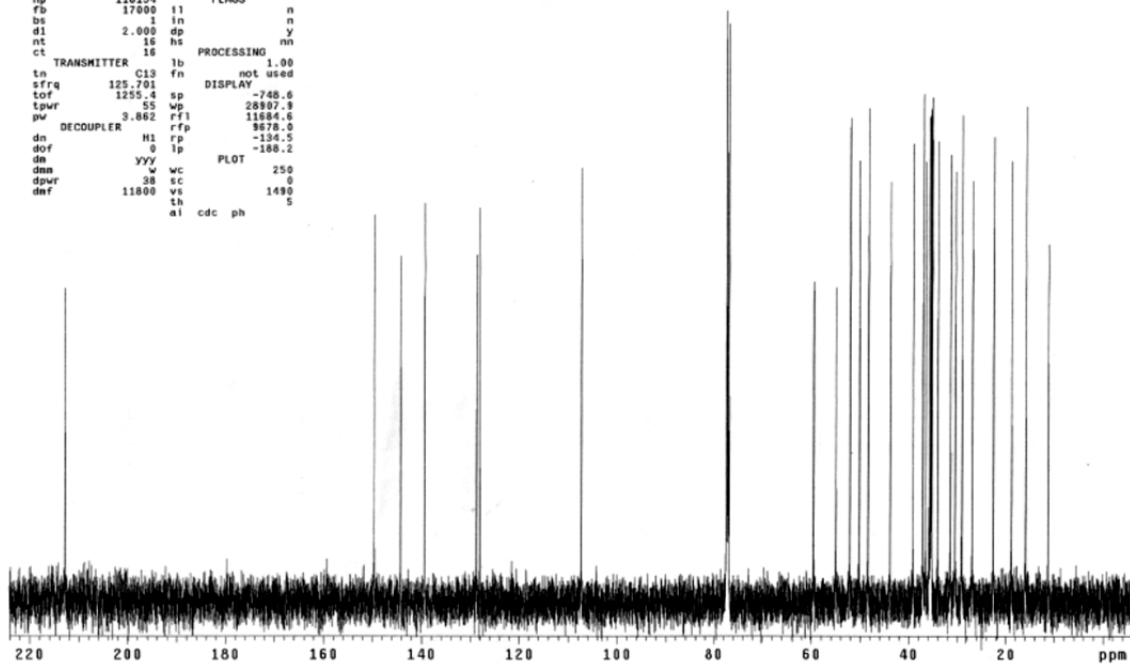


500 MHz var0

amc_cyclization_major_c13

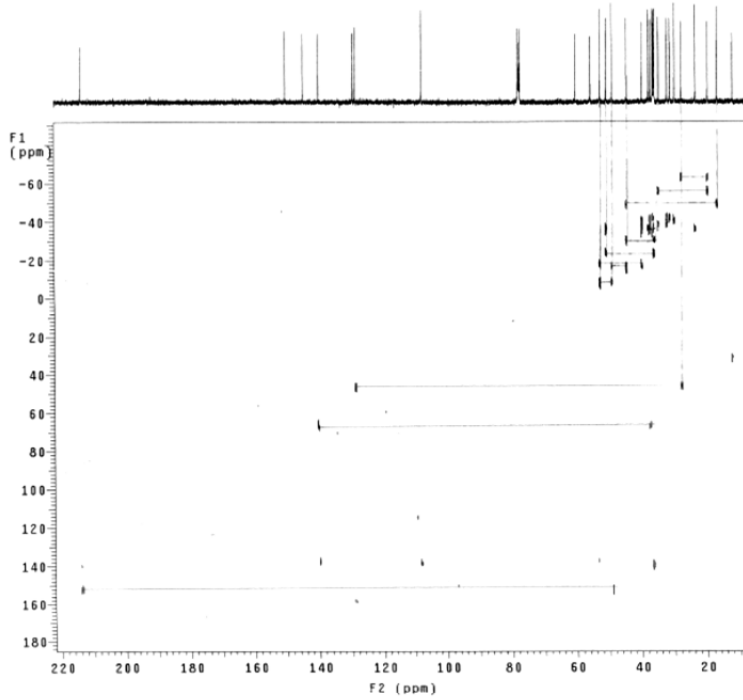
exp1 Carbon

SAMPLE		SPECIAL	
date	Oct 17 2012	temp	27.0
solvent	cdc13	gain	50
file	exp	spin	20
ACQUISITION			
sv	30165.3	pw90	11.000
at	1.358	a1fa	10.000
np	118154	FLAGS	
fb	17000	il	n
bs	1	ln	n
d1	2.000	dp	y
nt	16	hs	nn
ct	16	PROCESSING	
TRANSMITTER		lb	1.00
tn	C13	fn	not used
sfrq	125.701	DISPLAY	
tof	1255.4	sp	-740.6
tpwr	55	wp	28807.9
pw	3.862	rfl	11684.6
DECOUPLER		rfp	3678.0
dn	H1	rp	-134.5
dof	0	lp	-188.2
dn	yyy	PLOT	
dms	w	wc	250
dpwr	38	ec	0
dof	11800	vs	1490
		th	5
		a1	cdc ph



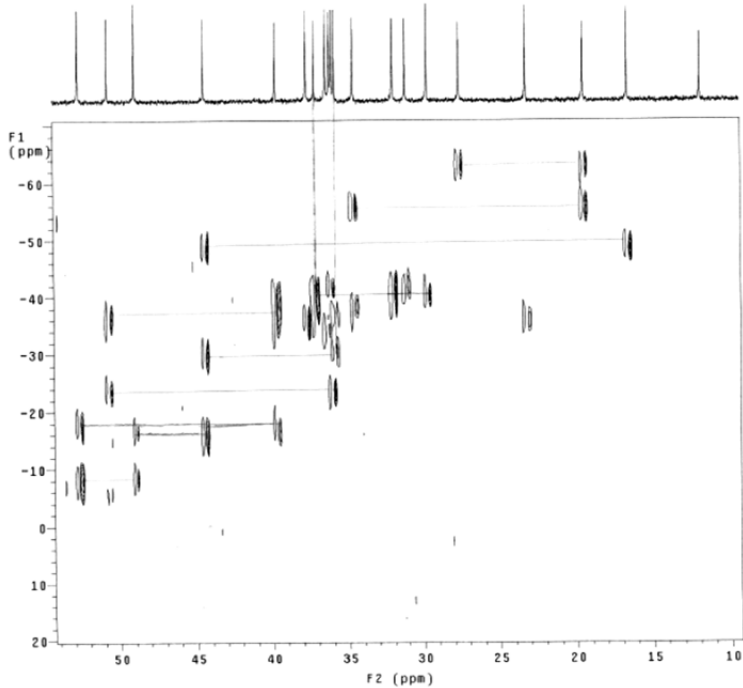
AKC_Major2

Sample Name:
AKC_Major2
Date Collected on:
Agilent-WR-vwrs400
Archive directory:
/hoss/elgin/vwrsys/data
Sample directory:
AKC_Major2_20121018_01
Fidfile: INADEQUATE_01
Pulse Sequence: INADEQUATE
Solvent: cdcl3
Data collected on: Oct 18 2012
Temp. 26.0 C / 299.1 K
Operator: elgin
Relax. delay 1.000 sec
Acq. time 0.002 sec
Width 25000.0 Hz
2D Width 50000.0 Hz
256 repetitions
2 x 64 increments
OBSERVE C13, 100.5226207 MHz
DECOUPLE H1, 399.7734871 MHz
Power 37 dB
continuously on
WALTZ-16 modulated
DATA PROCESSING
Gauss apodization 0.030 sec
F1 DATA PROCESSING
Gauss apodization 0.001 sec
F1 size 4096 x 4096
Total time 10 hr



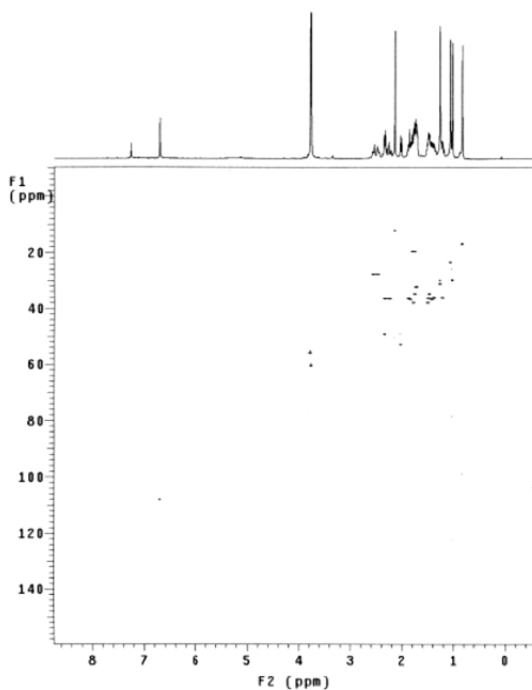
AKC_Major2

Sample Name:
AKC_Major2
Date Collected on:
Agilent-WR-vwrs400
Archive directory:
/hoss/elgin/vwrsys/data
Sample directory:
AKC_Major2_20121018_01
Fidfile: INADEQUATE_01
Pulse Sequence: INADEQUATE
Solvent: cdcl3
Data collected on: Oct 18 2012
Temp. 26.0 C / 299.1 K
Operator: elgin
Relax. delay 1.000 sec
Acq. time 0.002 sec
Width 25000.0 Hz
2D Width 50000.0 Hz
256 repetitions
2 x 64 increments
OBSERVE C13, 100.5226207 MHz
DECOUPLE H1, 399.7734871 MHz
Power 37 dB
continuously on
WALTZ-16 modulated
DATA PROCESSING
Gauss apodization 0.030 sec
F1 DATA PROCESSING
Gauss apodization 0.001 sec
F1 size 4096 x 4096
Total time 10 hr



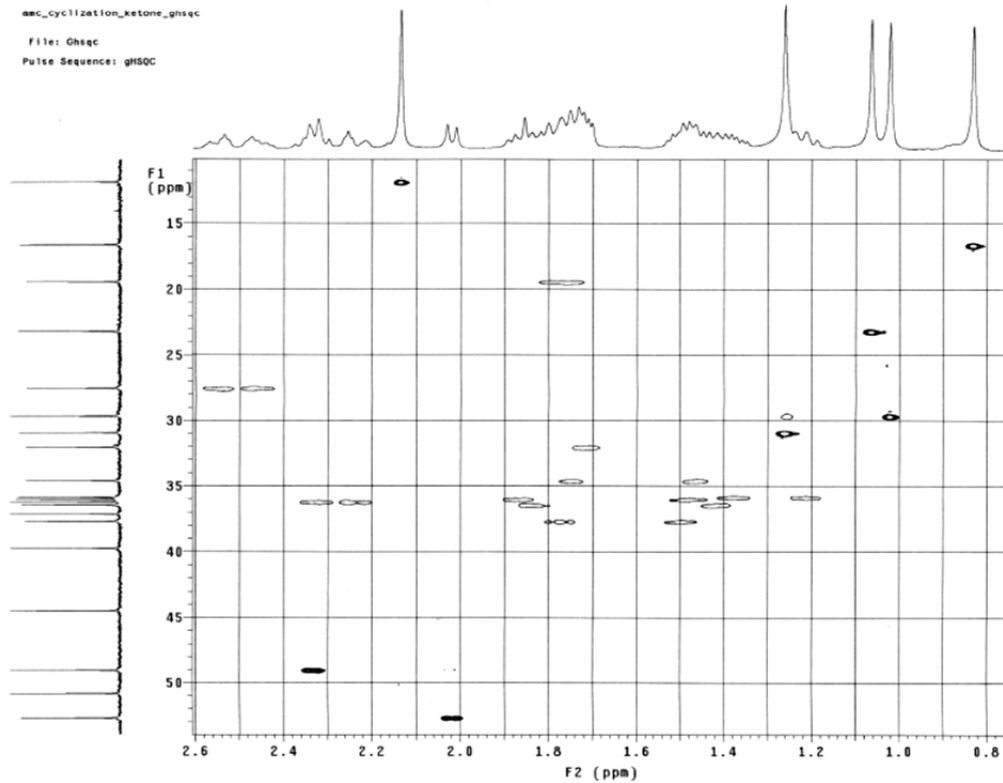
amc_cyclization_ketone_ghsec

```
exp6 Ghsec
SAMPLE
date Jan 26 2012 ns FLAGS n ACQUISITION ARRAYS
solvent cdc13 sspul y array phase
sample PFG1g y arraydim 1624
ACQUISITION hsqiv1 4694 1 phase
sw 4644.7 SPECIAL 27.0 2
at 0.188 temp 20
np 1952 gain 20
fb 3000 spn 0
ss 32 GRADIENTS
d1 2.000 gziv11 4694
nt 2 g11 0.002000
2D ACQUISITION gziv13 2355
sw1 21367.5 qt3 0.001000
nl 512 sntab 0.000500
phase arrayed F2 PROCESSING
PRESATURATION grf 0.892
satmode nnn gra not used
satdly 0 fn 4096
satfrra 499.8 F1 PROCESSING
satpwr -13 grf1 0.022
TRANSMITTER H1 proc1 lp
sfrq 499.867 fn1 4096
LOF -456.7 DISPLAY -275.8
LWR 57 sp -1278.4
pw 11.000 wp 4642.4
dn DECOUPLER C13 wp1 21357.1
dof -2515.3 rfp1 3626.2
de 000 rfp 3346.1
dmf 14285 rfp1 14857.4
dpr 40 rfp1 13567.6
pwxiv1 96 PLOT
pwx HSQC 9.500 wc 116.0
j1wh 140.0 wc2 116.0
multiflg 2 wcz 0
mult 2 vs 872
et cdc ph 2
```



amc_cyclization_ketone_ghsec

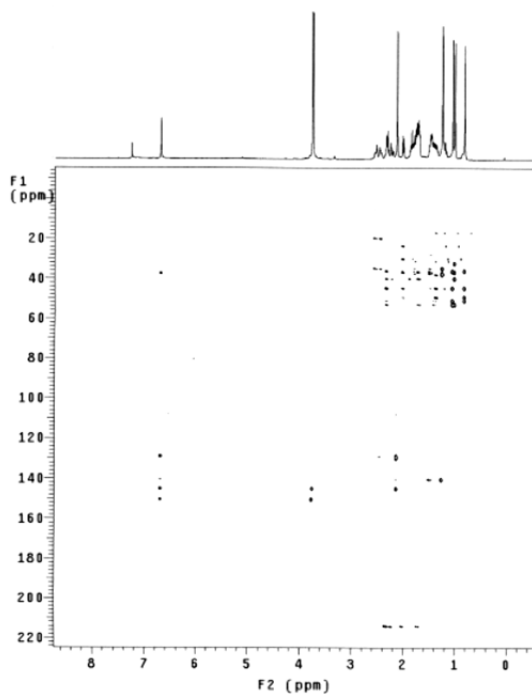
File: Ghsec
Pulse Sequence: gHSQC



amc_cyclization_ketone_ghabc

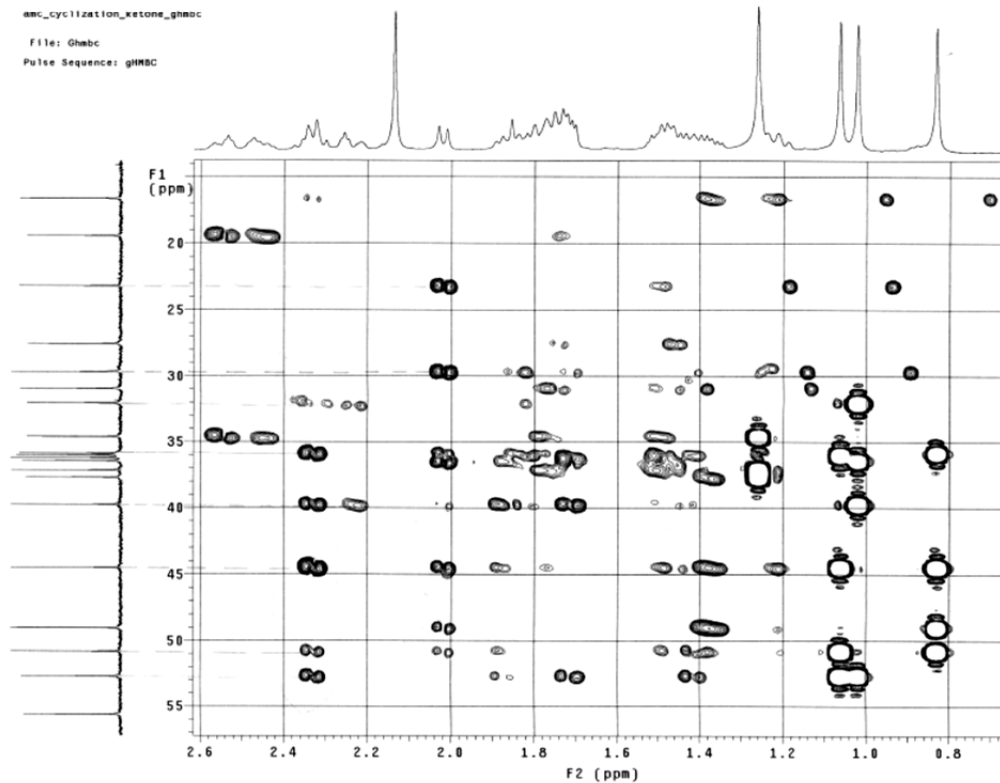
exp7 Ghabc

```
SAMPLE          hs   FLAGS          n
date    Jan 26 2010  cdcl3          n
solvent          cdcl3          n
sample          PFG1g            y
ACQUISITION     hzgvlv1          4684
sw          4644.7          SPECIAL 27.0
at          9.128          temp    0
np          1190          gain    8
fb          3000          sp10   0
ss          32          GRADIENTS 0
d1          2.000          g2lv11 4684
nt          8          g11      0.001000
2D ACQUISITION  g2lv13          2355
sw1         30185.9          g13      0.001000
nt          512          g1tab    0.000500
phase       0          F2 PROCESSING
PRESATURATION  sb          0.864
satmode       nnn          sbx          not used
satdly        0          fn          2048
satfrq        489.8          F1 PROCESSING
satpwr       -13          sb1          0.008
TRANSMITTER    HI          sb11         not used
tn           40          fml          4086
sfrq         489.867          DISPLAY
tof          -456.7          sp          -275.5
lwr         57          wp          4646.1
pw          11.000          sp1         -1805.5
DECOUPLER     C13          rfp1        30151.2
dn           13          rff1        1346.7
dor         1255.4          rfp        1086.7
dm          nnn          rff1        6586.8
dwr         14285          rfp1        4670.6
qpr         40          PLOT
pwxlv1       56          wc          116.0
pwx         9.500          sc          10.0
HWBC
j1xh         140.0          sc2         0
j1xh         8.0          vs          90976
          th
          ai cdc av          2
```



amc_cyclization_ketone_ghabc

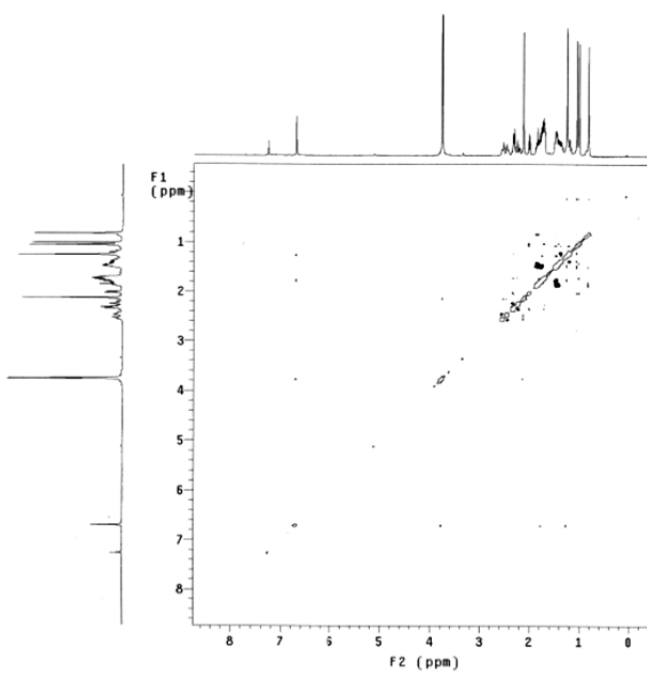
File: Ghabc
Pulse Sequence: gHWBC



amc_cyclization_ketone_noesy

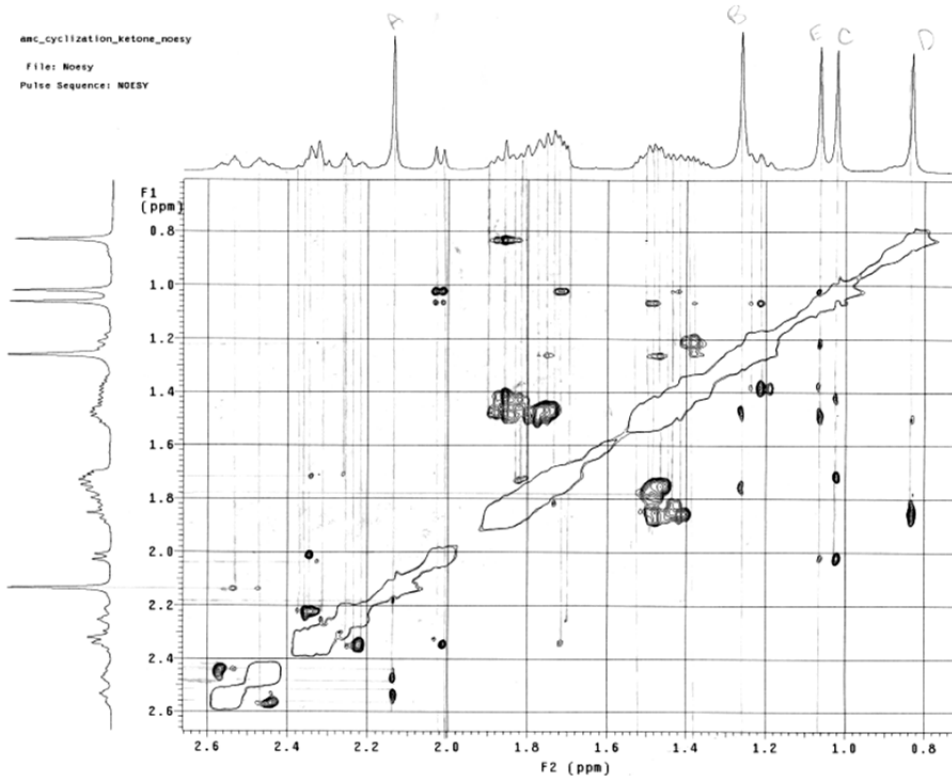
exp8 Noesy

```
SAMPLE          FLADS
date Jan 26 2012  hg      n
solvent cdc13      csu1    y
sample         PF01g     y
ACQUISITION    hsgv1    4694
sw 4644.7        SPECIAL
at 0.220        temp     27.0
sp 2686         gain     8
fb 3000         spin    0
ss 32          F2 PROCESSING
d1 2.000        gf       0.102
nt 8           fu       not used
2D ACQUISITION 8        f3 PROCESSING
sw1 4644.7     f3       4086
nt 250        gf1      0.051
TRANSMITTER    h1       proc1   1a
t1 499.867    f1       4086
tof -456.7    DISPLAY
spw 37        sp       -275.8
pw 11.000     wp       4642.4
NOESY         sp1      -276.4
mix 0.800     wp1      4642.4
PRESATURATION rf1      3907.0
satmode nnn   rfg      3629.0
satpwr -13     rf12     3907.7
satqly 0      rfp1     3629.0
satfrq 499.8 PLOT
DECOUPLER     wc       116.0
dn C13        cc       10.0
dm nnn        wc2      116.0
                cc2       0
                vs       209
                th       2
                al cdc ph
```

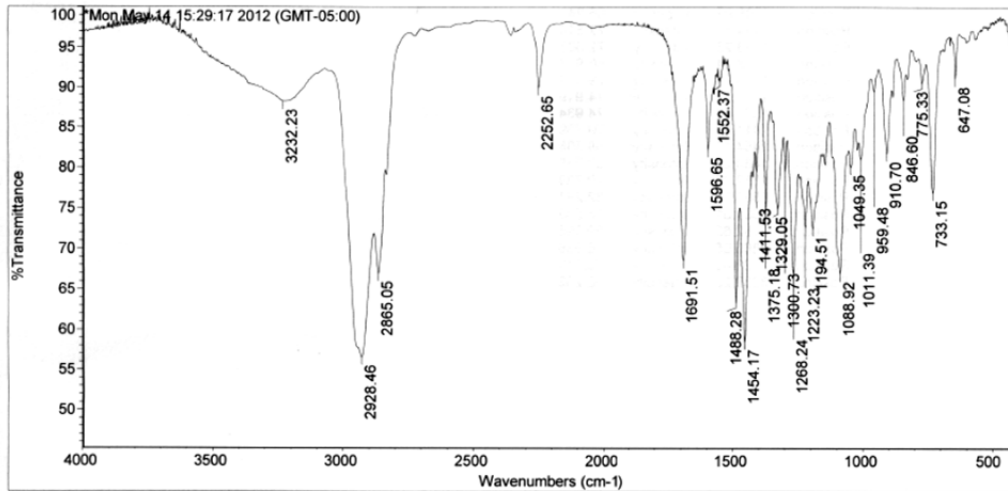
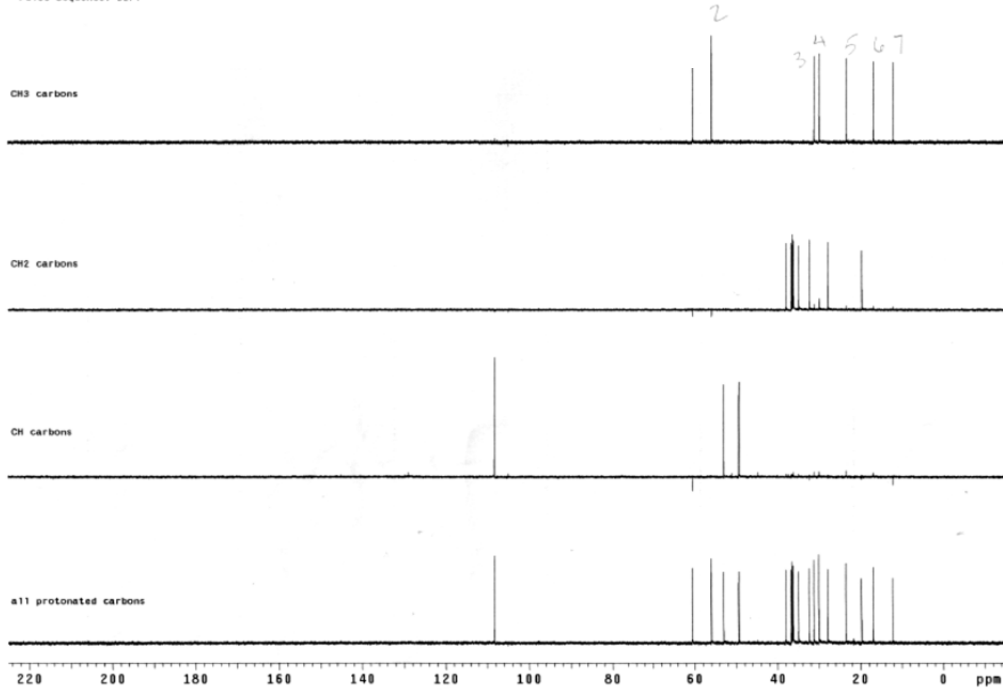


amc_cyclization_ketone_noesy

File: Noesy
Pulse Sequence: NOESY



aac_cyclization_ketone_dept
 File: Dept
 Pulse Sequence: DEPT



Mon May 14 15:32:57 2012 (GMT-05:00)

FIND PEAKS:

Spectrum: *Mon May 14 15:29:17 2012 (GMT-05:00)
 Region: 4000.00 400.00
 Absolute threshold: 92.042
 Sensitivity: 50

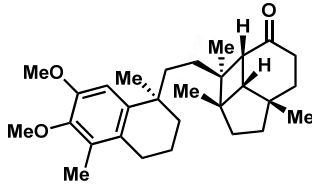
Position:	Intensity:
647.08	91.157
733.15	76.911
775.33	90.534
846.60	88.466
910.70	81.757
959.48	89.534
1011.39	81.037
1049.35	80.098

600 MHz nroox

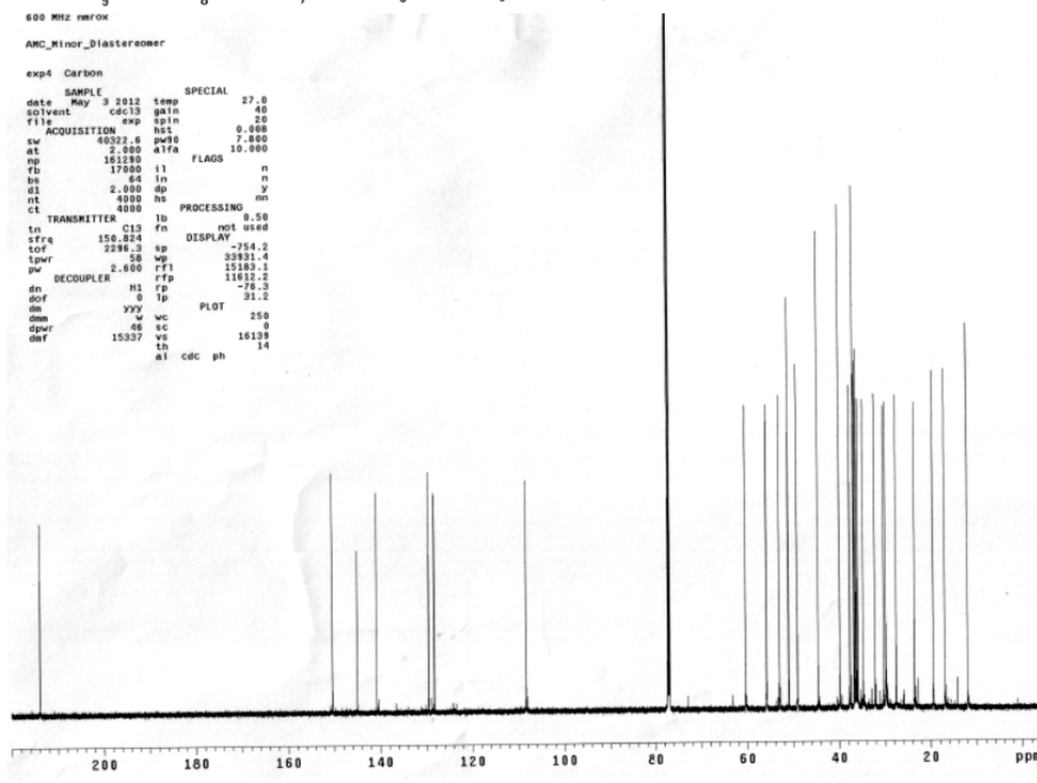
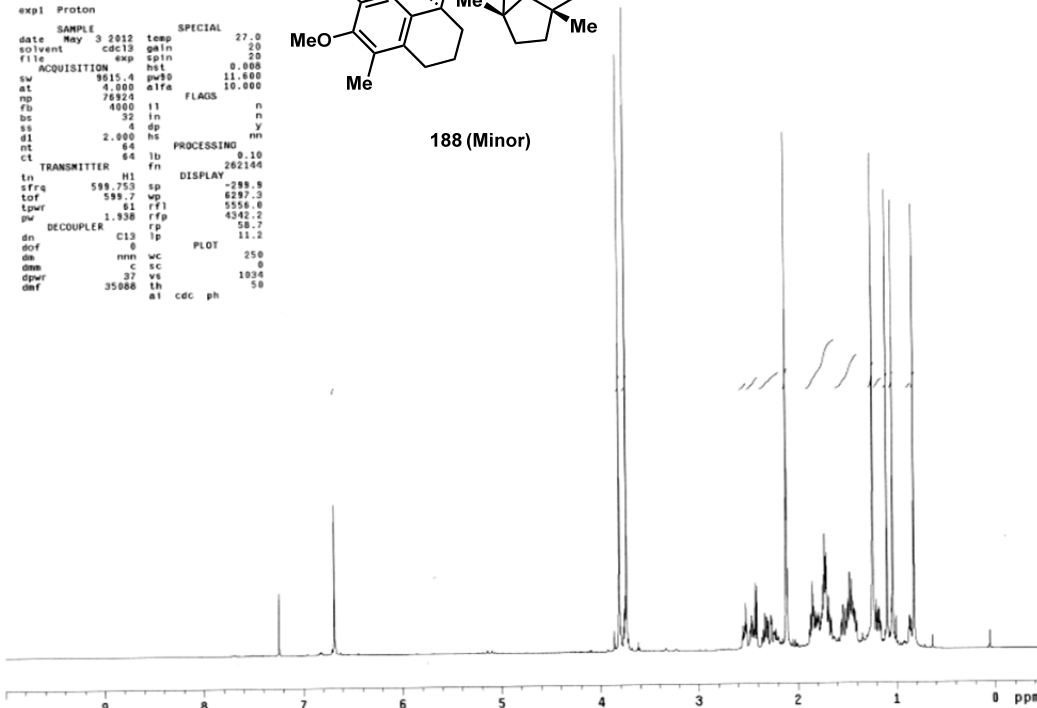
AMC_Minor_Diastereomer

exp1 Proton

```
SAMPLE SPECIAL 27.0
date May 3 2012 temp gain 20
solvent cdc13 gain 20
file exp sp1n 20
ACQUISITION hst 0.008
sw 9615.4 pw90 11.600
at 4.000 a1fa 10.000
np 76824 FLAGS
fb 4800 n
bs 32 in n
ss 4 dp y
g1 2.000 hs mn
nt 64 PROCESSING 0.10
ct 64 fb 262144
TRANSMITTER fn
tn H1 DISPLAY
sfrq 599.753 sp -288.9
tof 599.7 wp 6297.3
tpwr 61 rfl 5556.0
pw 1.938 rfp 4582.2
DECOUPLER rp 58.7
dn C13 lp 11.2
dof 6 PLOT
ds mn wc 250
dm c sc 0
dpr 37 vs 1034
dmf 35006 th 50
a1 cdc ph
```



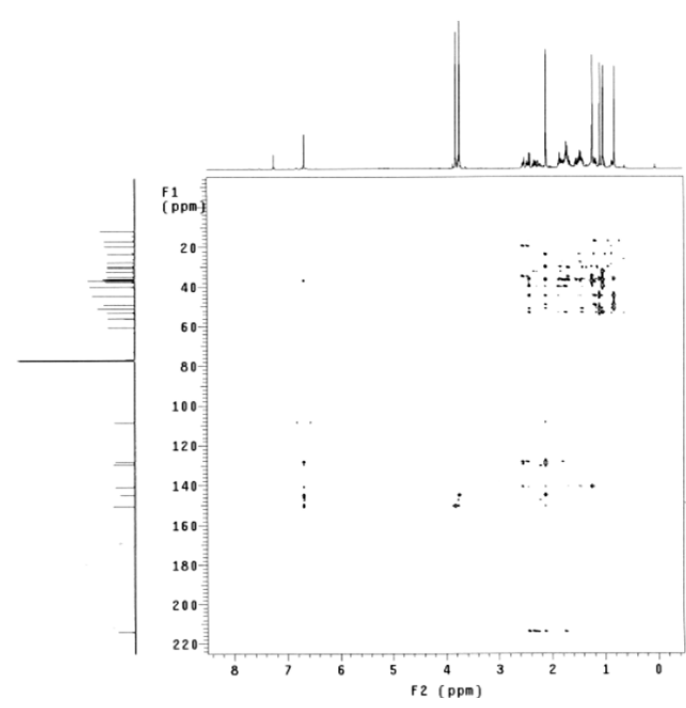
188 (Minor)



ANC_Minor_Diastereomer

```

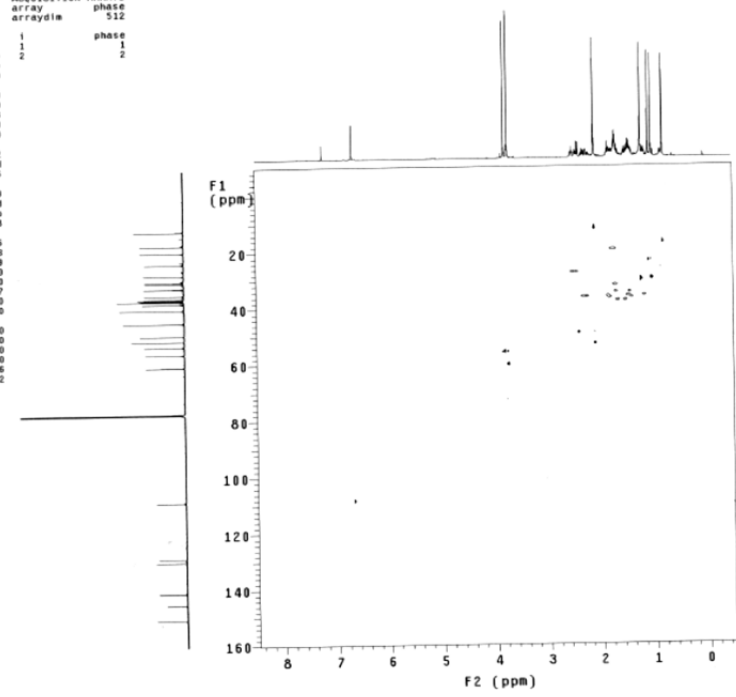
exp7 Qhbc
SAMPLE          FLAGS
date May 3 2012 hs n
solvent cdc13 sspul y
sample PFGfg 7664 y
ACQUISITION    hsglv1 SPECIAL
sw 5387.9
at 0.128 temp 27.0
np 1386 gain 2.0
fb 4800 spn 0
ss 32 GRADIENTS
d1 2.000 gzlv1 10219
nt 8 gt1 0.001000
2D ACQUISITION gzlv13 5138
sw1 36199.1 gt3 0.001000
nl 512 gstab 0.000500
phase
PRESATURATION sb 0.864
satmode mnn sbs not used
satdly 0 fn 4096
satfrs 499.8 f1 PROCESSING
satpwr -13 sb1 0.014
TRANSMITTER H1 sb1 not used
tn H1 proc1 lp
sfrq 599.752 fml 4096
tof -596.5 sp DISPLAY
tpwr 81 sp -289.0
pw 11.600 wp 5385.3
DECOUPLER C13 wp1 -2247.1
dn 1542.3 rf1 291.7
dm mny rfp 0
dwr 35088 rf11 2264.0
dpwr 37 rfp1 0
pwxlv1 57 PLOT
pwx HMBC 8.600 wc 116.0
j1xh 140.0 wc2 116.0
j1xh 8.0 sc2 0
wv th 231754
al cdc av 2
  
```



ANC_Minor_Diastereomer

```

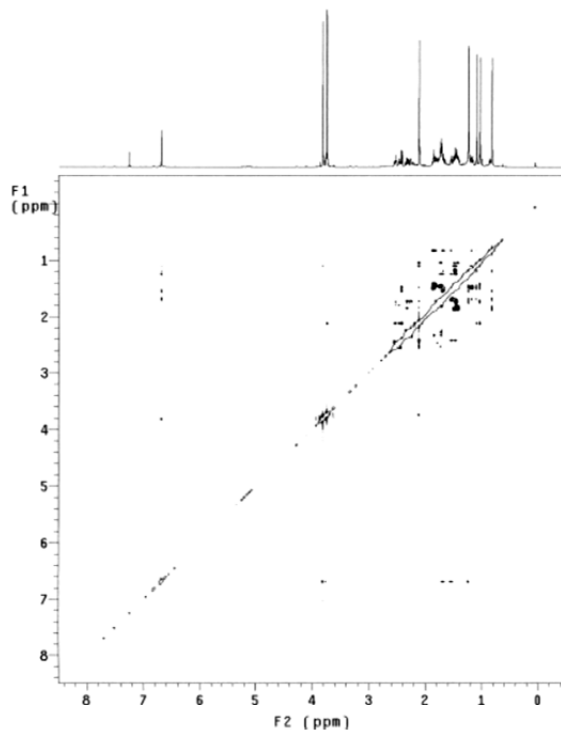
exp6 Qhbc
SAMPLE          FLAGS          ACQUISITION ARRAYS
date May 3 2012 hs n array phase
solvent cdc13 sspul y arraydim 512
sample PFGfg 7664 y
ACQUISITION    hsglv1 SPECIAL 1 phase
sw 5387.9
at 0.199 temp 27.0
np 2148 gain 3.0
fb 4800 spn 0
ss 8 GRADIENTS
d1 2.000 gzlv1 10219
nt 2 gt1 0.001000
2D ACQUISITION gzlv13 5138
sw1 25641.0 gt3 0.000500
nl 256 gstab 0.000500
phase arrayed f2 PROCESSING 1
PRESATURATION gf 0.092
satmode mnn gfs not used
satdly 9 fn 4096
satfrs 499.8 f1 PROCESSING
satpwr -13 gf1 0.000
TRANSMITTER H1 gf1 not used
tn H1 proc1 lp
sfrq 599.752 fml 2048
tof -596.5 sp DISPLAY
tpwr 81 sp -282.6
pw 11.600 wp 5385.3
DECOUPLER C13 wp1 -1484.9
dn -2881.9 rf1 2536.0
dm mny rfp 2240.7
dwr 35088 rf11 1510.0
dpwr 37 rfp1 0
pwxlv1 57 PLOT
pwx HSQC 8.400 wc 116.0
j1xh 140.0 wc2 116.0
mult 2 vs 6296
al cdc ph 2
  
```



AMC_Minor_Diastereomer

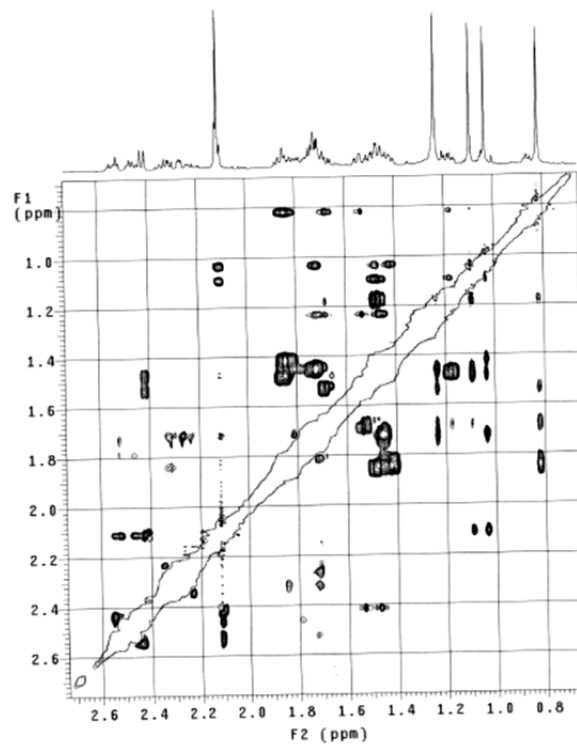
```

exp8 Noesy
SAMPLE          2D DISPLAY      ACQUISITION ARRAYS
date   May 3 2012   sp1          -291.5   array   phase
solvent cdc13      wp1          5382.7   arraydm 512
file    exp        sc2          0
ACQUISITION      wc2          116      phase
sfrq    599.752    rrf1         4638.9   1
tn       H1        rfp1         4342.2   2
at       0.190     dfrq         DEC. & VT
np       2048      dfrq         150.821
sw       5387.9    dn          C13
fb       4000      dpwr         31
bs       32        dor         0
ss       10        dm          n
tpwr     61        dsm         C
pw       11.6      dmf         29412
compH    1.0639    dseq
dl       2.000     dres        9.0
mix      0.800     homo        n
tof      -536.5    temp        27.0
nt       8
ct       8        dfrq2       0
gain     20       dn2         1
stpul    y       dpwr2       0
gt1      0.0025    dm2         n
gzlv11   8175     dm2         c
hg1      0.0020    dm2         n
hg1v1    6151     dm2         29412
satmode   nnn     dseq2       1.0
satpwr   -13     dres2       n
satdly    0       homo2       n
scuba     n        dfrq3       DEC3 0
zeflg     y       dn3         0
alt_grd   n        dn3         1
flags     n        dm3         n
in        n        dm3         n
dp        y       dm3         29412
hs        n        dm3         C
stpul    y       dseq3       1.0
2D ACQUISITION dres3
sw       5387.9    homo3       n
ni       256
phase    arrayed  gf          0.088
          DISPLAY  gfs         not used
sp       -291.4    wtfile      ft
wp       5382.7    proc        2048
vs       12991    fn          f
sc       10       math        not used
wc       116      sfilter     not used
hzmm     46.40    sorder      3
ls       5325.63  sstaps      3
rf1      4638.9   2D PROCESSING
rfp      4342.2   gf1         0.055
th       2       rfp1        not used
lms     100.000  wtfile1
al cdc ph      proci       1p
          fn1         2048
    
```



AMC_Minor_Diastereomer

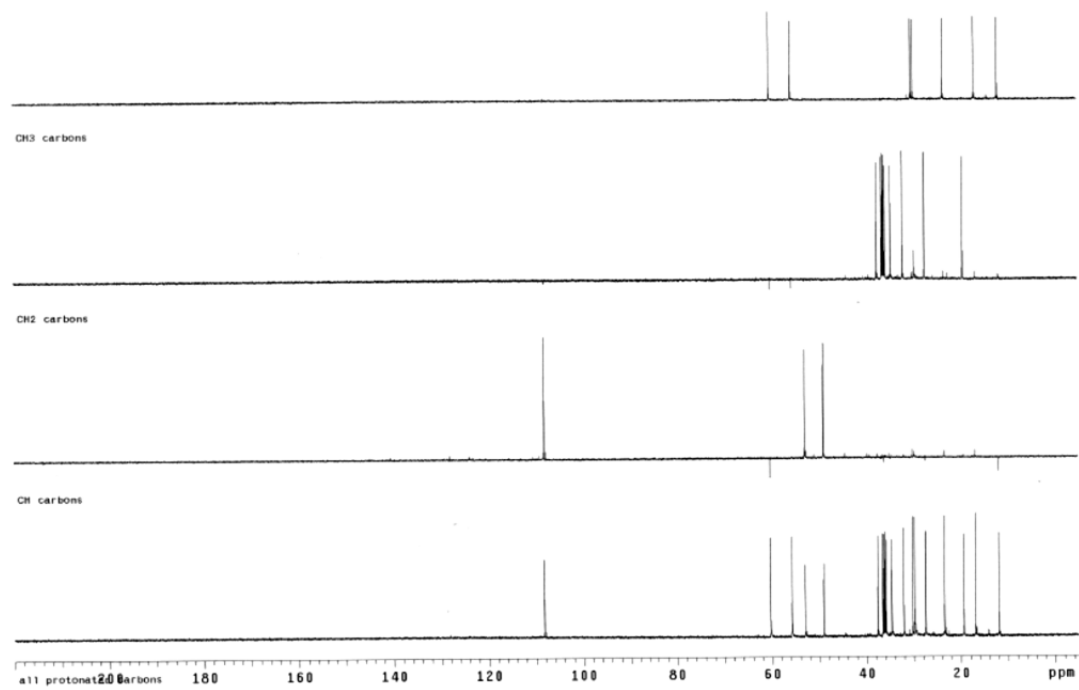
File: xp
Pulse Sequence: NOESY

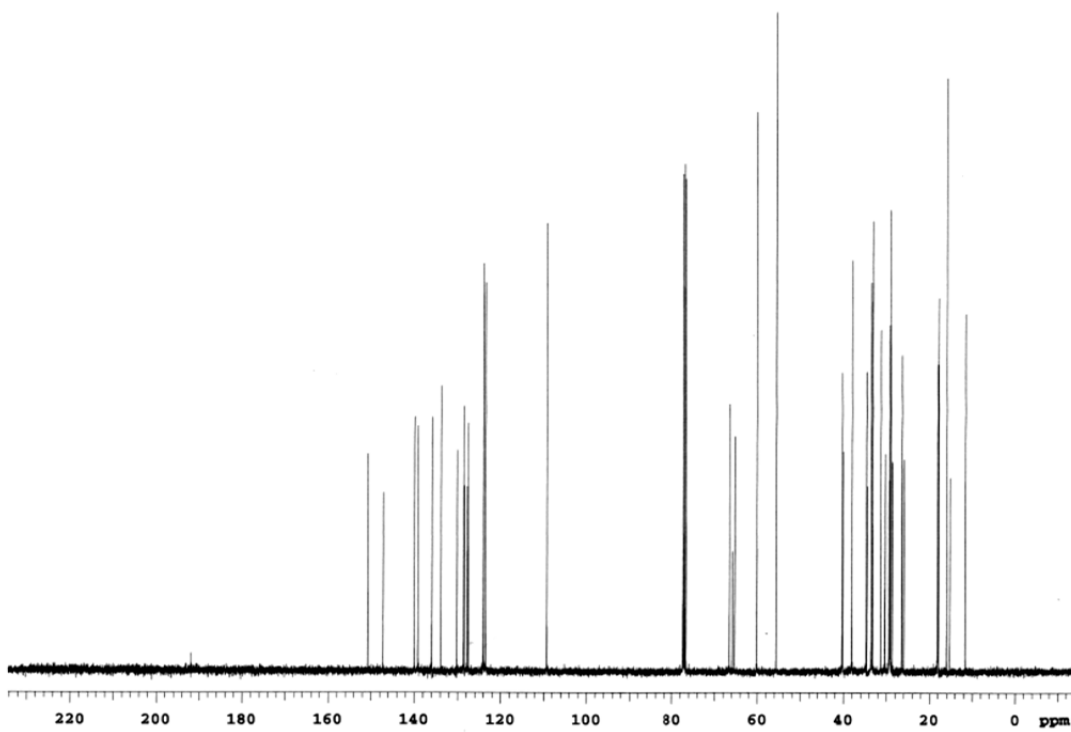
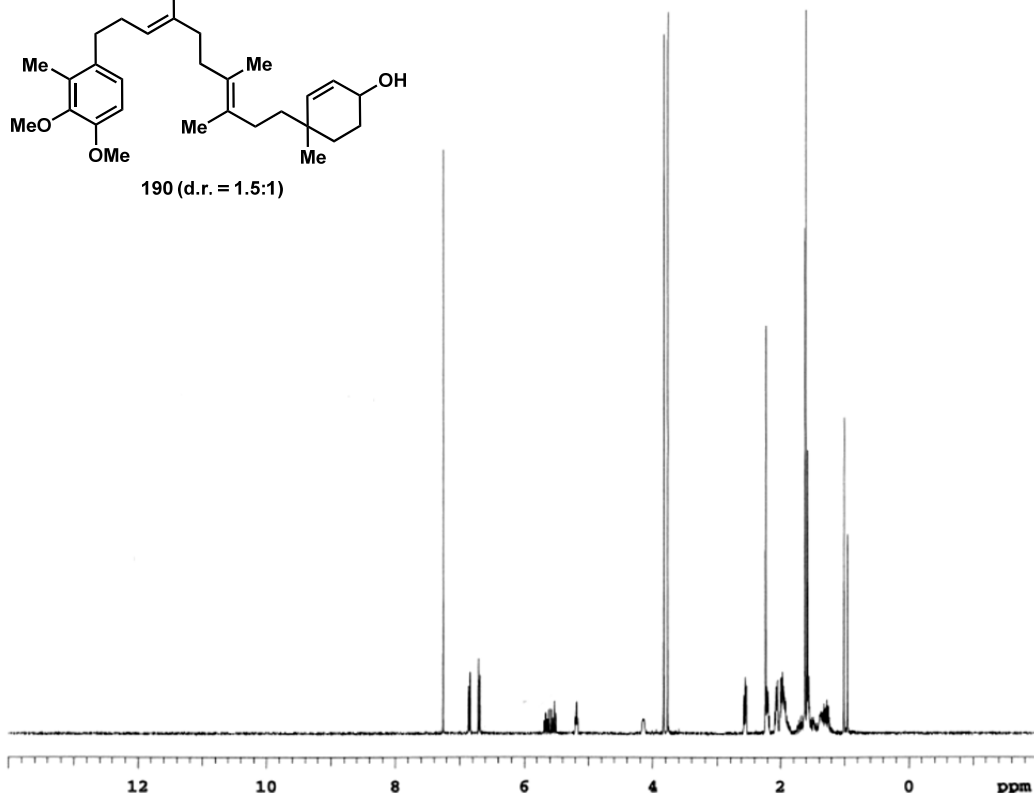
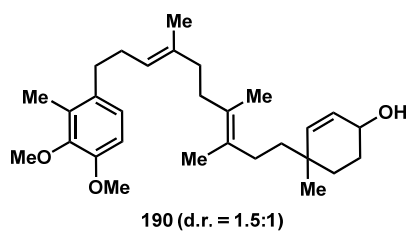


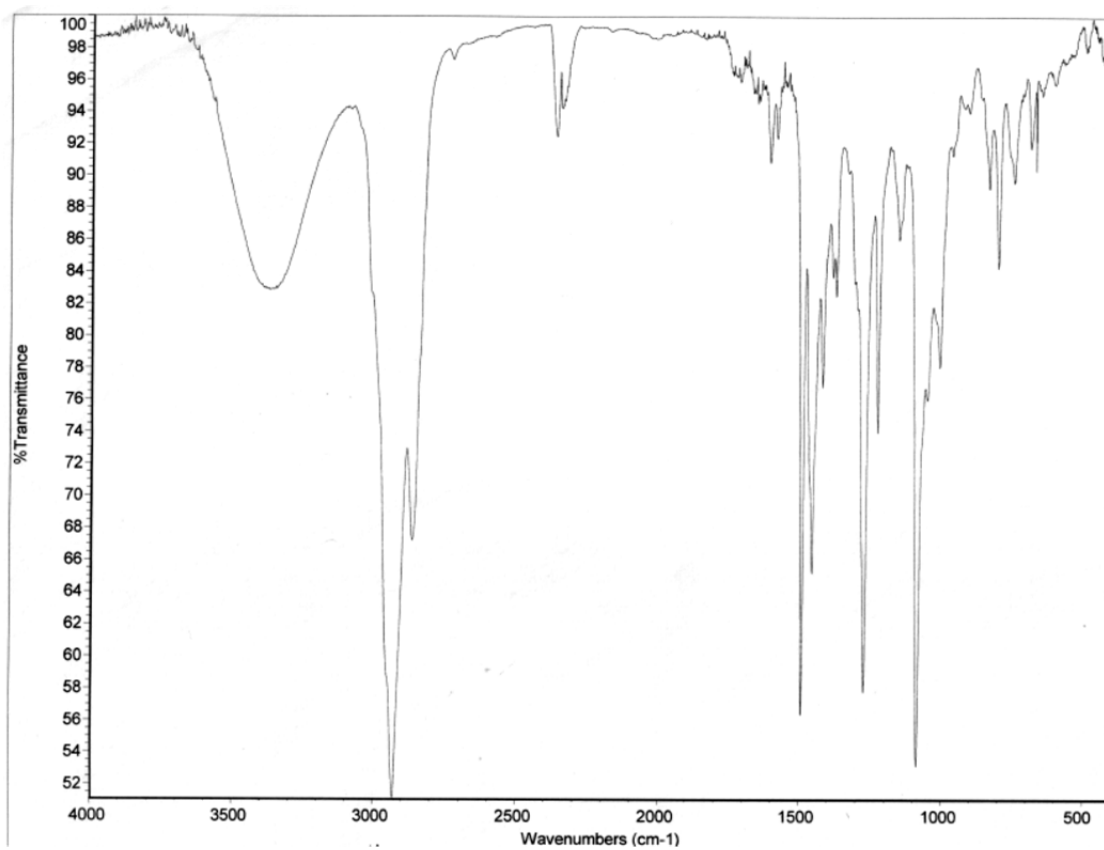
AMC_Minor_Diastereomer

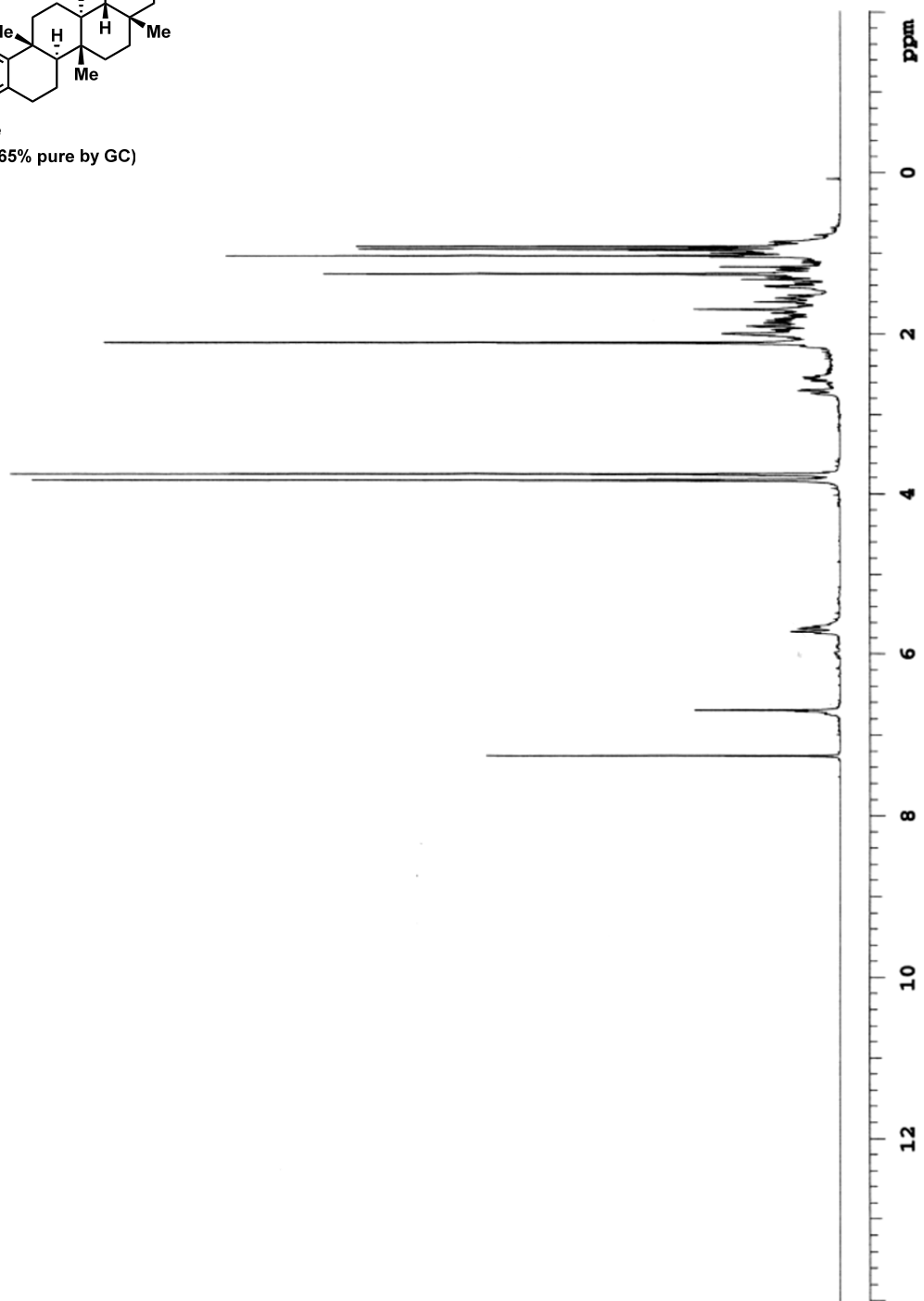
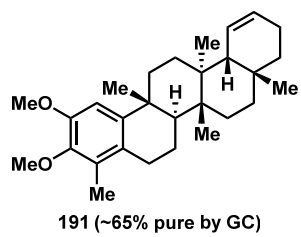
File: xp

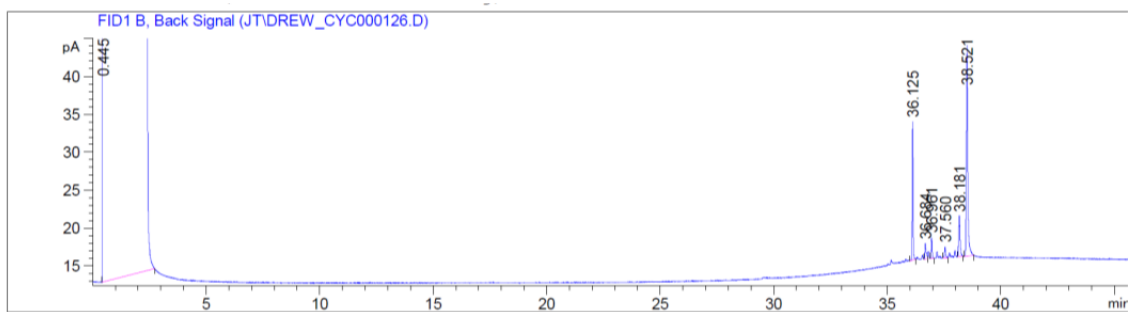
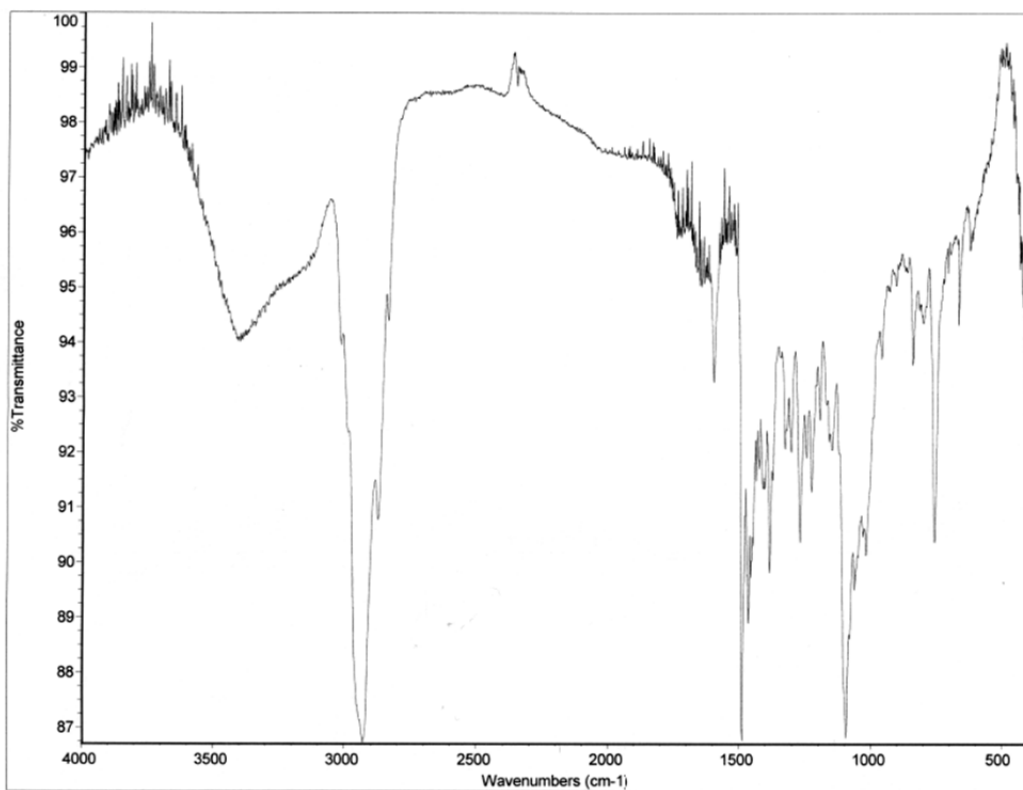
Pulse Sequence: dept







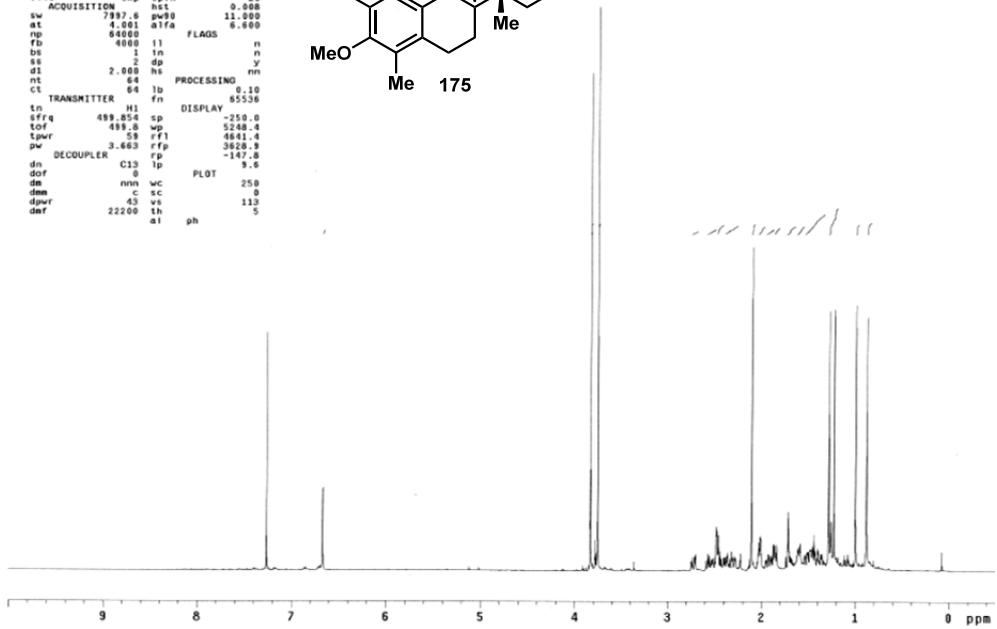
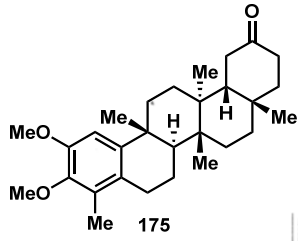




```

500 MHz nmr0
amc_celastrol_ketone_h1
exp1 Proton
SAMPLE
date Sep 18 2013 temp SPECIAL 27.0
solvent cdc13 gain 20
file exp sp1n 20
ACQUISITION hst 0.008
sw 797.6 pw90 11.000
at 4.001 atfa 6.000
np 60000 FLAGS
fb 4000 l1 n
ds 1 l1n n
ss 2 dp y
dl 2.000 hs PROCESSING nm
nt 64
ct TRANSMITTER 64 fb 0.10 65536
tn H1 DISPLAY
sfrq 499.854 sp -250.0
tof 499.8 wp 5240.4
tpwr 29 rfl 4641.4
pw 3.663 rfc 3928.8
DECOUPLER C13 rp -147.0
dn 0 lp PLOT 9.6
dm nnn wc 250
dmc c sc 0
dprf 43 vs 133
dnf 22200 al ph 5

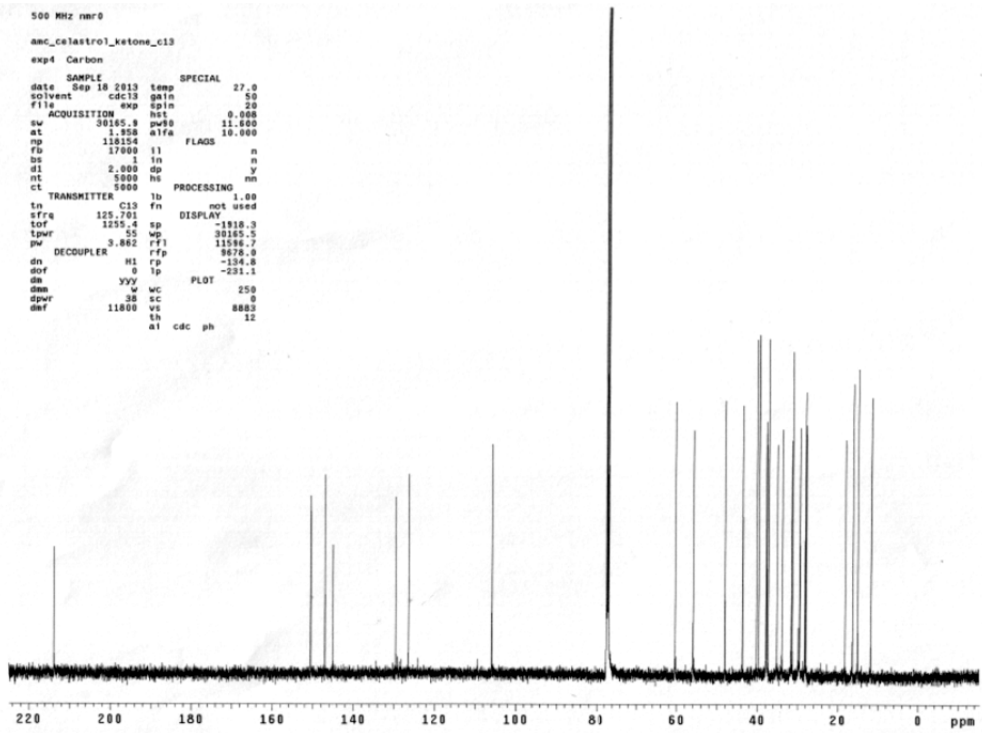
```



```

500 MHz nmr0
amc_celastrol_ketone_c13
exp4 Carbon
SAMPLE
date Sep 18 2013 temp SPECIAL 27.0
solvent cdc13 gain 50
file exp sp1n 20
ACQUISITION hst 0.008
sw 30185.8 pw90 11.000
at 1.958 atfa 10.000
np 101354 FLAGS
fb 17000 l1 n
ds 1 l1n n
ss 2 dp y
dl 2.000 hs PROCESSING nm
nt 5000
ct TRANSMITTER 1b fb 1.00 not used
tn C13 DISPLAY
sfrq 125.701 fn
tof 1255.4 sp -1918.3
tpwr 50 wp 30185.5
pw 3.882 rfl 11586.7
DECOUPLER H1 rfp 8678.0
dn 0 lp PLOT -231.1
dm YYY w wc 250
dmc 38 sc 0
dprf 11800 vs 8883
dnf 11800 al cdc ph 12

```



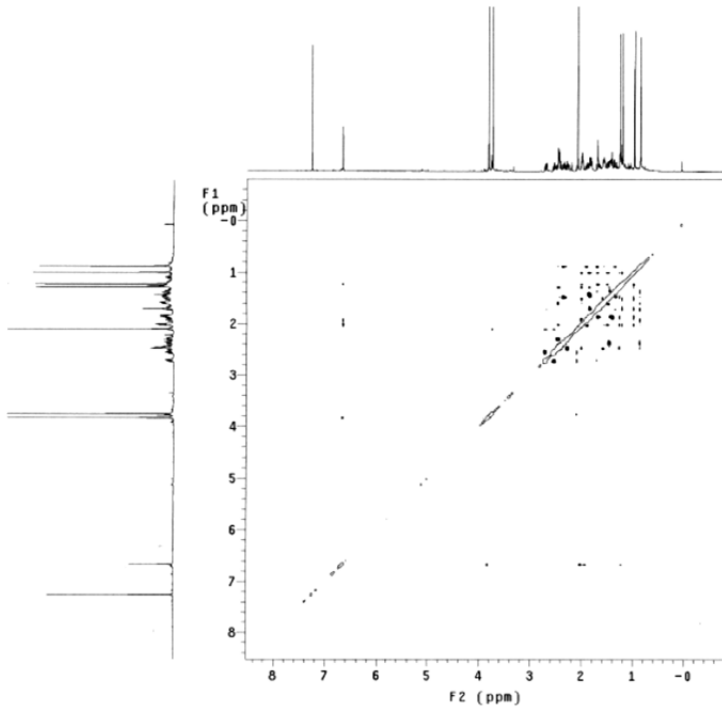
asc_celastrol_ketone_noesy

exp8 Noesy

```

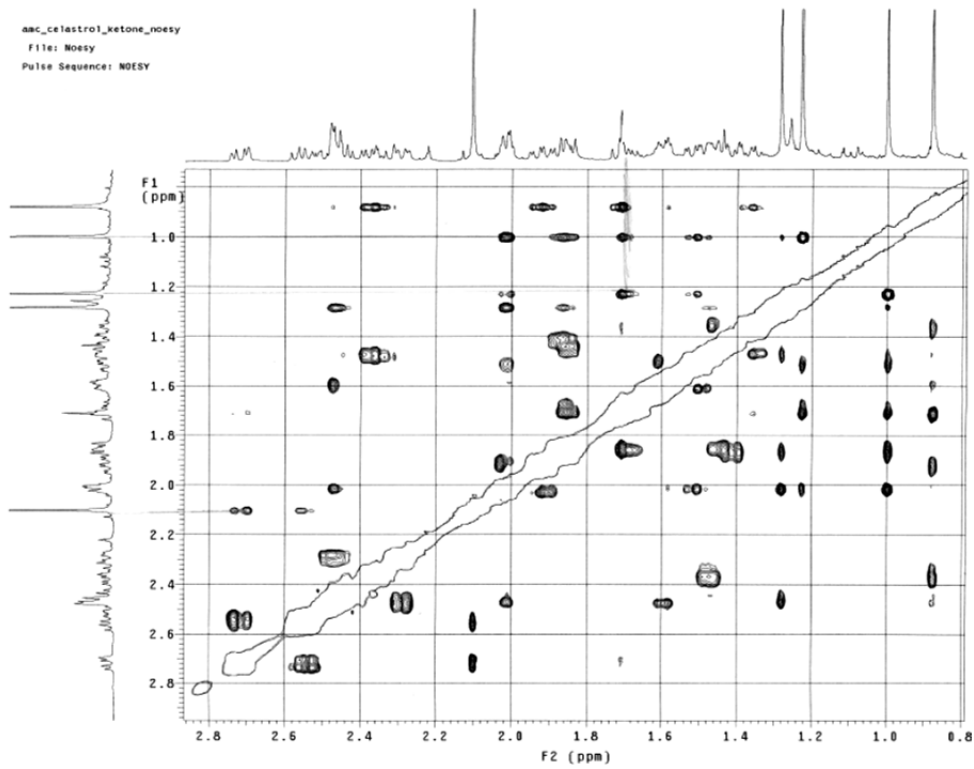
SAMPLE          FLAGS          n
date Sep 18 2013 hs              y
solvent cdc13 sspul             y
sample         PFG1g             y
ACQUISITION    hglv1            4694
sw 4661.7      SPECIAL          27.0
at 0.220      temp              30
np 2048       gain              0
fo 3000       spm              0
ss 32         F2 PROCESSING
dl 2.000      gf 0.101
nt 8          gfs not used
2D ACQUISITION fn 2048
sw1 4661.7    f1 PROCESSING
n1 256        gf1 0.051
tn TRANSMITTER N1 gfc1 not used
sfrq 499.853 fn1 2048
tof -556.1    DISPLAY
tpr 58        sp -397.9
pw NOESY 11.000 wp 4657.2
                    s1 -395.9
mix 0.800     wp1 4657.2
PRESATURATION rf1 3733.0
satmode nnn   rfe 3230.5
satpwr -13    rf11 3731.0
satolp 0      rfp1 3330.5
satfrq 499.8 PLOT
dn DECOUPLER  wc 116.0
                    sc 16.0
dm C13         nnc 116.0
                    vs 0
                    th 320
                    at cdc ph 2

```

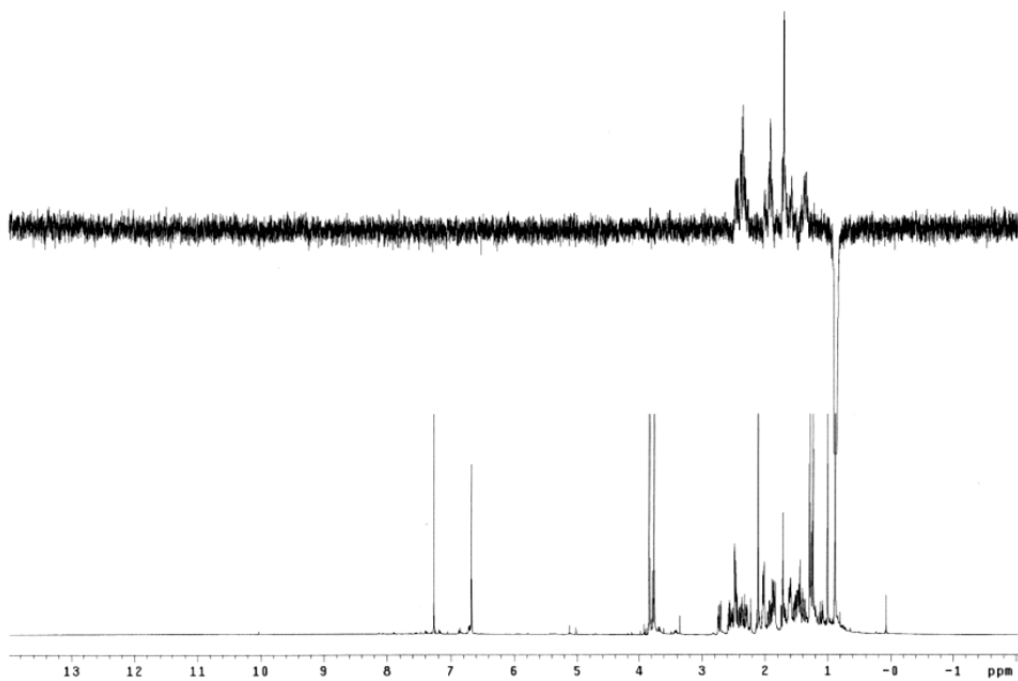


asc_celastrol_ketone_noesy

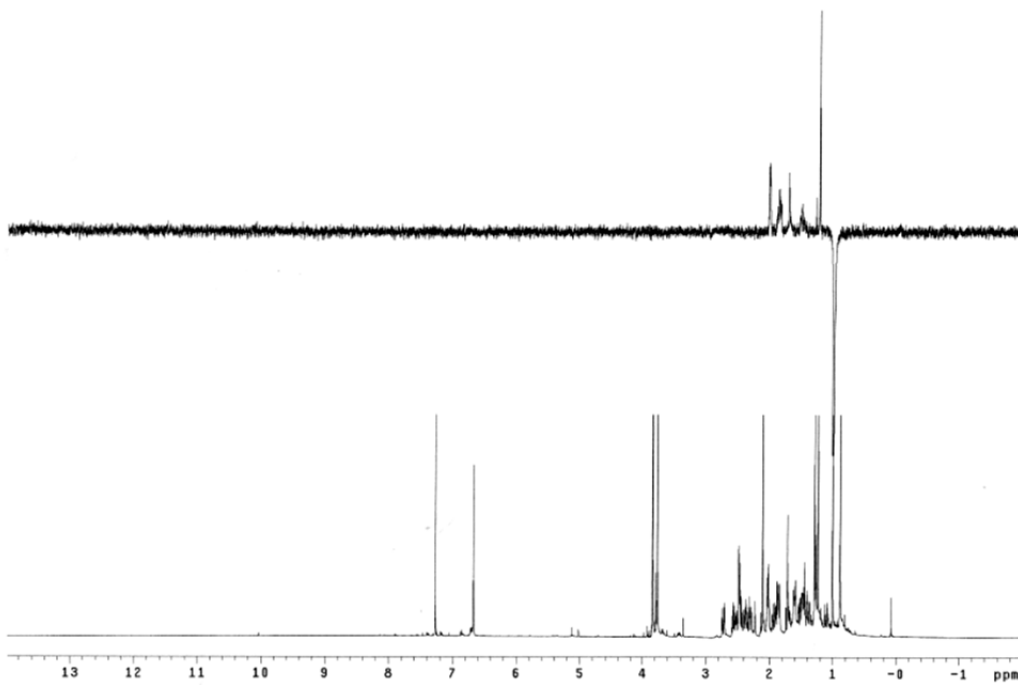
File: Noesy
Pulse Sequence: NOESY



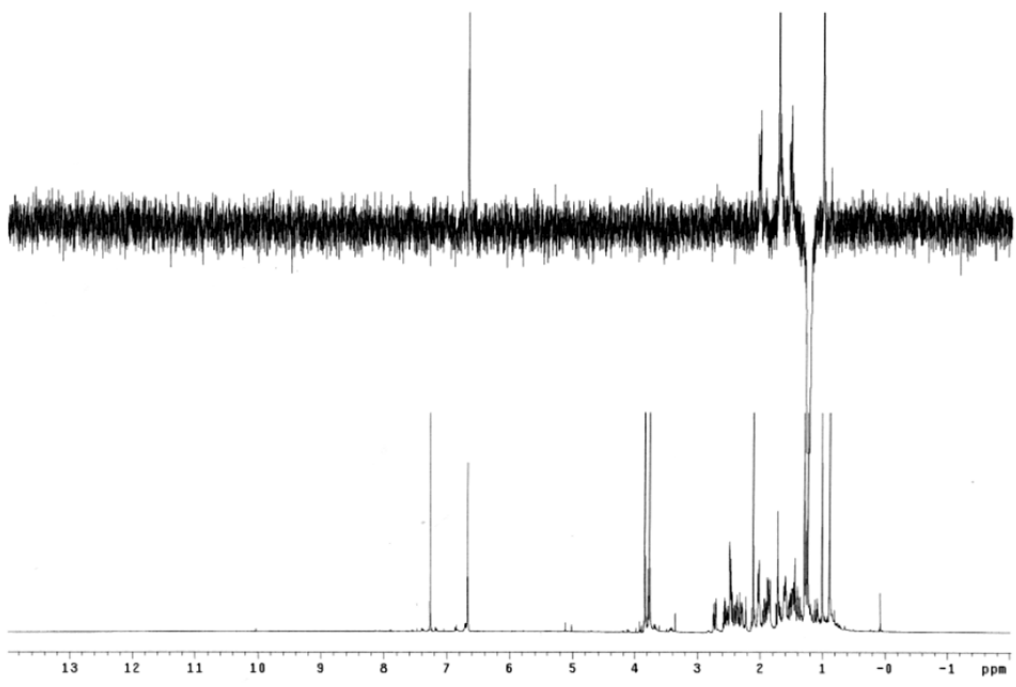
anc_celastrol_ketone_0_88p_idnoe
File: Noesy1d
Pulse Sequence: NOESY1D



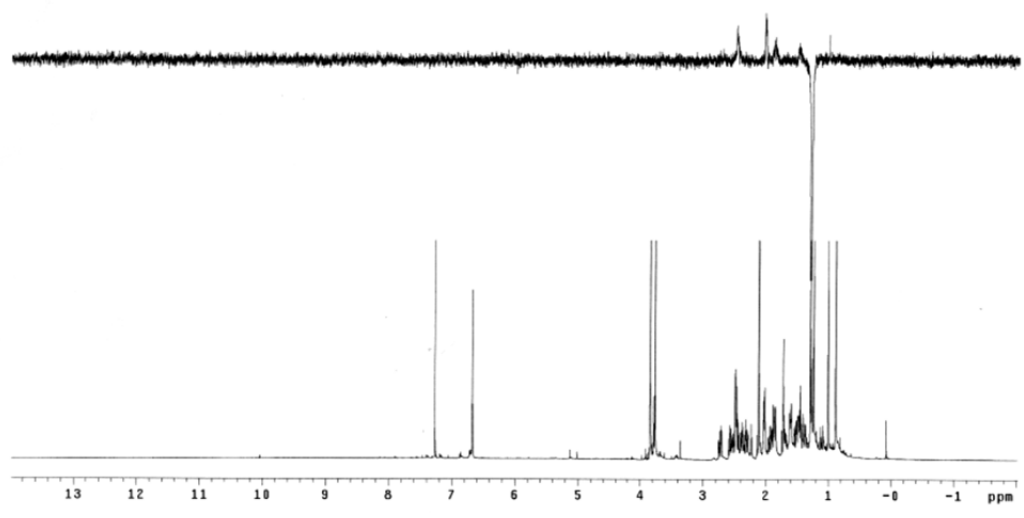
anc_celastrol_ketone_1_88p_idnoe
File: Noesy1d
Pulse Sequence: NOESY1D



anc_celastrol_ketone_1_23p
File: Noesy1d
Pulse Sequence: NOESY1D



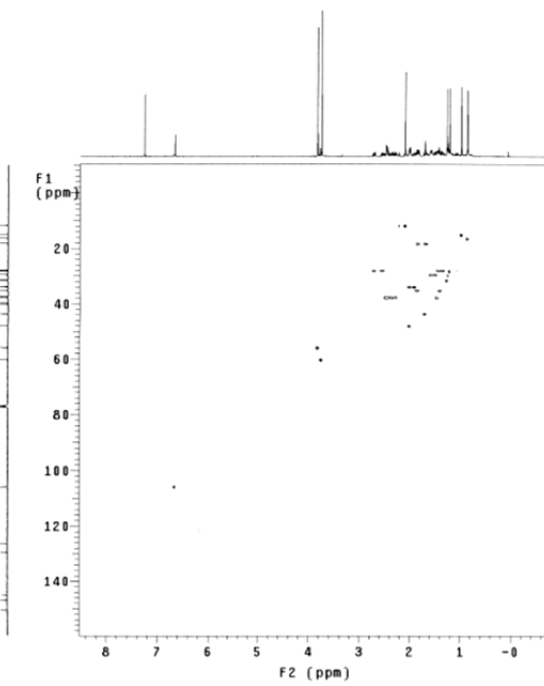
anc_celastrol_ketone_1_28p_idnoe
File: Noesy1d
Pulse Sequence: NOESY1D



```

amc_celestrol_ketone_h1
exp6 ghsqc
date Sep 18 2013 hs flags n ACQUISITION ARRAYS
solvent cdc13 sspul y arraydim 512
sample ACQUISITION hsglv 4684 1 phase
sv 4681.7 SPECIAL 1
at 0.199 temp 27.0 2
np 1800 gain 30
fp 3000 spin 0
ss 32 GRADIENTS 0
d1 2.000 g2lv11 4684
nt 4 g1 0.002000
2D ACQUISITION g2lv13 2347
sv1 23067.5 g13 0.001000
n1 250 g1ab 0.000500
phase arrayed f2 PROCESSING 0
PRESATURATION gf 0.092
satmode nnn gfs not used
satolv 0 f0 4096
satfrq 499.8 f1 PROCESSING
satpwr -13 gf1 0.011
TRANSMITTER hf1 not used
tn 55 sp -398.4
sfre 499.853 fnd 2048
tof -556.1 DISPLAY
tpwr 11.000 wp 4859.5
dn DECOUPLER C13 wp1 -1288.2
dor -2515.2 rf1 2276.1
dm nny rfg 1875.4
dpr 22200 rf11 8866.6
pwr 40 rfp1 7577.5
pocv1 55 PLOT
pwx 10.500 wc 116.0
hsoc 140.0 wcz 10.0
j1kh y sc2 116.0
nut1flg y vs 0
mult 2 vt 872
th 2
at cdc ph 2

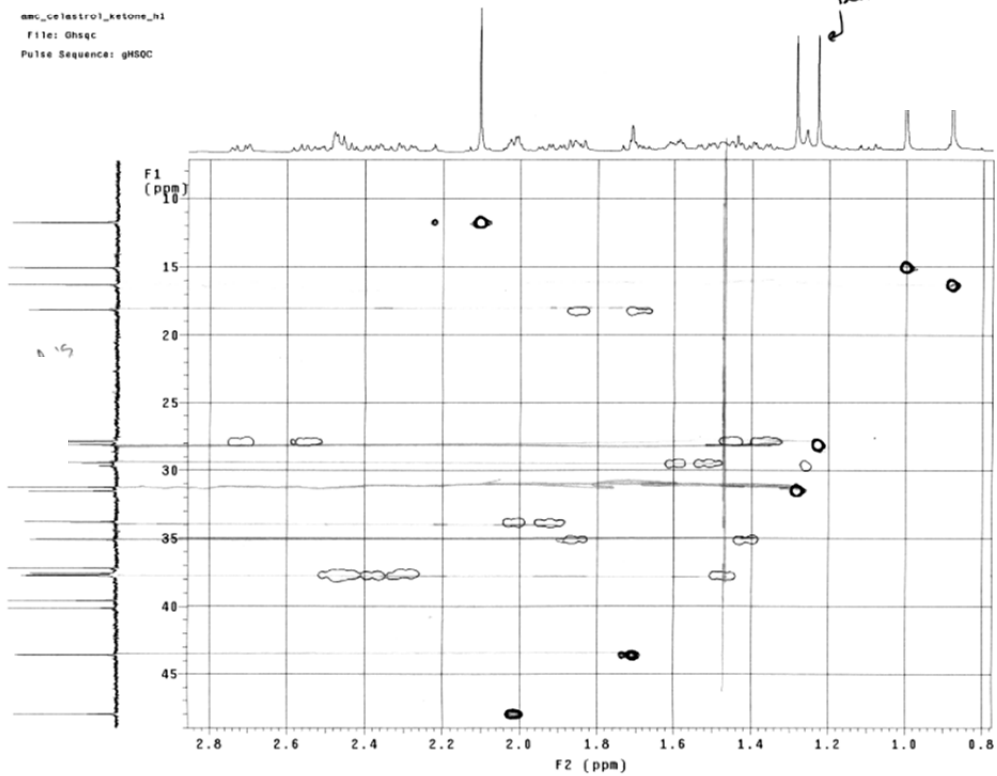
```



```

amc_celestrol_ketone_h1
File: ghsqc
Pulse Sequence: gHSOC

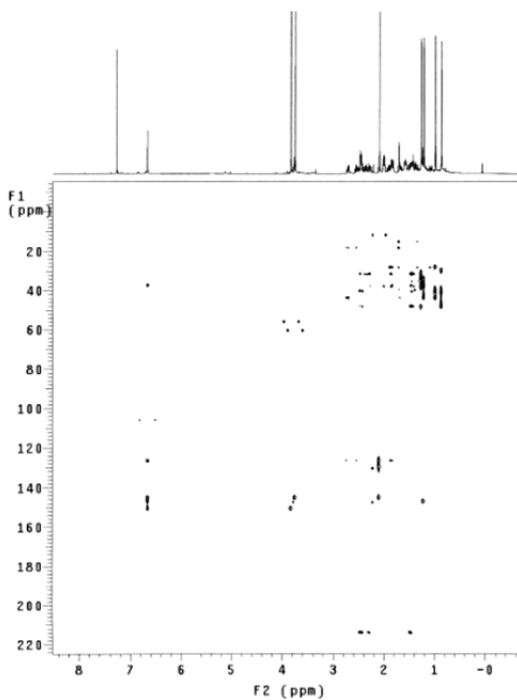
```




```

amc_celastrol_ketone_h1
exp7 Gmhc
date Sep 18 2013 hs FLAGS n
solvent cdc13 sspul n
sample PFO79 y
ACQUISITION hsqiv1 4694
sv 4661.7 SPECIAL
at 0.128 temp 27.0
np 1194 gain 30
ra 3000 spin 0
ss 32 GRADIENTS
d1 2.000 g2lv11 4684
nt 18 g11 0.001000
2D ACQUISITION g2lv13 2347
sv1 30165.3 g13 0.001000
nl 256 g1ab 0.000500
phase 0 F2 PROCESSING
PRESATURATION sb 0.064
satmode nnn sbs not used
selsly 0 fn 2048
satpr 499.8 f1 PROCESSING
satpwr -13 sb1 0.008
TRANSMITTER sbx1 not used
ln H1 proc1 1p
effe 499.853 fn1 2048
tof -556.1 DISPLAY
spwr 53 wp -386.5
pw 11.000 wp 4657.2
DECOUPLER C13 wpl -1893.6
dof 1255.4 rf1 30135.5
dm nnn rfp 2278.5
der 22200 rfp1 28781.6
dprw 43 rfp1 26868.6
puctv1 55 PLOT
pvx 10.500 wc 116.0
j1xh HNBC 140.0 cc 10.0
jnxh 0.0 cc2 116.0
vc 328
th
al cdc av 2

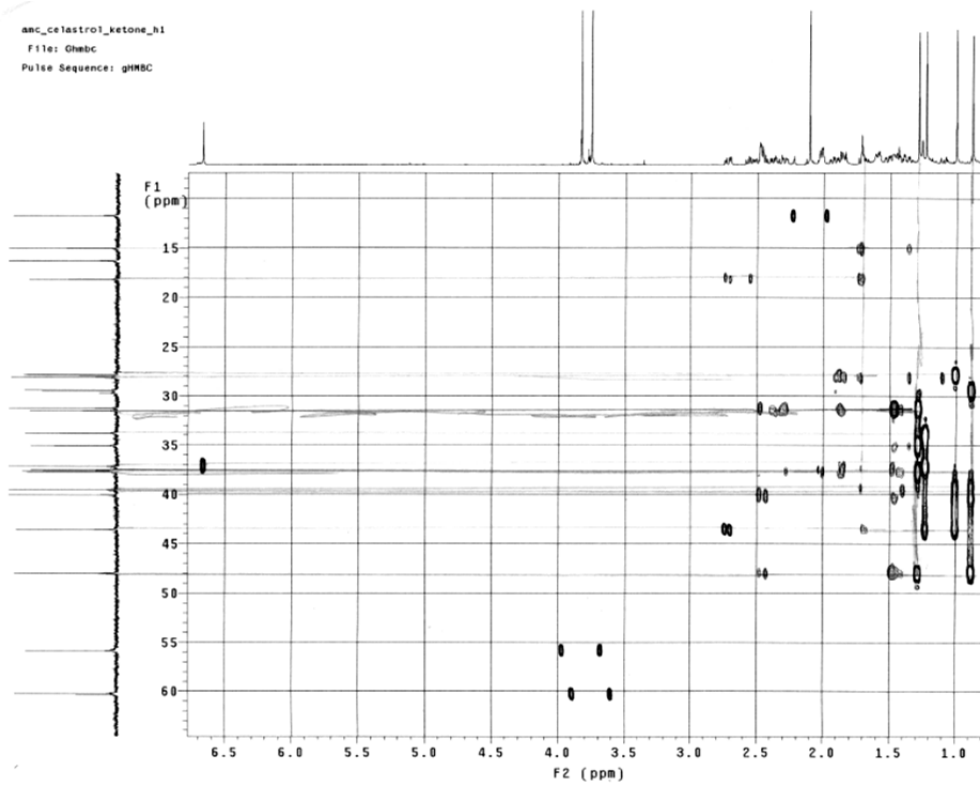
```



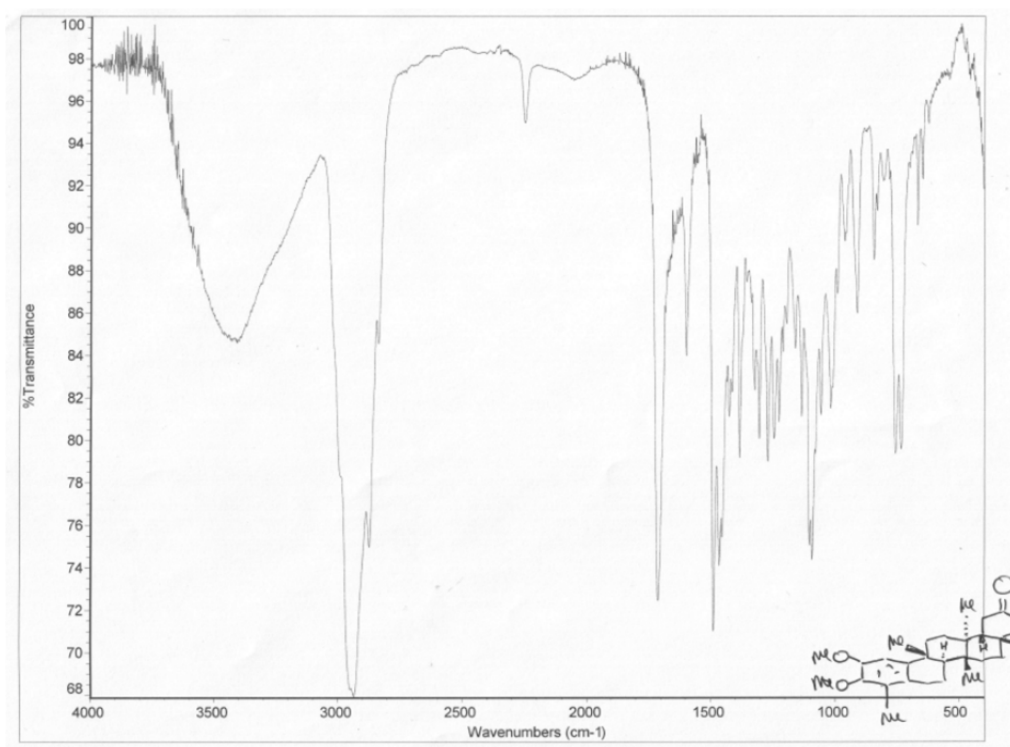
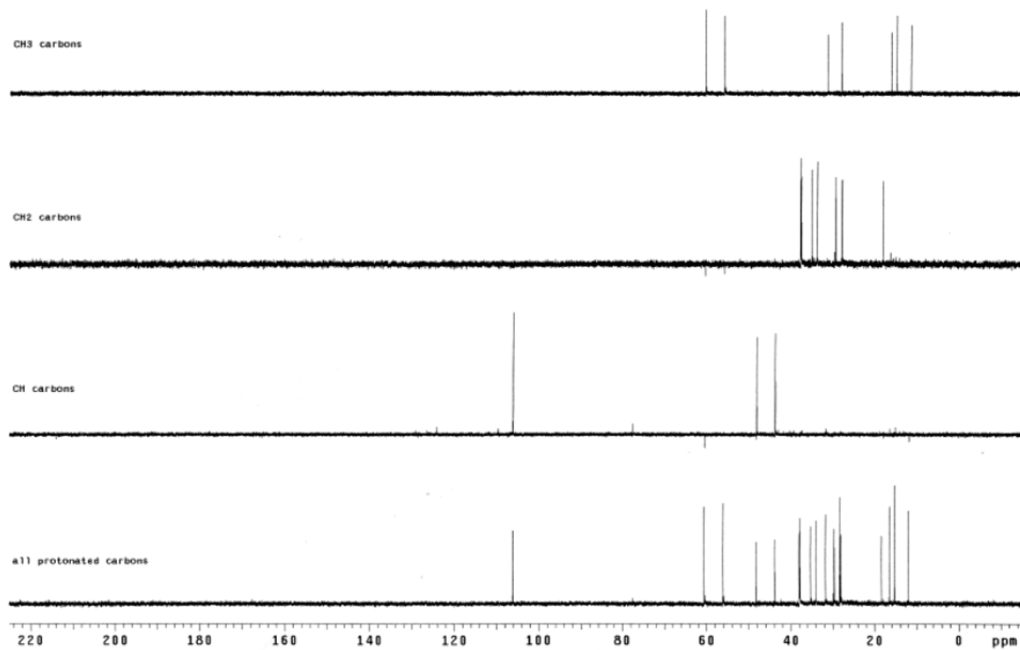
```

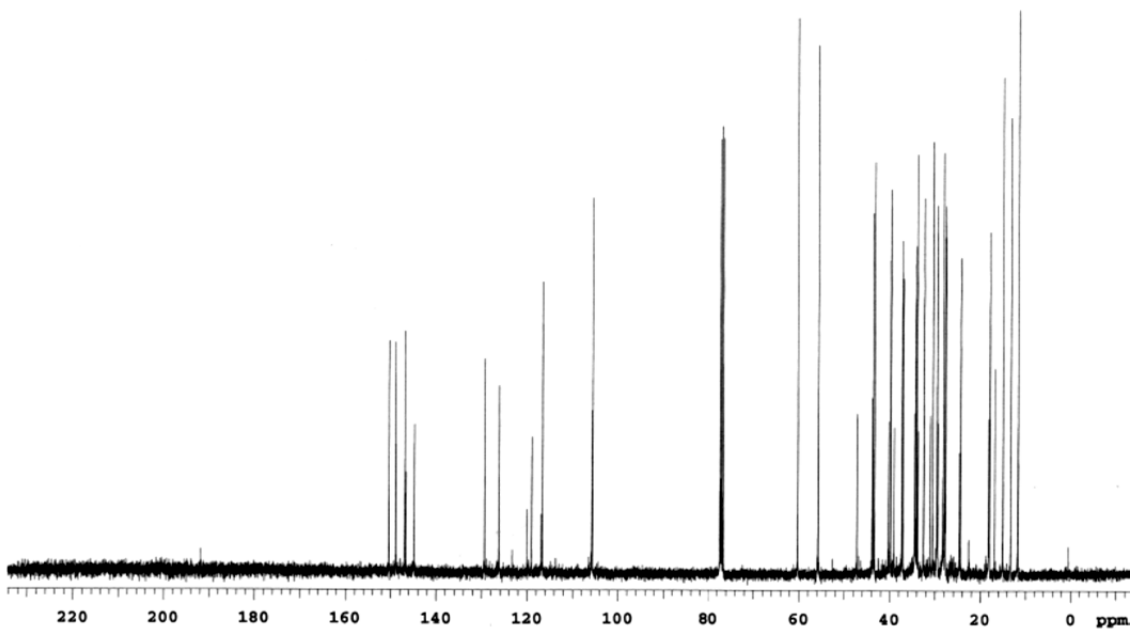
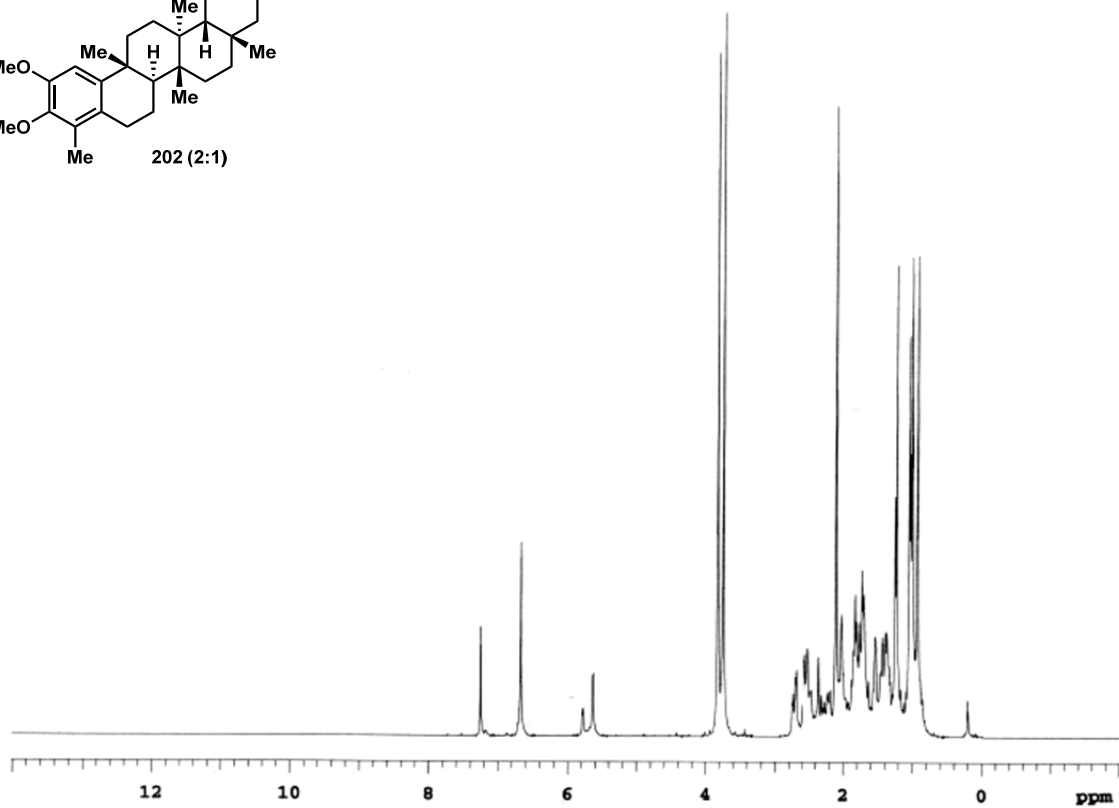
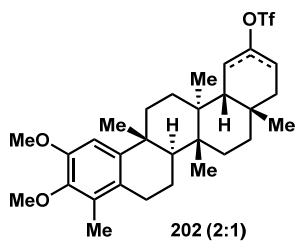
amc_celastrol_ketone_h1
File: Gmhc
Pulse Sequence: gHNBC

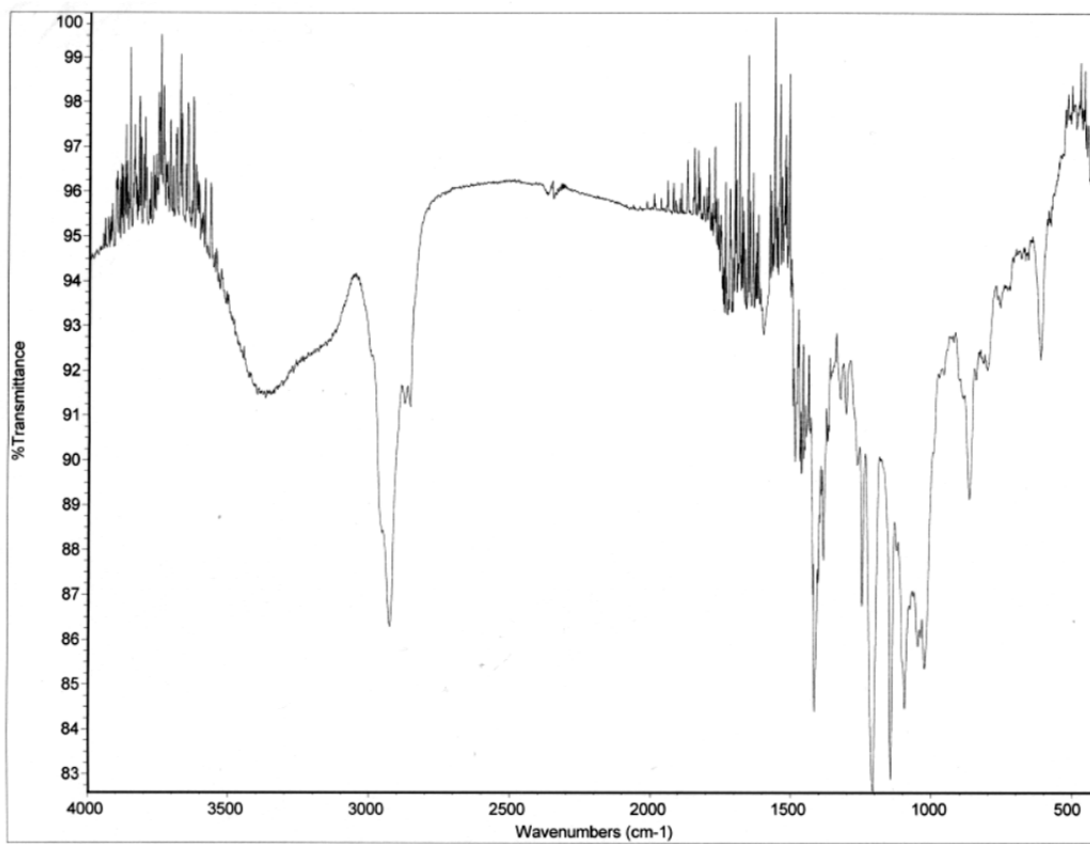
```

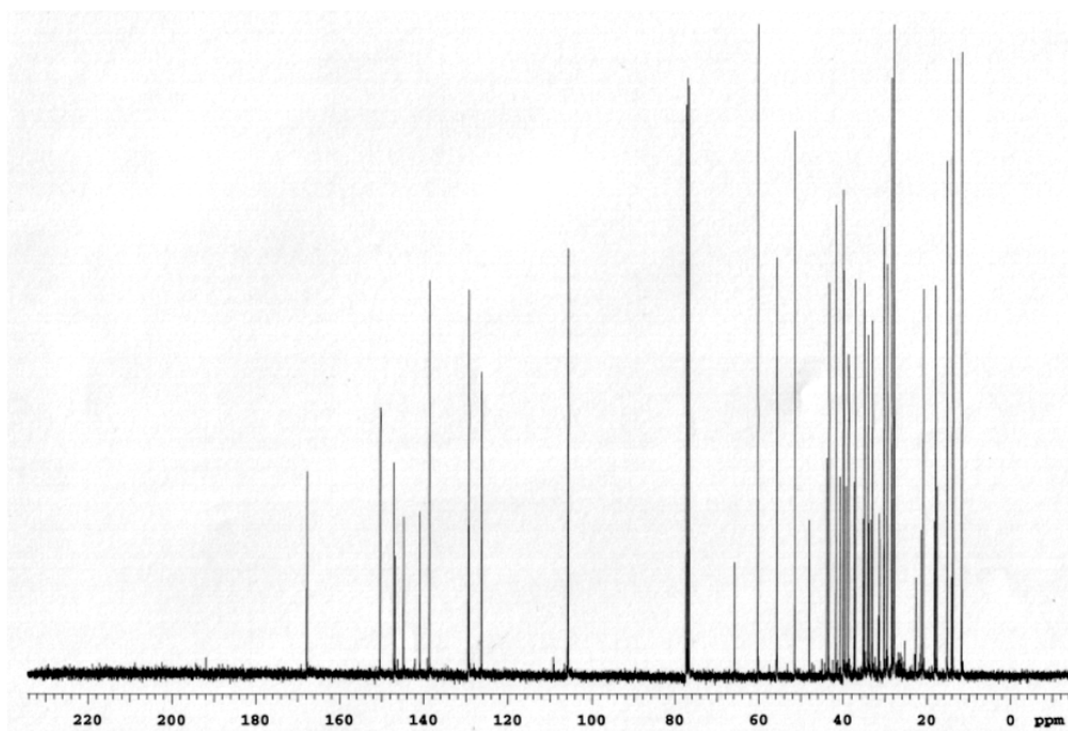
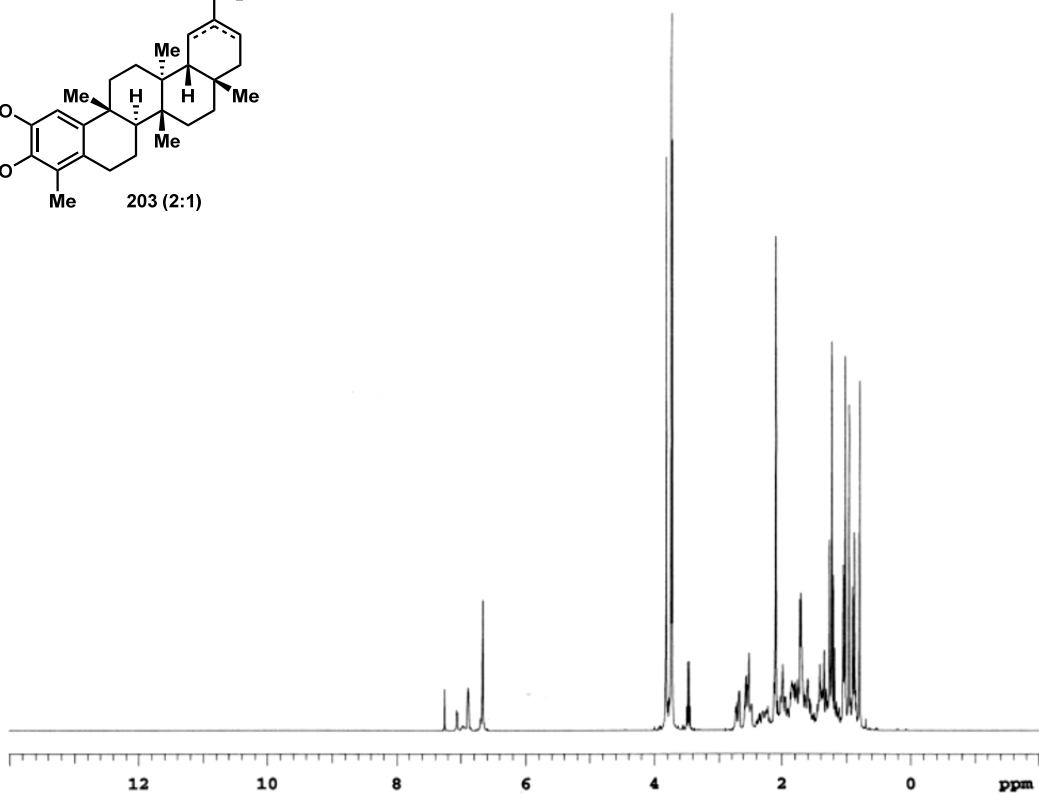
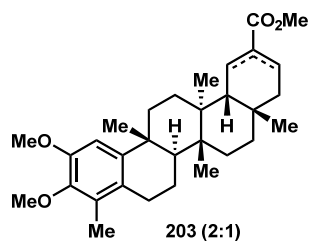


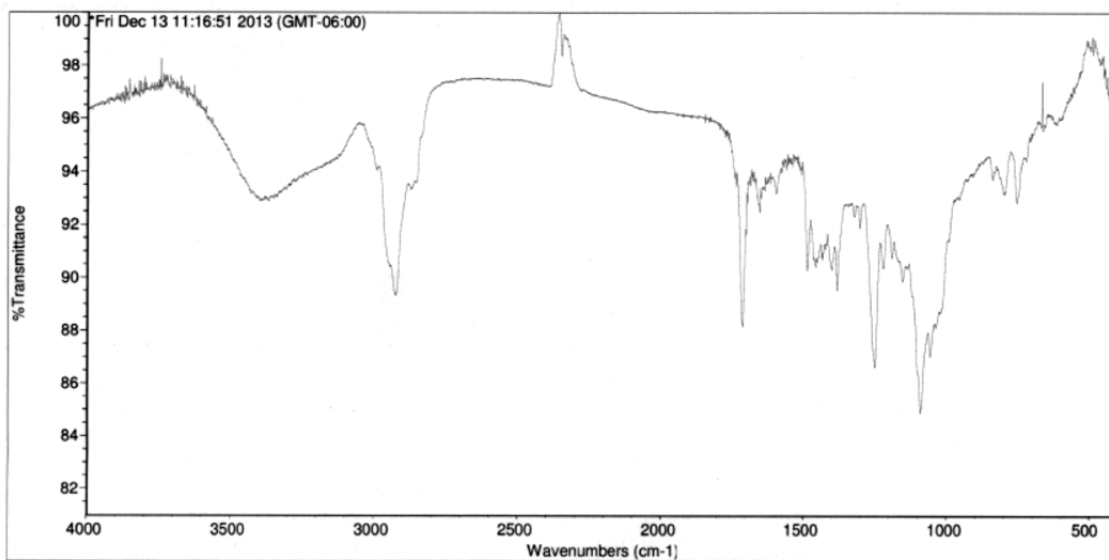
anc_celastrol_ketone_dept
File: Dept
Pulse Sequence: DEPT











Fri Dec 13 11:26:16 2013 (GMT-06:00)

FIND PEAKS:

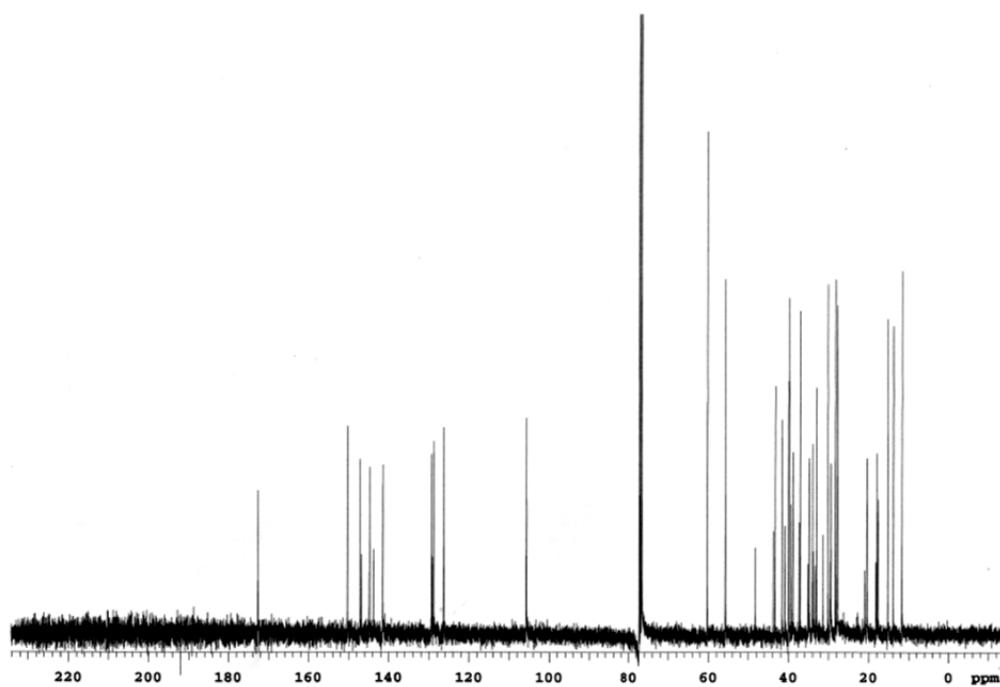
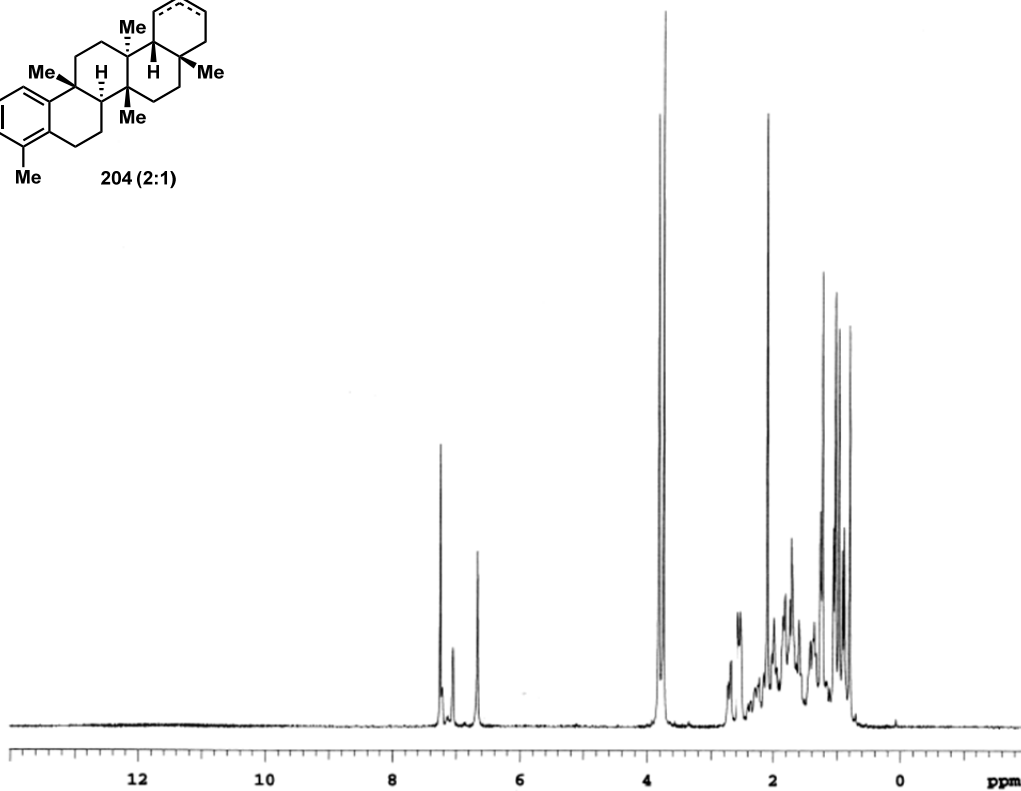
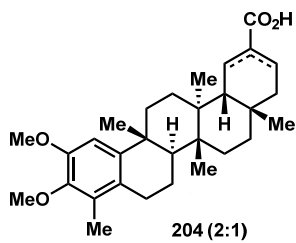
Spectrum: *Fri Dec 13 11:16:51 2013 (GMT-06:00)

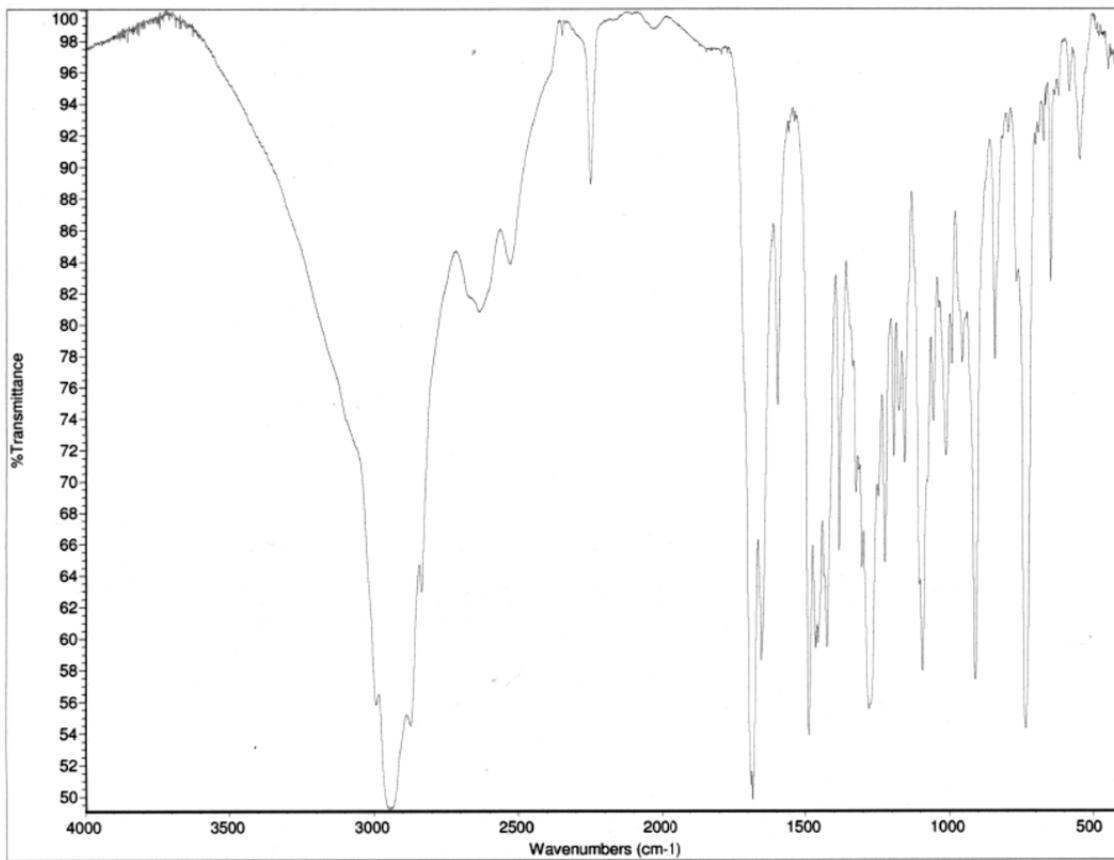
Region: 4000.00 400.00

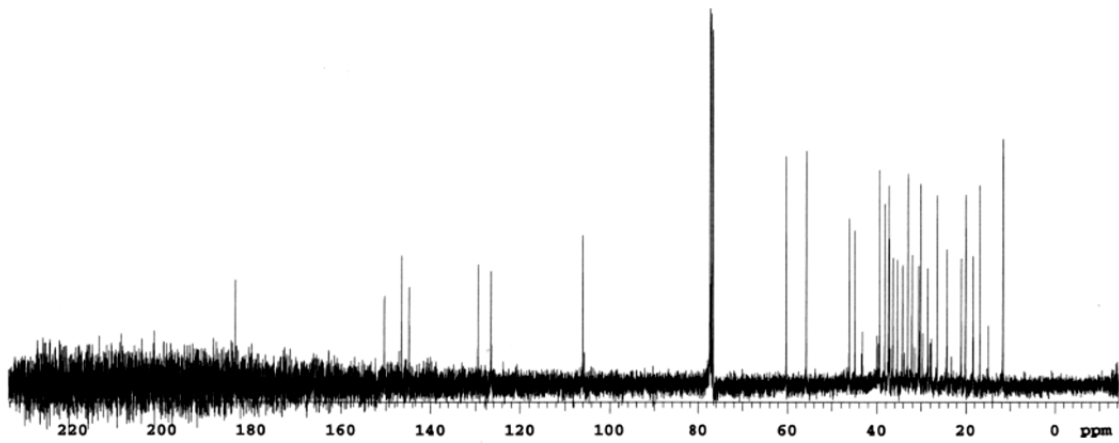
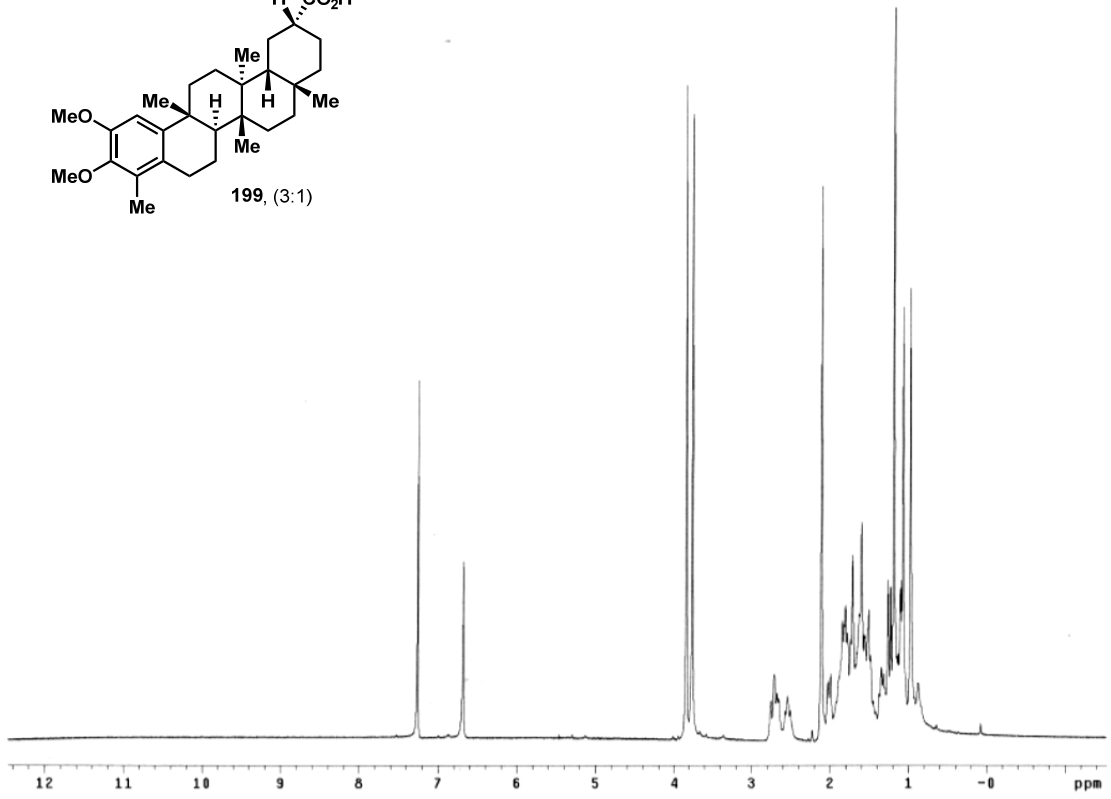
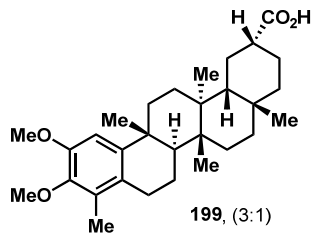
Absolute threshold: 82.305

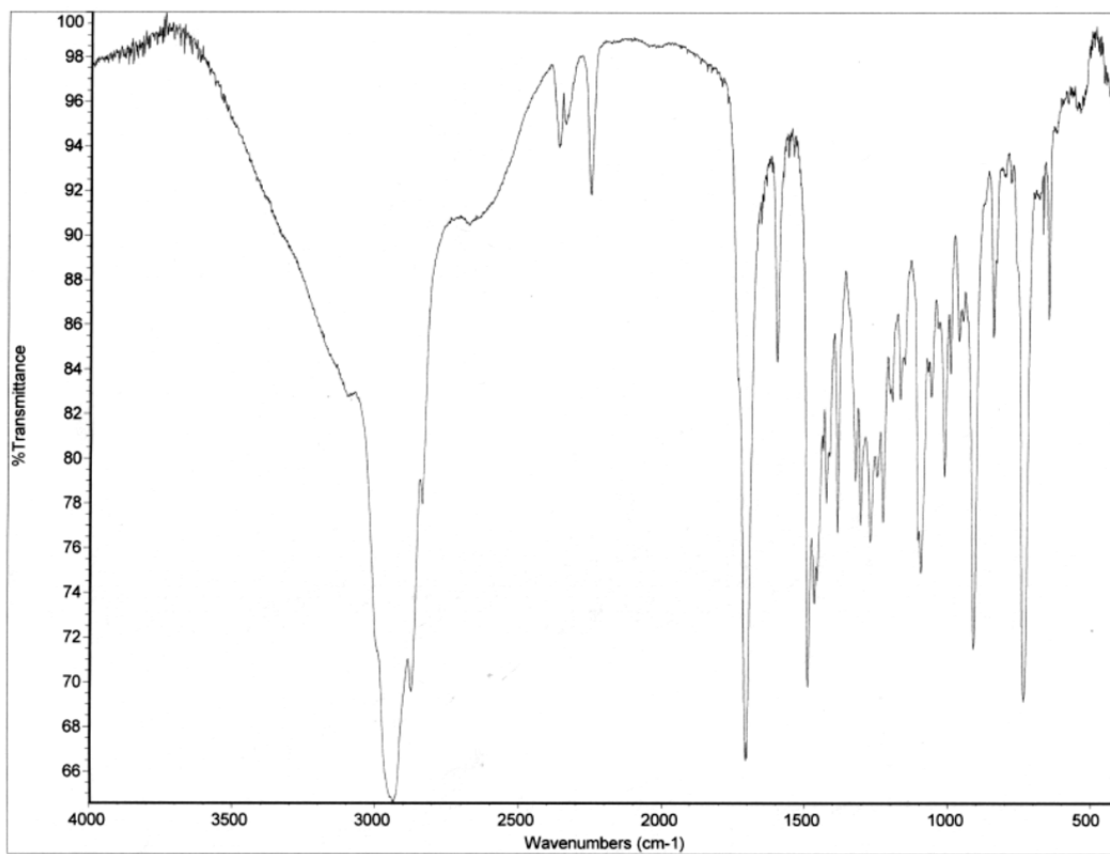
Sensitivity: 50

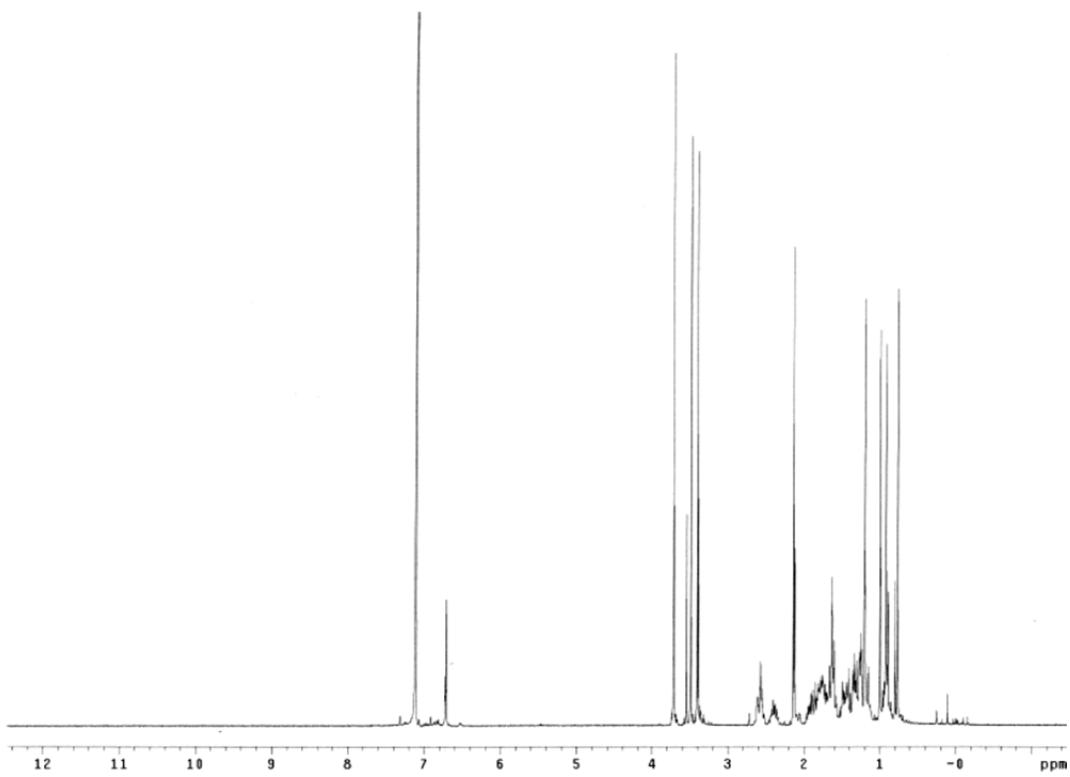
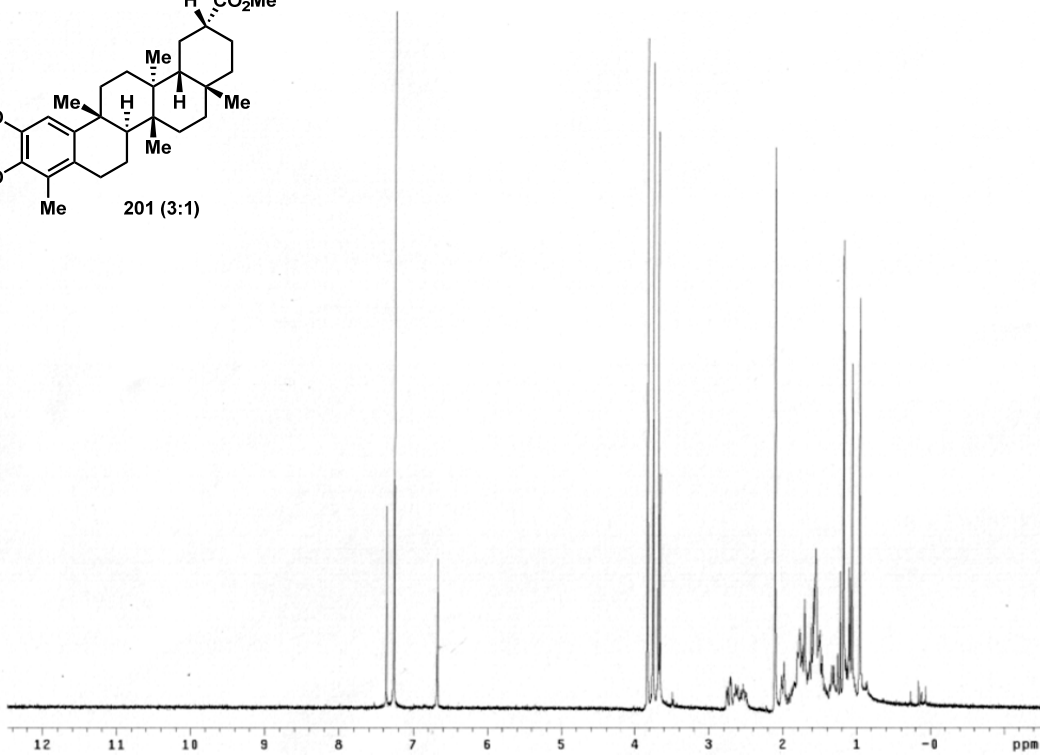
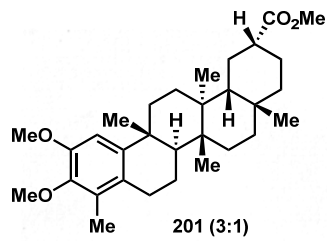
Peak list:

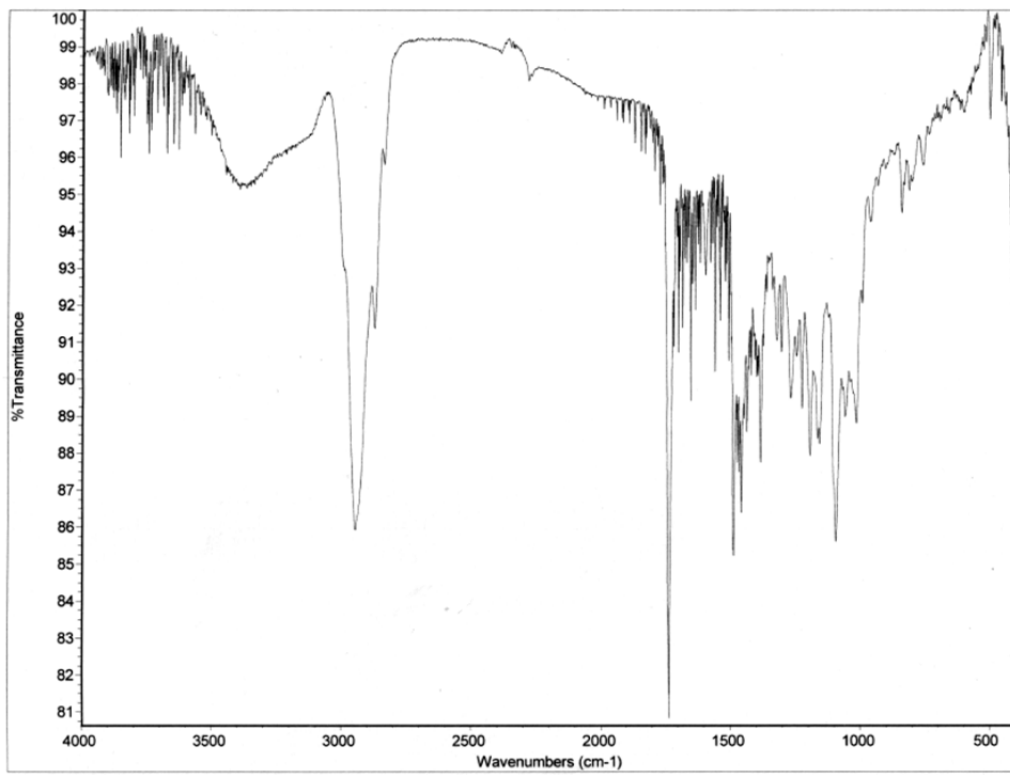
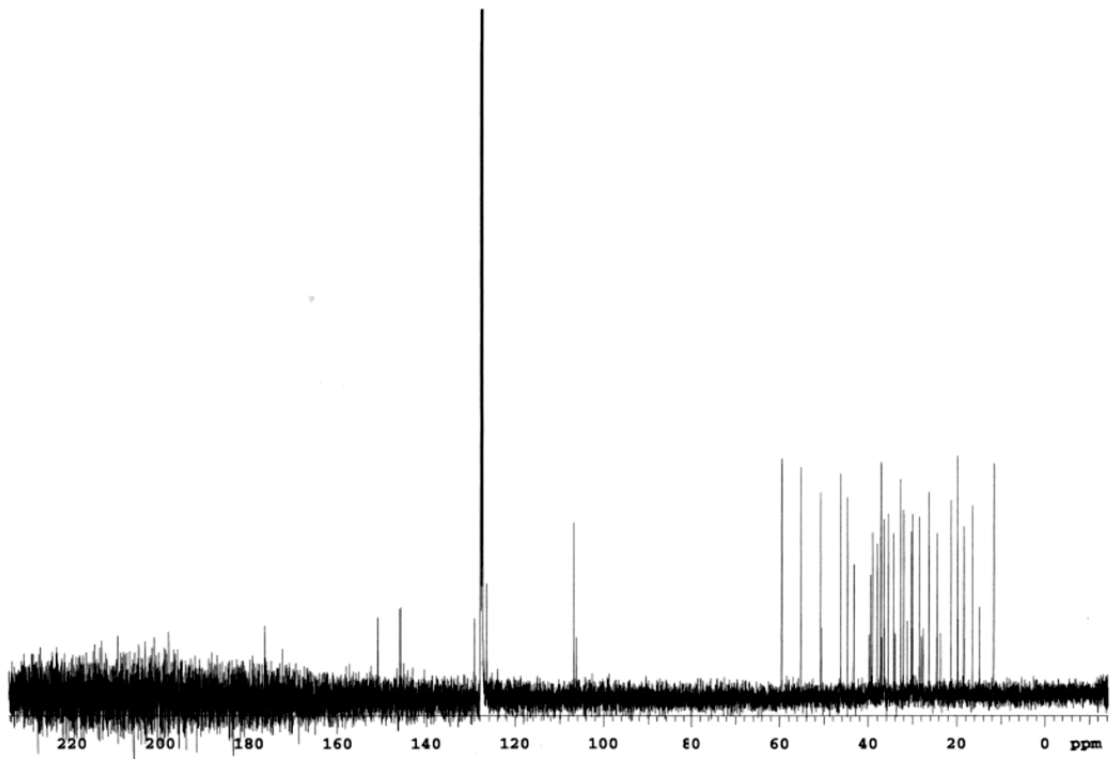


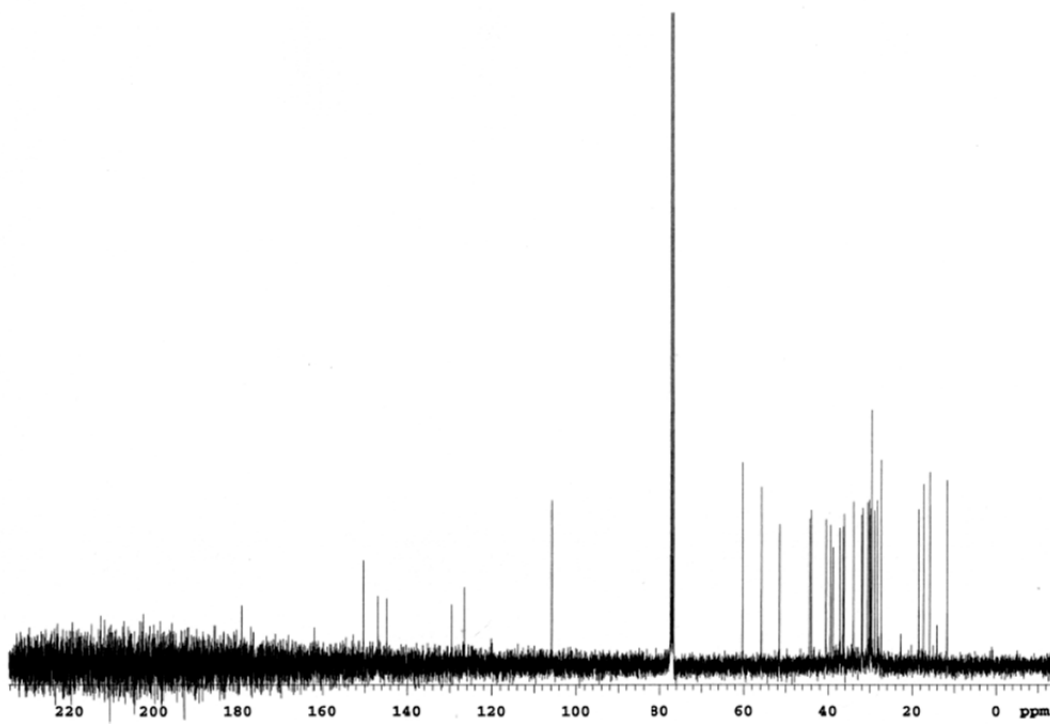
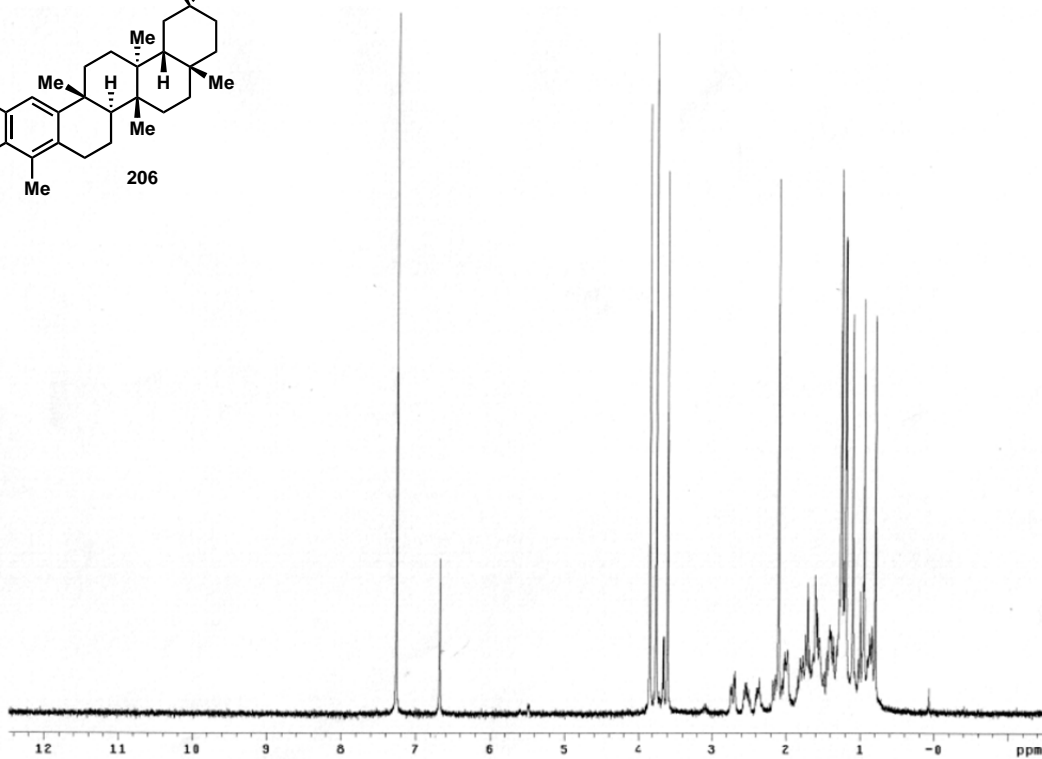
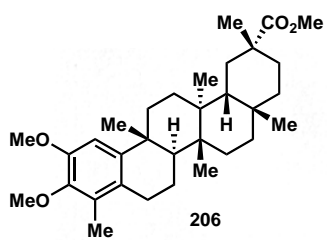


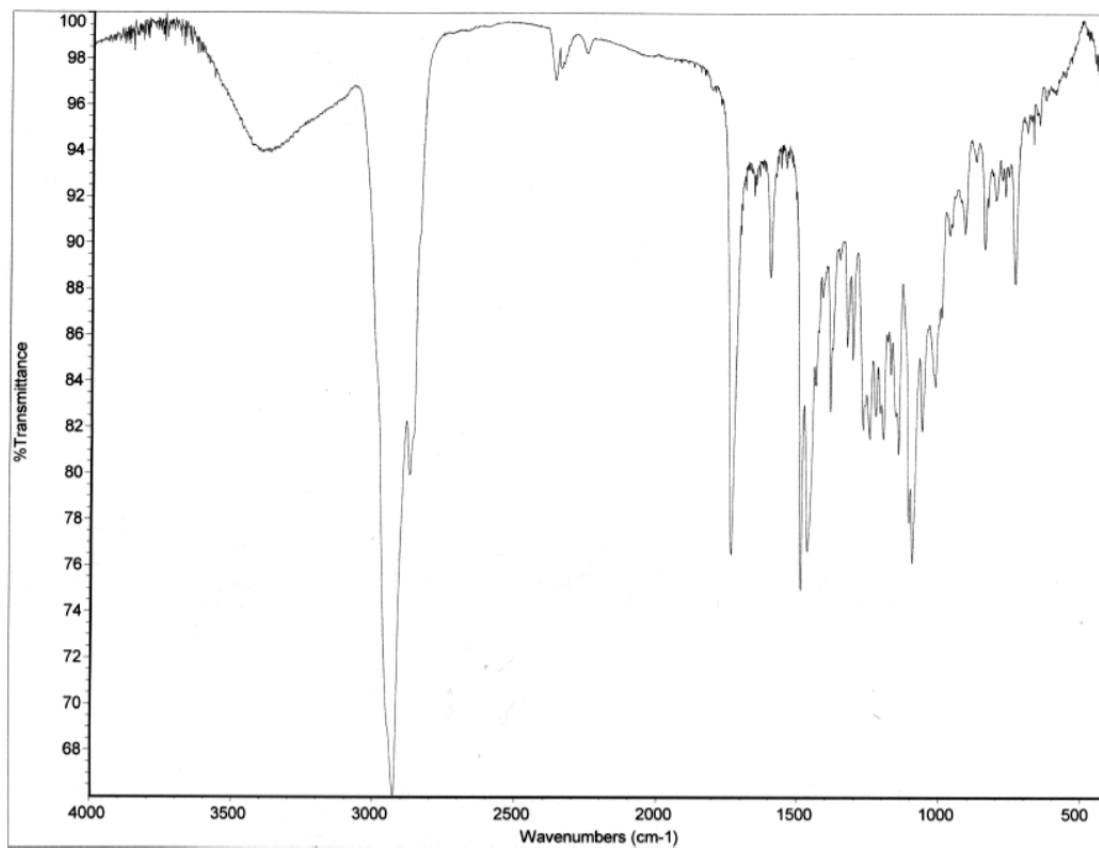


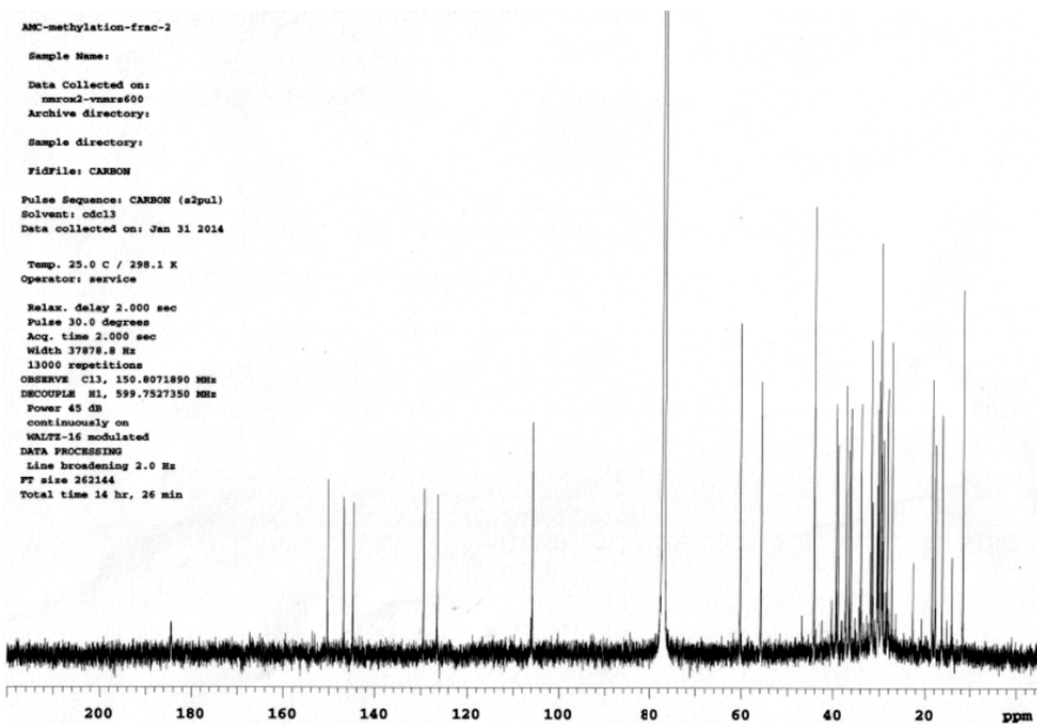
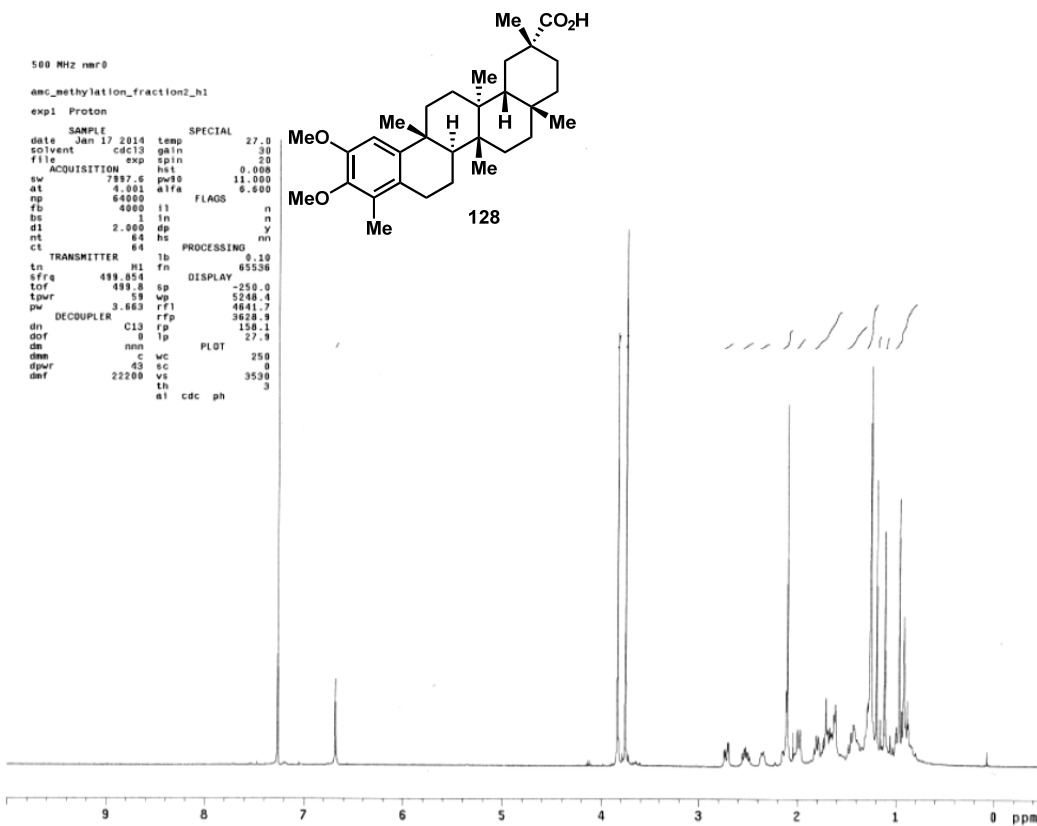










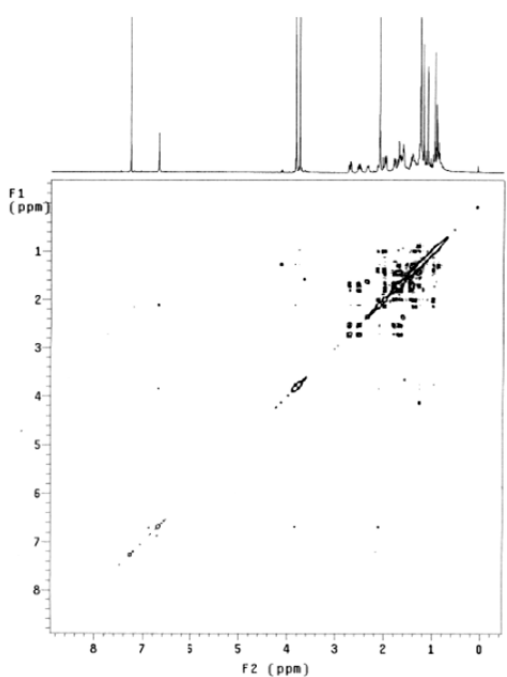
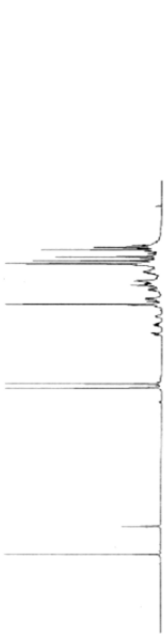


aac_methylation_fraction2_gcosy
exp3 gcosy

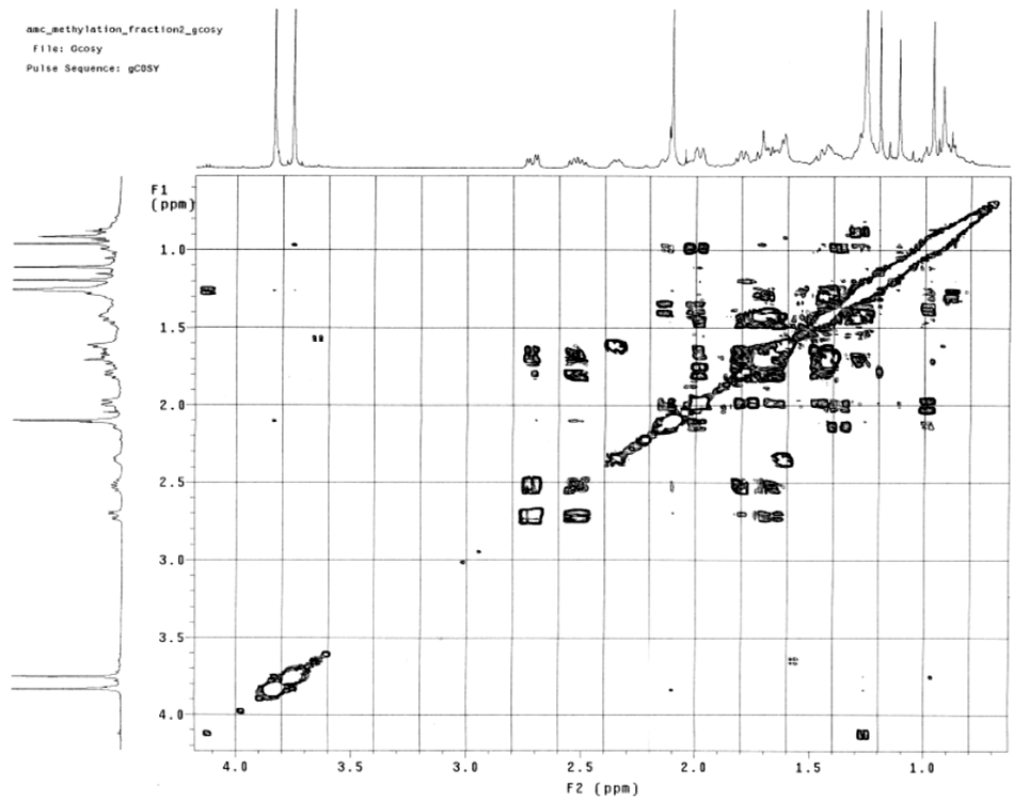
```

SAMPLE
date Jan 16 2014 hs FLAOS nn
solvent cdc13 hspul n
sample 4694
ACQUISITION hspul SPECIAL
sv 4882.7 temp 27.0
at 0.219 gain 30
np 2048 spin 0
fb 3000 f2 PROCESSING
ss 8 sb -0.109
d1 2.000 sbc not used
nt 1 fn 2048
2D ACQUISITION F1 PROCESSING
sw1 4882.7 sb1 -0.055
nl 256 sbc1 not used
PRESATURATION proc1 lp
satmode nnn fn1 2048
satply 0 DISPLAY
satfrq 499.8 sp -230.0
satpwr -13 wp 4678.2
TRANSMITTER sp1 -230.5
in H1 wp1 4678.2
sfrq 499.854 rf1 3883.5
tof -378.1 rfp 3828.8
tpr 53 rfl1 3884.0
pw 11.000 rfp1 3828.9
tprcf 1.000 FLOT
GRADIENTS wc 116.0
gzlv11 4884 uc 18.0
g11 0.001000 wc2 116.0
gtab 0.008500 uc2 0
DECOUPLER vs 872
dn C13 th 2
ds nnn al cdc av

```



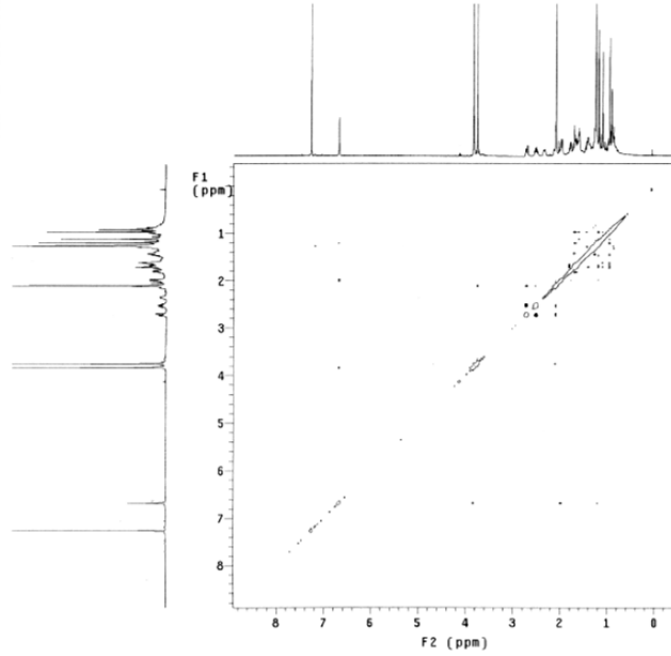
aac_methylation_fraction2_gcosy
File: gcosy
Pulse Sequence: gCOSY



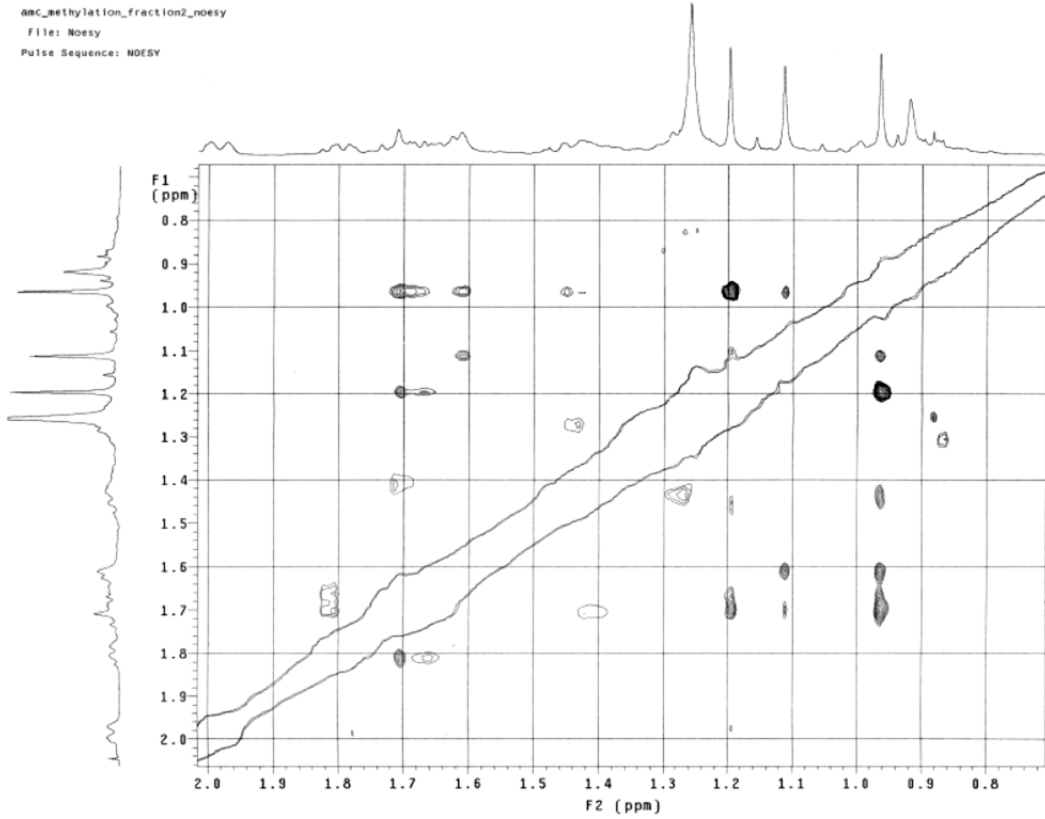
amc_methylation_fraction2_noesy

exp8 Noesy

```
date Jan 16 2014   no   FLAGS   n
solvent cdc13      sspul     7
sample  PF071g     hsp1v1  4695
ACQUISITION
sw 4682.7          SPECIAL 27.0
at 0.218          temp    30
np 2048           gain    0
fb 3000           sp1n    0
st 32            f2 PROCESSING
d1 2.000         gf      0.101
nt 0             gfs     not used
2D ACQUISITION
sw1 4682.7       f1 PROCESSING
n1 256           gf1     0.050
TRANSMITTER 256   gf1     not used
ln          n1   procl   1p
offq 498.854    fml     2048
topf -378.1     DISPLAY
lpwr 55         sp      -231.7
pw 11.000      wp      4878.2
NOESY 0.800    sp1     -230.7
n1x          wpt     4878.2
PRESATURATION rf1   3865.2
satmode      nnn   rfp     3820.8
satpw        -13   rf1    3865.2
sattdly      0    rfp1   3820.9
satfrq      498.8 PLOT
DECOUPLER   wc     116.0
dn          ac     10.0
dm          nnn   wc2    116.0
           vs     0
           sh     11802
           at   cdc ph 2
```



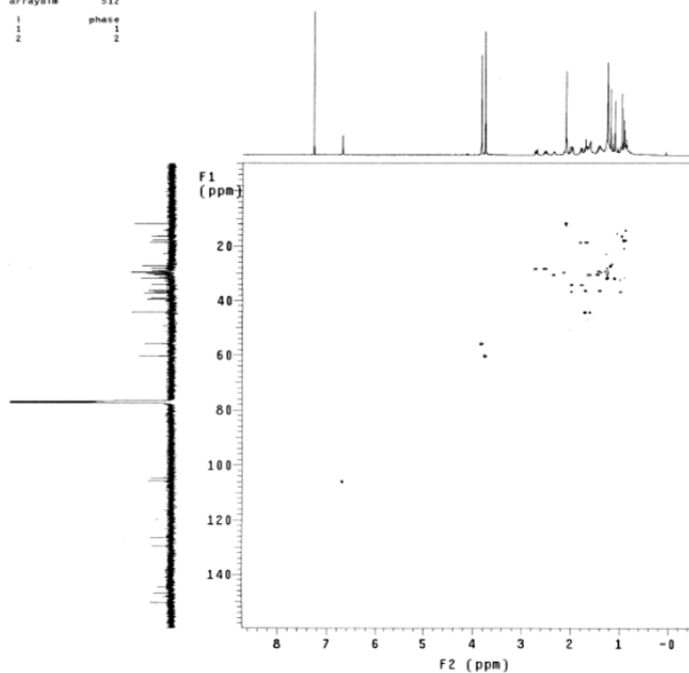
amc_methylation_fraction2_noesy
File: Noesy
Pulse Sequence: NOESY



```

amc_methylation_fraction2_ghsqc
exp6 Ghsqc
SAMPLE          FLAGS      ACQUISITION ARRAYS
date Jan 17 2014 ns          n array phase
solvent cdc13  sgal1      y arraydim 512
sample          PFGflg      y
ACQUISITION    hsglv1     4694      1      phase
sv 4756.2      SPECIAL 4694      1
at 0.199      temp 27.0      2
np 1896      gain 50
fb 3000      spin 0
ss 32      GRADIENTS
d1 2.000      g2lv11    4694
nt 16      gt1 0.002000
2D ACQUISITION g2lv13    2347
sw1 21367.5    gt3 0.001600
nt 256      g1tab 0.000500
phase arrayed  F2 PROCESSING
PRESATURATION  gf 0.092
satmode nnn  gfa not used
satdly 0      fn 4696
satfrq 499.8    F1 PROCESSING:
satpwr -13      gf1 0.011
tn TRANSMITTER M1  gfs1 not used
tof 499.853    fn1 2048
lpwr -516.6    DISPLAY -400.4
pv 11.000      wp 4753.9
DECOUPLER  sga -1258.0
dn C13  wp1 21346.7
dofr -2515.2    rf1 3741.2
dn nny  rfp 3338.5
dnf 22200      rf11 14598.4
dpr 43      rfp1 13308.7
pvc1v1 55      PLOT 116.0
pvc HSQC 10.500  wc 10.0
jsh 140.0      wc2 116.0
mult1 y      sc2 0
mult 2      vs 872
sh 1b
al cdc ph 2

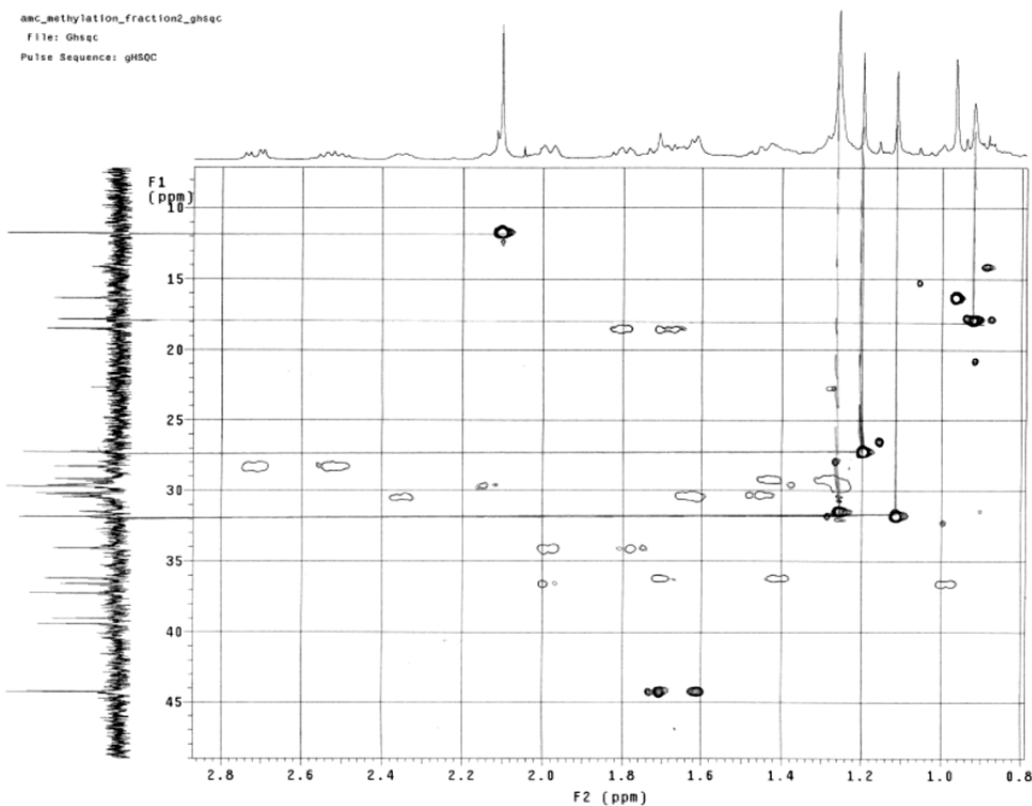
```



```

amc_methylation_fraction2_ghsqc
File: Ghsqc
Pulse Sequence: gHSQC

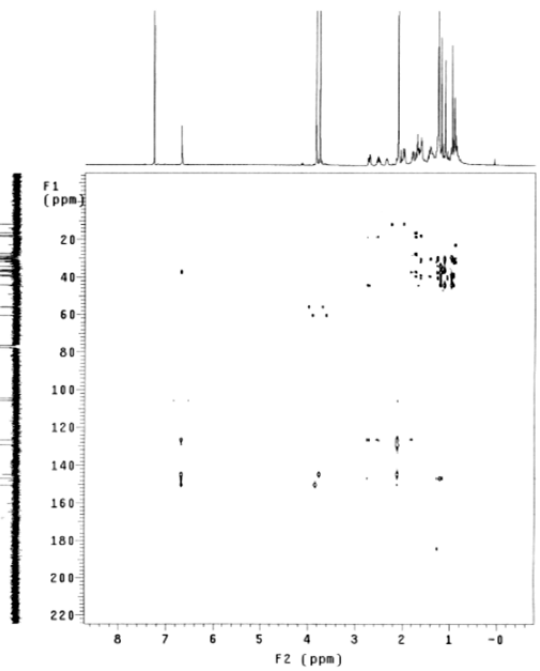
```



aac_methylation_fraction2_gmhc

exp7 gmhc

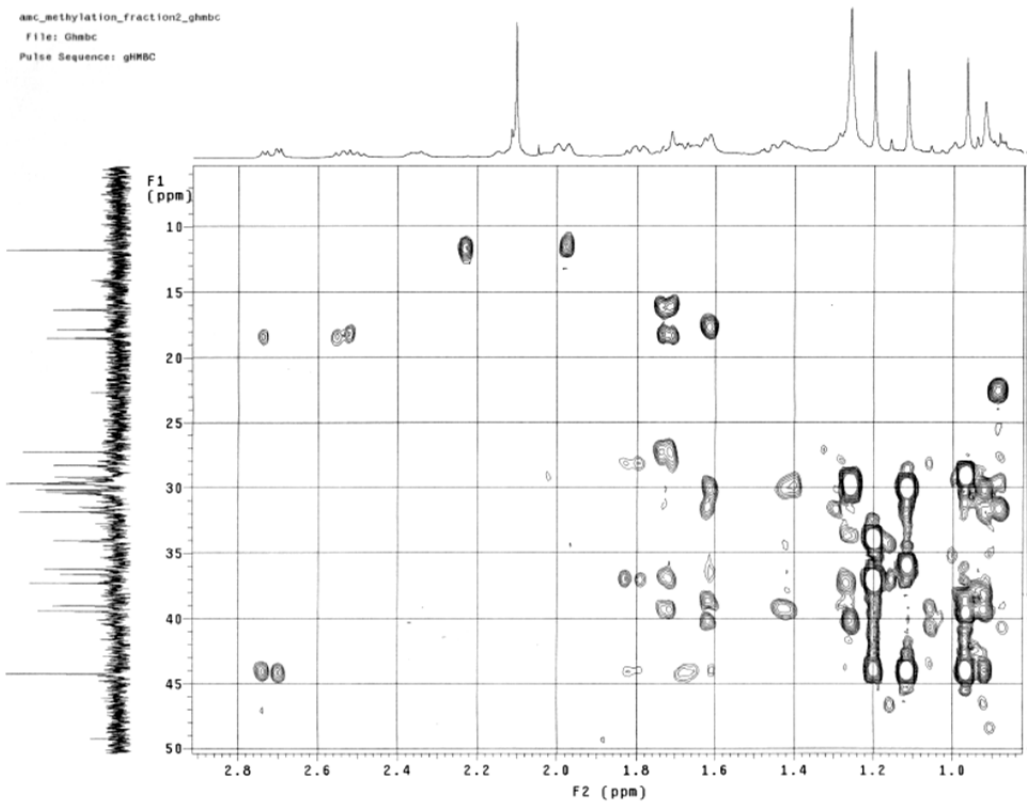
```
SAMPLE          FLAGS          n
date Jan 17 2014 hs              n
solvent cdc13  sgal            n
sample          PFG1g           Y
ACQUISITION    hsglv1          4694
sw 4756.2              SPECIAL
at 0.120 temp          27.0
rp 1228 gain           30
fb 3000 spin           0
ss 32 GRADIENTS        4694
d1 2.000 g2lv11        4694
nt 32 g11              0.001000
2D ACQUISITION g2lv13        2047
svl 30185.9 g13        0.001000
nl 206 g1tab           0.000500
phase 0 F2 PROCESSING
PRESATURATION  sb           0.064
satmode nnn sbs not used
satly 0 fn             2046
satfrq 499.8 F1 PROCESSING
satpwr -13 sb1         0.008
TRANSMITTER    sb11 not used
tn H1 proc1           lp
sfrq 499.853 sb11     4751.6
tof -510.6 fn1 DISPLAY 2046
tpwr 59 sp           -397.2
pw 11.000 wp         4751.6
dn DECOUPLER  C13 wp1    30136.5
dof 1255.4 rf1       3740.4
dm nnn rfe           3538.5
dof 22200 rf11       37449.3
dpr 43 rfp1         15905.5
pocv1 55 PLOT
pwx 10.500 wc        116.0
j1xh 140.8 wc2       116.0
j1xh 0.0 cc2         0
j1xh th             328
at cdc av           2
```



aac_methylation_fraction2_gmhc

File: gmhc

Pulse Sequence: gmhbc



AMC-methylation-frac-2

Sample Name:

Data Collected on:
nmr02-vmars600

Archive directory:

Sample directory:

Fidfile: DEPT

Pulse Sequence: DEPT

Solvent: cdcl3

Data collected on: Jan 31 2014

Temp. 25.0 C / 298.1 K

Operator: service

Relax. delay 2.000 sec

Pulse 90.0 degrees

Acq. time 2.000 sec

Width 37878.8 Hz

4000 repetitions

OBSERVE C13, 150.8071911 MHz

DECOUPLE H1, 599.7527350 MHz

Power 45 dB

on during acquisition

off during delay

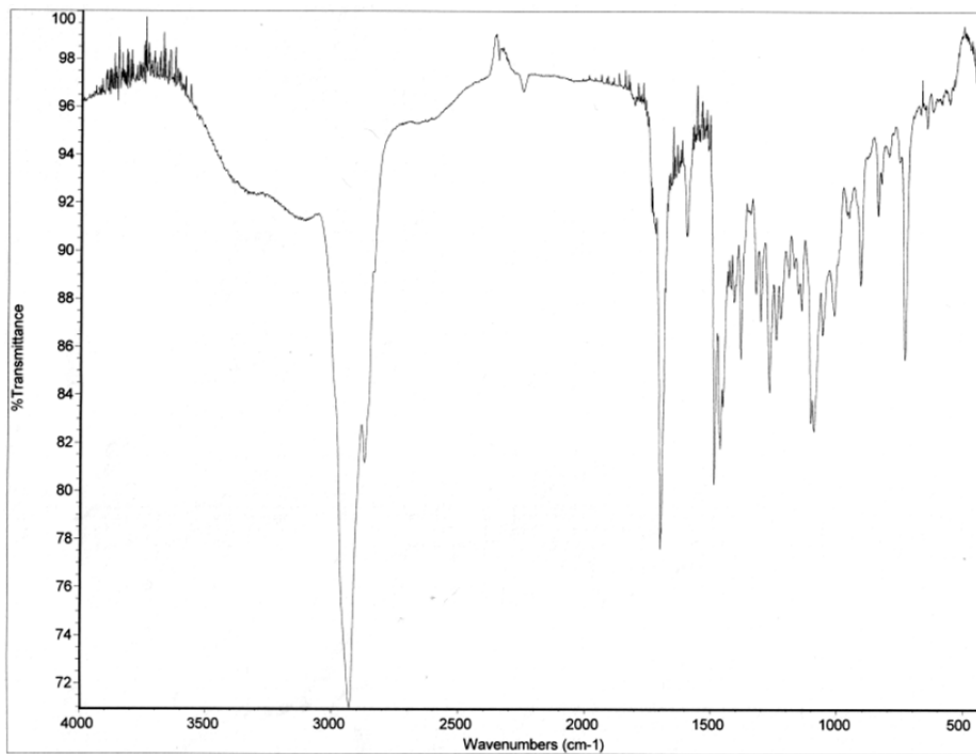
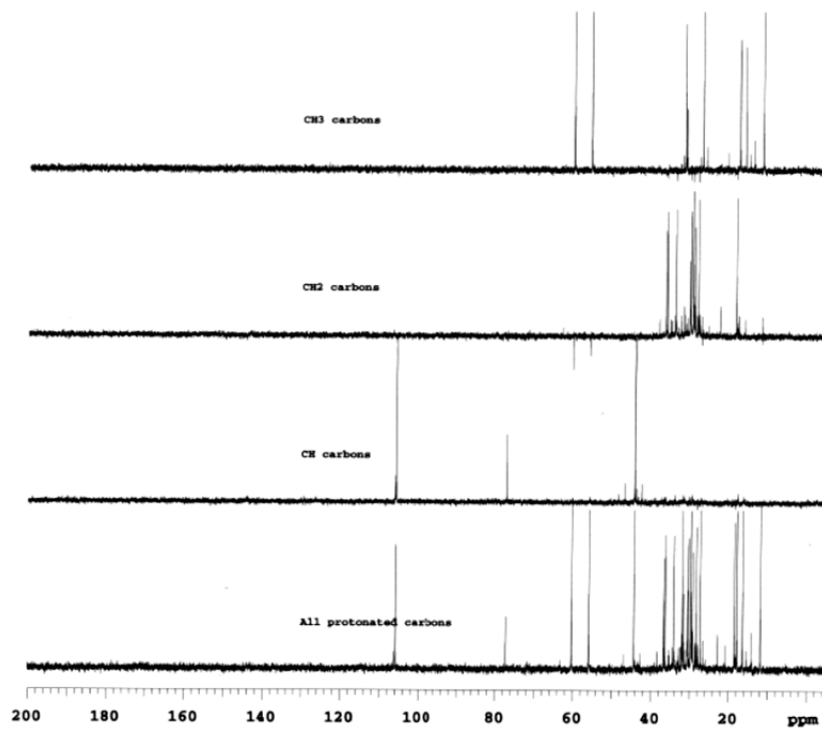
WALTZ-16 modulated

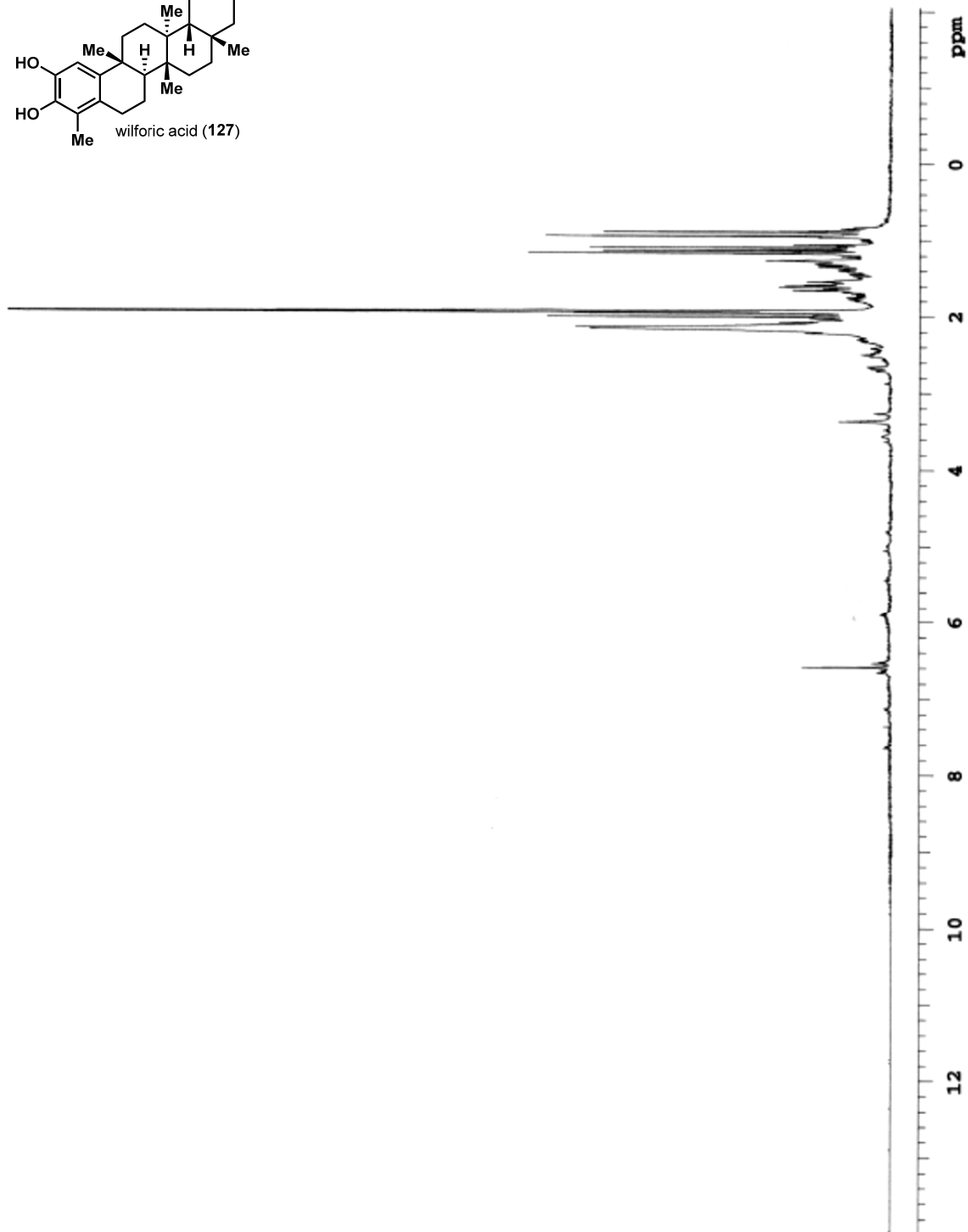
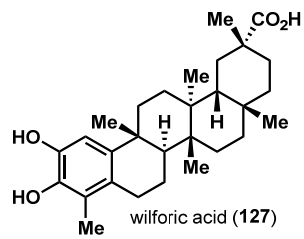
DATA PROCESSING

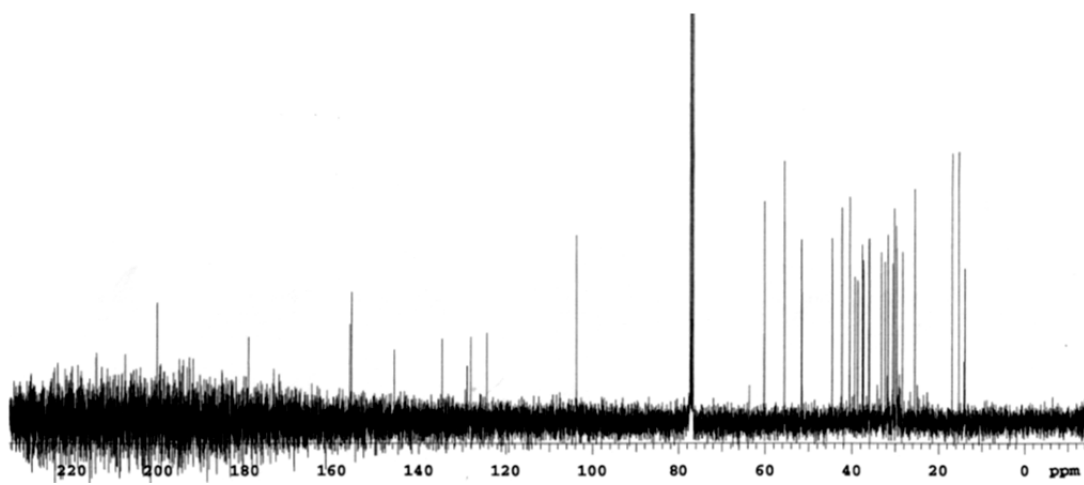
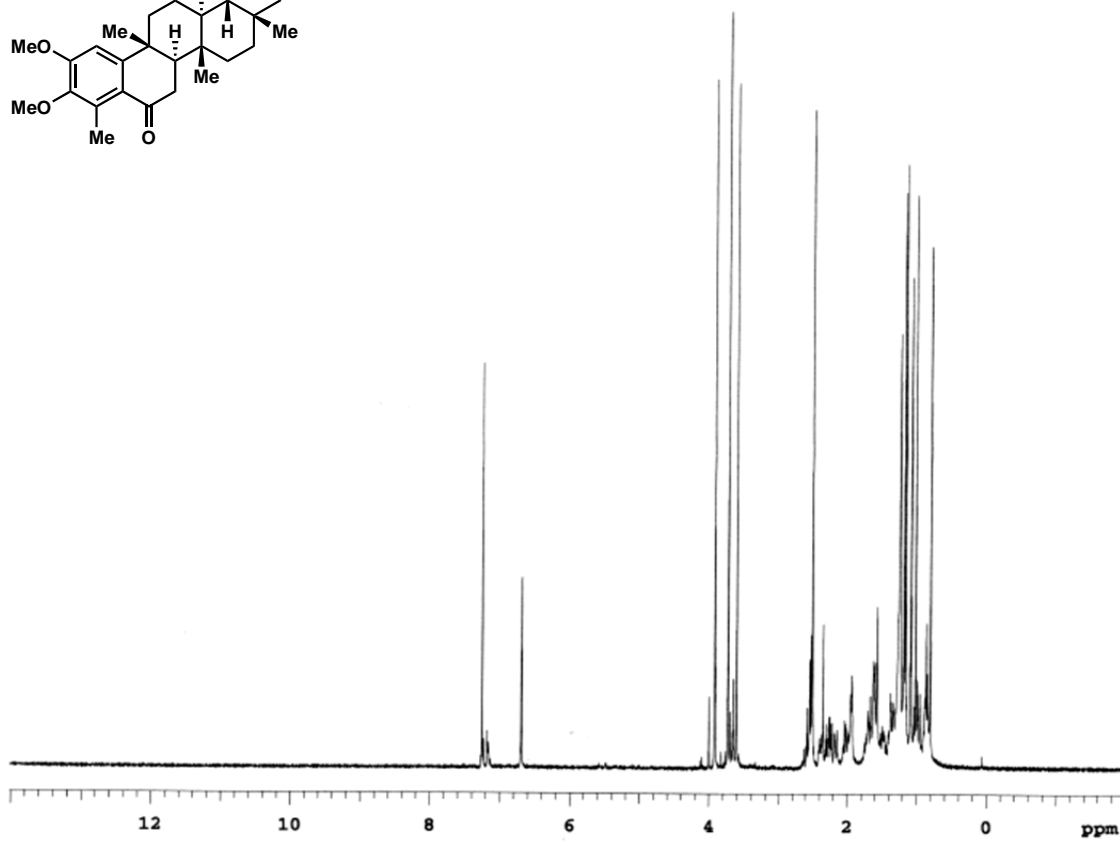
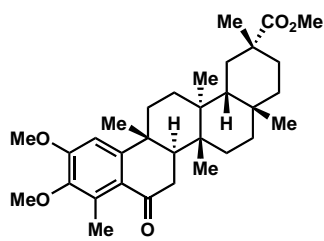
Line broadening 2.0 Hz

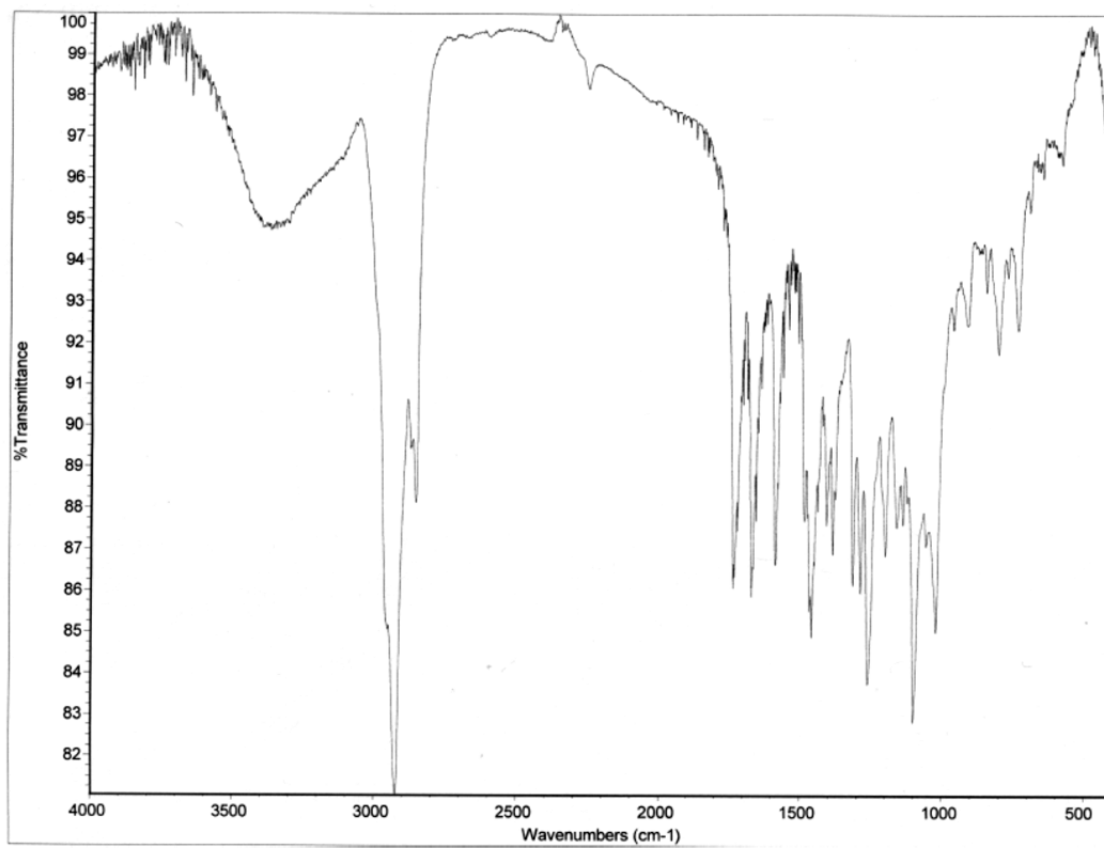
FT size 262144

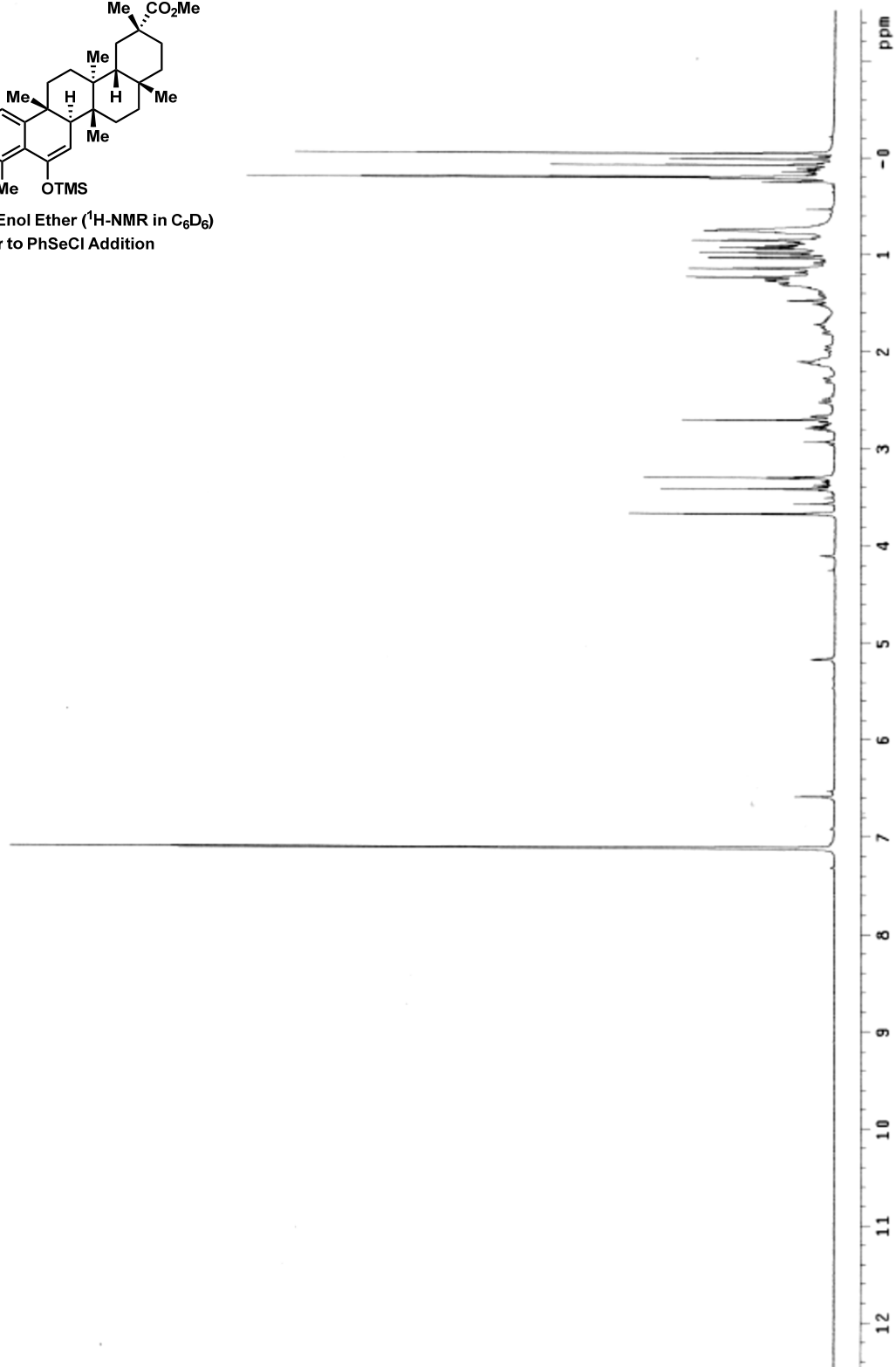
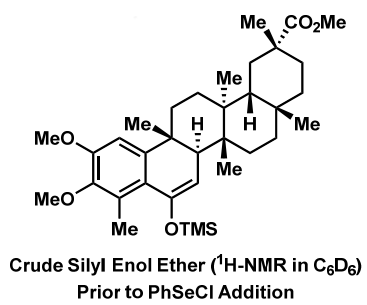
Total time 17 hr, 49 min





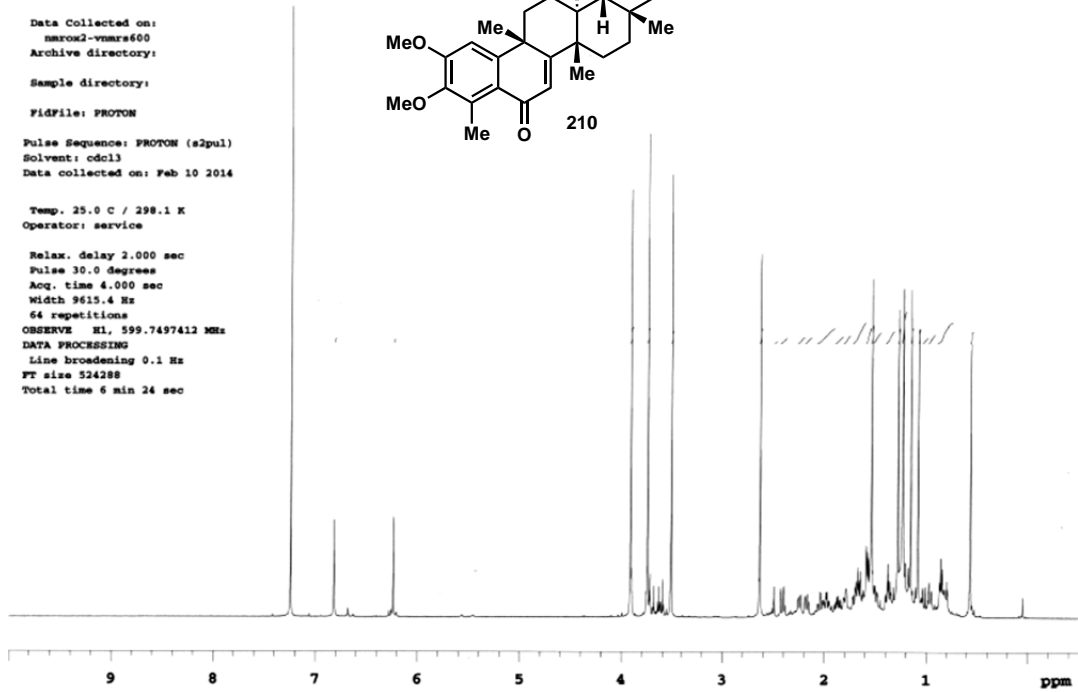
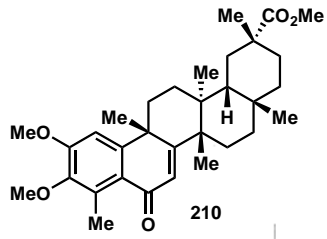




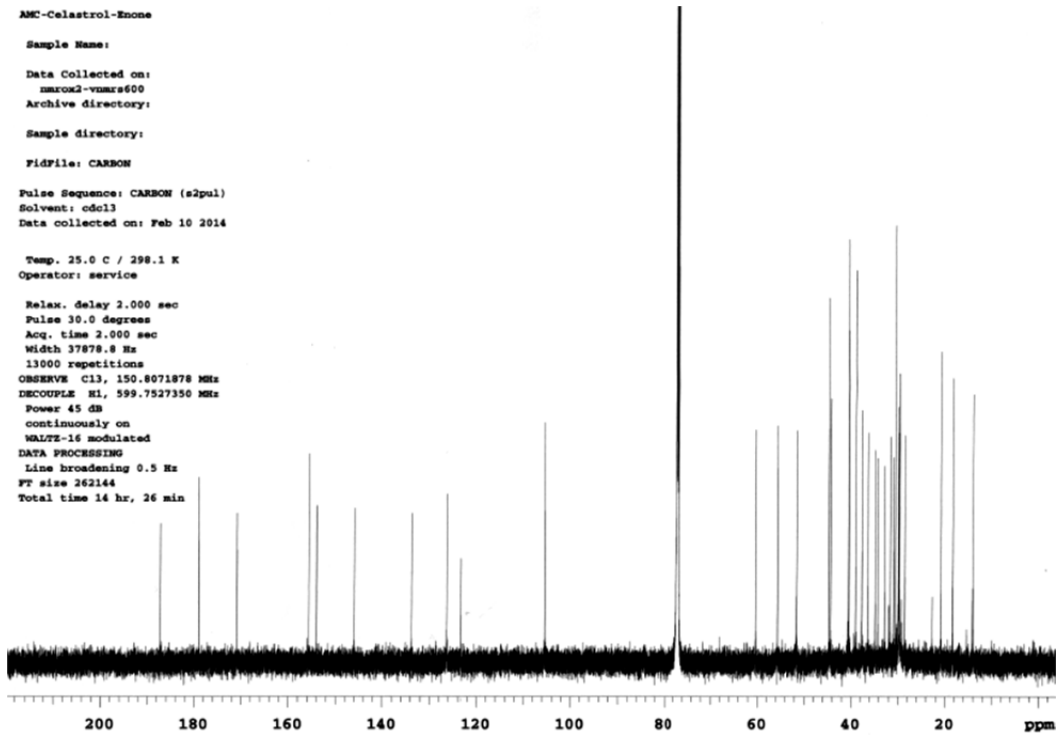


AMC-Celastrol-Enone
 Sample Name:
 Data Collected on:
 nmrox2-vnars600
 Archive directory:
 Sample directory:
 Fidfile: PROTON
 Pulse Sequence: PROTON (s2pul)
 Solvent: cdcl3
 Data collected on: Feb 10 2014

Temp. 25.0 C / 298.1 K
 Operator: service
 Relax. delay 2.000 sec
 Pulse 30.0 degrees
 Acq. time 4.000 sec
 Width 9615.4 Hz
 64 repetitions
 OBSERVE H1, 599.7497412 MHz
 DATA PROCESSING
 Line broadening 0.1 Hz
 FT size 524288
 Total time 6 min 24 sec



AMC-Celastrol-Enone
 Sample Name:
 Data Collected on:
 nmrox2-vnars600
 Archive directory:
 Sample directory:
 Fidfile: CARBON
 Pulse Sequence: CARBON (s2pul)
 Solvent: cdcl3
 Data collected on: Feb 10 2014
 Temp. 25.0 C / 298.1 K
 Operator: service
 Relax. delay 2.000 sec
 Pulse 30.0 degrees
 Acq. time 2.000 sec
 Width 37878.8 Hz
 13000 repetitions
 OBSERVE C13, 150.8071878 MHz
 DECOUPLE H1, 599.7527350 MHz
 Power 45 dB
 continuously on
 WALTZ-16 modulated
 DATA PROCESSING
 Line broadening 0.5 Hz
 FT size 262144
 Total time 14 hr, 26 min



AMC-Celastrol-Enone

Sample Name:

Data Collected on:
nmr02-vmr600
Archive directory:

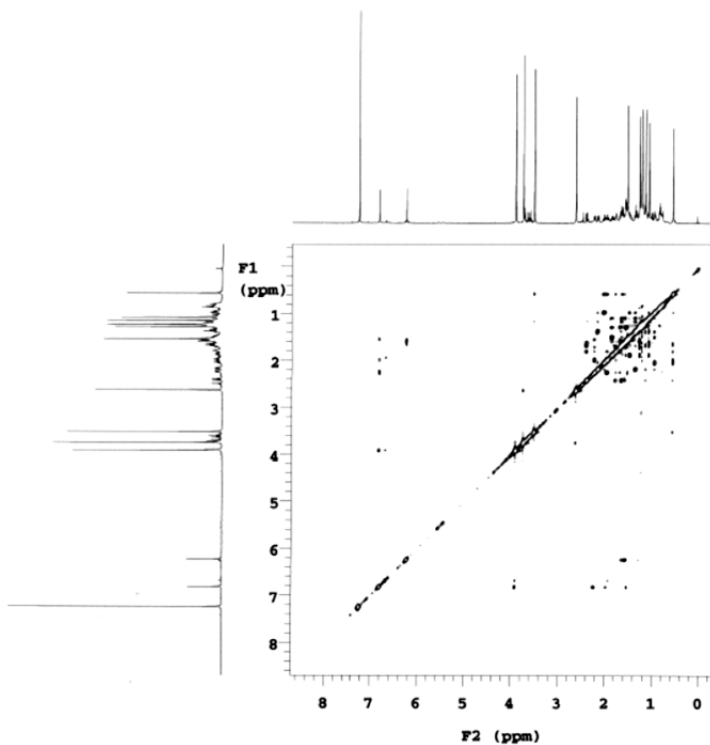
Sample directory:

FidFile: NOESY

Pulse Sequence: NOESY
Solvent: cdcl3
Data collected on: Feb 10 2014

Temp. 25.0 C / 298.1 K
Operator: service

Relax. Delay 2.000 sec
Acq. time 0.150 sec
Width 5506.6 Hz
2D Width 5506.6 Hz
8 repetitions
2 x 256 increments
OBSERVE H1, 599.7497412 MHz
DATA PROCESSING
Gauss apodization 0.049 sec
F1 DATA PROCESSING
Gauss apodization 0.024 sec
FT size 2048 x 2048
Total time 3 hr, 24 min



AMC-Celastrol-Enone

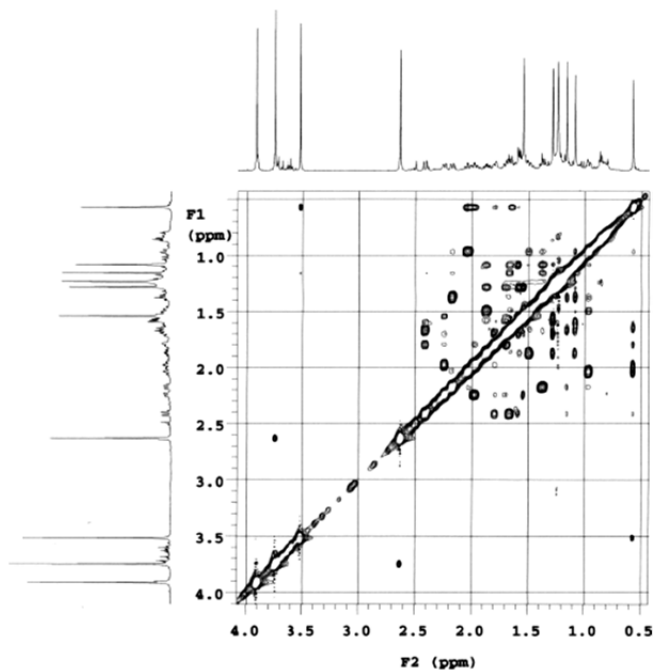
Sample Name:

Data Collected on:
nmr02-vmr600
Archive directory:

Sample directory:

FidFile: NOESY

Pulse Sequence: NOESY
Solvent: cdcl3
Data collected on: Feb 10 2014



AMC-Celastrol-Enone

Sample Name:

Data Collected on:

nmr02-vmar600

Archive directory:

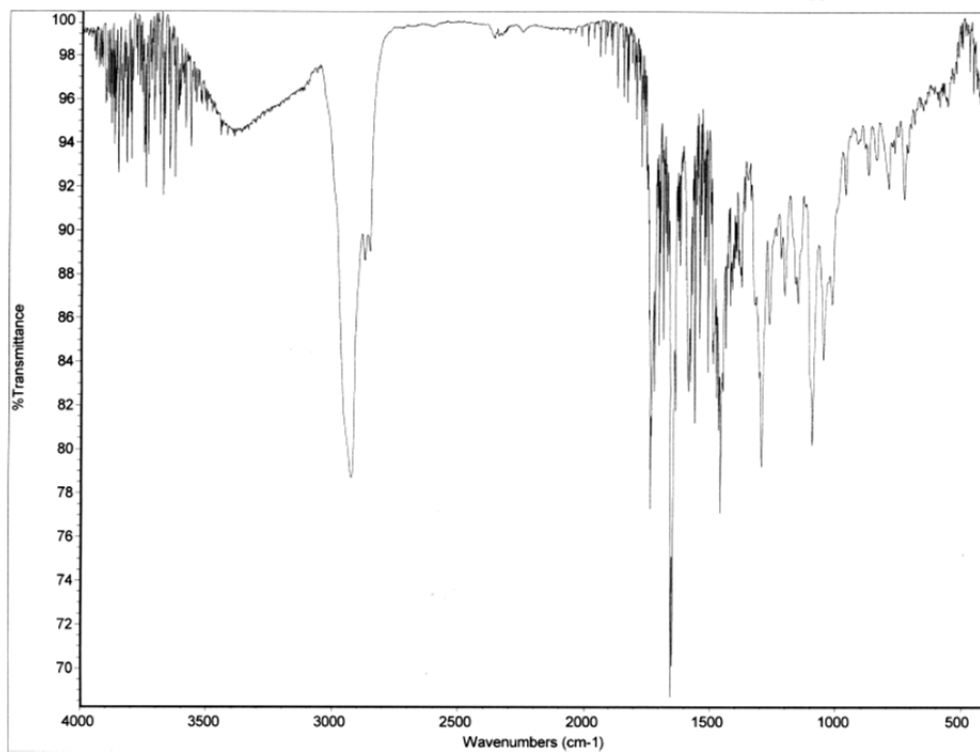
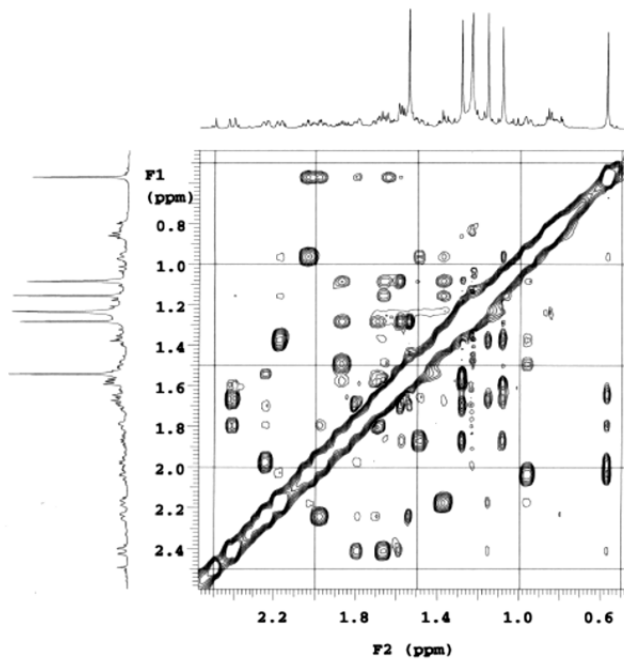
Sample directory:

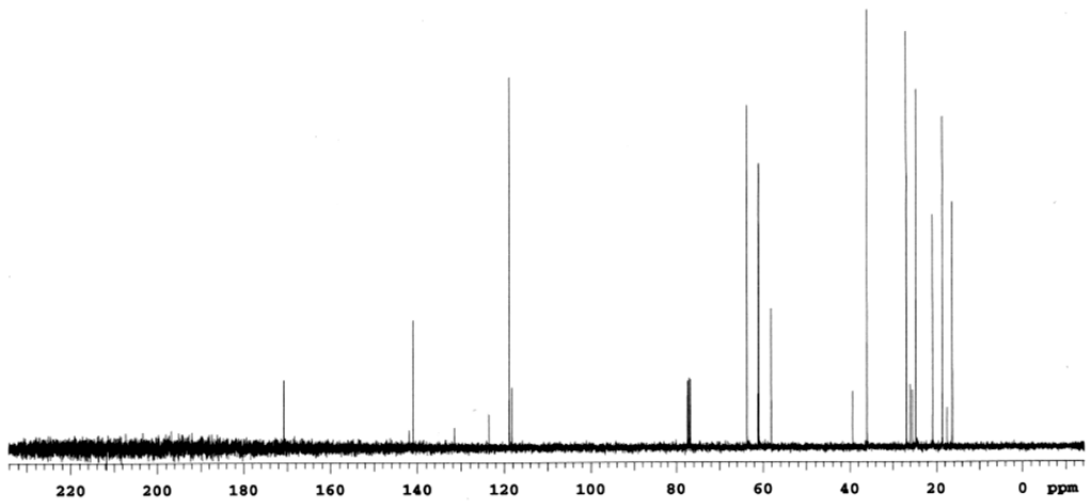
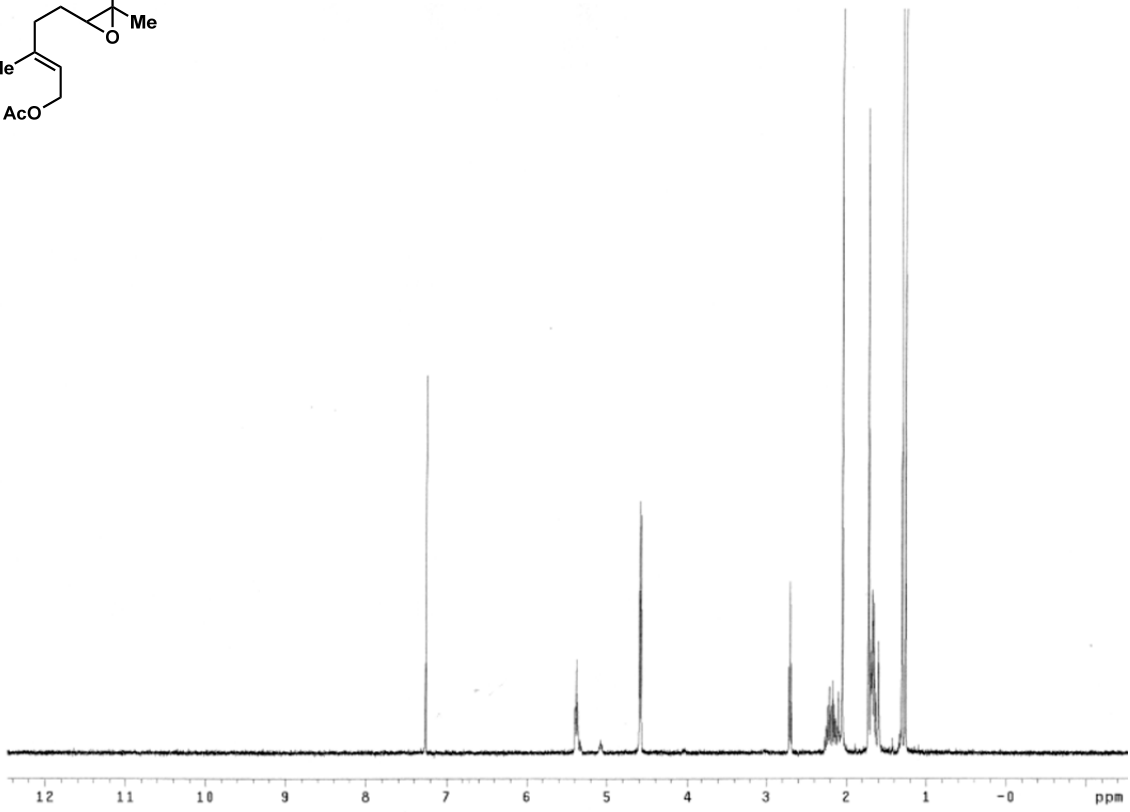
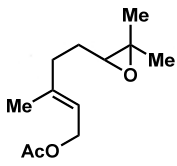
FidFile: NOESY

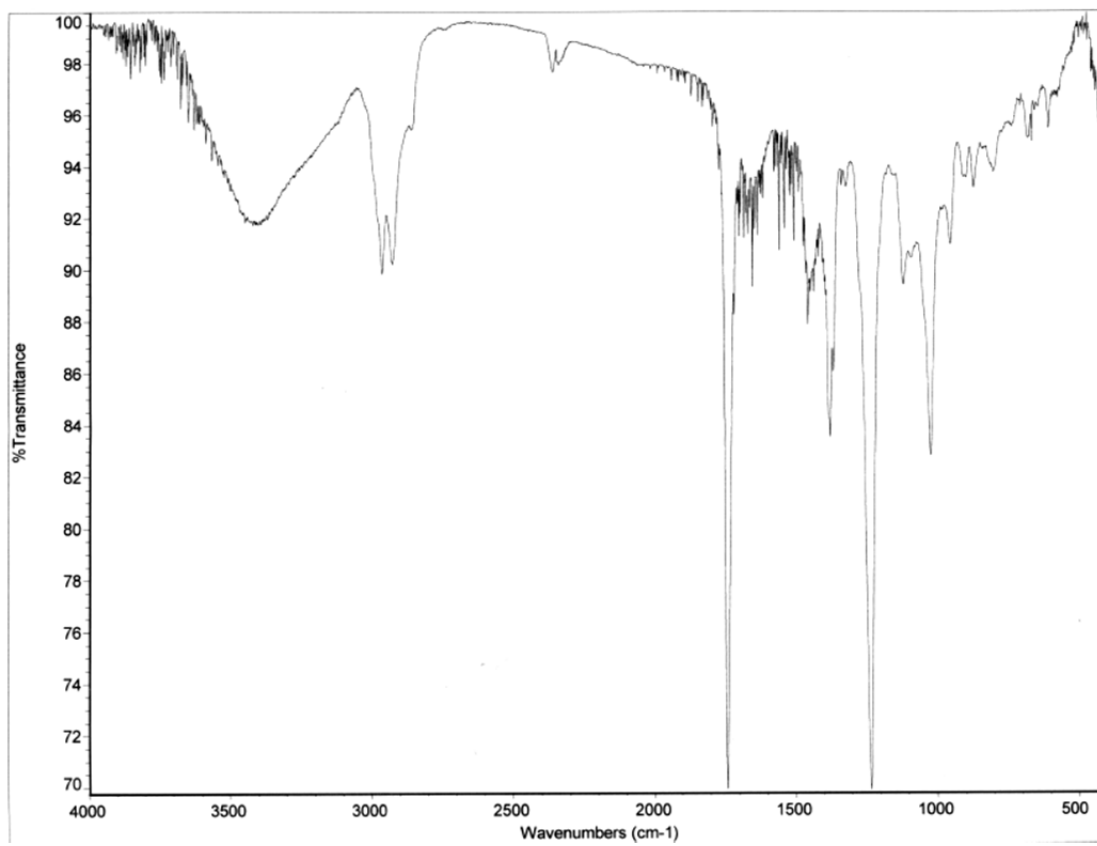
Pulse Sequence: NOESY

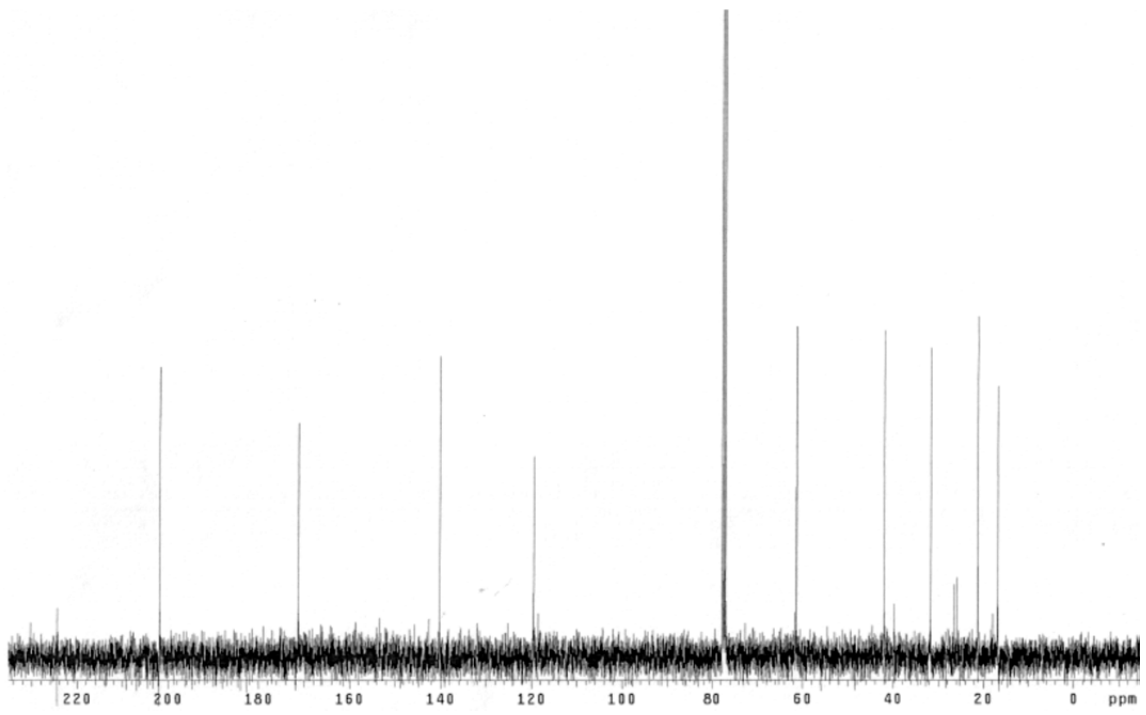
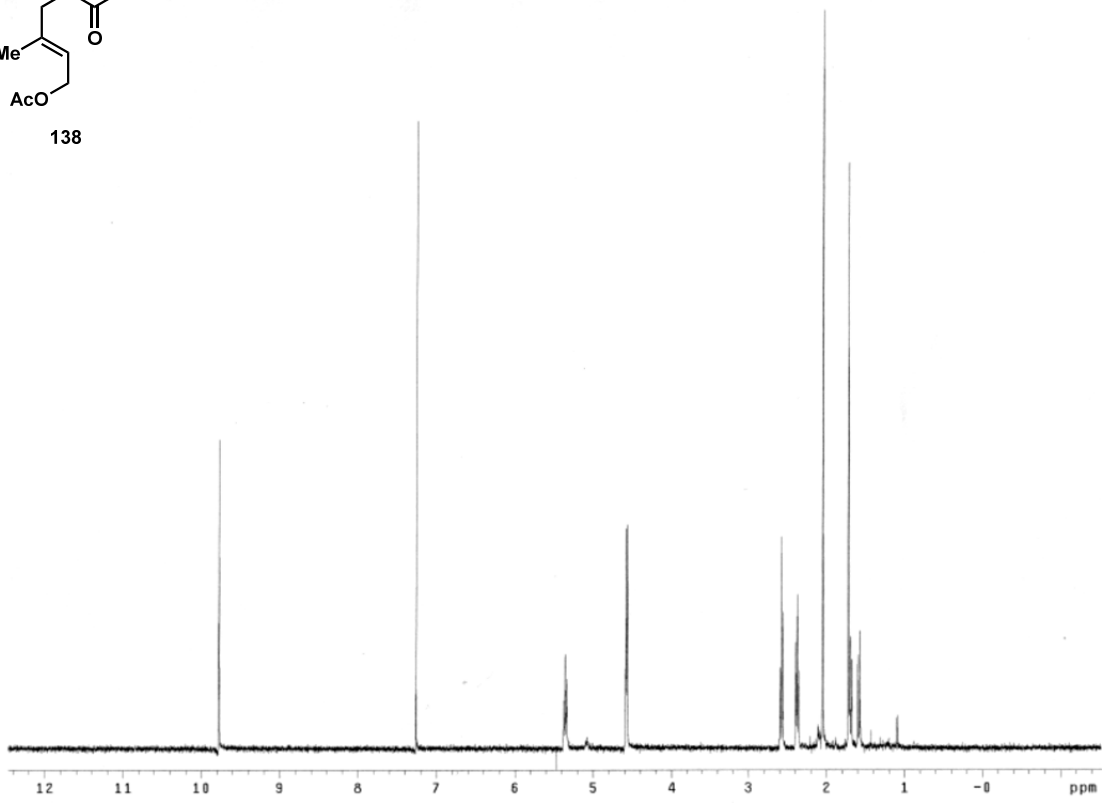
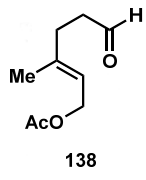
Solvent: cdcl3

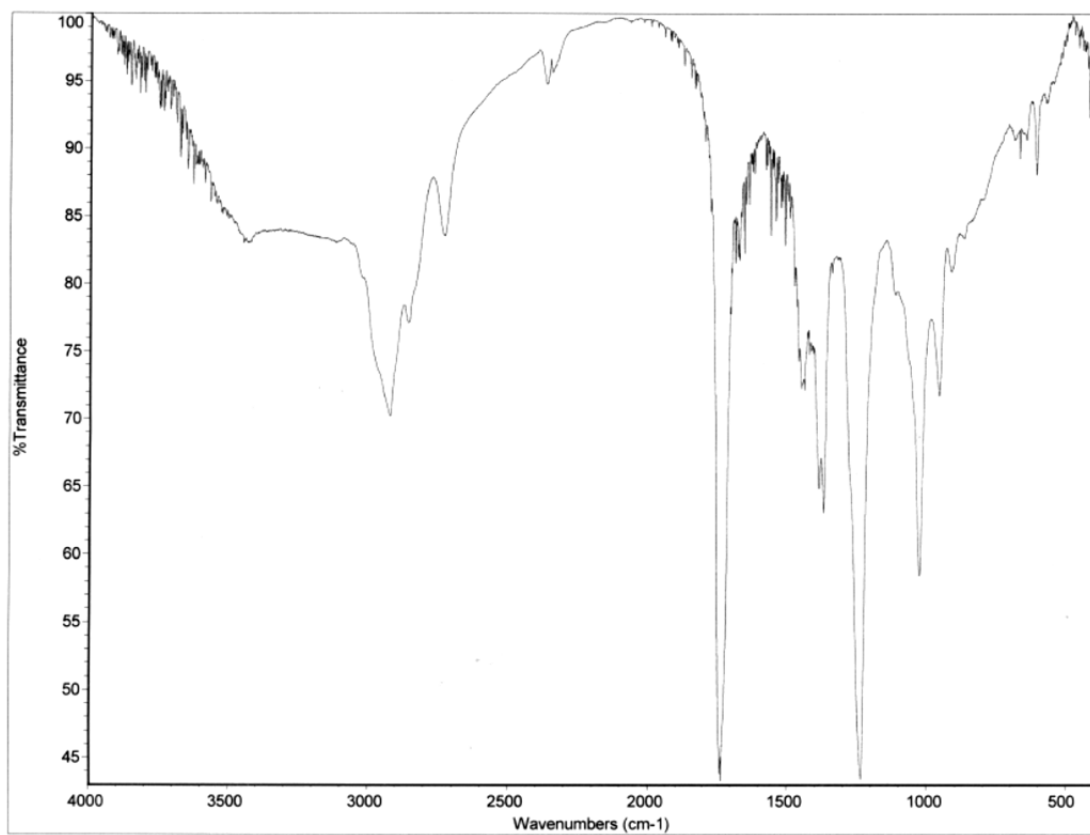
Data collected on: Feb 10 2014

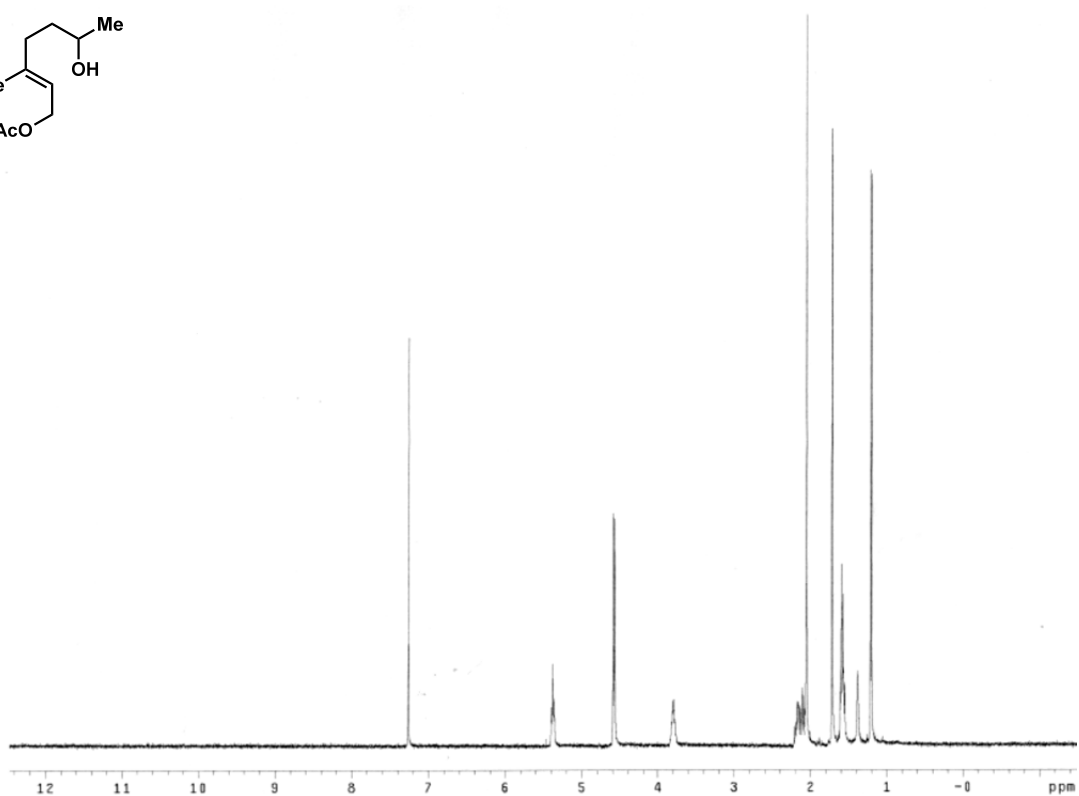
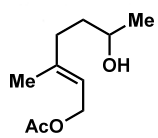




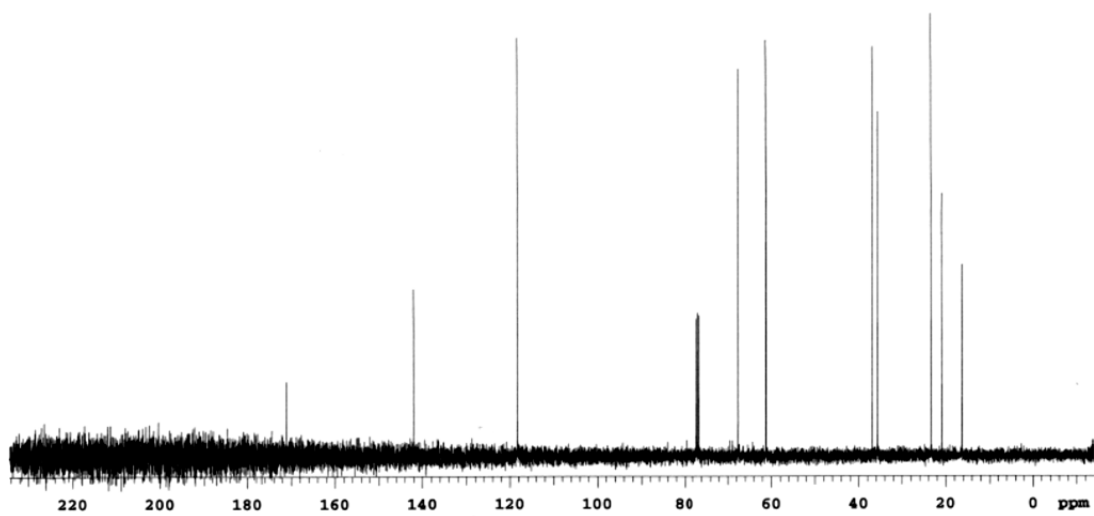


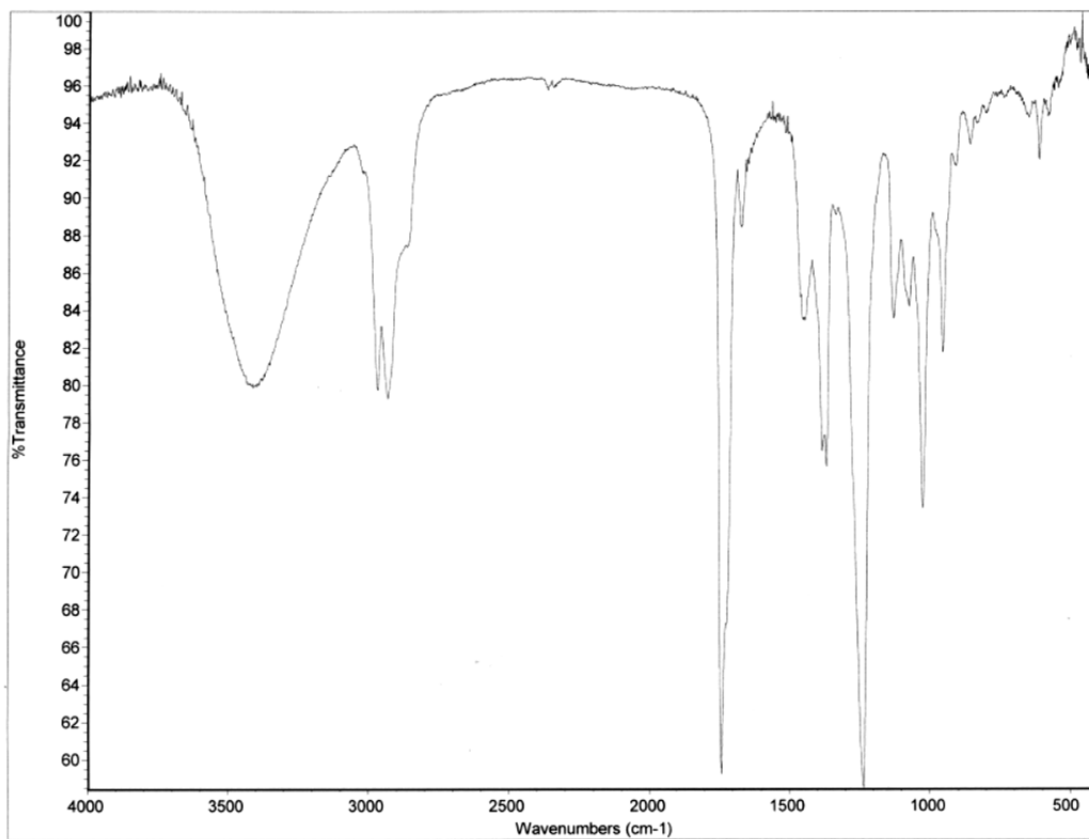


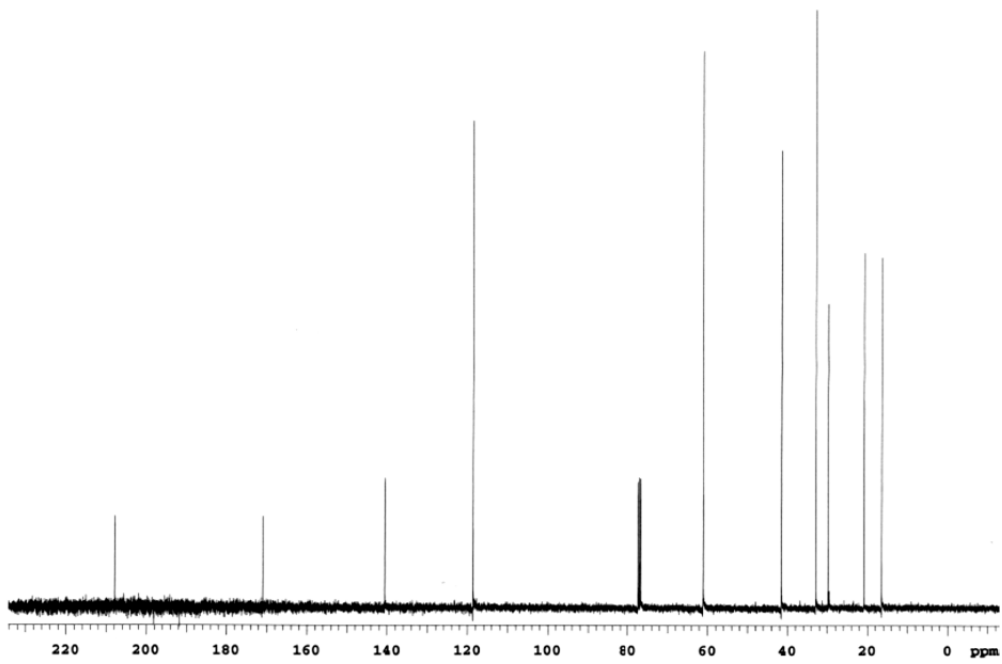
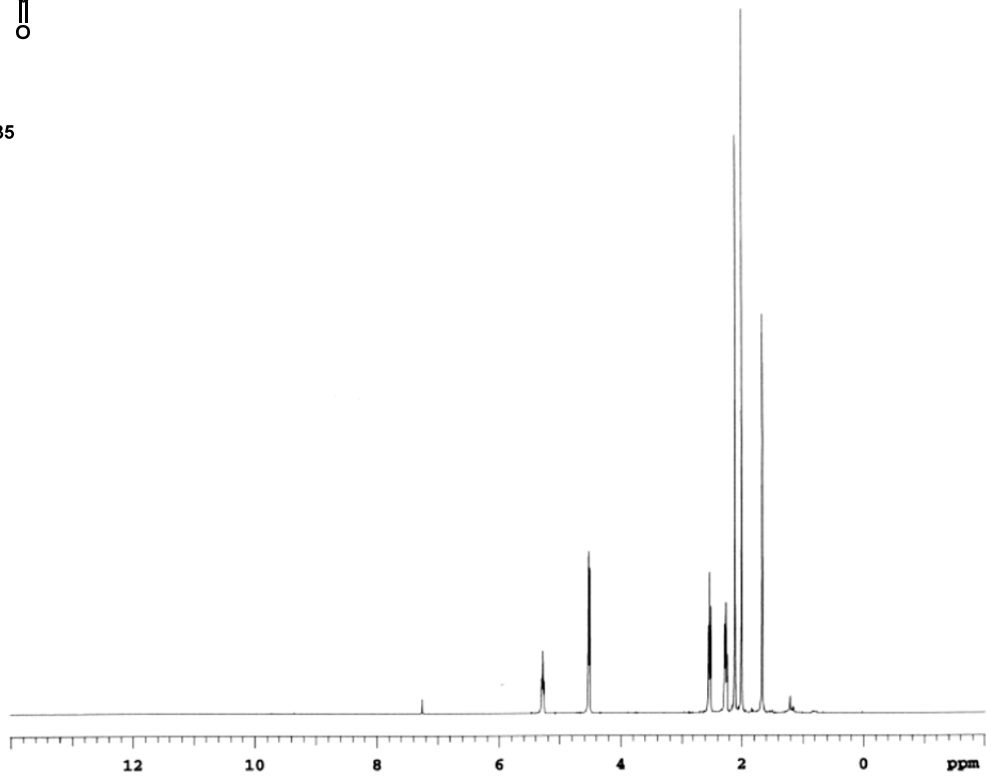
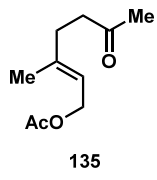


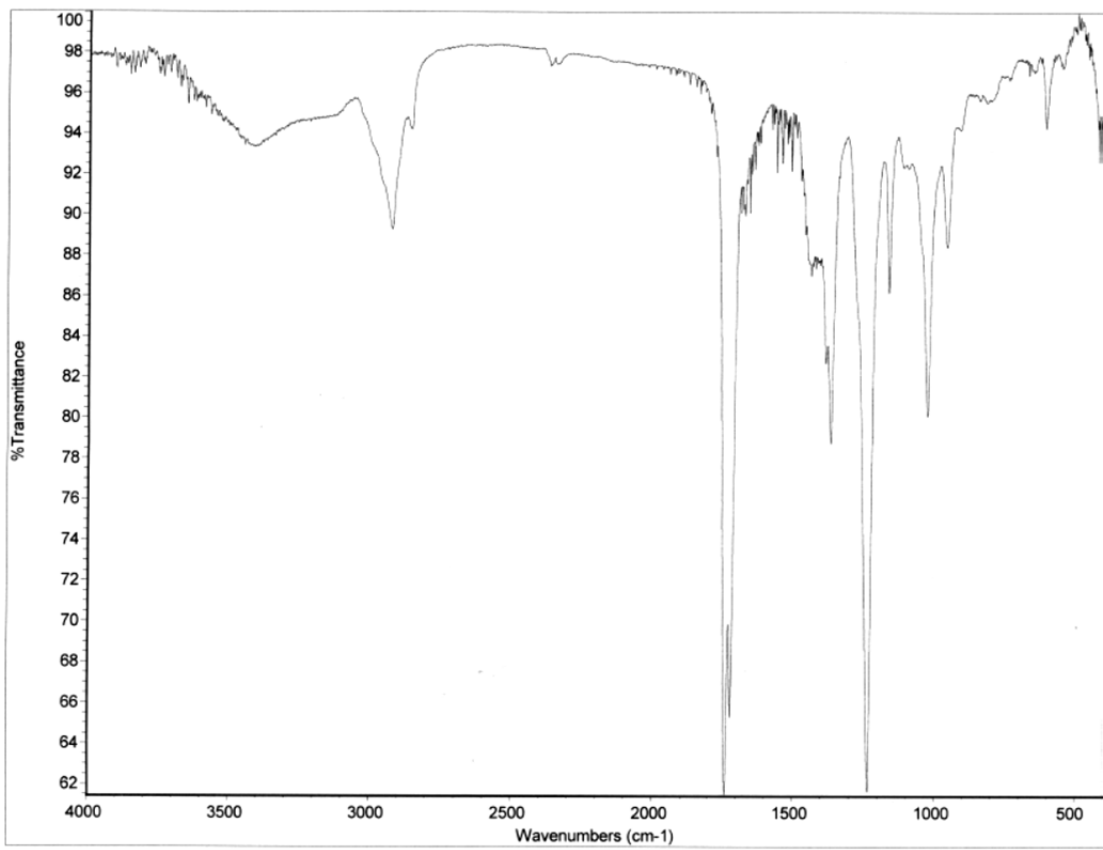


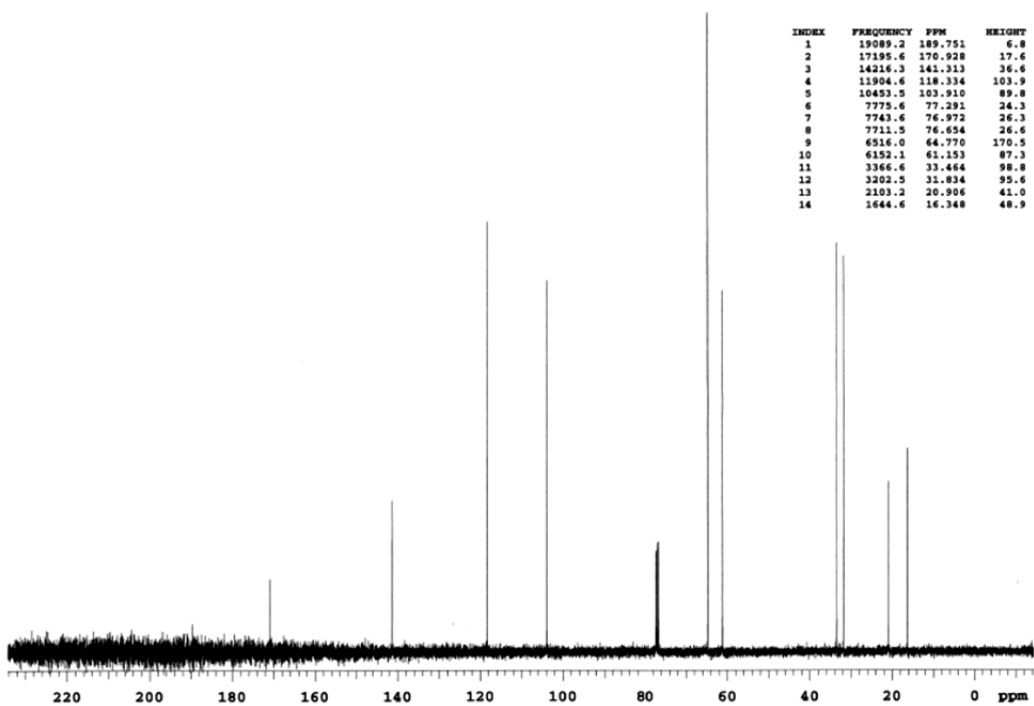
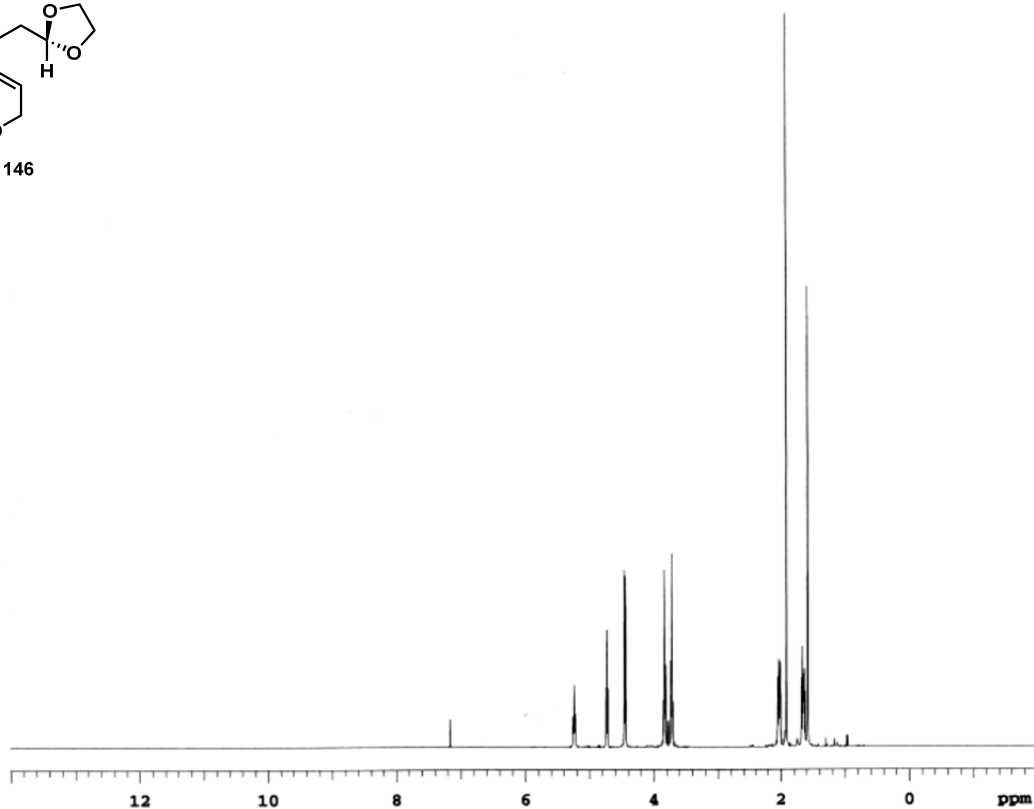
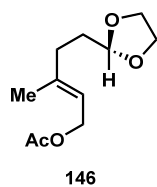
INDEX	FREQUENCY	PPM	HEIGHT
1	17210.1	171.072	17.2
2	14291.9	142.064	19.1
3	11901.6	118.304	95.8
4	7774.8	77.283	31.3
5	7742.8	76.965	32.7
6	7710.8	76.646	32.1
7	6800.6	67.599	88.6
8	6158.2	61.213	95.2
9	3708.4	36.862	93.7
10	3587.8	35.664	78.8
11	2354.9	23.408	101.2
12	2105.4	20.928	60.0
13	1643.1	16.333	43.6

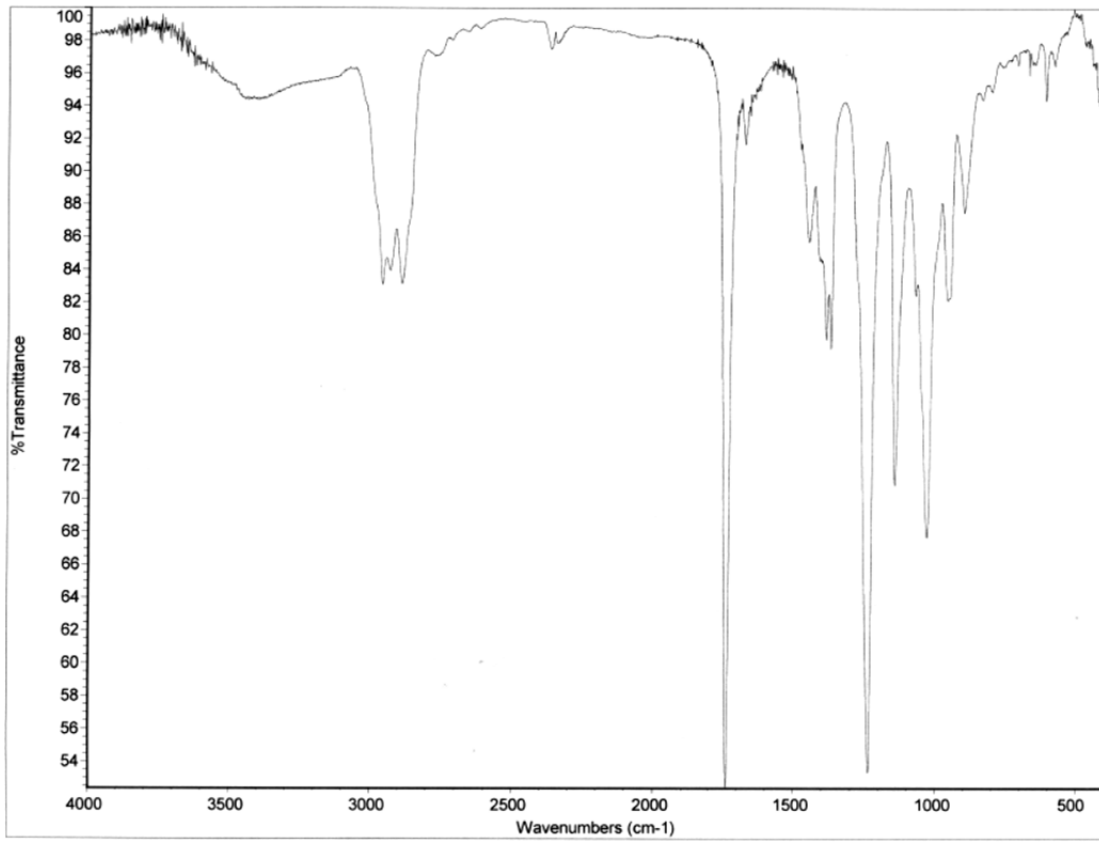


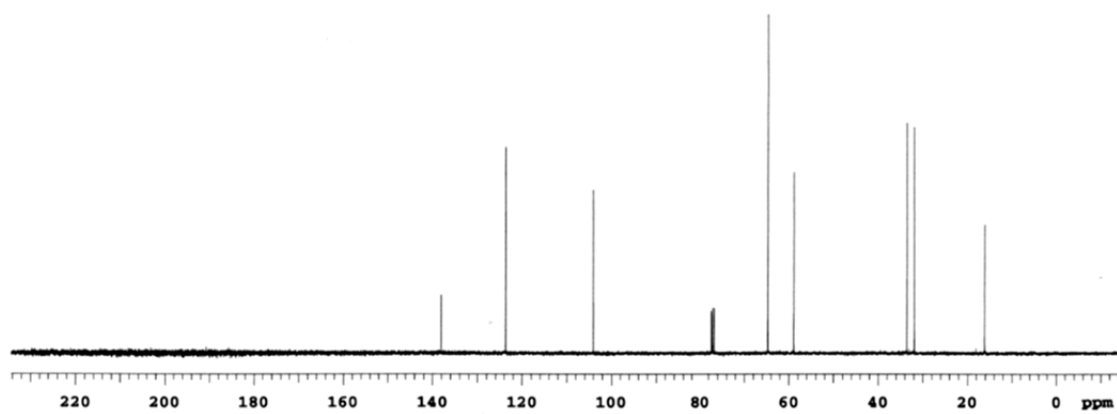
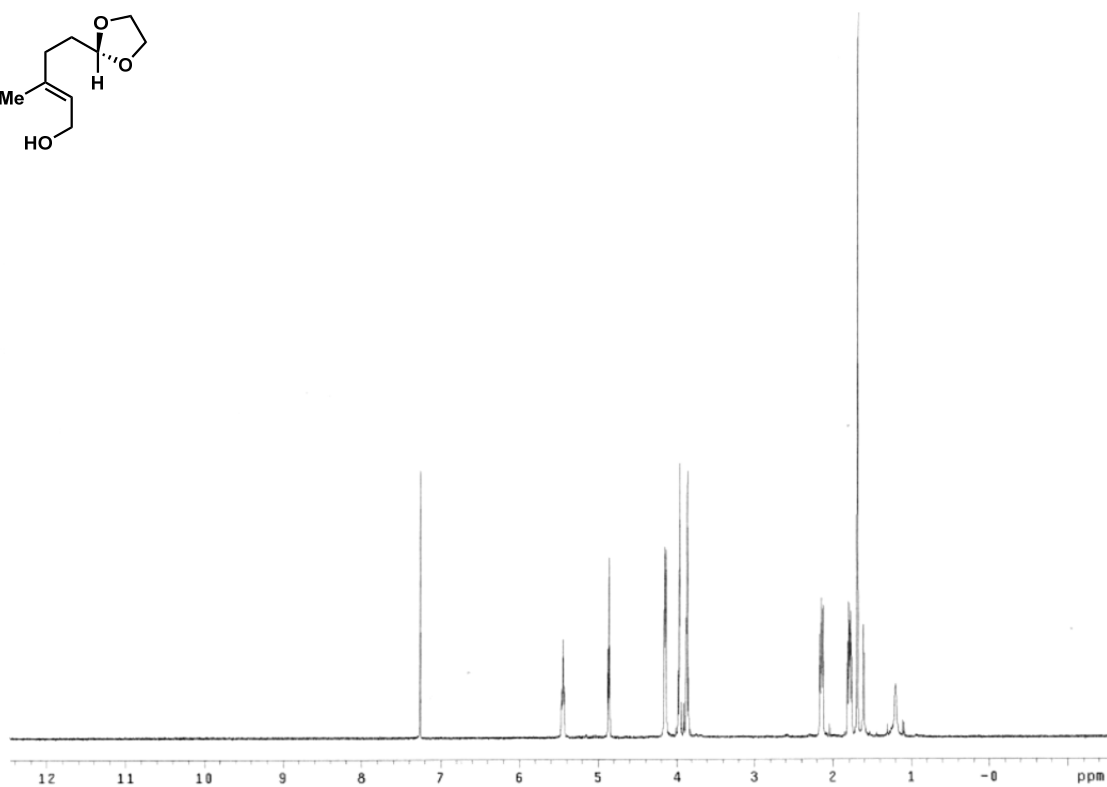
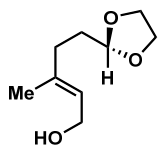


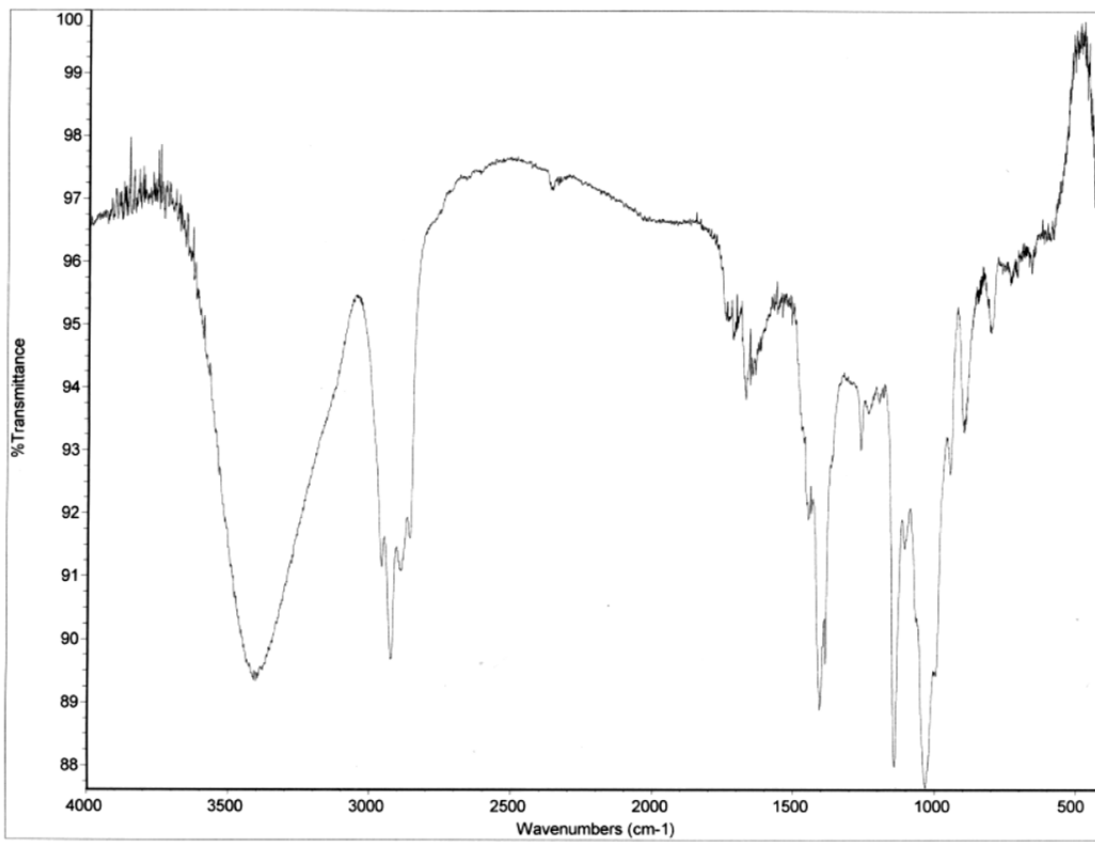


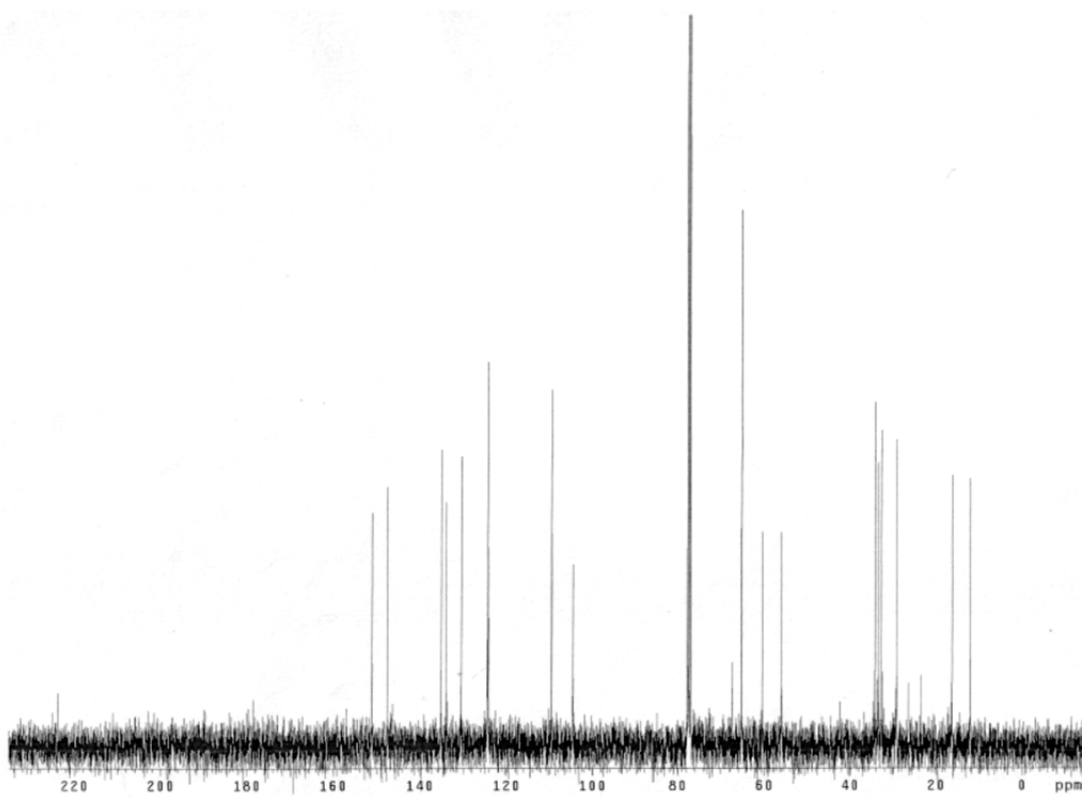
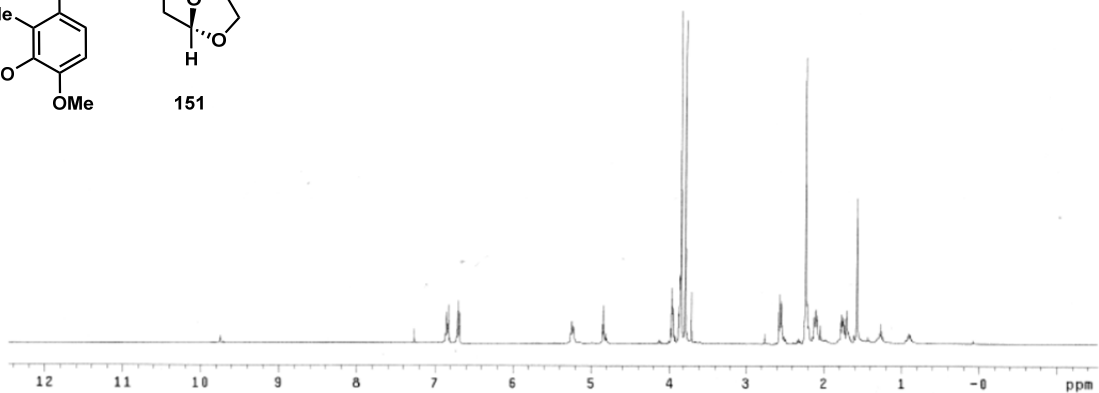
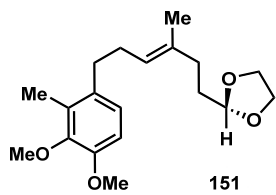


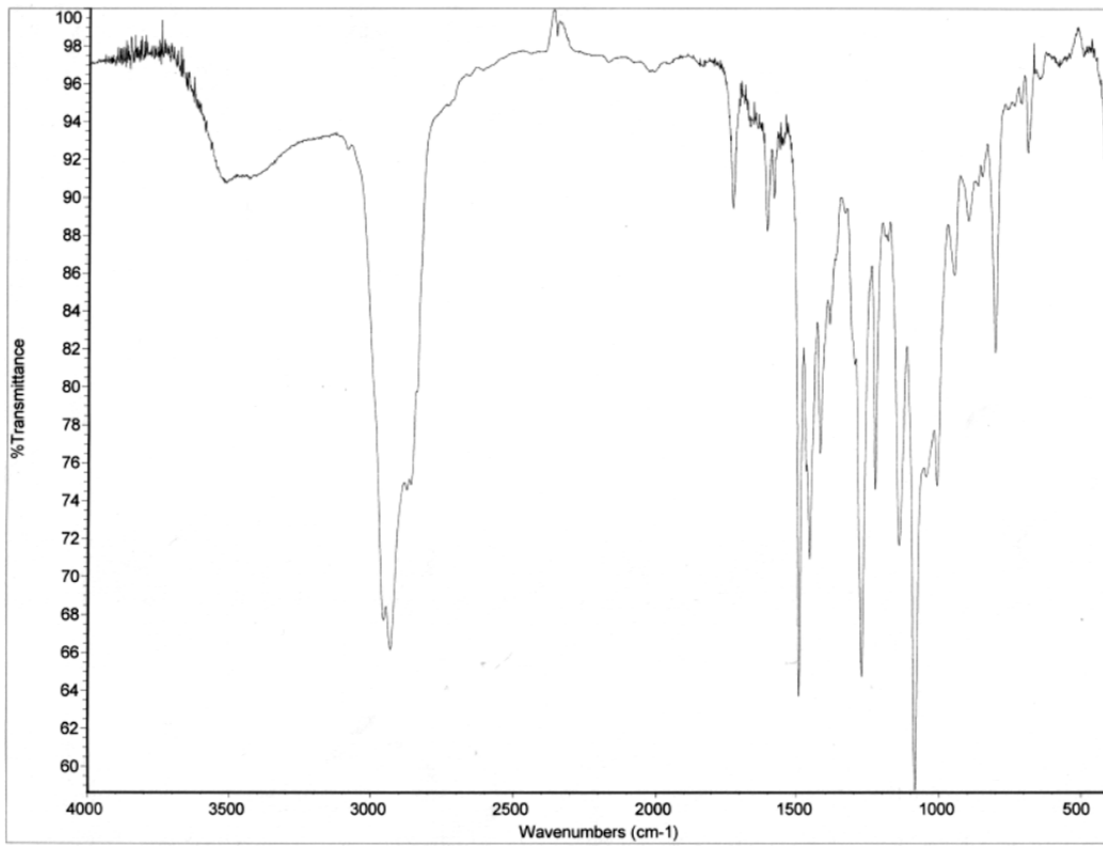


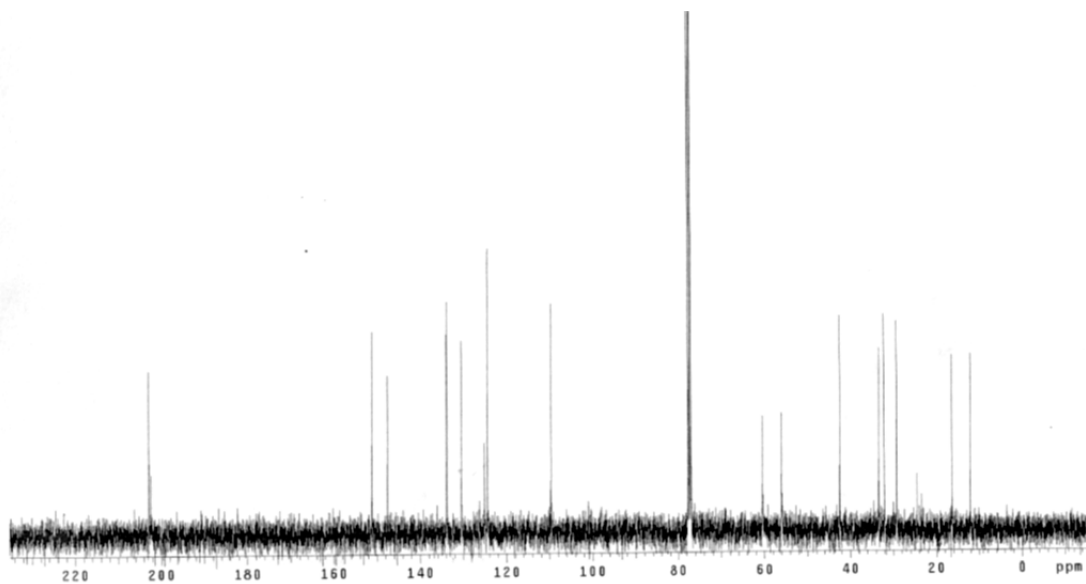
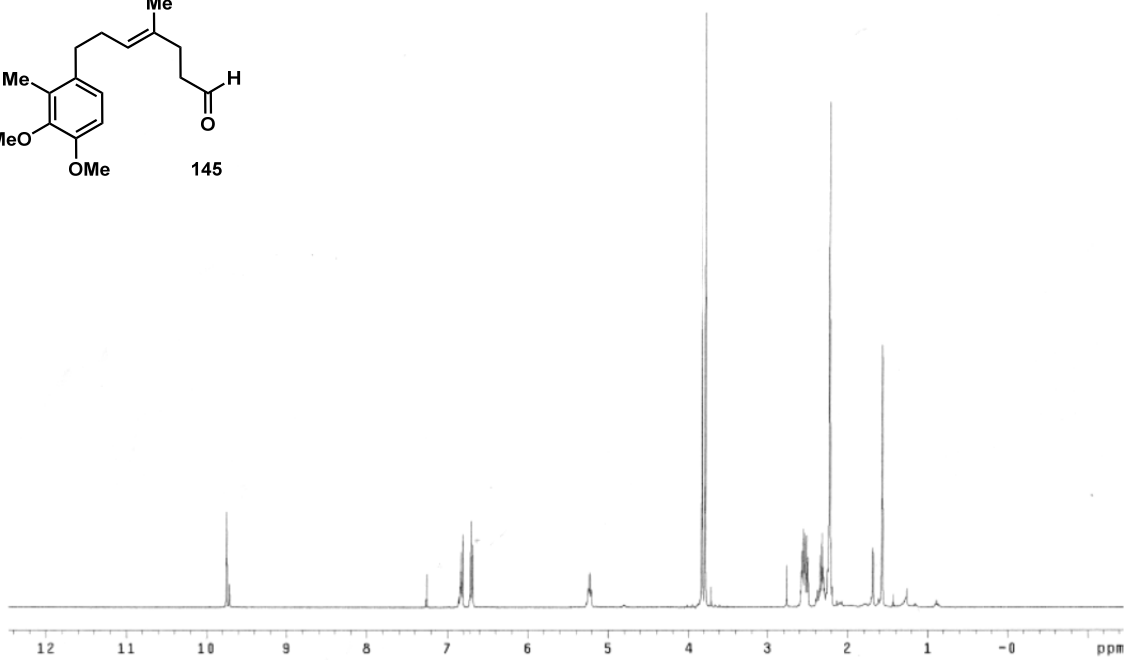
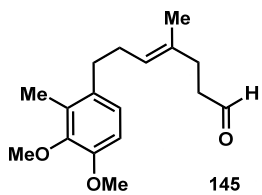


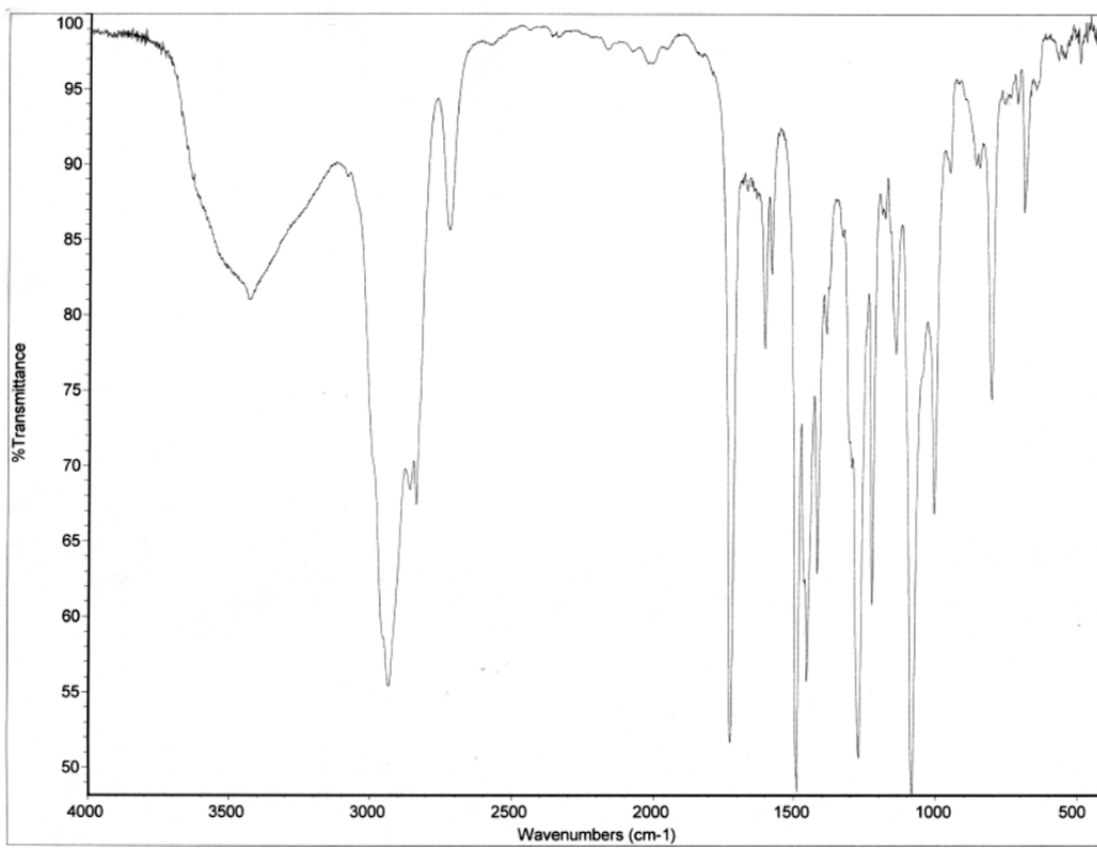


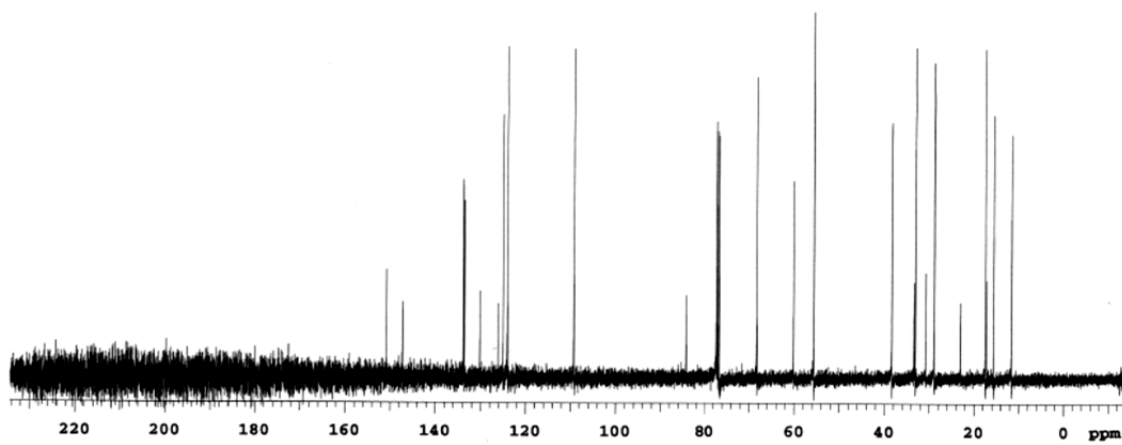
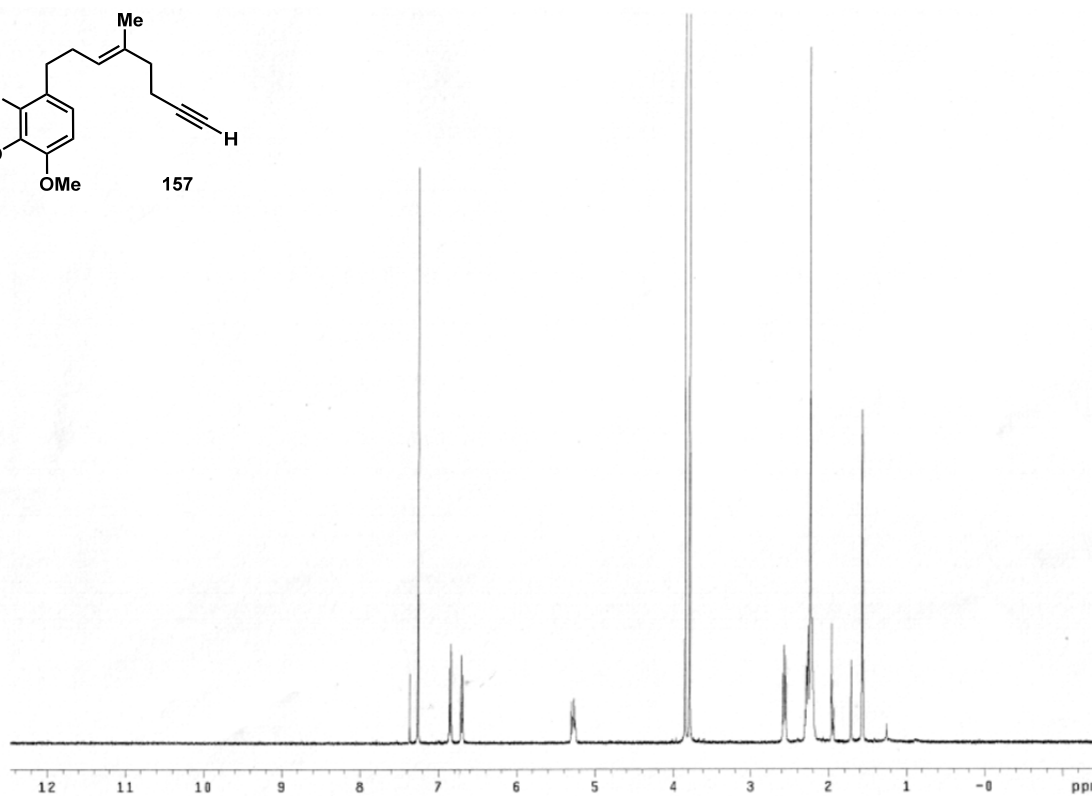
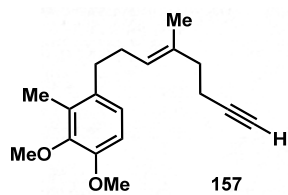


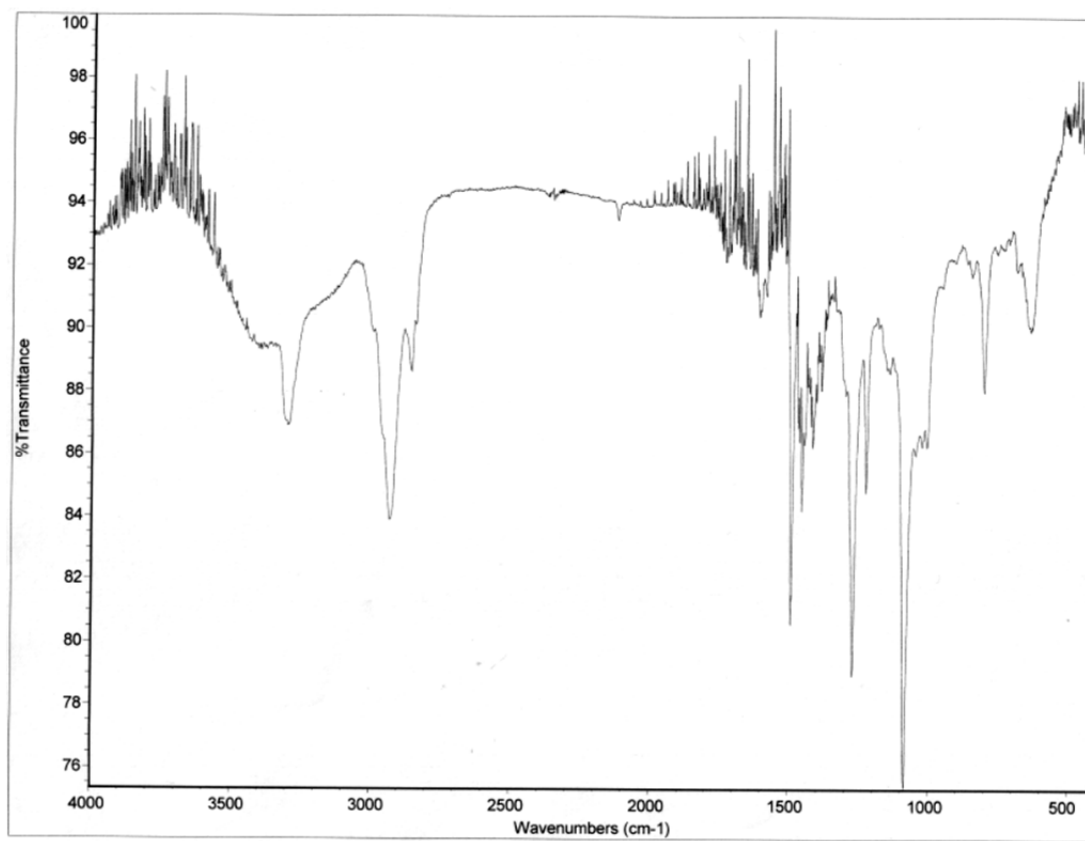


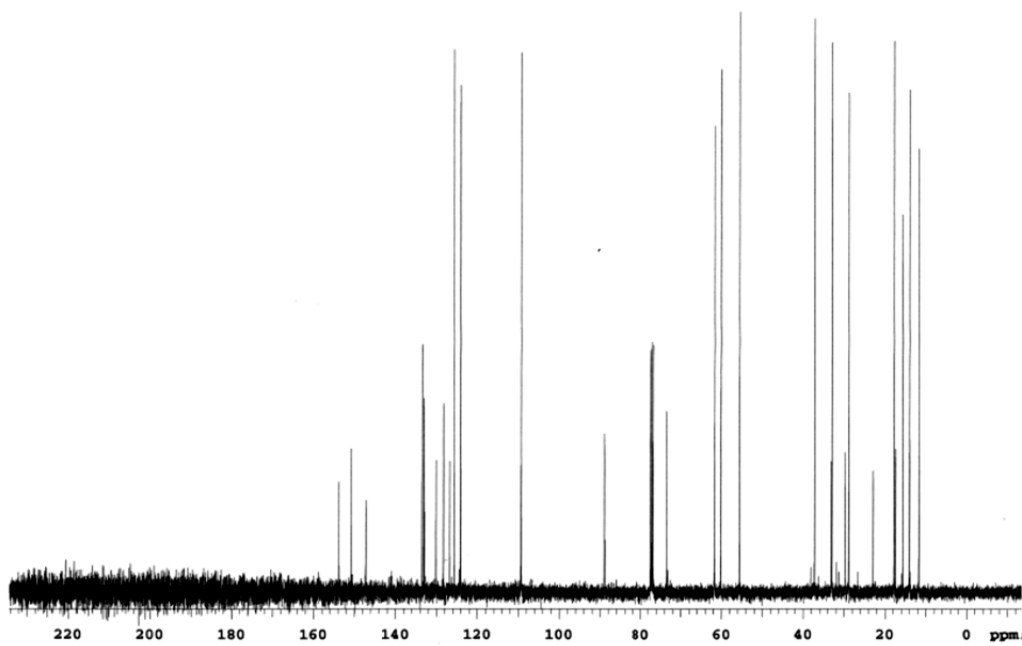
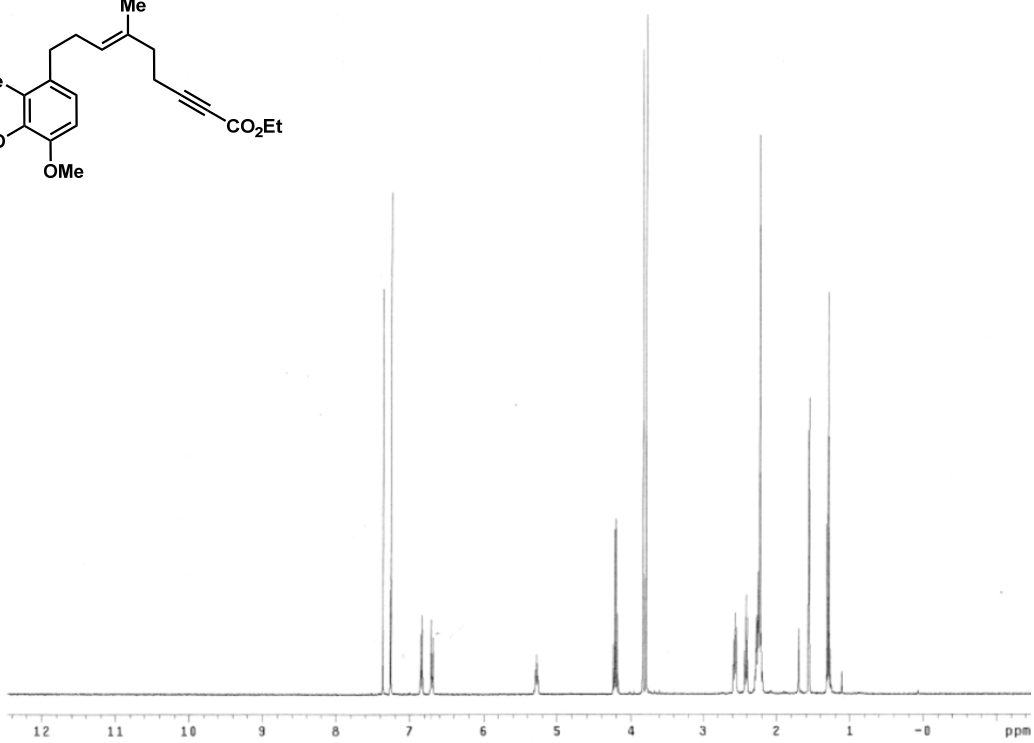
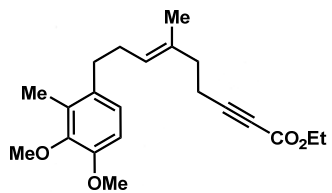


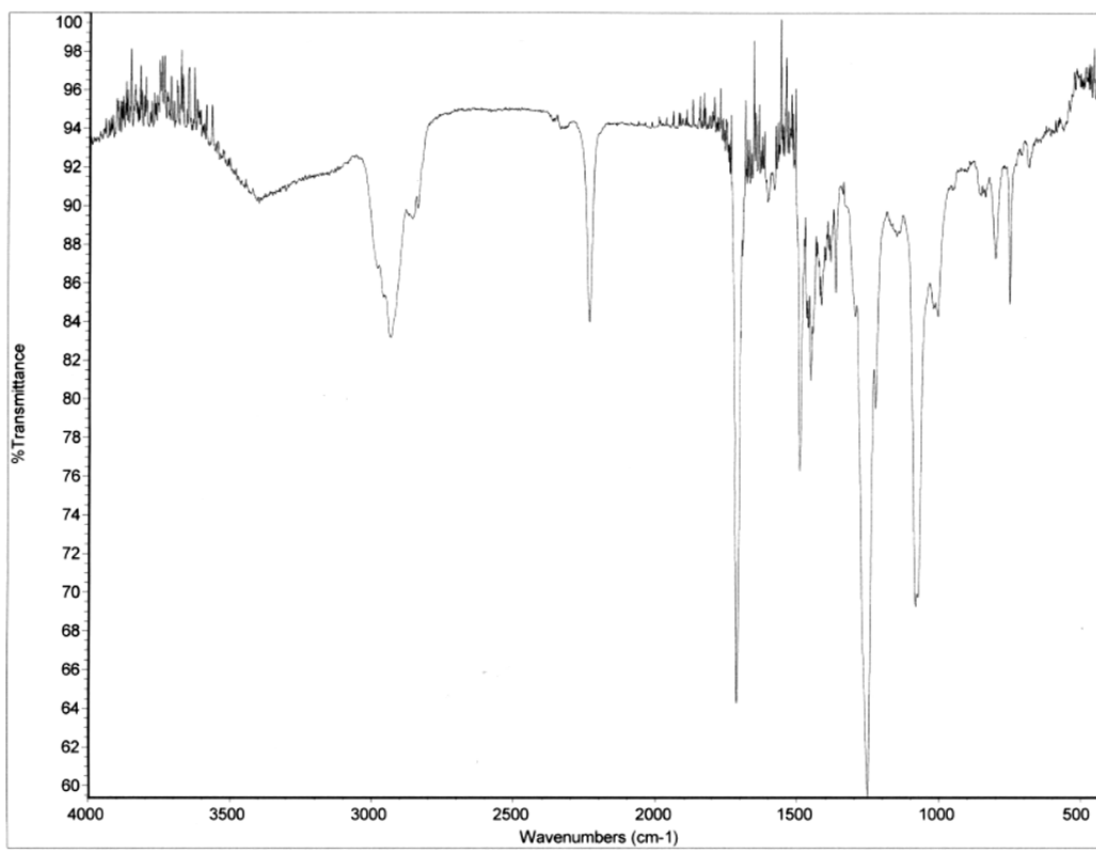


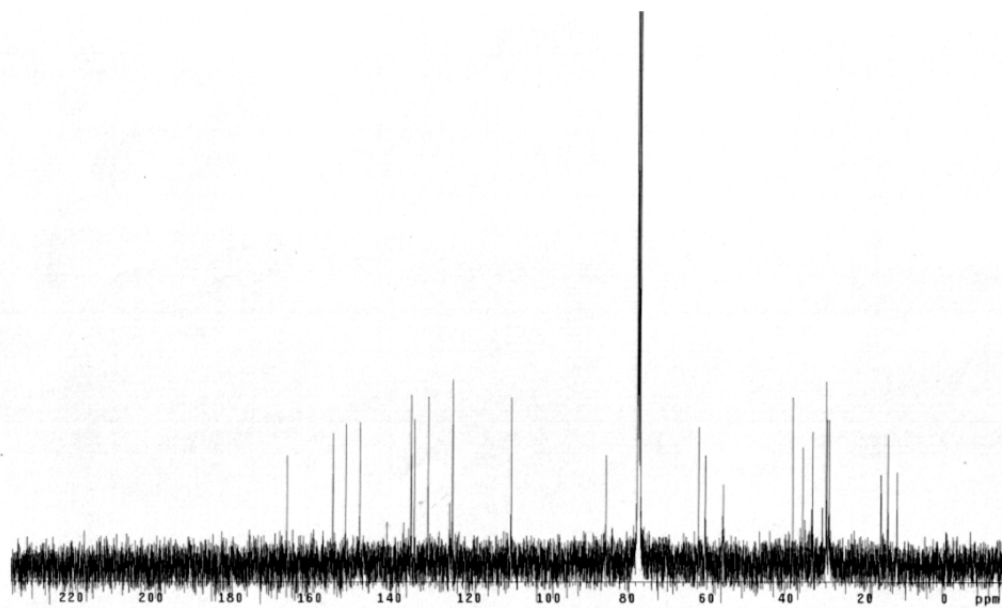
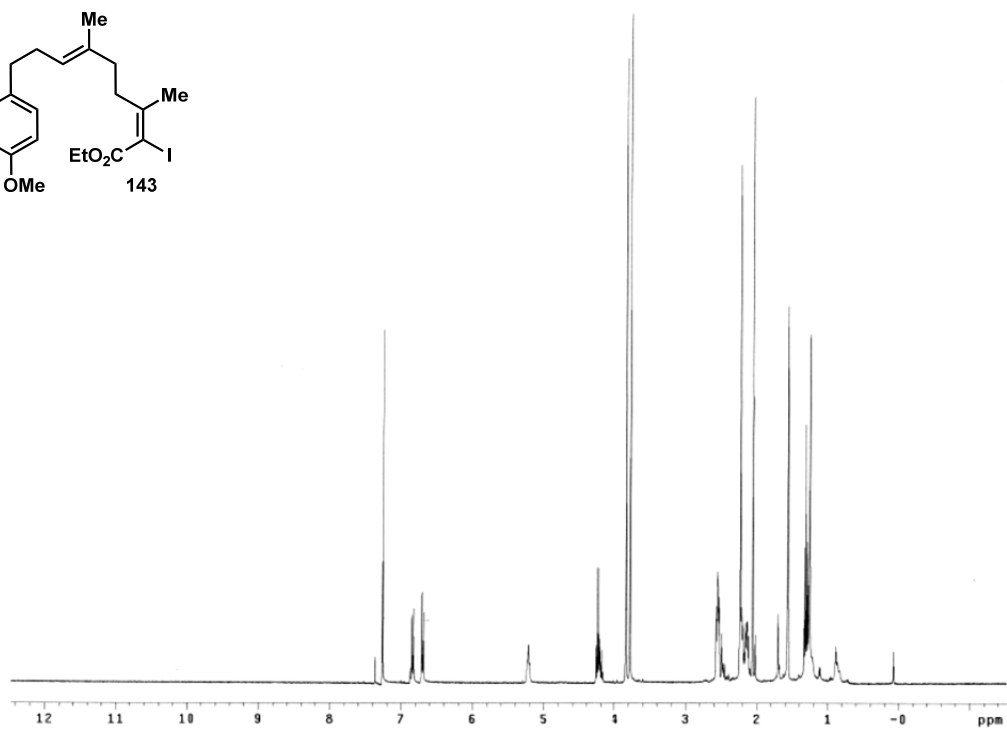
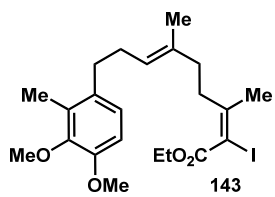


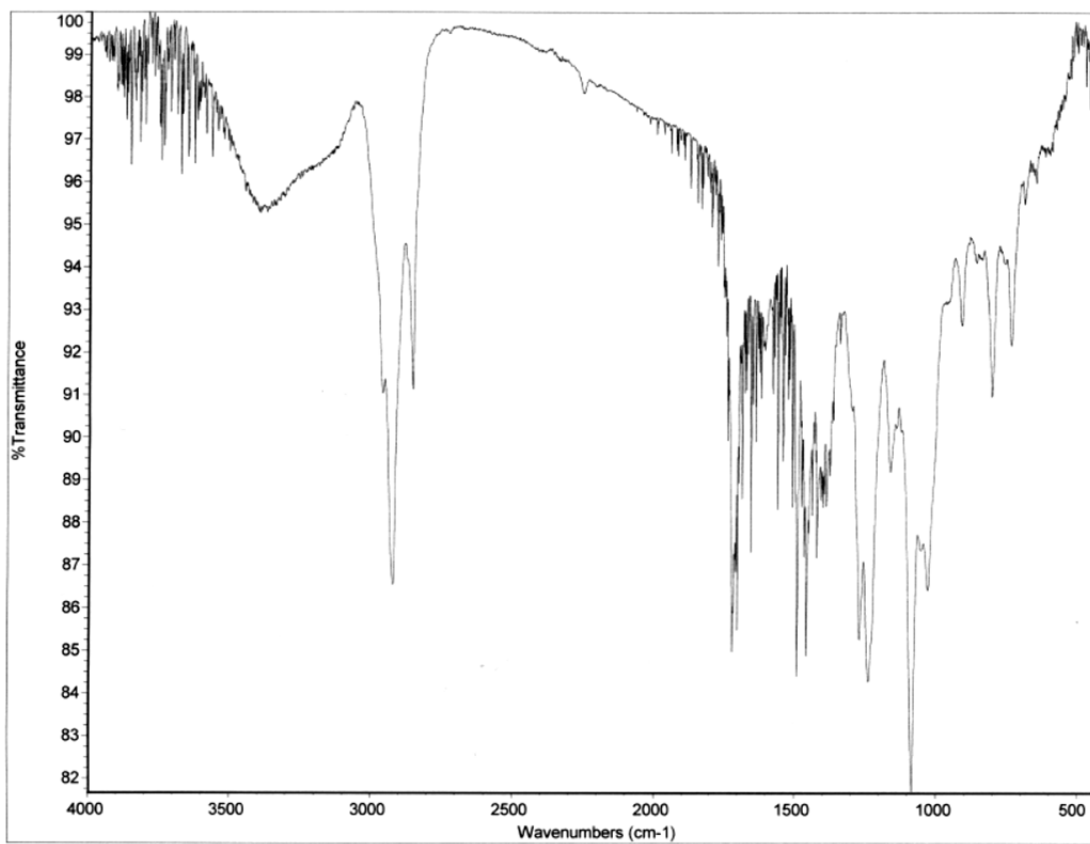


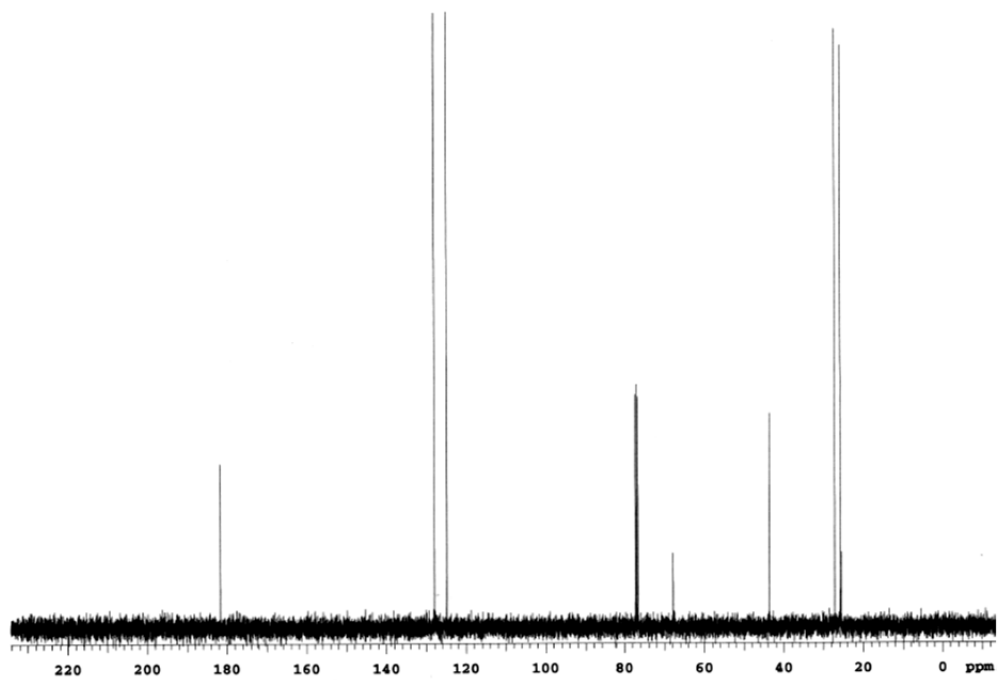
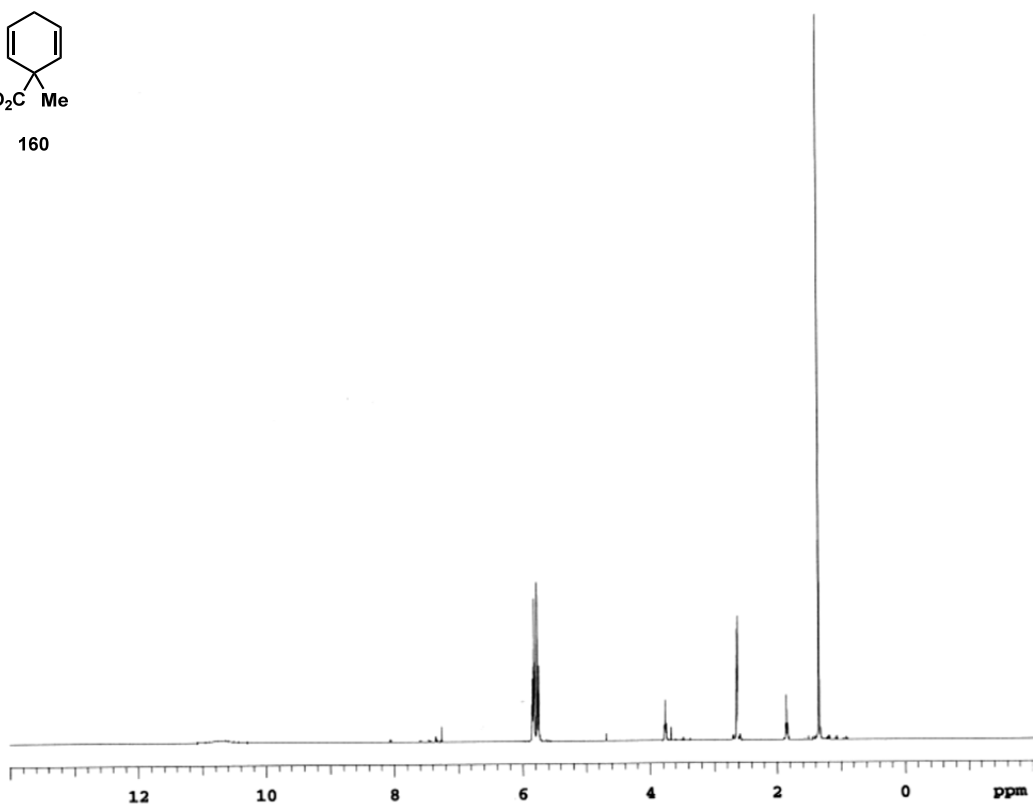
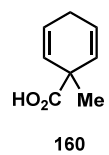


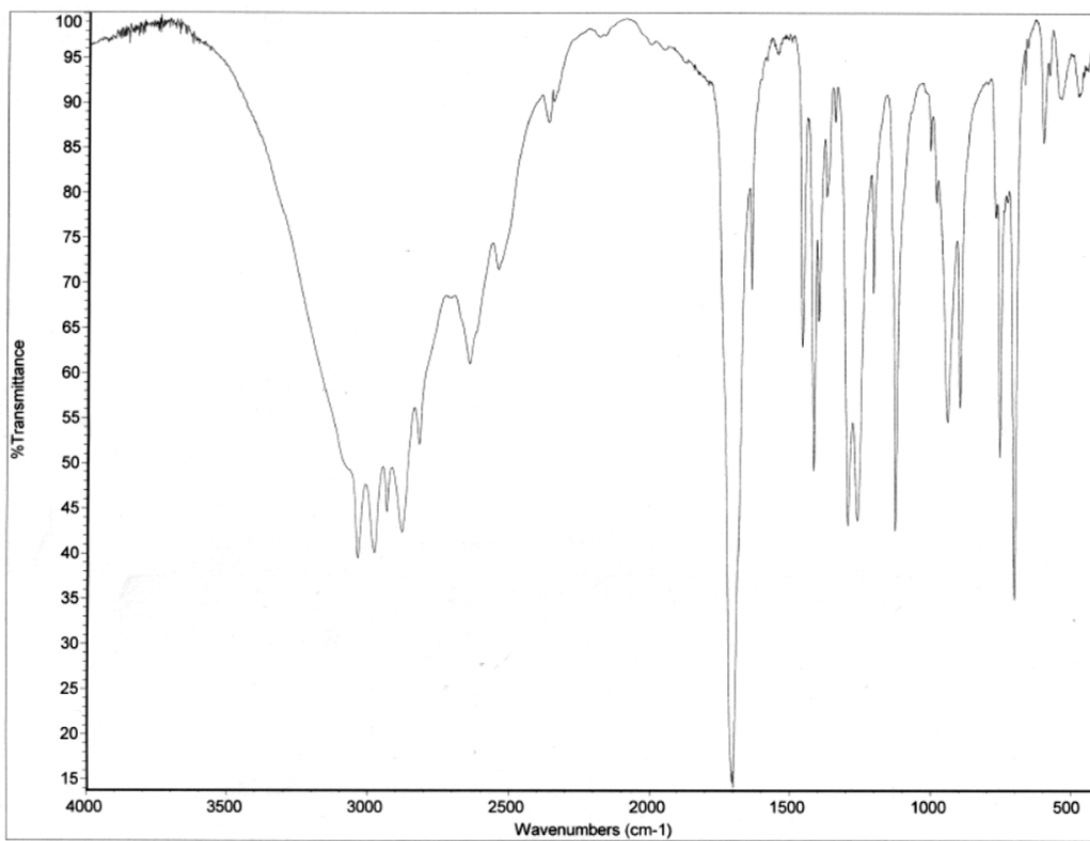


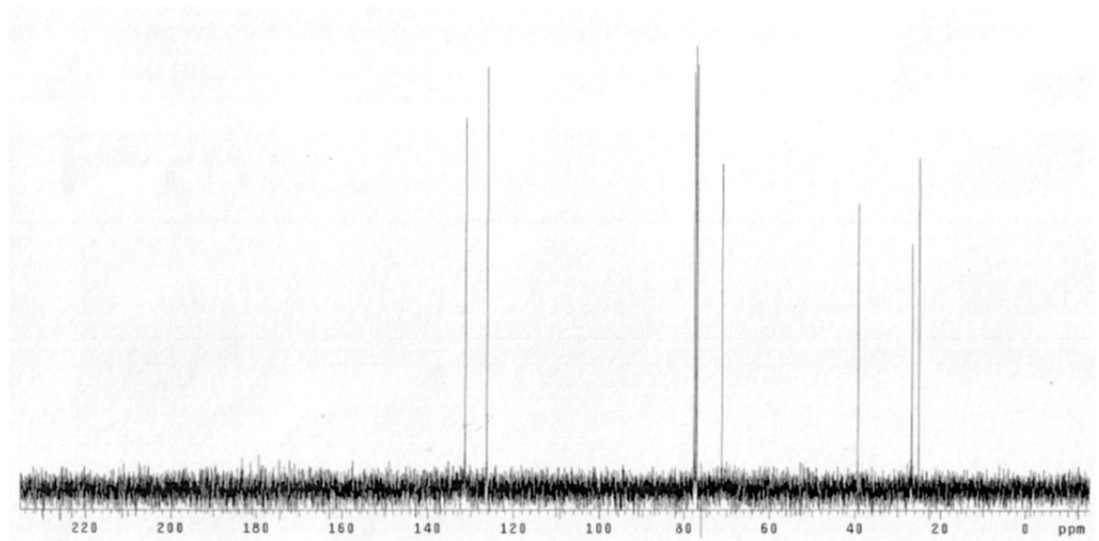
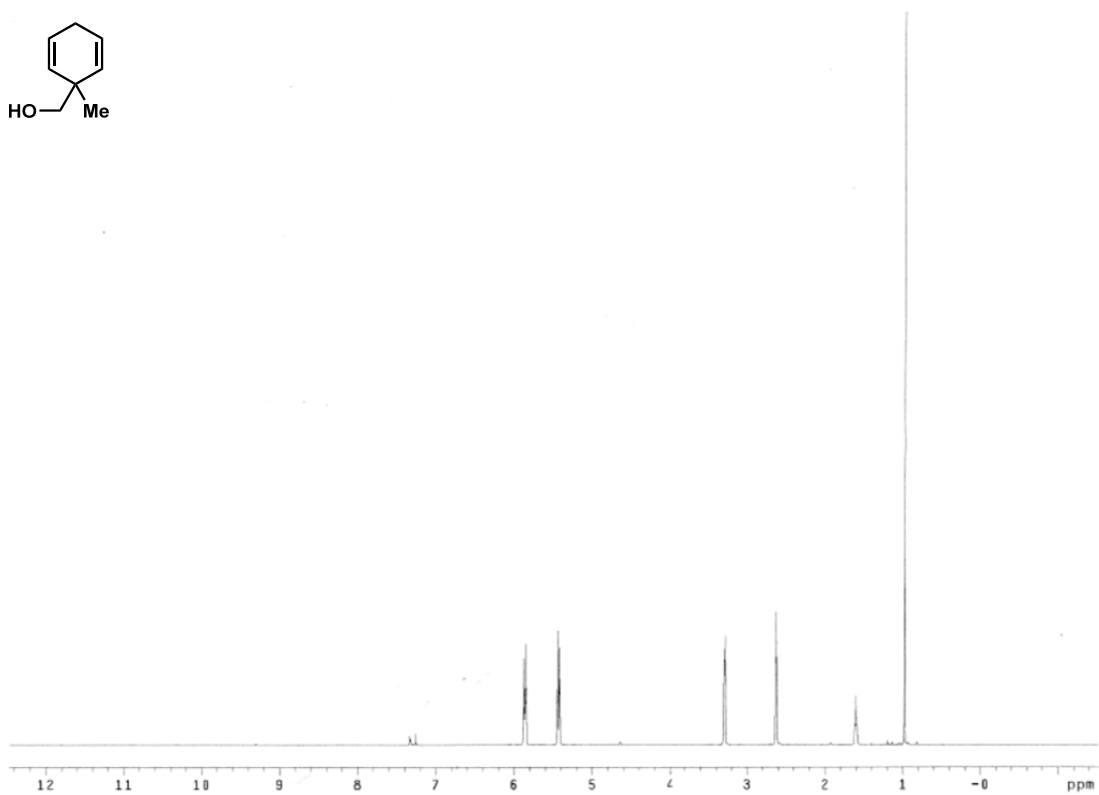
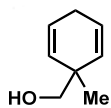


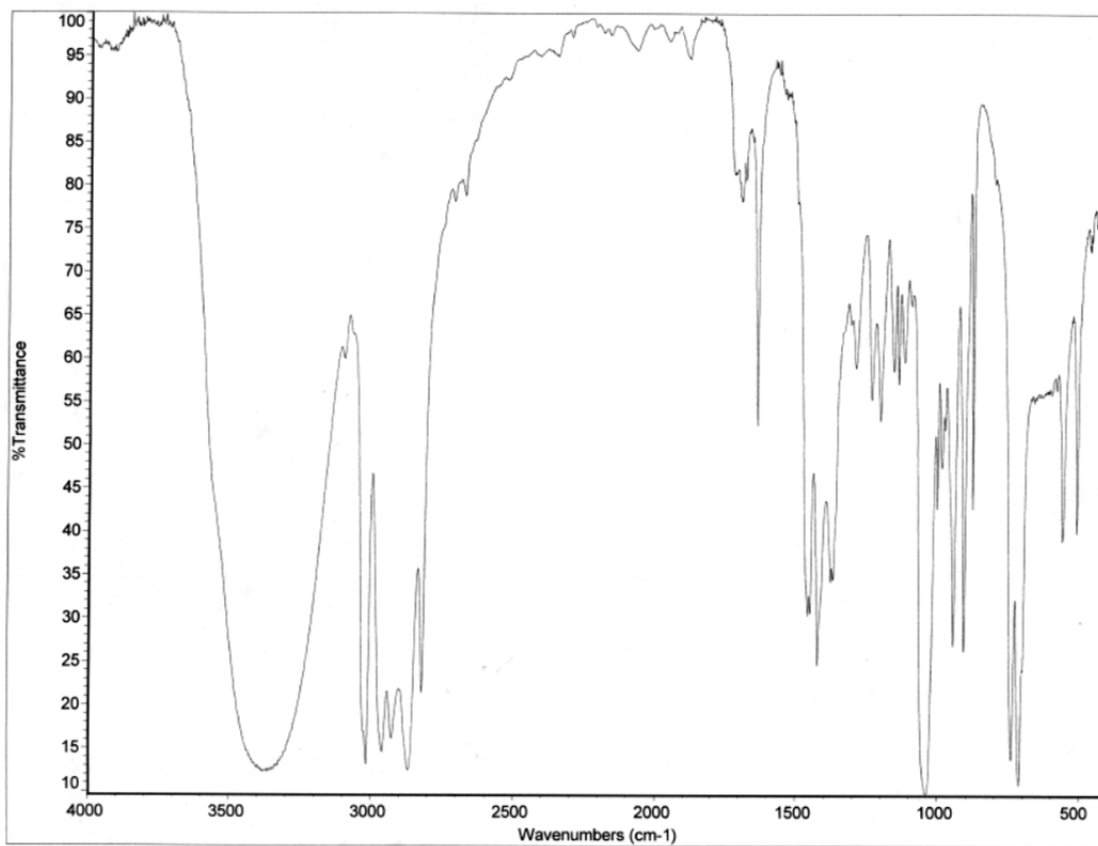


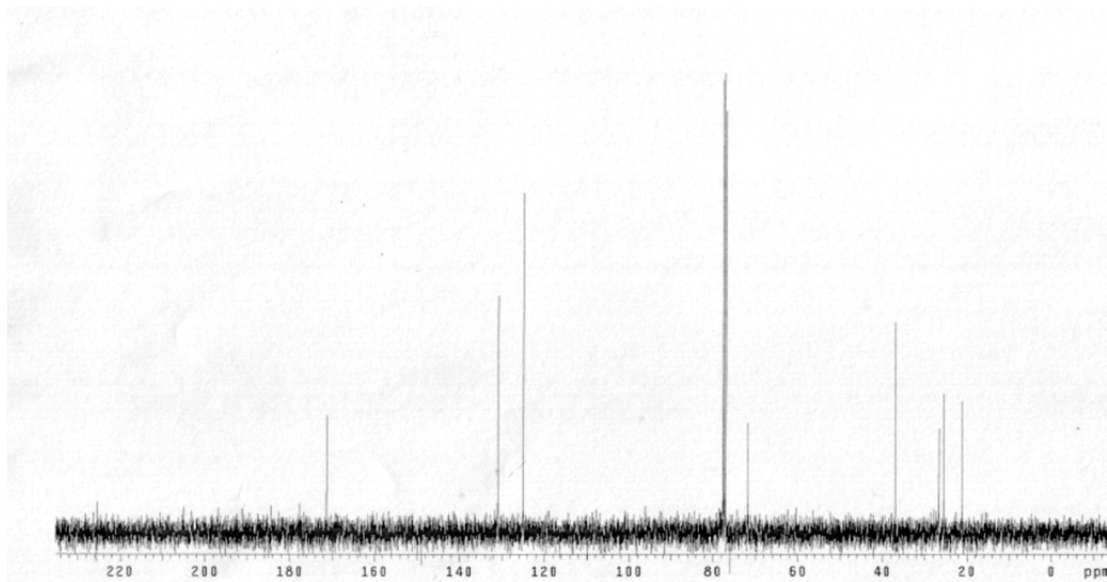
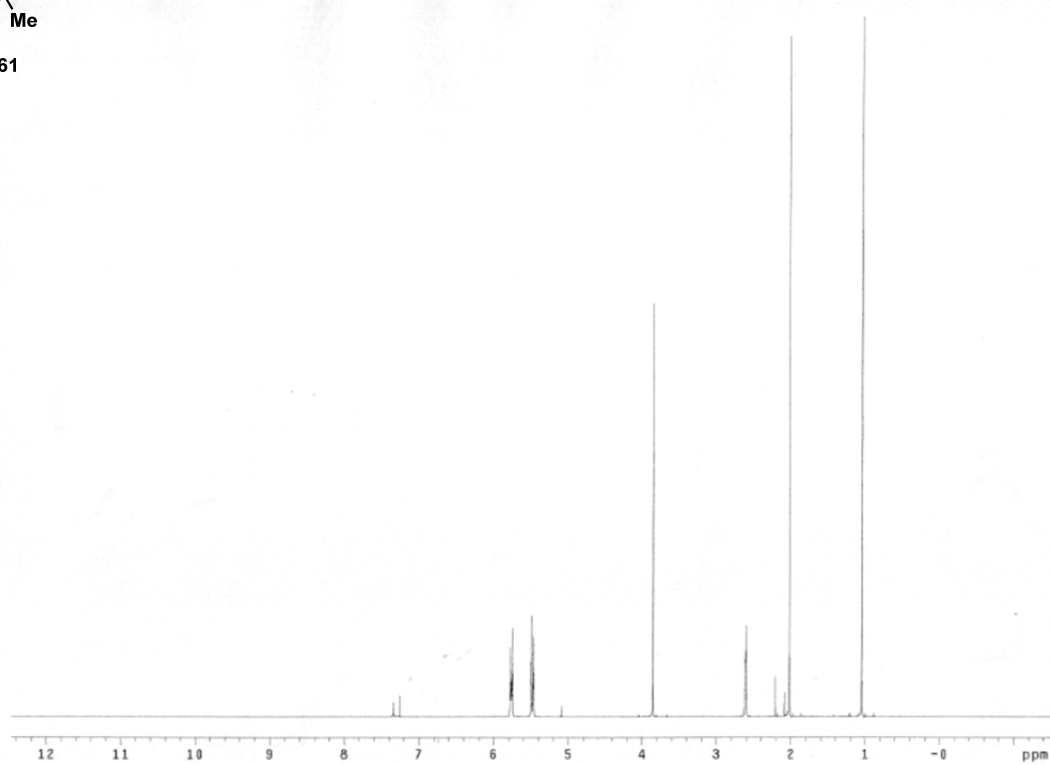
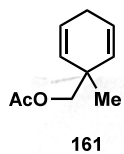


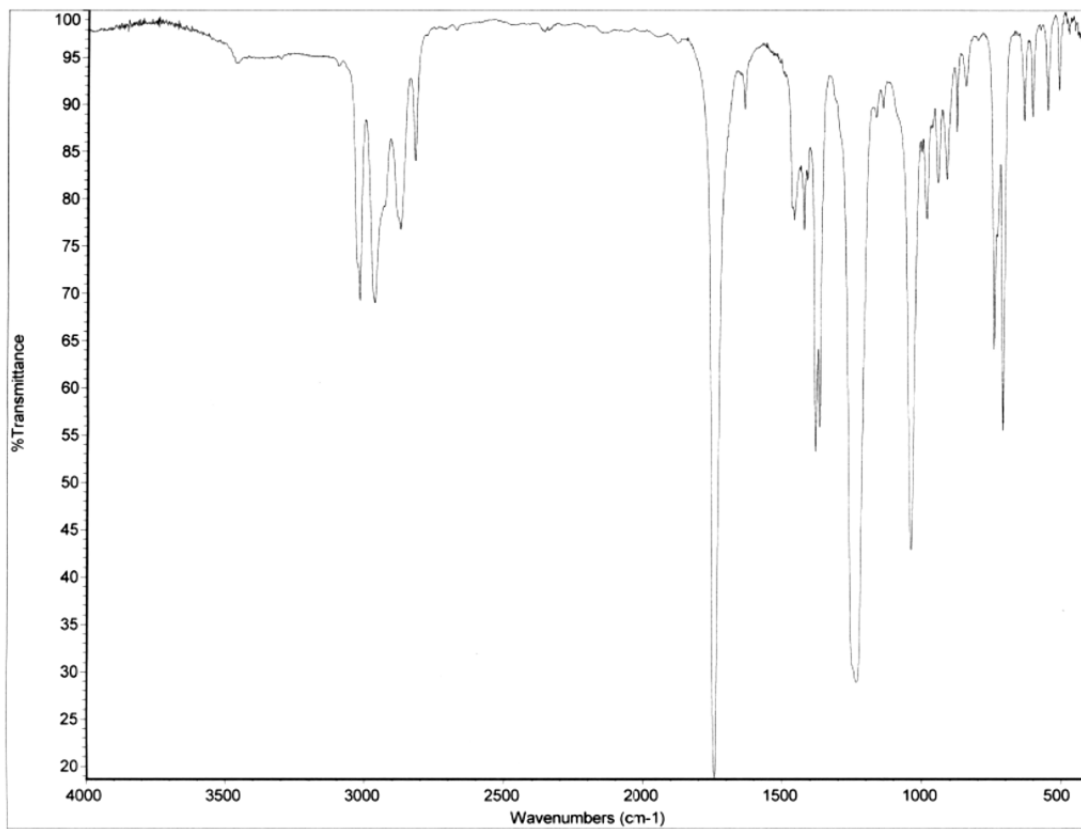


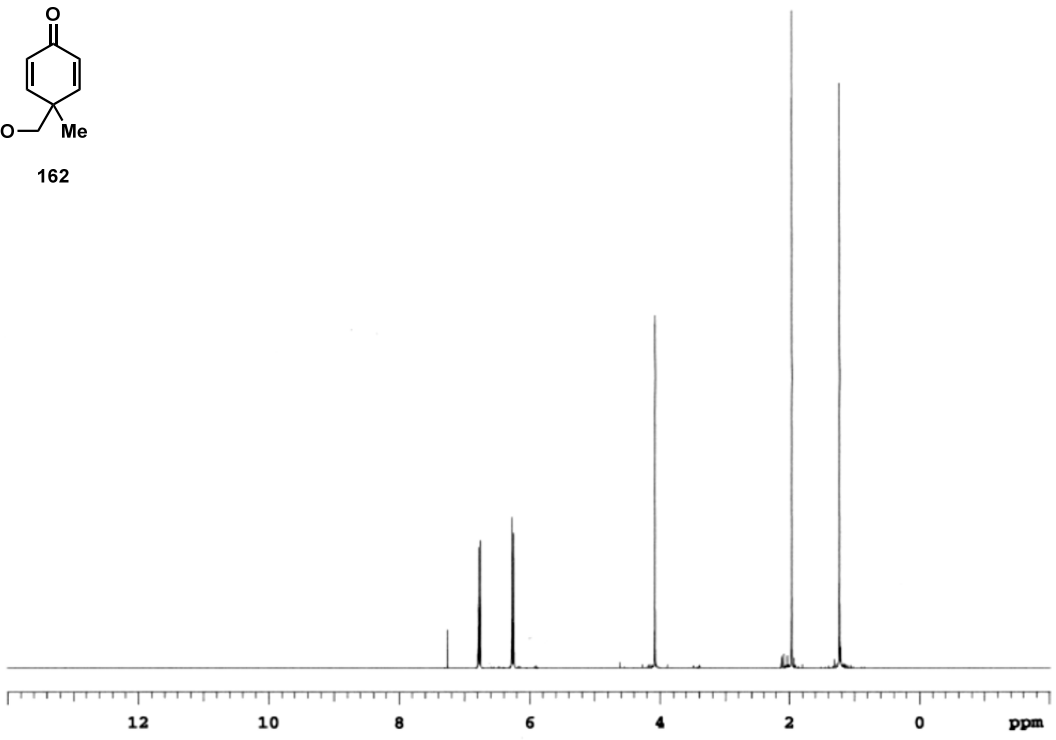
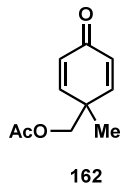




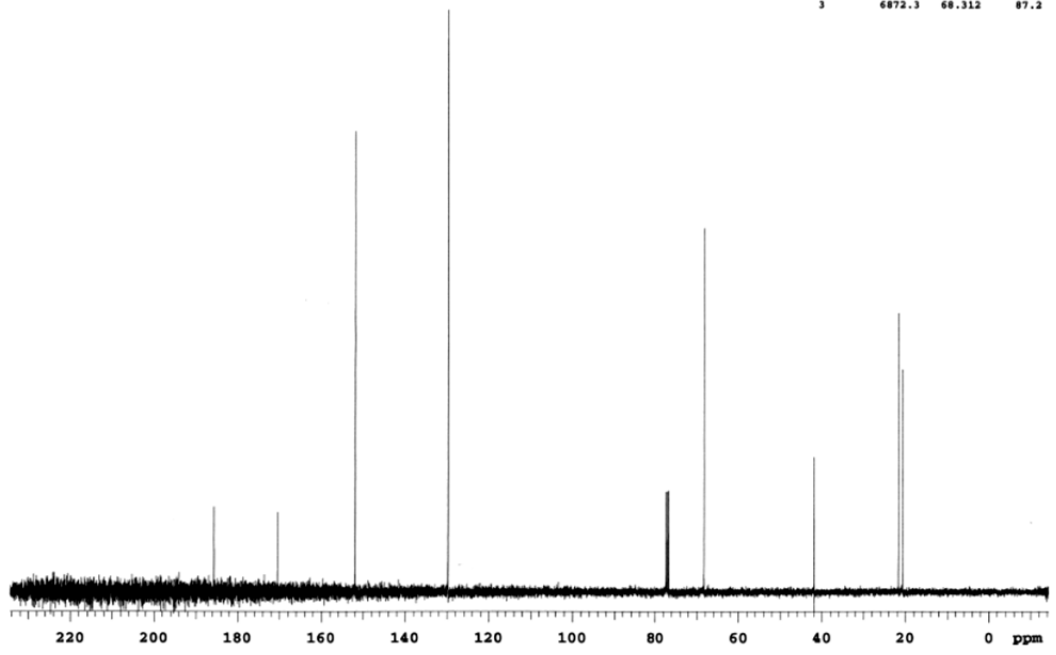


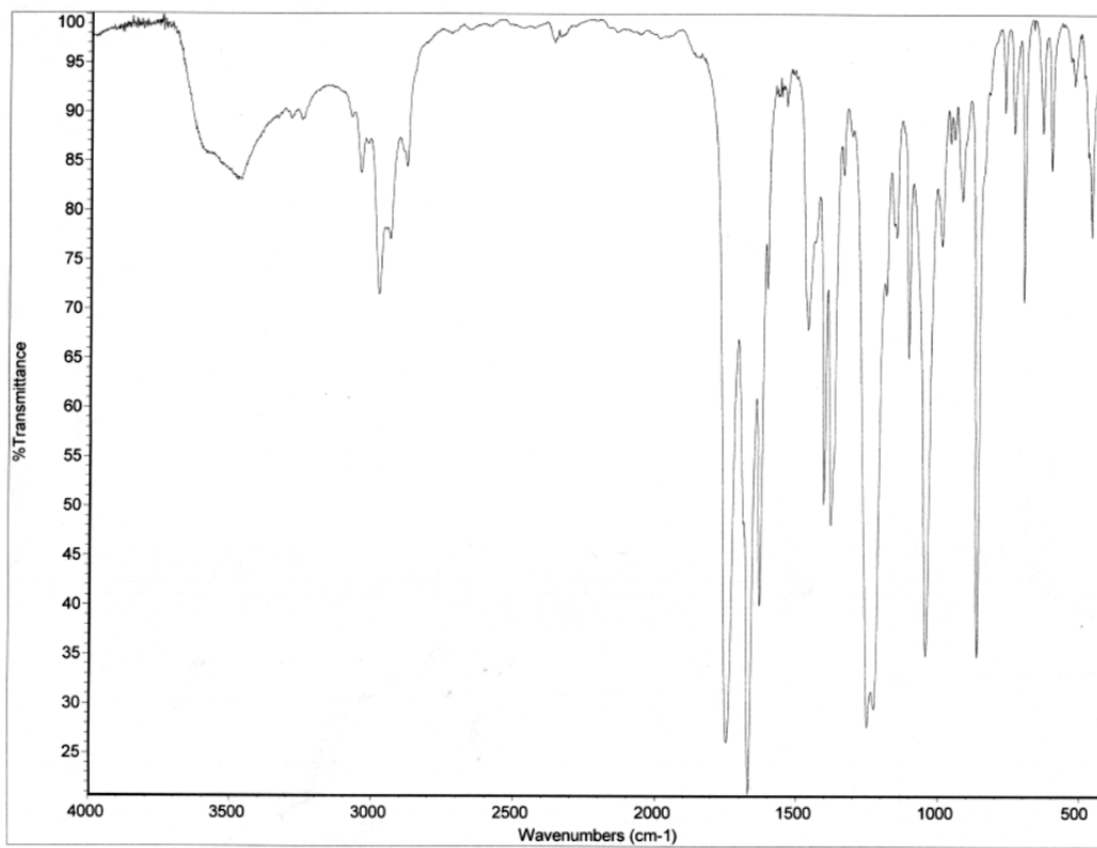


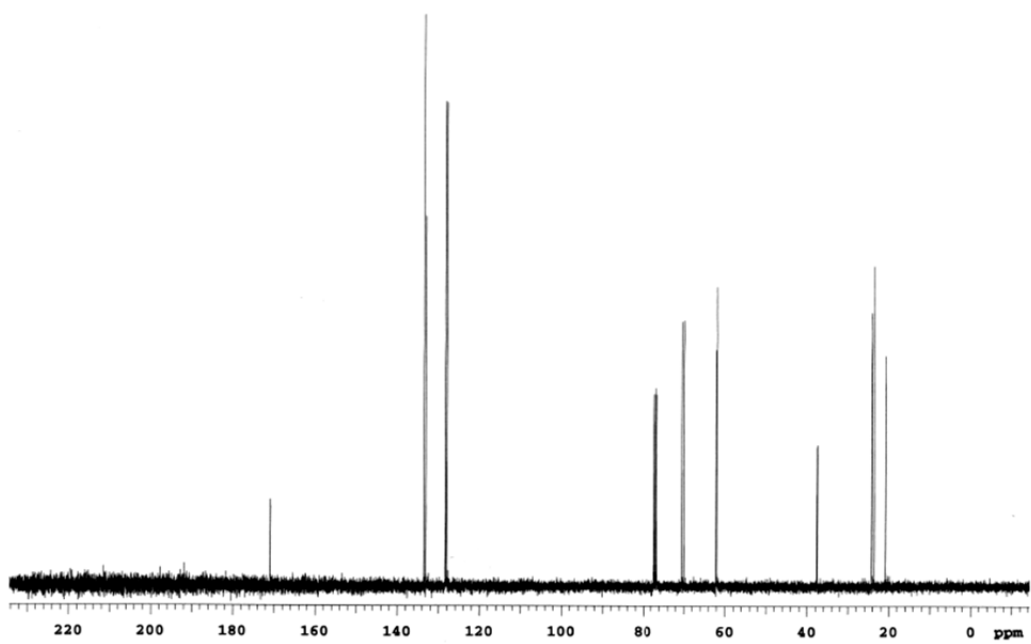
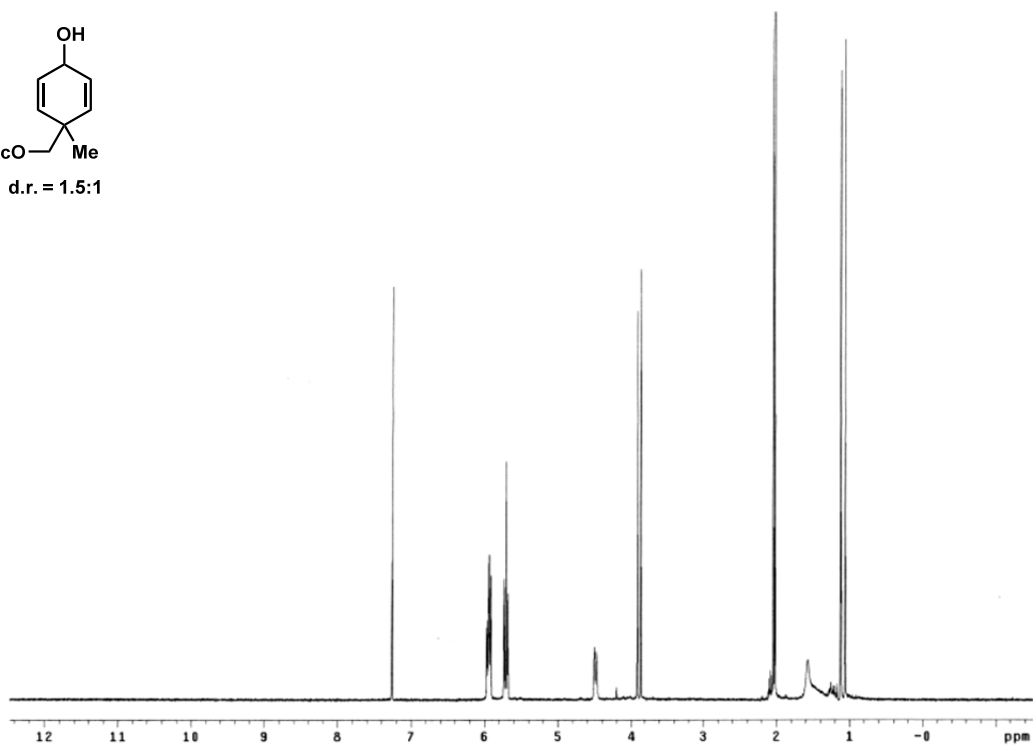
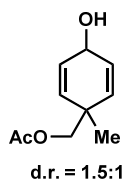


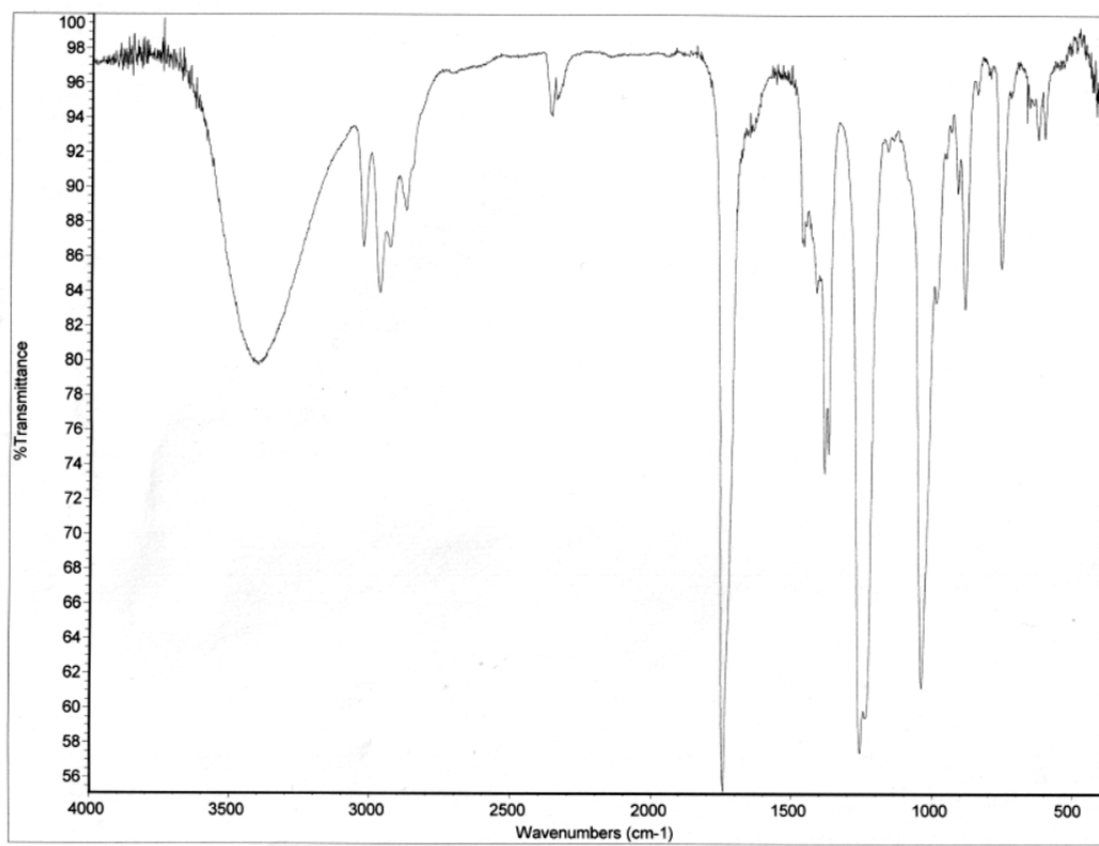


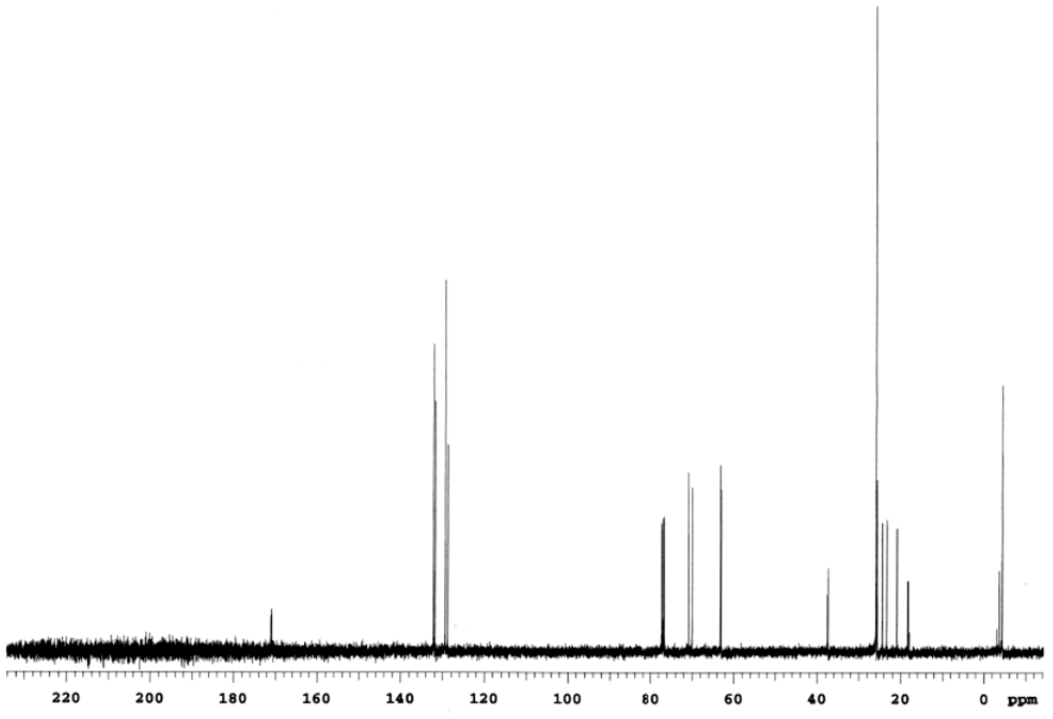
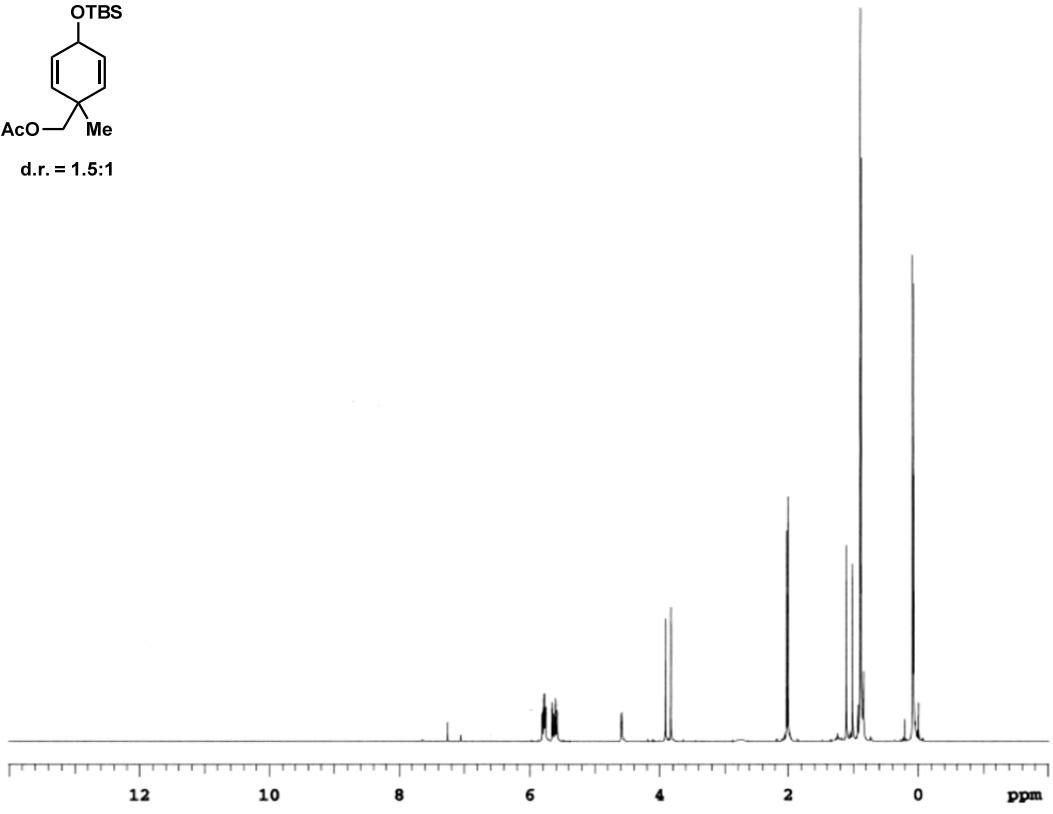
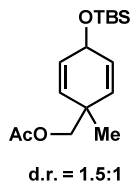
INDEX	FREQUENCY	PPM	HEIGHT
1	15285.3	151.938	110.3
2	13058.3	129.801	139.5
3	6872.3	68.312	87.2

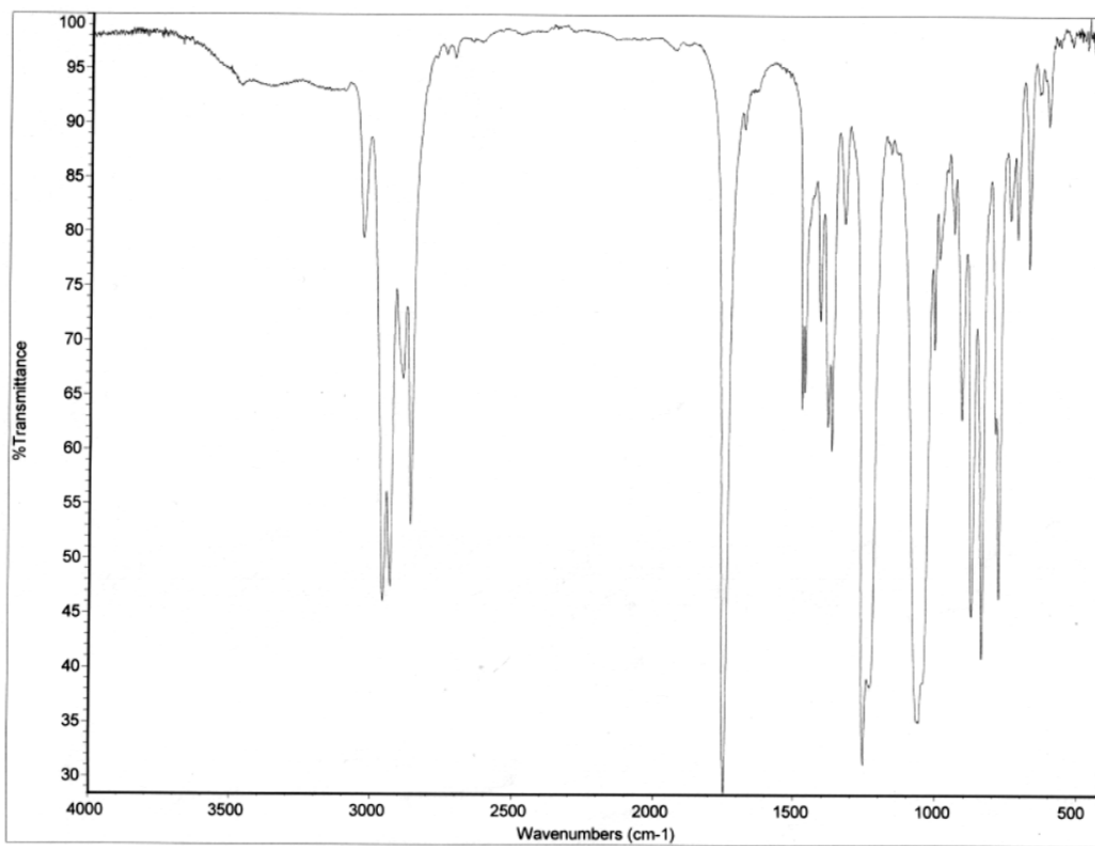


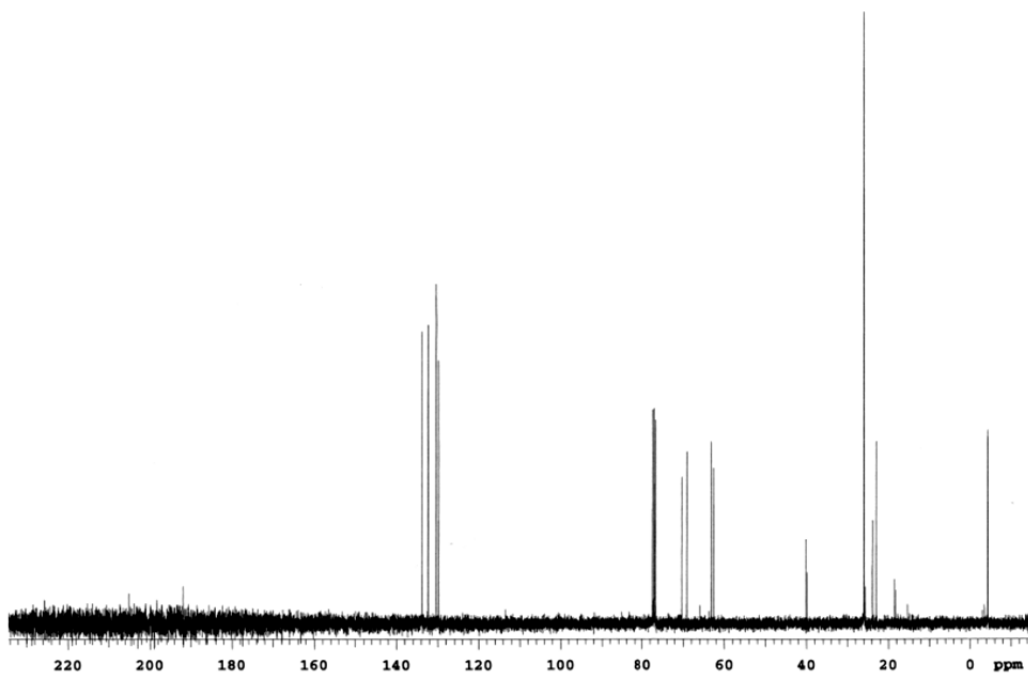
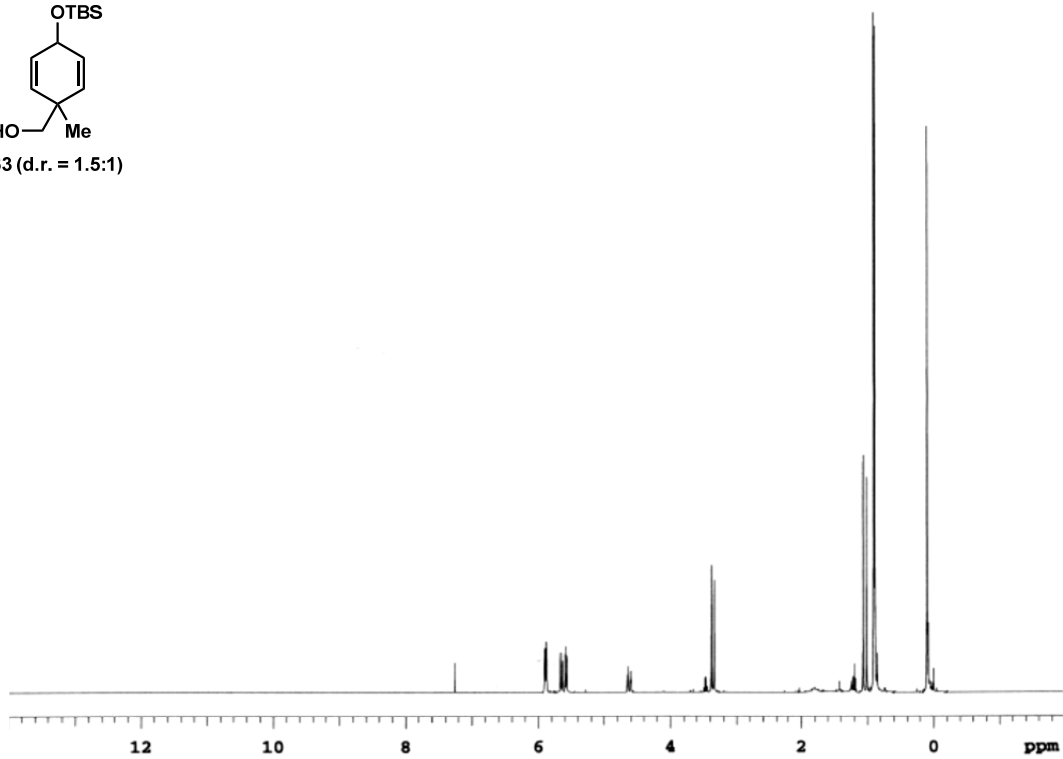
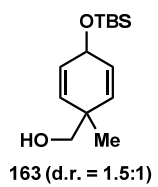


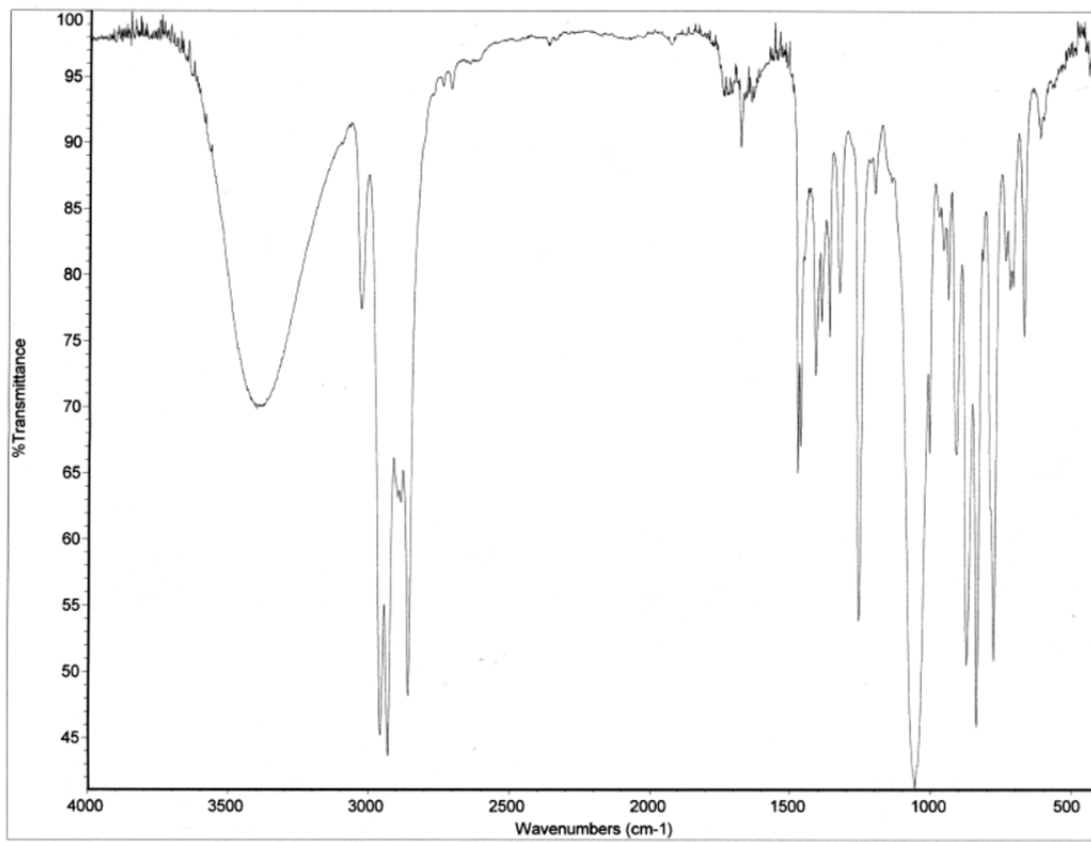


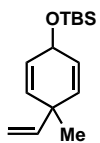




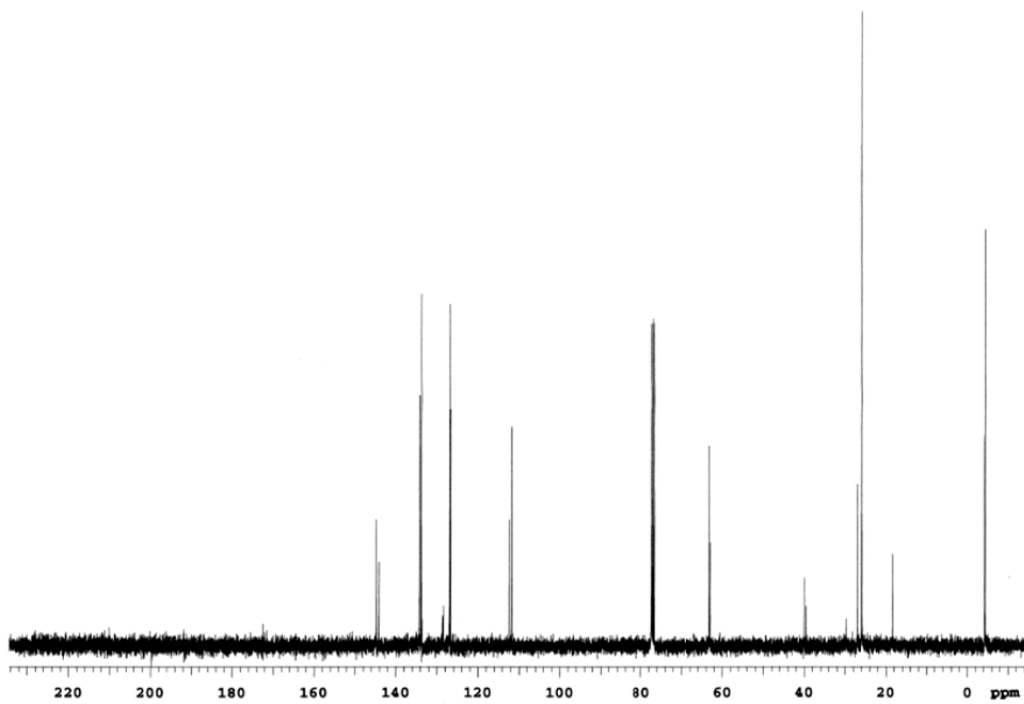
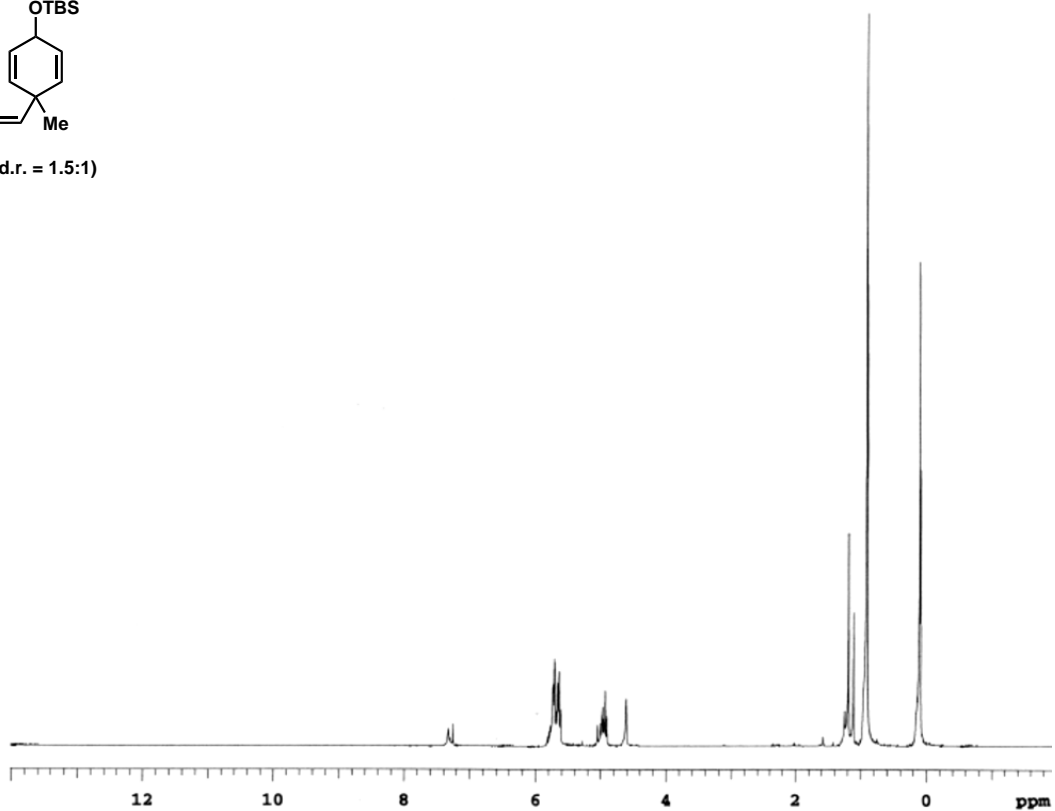


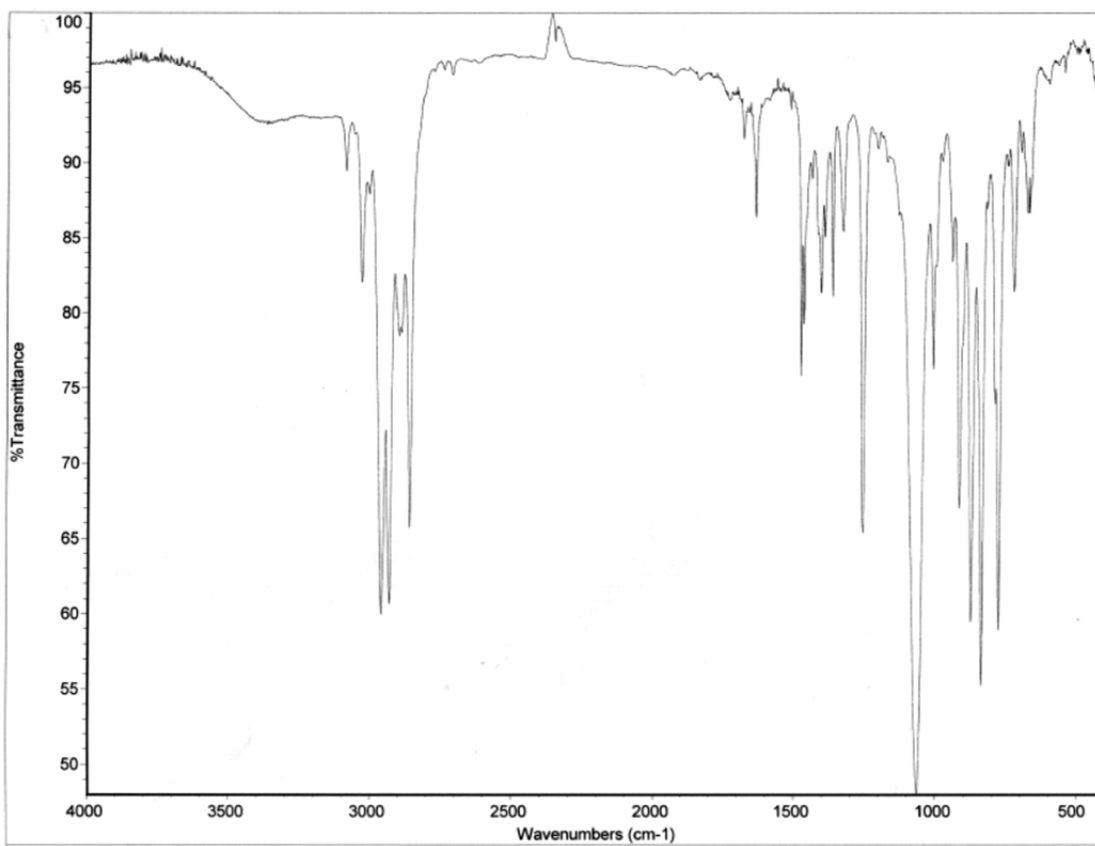






165 (d.r. = 1.5:1)





Chapter 3 – Aryl Hydroxylation Mediated by

4,5-Dichlorophthaloyl Peroxide

Phenols are fundamentally important molecules which possess broad utility and perform a suite of applications in the pharmaceutical, agricultural, and commodity chemical industries.¹³² Phenols are pharmacologically ubiquitous in drugs which serve a wide range of biological purposes.¹³³ During metabolism various aromatic compounds are also oxidized to phenols to increase their excretion from the body. The FDA mandates that metabolites generated in higher than 10% must be examined to elucidate their potential toxicity or side effects.¹³⁴ An effective synthetic protocol capable of accessing phenolic derivatives and potential metabolites of native pharmaceutical agents in an efficient, economical fashion would be an essential chemical and biological tool. Despite their vast importance, a procedure for the general, straightforward conversion of arenes to phenols does not exist. A protocol emulating cytochrome P450 which directly oxidizes aryl C-H bonds to C-OH bonds in a mild, selective manner is most ideal, but this rather rudimentary transformation poses many synthetic challenges.^{135,136} The major problem in developing hydroxylation reactions is that the phenolic products are more reactive than the starting materials which leads to over-oxidation. A protocol that is also tolerant to a multitude of functional groups also remains elusive.¹³⁷

Early hydroxylation reactions employed peroxides, but had limited success in generating mono-hydroxylated products, and when successful they had a limited scope.¹³⁸⁻¹⁴⁵ Methods to circumvent this problem using super acids to both activate the peroxides and subsequently deactivate the arenes were investigated.¹⁴⁶⁻¹⁴⁹ These

approaches lack generality because many functional groups cannot tolerate these exceptionally strong acids. Transition metal catalyzed oxidations of aromatics have improved upon the early acid-mediated processes which utilize peroxides, but these strategies are not ideal since they require precious metals and usually invoke directing groups to promote reactivity.¹⁵⁰⁻¹⁶¹ The use of directing groups inherently minimizes the substrate scope and the types of substituted phenols that can be accessed. The directing groups that are employed often need to be installed as well as removed creating an overall inefficient process with regard to step economy. Strategies that oxidize aryl silanes and aryl boronic acids or esters are also utilized to deliver phenols.¹⁶²⁻¹⁶⁶ Although potentially high yielding, these strategies require multiple steps starting from halogenated arenes and predominantly use transition metal catalysis to install the silane or boronate. Late-stage halogenations and the subsequent oxidation of the silanes or boronates on highly functionalized molecules can pose significant problems often rendering these strategies inferior to the widely used Friedel-Crafts/Baeyer-Villiger sequences for the installation of oxygen into arenes. Although effective, this multi-step process utilizes reagents that may not be suitable to latent functionality in the later stages of a synthetic strategy.¹⁶⁷⁻¹⁶⁹

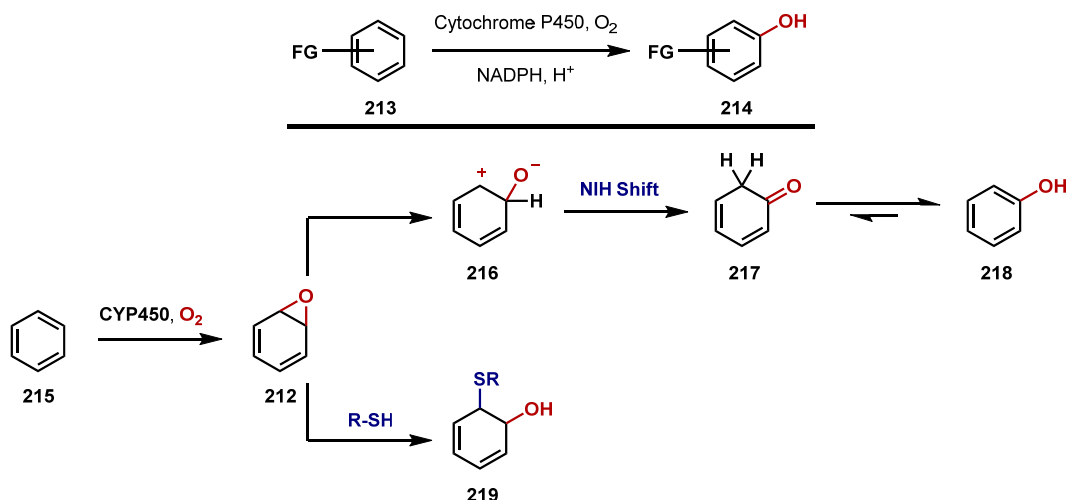
Phthaloyl peroxide (**211**), a reagent studied in detail by Greene in the 1950's, was recently shown to mono-hydroxylate arenes with a high degree of functional group tolerance.^{170,171} A major limitation to this protocol, however, is that electronically rich arenes are needed. Interestingly, computational analysis dictates that the reaction proceeds through a novel diradical reverse-rebound mechanism, not the expected electrophilic aromatic substitution (EAS) pathway. This is perplexing and several mechanistic questions remain since there is no experimental evidence to substantiate

these findings. Mechanistic evaluation and probing of different peroxide reagents could enhance this protocol thereby expanding the generality of the substrate scope to provide a more applicable strategy with higher utility.

Synthetic Protocols to Access Phenols

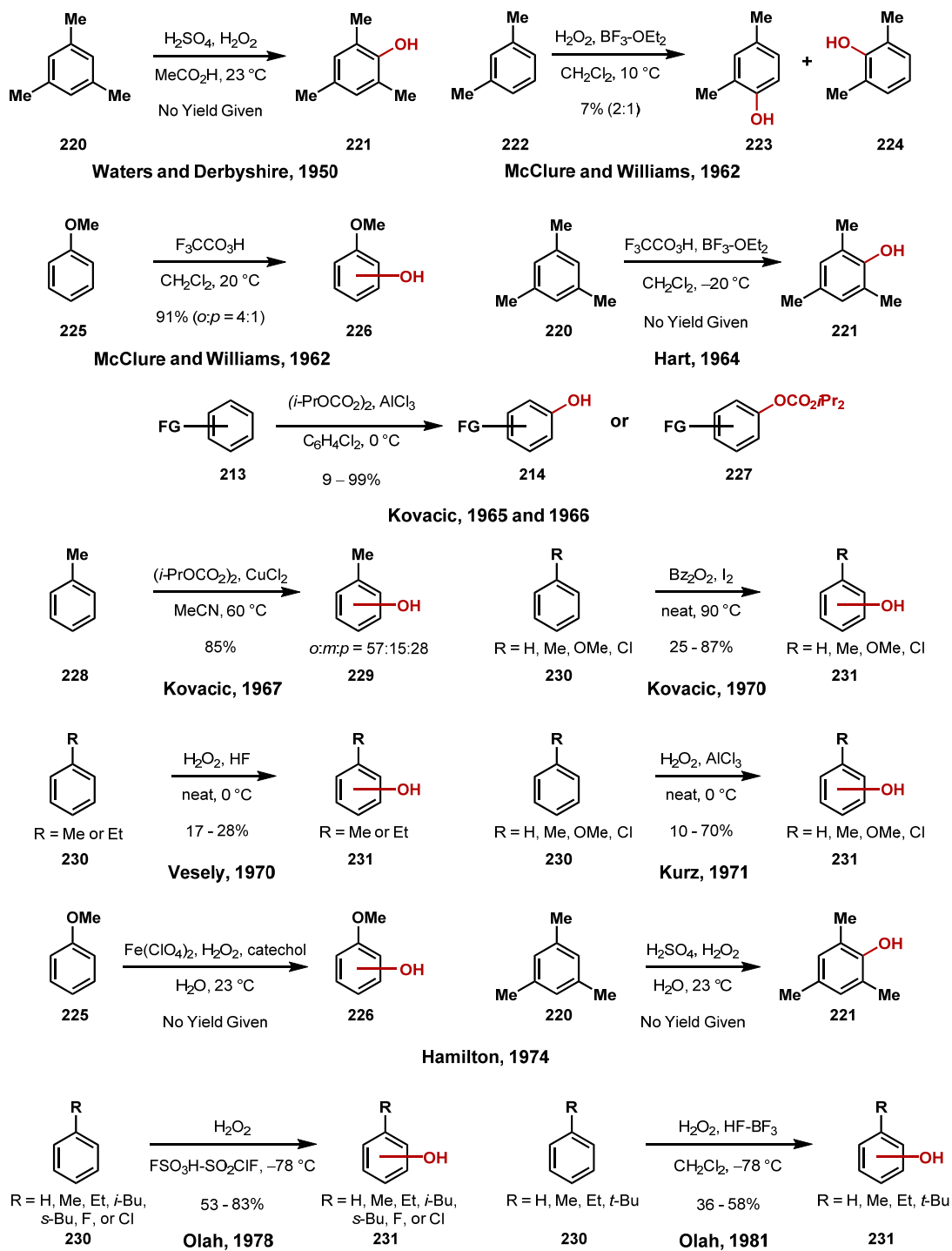
The monooxygenase super family of proteins that encompasses the cytochrome P450 catalyzes the oxidation of small molecules. These enzymes play an integral role in the biosynthesis of important compounds such as steroids and lipids, but they also metabolize drugs and foreign organic molecules to facilitate their excretion and clearance from the body.^{135,136} They are responsible for the oxidation of arenes like benzene and various poly-aromatic hydrocarbons (PAHs) through the direct conversion of the arene to an epoxide which undergoes an NIH shift to afford the phenolic metabolites (Scheme 3.1). The oxirane intermediate **212** can undergo another pathway involving covalent modification via nucleophilic addition of cysteine residues ultimately leading to the carcinogenic properties of these aromatics. Despite the deleterious toxicity, the overall transformation is fascinating from a synthetic perspective. An iron-oxygen complex containing an iron (V) core effects this overall transformation inside the active site of the enzyme which directly oxidizes the arene.

Scheme 3.1. CYP450 mediated hydroxylation of arenes.^{135,136}



Emulating this transformation chemically has proven to be quite difficult. Fenton's reagent affects this transformation but acts as an indiscriminate oxidant. It has limited utility because the arene is used in excess and the oxidant is the limiting reagent. Since the phenolic products are more reactive to further oxidation. Over-oxidation coupled with functional group liability severely limits this protocol. Its indiscriminate oxidation potential, however, has warranted its use in water purification to remove PAHs as well as other toxic organic molecules like tri- and tetrachloroethylene.¹³⁸ The use of strong acids, Lewis or Brønsted, in combination with peroxides has also affected this transformation, but again functional group liability severely limits these processes (Scheme 3.2).¹³⁹⁻¹⁴⁹ Additionally, these protocols typically use simple arenes in excess or as the solvent, further limiting the widespread synthetic utility of these approaches. Despite the major limitations these early developments laid significant groundwork in arene hydroxylation reactions.

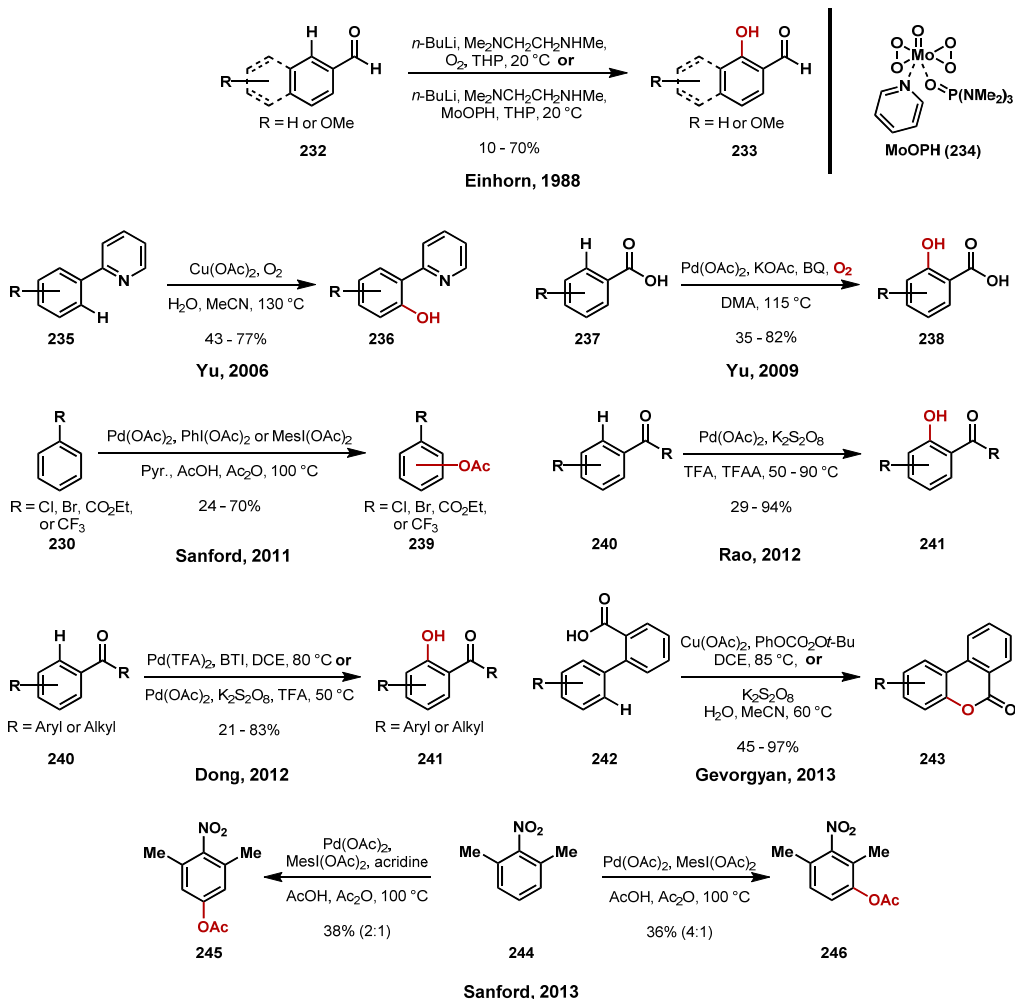
Scheme 3.2. Early peroxide mediated hydroxylation of arenes.¹³⁸⁻¹⁴⁹



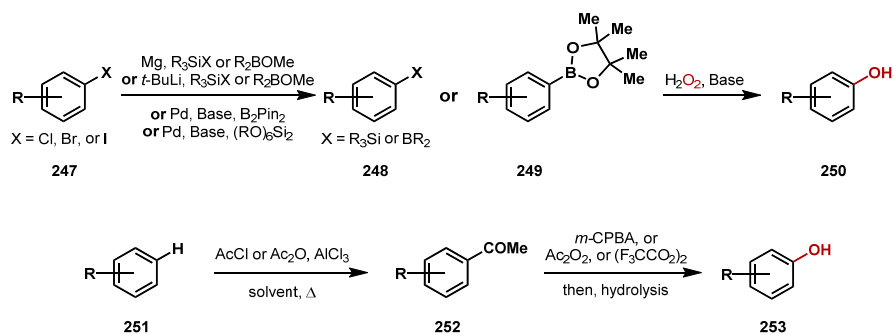
Remarkable achievements in the syntheses of phenols have recently been made using transition metal catalysis by researchers such as Crabtree, Sanford, Yu, Ritter, Gevorgyan, Dong, and Rao (Scheme 3.3).¹⁵⁰⁻¹⁶¹ These protocols can be effective, but tend to lack broad application due to the use of directing groups or contrived systems. The oxidation of aryl silanes or boronates is commonly implemented to provide phenols. Aryl silanes and boronic acids or esters, which essentially are masked phenols, are derived from the aryl halides through a cross-coupling approach such as the Miyaura boration or through anion mediated nucleophilic addition reactions.¹⁶⁷ Fleming-Tamao and boronate oxidation ultimately unmask the phenols.¹⁶²⁻¹⁶⁶ These strategies can be highly effective early in a synthetic strategy, but unselective aryl halogenation and peroxide mediated oxidations can be deleterious to common functional groups in the later stages of a synthetic strategy. This causes undesirable protecting group steps or alternative approaches. The universal protocol to synthesize a phenol is the Friedel-Crafts/Baeyer Villiger sequence.^{168,169} Although effective, this strategy usually requires protecting group manipulations and compatible functional groups which often limit its generality.

Scheme 3.3. Transition metal catalyzed and Friedel-Crafts/Baeyer Villiger syntheses of phenols.

Recently Developed Transition Metal Catalyzed Arene Hydroxylation Protocols:



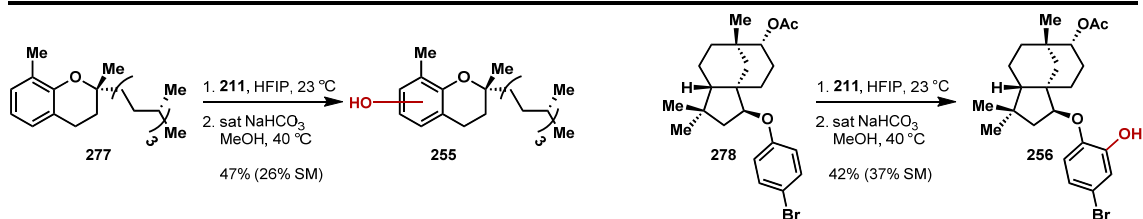
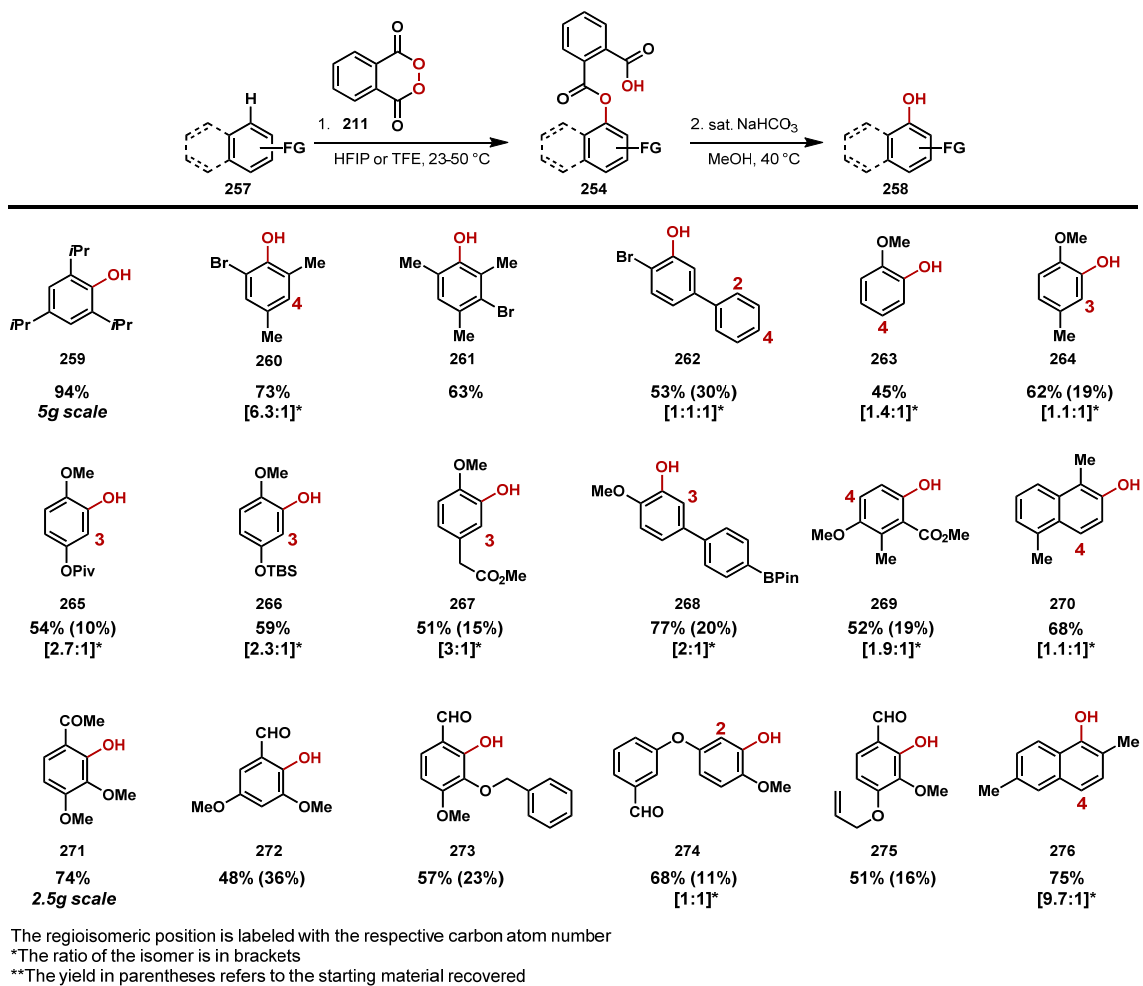
Fleming-Tamao/Boronate and Friedel-Crafts/Baeyer-Villiger Arene Oxidations:



Phthaloyl Peroxide Mediated Hydroxylation

Phthaloyl peroxide (**211**), originally studied in detail by Greene in the 1950's, has recently been exploited by our laboratory to oxidize arenes to phenols, converting C-H bonds to C-OH bonds (Table 3.1).^{170,171} The reaction is predictable, occurring in a similar fashion to the Friedel-Crafts reaction to afford the phenol in a two step sequence with minimal over-oxidation. The reaction is controlled by the formation of mixed phthaloyl ester-acid **254** which is reluctant to another oxidation by a second equivalent of phthaloyl peroxide. The mixed phthalate is then hydrolyzed using aqueous sodium bicarbonate in warm, deoxygenated methanol in the second step to provide the phenol. Remarkably, the peroxide and the overall protocol possess excellent functional group tolerance. Aldehydes, ketones, esters, alkenes, boronic esters, nitriles, allenes, alkynes, cyclopropanes, and cyclobutanes are all tolerated under these conditions. This protocol is also applicable to the late-stage oxidation of complex molecules and natural products including phenolic derivatives of tocopherol **255** as well as the advanced clovanemagnolol intermediate **256**. The major limitations to this protocol are that the reaction only works on electronically moderate to rich arenes and the *ortho/para* selectivity is low.

Table 3.1. Scope of arenes hydroxylated by phthaloyl peroxide.¹⁷¹

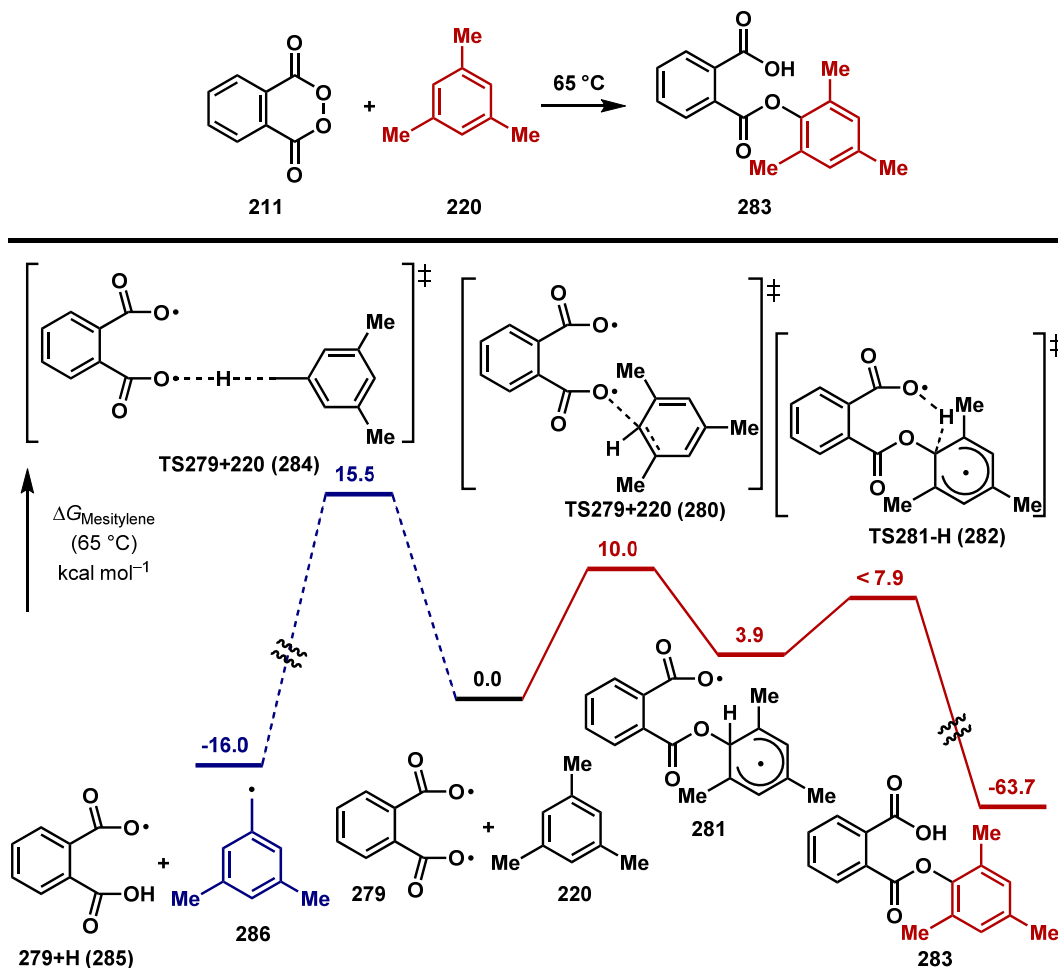


It was initially hypothesized that the reaction proceeded through an ionic pathway. This was substantiated by the selective oxidation of the arene over the alkyl substituents possessing benzylic hydrogens. In fact, no benzylic oxidation was observed

throughout the hydroxylation reaction in the cases of substrates **259-261**, **264**, **270**, **276**, or **277**. However, an ionic pathway contradicts the fact that no over-oxidation products were observed. The mixed phthaloyl ester-acid intermediate **254** would be more prone to oxidation than the starting arene through an EAS mechanism.¹⁷² These contradicting results prompted computational analysis to determine the most plausible mechanistic pathway. There are potentially four major reaction pathways: ionic, direct hydrogen abstraction, single electron transfer (SET), or a diradical reverse-rebound addition. Density functional theory (DFT) and *ab initio* calculations dictate that the lowest energetic reaction pathway is the diradical reverse-rebound. The energy required for this mechanism is 30.5 kcal/mol, which is approximately 5.2 kcal/mol lower than the ionic pathway.¹⁷¹

The reaction's selectivity for oxidizing the arene over the benzylic C-H bonds is rather surprising if a diradical process is actually occurring. Further DFT analysis using mesitylene (**220**) illustrated that benzylic oxidation via hydrogen abstraction is approximately 5.5 kcal/mol higher than aryl C-H oxidation (~10 kcal/mol), accounting for the arene selectivity (Scheme 3.4). The cyclohexadienyl diradical **281** then undergoes rearomatization via hydrogen abstraction which is expedited by the adjacent benzoyloxy radical to afford the mixed phthaloyl ester acid **283** as the sole product.

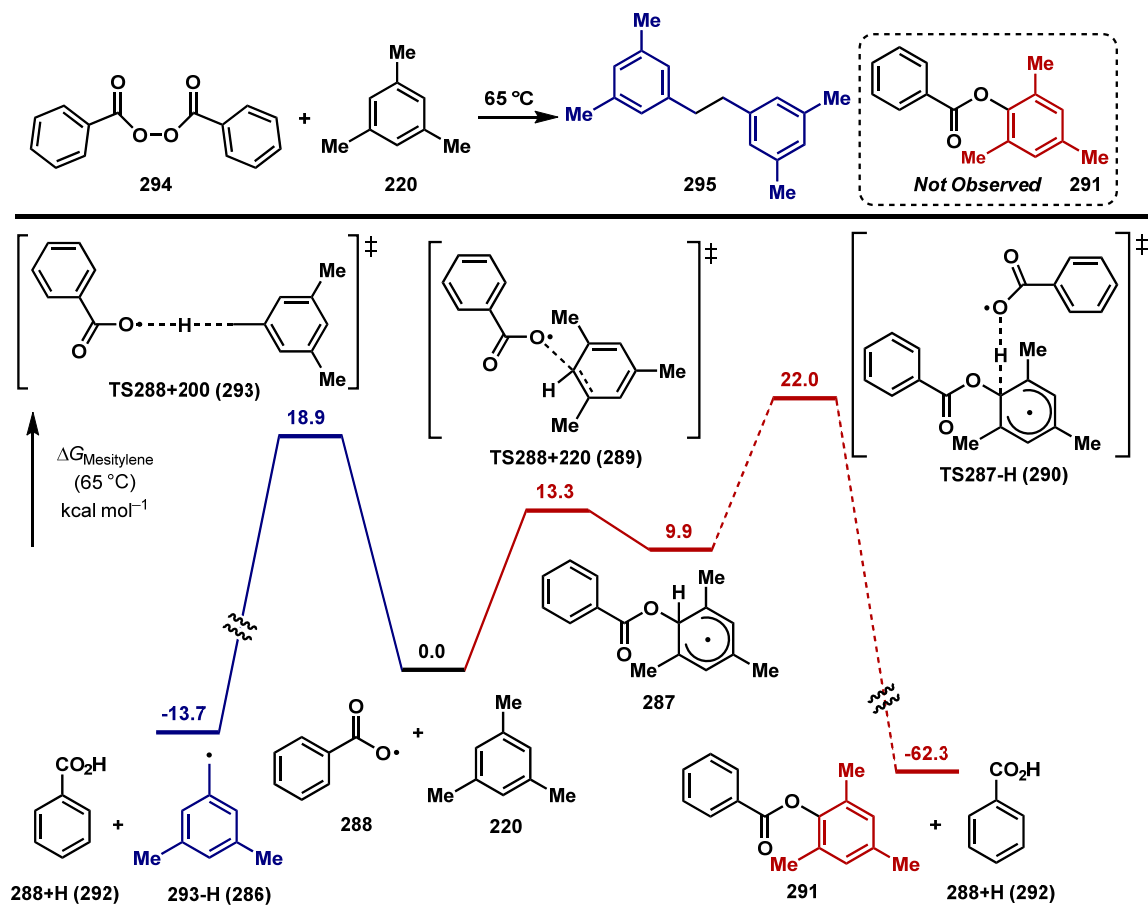
Scheme 3.4. CPCM-(U)B3LYP/6-31+G(d) computed free energy surfaces for aryl and benzylic functionalization of mesitylene using phthaloyl peroxide.



Phthaloyl peroxide is a special reagent in this process because peroxides such as benzoyl peroxide promote benzylic oxidation, not aryl oxidation (Scheme 3.5). Experimental observations confirm this result as no arene oxidation is observed when benzoyl peroxide is reacted with mesitylene. DFT and *ab initio* calculations on this process indicate that the aryl oxidation pathway for a mono-radical peroxide is lower in energy compared to the hydrogen abstraction pathway which forms the mesityl benzyl

radical (13.3 kcal/mol versus 18.9 kcal/mol).¹⁷¹ However, the energy associated with the rearomatization (25.8 kcal/mol) creates a barrier that is much higher compared to benzylic oxidation. Abstraction of the hydrogen from the cyclohexadienyl radical **287** requires a second benzoyloxy radical (**288**). This is entropically disfavored and causes the high energy penalty. Traversing this entropy barrier is nearly impossible under the reaction conditions so the only experimentally observed product is benzylic oxidation. Benzoyl peroxide is therefore a great oxidant in radical halogenations such as the Wohl-Ziegler reaction.¹⁷³ This entropic penalty does not exist when phthaloyl peroxide is used because the hydrogen abstraction is intramolecular.

Scheme 3.5. CPCM-(U)B3LYP/6-31+G(d) computed free energy surfaces for aryl and benzylic functionalization of mesitylene using benzoyl peroxide.



Development of an Arene Hydroxylation Protocol using

4,5-Dichlorophthaloyl Peroxide

Phthaloyl peroxide is a special oxidant which our laboratory has exploited to perform dihydroxylations of styrenes and, most notably, to oxidize arenes to phenols directly from the aryl C-H bond.^{171,174} The latter is of specific interest because it provides access to phenols in a functional group tolerant fashion amenable to late-stage hydroxylation reactions. This protocol can rapidly deliver small molecules that are potential metabolites as well as oxidized analogs of drugs and pharmaceutical agents. The restricted scope of the reaction warrants further development of peroxides with the capability to access new arenes. There is also minimal experimental evidence to substantiate the DFT and *ab initio* calculations that dictate the most energetically favorable mechanistic pathway is a diradical reverse-rebound addition. A stronger peroxide reagent could also help provide this experimental evidence that remains elusive.

In the pursuit of new phthaloyl peroxide reagents, computational analysis and prior research regarding the dihydroxylation of styrenes illustrated that symmetrically halogenated phthaloyl peroxides possessed the highest potential for effecting the arene hydroxylation.¹⁷⁴ In 2011, our laboratory had shown that 4,5-dichlorophthaloyl peroxide (**296**) dihydroxylated styrenes as well as non-styrenyl alkenes, a reaction not observed using other types of phthaloyl peroxides. Computational analysis using DFT and *ab initio* calculations conducted in collaboration with Yong Liang and Ken Houk dictated that this reagent could potentially be a more powerful oxidant than phthaloyl peroxide in the arene hydroxylation as well (Figure 3.1). Through comparing their reactivities with three separate arenes: mesitylene, benzene, and 1,3,5-trichlorobenzene, the calculations

delineated that the electron-rich arene is more reactive than the electron-deficient arene. This is predicated on the HOMO-SOMO interaction in the transition state illustrated by frontier molecular orbital (FMO) analysis. The energetic barrier for the transition state is lowered by enhancing the favorability of this interaction in elevating the HOMO energy of the arene. The barriers for the reactions are lowered by ~1-2 kcal/mol using 4,5-dichlorophthaloyl peroxide. The chlorides decrease the SOMO energy by approximately 0.2 eV as indicated by FMO analysis. This decrease in energy results in an increasingly favorable HOMO-SOMO interaction in the transition state. Overall, this suggests that 4,5-dichlorophthaloyl peroxide could react with benzene, an arene previously inaccessible in our hydroxylation reaction using phthaloyl peroxide.

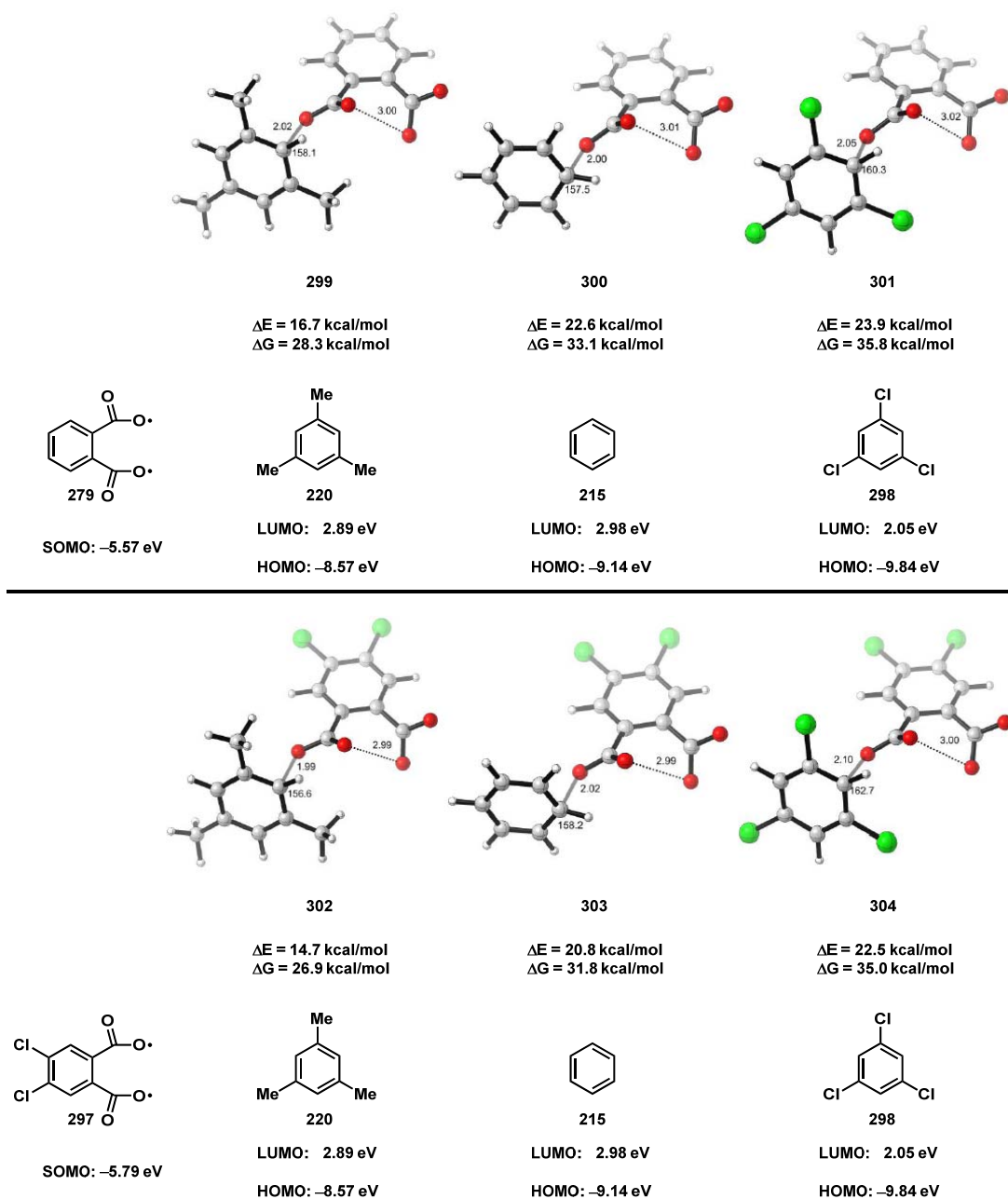


Figure 3.1. Arene reactivity difference between 4,5-dichloro- and phthaloyl peroxide via diradical addition.

Further computational investigation deciphered that 3,6-dichlorophthaloyl peroxide (**305**) would be a viable candidate for arene oxidation as well. Based on calculations conducted by Liang, the energetic barrier is only 16.7 kcal/mol for the oxidation of 1,3,5-trichlorobenzene using this reagent whereas the oxidation is 22.5 kcal/mol using 4,5-dichlorophthaloyl peroxide (Figure 3.2).

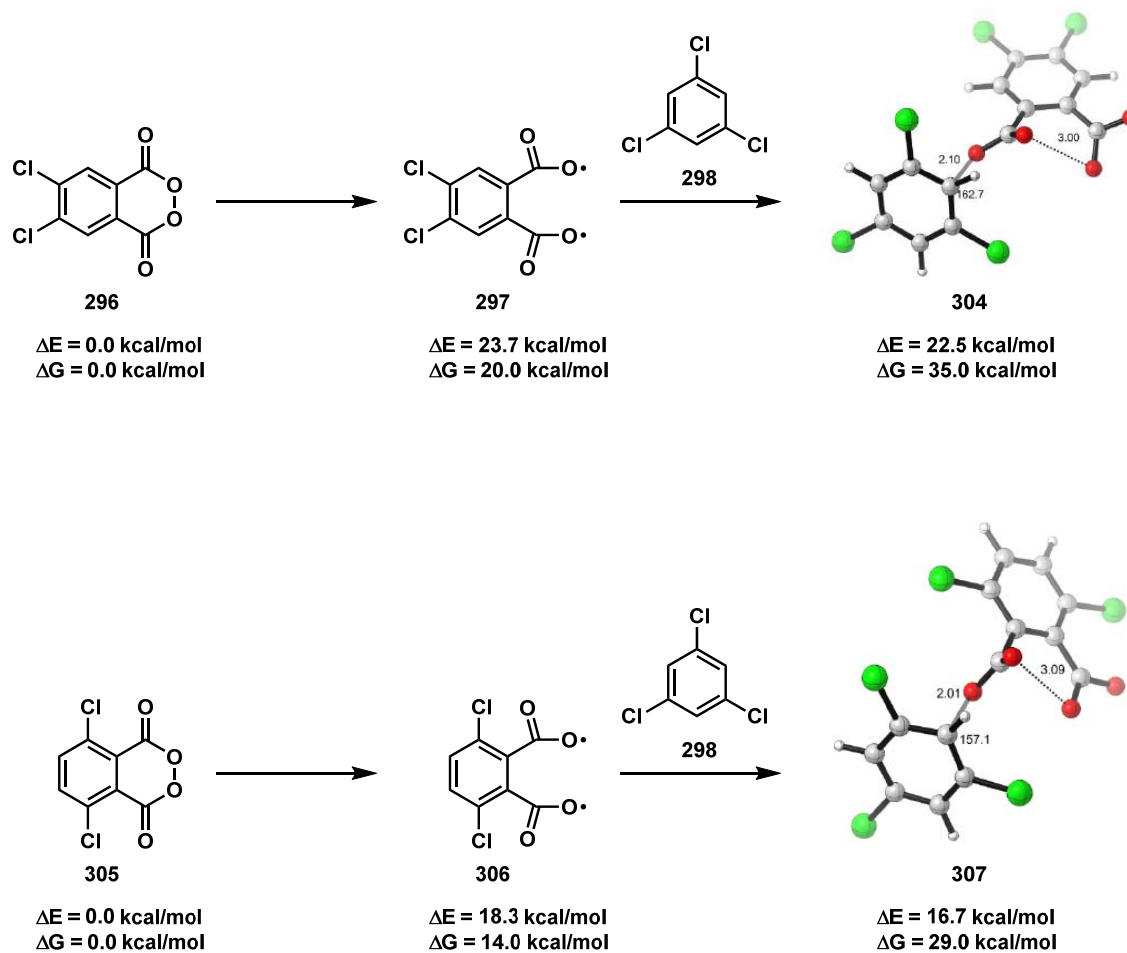


Figure 3.2. 4,5- and 3,6-dichlorophthaloyl peroxide oxidation of 1,3,5-trichlorobenzene.

The computational results combined with the previously observed reactivity mitigated by the dihydroxylation of alkenes provided plausibility for the synthesis of

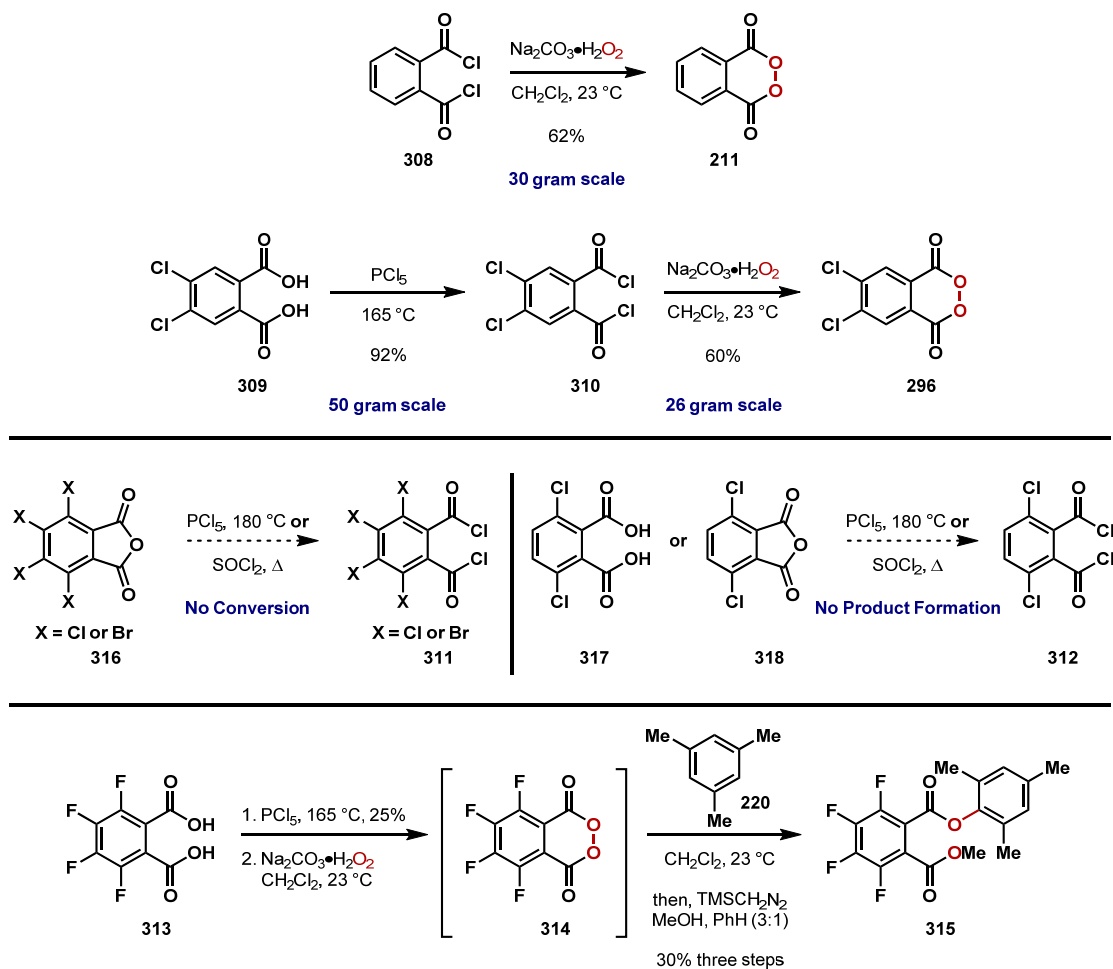
various halogenated peroxides. Phthaloyl peroxide is synthesized in one step from the cheap, commercially available phthaloyl chloride (**308**) using solid sodium percarbonate in wet methylene chloride (Scheme 3.6). This can be achieved on 30 gram scale to deliver the peroxide in 62% yield as a white, fluffy solid. This protocol has proven safe in repeatedly providing mass quantities of the peroxide without the occurrence of an explosion. 4,5-Dichlorophthaloyl peroxide was synthesized in a similar manner, but starting from the cheap, commercially available 4,5-dichlorophthalic acid (**309**). The diacid is first converted to the dichloride **310** by heating the solid acid to 165 °C in neat phosphorus pentachloride. After a three stage distillation the dichloride is afforded in 92% yield on 50 gram scale as a white, lacrimating solid. The dichloride was treated with solid sodium percarbonate in wet methylene chloride to afford the peroxide **296** in 60% yield as a white, flaky solid after recrystallization from benzene and pentane. It is important to note that both peroxides (**211** and **296**) can be stored under nitrogen in a freezer cooled to -20 °C for prolonged periods of time (months up to one year) without degradation or loss of reactivity.

The tetrachloro-, tetrabromo-, and 3,6-dichlorophthaloyl chlorides (**311** and **312**) could not be synthesized due to instability of the diacyl chlorides.¹⁷⁵ Therefore, the corresponding peroxides could not be synthesized. However, the tetrafluorophthaloyl dichloride was afforded by heating the diacid **313** to 165 °C in neat phosphorus pentachloride. After distillation, the product was accessed in 25% yield. Due to instability and resultant decomposition, the reaction forming the peroxide needed to be closely monitored by ¹³C-NMR. The tetrafluorophthaloyl peroxide (**314**) could not be purified or isolated due to degradation thereby the peroxide was treated *in situ* with mesitylene in methylene chloride at 23 °C. After five hours the solvent was removed and

the resulting viscous orange oil was dissolved in a solution of benzene/methanol (3:1) and treated with excess trimethylsilyl diazomethane to afford the crude mixed phthaloyl ester **315**. The golden yellow oil was purified by silica gel chromatography to provide the mixed ester in 30% yield over the three steps. The low yield is attributed to the decomposition of the tetrafluorophthaloyl peroxide in the peroxide formation reaction.

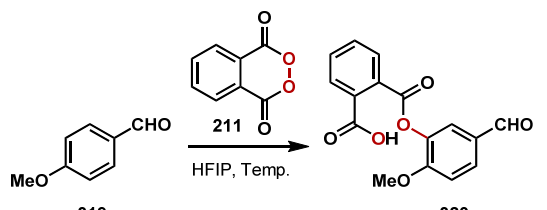
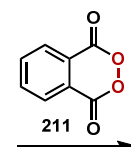
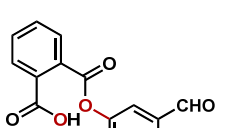
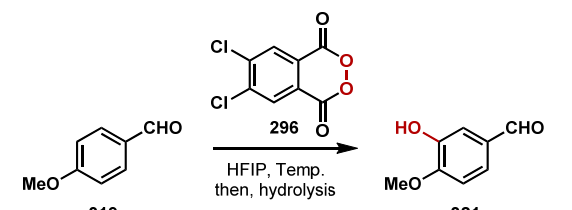
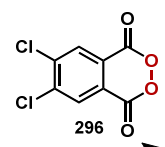
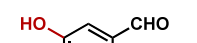
Despite the low yield, this was a good result because this type of reactivity was never observed using the parent phthaloyl peroxide or in non-fluorinated solvents. Fluorinated solvents such as HFIP and TFE at elevated temperatures are required when using phthaloyl peroxide to effect the arene hydroxylation in appreciable yields.

Scheme 3.6. Syntheses of different phthaloyl peroxides.



With multigram quantities of 4,5-dichlorophthaloyl peroxide available, its potential to hydroxylate arenes was initially examined using *p*-anisaldehyde (**319**). In comparison studies, the aldehyde was treated with four equivalents of phthaloyl peroxide in HFIP at 75 °C, however, this only promoted 6% conversion after 36 hours. Under identical conditions, but using the dichloroperoxide, *p*-anisaldehyde was oxidized with 80% conversion. After hydrolyzing the intermediate phthaloyl ester-acid, *isovanillin* (**321**) was isolated in a 69% yield (Table 3.2).

Table 3.2. Reactivity comparison between peroxides **211** and **296** using *p*-anisaldehyde.

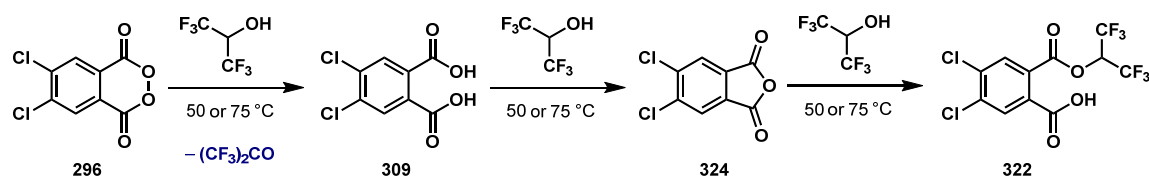
Reaction with Peroxide 211			Reaction with Peroxide 296		
					
Temperature (°C)	Peroxide equiv.	Conversion (%)	Temperature (°C)	Peroxide equiv.	Conversion (%)
50	1.3	0	50	1.3	10
50	2.5	0	50	2.5	32
75	2.5	2	75	2.5	28
75	4.0	6	75	4.0	80 (69% yield)

The use of four equivalents of the peroxide was surprising, but necessary as using less equivalents resulted in lower conversion of the starting material. The high temperature proved necessary because the reaction was sluggish at temperatures below 75 °C, but this temperature also warranted the use of excess peroxide due to a higher degree of peroxide decomposition. ¹H-NMR experiments were then conducted to analyze the cause of decomposition and the rate at which it was occurring. First, the peroxide was heated in deuterated HFIP at 50 and 75 °C. This showed that 15-20% and 35-40% decomposition of the peroxide occurred in deuterated HFIP at 50 and 75 °C respectively over 48 hours. By conducting the same experiment in HFIP and then analyzing the crude reaction material by ¹H-NMR, it was found that the peroxide had converted to the mixed phthaloyl ester acid **322** (Scheme 3.7). In order to confirm this result, the crude acid was esterified using trimethylsilyl diazomethane to provide the diester **323** which was purified and then fully characterized (see Experimental Section). Also observed in both NMR experiments was the formation of 4,5-dichlorophthaloyl

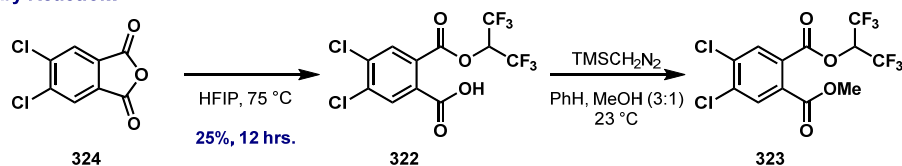
anhydride at the expense of the peroxide. The current hypothesis is that the peroxide oxidizes the solvent, leading to the diacid which is observed in both NMR experiments, and this material is then slowly converted to the anhydride (**324**) by the acidic reaction media. HFIP then reacts with the anhydride to form the ester **322**, and this was also confirmed by heating the anhydride in HFIP to 75 °C in a separate experiment. After 12 hours the solvent was removed and ¹H-NMR of the resultant crude yellow solid showed ~25% of the ester **322** and ~75% of the starting anhydride.

Scheme 3.7. Decomposition pathway of 4,5-dichlorophthaloyl peroxide in HFIP.

Observed by ¹H-NMR in CDCl₃ and (CF₃)₂CDOD:



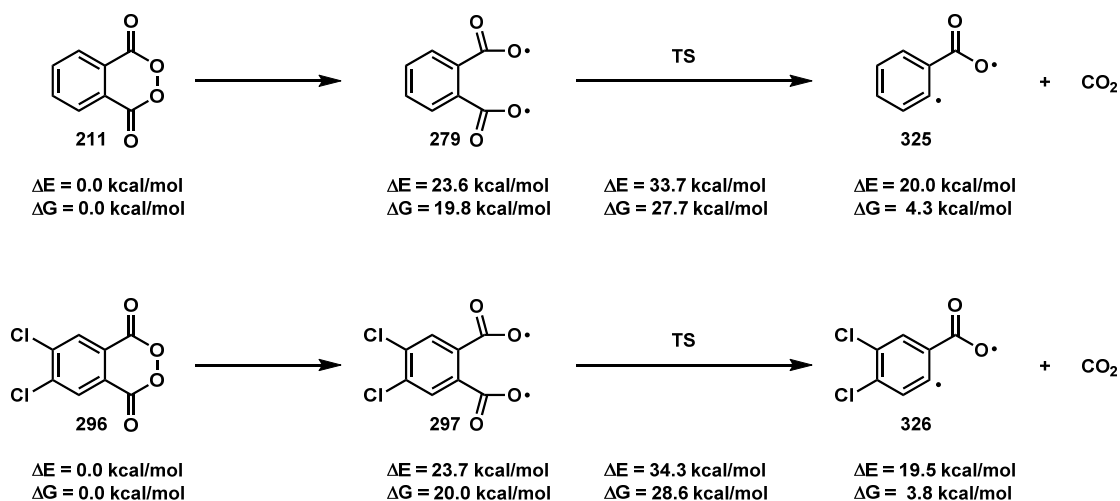
Observed by Reaction:



This decomposition was not observed in the original oxidation protocol developed by Changxia Yuan dictating that phthaloyl peroxide is more stable in fluorinated solvents. To understand the potential risks and dangers associated with using the new peroxide, DFT calculations were conducted to compare the thermal stabilities between the two oxidants (Scheme 3.8). Surprisingly, despite the enhanced reactivity, 4,5-

dichlorophthaloyl peroxide possesses slightly more thermal stability than phthaloyl peroxide, however, these computational experiments show another pathway for the peroxide decomposition. It is important to note that this type of decomposition was not observed in the original experiments examining the degradation, however, this internal decomposition has been observed during hydroxylation reactions on a small number of substrates using 4,5-dichlorophthaloyl peroxide.

Scheme 3.8. Thermal stability of 4,5-dichlorophthaloyl peroxide and phthaloyl peroxide.



The thermal stability of 4,5-dichlorophthaloyl peroxide was also investigated using thermogravimetric analysis (Figure 3.3). The TGA data indicates that the peroxide has a point of decomposition at 135 °C confirming that it is slightly more stable than phthaloyl peroxide which decomposes at 130 °C. These oxidants have remarkable thermal stability compared to benzoyl peroxide, which begins to gradually decompose at 105 °C. Unfortunately, both phthaloyl peroxides show a sharp decrease in mass at these

respective temperatures indicating that when they are heated above these points a potential explosion could occur. In light of this, all experiments were conducted at or below 75 °C.

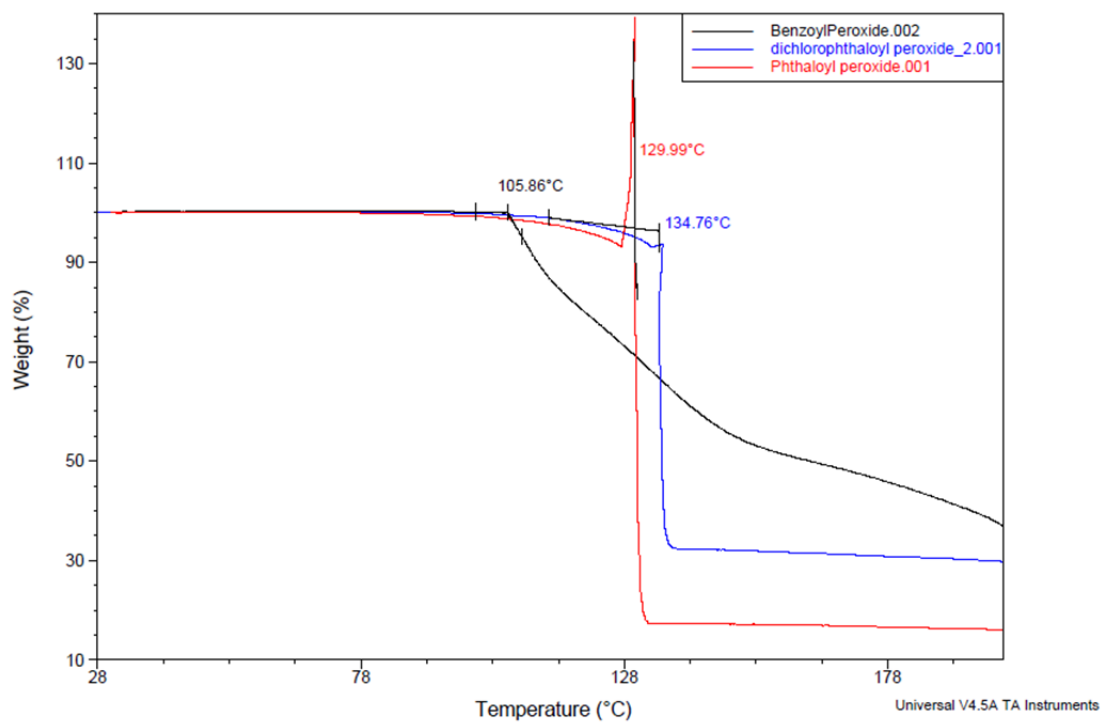
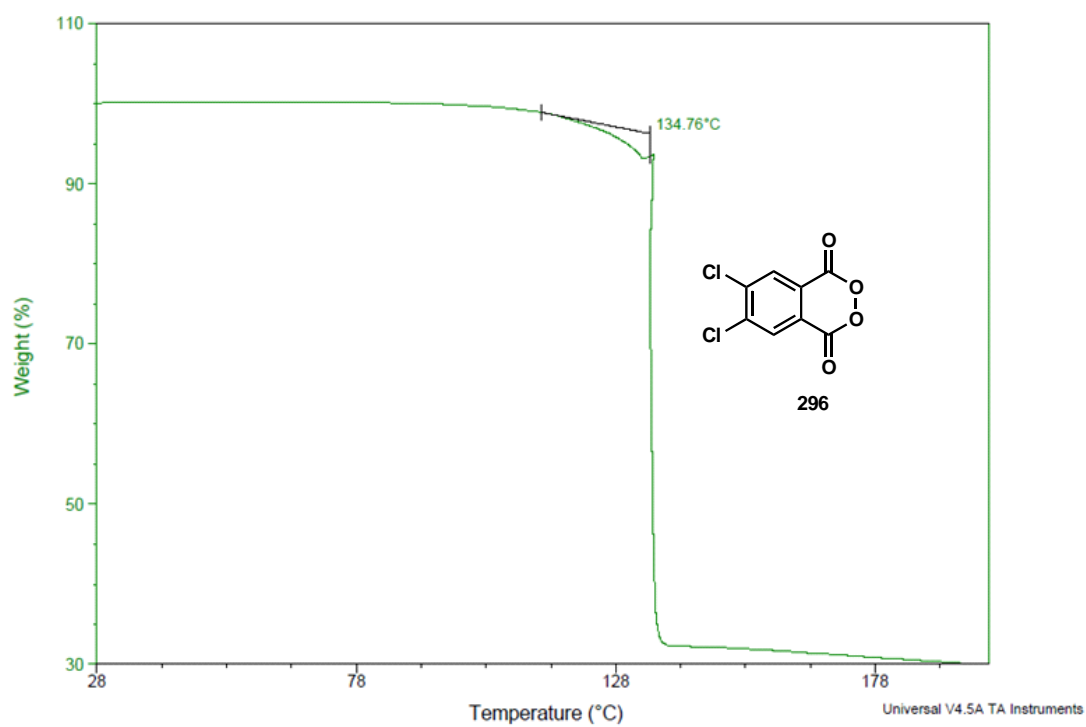


Figure 3.3. TGA data for 4,5-dichlorophthaloyl peroxide.

A full understanding of 4,5-dichlorophthaloyl peroxide's decomposition in HFIP, its thermal explosive potential, and the enhanced reactivity predicated on the oxidation of anisaldehyde, the hydroxylation reaction was next examined on previously inaccessible substrates. Two general sets of reaction conditions were developed. The oxidations were carried out using either 1.3 equivalents of 4,5-dichlorophthaloyl peroxide at 50 °C or 2.5 equivalents heated to 75 °C in HFIP. Operationally the reaction proceeds without the need for special exclusion of air or moisture and the use of commercial grade HFIP is sufficient. Karl Fisher titration on the HFIP routinely used in these reactions contained 924 ppm of water. Using purified HFIP rendered no difference in reactivity.

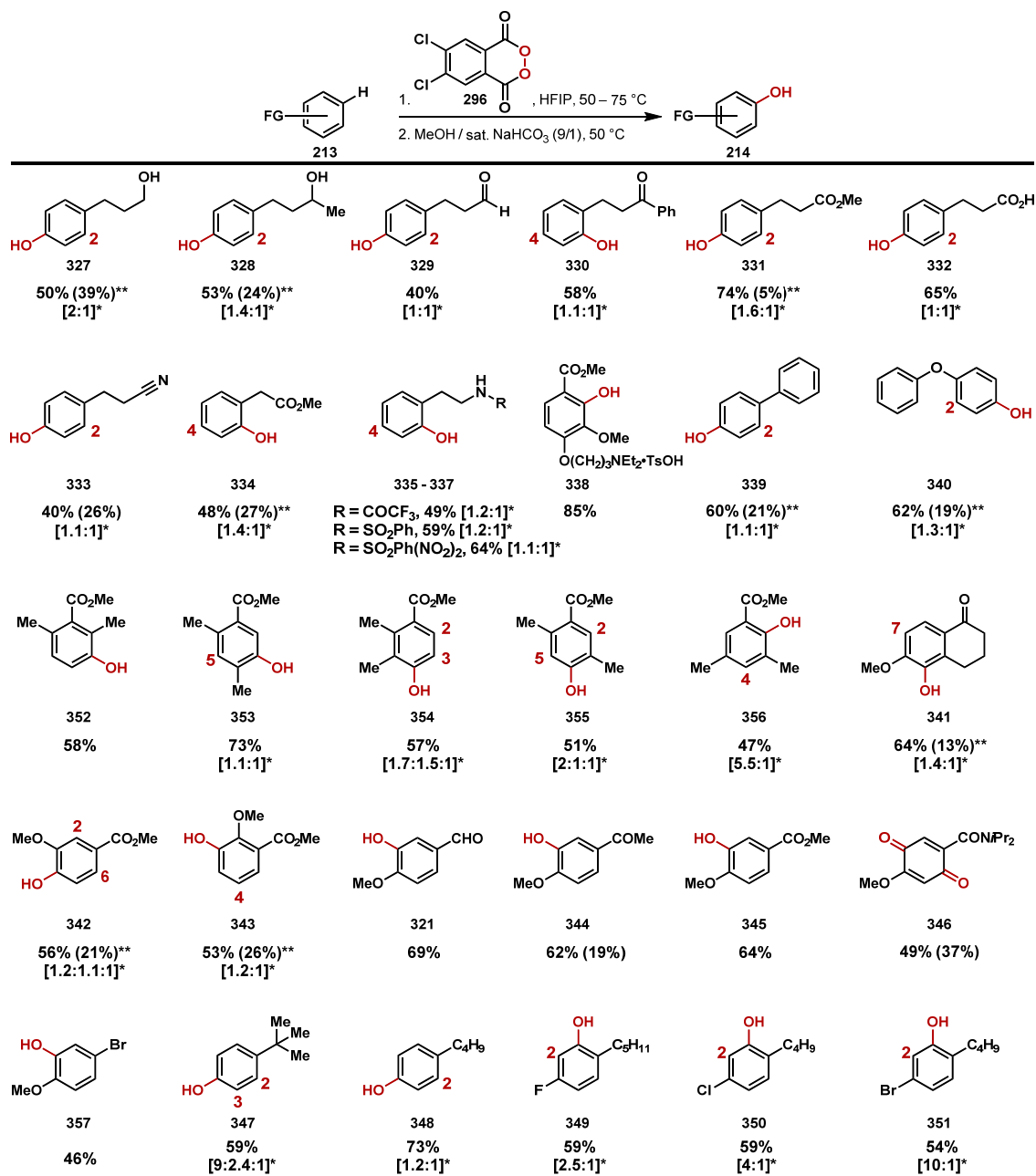
The products in Table 3.3 demonstrate the range of substituted arenes that can be successfully hydroxylated and the functional groups that are tolerated, adding to those already known.¹⁷¹ Primary and secondary alcohols are tolerated providing phenols **327** and **328**. Substrates possessing tertiary alcohols can be hydroxylated, but the yields are low due to ionization of the alcohols in these arenes. A series of hydrocinnamyl derivatives with higher degrees of oxidation participated well in the reaction to afford the phenols of the aldehyde **329**, ketone **330**, ester **331**, acid **332**, and nitrile **333**. Removal of one methylene led to a diminished yield of 48% for the oxidation to generate the ester **334**.

After examining different nitrogen protecting groups, the trifluoroacetamide **335**, sulfonamide **336**, and dinitrosulfonamide **337** were all produced in moderate to good yield representing some of the first substrates containing nitrogens successfully hydroxylated under this manifold. After testing additives it was found that amines (in their ammonium form) are also tolerated. The addition of *p*-toluenesulfonic acid monohydrate (1.0 equivalent) prior to that of 4,5-dichlorophthaloyl peroxide leads to

successful hydroxylation providing the aminophenol **338** in 85% yield. Hydroxylation of biphenyl (**339**), diphenyl ether (**340**), 6-methoxy tetralone (**341**) as well as methyl *m*-anisate (**342**) and methyl *o*-anisate (**343**) occurred in moderate to good yields, but provided mixtures of isomeric products. Single regioisomers were obtained in the hydroxylation of acetanisole (**344**), *p*-anisaldehyde (**319**), and methyl *p*-anisate (**345**) driven by synergistic regiochemical directing effects of the methyl ether and carbonyls. However, upon conducting the reaction using *p*-methoxy aryl amides, double hydroxylation of the arene occurred to afford the quinone **346**. Attempts to minimize this reaction to affect only mono-hydroxylation unfortunately were ineffective. Interchanging the methoxy group with a methyl or alkyl substituent rendered an unreactive arene and only returned the starting amide.

The oxidation of *tert*-butyl benzene delivered the *ortho*, *meta*, and *para* phenols **347** with the *para* isomer being the major product. This represented the first time a *meta* product was generated in the reaction and it potentially arose through rearrangement before aromatization to relieve steric strain of the *o*-phthalate intermediate. Butyl benzene (**348**) was converted in higher efficiency using 4,5-dichlorophthaloyl peroxide in 73% yield compared to 49% conversion using phthaloyl peroxide. A series of halogenated alkyl benzene derivatives (**349-351**) were oxidized to demonstrate the regioselectivities possible within these systems. As expected, the halogens were not as strong of a directing group as the alkyl substituents, and within these substrates fluorine is a stronger director than chlorine which in turn is more effective than bromine. Interestingly, the *ipso* products were formed in 2-5% yield replacing the halogen with a phenol.

Table 3.3. Hydroxylation of arenes mediated by 4,5-dichlorophthaloyl peroxide.



The regioisomeric position is labeled with the respective carbon atom number

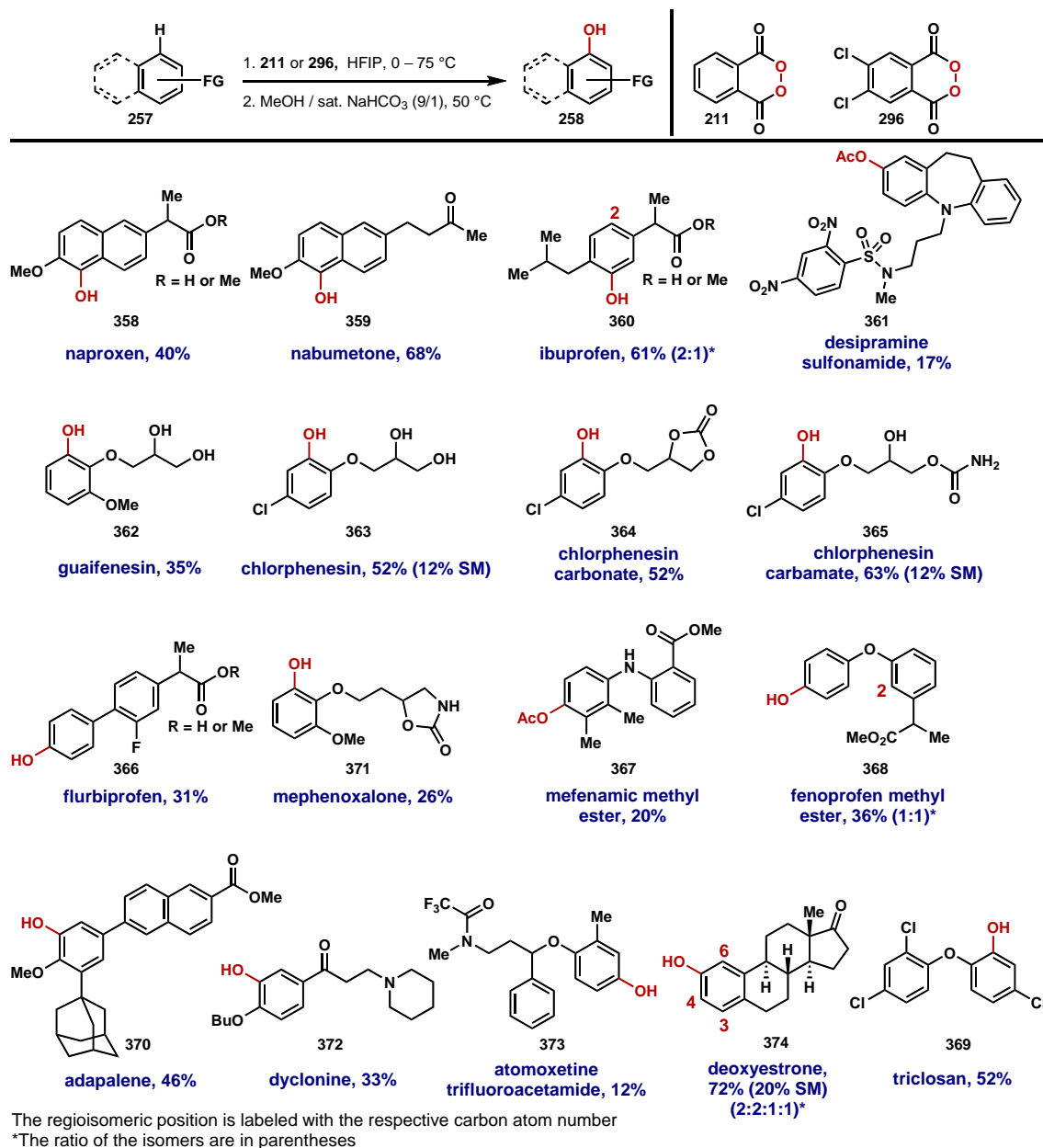
*The ratio of the isomer is in brackets

**The yield in parentheses refers to the starting material recovered

Since the oxidation proved highly tolerant to several functional groups, the protocol was applied to the syntheses of the phenolic derivatives of drugs as well as biocides in their native state (Table 3.4). Hydroxylation of the free acid as well as the esters of naproxen, nabumetone, and ibuprofen was achieved to generate the phenols **358**, **359**, and **360** in modest yield. Air oxidation of the electron rich naphthol led to the lower yields for the phenol **358**. Protection of the amine as the dinitrosulfonamide followed by oxidation provided the acetate derivative of desipramine (**361**) in 17% yield over three steps. The insipient phenol was protected as the acetate in order to separate the isomer from other minor isomers and to attain an accurate yield due to slight decomposition of the phenol during purification. Anilines do not participate well in the oxidation often leading to low selectivity as well as over-oxidized adducts and decomposition. As free alcohols were tolerated, guaifenesin and chlorphenesin glycol were hydroxylated to provide the phenols **362** and **363** in 35% and 52% yield respectively. The related carbonate and carbamate were similarly reacted to provide the corresponding phenols **364** and **365** in 52% and 63% yield. The NSAID flurbiprofen was also hydroxylated in 31% yield to provide the *para* phenol **366**. This phenol is a metabolite of flurbiprofen and has previously been synthesized through a Friedel-Crafts/Baeyer-Villiger sequence in an overall six steps and 20% yield, further substantiating the efficiency of our developed hydroxylation protocol.^{176,177} Treating the ester of mefenamic acid with 2 equivalents of the peroxide delivered the *para* phenol which was immediately protected to afford the acetate **367** in 20% yield over the three steps. The phenol was protected as the acetate in order to attain an accurate yield which had been difficult due to decomposition of the phenol during purification. Minimal conversion of the starting material was observed if only one equivalent was used. The hydroxylation strategy also provided an alternative

approach to access one of the metabolites of the NSAID fenoprofen **368** as well as the widely used household antibacterial and antifungal agent triclosan (**369**).^{178,179} Hydroxylation of 2,4,4'-trichlorodiphenylether was achieved regioselectively to synthesize triclosan in 52% yield. Adapalene, an effective drug for treating acne, was hydroxylated to afford the phenolic derivative **370** in 46% yield without any observation of adamantyl hydrogen abstraction or decomposition.¹⁸⁰ The residual material consisted of phenolic isomers as well as those associated with *ipso* substitution, replacing the adamantyl substituent with a phenol.

Table 3.4. Hydroxylation of drugs to provide phenolic derivatives and metabolites using phthaloyl and 4,5-dichlorophthaloyl peroxide.

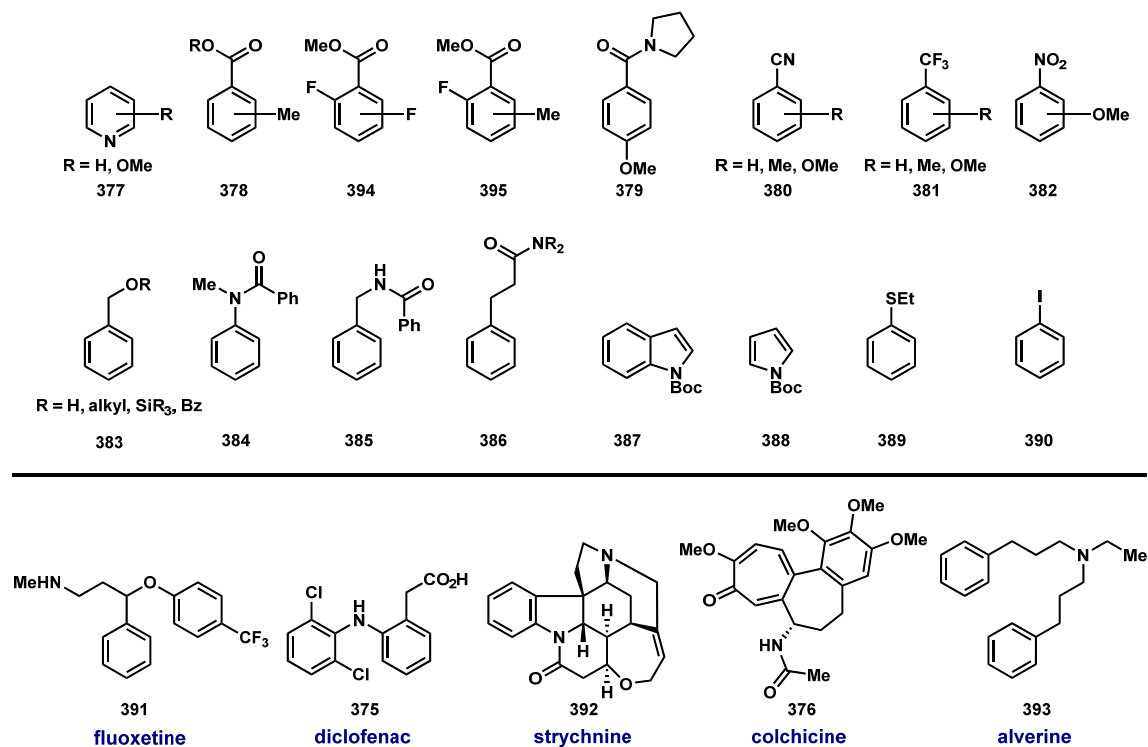


Although the hydroxylation proceeds well in a broadly functional group tolerant manner, incompatible functionality does exist (Table 3.5). Pyridines, thioethers, and aryl

iodides are oxidized at the heteroatom. Pyridines are oxidized quantitatively to the N-oxides, which are in turn reluctant to react further with the peroxides. Aryl thioethers are selectively oxidized to the sulfoxide using 1 equivalent of the peroxide, whereas 2 equivalents provide the sulfone quantitatively. Unfortunately, arenes containing aryl, benzyl, or alkyl amides do not react with the peroxide in a productive manner; only unreacted starting material is returned. The peroxide is fully consumed throughout the course of the reaction, but as to why no product is attained remains an unsolved problem. NMR experiments conducted in deuterated HFIP provided no evidence as to what was occurring or how the peroxide was decomposing. The use of different additives, either Brønsted or Lewis acids, did not aid this process.

Aryl nitriles, benzyl ethers, and arenes containing trifluoromethyl or nitro groups are extremely sluggish in the reaction. Alternatively, pyrroles and indoles react violently with the peroxide to afford no desirable product, only black tar. Lastly, extremely electron rich arenes such as diclofenac (**375**) and colchicine (**376**) were destroyed beyond structural assignment under the reaction conditions.

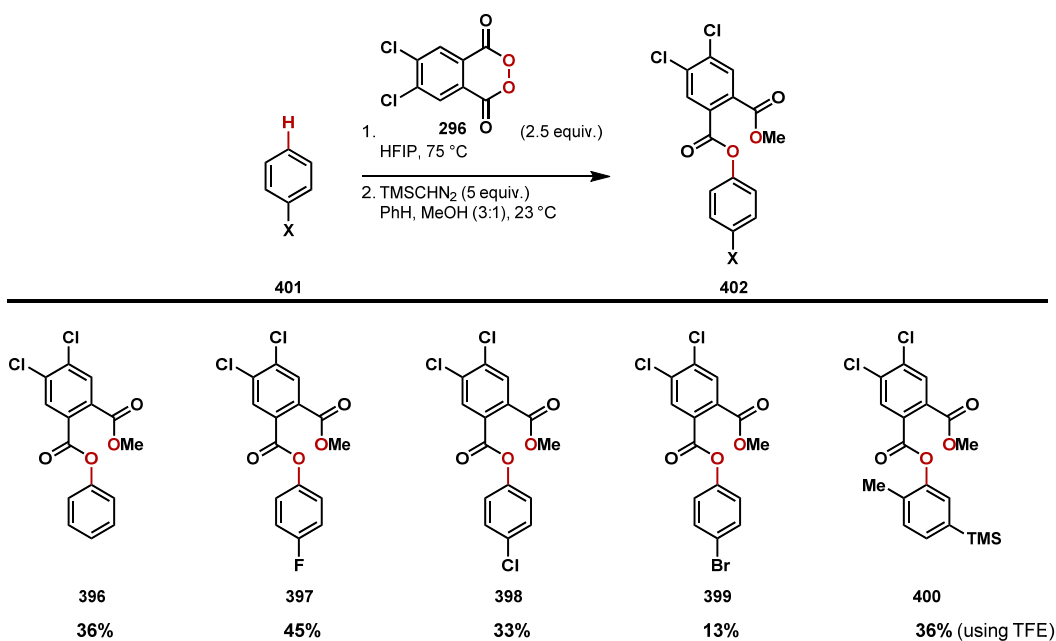
Table 3.5. Incompatible functional groups and arenes that are not oxidized using 4,5-dichlorophthaloyl peroxide.



The majority of previous arene oxidation procedures have focused on the hydroxylation of simple aromatics such as benzene, which is typically used as solvent and substrate. To showcase the unique reactivity of 4,5-dichlorophthaloyl peroxide, benzene, fluorobenzene, chlorobenzene, and bromobenzene were reacted with 2.5 equivalents of the peroxide in HFIP at 75 °C. *p*-Trimethylsilyl toluene was also reacted with the peroxide, but TFE was used instead because HFIP promoted desilylation (Table 3.6). As the phenolic products were volatile, the intermediate mixed phthaloyl ester-acids were esterified using trimethylsilyl diazomethane to generate the mixed phthalate esters **396** – **400**. After purifying these adducts via silica gel chromatography, they were then fully characterized. While the yields were modest, the reactivity of 4,5-

dichlorophthaloyl peroxide with these less reactive arenes is noteworthy as secondary oxidation of the products was not found to be competitive. Also, *p*-trimethylsilyl toluene was oxidized to afford the ester **400** as the major product. The minor product was the adduct containing the phthalate ester *ortho* to the silyl group which was isolated in 12% yield. The residual material is unreacted starting silane. No *ipso* substitution product was observed, which is interesting as aryl silanes tend to react through an EAS pathway with electrophiles to provide products of *ipso* substitution.¹⁸¹

Table 3.6. Oxidation of halobenzenes and *p*-trimethylsilyl toluene using 4,5-dichlorophthaloyl peroxide.



Early computational analysis indicated that the phthaloyl peroxide mediated arene oxidation proceeded through a diradical reverse-rebound reaction pathway.¹⁷¹ The 4,5-dichlorophthaloyl peroxide oxidation was initially hypothesized to proceed through an

ionic or EAS pathway. However, the reactions producing the phenols of the dimethylmethylbenzoates **354-356** (Table 3.3) and the phthalate ester of trimethylsilyl toluene contradict this theory. In light of these results and to fully elucidate the mechanism of this unique reaction, linear free energy relationships were examined to probe the transition state. Using the observed reactivity of benzene and the halobenzenes **397-399**, these relationships were assessed by reacting 5 equivalents of the corresponding arene and 5 equivalents of benzene with 1 equivalent of 4,5-dichlorophthaloyl peroxide in HFIP at 75 °C for 36 hours. The reaction mixture was then concentrated, re-dissolved in a mixture of benzene/methanol (3:1), and esterified using an excess of trimethylsilyl diazomethane. After concentration, the ratios of the crude phthalate esters were determined using ¹H-NMR. These experiments were conducted in duplicate to insure accuracy.

Examination of the reaction using the linear free energy relationships with σ vs. σ^+ values established a linear trend with a low negative *rho* value (-3.92), corresponding best using σ values which supports a single electron process (Figure 3.4). This is in juxtaposition to EAS which best fits to σ^+ values with large observed *rho* values (e.g. bromination, *rho* = -13).¹⁸²

DFT and *ab initio* calculations on the barriers for diradical addition and electrophilic aromatic substitution show a similar reactivity trend to that depicted in the Hammett plot. The calculations show that the EAS pathway is sensitive for electron-rich arenes. The activation free energy difference is approximately 7 kcal/mol for the reactions using anisole and benzene, whereas the activation energy difference is only about 4 kcal/mol for the diradical addition. This further substantiates that the slope obtained from the Hammett plot is closer to that for the diradical addition. Further

analysis of the transition state using kinetic isotope experiments (KIE) delineated that rearomatization via hydrogen abstraction is not the rate determining step extrapolated by the low KIE of 1.22.

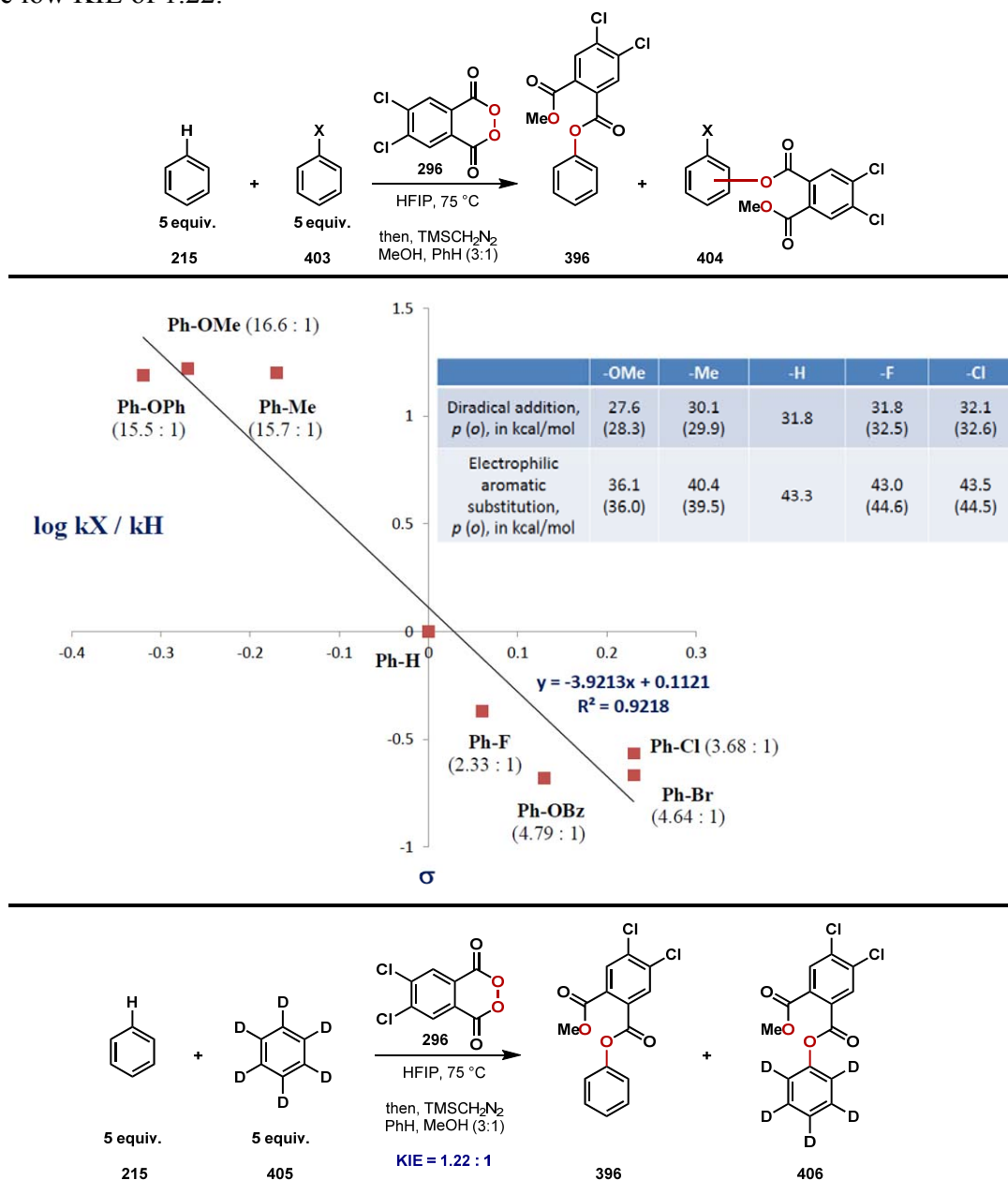
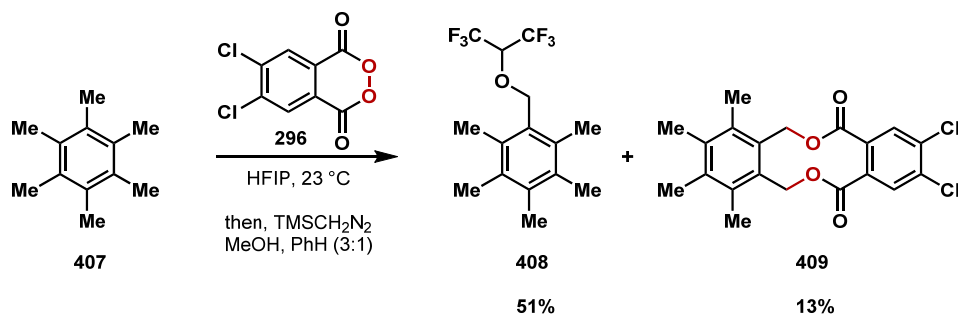


Figure 3.4. Linear free energy σ plot for the 4,5-dichlorophthaloyl peroxide mediated arene oxidation, computational analysis for the EAS and diradical addition pathways and KIE experiments depicting the major mechanistic pathway.

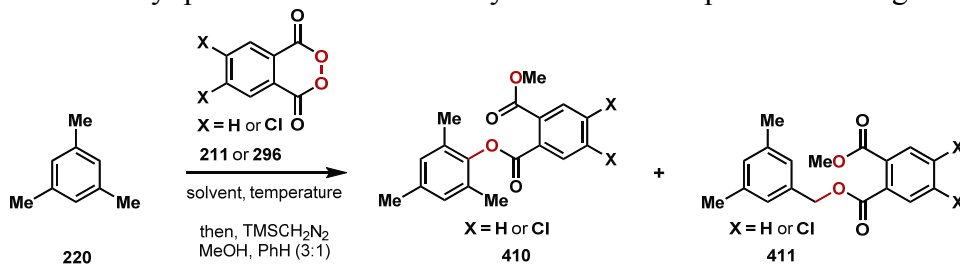
Hexamethylbenzene (**407**) was treated with 4,5-dichlorophthaloyl peroxide in HFIP at 23 °C to further indicate a diradical mechanism (Scheme 3.9). After concentration, the crude solid mixture was dissolved in a solution of benzene/methanol and esterified using trimethylsilyl diazomethane. The mixture was purified chromatographically to afford the ether **408** and the dibenzylester **409** which were then fully characterized. No products of *ipso* substitution or arene oxidation were observed.

Scheme 3.9. Reaction between hexamethylbenzene and 4,5-dichlorophthaloyl peroxide.



A surplus of evidence supports the major mechanistic pathway is the reverse-rebound diradical addition. To further confirm the presence of radicals, a series of benzylic oxidation experiments were conducted using mesitylene and both peroxides in different solvents at different temperatures. The hydroxylation reaction works optimally in the fluorinated solvents HFIP and TFE as the highest degree of oxidation is observed when using HFIP. These polar solvents can stabilize ionic intermediates and therefore can promote ionic reaction pathways. However, the experiments used to probe the transition state depict that the major reaction pathway is not ionic, but it is through a diradical addition process. HFIP and TFE can also stabilize radical intermediates through

hydrogen bonding effects which cause a remarkable increase in their persistence.^{183,184} This stabilization effect could in turn enhance the reaction's selectivity for arene oxidation over benzylic oxidation, whereas other solvents would not provide this stabilization (Schemes 3.4 and 3.5 depict the energetic barriers to effect these transformations). The hypothesis for these experiments is that if non-fluorinated solvents are used then significant amounts of benzylic oxidation should be observed compared to the use of HFIP and TFE. The use of non-protic halogenated solvents could potentially switch the mechanism to an ionic pathway, but if this were to occur then minimal benzylic oxidation should be observed, if any. This hypothesis proved to be correct as depicted in Table 3.7. When an excess of mesitylene was reacted with either peroxide in fluorinated or non-fluorinated solvents at different temperatures, a range of ratios for aryl versus benzylic oxidation was obtained. These ratios were assessed by ¹H-NMR analysis of the crude mixture and then confirmed by isolating the pure mixed phthalate esters after esterification. In HFIP at 23, 50 or 65 °C, this ratio was 99:1. The use of DCE at 65 °C promoted greater benzylic oxidation as observed by the ratio of 9:1. Using either cyclohexane or CCl₄ promoted more benzylic oxidation. Lastly, switching the solvent to benzene or conducting the reaction in neat mesitylene also increased the amount of benzylic oxidation.

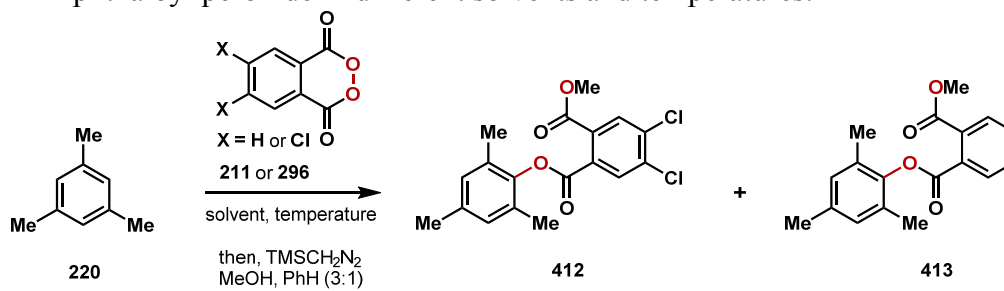
Table 3.7. Phthaloyl peroxide mediated benzylic oxidation experiments using mesitylene.

Peroxide	Solvent	Temperature	Ratio (410:411)	Isolated Yield
PPO (211)	HFIP	23 °C	>99:1	-----
PPO (211)	HFIP	50 °C	99:1	1.0% (411)
PPO (211)	HFIP	65 °C	99:1	1.3% (411)
DCPP (296)	HFIP	23 °C	>99:1	-----
DCPP (296)	HFIP	50 °C	99:1	1.0% (411)
PPO (211)	(CF₃)₂CH₂COH	65 °C	19:1	4.2% (411)
DCPP (296)	(CF₃)₂CH₂COH	65 °C	49:1	1.5% (411)
PPO (211)	TFE	23 °C	>99:1	-----
DCPP (296)	TFE	23 °C	>99:1	-----
DCPP (296)	DCE	65 °C	9:1	85%
DCPP (296)	PhH	65 °C	2.5:1	72%
PPO (211)	PhH	65 °C	1.9:1	66%
DCPP (296)	cyclohexane	65 °C	2.3:1	-----
DCPP (296)	CCl ₄	65 °C	2:1	-----
PPO (211)	Neat	50 °C	3:1	99%
DCPP (296)	Neat	23 °C	2.8:1	93%
DCPP (296)	Neat	50 °C	2.6:1	83%

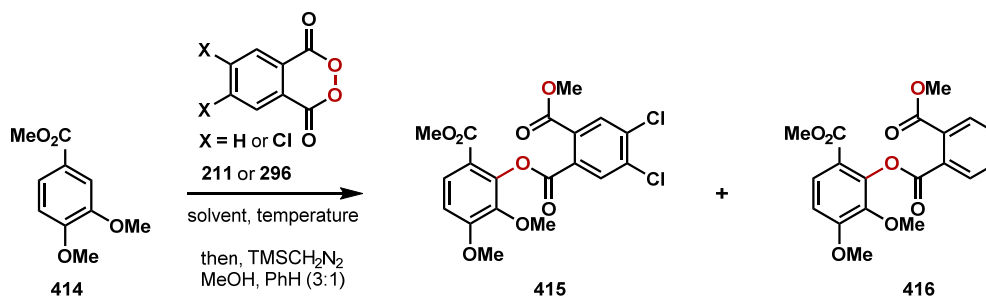
If the major reaction pathway was ionic then 4,5-dichlorophthaloyl peroxide should react much faster than phthaloyl peroxide, precluding the latter's reaction with a substrate especially in an ionizing solvent such as HFIP or TFE. However, this does not occur when a competition reaction is conducted using both peroxides (Table 3.8). Mesitylene was treated with 1 equivalent of phthaloyl peroxide and 1 equivalent of 4,5-dichlorophthaloyl peroxide in the same reaction vessel in different solvents at 23 or 65

°C. After concentration and esterification, the ratios of the phthalate adducts were determined by ¹H-NMR of the crude reaction mixture. As the solvent was changed from DCE to benzene, cyclohexane, and CCl₄ the ratio of phthalate adducts diminished drastically from 99:1 to 2:1. Also, when the reaction was conducted in HFIP or TFE at 23 °C the ratios were only 4.1:1 and 3.5:1 respectively. The experiments were also conducted using dimethoxy methylvanillate (**414**) at 23 and 65 °C as well. The same trend is observed thereby providing further evidence that the predominant pathway for the arene hydroxylation reaction using either peroxide is a diradical reverse-rebound addition. This does not exclude the possibility of an ionic mechanism, but this pathway is minor if it does occur.

Table 3.8. Competition experiments using mesitylene and dimethoxy methylvanillate comparing the rates of reactivity between 4,5-dichlorophthaloyl peroxide and phthaloyl peroxide in different solvents and temperatures.



Peroxide	Solvent	Temperature	Ratio (412:413)	Isolated Yield
PPO and DCPD	HFIP	23 °C	4.1:1	-----
PPO and DCPD	TFE	23 °C	3.5:1	-----
PPO and DCPD	DCE	65 °C	>99:1	85%
PPO and DCPD	PhH	65 °C	4.8:1	-----
PPO and DCPD	cyclohexane	65 °C	2:1	-----
PPO and DCPD	CCl₄	65 °C	2:1	-----



Peroxide	Solvent	Temperature	Ratio (415:416)	Isolated Yield
PPO and DCPD	HFIP	23 °C	23.5:1	-----
PPO and DCPD	TFE	23 °C	4.3:1	-----
PPO and DCPD	DCE	23 °C	4.2:1 (20 mg Scale)	-----
PPO and DCPD	DCE	23 °C	4.5:1 (50 mg Scale)	-----
PPO and DCPD	DCE	65 °C	8.9:1	-----
PPO and DCPD	PhH	23 °C	2.9:1	-----
PPO and DCPD	cyclohexane	23 °C	1:1	-----
PPO and DCPD	CCl ₄	23 °C	3.7:1	-----

Conclusion

A new protocol utilizing 4,5-dichlorophthaloyl peroxide has been developed to provide a novel, selective, and reliable strategy that oxidizes arenes to phenols. With enhanced reactivity relative to the parent phthaloyl peroxide, this reagent can hydroxylate a wide range of substrates. In addition, a variety of functional groups including alcohols, diols, amines, nitriles, carbamates, esters, aldehydes, ketones, and carboxylic acids are compatible, consistent with the hydroxylation reaction having broad applicability in synthesis. This enhanced protocol is amenable for rapidly accessing various phenolic derivatives of drugs constituting that the strategy efficiently generates oxygenated analogs and metabolites.

Computational analysis conducted by Houk and Liang depicted that the major reaction pathway is a diradical reverse-rebound addition. Experiments probing the transition state were conducted using linear free energy relationships. The resultant Hammett plot supported the diradical addition mechanism as the major pathway as predicted by DFT and *ab initio* calculations. This was further corroborated using a series of benzylic oxidation and competition experiments that provided substantial evidence of the diradical intermediate. These mechanistic insights provide valuable information regarding a novel protocol that achieves selective C-H functionalization thereby creating a platform for the discovery of new chemical transformations using diradicals.

Experimental Section

Arene Hydroxylation Mediated by 4,5-Dichlorophthaloyl Peroxide

Table of Contents

1. Safety Information	324
2. General Information	324
3. Experimental Procedure for 4,5-dichlorophthaloyl peroxide	326
4. Experimental Procedures	328
5. References	400
6. Catalog of Spectra	404

1. Safety Information

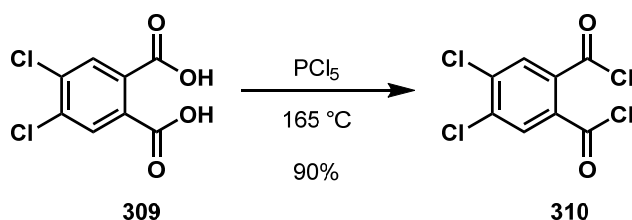
All peroxides can be dangerous when not handled correctly. The following procedures should be carried out by knowledgeable laboratory practitioners of organic synthesis. While we have not had a reaction using 4,5-dichlorophthaloyl peroxide detonate it is recommended that all reactions should be conducted with appropriate shielding as a precaution. Thermogravimetric analysis (TGA) data showed that 4,5-dichlorophthaloyl peroxide is stable below 115 °C, however, there is a rapid loss in mass at ~135 °C indicating a potential exothermic decomposition. Earlier work with 4,5-dichlorophthaloyl peroxide also describes the stability and proper handling of this compound.¹

2. General

Commercial reagents were purchased at the highest purity available and used without further purification. Trimethylsilyl diazomethane (TMSCHN₂) was purchased from Sigma-Aldrich as a 2.0 M solution in Et₂O. Reactions with 4,5-dichlorophthaloyl peroxide were performed without exclusion of air, other reactions were conducted under an atmosphere of N₂ unless otherwise indicated. Solvents (CH₂Cl₂ and Et₂O) were purified using a Pure-Solv MD-5 Solvent Purification System (Innovative Technology). 1,1,1,3,3,3-Hexafluoroisopropanol (HFIP) and 2,2,2-trifluoroethanol (TFE) were purchased from Oakwood Products and used without purification. Deoxygenated solvents were deoxygenated by sparging with nitrogen for at least 1 hour while stirring vigorously at a rate of 1000 rpm unless otherwise noted. HFIP, TFE, and methanol were removed by evaporation by positive flow of nitrogen. Other organic solutions were concentrated by evaporation using Buchi or Heidolph rotary evaporators. Analytical thin-layer chromatography (TLC) was carried out using 0.2 mm commercial glass-coated silica gel plates (silica gel 60, F254, EMD chemical). Thin layer chromatography plates were visualized by exposure to ultraviolet light and/or exposure to iodine powder, an acidic solution of ceric ammonium molybdate, or a basic solution of potassium permanganate followed by heating on a hot plate. The chromatographic purification of products was achieved using silica gel chromatography with positive N₂ pressure as described by Still.² Infrared spectral data were recorded on a Nicolet 380 FTIR using neat thin film technique. High-resolution mass spectral data (HRMS) were obtained on a Karatos MS9 and reported as m/z (relative intensity). Accurate masses are reported for the molecular ion [M+Na]⁺, [M+H]⁺, [M+2H]²⁺, [M], or [M-H]⁻. Nuclear magnetic resonance spectral data (¹H NMR and ¹³C NMR) were recorded with a Varian Gemini (400 MHz, ¹H at 400 MHz, ¹³C at 100 MHz, 500 MHz, ¹H at 500 MHz, ¹³C at 125 MHz, or 600 MHz, ¹H at 600 MHz, ¹³C at 150 MHz). For CDCl₃, C₆D₆, CD₃OD, and C₃D₆O solutions, chemical shifts are reported as parts per million (ppm) referenced to residual protium or carbon of the solvent; CHCl₃ δ 7.26 ppm, CDCl₃ δ 77.00 ppm, C₆D₅H δ 7.15 ppm, C₆D₆ δ 128.00 ppm, CD₂HOH δ 4.85 ppm, CD₃OD δ 47.60 ppm, C₃D₅HO δ 2.05 ppm, and C₃D₆O δ 29.00 ppm. Coupling constants are reported in Hertz (Hz). Data

for ^1H -NMR spectral data are reported as follows: chemical shift (ppm, referenced to protium); bs = broad singlet, s = singlet, br d = broad doublet, d = doublet, t = triplet, q = quartet, dd = doublet of doublets, dt = doublet of triplets, ddd = doublet of doublet of doublets, dddd = doublet of doublet of doublet of doublets, m = multiplet, integration, and coupling constant (Hz). Melting points were measured on a MEL-TEMP device with calibration using Benzoic Acid (M.P. = 122 °C) as the standard. Thermogravimetric analysis (TGA) was obtained from a TGA Q500 V20.13 analyzer.

3. Experimental Procedure for 4,5-dichlorophthaloyl peroxide

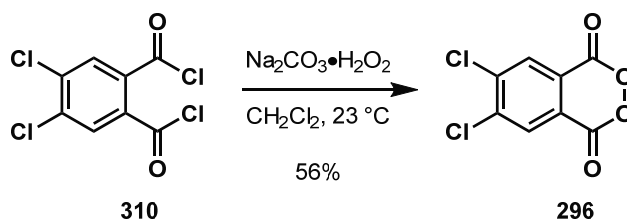


Solid 4,5-dichlorophthalic acid (**309**) (50.0 g, 213 mmol, 1.00 eq.) and solid phosphorus pentachloride (89.0 g, 427 mmol, 2.00 eq.) were added to a reaction vessel equipped under a continuous flow of nitrogen equipped with a reflux condenser and an output leading to a saturated aqueous mixture of NaHCO₃. The solid mixture was placed in an oil bath heated to 180 °C and stirred vigorously (600 rpm). **Caution: HCl Gas Evolution.** After 12 hrs the reaction vessel was removed from the oil bath, cooled to 23 °C, equipped with a fractional distillation apparatus and the dark grey-black liquid was purified by fractional distillation *in vacuo* to afford the dichloride **310** (55.1 g, 192 mmol, 90%, b.p. = 155 – 160 °C at 0.1 mmHg) as a clear colorless oil which solidified upon cooling to 23 °C. The spectral data and physical properties match that for 4,5-dichlorophthaloyl chloride.³

¹H-NMR (400 MHz, CDCl₃): δ 7.98 (s, 2H)

M.P. = 34 °C

B.P. = 155 – 160 °C (0.1 mmHg).



A mixture of solid 4,5-dichlorophthaloyl chloride **310** (25.5 g, 94 mmol, 1.00 eq.) and sodium percarbonate (16.2 g, 103 mmol, 1.10 eq.) were diluted with unpurified CH_2Cl_2 (469 mL). The white heterogeneous mixture was placed under an atmosphere of N_2 and stirred vigorously (1000 rpm). After 24 hrs the mixture was filtered over a pad of celite and carefully concentrated by rotary evaporation (water bath set to 23 °C) to afford a pale yellow solid. The solid was dissolved in benzene (110 mL) and then pentane (220 mL) was slowly added to the stirring solution inducing a slow precipitation of a white solid. The mixture was placed in an ice water bath cooled to 0 °C for 1 hr and filtered cold to afford the peroxide **296** as a white flakey solid (9.3 g, 40 mmol, 43%, 86% pure with 14% 4,5-dichlorophthaloyl anhydride). A second precipitation of the filtrate solution after concentration provided the peroxide **296** (2.7 g, 12 mmol, 13%, 86% pure with 14% 4,5-dichlorophthaloyl anhydride). Concentration of the filtrate solution after the second crop provided the starting 4,5-dichlorophthaloyl dichloride (5.7 g, 21 mmol, 22%). The spectral data data of **296** matches that for 4,5-dichlorophthaloyl peroxide.⁴

¹H NMR (400 MHz, CDCl_3): δ 8.34 (s, 2H)

¹³C NMR (100 MHz, CDCl_3): δ 160.4, 142.4, 131.8, 122.6

IR (neat film, cm^{-1}) 1748, 906 cm^{-1}

4. Experimental Procedures

General Procedure A:

To a flame-dried borosilicate flask equipped with a magnetic stir bar was added the corresponding arene as a solid or neat followed by the syringe addition of HFIP to provide a clear homogeneous solution with a substrate concentration of 0.1 M. In some cases, when noted, CHCl_3 was added to aid homogeneity. Solid 4,5-dichlorophthaloyl peroxide **296** was then added in one portion unless otherwise noted. After stirring at a rate of 500 rpm at 23 °C for 1 minute to provide full dissolution of the peroxide, the reaction vessel was capped with a polyethylene stopper, clamped, placed in an oil bath heated to 50 °C, and stirred at a rate of 500 rpm. After 24 or 48 hrs the reaction was removed from the oil bath and allowed to cool to 23 °C, the stopper was removed carefully, and the HFIP was evaporated by a continuous flow of N_2 to reveal a yellow, orange, or deep red solid mixture. The crude solid mixture was then placed under an atmosphere of N_2 , and a deoxygenated mixture of MeOH and saturated aqueous NaHCO_3 (9:1) was added by syringe under N_2 to provide an overall reaction concentration of 0.1 M. The heterogeneous mixture was placed in an oil bath heated to 50 °C and stirred at a rate of 500 rpm. After 1 hr the methanol was removed by a continuous flow of N_2 , and to the mixture was added Et_2O or EtOAc (10 mL) and an aqueous phosphate buffer (10 mL, 0.2 M, pH = 7). The mixture was vigorously stirred (800 rpm) at 23 °C for 2 minutes to provide a biphasic solution which was poured into a separatory funnel and partitioned. The organic layer was washed with an aqueous phosphate buffer (4 x 30 mL, 0.2 M, pH = 7) or with the combination of an aqueous saturated mixture of NaHCO_3 and brine (3 x 30 mL, 1:1). The residual organics were extracted from the aqueous layer with Et_2O (3 x 25 mL) or EtOAc (3 x 25 mL), dried over solid Na_2SO_4 , decanted, and concentrated carefully (**NOTE:** Some of phenolic products are volatile). The crude material was then purified by silica gel chromatography using the noted solvent mixture to afford the phenolic products.

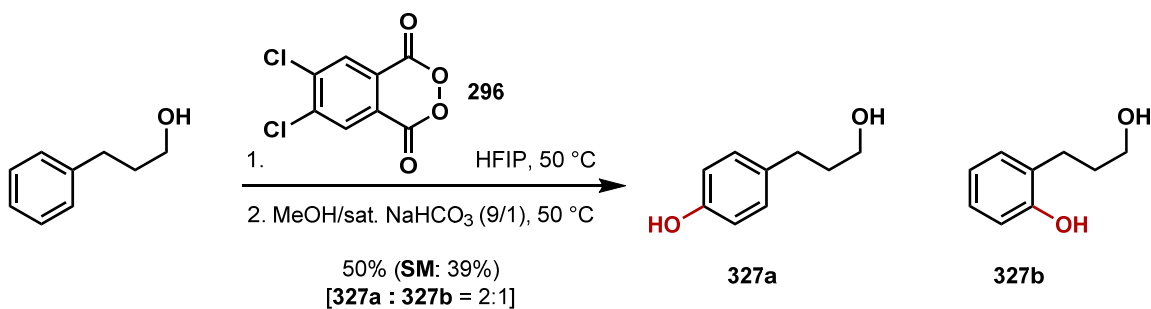
General Procedure B:

To a flame-dried borosilicate flask equipped with a magnetic stir bar was added the corresponding arene as a solid or neat followed by the syringe addition of HFIP to provide a clear homogeneous solution with a substrate concentration of 0.1 M. In some cases, when noted, CHCl_3 was added to aid homogeneity. Solid 4,5-dichlorophthaloyl peroxide **296** was then added in one portion. After stirring at a rate of 500 rpm at 23 °C for 1 minute to provide full dissolution of the peroxide, the reaction vessel was capped with a polyethylene stopper, clamped, placed in an oil bath heated to 75 °C, and stirred at a rate of 500 rpm. After 36 or 48 hours the reaction was removed from the oil bath and allowed to cool to 23 °C, the stopper was removed carefully, and the HFIP was evaporated by a continuous flow of N_2 to reveal a yellow, orange, or deep red solid

mixture. The crude solid mixture was then placed under an atmosphere of N₂, and a deoxygenated mixture of MeOH and saturated aqueous NaHCO₃ (9:1) was added by syringe under N₂ to provide an overall reaction concentration of 0.1 M. The heterogeneous mixture was then placed in an oil bath heated to 50 °C and stirred at a rate of 500 rpm. After 1 hr the methanol was removed by a continuous flow of N₂, and the mixture was diluted with Et₂O or EtOAc (10 mL) and an aqueous phosphate buffer (10 mL, 0.2 M, pH = 7). The mixture was vigorously stirred (800 rpm) at 23 °C for 2 minutes to provide a biphasic solution which was poured into a separatory funnel and partitioned. The organic layer was washed with an aqueous phosphate buffer (4 x 30 mL, 0.2 M, pH = 7) or with the combination of an aqueous saturated mixture of NaHCO₃ and brine (3 x 30 mL, 1:1). The residual organics were extracted from the aqueous layer with Et₂O (3 x 25 mL) or EtOAc (3 x 25 mL), dried over solid Na₂SO₄, decanted, and concentrated carefully (**NOTE:** Some of the phenolic products are volatile). The crude material was then purified by silica gel chromatography using the noted solvent mixture to provide the phenolic products.

General Procedure C:

To a flame-dried borosilicate flask equipped with a magnetic stir bar was added the corresponding arene as a solid or neat followed by the syringe addition of HFIP to provide a clear homogeneous solution with a substrate concentration of 0.1 M. Solid 4,5-dichlorophthaloyl peroxide was then added in one portion. After stirring at a rate of 500 rpm at 23 °C for 1 minute to provide full dissolution of the peroxide, the reaction vessel was capped with a polyethylene stopper, clamped, placed in an oil bath heated to 75 °C, and stirred at a rate of 500 rpm. After 36 hours the reaction was removed from the oil bath and allowed to cool to 23 °C. The stopper was removed carefully and the HFIP was evaporated to dryness by a continuous flow of N₂ to reveal a yellow solid mixture. The crude mixture was then dissolved in a benzene/methanol solution (3:1) providing an overall substrate concentration of 0.1 M and the clear yellow homogeneous solution was stirred at a rate of 500 rpm. TMSCHN₂ (5.00 eq., 0.2 M in Et₂O) was added in a slow dropwise fashion over 1 minute. **Caution: Rapid N₂ gas evolution.** After 30 minutes the deep yellow–orange solution was evaporated by a continuous flow of N₂ to provide a yellow–orange foam which was purified by silica gel chromatography using the noted solvent mixture to provide the mixed phthalate ester products.



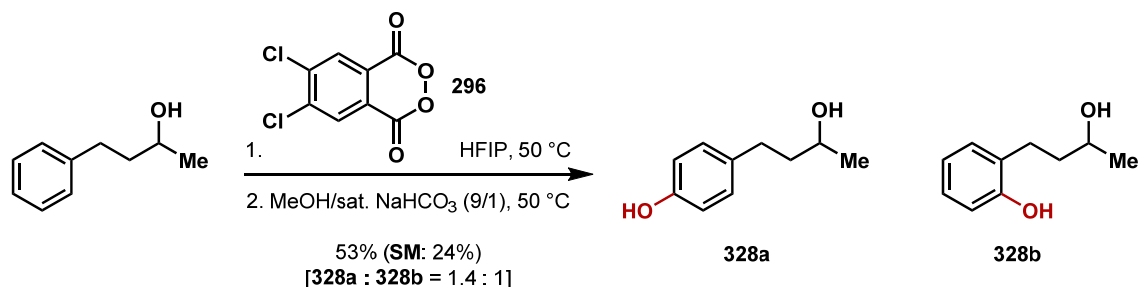
Diol 327a and 327b: Prepared following General Procedure A using hydrocinnamyl alcohol (100.0 mg, 0.73 mmol, 1.00 eq), 4,5-dichlorophthaloyl peroxide (256.0 mg, 0.96 mmol, 1.30 eq., 86%), and HFIP (7.3 mL) at 50 °C for 48 hrs. The crude brown foam was purified by silica gel chromatography; 2 – 30% EtOAc in CH₂Cl₂ and hexane (1:1) to provide the title compounds **327a** and **327b** (56.0 mg, 0.37 mmol, 50%, **327a** : **327b** = 2 : 1) as an orange foam and the starting alcohol (39.2 mg, 0.29 mmol, 39%) as a clear colorless oil. The spectral data of the title compounds match that for **327a** and **327b**.⁵⁻⁸

Major Isomer (327a):

¹H-NMR (400 MHz, CDCl₃): δ 7.07 (d, 1H, *J* = 8.6 Hz), 6.76 (d, 1H, *J* = 8.6 Hz), 3.67 (t, 2H, *J* = 6.5 Hz), 2.64 (t, 2H, *J* = 7.9 Hz), 1.92 – 1.82 (m, 2H).⁵⁻⁷

Minor Isomer (327b):

¹H-NMR (400 MHz, CDCl₃): δ 7.10 (d, 2H, *J* = 7.5 Hz), 6.88 (d, 1H, *J* = 7.5 Hz), 6.85 (d, 1H, *J* = 7.5 Hz), 3.66 (t, 2H, *J* = 5.8 Hz), 2.78 (dd, 2H, *J* = 6.5, 7.2 Hz), 1.92 – 1.82 (m, 2H).⁸



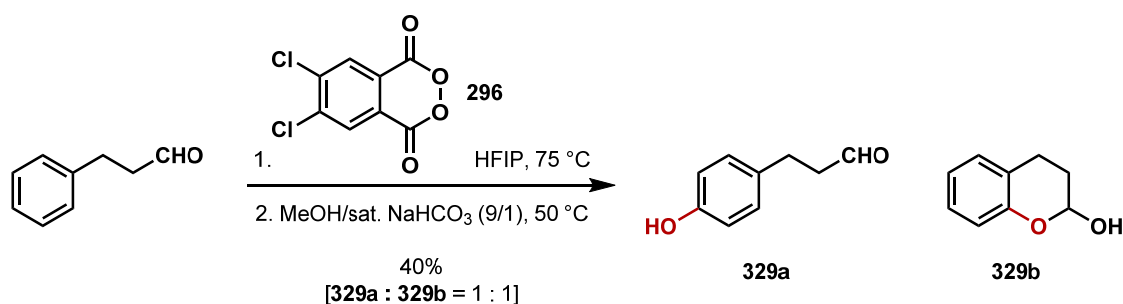
Diols 328a and 328b: Prepared following General Procedure A using methyl hydrocinnamyl alcohol (100.0 mg, 0.67 mmol, 1.00 eq), 4,5-dichlorophthaloyl peroxide (232.0 mg, 0.96 mmol, 1.30 eq., 87%), and HFIP (6.7 mL) at 50 °C for 48 hrs. The crude brown foam was purified by silica gel chromatography; 2 – 30% EtOAc in CH₂Cl₂ and hexane (1:1) to provide the title compounds **328a** and **328b** (59.0 mg, 0.36 mmol, 53%, **328a** : **328b** = 1.4 : 1) as an orange foam and the starting alcohol (24.0 mg, 0.16 mmol, 24%) as a clear colorless oil. The spectral data of the title compounds match that for **328a** and **328b**.⁹⁻¹⁰

Major Isomer (328a):

¹H-NMR (400 MHz, CDCl₃): δ 7.07 (d, 2H, *J* = 8.6 Hz), 6.75 (d, 2H, *J* = 8.6 Hz), 3.82 (m, 1H), 2.89 (m, 2H), 2.72 – 2.57 (m, 2H), 1.22 (d, 3H, *J* = 6.1 Hz).⁹

Minor Isomer (328b):

¹H-NMR (400 MHz, CDCl₃): δ 7.09 (m, 2H), 6.88 (m, 2H), 3.76 (m, 1H), 2.89 (m, 2H), 2.72 – 2.57 (m, 2H), 1.22 (d, 3H, *J* = 6.1 Hz).¹⁰



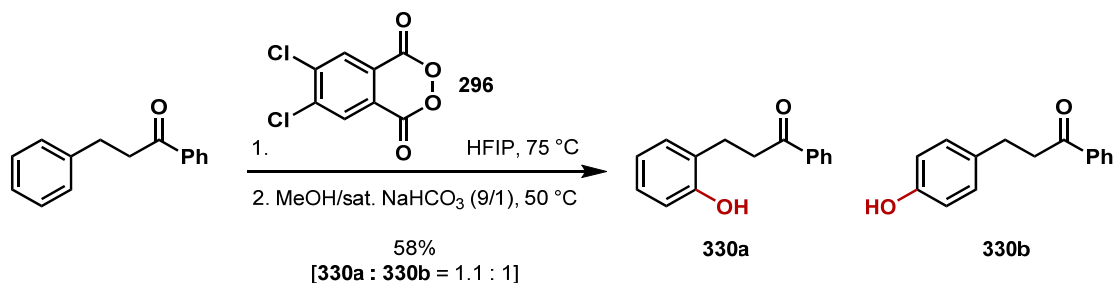
Aldehyde 329a and Lactol 329b: Prepared following [General Procedure B](#) using the hydrocinnamyl aldehyde (100.0 mg, 0.71 mmol, 1.00 eq., 95% pure), 4,5-dichlorophthaloyl peroxide (480.0 mg, 1.77 mmol, 2.50 eq., 86%), and HFIP (7.1 mL) at 75 °C for 36 hrs. The crude brown foam was purified by silica gel chromatography; 1 – 5% Et₂O in CH₂Cl₂ / hexane (1:1) to provide the aldehyde **329a** (21.0 mg, 0.14 mmol, 20%) and the lactol **329b** (21.0 mg, 0.14 mmol, 20%) as yellow foams. The spectral data of the title compounds match that for **329a** and **329b**.¹¹⁻¹²

Aldehyde 329a:

¹H-NMR (400 MHz, CDCl₃): δ 9.81 (t, 1H, *J* = 1.7 Hz), 7.06 (d, 2H, *J* = 8.6 Hz), 6.76 (d, 2H, *J* = 8.6 Hz), 4.59 (bs, 1H), 2.89 (t, 2H, *J* = 7.5 Hz), 2.74 (dd, 2H, *J* = 1.7, 7.5 Hz).¹¹

Lactol 329b:

¹H-NMR (400 MHz, CDCl₃): δ 7.12 (t, 1H, *J* = 7.9 Hz), 7.07 (d, 1H, *J* = 7.2 Hz), 6.89 (t, 1H, *J* = 7.2 Hz), 6.82 (d, 1H, *J* = 7.9 Hz), 5.62 (m, 1H), 3.03 (bs, 1H), 2.99 (m, 1H), 2.71 (dt, 1H, *J* = 5.1, 5.5 Hz), 2.06 – 1.99 (m, 2H).¹²



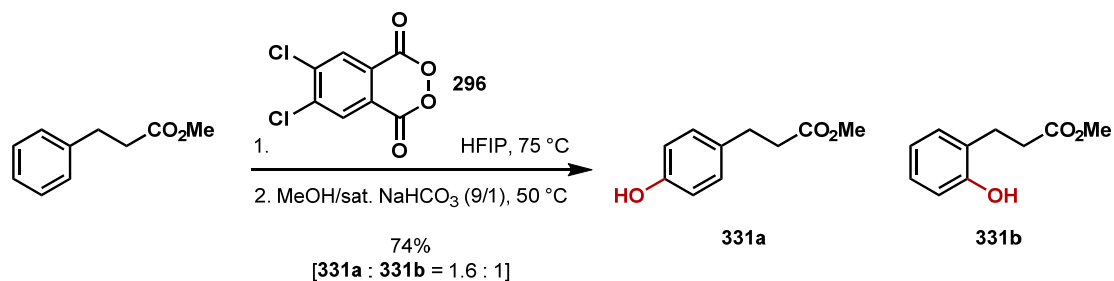
Ketones 330a and 330b: Prepared following General Procedure B using the hydrocinnamyl aryl ketone (100.0 mg, 0.48 mmol, 1.00 eq.), 4,5-dichlorophthaloyl peroxide (322.0 mg, 1.19 mmol, 2.50 eq., 86%), and HFIP (4.8 mL) at 75 °C for 36 hours. The crude brown foam was purified by silica gel chromatography; 1 – 10% Et₂O in CH₂Cl₂ / hexane (1:1) to provide the ketone **330a** (32.3 mg, 0.14 mmol, 30%) and the ketone **330b** (30.0 mg, 0.13 mmol, 28%) as orange foams. The spectral data of the title compounds match that for **330a** and **330b**.¹³⁻¹⁴

Major Isomer (330a):

¹H-NMR (400 MHz, CDCl₃): δ 7.98 (d, 2H, *J* = 7.2 Hz), 7.88 (bs, 1H), 7.58 (t, 1H, *J* = 7.2 Hz), 7.45 (t, 2H, *J* = 7.5 Hz), 7.11 (dd, 2H, *J* = 7.2, 7.5 Hz), 6.91 (d, 1H, *J* = 7.9 Hz), 6.85 (t, 1H, *J* = 7.5 Hz), 3.46 (dd, 2H, *J* = 5.8, 6.2 Hz), 3.04 (dd, 2H, *J* = 5.8, 6.2 Hz).¹³

Minor Isomer (330b):

¹H-NMR (400 MHz, CDCl₃): δ 7.95 (d, 2H, *J* = 6.8 Hz), 7.56 (t, 1H, *J* = 7.5 Hz), 7.45 (t, 2H, *J* = 7.5 Hz), 7.12 (d, 2H, *J* = 8.6 Hz), 6.77 (d, 2H, *J* = 8.6 Hz), 4.58 (bs, 1H), 3.26 (t, 2H, *J* = 7.7 Hz), 3.00 (dd, 2H, *J* = 7.7 Hz).¹⁴



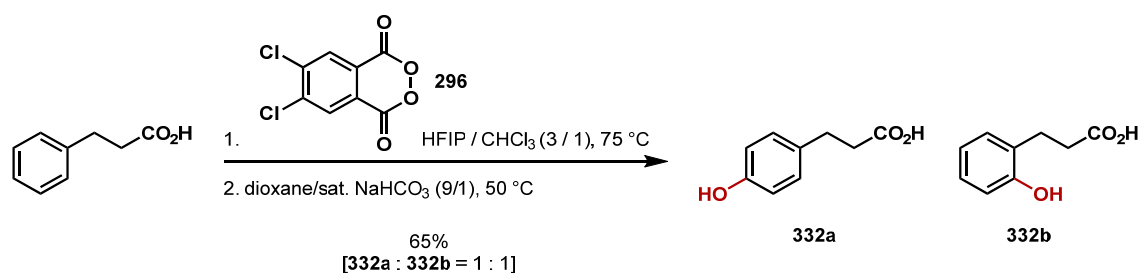
Esters 331a and 331b: Prepared following General Procedure B using the hydrocinnamyl methyl ester (100.0 mg, 0.61 mmol, 1.00 eq.), 4,5-dichlorophthaloyl peroxide (399.0 mg, 1.52 mmol, 2.50 eq., 89%), and HFIP (6.1 mL) at 75 °C for 36 hrs. The crude brown foam was purified by silica gel chromatography; 1 – 5% Et₂O in CH₂Cl₂ / hexane (1:1) to provide the esters **331a** and **331b** (81.3 mg, 0.55 mmol, 74%, **331a** : **331b** = 1.6 : 1) as a pale yellow foam and the starting ester (5.1 mg, 0.03 mmol, 5%) as a clear colorless oil. The spectral data of the title compounds match that for **331a** and **331b**.¹⁵⁻¹⁶

Major Isomer (331a):

¹H-NMR (400 MHz, CDCl₃): δ 7.26 (bs, 1H), 7.06 (d, 2H, *J* = 8.6 Hz), 6.88 (d, 2H, *J* = 8.6 Hz), 3.69 (s, 3H), 2.91 (t, 2H, *J* = 6.8 Hz), 2.73 (t, 2H, *J* = 6.8 Hz).¹⁵

Minor Isomer (331b):

¹H-NMR (400 MHz, CDCl₃): δ 7.11 (m, 2H), 6.75 (d, 2H, *J* = 8.6 Hz), 3.66 (s, 3H), 2.88 (t, 2H, *J* = 7.9 Hz), 2.59 (t, 2H, *J* = 7.9 Hz).¹⁶



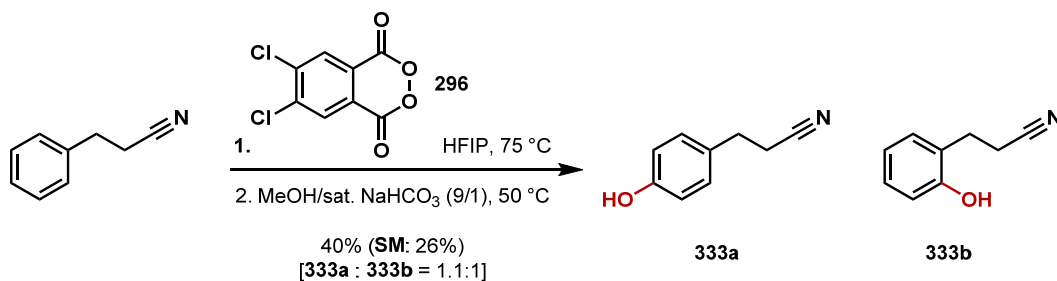
Acids 332a and 332b: Prepared following General Procedure B using hydrocinnamic acid (100.0 mg, 0.67 mmol, 1.00 eq.), 4,5-dichlorophthaloyl peroxide (451.0 mg, 1.67 mmol, 2.50 eq., 86%), CHCl_3 (1.7 mL), and HFIP (5.0 mL) at 75 °C for 48 hrs. After removal of the HFIP and CHCl_3 by continuous positive flow of nitrogen, the mixed phthalate diacid was placed under an atmosphere of N_2 , suspended in 1,4-dioxane (6.0 mL) added via syringe, and then a saturated aqueous mixture of NaHCO_3 (0.7 mL) was added via a syringe. The red-orange suspension was placed in an oil bath heated to 50 °C and stirred vigorously (700 rpm). After 1 hour the red solution was removed from the oil bath, acidified to a pH = 2 using 1 N HCl (3 mL), diluted with EtOAc (20 mL), poured into a separatory funnel containing brine (20 mL), and the layers were partitioned. The organics were washed with an aqueous phosphate buffer (2 x 20 mL, 0.2 M, pH = 4) and the residual organics were extracted from the aqueous layer with a mixture of EtOAc and brine (4 x 30 mL, 1:1). The combined organics were dried over solid Na_2SO_4 , decanted, and concentrated to reveal an orange solid. The orange solid was suspended in CH_2Cl_2 (30 mL), heated for 5 minutes with a heat gun, and sonicated for 1 minute. The residual orange mixture was filtered to remove the insoluble white solid 4,5-dichlorophthalic acid. The orange filtrate solution was concentrated to reveal an orange solid which was purified by silica gel chromatography; 1% CH_3OH and 1% AcOH in CH_2Cl_2 to provide the acids **332a** and **332b** (71.8 mg, 0.43 mmol, 65%, **332a** : **332b** = 1 : 1) as an orange solid mixture and the starting acid (12.0 mg, 0.08 mmol, 12%) as a white solid. The spectral data of the title compounds match that for **332a** and **332b**.^{17,18}

Acid 332a:

¹H-NMR (400 MHz, CDCl_3): δ 7.08 (d, 2H, $J = 8.6$ Hz), 6.76 (d, 2H, $J = 8.6$ Hz), 2.90 (t, 2 H, $J = 7.5$ Hz), 2.65 (t, 2 H, $J = 7.5$ Hz).¹⁷

Acid 332b:

¹H-NMR (400 MHz, CDCl_3): δ 7.11 (d, 2H, $J = 8.6$ Hz), 6.82 – 6.89 (m, 2H, $J = 8.6$ Hz), 2.92 (t, 2 H, $J = 6.5$ Hz), 2.78 (t, 2 H, $J = 6.5$ Hz).¹⁸



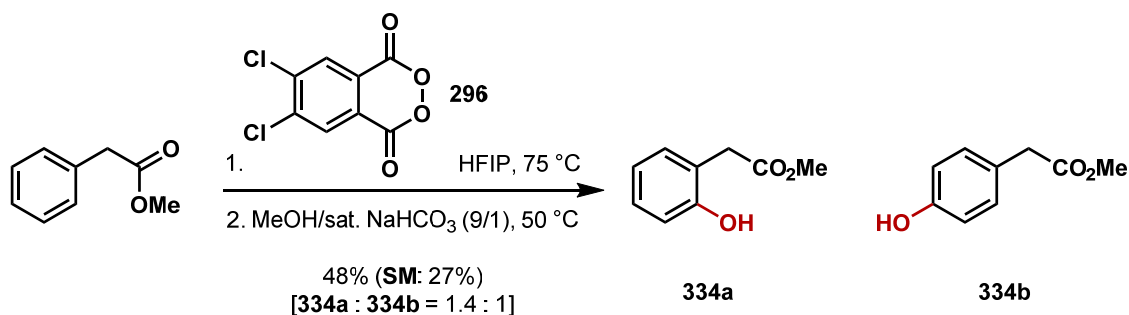
Nitriles 333a and 333b: Prepared following General Procedure B using the hydrocinnamyl nitrile (100.0 mg, 0.76 mmol, 1.00 eq.), 4,5-dichlorophthaloyl peroxide (516.0 mg, 1.91 mmol, 2.50 eq., 86%), and HFIP (7.6 mL) at 75 °C for 36 hrs. The crude brown foam was purified by silica gel chromatography; 1 – 10% Et₂O in CH₂Cl₂ / hexane (1:1) to provide the nitriles **333a** (23.1 mg, 0.16 mmol, 21%) and **333b** (21.0 mg, 0.14 mmol, 19%) as pale yellow foams and the starting nitrile (25.8 mg, 0.20 mmol, 26%) as a clear colorless oil. The spectral data of the title compounds match that for **333a** and **333b**.^{19,20}

Nitrile 333a:

¹H-NMR (400 MHz, CDCl₃): δ 7.11 (d, 2H, *J* = 8.6 Hz), 6.80 (d, 2H, *J* = 8.6 Hz), 4.67 (bs, 1H), 2.89 (t, 2H, *J* = 7.5 Hz), 2.58 (t, 2H, *J* = 7.5 Hz).¹⁹

Nitrile 333b:

¹H-NMR (400 MHz, CDCl₃): δ 7.17 (dd, 1H, *J* = 1.7, 7.2 Hz), 7.13 (dd, 1H, *J* = 1.7, 7.9 Hz), 6.91 (dt, 1H, *J* = 1.7, 7.2 Hz), 6.73 (d, 1H, *J* = 7.9 Hz), 4.85 (bs, 1H), 2.98 (t, 2H, *J* = 7.5 Hz), 2.67 (t, 2H, 7.5 Hz).²⁰



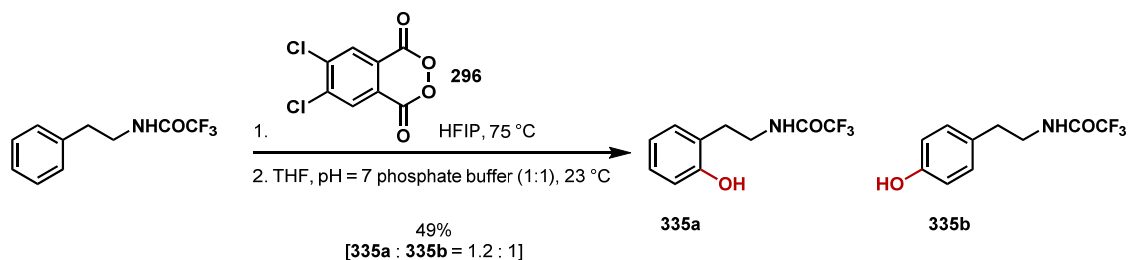
Esters 334a and 334b: Prepared following General Procedure B using the starting methyl ester (100.0 mg, 0.67 mmol, 1.00 eq.), 4,5-dichlorophthaloyl peroxide (436.0 mg, 1.67 mmol, 2.50 eq., 89%), and HFIP (6.7 mL) at 75 °C for 36 hrs. The crude orange foam was purified by silica gel chromatography; 1 – 10% Et₂O in CH₂Cl₂ / hexane (1:1) to provide the esters **334a** and **334b** (52.4 mg, 0.32 mmol, 48%, **334a** : **334b** = 1.4 : 1) as a pale yellow foam and the starting ester (27.1 mg, 0.18 mmol, 27%) as a clear colorless oil. The spectral data of the title compounds match that for **334a** and **334b**.²¹⁻²²

Major Isomer (334a):

¹H-NMR (400 MHz, CDCl₃): δ 7.33 (bs, 1H), 7.20 (m, 1H), 7.10 (dd, 1H, *J* = 1.6, 7.4 Hz), 6.94 (d, 1H, *J* = 8.2 Hz), 6.89 (dt, 1H, *J* = 1.2, 7.4 Hz), 3.75 (s, 3H), 3.68 (s, 2H).²¹

Minor Isomer (334b):

¹H-NMR (400 MHz, CDCl₃): δ 7.15 (d, 2H, *J* = 8.2 Hz), 6.78 (d, 2H, *J* = 8.2 Hz), 3.72 (s, 3 H), 3.58 (s, 2 H).²²



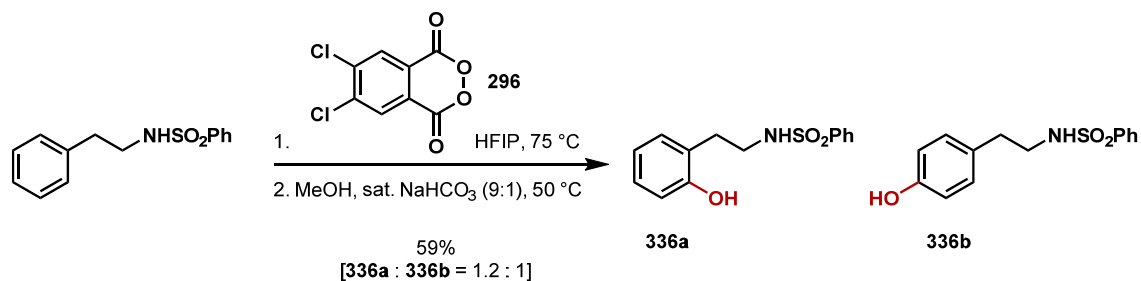
Amides 335a and 335b: Prepared following General Procedure B using the starting trifluoroacetamide (100.0 mg, 0.46 mmol, 1.00 eq.), 4,5-dichlorophthaloyl peroxide (523.0 mg, 1.84 mmol, 4.00 eq., 82%), and HFIP (4.6 mL) at 75 °C for 72 hrs. After removal of the HFIP by continuous positive flow of nitrogen, the mixed phthalate ester-acid was placed under an atmosphere of N₂, THF (2.3 mL) was added via syringe, and an aqueous phosphate buffer (2.3 mL, pH = 7, 0.2 M) was added via syringe. The yellow biphasic solution was stirred vigorously (1000 rpm) at 23 °C. After 24 hrs the solution was diluted with EtOAc (20 mL), poured into a separatory funnel containing an aqueous phosphate buffer (10 mL, pH = 7, 0.2 M), and the layers were partitioned. The organics were washed with an aqueous phosphate buffer (4 x 20 mL, 0.2 M, pH = 7) and the residual organics were extracted from the aqueous layer with EtOAc (4 x 30 mL). The combined organics were dried over solid Na₂SO₄, decanted, and concentrated. The crude brown foam was purified by silica gel chromatography; hexane → 25% acetone in hexane to provide the amides **335a** (28.8 mg, 0.12 mmol, 27%) and **335b** (23.6 mg, 0.10 mmol, 22%) as pale yellow foams.²³

Amide 335a:

¹H-NMR (400 MHz, CDCl₃): δ 7.17 – 7.10 (m, 2H), 7.05 (bs, 1H), 6.91 (dt, 1H, *J* = 1.0, 7.5 Hz), 6.80 (d, 1H, 8.2 Hz), 3.60 (q, 2H, *J* = 6.5 Hz), 2.93 (t, 2H, *J* = 6.5 Hz)

Amide 335b:

¹H-NMR (400 MHz, CDCl₃): δ 7.05 (d, 2H, *J* = 8.2 Hz), 6.80 (d, 2H, *J* = 8.2 Hz), 6.25 (bs, 1H), 3.58 (q, 2H, *J* = 6.5 Hz), 2.81 (t, 2H, *J* = 6.5 Hz).



Sulfonamides 336a and 336b: Prepared following General Procedure B using the sulfonamide (100.0 mg, 0.38 mmol, 1.00 eq.), 4,5-dichlorophthaloyl peroxide (265.0 mg, 0.96 mmol, 2.50 eq., 84%), and HFIP (3.8 mL) at 75 °C for 72 hrs. The crude orange foam was purified by silica gel chromatography; hexane – 25% acetone in hexane to provide the sulfonamide **336a** (34.8 mg, 0.13 mmol, 33%) as a yellow amorphous foam and **336b** (27.8 mg, 0.10 mmol, 26%) as a white solid.

Sulfonamide 336a:

$R_f = 0.40$ (35% acetone in hexane)

$^1\text{H-NMR}$ (400 MHz, CDCl_3): δ 7.78 (d, 2H, $J = 7.2$ Hz), 7.53 (d, 1H, $J = 7.9$ Hz), 7.45 (dt, 2H, $J = 7.2, 7.9$ Hz), 7.08 (t, 1H, 7.9 Hz), 6.97 (dd, 1H, $J = 1.4, 7.5$ Hz), 6.81 (t, 1H, $J = 7.5$ Hz), 6.75 (d, 1H, $J = 7.9$ Hz), 5.62 (bs, 1H), 4.99 (bs, 1H), 3.23 (m, 2H), 2.79 (t, 2H, $J = 6.5$ Hz)

$^{13}\text{C-NMR}$ (100 MHz, CDCl_3): δ 153.86, 139.46, 132.80, 132.60, 130.92, 129.07, 128.21, 127.00, 126.38, 124.40, 120.94, 115.60, 43.58, 30.39

IR (neat film, cm^{-1}): 3274, 1457, 1447, 1322, 1157, 1093, 755

HRMS (EC-CI): calcd. for $\text{C}_{14}\text{H}_{15}\text{NO}_3\text{S}$ [M] 277.0773, found 277.0779.

Sulfonamide 336b:

$R_f = 0.33$ (35% acetone in hexane)

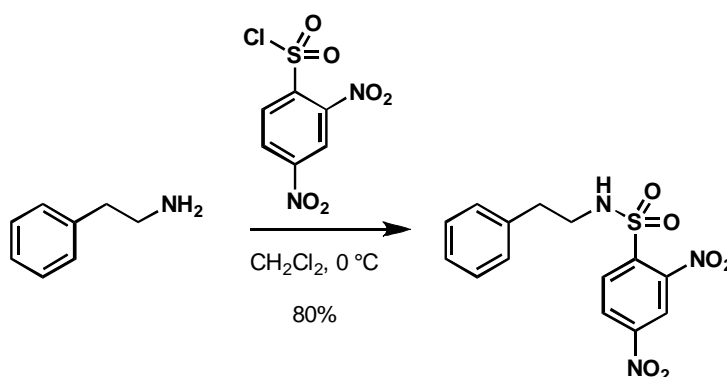
$^1\text{H-NMR}$ (400 MHz, $\text{C}_3\text{D}_6\text{O}$): δ 8.14 (bs, 1H), 7.85 (m, 2H), 7.60 (m, 3H), 6.97 (d, 2H, $J = 8.6$ Hz), 6.71 (d, 2H, $J = 8.6$ Hz), 6.45 (bs, 1H), 3.09 (m, 2H), 2.67 (t, 2H, $J = 7.2$ Hz)

$^{13}\text{C-NMR}$ (100 MHz, CDCl_3): δ 156.73, 142.01, 133.06, 130.51, 130.21, 129.88, 127.71, 115.99, 45.70, 35.86

IR (neat film, cm^{-1}): 3391, 3019, 2924, 1215, 757

HRMS (EC-Cl): calcd. for $\text{C}_{14}\text{H}_{15}\text{NO}_3\text{S}$ [M] 277.0773, found 277.0776.

M.P.: 116 – 121 °C



A solution of phenethylamine (0.29 g, 0.30 mL, 2.36 mmol, 2.10 eq.) in methylene chloride (11 mL) was placed in an ice water bath cooled to $0\text{ }^\circ\text{C}$ for 20 minutes upon which solid dinitrobenzene sulfonyl chloride (0.30 g, 1.13 mmol, 1.00 eq.) was added under a positive flow of nitrogen. After 2 hrs the golden yellow-orange solution was diluted with an aqueous phosphate buffer (20 mL, $\text{pH} = 7$, 0.2 M), poured into a separatory funnel, partitioned, and the organic layer was washed with an aqueous phosphate buffer (2 x 10 mL, $\text{pH} = 7$, 0.2 M). Residual organics were extracted from the aqueous layer with methylene chloride (2 x 10 mL), dried over solid Na_2SO_4 , decanted, and concentrated. The crude yellow-orange solid mixture was purified by silica gel chromatography; 10% acetone in hexane to afford the dinitrobenzene sulfonamide product as a yellow solid (0.32 g, 0.90 mmol, 80%).

$R_f = 0.61$ (50% acetone in hexane)

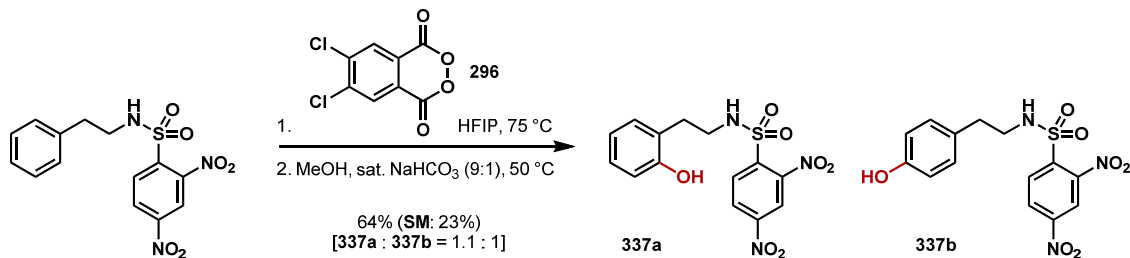
$^1\text{H-NMR}$ (400 MHz, CDCl_3): δ 8.59 (d, 1H, $J = 2.0$ Hz), 8.45 (dd, 1H, $J = 2.4, 8.6$ Hz), 8.19 (d, 1H, $J = 8.6$ Hz), 7.21 – 7.13 (m, 3H), 7.08 – 7.06 (m, 2H), 5.36 (t, 1H, $J = 5.8$ Hz), 3.50 (q, 2H, $J = 6.5$ Hz), 2.85 (t, 2H, $J = 6.5$ Hz)

$^{13}\text{C-NMR}$ (100 MHz, CDCl_3): δ 149.58, 147.80, 139.30, 137.15, 132.26, 128.76, 128.71, 127.13, 127.02, 120.73, 45.38, 36.01

IR (neat film, cm^{-1}): 1549, 1537, 1349, 1167, 747

HRMS (EC-CI): calcd. for C₁₄H₁₃N₃O₆S [M] 352.0603, found 352.0602.

M.P.: 117 – 120 °C



Sulfonamides 337a and **337b**: Prepared following General Procedure B using the starting dinitrosulfonamide (100.0 mg, 0.29 mmol, 1.00 eq.), 4,5-dichlorophthaloyl peroxide (197.0 mg, 0.71 mmol, 2.50 eq., 84%), and HFIP (2.9 mL) at 75 °C for 72 hrs. The crude orange foam was purified by silica gel chromatography; hexane – 25% acetone in hexane to provide the dinitrosulfonamides **337a** (34.1 mg, 0.09 mmol, 33%) and **337b** (33.2 mg, 0.09 mmol, 32%) as yellow solids and the starting dinitrosulfonamide as a yellow solid (22.7 mg, 0.07 mmol, 23%).

Sulfonamide **337a**:

R_f = 0.56 (50% acetone in hexane)

¹H-NMR (400 MHz, C₃D₆O): δ 8.70 (d, 1H, *J* = 2.4 Hz), 8.59 (dd, 1H, *J* = 2.4, 8.9 Hz), 8.27 (d, 1H, *J* = 8.9 Hz), 7.04 (dd, 1H, 1.7, 7.5 Hz), 6.95 (dt, 1H, *J* = 1.7, 7.5 Hz), 6.71 (dd, 1H, *J* = 1.0, 7.5 Hz), 6.63 (dt, 1H, *J* = 1.0, 7.5 Hz), 3.49 (t, 2H, *J* = 7.1 Hz), 2.85 (t, 2H, *J* = 7.1 Hz)

¹³C-NMR (100 MHz, CDCl₃): δ 155.13, 149.58, 147.80, 138.80, 132.04, 130.92, 127.75, 127.14, 124.44, 120.31, 119.55, 114.80, 43.58, 30.60

IR (neat film, cm⁻¹): 3349, 1538, 1350, 1167, 748

HRMS (EC-CI): calcd. for C₁₄H₁₃N₃O₇S [M] 367.0474, found 367.0471.

M.P.: 128 – 130 °C

Sulfonamide **336b**:

R_f = 0.53 (50% acetone in hexane)

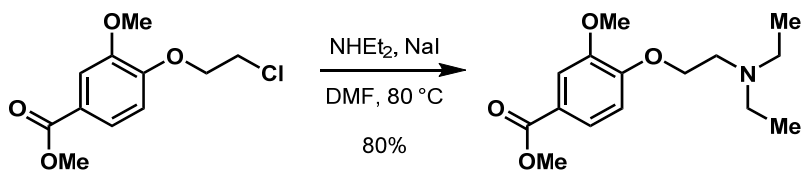
¹H-NMR (400 MHz, C₃D₆O): δ 8.70 (d, 1H, *J* = 1.2 Hz), 8.57 (m, 1H), 8.16 (dd, 1H, *J* = 1.6, 8.6 Hz), 6.97 (d, 2H, *J* = 8.2 Hz), 6.58 (d, 2H, *J* = 8.2 Hz), 3.46 (t, 2H, *J* = 7.1 Hz), 2.77 (t, 2H, *J* = 7.1 Hz)

¹³C-NMR (100 MHz, CDCl₃): δ 139.02, 132.01, 129.89, 128.93, 127.25, 120.22, 115.03, 45.62, 34.82

IR (neat film, cm⁻¹): 3391, 1538, 1350, 1165, 747

HRMS (EC-Cl): calcd. for C₁₄H₁₃N₃O₇S [M] 367.0474, found 367.0470.

M.P.: 134 – 136 °C



To a solution of methyl 4-(3-chloropropoxy)-3-methoxybenzoate (1.37 g, 5.30 mmol, 1.00 eq.) in dimethylformamide (28.5 mL) was added NaI (1.59 g, 10.59 mmol, 2.00 eq.) and diethylamine (1.64 mL, 15.89 mmol, 3.00 eq.). The flask was purged with N₂ and placed in an oil bath heated to 80 °C. After 24 hrs the solution was removed from the oil bath and allowed to cool to 23 °C, poured into a separatory funnel containing 3 N LiCl (150 mL), partitioned, and the organics were extracted from the aqueous layer with EtOAc (4 x 50 mL). The combined organics were washed with 3 N LiCl (1 x 50 mL) to remove residual DMF, washed with brine (1 x 50 mL), dried over solid Na₂SO₄, decanted, and concentrated. The crude mixture was purified by silica gel chromatography; 1% CH₃OH and 1% Et₃N in CH₂Cl₂ to provide the amine as an amber oil (1.25 g, 4.24 mmol, 80%).

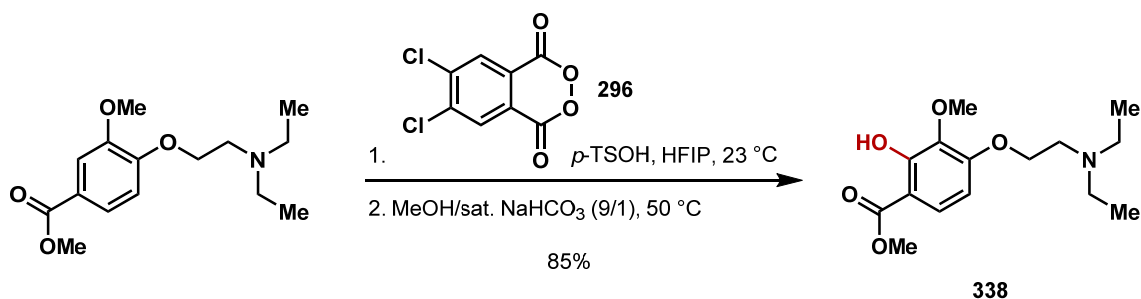
R_f = 0.40 (2% CH₃OH and 2% Et₃N in CH₂Cl₂)

¹H-NMR (400 MHz, CDCl₃): δ 7.64 (dd, 1H, *J* = 2.0, 8.6 Hz), 7.53 (d, 1H, *J* = 2.0 Hz), 6.90 (d, 1H, *J* = 8.2 Hz), 4.12 (t, 2H, *J* = 6.6 Hz), 3.90 (s, 3H), 3.89 (s, 3H), 2.61 (t, 2H, *J* = 7.1 Hz), 2.54 (q, 4H, *J* = 7.4 Hz), 1.99 (m, 2H), 1.01 (t, 6H, *J* = 7.4 Hz)

¹³C-NMR (100 MHz, CDCl₃): δ 166.92, 152.53, 148.81, 123.49, 122.4, 112.28, 111.52, 67.39, 56.01, 51.93, 49.07, 46.92, 26.61, 11.70

IR (neat film, cm⁻¹): 2967, 2809, 1717, 1293

HRMS (EC-CI): [M+Na]⁺ calc'd for C₁₆H₂₅NO₄: 318.16758. Found: 318.16729.



To a stirred solution of the starting amine (75.0 mg, 0.254 mmol, 1.00 eq.) in HFIP (2.5 mL) at 23 °C was added *p*-toluenesulfonic acid (43.7 mg, 0.254 mmol, 1.00 eq.). After 2 minutes 4,5-dichlorophthaloyl peroxide (89.0 mg, 0.33 mmol, 1.30 eq., 86%) was added. After 4 hrs the solvent was removed by a continuous flow of N₂ providing the mixed phthalate acid as a red solid. The crude solid was placed under an atmosphere of N₂, suspended in a deoxygenated mixture of methanol and saturated aqueous NaHCO₃ (9:1, 2.5 mL), and placed in an oil bath heated to 50 °C for 1 hr. The mixture was removed from the oil bath, cooled to 23 °C and an aqueous phosphate buffer (5 mL, 0.2 M, pH = 10) was added. The biphasic mixture was poured into a separatory funnel, partitioned, and the residual organics were extracted from the aqueous layer with EtOAc (3 x 5 mL). The combined organics were washed with an aqueous phosphate buffer (1 x 5 mL, 0.2 M, pH = 10), brine (1 x 5 mL), dried over solid Na₂SO₄, and concentrated. The crude mixture was purified by silica gel chromatography; 1% methanol and 1% triethylamine in CH₂Cl₂ to afford the phenol **338** as a clear colorless oil (67.7 mg, 0.22 mmol, 85%).

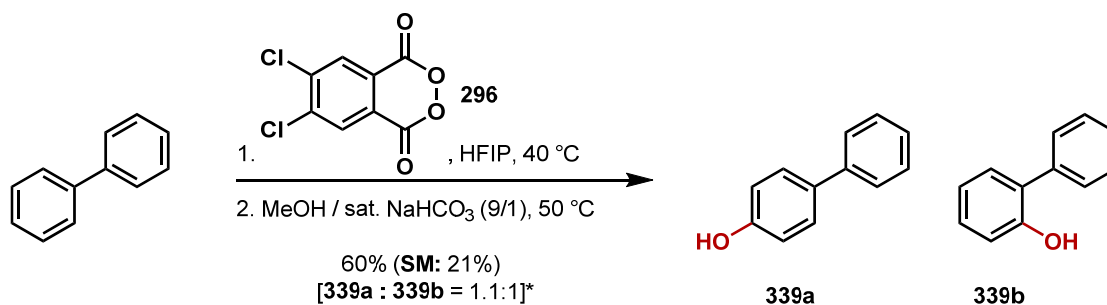
R_f = 0.40 (2% methanol and 2% triethylamine in CH₂Cl₂)

¹H NMR (400 MHz, CDCl₃): δ 10.79 (s, 1 H), 7.55 (d, 1H, *J* = 9.0 Hz), 6.48 (d, 1H, *J* = 9.0 Hz), 4.12 (m, 2H), 3.92 (s, 3H), 3.87 (s, 3H), 2.65 (t, 2H, *J* = 7.0 Hz), 2.57 (q, 4H, *J* = 7.0 Hz), 1.99 (t, 2H, *J* = 7.0 Hz), 1.04 (t, 6H, *J* = 7.0 Hz)

¹³C NMR (100 MHz, CDCl₃): δ 170.14, 157.28, 155.71, 136.35, 125.27, 106.52, 103.90, 66.84, 60.31, 51.76, 48.86, 46.66, 26.37, 11.21

IR (neat film, cm⁻¹): 3369, 2966, 2917, 1720, 1240

HRMS (EC-CI): [M+H]⁺ calc'd for C₁₆H₂₆NO₅: 312.1806; found: 312.1800.



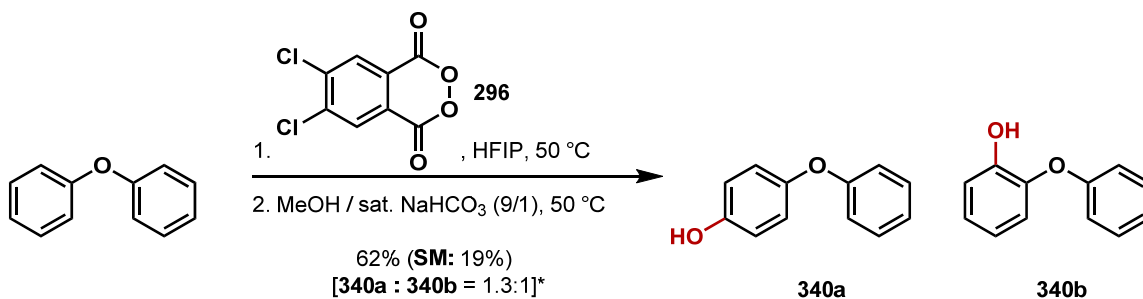
Phenols 339a and 339b: Prepared following General Procedure A using biphenyl (100.0 mg, 0.65 mmol, 1.00 eq.), 4,5-dichlorophthaloyl peroxide (226.0 mg, 0.84 mmol, 1.30 eq., 87%), and HFIP (6.5 mL) at 40 °C for 24 hrs. The crude orange foam was purified by silica gel chromatography; 1 – 10% Et₂O in CH₂Cl₂ / hexane (1:1) to afford the phenols **339a** (35.0 mg, 0.21 mmol, 32%) and **339b** (31.0 mg, 0.18 mmol, 28%) as pale yellow solids and the starting biphenyl as a white solid (21.1 mg, 0.13 mmol, 21%). The spectral data of the title compounds match that of the phenols **339a** and **339b**.⁵

Phenol 339a:

¹H NMR (400 MHz, CDCl₃): δ 7.53 (m, 2H), 7.48 (d, 2H, *J* = 8.6 Hz), 7.41 (t, 2H, *J* = 7.9 Hz), 7.30 (t, 1H, *J* = 7.9 Hz), 7.25 (m, 1H), 6.91 (d, 2H, *J* = 8.6 Hz), 4.70 (bs, 1H)

Phenol 339b:

¹H NMR (400 MHz, CDCl₃): δ 7.48 (m, 4H), 7.40 (m, 1H), 7.26 (m, 2H), 7.00 (dt, 1H, *J* = 1.3, 6.1 Hz), 6.99 (d, 1H, *J* = 7.8 Hz), 5.18 (bs, 1H)



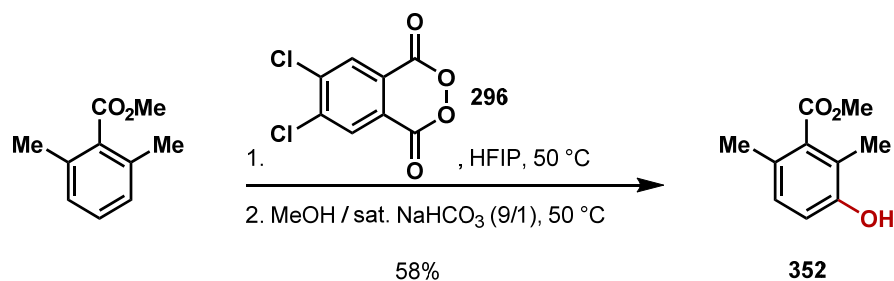
Phenols 340a and 340b: Prepared following General Procedure A using diphenyl ether (100.0 mg, 0.59 mmol, 1.00 eq.), 4,5-dichlorophthaloyl peroxide (207.0 mg, 0.76 mmol, 1.30 eq., 86%), and HFIP (6.5 mL) at 50 °C for 24 hrs. The crude orange foam was purified by silica gel chromatography; 1 – 10% Et₂O in CH₂Cl₂ / hexane (1:1) to afford the phenols **340a** (37.6 mg, 0.20 mmol, 35%) and **340b** (29.0 mg, 0.16 mmol, 27%) as pale yellow amorphous oils and the starting diphenyl ether as a clear colorless oil (18.6 mg, 0.11 mmol, 19%). The spectral data of the title compounds match that of the phenols **340a** and **340b**.⁵

Phenol 340a:

¹H NMR (400 MHz, CDCl₃): δ 7.30 (m, 2H), 7.04 (t, 1H, *J* = 7.5 Hz), 6.93 (m, 4H, *J* = 7.9 Hz), 6.81 (d, 1H, *J* = 9.2 Hz) 4.56 (bs, 1H)

Phenol 340b:

¹H NMR (400 MHz, CDCl₃): δ 7.34 (dd, 2H, *J* = 7.5, 8.5 Hz), 7.12 (t, 1H, *J* = 7.5 Hz), 7.04 (m, 4H), 6.90 – 6.84 (m, 2H), 5.55 (bs, 1H)



Phenol 352: Prepared following General Procedure B using 2,6-dimethyl methylbenzoate (100.0 mg, 0.61 mmol, 1.00 eq.), 4,5-dichlorophthaloyl peroxide (422.0 mg, 1.52 mmol, 2.50 eq., 84%), and HFIP (6.1 mL) at 75 °C for 48 hrs. The crude orange foam was purified by silica gel chromatography; pentane and then hexane → 15% acetone in hexane to afford the phenol **352** as a pale yellow amorphous oil (63.0 mg, 0.35 mmol, 58%).

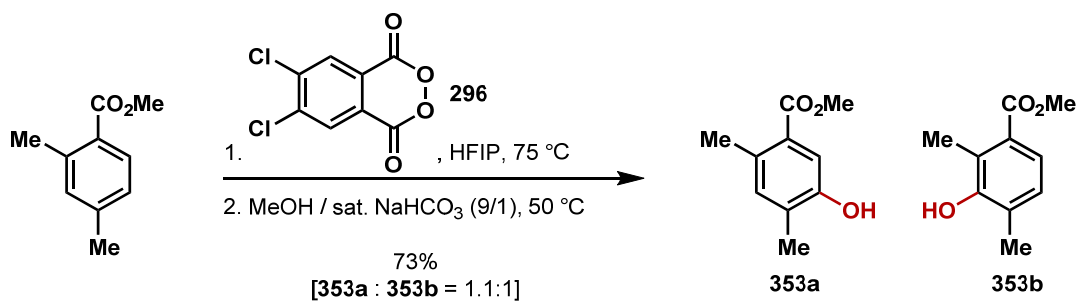
$R_f = 0.46$ (50% Et₂O in hexane)

¹H NMR (400 MHz, CDCl₃): δ 6.91 (d, 1H, $J = 8.2$ Hz), 6.72 (d, 1H, $J = 8.2$ Hz), 4.64 (bs, 1H), 3.91 (s, 3H), 2.22 (s, 3H), 2.18 (s, 3H)

¹³C NMR (100 MHz, CDCl₃): δ 170.77, 151.81, 135.07, 128.30, 126.50, 121.10, 116.06, 52.14, 18.87, 12.85

IR (neat film, cm⁻¹): 3399, 2360, 2341, 1706, 1293, 1047

HRMS (EC-CI): calcd. for C₁₀H₁₂O₃ [M] 180.0786, found 180.0787.



Phenols 353a and **353b**: Prepared following General Procedure B using 2,4-dimethyl methylbenzoate (150.0 mg, 0.91 mmol, 1.00 eq.), 4,5-dichlorophthaloyl peroxide (649.0 mg, 2.28 mmol, 2.50 eq., 82%), and HFIP (9.1 mL) at 75 °C for 48 hrs. The crude orange foam was purified by silica gel chromatography; pentane and then hexane → 30% EtOAc in hexane to afford the phenol **353a** as a pale yellow amorphous oil (63.2 mg, 0.35 mmol, 38%) and phenol **353b** as a pale yellow oil (57.4 mg, 0.22 mmol, 35%). The spectral data for the title compound matches that of phenol **353a**.²⁴

Phenol 353a:

¹H NMR (400 MHz, CDCl₃): δ 7.36 (s, 1H), 6.99 (s, 1H), 3.86 (s, 3H), 2.48 (s, 3H), 2.25 (s, 3H)

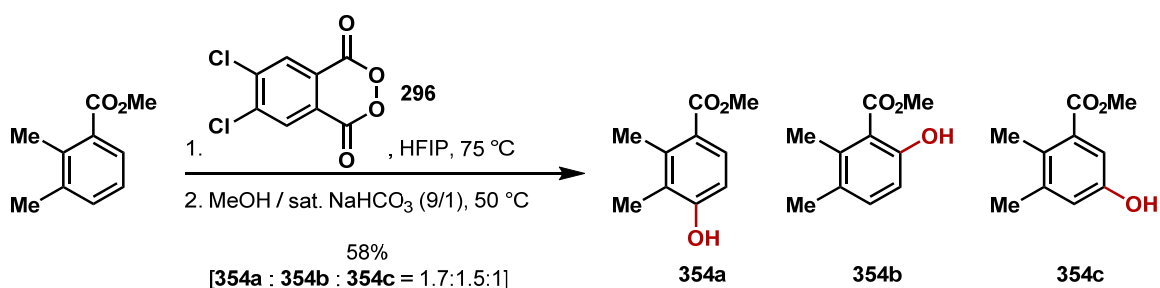
Phenol 353b:

¹H NMR (400 MHz, CDCl₃): δ 7.37 (d, 1H, *J* = 7.8 Hz), 7.00 (d, 1H, *J* = 7.8 Hz), 4.91 (bs, 1H), 3.87 (s, 3H), 2.48 (s, 3H), 2.28 (s, 3H)

¹³C NMR (100 MHz, CDCl₃): δ 168.41, 152.57, 132.98, 129.10, 127.63, 124.65, 122.46, 51.87, 16.44, 12.63

IR (neat film, cm⁻¹): 3477, 2952, 1702, 1435, 1273, 1054

HRMS (EC-CI): calcd. for C₁₀H₁₃O₃ [M+H]⁺ 181.0865, found 181.0865.



Phenols 354a, 354b, and 354c: Prepared following [General Procedure B](#) using 2,3-dimethyl methylbenzoate (100.0 mg, 0.61 mmol, 1.00 eq.), 4,5-dichlorophthaloyl peroxide (422.0 mg, 1.52 mmol, 2.50 eq., 84%), and HFIP (6.1 mL) at 75 °C for 48 hrs. The crude orange foam was purified by silica gel chromatography; 1 – 5% Et₂O in hexane / CH₂Cl₂ (1:1) to afford the phenols **354a** as a pale yellow amorphous oil (25.9 mg, 0.14 mmol, 24%), **354b** as a pale yellow amorphous oil (21.8 mg, 0.12 mmol, 20%), and **354c** as a pale yellow foam (14.9 mg, 0.08 mmol, 14%). The spectral data for the title compounds matches that for phenols **354a** and **354b**.^{25, 26}

Phenol 354a:

¹H NMR (400 MHz, CDCl₃): δ 7.65 (d, 1H, *J* = 8.2 Hz), 6.63 (d, 1H, *J* = 8.2 Hz), 3.85 (s, 3H), 2.51 (s, 3H), 2.20 (s, 3H)

Phenol 354b:

¹H NMR (400 MHz, CDCl₃): δ 10.58 (bs, 1H), 7.28 (d, 1H, *J* = 7.8 Hz), 7.13 (d, 1H, *J* = 7.8 Hz), 3.88 (s, 3H), 2.45 (s, 3H), 2.32 (s, 3H)

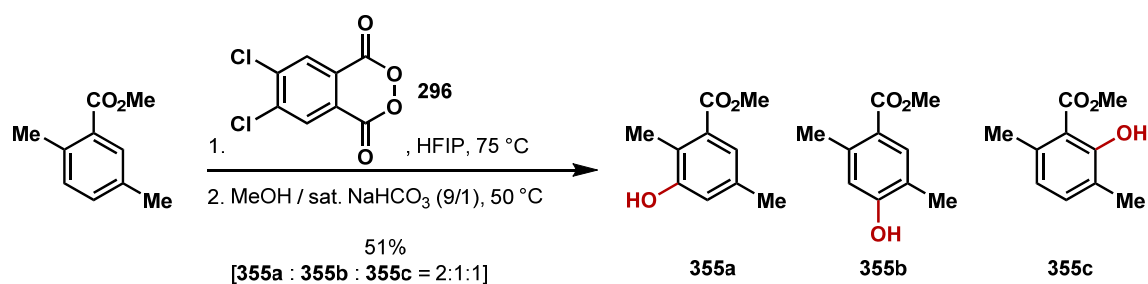
Phenol 354c:

¹H NMR (400 MHz, CDCl₃): δ 7.10 (d, 1H, *J* = 2.7 Hz), 6.80 (d, 1H, *J* = 2.7 Hz), 5.25 (bs, 1H), 3.87 (s, 3H), 2.35 (s, 3H), 2.26 (s, 3H)

¹³C NMR (125 MHz, CDCl₃): δ 168.74, 152.61, 139.69, 131.72, 129.79, 120.41, 114.08, 51.99, 20.69, 15.80

IR (neat film, cm⁻¹): 3398, 1718, 1436, 1225

HRMS (EC-CI): calcd. for C₁₀H₁₃O₃ [M] 180.0786, found 180.0785.



Phenols 355a, 355b, and 355c: Prepared following General Procedure B using 2,5-dimethyl methylbenzoate (100.0 mg, 0.61 mmol, 1.00 eq.), 4,5-dichlorophthaloyl peroxide (422.0 mg, 1.52 mmol, 2.50 eq., 84%), and HFIP (6.1 mL) at 75 °C for 48 hrs. The crude orange foam was purified by silica gel chromatography; pentane and then hexane → 15% acetone in hexane to afford the phenols **355a** (27.7 mg, 0.15 mmol, 25%) and **355b** (14.5 mg, 0.08 mmol, 13%) as pale yellow foams, and **355c** as a pale yellow solid (13.9 mg, 0.08 mmol, 13%). The spectral data for the title compounds matches that for phenols **355a**, **355b**, and **355c**.^{27,28}

Phenol 355a:

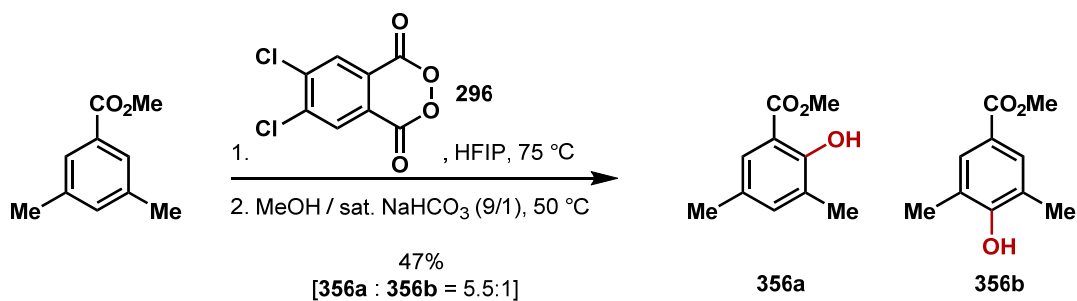
¹H NMR (400 MHz, CDCl₃): δ 7.23 (s, 1H), 6.77 (s, 1H), 5.22 (bs, 1H), 3.88 (s, 3H), 2.40 (s, 3H), 2.27 (s, 3H)

Phenol 355b:

¹H NMR (400 MHz, CDCl₃): δ 7.77 (s, 1H), 6.62 (s, 1H), 5.57 (bs, 1H), 3.85 (s, 3H), 2.52 (s, 3H), 2.22 (s, 3H)

Phenol 355c:

¹H NMR (400 MHz, CDCl₃): δ 11.58 (bs, 1H), 7.15 (d, 1H, *J* = 7.5 Hz), 6.62 (d, 1H, *J* = 7.5 Hz), 3.95 (s, 3H), 2.50 (s, 3H), 2.22 (s, 3H)



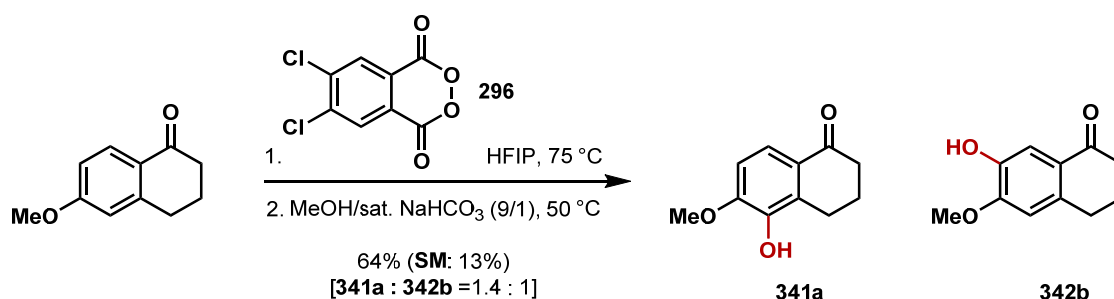
Phenols 356a and 356b: Prepared following General Procedure B using 3,5-dimethyl methylbenzoate (100.0 mg, 0.61 mmol, 1.00 eq.), 4,5-dichlorophthaloyl peroxide (422.0 mg, 1.52 mmol, 2.50 eq., 84%), and HFIP (6.1 mL) at 75 °C for 48 hrs. The crude orange foam was purified by silica gel chromatography; pentane and then hexane \rightarrow 15% acetone in hexane to afford the phenol **356a** (44.0 mg, 0.24 mmol, 40%) as a white solid and the phenol **356b** (7.8 mg, 0.04 mmol, 7%) as a pale yellow foam. The spectral data for the title compounds matches that for phenols **356a** and **356b**.^{26, 29}

Phenol 356a:

¹H NMR (400 MHz, CDCl₃): δ 10.83 (bs, 1H) 7.48 (bs, 1H), 7.15 (bs, 1H), 3.93 (s, 3H), 2.25 (s, 3H), 2.23 (s, 3H)

Phenol 356b:

¹H NMR (400 MHz, CDCl₃): δ 7.80 (s, 2H), 5.34 (bs, 1H), 3.87 (s, 3H), 2.27 (s, 6H)



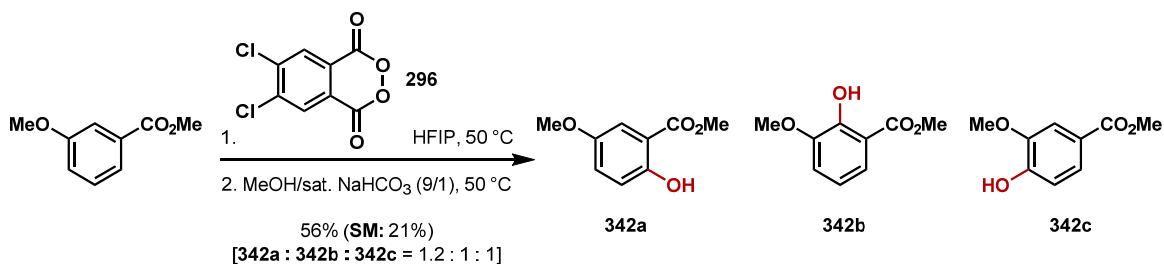
Tetralones 341a and 341b: Prepared following General Procedure B using 6-methoxy tetralone (100.0 mg, 0.57 mmol, 1.00 eq.), 4,5-dichlorophthaloyl peroxide (367.0 mg, 1.42 mmol, 2.50 eq., 90%), and HFIP (5.7 mL) at 75 °C for 36 hrs. The crude brown foam was purified by silica gel chromatography; 1 – 20% EtOAc in CH₂Cl₂ / hexane (1:1) to afford the phenols **341a** (41.0 mg, 0.21 mmol, 38%) and **341b** (29.0 mg, 0.15 mmol, 48%) as yellow solids and the starting tetralone (13.0 mg, 0.07 mmol, 13%) as a pale yellow solid. The spectra of the title compounds match that for **341a** and **341b**.^{30,31}

Major Isomer (341a):

¹H-NMR (400 MHz, CDCl₃): δ 7.68 (d, 1H, *J* = 8.6 Hz), 6.84 (d, 1H, *J* = 8.6 Hz), 5.71 (bs, 1H), 3.96 (s, 3H), 2.93 (t, 2H, *J* = 6.2 Hz), 2.60 (t, 2H, *J* = 6.2 Hz), 2.11 (ddd, 2H, *J* = 6.2 Hz).³⁰

Minor Isomer (341b):

¹H-NMR (400 MHz, CDCl₃): δ 7.56 (s, 1H), 6.66 (s, 1H), 5.52 (bs, 1H), 3.95 (s, 3H), 2.88 (t, 2H, *J* = 6.5 Hz), 2.59 (t, 2H, *J* = 6.5 Hz), 2.10 (ddd, 2H, *J* = 6.5 Hz).³¹



Phenols 342a, 342b, and 342c: Prepared following General Procedure A using 3-methoxy methylbenzoate (100.0 mg, 0.60 mmol, 1.00 eq.), 4,5-dichlorophthaloyl peroxide (212.0 mg, 0.78 mmol, 1.30 eq., 86%), and HFIP (6.0 mL) at 50 °C for 24 hrs. The crude brown foam was purified by silica gel chromatography; 1 – 20% Et₂O in CH₂Cl₂ / hexane (1:1) to provide the phenols **342a** (22.1 mg, 0.12 mmol, 20%), **342b** (19.7 mg, 0.11 mmol, 18%), **342c** (18.8 mg, 0.10 mmol, 17%) as pale yellow solids and the starting benzoate (20.9 mg, 0.13 mmol, 21%) as a clear colorless oil. The spectra of the title compounds match that for **342a**, **342b**, and **342c**.^{5,6,32,33}

Major Isomer (342a):

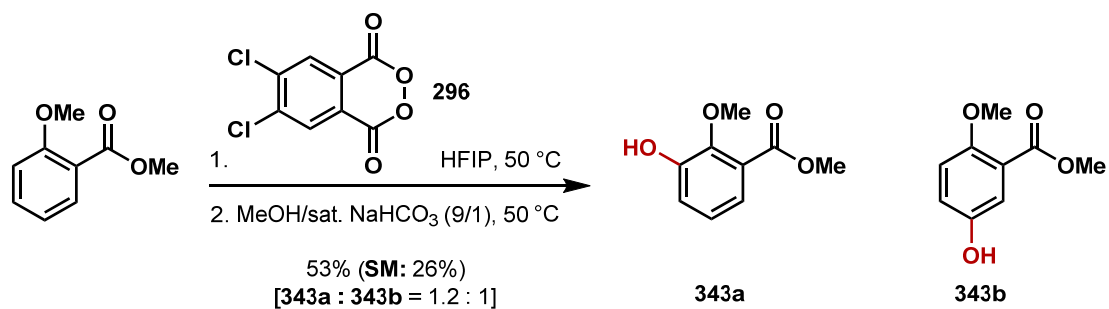
¹H-NMR (400 MHz, CDCl₃): δ 10.37 (bs, 1H), 7.29 (d, 1H, *J* = 3.3 Hz), 7.08 (dd, 1H, *J* = 3.3, 8.9 Hz), 6.92 (d, 1H, *J* = 8.9 Hz), 3.95 (s, 3H), 3.78 (s, 3H).³²

Minor Isomer (342b):

¹H-NMR (400 MHz, CDCl₃): δ 11.00 (bs, 1H), 7.43 (dd, 1H, *J* = 1.5, 8.2 Hz), 7.04 (d, 1H, *J* = 8.2 Hz), 6.83 (t, 1H, *J* = 8.2 Hz), 3.95 (s, 3H), 3.91 (s, 3H).^{5,6,33}

Minor Isomer (342c):

¹H-NMR (400 MHz, CDCl₃): δ 7.64 (d, 1H, *J* = 8.2 Hz), 7.55 (d, 1H, *J* = 2.1 Hz), 6.94 (d, 1H, *J* = 8.2 Hz), 5.97 (bs, 1H), 3.95 (s, 3H), 3.89 (s, 3H).^{5,6}



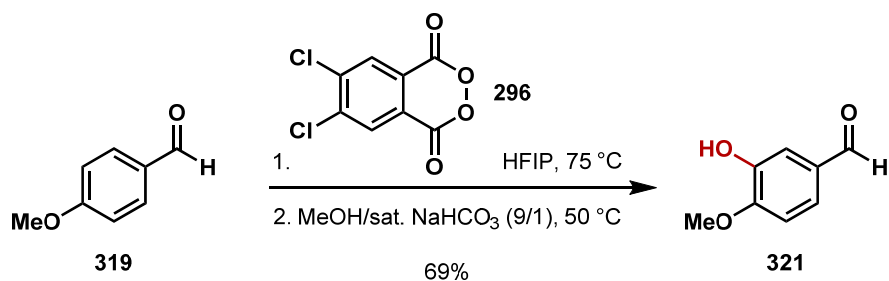
Phenols 343a and 343b: Prepared following [General Procedure A](#) using methyl salicylate (100.0 mg, 0.60 mmol, 1.00 eq.), 4,5-dichlorophthaloyl peroxide (212.0 mg, 0.78 mmol, 1.30 eq., 86%), and HFIP (6.0 mL) at 50 °C for 24 hrs. The crude brown foam was purified by silica gel chromatography; 1 – 20% Et₂O in CH₂Cl₂ and hexane (1:1) to afford the phenols **343a** (31.0 mg, 0.17 mmol, 28%) and **343b** (27.2 mg, 0.15 mmol, 25%) as yellow solids and the starting salicylate (25.6 mg, 0.15 mmol, 26%) as a clear colorless oil. The spectra of the title compounds match that for **343a** and **343b**.^{34, 35}

Major Isomer (343a):

¹H-NMR (400 MHz, CDCl₃): δ 7.40 (dd, 1H, *J* = 1.7, 8.2 Hz), 7.15 (dd, 1H, *J* = 1.7, 8.2 Hz), 7.05 (t, 1H, *J* = 8.2 Hz), 5.91 (bs, 1H), 3.93 (s, 3H), 3.92 (s, 3H).³⁴

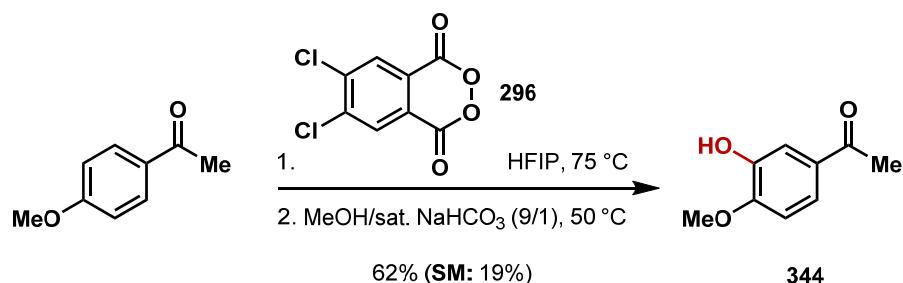
Minor Isomer (343b):

¹H-NMR (400 MHz, CDCl₃) δ 7.29 (d, 1H, *J* = 3.4 Hz), 6.97 (dd, 1H, *J* = 3.4, 8.9 Hz), 6.88 (d, 1H, *J* = 8.9 Hz), 4.52 (bs, 1H), 3.89 (s, 3H), 3.86 (s, 3H).³⁵



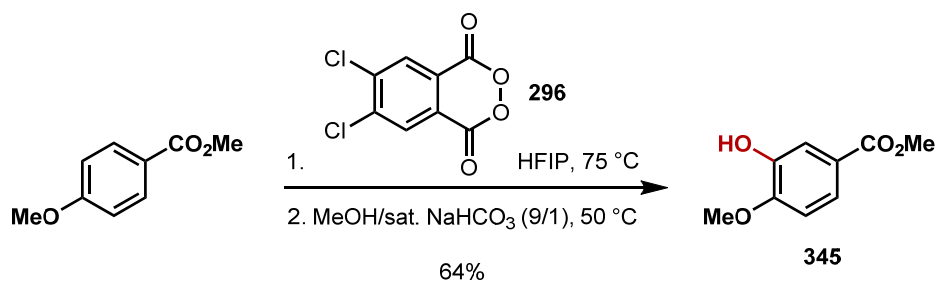
Isovanillin 321: Prepared following [General Procedure B](#) using *p*-anisaldehyde (**319**) (30.0 mg, 0.22 mmol, 1.00 eq.), 4,5-dichlorophthaloyl peroxide (239.0 mg, 0.88 mmol, 4.00 eq., 86%), and HFIP (2.2 mL) at 75 °C for 36 hrs. The crude golden orange foam was purified by silica gel chromatography; 1 – 10% Et₂O in CH₂Cl₂ and hexane (1:1) to afford *isovanillin* (**321**) (23.0 mg, 0.15 mmol, 69%) as a yellow solid. The spectra of the title compound matches that for **321**.^{5,6}

¹H-NMR (400 MHz, CDCl₃): δ 9.85 (s, 1H), 7.45 (s, 1H), 7.44 (dd, 1H, *J* = 2.1, 6.5 Hz), 6.98 (d, 1H, *J* = 9.9 Hz), 6.72 (s, 1H), 3.99 (s, 3H).^{5,6}



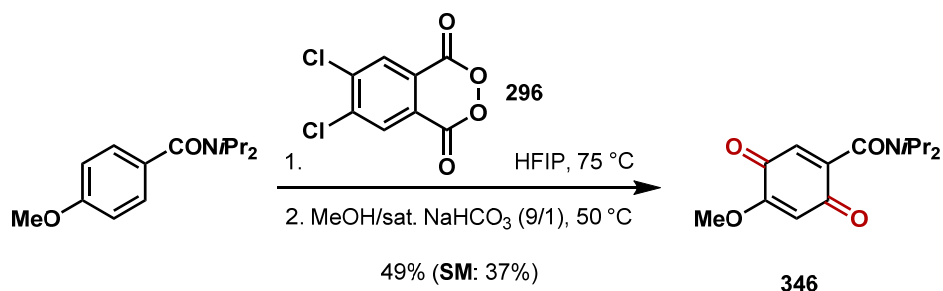
Ketone 344: Prepared following General Procedure B using 4-methoxy acetophenone (100.0 mg, 0.67 mmol, 1.00 eq.), 4,5-dichlorophthaloyl peroxide (446.0 mg, 1.67 mmol, 2.50 eq., 86%), and HFIP (6.7 mL) at 75 °C for 36 hrs. The crude brown foam was purified by silica gel chromatography; 1 – 10% Et₂O in CH₂Cl₂ and hexane (1:1) to afford the ketone **344** (68.5 mg, 0.41 mmol, 62%) as a yellow solid and the starting acetophenone (18.8 mg, 0.13 mmol, 19%) as a white solid. The spectra of the title compound matches that for **344**.³⁶

¹H-NMR (400 MHz, CDCl₃): δ 7.54 (dd, 1H, *J* = 2.1, 10.6 Hz), 7.53 (s, 1H), 6.89 (d, 1H, *J* = 8.2 Hz), 5.64 (bs, 1H), 3.97 (s, 3H), 2.55 (s, 3H).³⁶



Phenol 345: Prepared following General Procedure B using 4-methoxy methylbenzoate (100.0 mg, 0.60 mmol, 1.00 eq.), 4,5-dichlorophthaloyl peroxide (408.0 mg, 1.50 mmol, 2.50 eq., 86%), and HFIP (6.0 mL) at 75 °C for 36 hrs. The crude brown foam was purified by silica gel chromatography; 1 – 20% Et₂O in CH₂Cl₂ and hexane (1:1) to afford the phenol **345** (70.0 mg, 0.39 mmol, 64%) as a yellow solid and the starting benzoate (5.0 mg, 0.03 mmol, 5%) as a white solid. The spectra of the title compound matches that for **345**.³⁷

¹H-NMR (400 MHz, CDCl₃): δ 7.62 (dd, 1H, *J* = 2.0, 8.6 Hz), 7.59 (d, 1H, *J* = 2.0 Hz), 6.87 (d, 1H, *J* = 8.6 Hz), 5.61 (s, 1H), 3.95 (s, 3H), 3.88 (s, 3H).³⁷



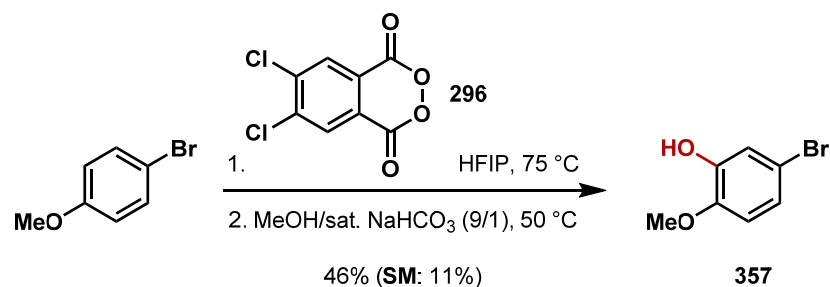
***p*-Quinone 346:** Prepared following General Procedure B using 4-methoxy diisopropylamide (90.0 mg, 0.35 mmol, 1.00 eq.), 4,5-dichlorophthaloyl peroxide (259.0 mg, 0.96 mmol, 2.50 eq., 86%), and HFIP (3.8 mL) at 75 °C for 36 hrs. The crude brown foam was purified by silica gel chromatography; 1 – 30% EtOAc in CH₂Cl₂ and hexane (1:1) to afford the quinone **346** (50.0 mg, 0.19 mmol, 49%) as a dark yellow solid and the starting amide (33.7 mg, 0.14 mmol, 37%) as a viscous yellow oil.

¹H-NMR (500 MHz, C₃D₆O): δ 6.56 (s, 1H), 6.04 (s, 1H), 3.87 (s, 3H), 3.79 (ddd, 1H, *J* = 6.6 Hz), 3.56 (ddd, 1H, *J* = 6.9 Hz), 1.44 (bs, 6H), 1.14 (bs, 1H)

¹³C-NMR (500 MHz, C₃D₆O): δ 186.09, 182.53, 163.92, 160.03, 145.74, 129.05, 107.78, 56.80, 51.68, 46.24, 20.71, 20.59, 20.45, 20.17

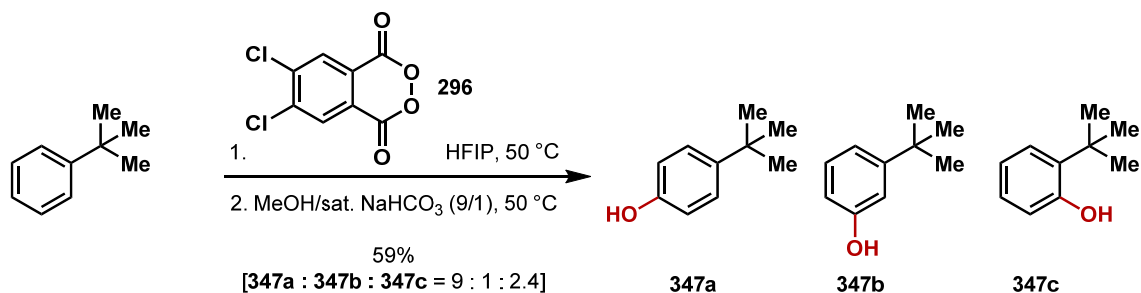
IR (neat film, cm⁻¹): 3419, 1637

HRMS (EC-Cl): calcd. for C₁₄H₂₁NO₄ [M+2H]²⁺ 267.1471, found 267.1474.



Phenol 357: Prepared following General Procedure A using 4-bromoanisole (100.0 mg, 0.54 mmol, 1.00 eq.), 4,5-dichlorophthaloyl peroxide (186.0 mg, 0.70 mmol, 1.30 eq., 87%), and HFIP (5.4 mL) at 50 °C for 24 hrs. The crude brown foam was purified by silica gel chromatography; 1 – 10% Et₂O in CH₂Cl₂ and hexane (1:1) to afford the phenol **357** (50.0 mg, 0.25 mmol, 46%) as a pale yellow amorphous oil and the starting 4-bromoanisole (11.0 mg, 0.05 mmol, 11%) as a clear colorless oil. The spectra of the title compound matches that for **357**.³⁸

¹H-NMR (400 MHz, CDCl₃): δ 7.06 (d, 1H, *J* = 2.4 Hz), 6.96 (dd, 1H, *J* = 2.4, 8.6 Hz), 6.71 (d, 1H, *J* = 8.6 Hz), 5.63 (bs, 1H), 3.87 (s, 3H).³⁸



Phenols 347a, 347b, and 347c: Prepared following General Procedure A using *tert*-butyl benzene (100.0 mg, 0.75 mmol, 1.00 eq.), 4,5-dichlorophthaloyl peroxide (259.0 mg, 0.97 mmol, 1.30 eq., 87%), and HFIP (7.5 mL) at 50 °C for 24 hrs. The crude brown foam was purified by silica gel chromatography; 1 – 5% Et₂O in CH₂Cl₂ and hexane (1:1) to afford the phenols **347a** and **347b** (53.4 mg, 0.36 mmol, 48%, **347a** : **347b** = 9 : 1) as an orange foam and **347c** (12.6 mg, 0.08 mmol, 11%) as a pale yellow foam. The spectra of the title compounds match that for **347a**, **347b**, and **347c**.⁵⁻⁶

Major Isomer (347a):

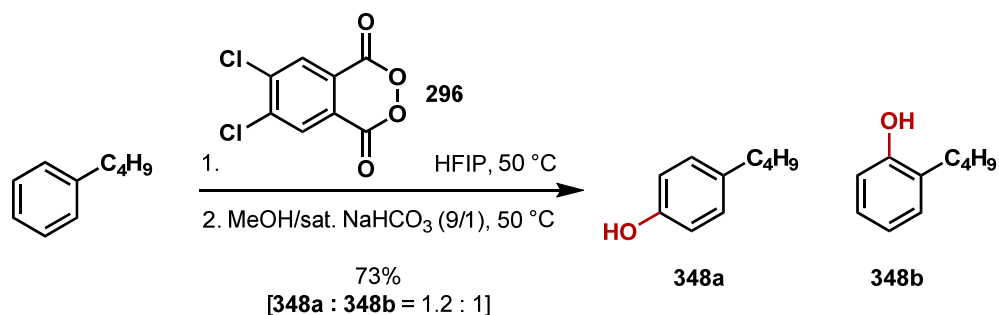
¹H-NMR (400 MHz, CDCl₃): δ 7.26 (d, 2H, *J* = 8.9 Hz), 6.77 (d, 2H, *J* = 8.9 Hz), 4.54 (bs, 1H), 1.29 (s, 9H).⁵

Minor Isomer (347b):

¹H-NMR (400 MHz, CDCl₃): δ 7.17 (t, 1H, *J* = 7.9 Hz), 6.97 (m, 1H), 6.87 (dd, 1H, *J* = 2.1, 2.4 Hz), 6.64 (m, 1H), 4.60 (bs, 1H), 1.30 (s, 9H).⁵

Minor Isomer (347c):

¹H-NMR (400 MHz, CDCl₃): δ 7.27 (d, 1H, *J* = 8.6 Hz), 7.07 (t, 1H, *J* = 6.5 Hz), 6.88 (dd, 1H, *J* = 6.5, 8.6 Hz), 6.66 (d, 1H, *J* = 8.6 Hz), 4.71 (bs, 1H), 1.41 (s, 9H).⁶



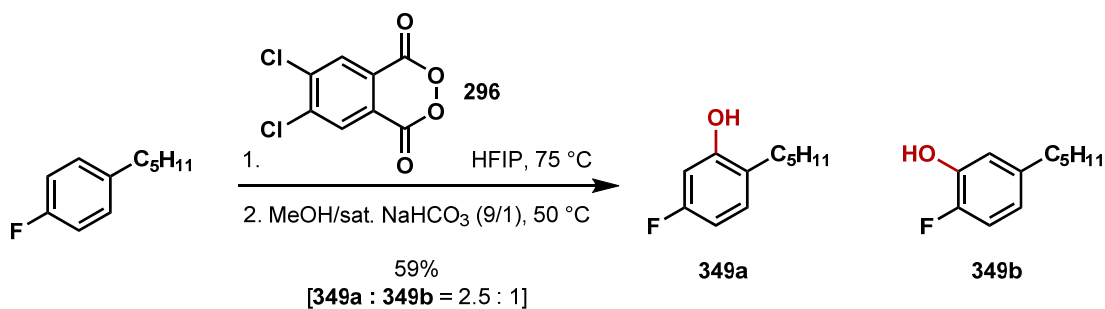
Phenols 348a and 348b: Prepared following General Procedure A using butyl benzene (100.0 mg, 0.75 mmol, 1.00 eq.), 4,5-dichlorophthaloyl peroxide (262.0 mg, 0.97 mmol, 1.30 eq., 86%), and HFIP (7.5 mL) at 50 °C for 24 hrs. The crude orange foam was purified by silica gel chromatography; 1 – 5% Et₂O in CH₂Cl₂ and hexane (1:1) to afford the phenols **348a** and **348b** (81.1 mg, 0.54 mmol, 73%, **348a** : **348b** = 1.2 : 1) as a pale yellow foam. The spectra of the title compounds match that for **348a** and **348b**.^{5, 6, 39}

Major Isomer (348a):

¹H-NMR (400 MHz, CDCl₃): δ 7.04 (d, 2H, *J* = 8.6 Hz), 6.74 (d, 2H, *J* = 8.6 Hz), 4.56 (bs, 1H), 2.54 (t, 2H, *J* = 7.8 Hz), 1.64 – 1.52 (m, 2H), 1.44 – 1.31 (m, 2H), 0.92 (t, 3H, *J* = 7.1 Hz).^{5, 6, 39}

Minor Isomer (348b):

¹H-NMR (400 MHz, CDCl₃): δ 7.13 – 7.05 (m, 2H), 6.87 (dt, 1H, *J* = 1.1, 7.4 Hz), 6.77 – 6.74 (m, 1H), 4.64 (bs, 1H), 2.61 (t, 2H, *J* = 7.9 Hz), 1.64 – 1.52 (m, 2H), 1.44 – 1.31 (m, 2H), 0.94 (t, 3H, *J* = 7.5 Hz).^{6, 39}



Fluorophenols 349a and 349b: Prepared following General Procedure B using 4-pentyl fluorobenzene (100.0 mg, 0.60 mmol, 1.00 eq.), 4,5-dichlorophthaloyl peroxide (403.0 mg, 1.50 mmol, 2.50 eq., 87%), and HFIP (6.0 mL) at 75 °C for 36 hrs. The crude brown foam was purified by silica gel chromatography; 1% Et₂O in CH₂Cl₂ and hexane (1:1) to afford the fluorophenols **349a** and **349b** (64.3 mg, 0.35 mmol, 59%, **349a** : **349b** = 2.5 : 1) as a yellow oil. The spectra of the title compound matches that for **349b**.⁴⁰

$R_f = 0.57$ (3% Et₂O in 49% hexane and 48% CH₂Cl₂);

Major Isomer (349a):

¹H-NMR (400 MHz, CDCl₃): δ 7.03 (dd, 1H, *J* = 6.8, 8.6 Hz), 6.57 (dt, 1H, *J* = 5.8, 8.2 Hz), 6.52 (dd, 1H, *J* = 2.4, 9.9 Hz), 4.82 (bs, 1H), 2.53 (q, 2H, *J* = 8.2 Hz), 1.58 (m, 2H), 1.35 (m, 4H), 0.90 (m, 3H)

¹³C-NMR (100 MHz, CDCl₃): δ 161.43, 154.21, 130.66, 124.80, 107.50, 103.00, 31.59, 29.48, 29.29, 22.54, 14.02

IR (neat film, cm⁻¹): 3391, 2929, 1609, 1514, 1279, 1112

HRMS (EC-CI): calcd. for C₁₁H₁₅OF [M+H]⁺ 182.1107, found 182.1106.

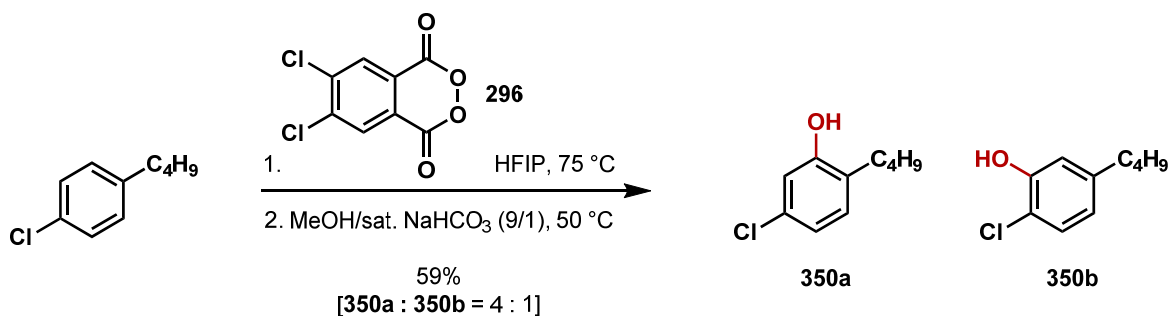
Minor Isomer (349b)⁴⁰:

¹H-NMR (400 MHz, CDCl₃): δ 6.95 (dd, 1H, *J* = 8.2, 10.3 Hz), 6.84 (dd, 1H, *J* = 2.1, 8.2 Hz), 6.66 - 6.63 (m, 1H), 5.01 (bs, 1H), 2.53 (q, 2H, *J* = 8.2 Hz), 1.58 (m, 2H), 1.35 (m, 4H), 0.90 (m, 3H)

¹³C-NMR (100 MHz, CDCl₃): δ 149.28, 142.97, 139.89, 130.92, 120.52, 116.97, 114.97, 35.26, 31.35, 31.08, 22.51, 14.02

IR (neat film, cm⁻¹): 3391, 2929, 1609, 1514, 1279, 1112

HRMS (EC-Cl): calcd. for C₁₁H₁₅O₂F [M+H]⁺ 182.1107, found 182.1106



Chlorophenols 350a and 350b: Prepared following General Procedure B using 4-butylchlorobenzene (100.0 mg, 0.59 mmol, 1.00 eq.), 4,5-dichlorophthaloyl peroxide (406.0 mg, 1.48 mmol, 2.50 eq., 85%), and HFIP (5.9 mL) at 75 °C for 36 hrs. The crude brown foam was purified by silica gel chromatography; 1% Et₂O in CH₂Cl₂ and hexane (1:1) to afford the chlorophenols **350a** and **350b** (64.4 mg, 0.35 mmol, 59%, **350a** : **350b** = 4 : 1) as a yellow oil.

R_f = 0.57 (3% Et₂O in 49% hexane and 48% CH₂Cl₂);

Major Isomer (350a):

¹H-NMR (400 MHz, CDCl₃): δ 7.02 (d, 1H, *J* = 8.2 Hz), 6.5 (dd, 1H, *J* = 2.1, 8.2 Hz), 6.78 (d, 1H, *J* = 2.1 Hz), 4.69 (bs, 1H), 2.56 (t, 2H, *J* = 7.5 Hz), 1.57 (ddd, 2H, *J* = 7.5 Hz), 1.37 (dddd, 2H, *J* = 7.5 Hz), 0.94 (t, 3H, *J* = 7.5 Hz)

¹³C-NMR (100 MHz, CDCl₃): δ 154.20, 132.00, 131.18, 127.44, 121.10, 115.76, 31.98, 29.38, 22.70, 14.16

IR (neat film, cm⁻¹): 3412, 2957, 2930, 1603, 1588, 1413

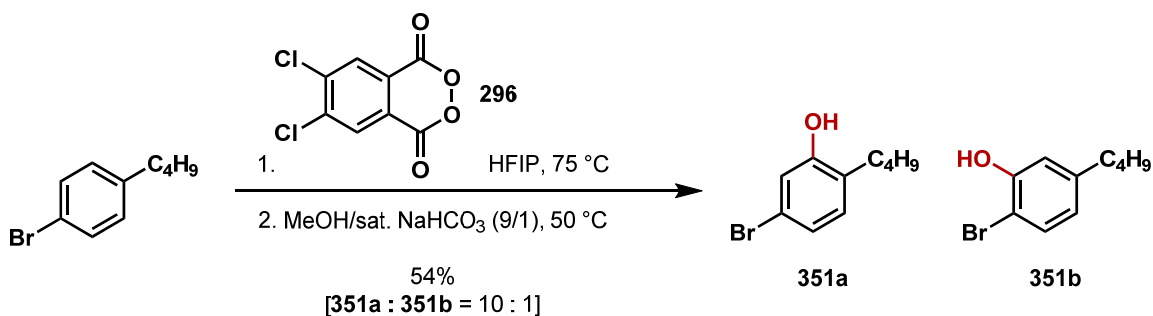
HRMS (EC-Cl): calcd. for C₁₀H₁₃OCl [M+H]⁺ 184.0655, found 184.0653.

Minor Regioisomer (350b):

¹H-NMR (400 MHz, CDCl₃): δ 7.19 (d, 1H, *J* = 8.2 Hz), 6.86 – 6.83 (m, 1H), 6.69 (dd, 1H, *J* = 2.05, 8.2 Hz), 5.43 (bs, 1H), 2.54 (t, 2H, *J* = 7.5 Hz), 1.57 (ddd, 2H, *J* = 7.5 Hz), 1.37 (dddd, 2H, *J* = 7.5 Hz), 0.92 (t, 3H, *J* = 7.5 Hz)

IR (neat film, cm⁻¹): 3412, 2957, 2930, 1603, 1588, 1413

HRMS (EC-CI): calcd. for C₁₀H₁₃OCl [M+H]⁺ 184.0655, found 184.0653.



Bromophenols 351a and 351b: Prepared following General Procedure B using 4-butyl bromobenzene (100.0 mg, 0.47 mmol, 1.00 eq.), 4,5-dichlorophthaloyl peroxide (321.0 mg, 1.17 mmol, 2.50 eq., 85%), and HFIP (4.7 mL) at 75 °C for 36 hrs. The crude brown foam was purified by silica gel chromatography; 1% Et₂O in CH₂Cl₂ and hexane (1:1) to afford the bromophenols **351a** and **351b** (58.3 mg, 0.25 mmol, 54%, **351a** : **351b** = 10 : 1) as a dark yellow oil.

R_f = 0.57 (3% Et₂O in 49% hexane and 48% CH₂Cl₂)

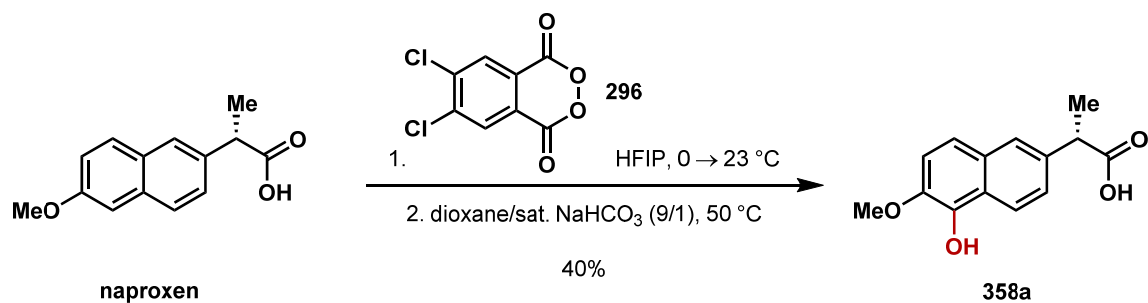
¹H-NMR (400 MHz, CDCl₃) δ 6.98 (d, 1H, *J* = 1.7 Hz), 6.97 (bs, 1H), 6.93 (d, 1H, *J* = 1.7 Hz), 4.72 (bs, 1H), 2.55 (t, 2H, *J* = 7.5 Hz), 1.60 – 1.53 (m, 2H), 1.42 – 1.33 (dddd, 2H, *J* = 7.5 Hz), 0.93 (t, 3H, *J* = 7.5 Hz)

¹H-NMR (400 MHz, C₆D₆): δ 6.88 (dd, 1H, *J* = 2.1, 8.2 Hz), 6.58 (d, 1H, *J* = 8.2 Hz), 6.29 (bs, 1H), 3.90 (bs, 1H), 2.36 (t, 2H, *J* = 7.9 Hz), 1.40 (ddd, 2H, *J* = 7.9 Hz), 1.17 (dddd, 2H, *J* = 7.5 Hz), 0.80 (t, 3H, *J* = 7.5 Hz)

¹³C-NMR (100 MHz, CDCl₃): δ 154.45, 131.56, 128.04, 123.99, 119.63, 118.59, 31.91, 29.45, 22.70, 14.17

IR (neat film, cm⁻¹): 3390, 2957, 2928, 1408, 1123

HRMS (EC-CI): calcd. for C₁₀H₁₂OBr [M+H]⁺ 228.0150, found 228.0149.



Acid 358a: Prepared following General Procedure A using naproxen (100 mg, 0.43 mmol, 1.00 eq.), 4,5-dichlorophthaloyl peroxide (153.0 mg, 0.57 mmol, 1.30 eq.), and HFIP (4.3 mL) at 0 °C gradually warming to 23 °C over 24 hrs. After removal of the HFIP by continuous positive flow of nitrogen, the mixed phthalate diacid was placed under an atmosphere of argon. The crude brown solid was suspended in a deoxygenated mixture composed of dioxane and aqueous saturated NaHCO₃ (9:1, 2.1 mL) and placed in an oil heated to 50 °C. After 20 minutes the brown solution was poured into an aqueous phosphate buffer (20 mL, 0.2 M, pH = 2) and adjusted to pH = 4. EtOAc (20 mL) was added and the layers were partitioned. The residual organics were extracted from the aqueous layer with EtOAc (2 x 20 mL), combined, dried over solid Na₂SO₄, filtered, and concentrated. The crude brown foam was purified by silica gel chromatography; 40% Et₂O and 1% acetic acid in hexane to afford the phenol **358a** (43.0 mg, 0.18 mmol, 40%) as a colorless solid that decomposes in air.

R_f = 0.09 (40% Et₂O and 1% AcOH in hexane)

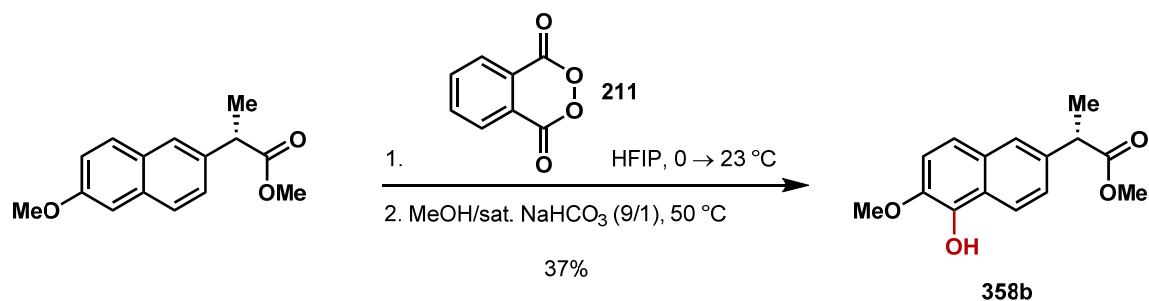
¹H-NMR (400 MHz, CDCl₃): δ 8.11 (d, 1H, *J* = 8.9 Hz), 7.66 (d, 1H, *J* = 1.4 Hz), 7.41 (dd, 1H, *J* = 8.9, 1.7 Hz), 7.36 (d, 1H, *J* = 8.9 Hz), 7.24 (d, 1H, *J* = 8.9 Hz), 4.00 (s, 3H), 3.9 (q, 1H, *J* = 7.2 Hz), 1.59 (d, 3H, *J* = 7.2 Hz)

¹³C-NMR (125 MHz, CDCl₃): δ 179.5, 141.3, 139.7, 135.5, 129.5, 125.9, 125.2, 123.2, 121.9, 119.5, 113.6, 57.2, 45.2, 18.1

IR (neat film cm⁻¹): 3433, 2937, 1704, 1275

HRMS (EC-CI): calcd. for C₁₄H₁₄O₄: 246.0892, found 246.0894.

M.P. = 132 – 134 °C.



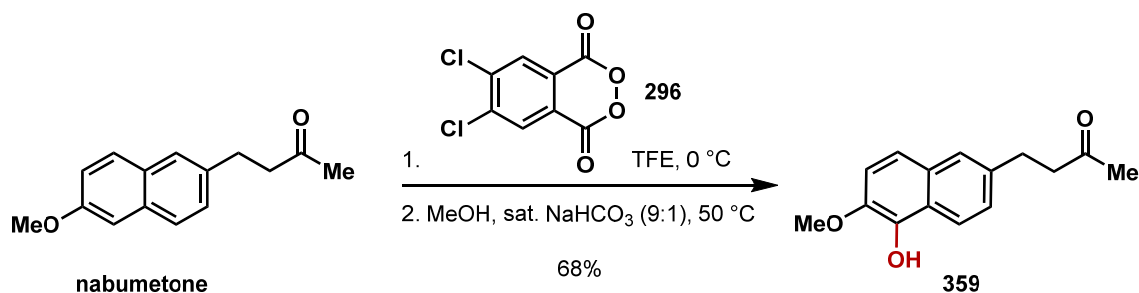
Ester 358b: Prepared following General Procedure A using the naproxen methyl ester (150.0 mg, 0.61 mmol, 1.00 eq.) which was dissolved in HFIP (6.1 mL), placed in an ice water bath cooled to 0 °C for 1 hr, and then phthaloyl peroxide (131.0 mg, 0.80 mmol, 1.30 eq.) was added over 15 minutes in six portions causing the solution to change to a dark turquoise color. After 20 minutes the HFIP was removed from the black mixture by continuous positive flow of nitrogen. The black mixture was placed under an atmosphere of nitrogen, a deoxygenated mixture of methanol and aqueous saturated NaHCO₃ (9:1, 6.1 mL) was added, and the black solution was placed in an oil bath heated to 50 °C. After 12 hrs the black solution was removed from the oil bath, cooled to 23 °C, diluted with an aqueous phosphate buffer (10 mL, pH = 7, 0.2 M) and EtOAc (10 mL), poured into a separatory funnel, partitioned, and the organic layer was washed with an aqueous phosphate buffer (3 x 20 mL, 0.2 M, pH = 7). Residual organics were extracted from the aqueous layer with EtOAc (3 x 20 mL), combined, dried over solid Na₂SO₄, filtered, and concentrated. The crude dark brown mixture was purified by silica gel chromatography; hexane – 10% EtOAc in hexane to afford the phenol **358b** (58.5 mg, 0.23 mmol, 37%) as an off white solid that decomposes in air.

¹H-NMR (400 MHz, CDCl₃): δ 8.10 (d, 1H, *J* = 8.9 Hz), 7.63 (d, 1H, *J* = 1.7 Hz), 7.39 (dd, 1H, *J* = 1.7, 8.9 Hz), 7.36 (d, 1H, *J* = 8.9 Hz), 7.25 (d, 1H, *J* = 8.9 Hz), 5.98 (bs, 1H), 3.99 (s, 3H), 3.86 (q, 1H, *J* = 7.2 Hz), 3.66 (s, 3H), 1.57 (d, 3H, *J* = 7.2 Hz)

¹³C-NMR (125 MHz, CDCl₃): δ 175.11, 141.24, 139.71, 136.29, 129.56, 126.63, 125.24, 123.06, 121.78, 119.41, 113.54, 57.15, 52.07, 45.43, 18.50

IR (neat film cm⁻¹): 3434, 1731, 1594, 1475, 1263, 1072

M.P. = 78 – 79 °C.



Phenol 359: Prepared following General Procedure A: A clear colorless solution of nabumetone (250.0 mg, 1.10 mmol, 1.00 eq.) in TFE (11.0 mL) was placed in an ice water bath cooled to 0 °C for 1 hr. 4,5-dichlorophthaloyl peroxide (405.0 mg, 1.42 mmol, 1.30 eq.) was added in 8 portions over 10 minutes causing the solution to change to a dark brown mixture. After 1 hr the TFE was removed from the black mixture by continuous positive flow of nitrogen. The brown solid mixture containing the mixed phthalate ester-acid was placed under an atmosphere of nitrogen and a deoxygenated mixture composed of methanol and aqueous saturated NaHCO₃ (9:1, 11.0 mL) was added. The black solution was placed in an oil bath heated to 50 °C and after 2 hrs the black solution was removed from the oil bath, cooled to 23 °C, diluted with an aqueous phosphate buffer (10 mL, pH = 7, 0.2 M) and EtOAc (10 mL), poured into a separatory funnel, partitioned, and the organic layer was washed with an aqueous phosphate buffer (3 x 30 mL, pH = 7, 0.2 M). Residual organics were extracted from the aqueous layer with EtOAc (3 x 20 mL), combined, dried over solid Na₂SO₄, filtered, and concentrated. The crude dark brown foam was purified by silica gel chromatography; hexane – 30% EtOAc in hexane to afford the phenol **359** (183.0 mg, 0.75 mmol, 68%) as an off white amorphous foam that decomposes in air.

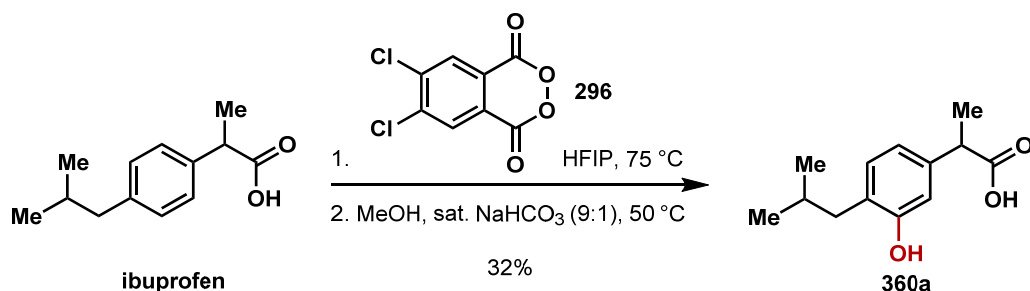
$R_f = 0.14$ (25% EtOAc in hexane)

¹H-NMR (400 MHz, CDCl₃): δ 8.07 (d, 1H, $J = 8.9$ Hz), 7.52 (bs, 1H), 7.32 (d, 1H, $J = 8.9$ Hz), 7.28 (dd, 1H, $J = 8.9, 2.1$ Hz), 7.23 (d, 1H, $J = 8.9$ Hz), 5.99 (bs, 1H), 3.99 (s, 3H), 3.03 (t, 2H, $J = 7.9$ Hz), 2.83 (t, 2H, $J = 7.9$ Hz), 2.15 (s, 3H)

¹³C-NMR (100 MHz, CDCl₃): δ 208.1, 140.9, 139.7, 136.7, 129.7, 126.5, 125.9, 122.5, 121.5, 119.0, 113.5, 57.2, 45.1, 30.2, 29.8

IR (neat film, cm⁻¹): 3407, 2923, 1710, 1363, 1273

HRMS (EC-CI) calcd. for C₁₅H₁₆O₃: 244.1099. Found: 244.1100.



Phenol 360a: Prepared following General Procedure B using ibuprofen (50.0 mg, 0.24 mmol, 1 eq.), HFIP (0.5 mL), and 4,5-dichlorophthaloyl peroxide (164.0 mg, 0.61 mmol, 2.50 eq.) at 75 °C for 24 hrs. HFIP was removed *in vacuo* yielding a brown solid which was suspended in a deoxygenated mixture composed of methanol and aqueous saturated NaHCO₃ (9:1, 2.1 mL), placed in an oil bath heated to 50 °C, and after 1 hr the mixture was removed from the oil bath, cooled to 23 °C, diluted with an aqueous phosphate buffer (20 mL, pH = 2, 0.2 M) and adjusted to pH = 4. Ethyl ether (20 mL) was added and the layers were partitioned. Residual organics were extracted from the aqueous layer with ether (2 x 20 mL), combined, dried over solid MgSO₄, and concentrated. The crude brown foam was purified by silica gel chromatography; 40% Et₂O and 1% AcOH in hexane to afford the phenol **360a** as an amorphous yellow oil (17.2 mg, 0.08 mmol, 32%).

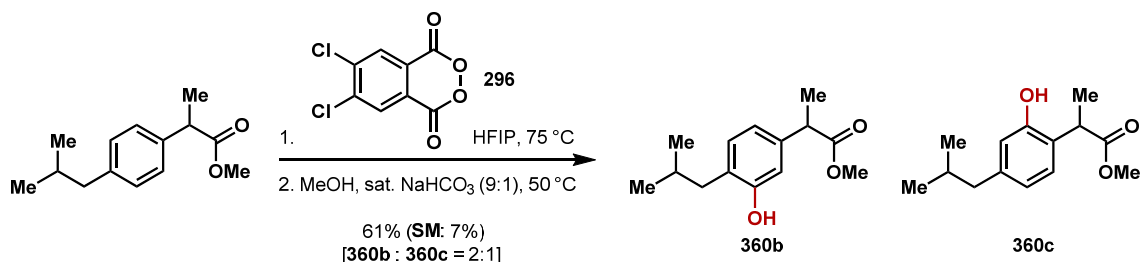
$R_f = 0.26$ (40% Et₂O and 1% AcOH in hexane)

¹H-NMR (400 MHz, CDCl₃): δ 7.02 (d, 1H, $J = 7.9$ Hz), 6.80 (dd, 1H, $J = 7.5, 1.7$ Hz), 6.74 (d, 1H, $J = 1.7$ Hz), 3.66 (q, 1H, $J = 7.2$ Hz), 2.44 (d, 2H, $J = 7.5$ Hz), 1.91 (dddd, 1H, $J = 6.8$ Hz), 1.48 (d, 3H, $J = 7.2$ Hz), 0.92 (d, 6H, $J = 6.8$ Hz)

¹³C-NMR (100 MHz, CDCl₃): δ 179.9, 153.7, 138.7, 131.4, 126.7, 119.8, 114.3, 44.7, 39.0, 28.8, 22.5, 18.0

IR (neat film, cm⁻¹): 3399, 2955, 1707

HRMS (EC-CI): calcd. For C₁₃H₁₈O₃: 222.1256. Found: 222.1255.



Phenols 360b and 360c: Prepared following General Procedure B using ibuprofen methyl ester (300.0 mg, 1.36 mmol, 1.00 eq.), 4,5-dichlorophthaloyl peroxide (747.0 mg, 2.72 mmol, 2.50 eq., 85%), and HFIP (13.6 mL) at 75 °C for 24 hrs. The crude brown tar was purified by silica gel chromatography; hexane – 4% EtOAc in hexane to provide the starting ester (22.3 mg, 0.10 mmol, 7%) as a clear colorless oil and the phenols as a mixture which were then further purified by silica gel chromatography; 1 - 2 % Et₂O in CH₂Cl₂ and hexane (1:1) to afford the phenol **360b** (130.0 mg, 0.55 mmol, 40%) and **360c** (66.0 mg, 0.28 mmol, 21%) as pale yellow amorphous oils.

Major Isomer (360b):

¹H-NMR (400 MHz, CDCl₃): δ 7.01 (d, 1H, *J* = 7.7 Hz), 6.78 (dd, 1H, *J* = 1.6, 7.7 Hz), 6.75 (d, 1H, *J* = 1.6 Hz), 5.22 (bs, 1H), 3.67 (s, 1H), 3.65 (q, 1H, *J* = 7.2 Hz), 2.45 (d, 2H, *J* = 7.2 Hz), 1.92 (dddd, 1H, *J* = 6.7 Hz), 1.47 (d, 3H, *J* = 7.2 Hz), 0.92 (d, 6H, *J* = 6.7 Hz)

¹³C-NMR (100 MHz, CDCl₃): δ 175.46, 153.96, 139.35, 131.30, 126.57, 119.56, 114.04, 52.13, 45.00, 38.99, 28.75, 22.53, 18.51

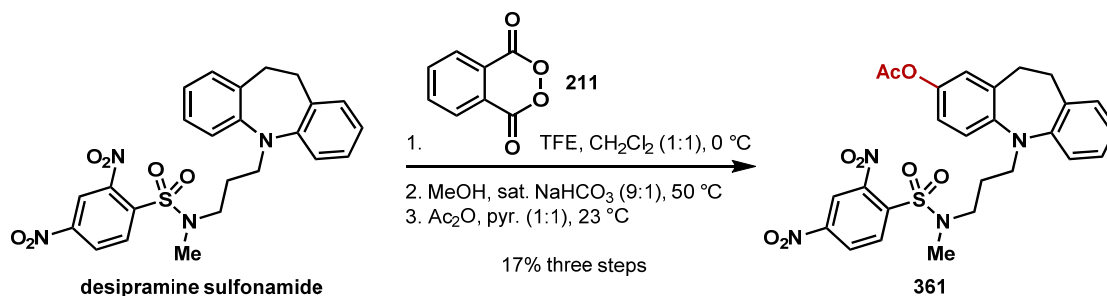
IR (neat film, cm⁻¹): 3401, 2953, 2360, 2342, 1715

Minor Isomer (361b):

¹H-NMR (400 MHz, CDCl₃): δ 7.43 (bs, 1H), 6.98 (d, 1H, *J* = 7.9 Hz), 6.71 (d, 1H, *J* = 1.7 Hz), 6.67 (dd, 1H, *J* = 1.7, 7.9 Hz), 3.84 (q, 1H, *J* = 7.2 Hz), 3.73 (s, 1H), 2.39 (d, 2H, *J* = 7.2 Hz), 1.84 (dddd, 1H, *J* = 6.8 Hz), 1.54 (d, 3H, *J* = 7.2 Hz), 0.89 (d, 6H, *J* = 6.8 Hz)

¹³C-NMR (100 MHz, CDCl₃): δ 177.57, 154.30, 142.84, 128.48, 122.92, 121.66, 118.33, 52.65, 44.95, 42.03, 30.01, 22.42, 16.57

IR (neat film, cm⁻¹): 3401, 2953, 2360, 2342, 1734



Acetate 361: Prepared following General Procedure A: A clear yellow solution of the desipramine dinitrosulfonamide (95.0 mg, 0.19 mmol, 1.00 eq.) in TFE and CH₂Cl₂ (4.0 mL, 1:1) was placed in an ice water bath cooled to 0 °C for 1 hr. Phthaloyl peroxide (40.0 mg, 0.25 mmol, 1.30 eq.) was added in 5 portions over 5 minutes causing the solution to change to a dark black mixture. After 1 hr the TFE and CH₂Cl₂ were removed from the black mixture by continuous positive flow of nitrogen. The black solid tar containing the mixed phthalate ester-acid was placed under an atmosphere of nitrogen and a deoxygenated mixture composed of methanol and aqueous saturated NaHCO₃ (9:1, 4.0 mL) was added. The black solution was placed in an oil bath heated to 50 °C. After 12 hrs the black solution was removed from the oil bath, cooled to 23 °C, diluted with an aqueous phosphate buffer (10 mL, pH = 7, 0.2 M) and EtOAc (10 mL), poured into a separatory funnel, partitioned, and the organic layer was washed with an aqueous phosphate buffer (3 x 30 mL, pH = 7, 0.2 M). Residual organics were extracted from the aqueous layer with EtOAc (3 x 20 mL), combined, dried over solid Na₂SO₄, filtered, and concentrated. The crude black tar was dissolved in CH₂Cl₂ (3.0 mL), pyridine (0.5 mL) and acetic anhydride (0.5 mL) were added sequentially, and the brown solution was allowed to stir at 23 °C. After 24 hrs the dark brown solution was diluted with an aqueous phosphate buffer (10 mL, pH = 4, 0.2 M) and EtOAc (10 mL), poured into a separatory funnel, partitioned, and the organic layer was washed with an aqueous phosphate buffer (2 x 10 mL, pH = 7, 0.2 M). Residual organics were extracted from the aqueous layer with EtOAc (2 x 10 mL), dried over solid Na₂SO₄, decanted, and concentrated. The crude dark brown foam was purified by silica gel chromatography; hexane – 20% EtOAc in hexane to afford the acetate **361** (18.2 mg, 0.03 mmol, 17%) as a golden yellow amorphous foam.

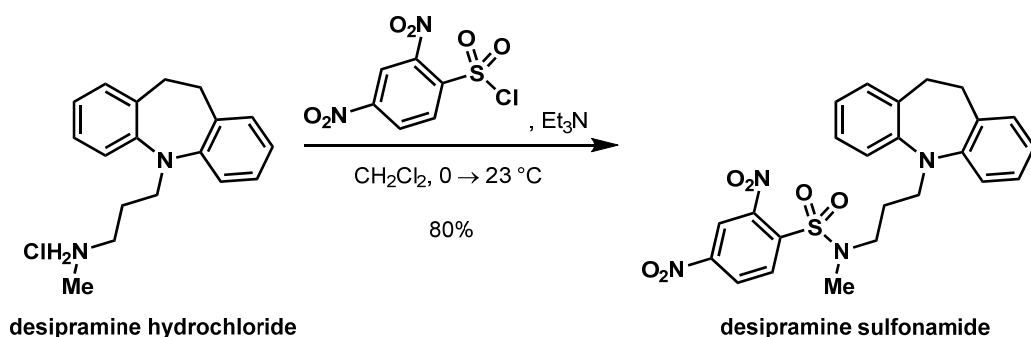
$R_f = 0.66$ (50% EtOAc in hexane)

¹H-NMR (400 MHz, CDCl₃): δ 8.38 (d, 1H, $J = 2.4$ Hz), 8.34 (dd, 1H, $J = 2.4$ Hz, 8.6 Hz), 8.03 (d, 1H, $J = 8.6$ Hz), 7.11 – 7.05 (m, 3H), 6.98 (t, 2H, $J = 7.4$ Hz), 6.90 (dd, 1H, $J = 2.3$ Hz, 7.4 Hz), 6.84 (dt, 1H, $J = 1.1$ Hz, 7.4 Hz), 3.88 – 3.82 (m, 1H), 3.60 – 3.48 (m, 2H), 3.35 – 3.24 (m, 3H), 2.93 – 2.87 (m, 1H), 2.85 (s, 3H), 2.76 (dt, 1H, $J = 4.0$ Hz, 12.9 Hz), 2.33 (s, 3H), 1.74 (ddd, 2H, $J = 7.3$ Hz)

¹³C-NMR (125 MHz, CDCl₃): δ 168.98, 149.49, 148.00, 146.33, 145.11, 142.04, 139.56, 138.12, 132.41, 131.54, 130.38, 126.42, 126.00, 125.67, 125.57, 121.77, 121.36, 119.93, 119.61, 49.21, 48.46, 34.48, 33.53, 31.05, 26.08, 21.21

IR (neat film, cm⁻¹): 1765, 1553, 1537, 1475, 1367, 1351, 1200, 1165, 750, 736

HRMS (EC-CI): calc'd. for C₂₆H₂₇N₄O₈S [M+H]⁺: 555.1550. Found: 555.1542.



A solution of desipramine hydrochloride (200.0 mg, 0.69 mmol, 1.00 eq.) in CH_2Cl_2 (6.9 mL) was placed in an ice water bath cooled to $0\text{ }^\circ\text{C}$ for 20 minutes. Freshly distilled triethylamine (0.15 g, 0.2 mL, 1.52 mmol, 2.20 eq.) was added followed by solid dinitrosulfonyl chloride (185.0 mg, 0.69 mmol, 1.00 eq.) under a positive flow of nitrogen. The golden yellow solution was warmed gradually to $23\text{ }^\circ\text{C}$ over 12 hrs, diluted with an aqueous phosphate buffer (10 mL, pH = 4, 0.2 M) and EtOAc (20 mL), poured into a separatory funnel, partitioned, and the aqueous layer was washed with an aqueous phosphate buffer (2 x 10 mL, pH = 4, 0.2 M). Residual organics were extracted from the aqueous layer with EtOAc (2 x 10 mL), dried over solid Na_2SO_4 , decanted, and concentrated. The crude orange mixture was purified by silica gel chromatography; 10% EtOAc in hexane to afford the desipramine sulfonamide as a dark yellow-orange solid (267.0 mg, 0.55 mmol, 80%).

$R_f = 0.66$ (50% EtOAc in hexane)

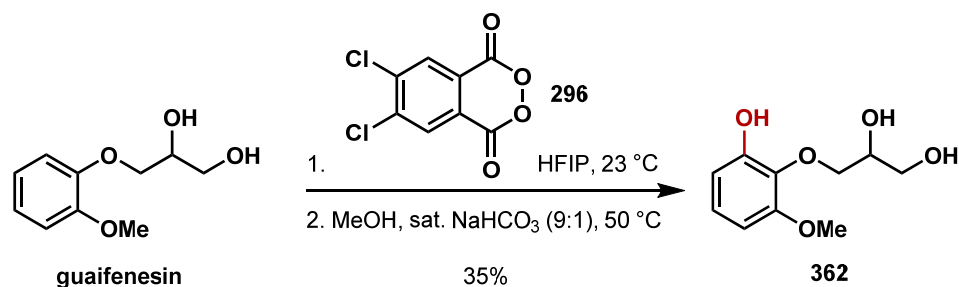
$^1\text{H-NMR}$ (400 MHz, CDCl_3): δ 8.34 (d, 1H, $J = 2.0$ Hz), 8.26 (dd, 1H, $J = 2.0$ Hz, 8.9 Hz), 8.0 (d, 1H, $J = 8.9$ Hz), 7.09 (d, 3H, $J = 7.5$ Hz), 6.98 (d, 2H, $J = 7.5$ Hz), 6.90 (t, 1H, $J = 7.5$ Hz), 3.71 (t, 2H, $J = 6.1$ Hz), 3.34 (t, 2H, $J = 6.7$ Hz), 3.14 (s, 4H), 2.87 (s, 3H), 1.80 (m, 2H)

$^{13}\text{C-NMR}$ (100 MHz, CDCl_3): δ 149.49, 147.70, 138.14, 134.18, 132.30, 130.03, 126.53, 126.03, 122.97, 119.62, 119.56, 48.19, 46.87, 34.56, 32.04, 25.43

IR (neat film, cm^{-1}): 1603, 1573, 1351, 1163, 751

HRMS (EC-CI): calc'd. for $\text{C}_{24}\text{H}_{25}\text{N}_4\text{O}_6\text{S}$ $[\text{M}+\text{H}]^+$: 497.1495. Found: 497.1490.

M.P.: $52 - 56\text{ }^\circ\text{C}$



Phenol 362: Prepared following General Procedure A using (±)-guaifenesin (75.0 mg, 0.38 mmol, 1.00 eq.), 4,5-dichlorophthaloyl peroxide (133.0 mg, 0.49 mmol, 1.30 eq.) in HFIP (3.8 mL) at 23 °C for 24 hrs. The crude dark brown foam was purified by silica gel chromatography; 50% EtOAc in hexane to afford the phenol **362** as an opaque colorless oil (27.9 mg, 0.13 mmol, 35%).

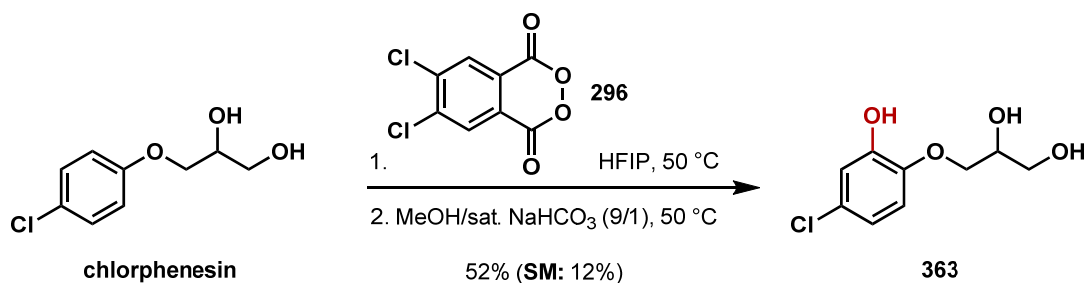
$R_f = 0.55$ (100% EtOAc)

$^1\text{H-NMR}$ (500 MHz, CDCl_3): δ 6.94 (t, 1H, $J = 8.3$ Hz), 6.59 (dd, 1H, $J = 1.2, 8.3$ Hz), 6.45 (dd, 1H, $J = 1.2, 8.3$ Hz), 4.16 (dd, 1H, $J = 2.7, 10.3$ Hz), 4.04 (m, 1H), 4.01 (t, 1H, $J = 4.2$ Hz), 3.85 (s, 3H), 3.82 (d, 1H, $J = 3.7$ Hz), 3.77 (m, 1H)

$^{13}\text{C-NMR}$ (125 MHz, CDCl_3): δ 152.92, 150.38, 135.14, 124.62, 109.22, 103.45, 74.89, 70.76, 63.69, 55.83.

IR (neat film, cm^{-1}): 3371, 1236, 1201.

HRMS (EC-CI): calc'd for $\text{C}_{10}\text{H}_{14}\text{O}_5\text{Na}$ $[\text{M}+\text{Na}]^+$: 237.07334. Found: 237.07352.



Triol 363: Prepared following General Procedure A using chlorphenesin (95.0 mg, 0.47 mmol, 1.00 eq.), 4,5-dichlorophthaloyl peroxide (165.0 mg, 0.61 mmol, 1.30 eq., 86%), and HFIP (4.7 mL) at 50 °C for 24 hrs. The crude brown solid was purified by silica gel chromatography; 5 - 50% acetone in hexane to provide the triol **363** (53.0 mg, 0.24 mmol, 52%) as a pale yellow foam and chlorphenesin (11.0 mg, 0.05 mmol, 12%) as a white solid.

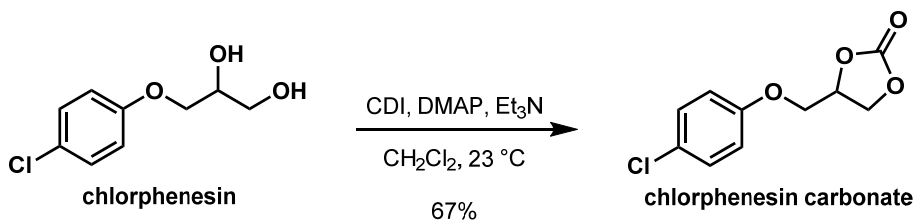
$R_f = 0.47$ (50% acetone in hexane)

¹H-NMR (400 MHz, C₃D₆O): δ 8.21 (bs, 1H), 6.98 (d, 1H, $J = 8.6$ Hz), 6.85 (d, 1H, $J = 2.4$ Hz), 6.79 (dd, 1H, $J = 2.4, 8.6$ Hz), 4.39 (bs, 1H), 4.14 (d, 1H, $J = 5.8$ Hz), 4.01 (m, 2H), 3.84 (t, 1H, $J = 5.4$ Hz), 3.67 (t, 2H, $J = 5.4$ Hz)

¹³C-NMR (125 MHz, C₃D₆O): δ 148.14, 145.93, 125.81, 119.06, 115.47, 114.63, 71.43, 70.44, 62.88

IR (neat film, cm⁻¹): 3410, 2935, 1634, 1592, 1504, 1268, 1215

HRMS (EC-ESI): calc'd. for C₉H₁₁ClNaO₄ [M+Na]⁺ 241.0238, found 241.0234.



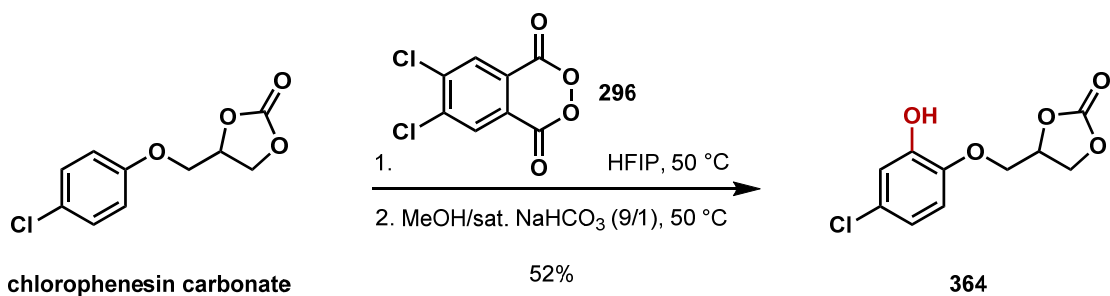
Chlorphenesin carbonate: To a white solid mixture of chlorphenesin (0.40 g, 1.97 mmol, 1.00 eq.), 1,1'-carbonyldiimidazole (0.48 g, 3.00 mmol, 1.50 eq.), and 4-*N,N'*-dimethylaminopyridine (0.01 g, 0.10 mmol, 0.05 eq.) in CH_2Cl_2 (19.7 mL) was added freshly distilled Et_3N (1.00 g, 1.4 mL, 9.87 mmol, 5.00 eq.). After 18 hrs at 23 °C the pale yellow homogeneous solution was diluted with Et_2O (30 mL) and residual CDI, DMAP, and Et_3N were quenched with an aqueous phosphate buffer (50 mL, pH = 7, 0.2 M), poured into a separatory funnel, and partitioned. The residual organics were extracted from the aqueous layer with Et_2O (4 x 20 mL), dried over solid Na_2SO_4 , decanted, and concentrated. The crude off white solid was purified by silica gel chromatography; 5 – 25% acetone in hexane to afford the chlorphenesin carbonate as a white solid (0.30 g, 1.31 mmol, 67%). The spectra of the title compound matches that for carbonate.⁴¹

R_f = (40% acetone in hexane)

$^1\text{H-NMR}$ (500 MHz, CDCl_3): δ 7.27 (d, 2H, J = 8.9 Hz), 6.85 (d, 2H, J = 8.9 Hz), 5.02 (m, 1H), 4.62 (t, 1H, J = 8.6 Hz), 4.52 (dd, 1H, J = 5.8, 8.6 Hz), 4.22 (dd, 1H, J = 4.1, 10.6 Hz), 4.12 (dd, 1H, J = 3.4, 10.6 Hz)

$^{13}\text{C-NMR}$ (125 MHz, CDCl_3): δ 156.32, 154.49, 129.60, 127.04, 115.92, 73.90, 67.25, 66.08

IR (neat film, cm^{-1}) 1790, 1492, 1243, 1169



Phenol 364: Prepared following General Procedure A using chlorophenesin carbonate (50.0 mg, 0.22 mmol, 1.00 eq.), 4,5-dichlorophthaloyl peroxide (138.0 mg, 0.51 mmol, 2.50 eq., 86%), and HFIP (2.0 mL) at 50 °C for 24 hrs. The crude brown foam was purified by silica gel chromatography; 5 - 30% acetone in hexane to provide the phenol **364** (28.0 mg, 0.11 mmol, 52%) as an off white solid.

R_f = 0.46 (40% acetone in hexane)

$^1\text{H-NMR}$ (400 MHz, CDCl_3): δ 6.98 (d, 1H, J = 2.4 Hz), 6.84 (dd, 1H, J = 2.4, 8.6 Hz), 6.78 (d, 1H, J = 8.6 Hz), 5.48 (bs, 1H), 5.07 (m, 1H), 4.66 (dd, 1H, J = 7.8, 8.9 Hz), 4.47 (dd, 1H, J = 5.8, 8.9 Hz), 4.30 (dd, 1H, J = 3.4, 10.9 Hz), 4.20 (dd, 1H, J = 4.4, 10.9 Hz)

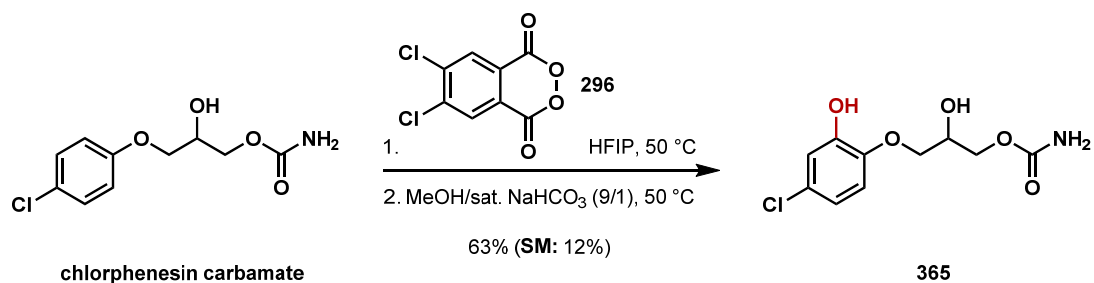
$^1\text{H-NMR}$ (400 MHz, $\text{C}_3\text{D}_6\text{O}$): δ 8.39 (bs, 1H), 7.01 (d, 1H, J = 8.7 Hz), 6.88 (d, 1H, J = 2.6 Hz), 6.80 (dd, 1H, J = 2.6, 8.7 Hz), 5.20 (m, 1H), 4.71 (t, 1H, J = 8.4 Hz), 4.56 (dd, 1H, J = 6.9, 8.5 Hz), 4.39 (dd, 1H, J = 3.4, 11.2 Hz), 4.33 (dd, 1H, J = 4.7, 11.2 Hz)

$^{13}\text{C-NMR}$ (100 MHz, $\text{C}_3\text{D}_6\text{O}$): δ 155.48, 148.85, 146.29, 127.20, 120.04, 116.79, 115.78, 75.67, 69.51, 66.69

IR (neat film, cm^{-1}): 3400, 2922, 1783, 1634

HRMS (EC-CI): calcd. for $\text{C}_{10}\text{H}_9\text{ClO}_5$ [M], 244.0139, found 244.0141

M.P. = 122 - 125°C.



Carbamate 365: Prepared following General Procedure A using chlorphenesin carbamate (85.0 mg, 0.35 mmol, 1.00 eq.), 4,5-dichlorophthaloyl peroxide (122.0 mg, 0.45 mmol, 1.30 eq., 86%), and HFIP (3.5 mL) at 50 °C for 24 hrs. The crude brown solid mixture was purified by silica gel chromatography; 5 - 35% acetone in hexane to afford the carbamate **365** (57.0 mg, 0.22 mmol, 63%) as an off-white solid and the starting chlorphenesin carbamate (10.2 mg, 0.04 mmol, 12%).

$R_f = 0.45$ (50% acetone in hexane)

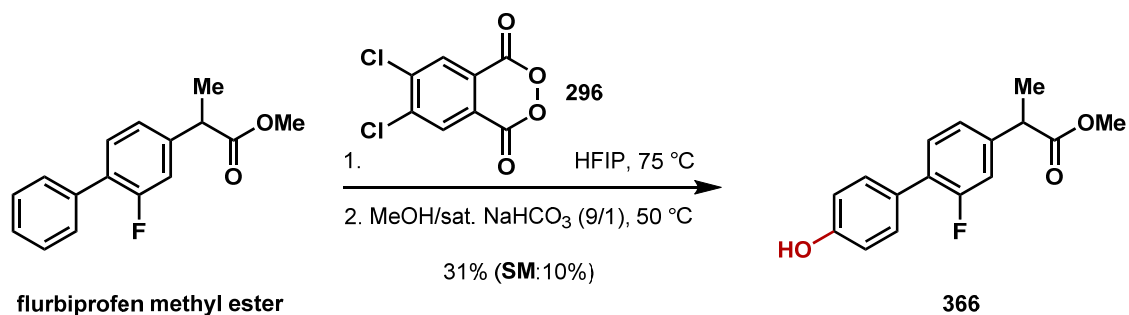
$^1\text{H-NMR}$ (400 MHz, CD₃OD): δ 6.88 (d, 1H, $J = 8.6$ Hz), 6.80 (d, 1H, $J = 2.7$ Hz), 6.74 (dd, 1H, $J = 2.7, 8.6$ Hz), 4.16 (m, 3H), 4.06 (m, 1H), 3.98 (m, 1H)

$^{13}\text{C-NMR}$ (100 MHz, C₃D₆O): δ 158.25, 147.58, 145.60, 125.98, 118.86, 115.51, 113.82, 70.04, 68.05, 64.92

IR (neat film, cm⁻¹): 3369, 1706, 1501

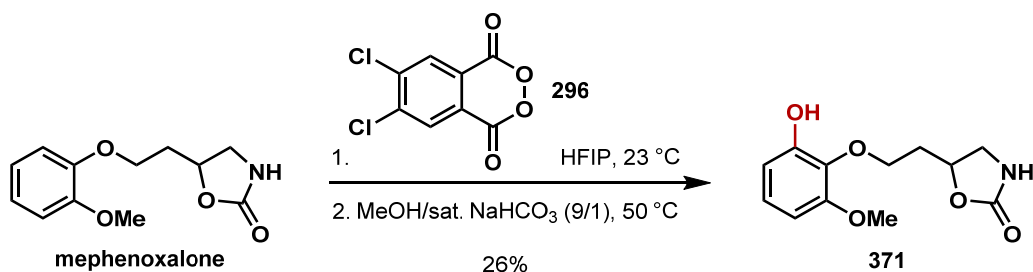
HRMS (EC-ESI): calc'd. for C₁₀H₁₂ClNNaO₅ [M+Na]⁺ 284.0296, found 284.0293

M.P. = 124 - 127°C.



Phenol 366: Prepared following [General Procedure B](#) using flurbiprofen methyl ester (210.0 mg, 0.81 mmol, 1.00 eq.), 4,5-dichlorophthaloyl peroxide (446.0 mg, 1.63 mmol, 2.00 eq., 85%), and HFIP (8.1 mL) at 75 °C for 24 hrs. The crude dark yellow solid mixture was purified by silica gel chromatography; 1% 1,4-dioxane in benzene to afford the phenol **366** (69.0 mg, 0.25 mmol, 31%) as a pale yellow foam and the starting flurbiprofen (20.9 mg, 0.08 mmol, 10%). The spectral data of the title compound matches that for the phenol **366**.^{42,43}

¹H-NMR (400 MHz, CDCl₃): δ 7.42 (dd, 2H, *J* = 1.5, 7.1 Hz), 7.34 (t, 1H, *J* = 7.4 Hz), 7.11 (m, 2H), 6.89 (d, 2H, *J* = 8.6 Hz), 4.99 (bs, 1H), 3.75 (q, 2H, *J* = 7.0 Hz), 3.70 (s, 3H), 1.53 (d, 3H, *J* = 7.0 Hz)^{42,43}



Phenol 371: Prepared following General Procedure B using (±)-mephenoxalone (50.0 mg, 0.22 mmol, 1.00 eq.), 4,5-dichlorophthaloyl peroxide (67.8 mg, 0.29 mmol, 1.30 eq.), and HFIP (2.2 mL). The crude dark brown foam was purified by silica gel chromatography; 50% EtOAc in hexane to afford phenol **371** as an opaque pale yellow oil (13.9 mg, 0.06 mmol, 26%).

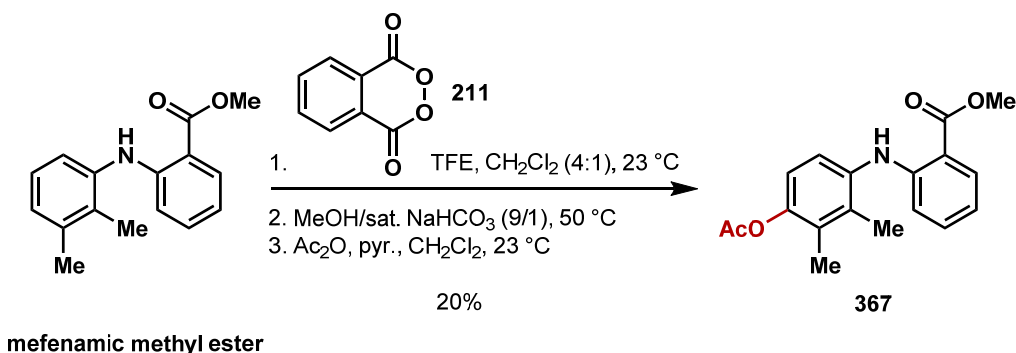
$R_f = 0.47$ (100% EtOAc)

¹H-NMR (400 MHz, CDCl₃): δ 6.95 (t, 1H, $J = 8.2$ Hz), 6.61 (dd, 1H, $J = 1.6, 8.2$ Hz), 6.46 (dd, 1H, $J = 1.2, 8.2$ Hz), 6.02 (s, 1H), 5.45 (s, 1H), 4.93 (m, 1H), 4.29 (dd, 1H, $J = 3.5, 11.0$ Hz), 4.14 (dd, 1H, $J = 5.9, 11.0$ Hz), 3.84 (s, 3H), 3.74 (t, 1H, $J = 8.6$ Hz), 3.58 (t, 1H, $J = 6.6$ Hz).

¹³C-NMR (100 MHz, CDCl₃): δ 158.94, 152.40, 149.72, 133.87, 124.73, 108.77, 103.77, 74.76, 73.13, 55.81, 41.90

IR (neat film, cm⁻¹): 3346, 1733, 1253, 1198

HRMS (EC-CI): calc'd for C₁₁H₁₃NO₅Na [M+Na]⁺: 262.06859. Found: 262.06826.



Acetate 367: Prepared using General Procedure A: A clear colorless solution of mefenamic methyl ester (50.0 mg, 0.20 mmol, 1.00 eq.) in TFE and CH₂Cl₂ (4.0 mL, 4:1) was placed in an ice water bath cooled to 0 °C for 30 minutes. Phthaloyl peroxide (71.0 mg, 0.43 mmol, 2.20 eq.) was added in 5 portions over 5 minutes causing the solution to change to a dark black mixture. The mixture was allowed to warm gradually to 23 °C over 12 hrs following which the TFE and CH₂Cl₂ were removed from the black mixture by continuous positive flow of nitrogen. The black solid tar was placed under an atmosphere of nitrogen and a deoxygenated mixture composed of methanol and aqueous saturated NaHCO₃ (9:1, 4.0 mL) was added. The black solution was placed in an oil bath heated to 50 °C. After 12 hrs the black solution was removed from the oil bath, cooled to 23 °C, diluted with an aqueous phosphate buffer (10 mL, pH = 7, 0.2 M) and EtOAc (10 mL), poured into a separatory funnel, partitioned, and the organic layer was washed with an aqueous phosphate buffer (3 x 30 mL, pH = 7, 0.2 M). Residual organics were extracted from the aqueous layer with EtOAc (3 x 20 mL), combined, dried over solid Na₂SO₄, decanted, and concentrated. The crude black tar was dissolved in CH₂Cl₂ (4.0 mL) upon which pyridine (155.0 mg, 0.2 mL, 1.96 mmol, 10.0 eq.) and acetic anhydride (60.0 mg, 0.1 mL, 0.59 mmol, 3.00 eq.) were added sequentially. After 24 hrs at 23 °C the dark brown solution was diluted with an aqueous phosphate buffer (10 mL, pH = 4, 0.2 M) and EtOAc (10 mL), poured into a separatory funnel, partitioned, and the organic layer was washed with an aqueous phosphate buffer (2 x 10 mL, pH = 7, 0.2 M). Residual organics were extracted from the aqueous layer with EtOAc (2 x 10 mL), dried over solid Na₂SO₄, decanted, and concentrated. The crude dark brown foam was purified by silica gel chromatography; hexane – 2% EtOAc in hexane to afford the acetate **367** (12.3 mg, 0.04 mmol, 20%) as a golden yellow amorphous foam.

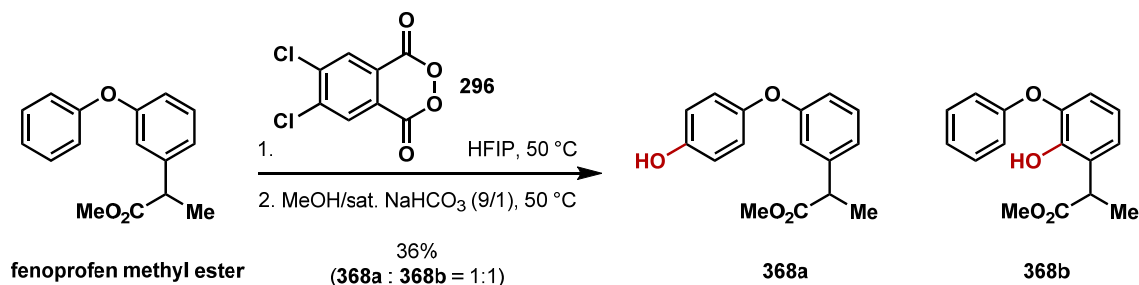
R_f = 0.59 (40% EtOAc in hexane)

¹H-NMR (500 MHz, CDCl₃): δ 9.19 (bs, 1H), 7.95 (dd, 1H, *J* = 1.4, 7.1 Hz), 7.24 (m, 1H), 7.16 (d, 1H, *J* = 8.3 Hz), 6.88 (d, 1H, *J* = 8.3 Hz), 6.71 (dd, 1H, *J* = 1.1, 8.3 Hz), 6.66 (dt, 1H, *J* = 1.2, 5.9 Hz), 3.91 (s, 3H), 2.34 (s, 3H), 2.20 (s, 3H), 2.13 (s, 3H)

¹³C-NMR (125 MHz, CDCl₃): δ 169.56, 169.11, 149.44, 146.53, 136.61, 134.60, 134.21, 134.46, 130.05, 123.90, 119.75, 116.19, 113.67, 110.81, 51.69, 20.86, 14.63, 13.30

IR (neat film, cm⁻¹): 2918, 2360, 2340, 1760, 1703, 1252, 1195, 1090

HRMS (EC-CI): calcd. for C₁₇H₁₆NO₃ [M+H]⁺ 282.1130, found 282.1131.



Phenols 368a and 368b: Prepared following General Procedure A using fenoprofen methyl ester (128.0 mg, 0.50 mmol, 1.00 eq.), 4,5-dichlorophthaloyl peroxide (181.0 mg, 0.65 mmol, 1.30 eq.), and HFIP (5.0 mL) at 50 °C for 24 hrs. The crude orange foam was purified by silica gel chromatography; hexane – 12% EtOAc in hexane to afford the phenol **368a** as a white solid (24.0 mg, 0.09 mmol, 18%) and phenol **368b** as a pale yellow foam (24.2 mg, 0.09 mmol, 18%).

Phenol 368a:

R_f = 0.56 (30% EtOAc in hexane)

¹H-NMR (500 MHz, CDCl₃): δ 7.25 (m, 3H), 6.97 (d, 1H, *J* = 7.2 Hz), 6.92 (d, 2H, *J* = 8.8 Hz), 6.91 (bs, 1H), 6.81 (d, 2H, *J* = 8.8 Hz), 3.67 (q, 1H, *J* = 7.2 Hz), 1.47 (d, 3H, *J* = 7.2 Hz)

¹³C-NMR (125 MHz, CDCl₃): δ 175.05, 158.70, 152.03, 149.75, 142.22, 129.74, 121.47, 121.07, 116.83, 116.33, 115.97, 52.20, 45.30, 18.43

IR (neat film, cm⁻¹): 3411, 2922, 1732, 1587, 1471, 1266, 1215

HRMS (EC-CI): calcd. for C₁₆H₁₆O₄ [M] 272.1049, found 272.1049.

M.P. = 102 – 105 °C

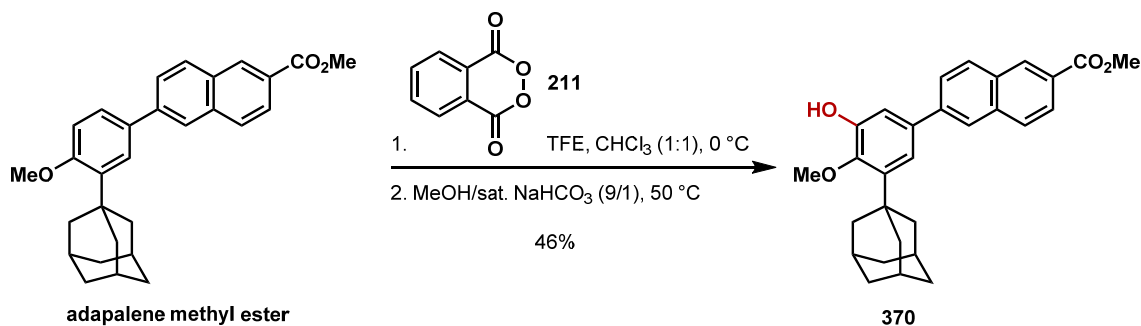
Phenol 368b:

¹H-NMR (500 MHz, CDCl₃): δ 7.35 (dd, 2H, *J* = 1.2, 7.2 Hz), 7.13 (dt, 1H, *J* = 1.0, 7.2 Hz), 7.04 (m, 2H), 6.99 (dd, 1H, *J* = 2.0, 7.2 Hz), 6.83 – 6.79 (m, 2H), 5.99 (bs, 1H), 4.12 (q, 1H, *J* = 7.1 Hz), 3.71 (s, 3H), 1.53 (d, 3H, *J* = 7.1 Hz)

¹³C-NMR (125 MHz, CDCl₃): δ 175.36, 156.57, 145.01, 143.86, 129.87, 128.21, 123.74, 123.12, 120.13, 118.32, 117.07, 52.14, 39.32, 17.24

IR (neat film, cm⁻¹): 3411, 2922, 1732, 1587, 1471, 1266, 1215

HRMS (EC-CI): calcd. for C₁₆H₁₆O₄ [M] 272.1049, found 272.1050.



Phenol 370: Prepared using General Procedure A: A clear colorless solution of adapalene methyl ester (100.0 mg, 0.23 mmol, 1.00 eq.) in TFE and CHCl₃ (9.4 mL, 1:1) was placed in an ice water bath cooled to 0 °C for 1 hr. Phthaloyl peroxide (46.0 mg, 0.28 mmol, 1.20 eq.) was added in 10 portions over 10 minutes changing the colorless solution to a dark brown mixture. After 2 hrs the TFE and CHCl₃ were removed from the brown mixture by continuous positive flow of nitrogen. The black solid containing the mixed phthalate ester-acid was placed under an atmosphere of nitrogen and a deoxygenated mixture composed of methanol and aqueous saturated NaHCO₃ (9:1, 4.0 mL) was added. The brown solution was placed in an oil bath heated to 50 °C. After 12 hrs the brown solution was removed from the oil bath, cooled to 23 °C, diluted with an aqueous phosphate buffer (10 mL, pH = 7, 0.2 M) and EtOAc (10 mL), poured into a separatory funnel, partitioned, and the organic layer was washed with an aqueous phosphate buffer (3 x 30 mL, pH = 7, 0.2 M). Residual organics were extracted from the aqueous layer with EtOAc (3 x 20 mL), combined, dried over solid Na₂SO₄, filtered, and concentrated. The crude dark brown foam was purified by silica gel chromatography; hexane – 20% EtOAc in hexane and then purified again by silica gel chromatography; 12% 1,4-dioxane in hexane to afford the phenol **370** as a white solid (48.0 mg, 0.11 mmol, 46%).

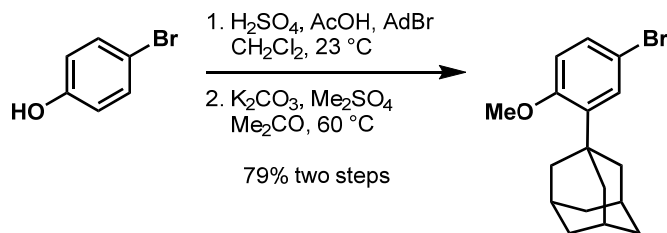
R_f = 0.78 (40% 1,4-dioxane in hexane)

¹H-NMR (400 MHz, CDCl₃): δ 8.62 (s, 1H), 8.07 (d, 1H, *J* = 8.6 Hz), 8.00 (s, 1H), 7.98 (d, 1H, *J* = 8.6 Hz), 7.91 (d, 1H, *J* = 8.6 Hz), 7.76 (d, 1H, *J* = 8.6 Hz), 7.20 (d, 1H, 2.0 Hz), 5.41 (bs, 1H), 3.99 (s, 3H), 3.90 (s, 3H), 2.15 (bs, 7H), 2.12 (bs, 2H), 1.81 (bs, 6H)

¹³C-NMR (100 MHz, CDCl₃): δ 167.31, 149.96, 147.28, 143.88, 140.97, 136.45, 135.79, 131.50, 130.82, 129.73, 128.33, 127.16, 126.42, 125.25, 118.24, 113.35, 61.36, 52.25, 41.78, 37.65, 36.91, 29.70, 29.10

IR (neat film, cm⁻¹): 3445, 1656

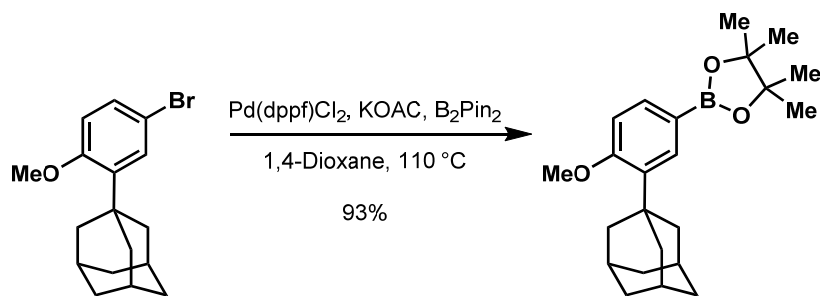
M.P. = 240 – 242 °C



To a solution of *p*-bromophenol (750.0 mg, 4.34 mmol, 1.00 eq.) in CH_2Cl_2 (2.2 mL) and AcOH (1.25 mL) was added sulfuric acid (0.3 mL, 4.69 mmol, 1.08 eq., 98%) and then 1-adamantyl alcohol (660.0 mg, 4.34 mmol, 1.00 eq.) at 23 °C. After 36 hrs the pale yellow solution was poured into a separatory funnel containing an aqueous phosphate buffer (30 mL, pH = 7, 0.2 M) and CH_2Cl_2 (20 mL), partitioned, and the organics were washed with a saturated aqueous mixture of NaHCO_3 (1 x 20 mL). Residual organics were extracted from the aqueous layer with CH_2Cl_2 (2 x 10 mL), combined, washed with brine (2 x 10 mL), dried over solid Na_2SO_4 , decanted, and concentrated. The phenolic product was carried into the next reaction without further purification or characterization.

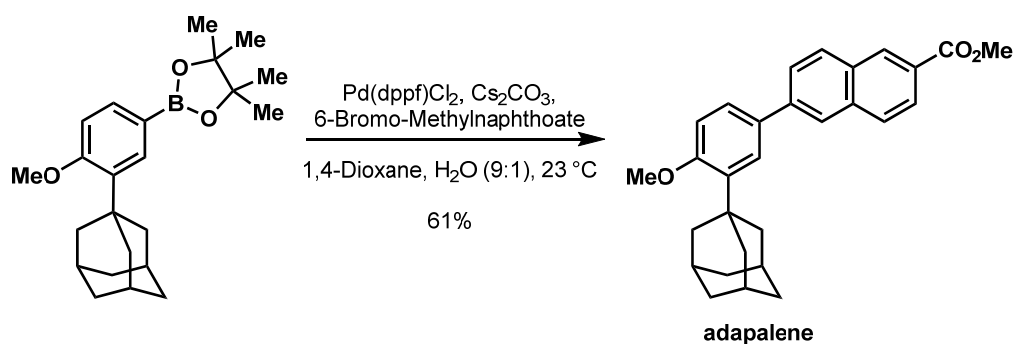
A mixture of the crude adamantyl *p*-bromophenol, K_2CO_3 (1.80 g, 13.0 mmol, 3.00 eq.), and Me_2SO_4 (0.41 mL, 4.34 mmol, 1.00 eq.) in acetone (44 mL) was purged with nitrogen and stoppered with a plastic PTFE cap. The mixture was placed in an oil bath heated to 60 °C and stirred vigorously (1000 rpm). After 24 hrs the white heterogeneous mixture was removed from the oil bath, cooled to 23 °C, suction filtered over a pad of celite, and concentrated. The pale yellow foam was dissolved in Et_2O (20 mL), poured into a separatory funnel, and washed with an aqueous NaOH solution (3 x 20 mL, 1 N) to remove the unreacted phenol. Residual organics were extracted from the aqueous layer with Et_2O (2 x 15 mL), combined, dried over solid Na_2SO_4 , decanted, and fully concentrated *in vacuo* to remove any residual unreacted *p*-bromoanisole to afford the adamantyl *p*-bromoanisole as a pale yellow solid (1.10 g, 3.42 mmol, 79%, two steps). The spectral data of the title compound matches that of 3-adamantyl *p*-bromoanisole.⁴⁴

¹H-NMR (400 MHz, CDCl_3): δ 7.29 – 7.24 (m, 2H), 6.73 (d, 1H, J = 8.6 Hz), 3.81 (s, 3H), 2.05 bs, 9H), 1.75 (bs, 6H)



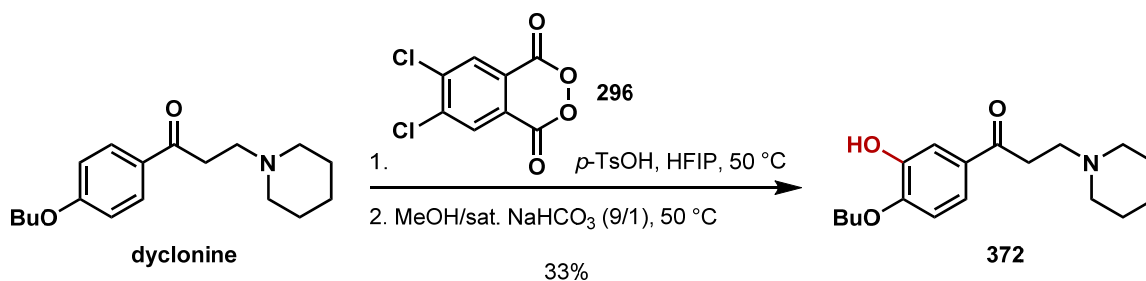
To a solution of 3-adamantyl *p*-bromoanisole (320.0 mg, 1.00 mmol, 1.00 eq.), KOAc (303.0 mg, 3.09 mmol, 3.10 eq.), and B₂Pin₂ (278.0 mg, 1.10 mmol, 1.10 eq.) in 1,4-dioxane (10 mL) was added Pd(dppf)Cl₂-CH₂Cl₂ (49.0 mg, 0.06 mmol, 0.06 eq.) under a positive flow of nitrogen. The red mixture was sparged with nitrogen, stoppered with a plastic PTFE cap, and placed into an oil bath heated to 110 °C. After 4 hrs the black mixture was removed from the oil bath, cooled to 23 °C, concentrated, and residual 1,4-dioxane was azeotropically removed with CHCl₃ (3 x 3 mL). The black mixture was dissolved in a solution of CHCl₃ and hexane (2 mL, 1:1), loaded directly onto silica gel, and purified by silica chromatography; hexane – 5% EtOAc in hexane to afford the boronic ester as a pale yellow foam which solidified upon standing at 23 °C (340.0 mg, 0.92 mmol, 93%). The boronic ester was carried onto to the next reaction without full characterization.

¹H-NMR (400 MHz, CDCl₃): δ 7.66 – 7.64 (m, 2H), 6.86 (d, 1H, *J* = 7.8 Hz), 3.85 (s, 3H), 2.12 bs, 6H), 2.05 (bs, 3H), 1.76 (bs, 6H), 1.32 (s, 12H)



To a solution of the boronic ester (340.0 mg, 0.92 mmol, 1.00 eq.) in 1,4-dioxane and water (9.2 mL, 9:1) was added Pd(dppf)Cl₂-CH₂Cl₂ (75.0 mg, 0.09 mmol, 0.10 eq.) and Cs₂CO₃ (932.0 mg, 2.86 mmol, 3.10 eq.) under a positive flow of nitrogen. 6-bromo-methylnaphthoate (269.0 mg, 1.02 mmol, 1.10 eq.) was added under a positive flow of nitrogen to the now black mixture. After stirring rapidly (800 rpm) at 23 °C for 16 hrs the black mixture was poured into a separatory funnel containing CH₂Cl₂ (20 mL) and brine (10 mL), partitioned, and the residual organics were extracted from the aqueous layer with CH₂Cl₂ (1 x 10 mL), dried over solid Na₂SO₄, suction filtered over a pad of celite, and concentrated. The crude pale yellow mixture was purified by silica gel chromatography to afford the adapalene methyl ester as a white solid (241.0 mg, 0.57 mmol, 61%). The spectral data of the title compound matches that of the adapalene methyl ester.⁴⁴

¹H-NMR (400 MHz, CDCl₃): δ 8.61 (s, 1H), 8.07 (dd, 1H, *J* = 1.4, 8.9 Hz), 8.01 (d, 1H, *J* = 1.4 Hz), 7.98 (d, 1H, *J* = 8.6 Hz), 7.92 (d, 1H, *J* = 8.2 Hz), 7.79 (dd, 1H, *J* = 1.7, 8.6 Hz), 7.60 (d, 1H, *J* = 2.3 Hz), 7.54 (dd, 1H, *J* = 2.4, 8.6 Hz), 7.00 (d, 1H, *J* = 8.2 Hz), 3.99 (s, 3H), 3.91 (s, 3H), 2.18 (bs, 6H), 2.10 (bs, 3H), 1.80 (bs, 6H)



Phenol 372: Prepared following General Procedure A: To a solution of dyclonine (131.0 mg, 0.45 mmol, 1.00 eq.) in HFIP (4.5 mL) was added *p*-toluenesulfonic acid monohydrate (86.0 mg, 0.45 mmol, 1.00 eq.). The pale yellow solution was stirred for 2 minutes at 23 °C upon which 4,5-dichlorophthaloyl peroxide (514.0 mg, 1.81 mmol, 4.00 eq., 82%) was added. The pale yellow solution was stoppered with a plastic PTFE cap and placed in an oil bath heated to 50 °C. After 12 hrs the red solution was removed from the oil bath, cooled to 23 °C, and HFIP was removed by a continuous flow of nitrogen. The dark red mixture was placed under an atmosphere of nitrogen upon which a deoxygenated mixture of methanol and a saturated aqueous mixture of NaHCO_3 (4.5 mL, 9:1) was added. The dark red solution was placed in an oil bath heated to 50 °C. After 2 hrs the dark red solution was removed from the oil bath, cooled to 23 °C, diluted with a saturated aqueous mixture of NaHCO_3 (10 mL) and EtOAc (10 mL), poured into a separatory funnel, partitioned, and the aqueous layer was washed with a saturated aqueous mixture of NaHCO_3 and brine (3 x 30 mL, 1:1). Residual organics were extracted from the aqueous layer with a combination of EtOAc and brine (3 x 30 mL, 2:1), combined, dried over solid Na_2SO_4 , decanted, and concentrated. The crude black foam was purified by silica gel chromatography; 1 – 5% MeOH in CH_2Cl_2 , then 1% MeOH and 1% Et_3N in CH_2Cl_2 to afford the aminophenol **372** as a red solid (50.6 mg, 0.15 mmol, 33%, 90% pure by $^1\text{H-NMR}$).

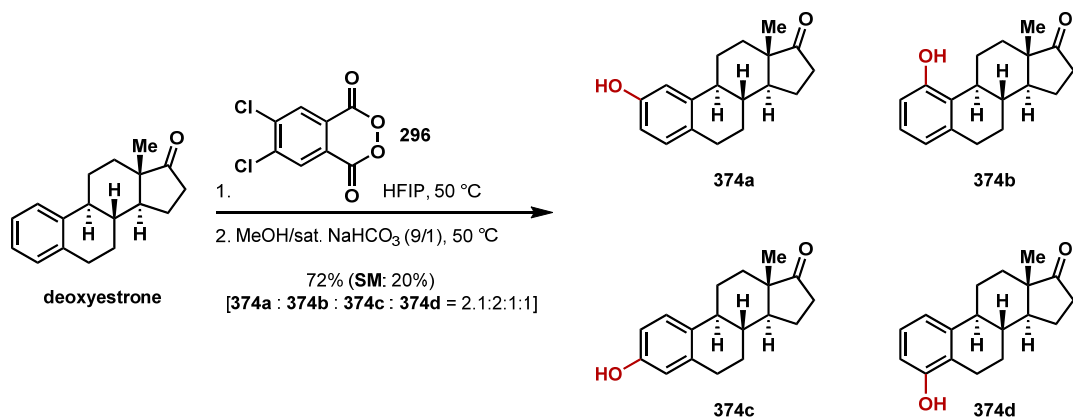
R_f = 0.50 (5% MeOH in CH_2Cl_2)

$^1\text{H-NMR}$ (400 MHz, CDCl_3): δ 7.58 (dd, 1H, J = 2.0, 8.2 Hz), 7.56 (d, 1H, 2.0 Hz), 6.86 (d, 1H, J = 8.2 Hz), 4.12 (t, 2H, J = 6.8 Hz), 3.64 (t, 2H, J = 6.8 Hz), 3.36 (t, 2H, J = 6.8 Hz), 3.03 (bs, 4H), 1.97 (bs, 4H), 1.83 (ddd, 2H, J = 7.8 Hz), 1.63 (bs, 2H), 1.51 (ddd, 2H, J = 7.8 Hz), 1.00 (t, 3H, J = 7.8 Hz)

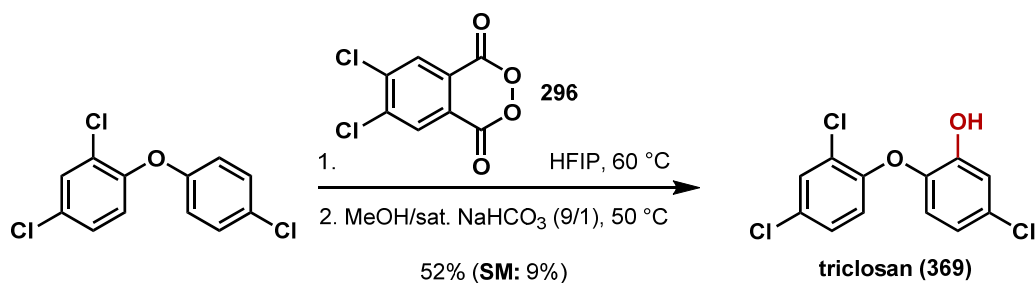
$^{13}\text{C-NMR}$ (100 MHz, CDCl_3): δ 195.14, 151.12, 145.90, 129.10, 122.04, 114.15, 110.83, 68.83, 53.73, 52.27, 33.07, 30.97, 22.92, 22.18, 19.12, 13.78

IR (neat film, cm^{-1}): 3401, 2957, 2873, 1673, 1604, 1435, 1276,

M.P. = 140 – 144 °C

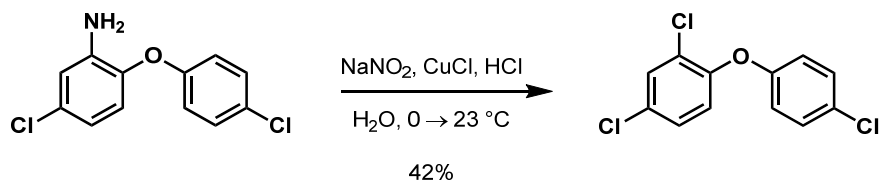


Phenols 374a – 374d: Prepared following General Procedure A using deoxyestrone (100.0 mg, 0.39 mmol, 1.00 eq.), 4,5-dichlorophthaloyl peroxide (142.0 mg, 0.51 mmol, 1.30 eq., 84%), and HFIP (3.9 mL) at 50 °C for 24 hrs. The crude pale yellow solid was purified by silica gel chromatography; 5 - 20% EtOAc in CH₂Cl₂ and hexane (1:1) to afford the mixture of estrone phenols **374a**, **374b**, **374c**, and **374d** (76.4 mg, 0.28 mmol, 72%, **374a** : **374b** : **374c** : **374d** = 2.1:2:1:1) as a white solid and the starting deoxyestrone as a white solid (19.5 mg, 0.08 mmol, 20%). The spectra of the title compounds match that for **374a**, **374b**, **374c**, and **374d**.^{45,46}



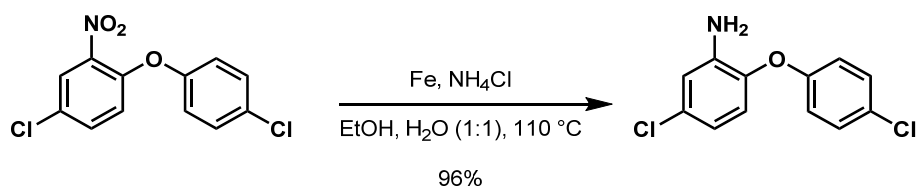
Triclosan (369): Prepared following General Procedure B using 2,4,4'-trichlorophenylether (95.0 mg, 0.35 mmol, 1.00 eq.), 4,5-dichlorophthaloyl peroxide (188.0 mg, 0.70 mmol, 2.00 eq., 86%), and HFIP (3.5 mL) at 60 °C for 24 hrs. The crude brown foam was purified by silica gel chromatography; 1 – 10% Et₂O in pentane to provide triclosan (**369**) (52.0 mg, 0.18 mmol, 52%) as a pale yellow foam and the starting trichloride (8.4 mg, 0.03 mmol, 9%). The spectra of the title compound matches that of triclosan (**369**).⁴⁷

¹H-NMR (400 MHz, CDCl₃)⁴⁷: δ 7.48 (d, 1H, *J* = 2.2 Hz), 7.22 (dd, 1H, *J* = 2.2, 8.5 Hz), 7.07 (d, 1H, *J* = 2.2 Hz), 6.95 (d, 1H, *J* = 8.5 Hz), 6.81 (dd, 1H, *J* = 2.2, 8.5 Hz), 6.66 (d, 1H, *J* = 8.5 Hz), 5.63 (bs, 1H)



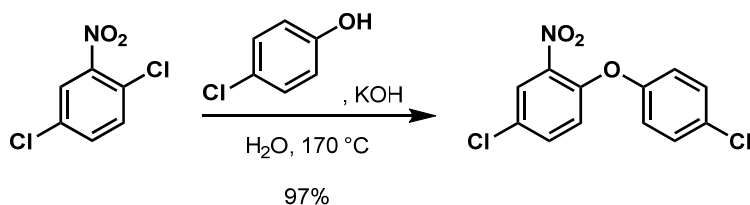
The aniline (2.96 g, 11.7 mmol, 1.00 eq.) was suspended in water (9 mL) and concentrated HCl (7 mL, 87.0 mmol, 7.45 eq., 38%, 12.4 M). The orange solid mixture was placed in an ice water bath cooled to 0 °C and stirred vigorously (400 rpm). After 5 minutes NaNO₂ (0.88 g, 12.8 mmol, 1.10 eq.) was added all at once and the mixture immediately changed to a deep red-orange color. After 25 minutes, CuCl (1.73 g, 17.5 mmol, 1.50 eq.) was added all at once followed by concentrated HCl (1.5 mL, 18.0 mmol, 1.55 eq., 38%, 12.4 M). The dark red-orange solution was removed from the cooling bath and stirred vigorously (400 rpm) at 23 °C. After 30 minutes the dark orange biphasic mixture was diluted with Et₂O (20 mL), poured into a separatory funnel, partitioned, and the organic layer was washed with 1 N HCl (3 x 25 mL). Residual organics were extracted from the aqueous layer with Et₂O (3 x 25 mL), combined, dried over solid Na₂SO₄, decanted, and concentrated. The crude dark yellow solid was purified by silica gel chromatography; hexane to provide the known 2,4,4'-trichlorophenylether (1.34 g, 4.90 mmol, 42%) as a white crystalline solid.⁴⁸ The spectra of the title compound matches that of the trichloride.⁴⁸

¹H-NMR (400 MHz, CDCl₃): δ 7.47 (d, 1H, *J* = 2.7 Hz), 7.29 (d, 2H, *J* = 8.9 Hz), 7.21 (dd, 1H, *J* = 2.7, 8.9 Hz), 6.92 (d, 1H, *J* = 8.9 Hz), 6.88 (d, 2H, *J* = 8.9 Hz)



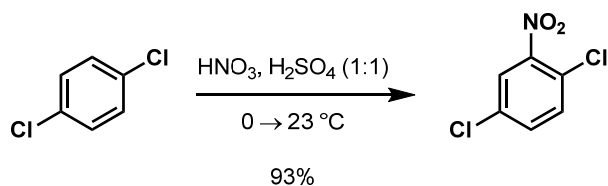
To a suspension of 2-nitro-4,4'-dichlorophenyl ether (3.43 g, 12.1 mmol, 1.00 eq.) in ethanol (48.3 mL) and water (48.3 mL) was added iron powder (1.82 g, 32.6 mmol, 2.70 eq.) and solid NH_4Cl (2.91 g, 54.3 mmol, 4.50 eq.). The reaction vessel was equipped with a reflux condenser, purged with N_2 , and the black mixture was placed in an oil bath heated to $110\text{ }^\circ\text{C}$ stirring vigorously (800 rpm). After 12 hrs the black mixture was suction filtered over celite to remove the iron and the filtrate solution was concentrated to remove the EtOH. The resultant yellow solid mixture was diluted with CH_2Cl_2 (50 mL) and an aqueous phosphate buffer (50 mL, 0.2 M, pH = 10), poured into a separatory funnel, partitioned, and the organics were washed with an aqueous phosphate buffer (1 x 25 mL, 0.2 M, pH = 10). Residual organics were extracted from the aqueous with CH_2Cl_2 (2 x 30 mL), combined, dried over solid Na_2SO_4 , decanted, and concentrated to provide the known aniline (2.96 g, 11.7 mmol, 96%) pure as a yellow solid.⁴⁸

$^1\text{H-NMR}$ (400 MHz, CDCl_3): δ 7.26 (d, 2H, $J = 5.5$ Hz), 6.89 (d, 2H, $J = 9.2$ Hz), 6.80 (d, 1H, $J = 2.4$ Hz), 6.76 (d, 1H, $J = 8.6$ Hz), 6.67 (dd, 1H, $J = 2.4, 8.6$ Hz), 3.86 (bs, 2H).



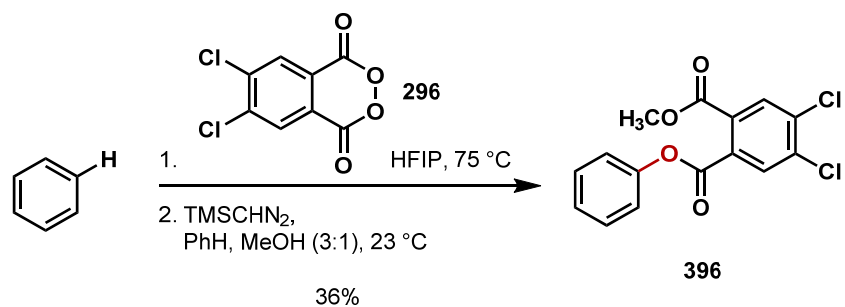
The solid mixture of 1,4,-dichloro-2-nitrobenzene (2.40 g, 12.50 mmol, 1.00 eq.), KOH (0.74 g, 13.13 mmol, 1.05 eq.), and 4-chlorophenol (1.77 g, 13.75 mmol, 1.10 eq.) was suspended in water (1 mL), placed in an oil bath heated to 170 °C, and stirred rapidly (400 rpm). After 2.5 hrs the reddish-brown liquid was removed from the oil bath, cooled to 23 °C, diluted with Et₂O (20 mL), and residual 4-chlorophenol was quenched with 4 N NaOH (20 mL). The biphasic mixture was then poured into a separatory funnel. 4 N NaOH (20 mL) and Et₂O (20 mL) was added to the reaction vessel to dissolve residual solids with the aid of sonication, and this yellow-orange mixture was added to the separatory funnel. The layers were partitioned and the organic layer was washed with 4 N NaOH (3 x 20 mL) to remove the excess 4-chlorophenol. The residual organics were extracted from the aqueous layer with Et₂O (3 x 20 mL), combined, dried over solid Na₂SO₄, decanted, and concentrated to reveal the known 2-nitro-4,4'-dichlorophenyl ether (3.43 g, 12.07 mmol, 97%) pure as a dark yellow solid.⁴⁸

¹H-NMR (400 MHz, CDCl₃): δ 7.95 (d, 1H, *J* = 2.4 Hz), 7.48 (dd, 1H, *J* = 2.4, 8.9 Hz), 7.35 (d, 2H, *J* = 8.9 Hz), 6.97 (d, 3H, *J* = 8.9 Hz).



Concentrated H_2SO_4 (6.7 mL, 18 M, 98%) was slowly added to fuming HNO_3 (6.7 mL, 90%) in an ice water bath cooled to $0\text{ }^\circ\text{C}$. After 5 minutes *p*-dichlorobenzene (2.00 g, 13.61 mmol, 1.00 eq.) was added all at once. After 2 minutes the cold bath was removed and the yellow heterogeneous mixture was stirred vigorously (500 rpm) at $23\text{ }^\circ\text{C}$. After 15 minutes the yellow homogeneous solution was poured into ice water (250 mL), and the resultant yellow solid was filtered. The yellow solid was then dried *in vacuo* with heating ($100\text{ }^\circ\text{C}$) for 30 minutes to remove excess H_2O to afford the known 2-nitro-4-dichlorobenzene (2.43 g, 12.66 mmol, 93%) pure as a yellow solid which solidified upon cooling to $23\text{ }^\circ\text{C}$.⁴⁸

$^1\text{H-NMR}$ (400 MHz, CDCl_3): δ 7.89 (bs, 1H), 7.50 (d, 2H, $J = 1.0\text{ Hz}$).



Phthalate Ester 396: Prepared following General Procedure C using benzene (10.0 mg, 0.13 mmol, 1.00 eq), 4,5-dichlorophthaloyl peroxide (87.0 mg, 0.32 mmol, 2.50 eq., 86%), HFIP (1.3 mL), and TMSCHN₂ (0.3 mL, 0.64 mmol, 5.00 eq., 2.0 M). The crude yellow foam was purified by silica gel chromatography; benzene to provide the phthalate ester **396** (15.1 mg, 0.05 mmol, 36%) as a clear amorphous solid.

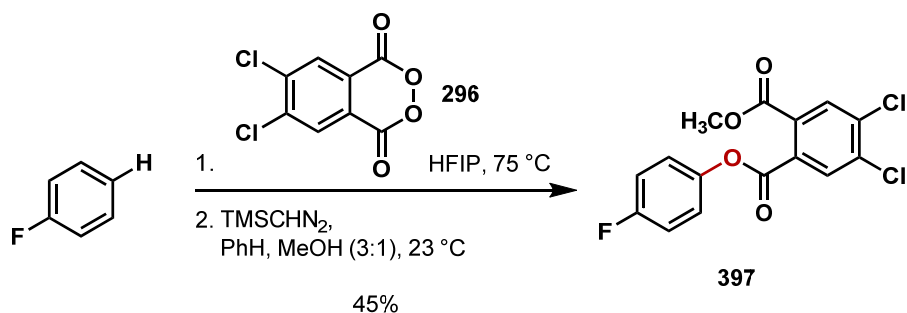
R_f = 0.56 (benzene)

¹H-NMR (400 MHz, CDCl₃): δ 7.97 (s, 1H), 7.91 (s, 1H), 7.44 (t, 2H, *J* = 7.9 Hz), 7.29 (t, 1H, *J* = 7.9), 7.25 (d, 2H, *J* = 7.9), 3.93 (s, 3H)

¹³C-NMR (100 MHz, CDCl₃): δ 165.93, 164.47, 150.79, 136.44, 136.37, 131.53, 131.45, 131.40, 129.86, 128.55, 126.60, 121.47, 53.42

IR (neat film, cm⁻¹): 2955, 1733, 1436, 1288, 1069

HRMS (EC-CI): calcd. for C₁₅H₁₀O₄Cl₂ [M+H]⁺ 325.0034, found 325.0028.



Phthalate Ester 397: Prepared following General Procedure C using fluorobenzene (10.0 mg, 0.10 mmol, 1.00 eq.), 4,5-dichlorophthaloyl peroxide (69.0 mg, 0.26 mmol, 2.50 eq., 88%), HFIP (1.0 mL), and TMSCHN₂ (0.3 ml, 0.52 mmol, 5.00 eq., 2.0 M). The crude yellow foam was purified by silica gel chromatography; benzene to provide the phthalate ester **397** (16.0 mg, 0.05 mmol, 45%) as a white solid.

R_f = 0.63 (benzene)

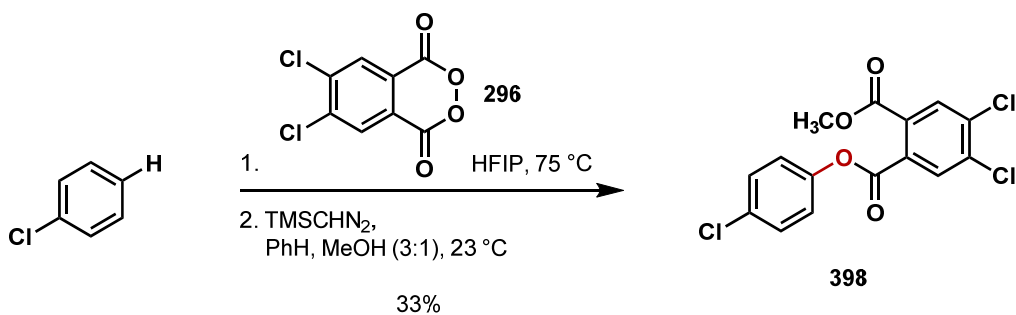
¹H-NMR (400 MHz, CDCl₃): δ 7.94 (s, 1H), 7.93 (s, 1H), 7.24 – 7.21 (m, 2H), 7.12 (dd, 2H, *J* = 8.2, 8.9), 3.93 (s, 3H)

¹³C-NMR (100 MHz, CDCl₃) δ 165.76, 164.62, 161.98, 146.60, 136.52, 136.48, 131.54, 131.36, 131.31, 131.28, 123.00, 116.23, 53.42

IR (neat film, cm⁻¹): 2924, 2356, 1733, 1503, 1291, 1116

HRMS (EC-Cl): calcd. for C₁₅H₉O₄Cl₂F [M+H]⁺ 342.9940, found 342.9934.

M.P. = 96 – 99 °C.



Phthalate Ester 398: Prepared following General Procedure C using chlorobenzene (10.0 mg, 0.09 mmol, 1.00 eq.), 4,5-dichlorophthaloyl peroxide (60.0 mg, 0.22 mmol, 2.50 eq., 86%), HFIP (0.88 mL), and TMSCHN₂ (0.2 mL, 0.44 mmol, 5.00 eq., 2.0 M). The crude yellow foam was purified by silica gel chromatography; benzene to provide the phthalate ester **398** (10.3 mg, 0.03 mmol, 33%) as a clear foam.

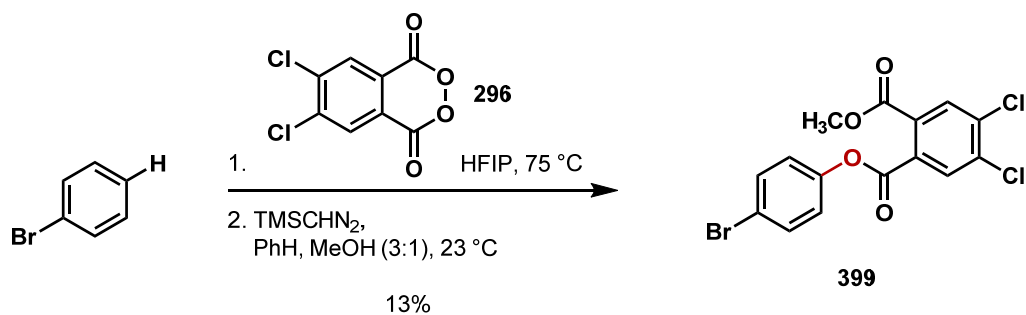
R_f = 0.69 (benzene)

¹H-NMR (400 MHz, CDCl₃): δ 7.93 (s, 2H), 7.40 (d, 2H, *J* = 8.9 Hz), 7.21 (d, 2H, *J* = 8.9 Hz), 3.92 (s, 3H)

¹³C-NMR (100 MHz, CDCl₃): δ 165.48, 164.16, 149.00, 136.33, 136.30, 131.80, 131.33, 131.08, 131.03, 130.99, 129.70, 122.66, 53.22

IR (neat film, cm⁻¹): 2955, 2924, 1733, 1503, 1487, 1288

HRMS (EC-Cl) calcd. for C₁₅H₉O₄Cl₃ [M+H]⁺ 358.9645, found 358.9636.



Phthalate Ester 399: Prepared following [General Procedure C](#) using bromobenzene (10.0 mg, 0.06 mmol, 1.00 eq.), 4,5-dichlorophthaloyl peroxide (43.0 mg, 0.16 mmol, 2.50 eq., 86%), HFIP (0.6 mL), and TMSCHN₂ (0.2 ml, 0.32 mmol, 5.00 eq., 2.0 M). The crude yellow foam was purified by silica gel chromatography; hexane – 3% EtOAc in hexane to afford the phthalate **399** (3.2 mg, 0.01 mmol, 13%) as a colorless foam.

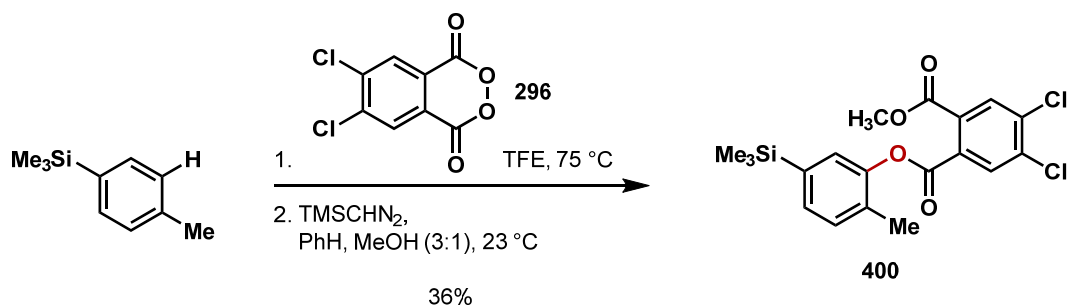
R_f = 0.40 (10% EtOAc in hexane)

¹H-NMR (400 MHz, CDCl₃): δ 7.93 (s, 2H), 7.55 (d, 2H, *J* = 8.9 Hz), 7.15 (d, 2H, *J* = 8.9 Hz), 3.92 (s, 3H)

¹³C-NMR (100 MHz, CDCl₃): δ 165.48, 164.08, 149.55, 136.32, 132.68, 131.33, 131.08, 131.02, 131.00, 123.08, 119.53, 53.22

IR (neat film, cm⁻¹) 2952, 1731, 1513, 1286

HRMS (EC-ESI): calcd. for C₁₅H₉O₄Cl₂Br [M+Na]⁺ 426.8931, found 426.8923.



Phthalate Ester 400: Prepared following General Procedure C using *p*-trimethylsilyl toluene (30.0 mg, 0.18 mmol, 1.00 eq.), 4,5-dichlorophthaloyl peroxide (124.0 mg, 0.46 mmol, 2.50 eq., 86%), TFE (1.8 mL), and TMSCHN₂ (0.5 ml, 0.91 mmol, 5.00 eq., 2.0 M). The crude yellow foam was purified by silica gel chromatography; benzene to afford the phthalate **400** (27.1 mg, 0.07 mmol, 36%) as a colorless foam.

$R_f = 0.70$ (benzene)

¹H-NMR (400 MHz, C₆D₆): δ 7.74 (s, 1H), 7.59 (s, 1H), 7.42 (s, 1H), 7.25 (d, 1H, *J* = 6.6 Hz), 7.08 (d, 1H, *J* = 6.6 Hz), 3.42 (s, 3H), 2.13 (s, 3H), 0.20 (s, 9H)

¹³C-NMR (100 MHz, CDCl₃): δ 165.64, 163.48, 149.87, 139.95, 136.25, 135.79, 132.60, 131.63, 131.37, 131.35, 131.24, 131.23, 131.20, 126.60, 52.47, 16.22, 1.19

IR (neat film, cm⁻¹) 1738, 1287, 1249

5. References

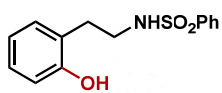
1. (a) Russell, K. E.. *The Journal of the American Chemical Society* **1955**, 77, 4814-4815.
(b) Greene, F. D *The Journal of the American Chemical Society* **1956**, 78, 2246-2250 (1956).
2. Still, W. C., Kahn, M. and Mitra, A. J. *The Journal of Organic Chemistry* **1978**, 43, 2923-2925.
3. Vangeneugden, D.; Kiebooms, R.; Adriaensens, P.; Vanderzande, D.; Gelan, J.; Desmet, J.; and Huyberechts, G. *Acta Polymerica* **1998**, 49 (12), 687 – 692.
4. Yuan, C.; Axelrod, A.; Valera, M.; Danysh, L.; and Siegel, D. *Tetrahedron Letters* **2011**, 52, 2540 – 2542.
5. Sigma-Aldrich website: <http://www.sigmaaldrich.com/united-states.html>.
6. Spectral data Database for Organic Compounds SDBS
http://riodb01.ibase.aist.go.jp/sdbs/cgi-bin/cre_index.cgi?lang=eng.
7. Szostak, M.; Spain, M.; and Procter, D. J. *Organic Letters* **2012**, 14(3), 840-843.
8. Szostak, M.; Spain, M.; and Procter, D. J. *The Journal of Organic Chemistry* **2012**, 77 (7), 3049.
9. Yuasa, Y.; Shibuya, S.; Yuasa, Y. *Synthetic Communications* **2003**, 33(9), 1469-1475.
10. Kelly, B. D. and Lambert, T. H. *Organic Letters* **2011**, 13(4), 740-743.
11. Schmidt, B.; Holter, F.; Kelling, A; and Schilde, U. *The Journal of Organic Chemistry* **2011**, 76, 3357.
12. Martin, P.; Trobe, M.; Tan, H.; Kleineweischede, R.; and Breinbauer, R. *Chemistry – A European Journal* **2013**, 19 (7), 2442.
13. Maiti, G.; Kayal, U.; Karmahar, R.; and Bhattacharya, R. N. *Tetrahedron Letters* **2012**, 53, 6321.
14. Alcaide, B.; Almedros, P.; Quiros, M. T.; Lopez, R.; Menendez, M. I.; Sochacha-Cwichla, A. *The Journal of the American Chemical Society* **2013**, 135, 898.

15. Rauniyar, V. and Hall, D. G. *The Journal of Organic Chemistry* **2009**, 74 (11), 4236
16. Marumoto, S. and Miyazawa, M. *Tetrahedron* **2011**, 67, 495.
17. Chen, H.; Wang, J.; Hong, X.; Zhou, H-B.; Dong, C. *The Canadian Journal of Chemistry* **2012**, 90(9), 758-761.
18. Rao, G. K.; Gowda, N. B.; and Ramakrishna; R. A. *Synthetic Communications* **2012**, 42, 893.
19. Dong, C-Z.; Ahamada-Himidi, A.; Plocki, S.; Aoun, D.; Touaibia, M.; Meddad-Bel Habich, N.; Huet, J.; Redeuilh, C.; Ombetta, J-E.; Godfroid, J-J.; Massicot, F.; and Heymans, F. *Bioorganic & Medicinal Chemistry* **2005**, 13(6), 1989.
20. Peters Martin, P.; Trobe, M.; Tan, H.; Kleineweischede, R.; and Breinbauer, R. *Chemistry – A European Journal* **2013**, 19 (7), 2442.
21. Fleming, P. and O’Shea, D. F. *The Journal of the American Chemical Society* **2011**, 133, 1698.
22. Murr, M. D-E.; Nowaczyk, S.; Le Gall, T.; and Mioskowski, C. *The European Journal of Organic Chemistry* **2006**, 1489.
23. a) Kirk, K. L. *The Journal of Fluorine Chemistry* **1992**, 59, 197. b) Weinstock, J.; Gaitanopoulos, D. E.; Stringer, O. D.; Franz, R. G.; Hieble, J. P.; Kinter, L. B.; Mann, W. A.; Flaim, K. E.; and Gessner, G. *The Journal of Medicinal Chemistry* **1987**, 30, 1166.
24. Cabaret, D.; Adediran, A. S.; Garcia Gonzalez, M. J.; Pratt, R. F.; and Wakselman, M. *The Journal of Organic Chemistry* **1999**, 64, 713.
25. Fujii, S.; Chang, S. Y.; and Burke, M. *Angewandte Chemie, International Edition* **2011**, 50, 7862.
26. Snider, B. B. and Patricia, J. J. *The Journal of Organic Chemistry* **1989**, 54, 38.
27. Fujiwara, A. N. and Acton, E. M. *The Canadian Journal of Chemistry* **1970**, 48, 1346.
28. Mrob, G.; Ladzik, S.; Reinke, H.; Spannenberg, A.; Fischer, C.; and Langer, P. *Synthesis* **2009**, 13, 2236.

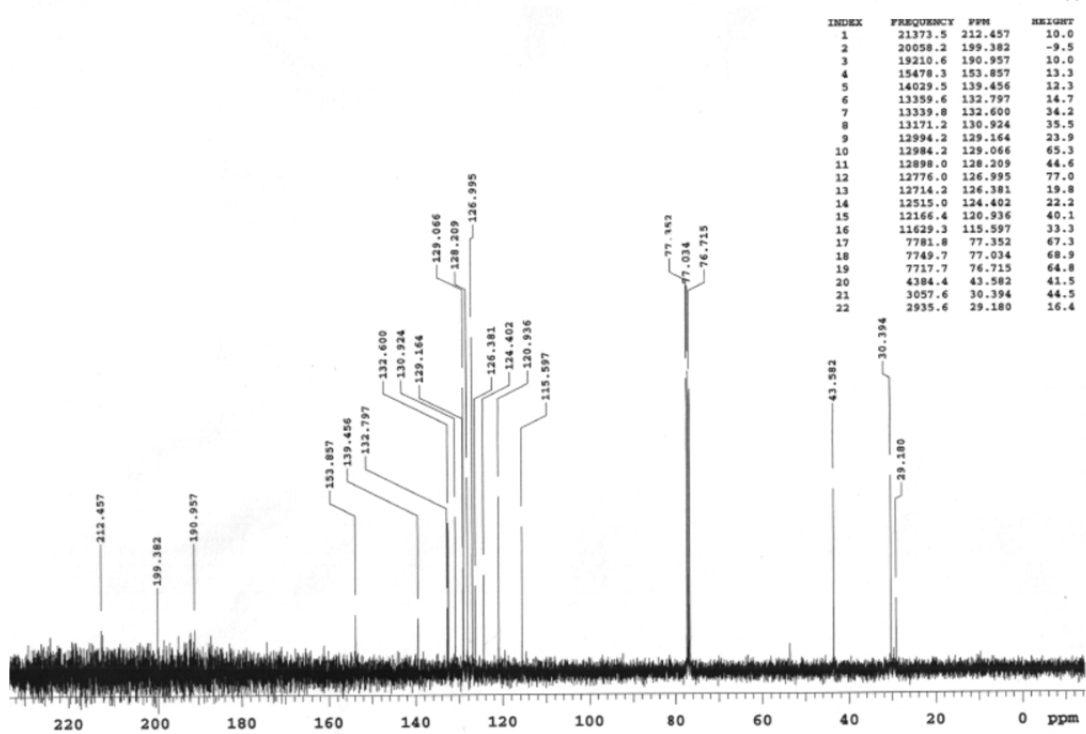
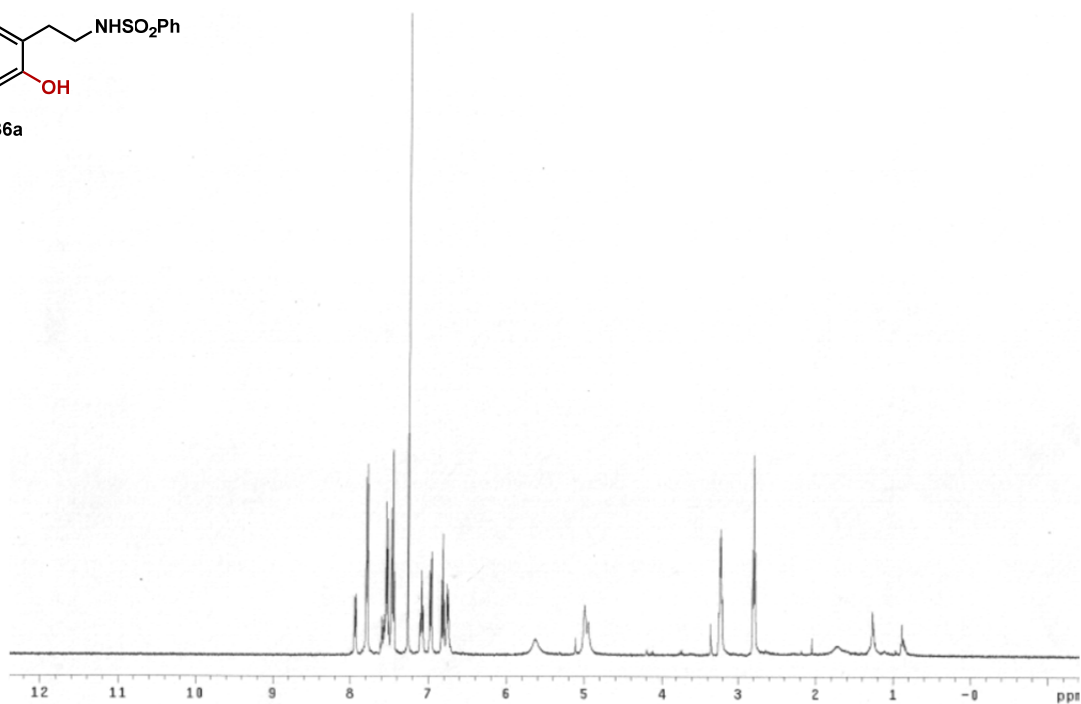
29. Lu, Y.; Lum, T. K.; Augustine, Y. W. L.; Weltrowska, G.; Nguyen, T. M.-D.; Lemieux, C.; Chung, N. N.; and Schiller, P. W. *The Journal of Medicinal Chemistry* **2006**, 49, 5382.
30. Ghatak, A.; Dorsey, J. M.; Garner, C. M.; and Pinney, K. G. *Tetrahedron Letters* **2003**, 44(21), 4145.
31. Ramdayal, F. D.; Kiemle, D. J.; and LaLonde, R. T. *The Journal of Organic Chemistry* **1999**, 64(13), 4607.
32. Petrovic, D. and Bruckner, R. *Organic Letters* **2011**, 13(24), 6524.
33. Sher, M.; Dang, T. H.; Tam, A.; Zafar, R.; Muhammad, A.; Fischer, C.; and Langer, P. *The Journal of Organic Chemistry* **2007**, 72(16), 6284.
34. Churcher, I.; Hallett, D.; and Magnus, P. *Tetrahedron* **1999**, 55 (6), 1597.
35. Legrand, S.; Nordlander, G.; Nordnehem, H.; Borg-Karlson, A.; and Ghiellus, C. R.; *Zeitschrift fuer Naturforschung, B: Chemical Sciences* **2004**, 59 (7), 829.
36. Rosiak, A.; Frey, W.; and Christoffers, J. *The European Journal of Organic Chemistry* **2006**, 4044.
37. Payne, R. J.; Toscano, M. D.; Bulloch, E. M. M.; Abell, A. D.; and Abell, C. *Organic & Biomolecular Chemistry* **2005**, 3, 2271 – 2281.
38. Woodring, J. L.; Bland, N. D.; Ochiana, S. O.; Campbell, R. K.; and Pollastri, M. P. *Bioorganic & Medicinal Chemistry Letters* **2013**, 23, 5971.
39. Yuan, C.; Liang, Y.; Hernandez, T. M.; Berriochoa, A.; Houk, K. N.; and Siegel, D. *Nature* **2013**, 499, 192.
40. Claudi, F.; Cardellini, M.; Cingolani, G. M.; Piergentili, A.; Peruzzi, G.; and Balduini, W. *The Journal of Medicinal Chemistry* **1990**, 33(9), 2408 – 2412.
41. Aoyagi, N.; Furusho, Y.; and Endo, T. *The Journal of Polymer Science, Part A: Polymer Chemistry*, **2013**, 51(5), 1230 – 1242.
42. Risdall, P. C.; Adams, S. S.; Crampton, E. L.; and Marchant, B. *Xenobiotica* **1978**, 8, 691.

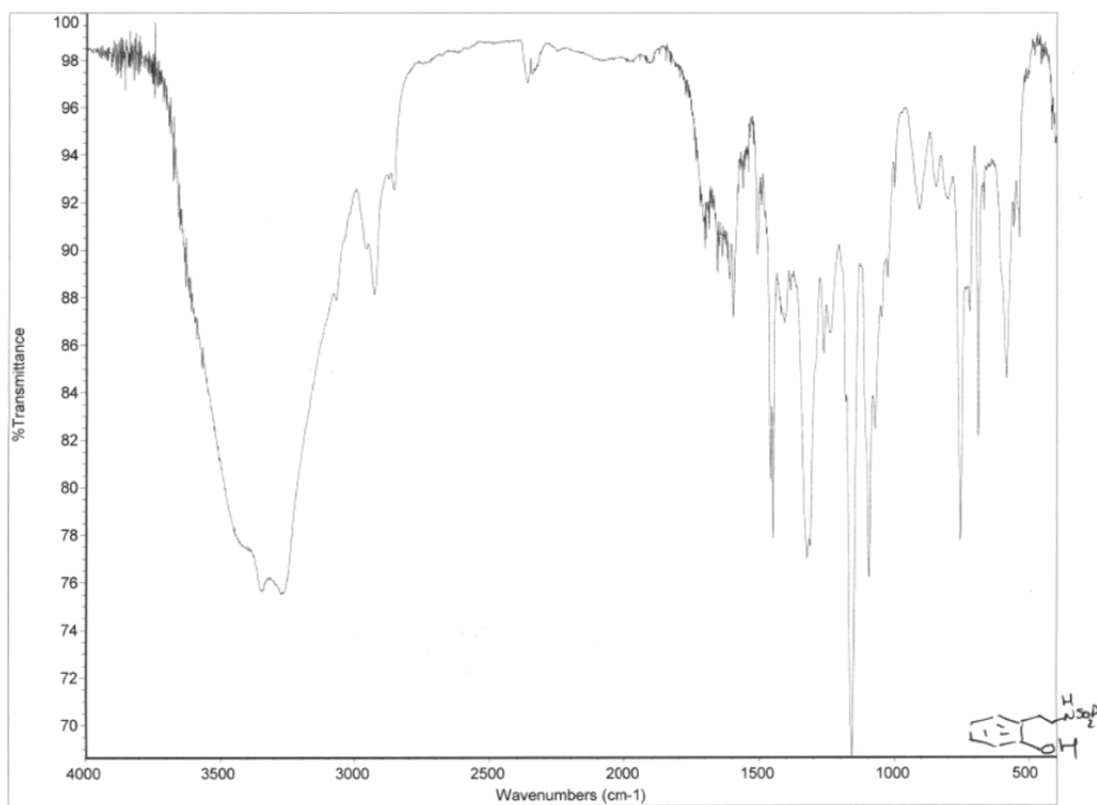
43. a) Bayly, C. I.; Black, W. C.; Leger, S.; Ouimet, N.; Ouellet, M.; and Percival, M. D. *Bioorganic & Medicinal Chemistry Letters* **1999**, 9, 307. b) Chen, Y.; Sun, J.; Huang, Z.; Liao, H.; Peng, S.; Lehmann, J.; and Zhang, Y. *Bioorganic & Medicinal Chemistry* **2013**, 21, 2462.
44. Liu, Z. and Xiang, J. *Organic Process Research and Development* **2006**, 10, 285.
45. Park, J. and Chae, J. *Synlett* **2010**, 11, 1651
46. Funk, R. L. and Vollhardt, P. C. *The Journal of the American Chemical Society* **1980**, 102, 5253.
47. Wilson, K. A. and Beck, J. J. *Chemical Educator* **2007**, 12 (5), 338.
48. a) Groves, L. G.; Turner, E. E.; and Sharp, G. I. *The Journal of the American Chemical Society* **1929**, 512. b) Nostrolm, A. and Andersson, K. *Chemosphere* **1977**, 6 (5), 237.

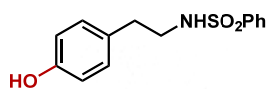
6. Catalog of Spectra



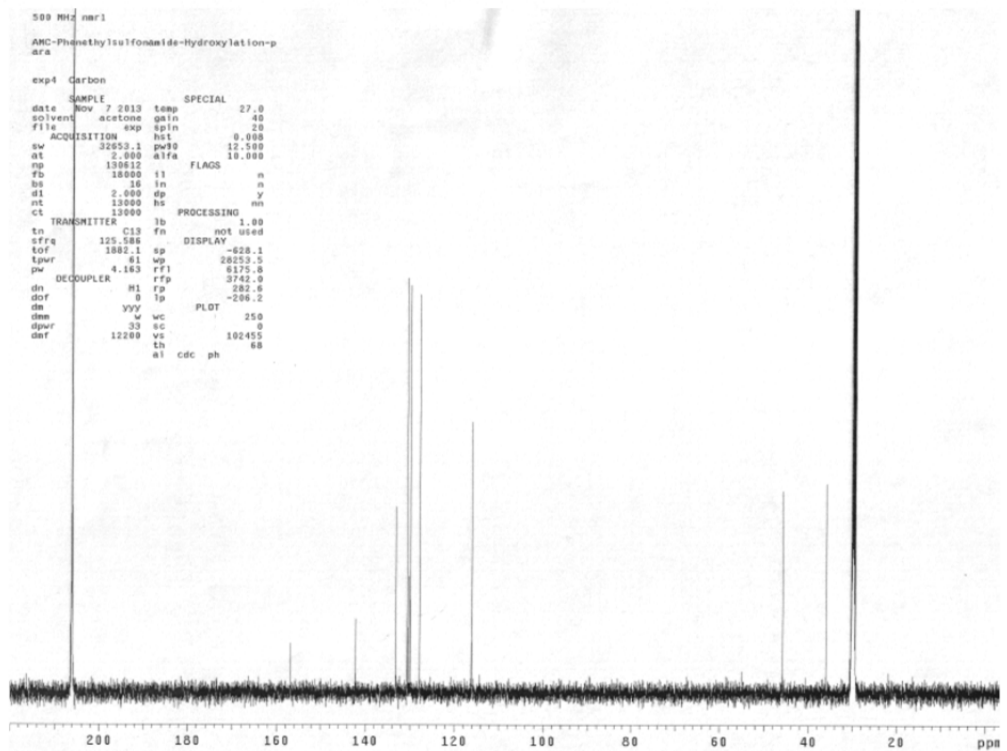
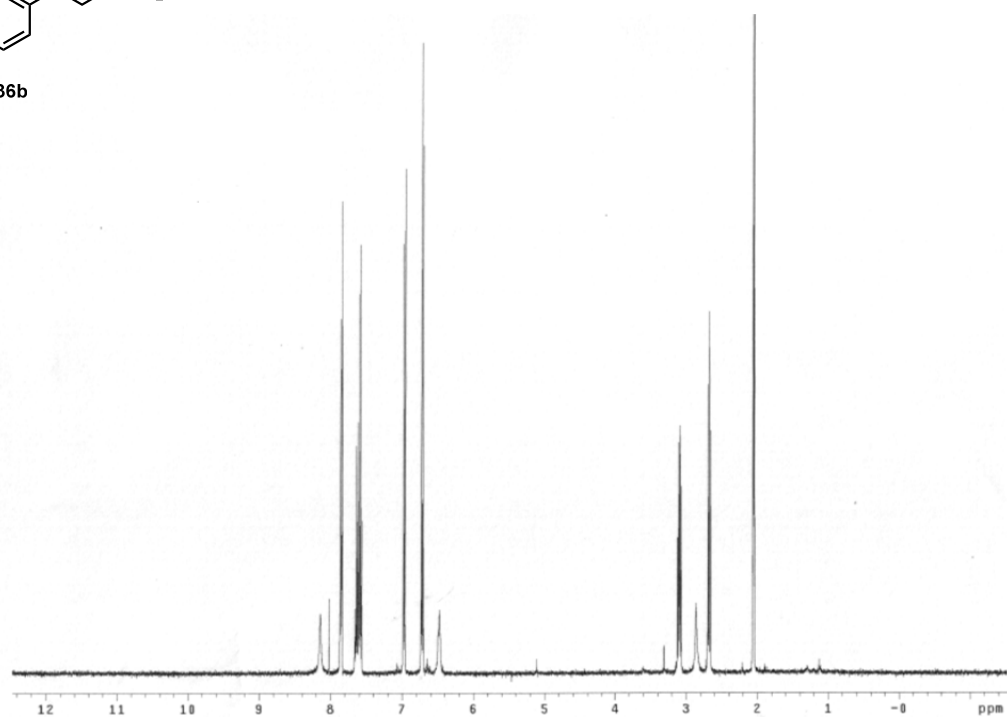
336a

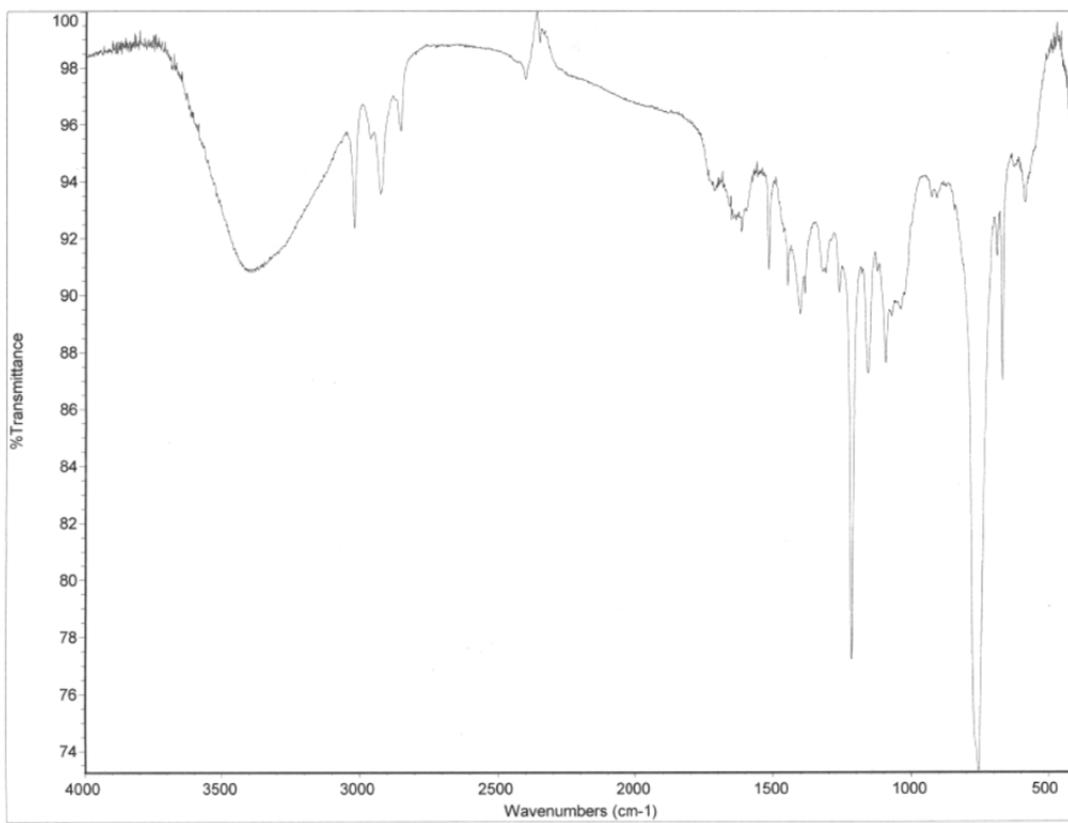


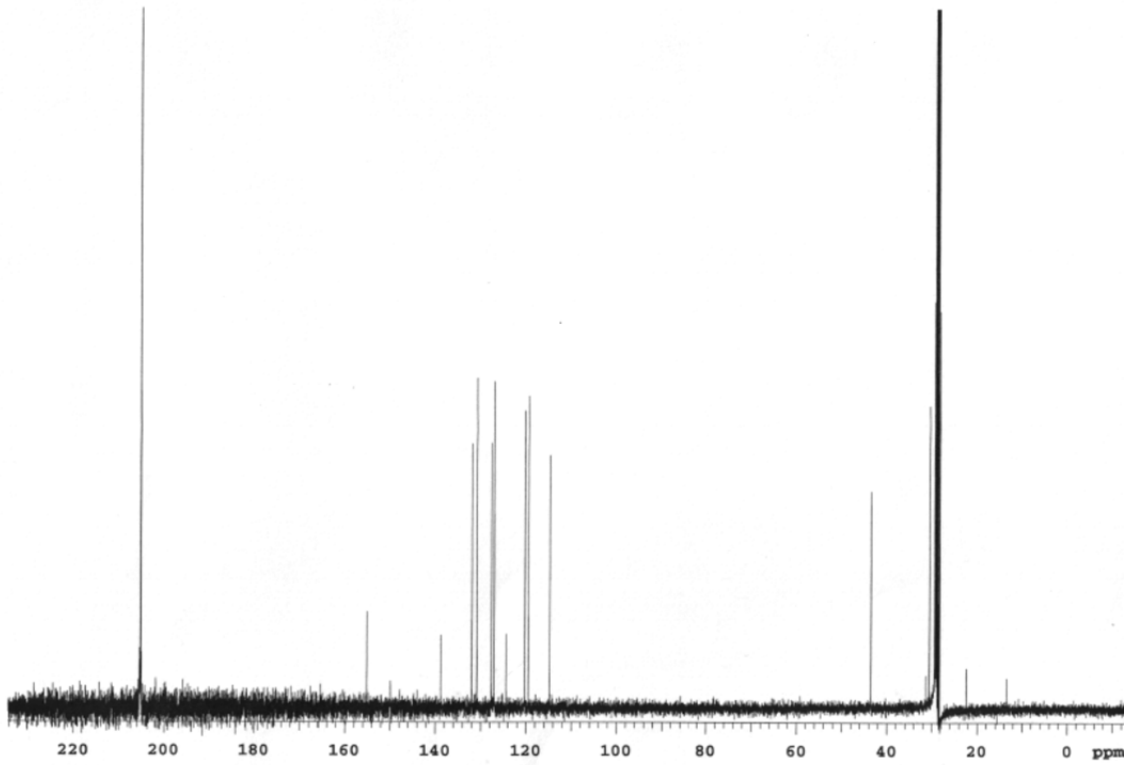
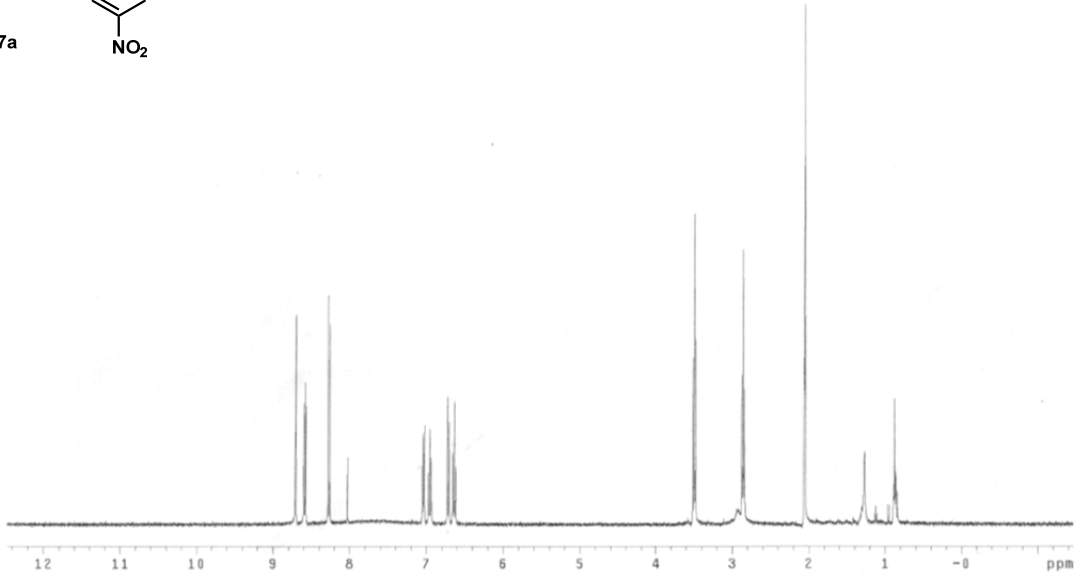
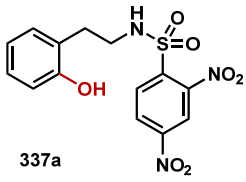


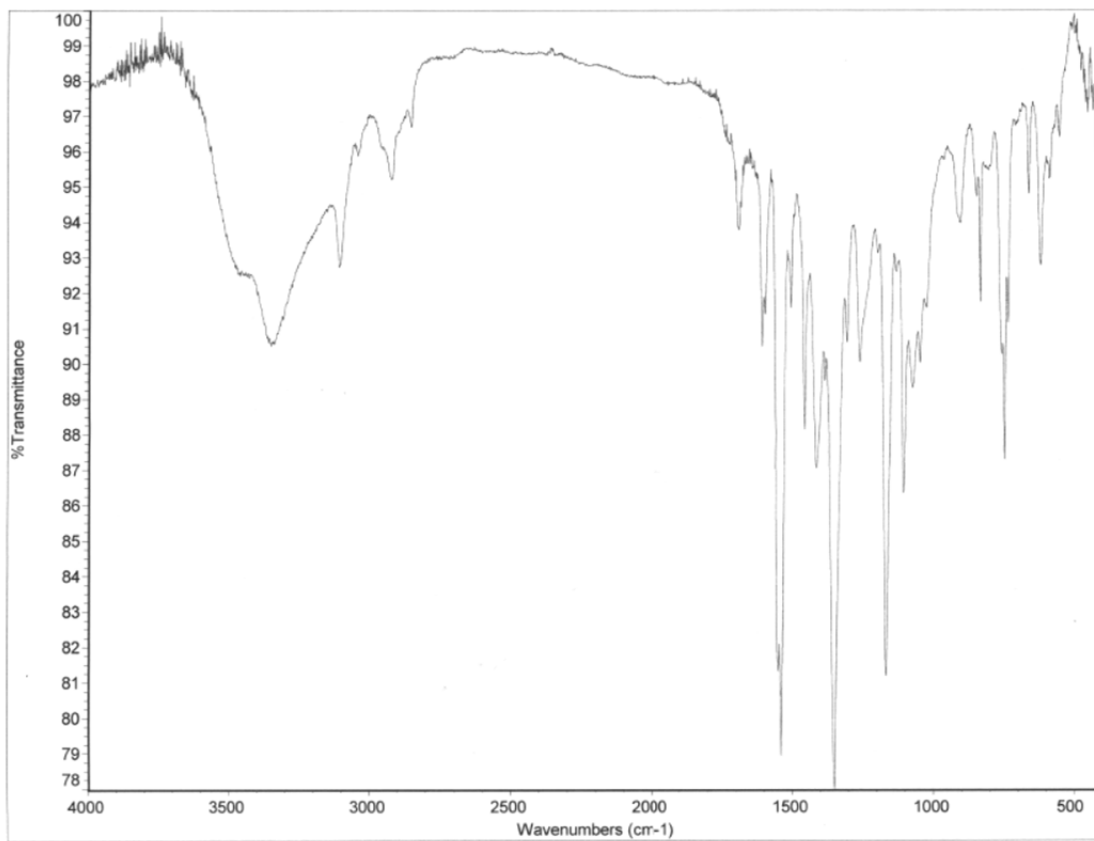


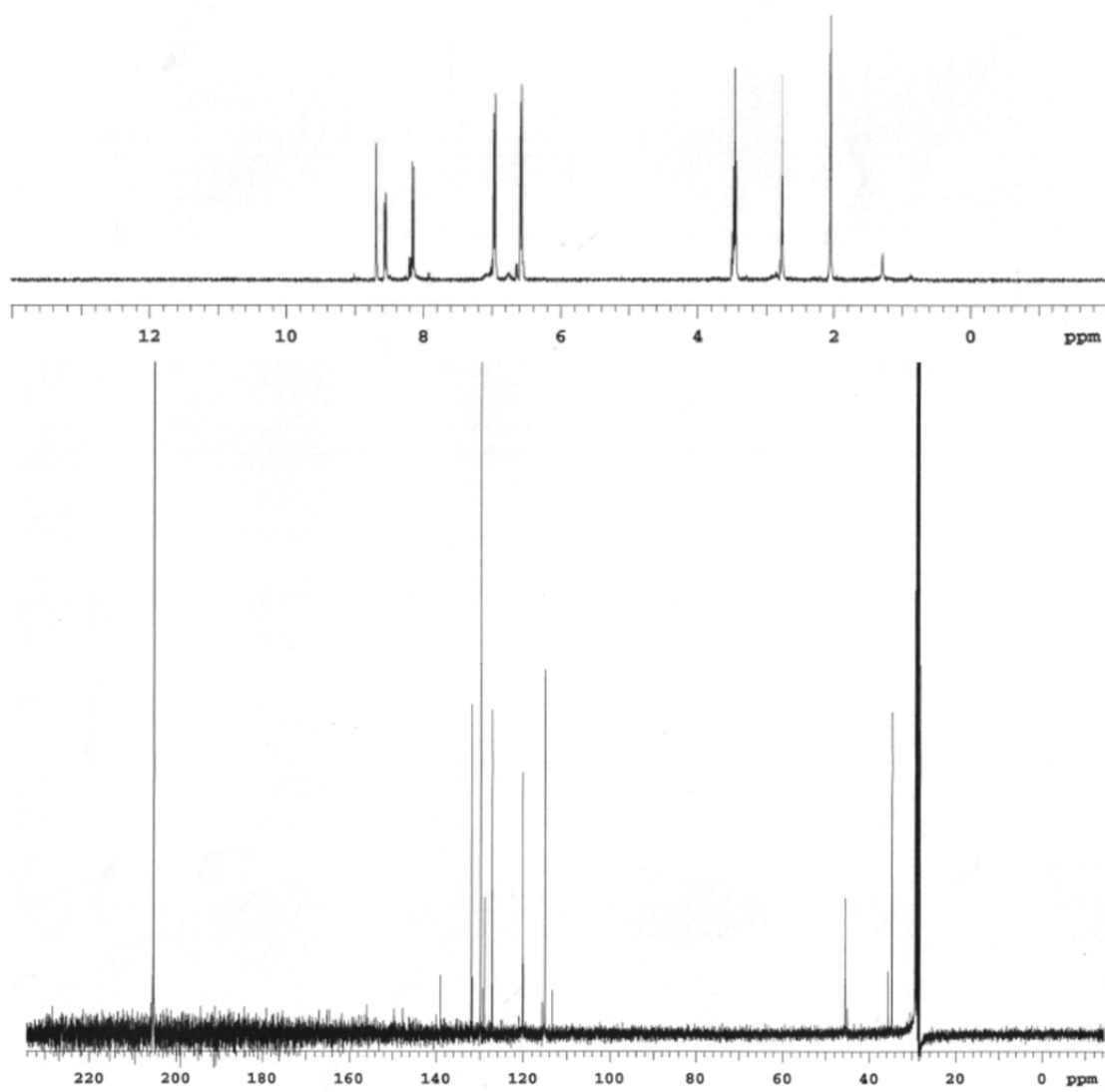
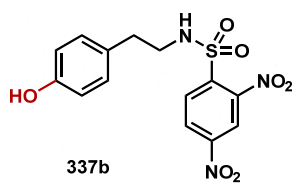
336b

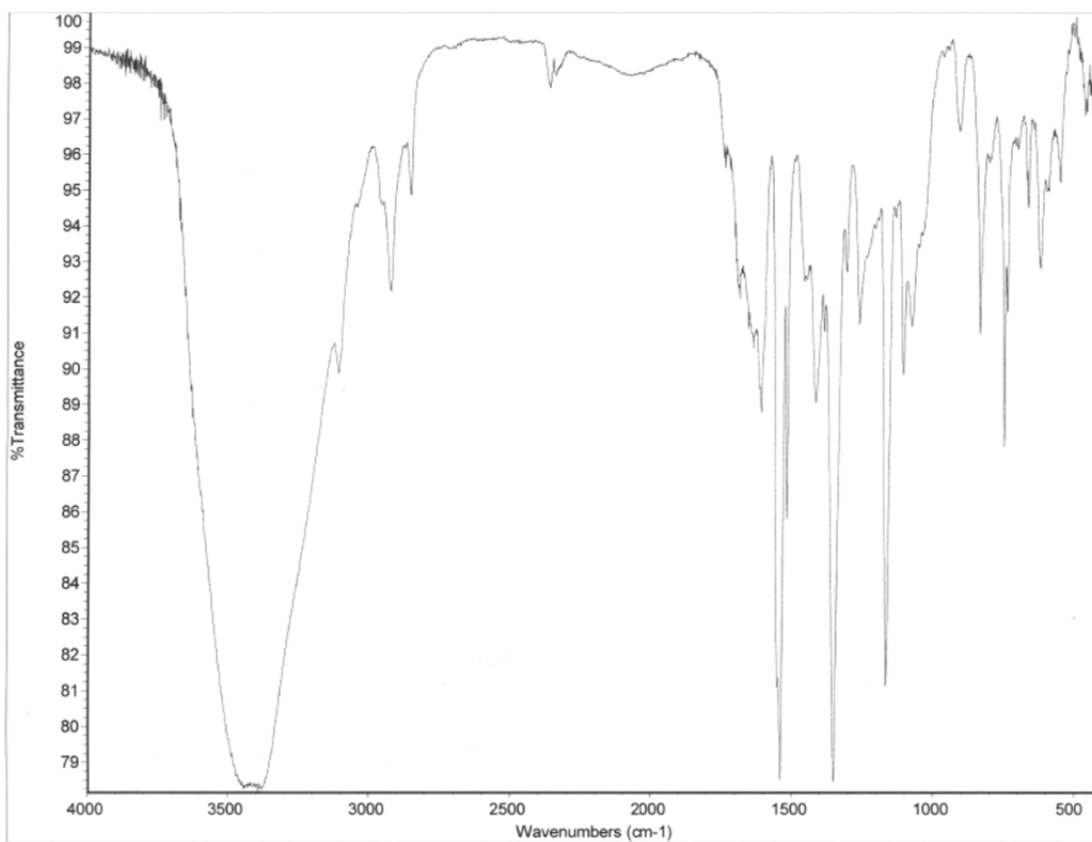


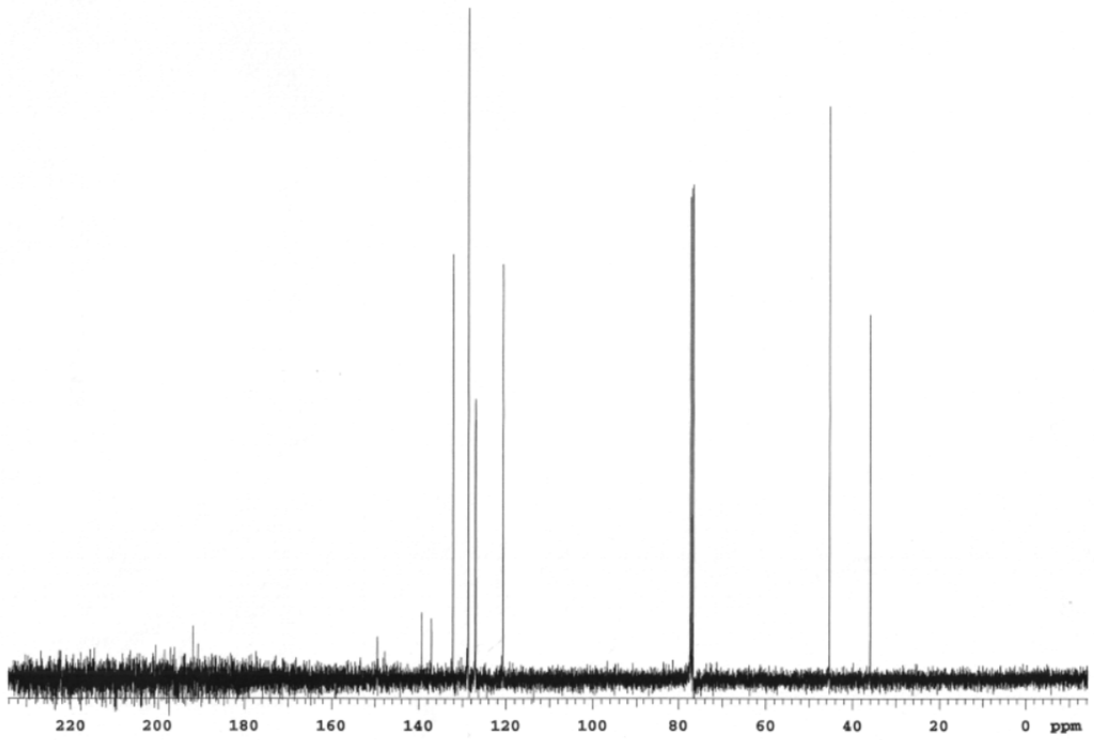
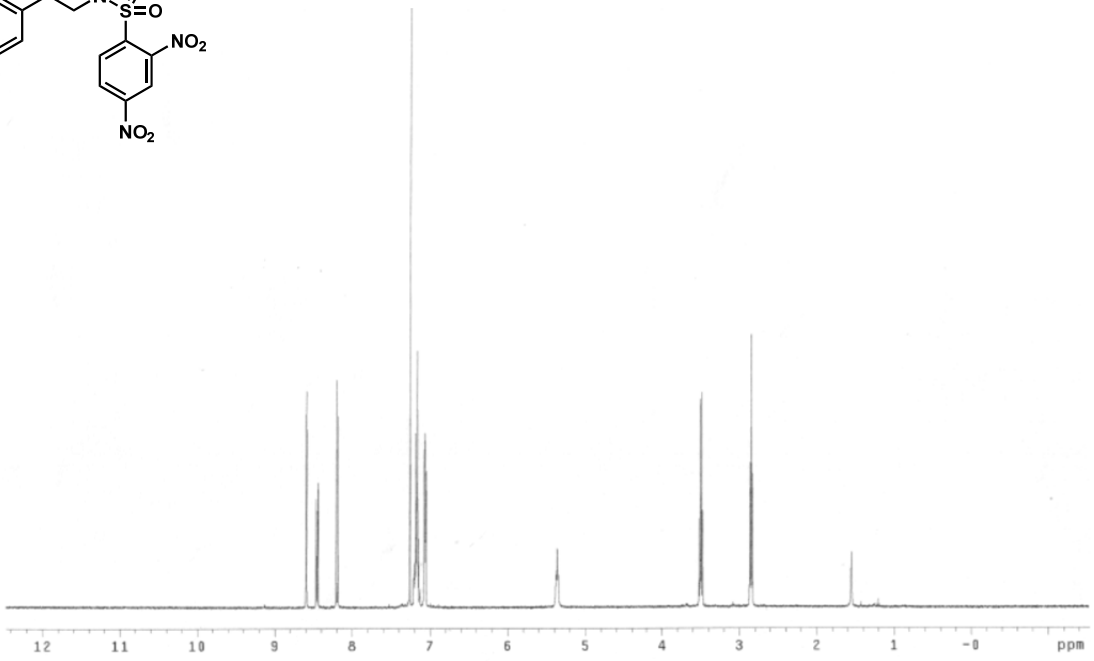
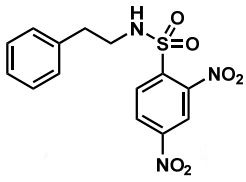


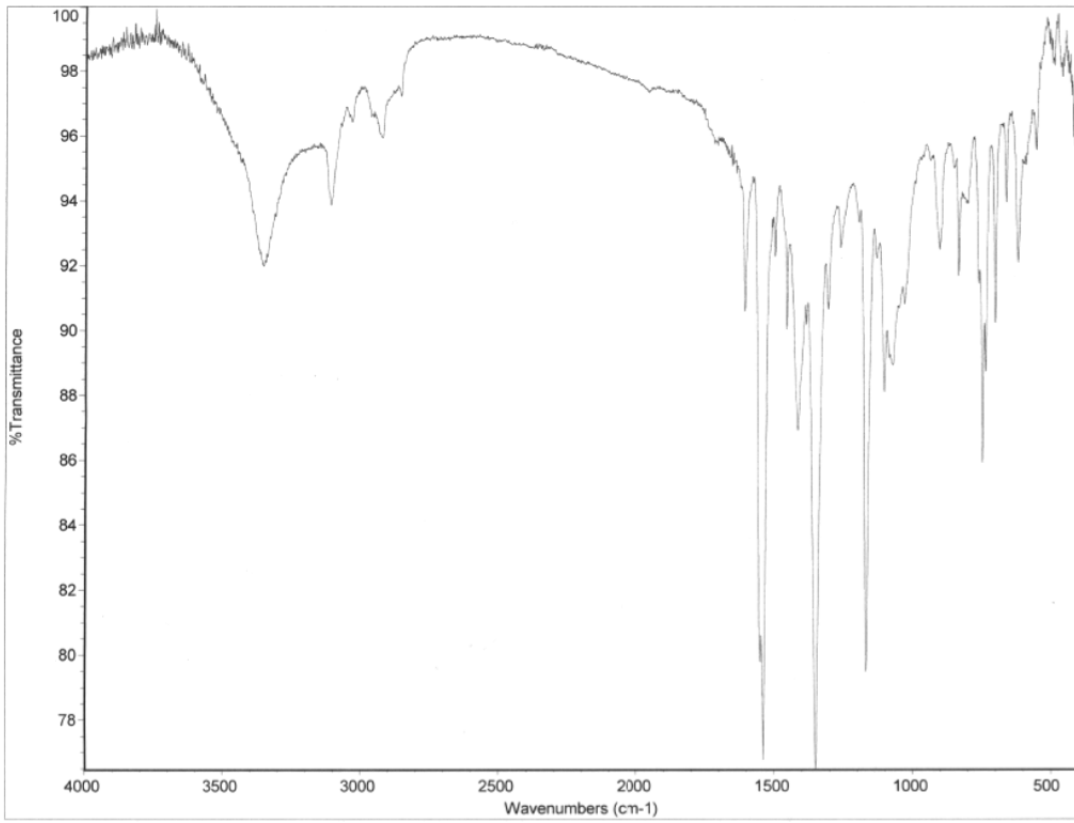


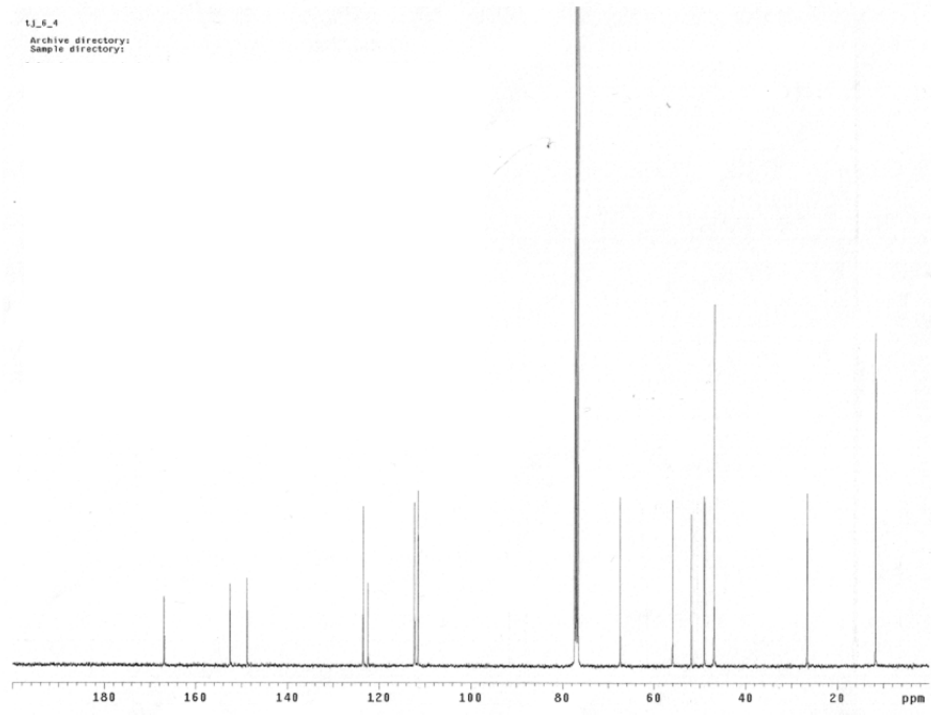
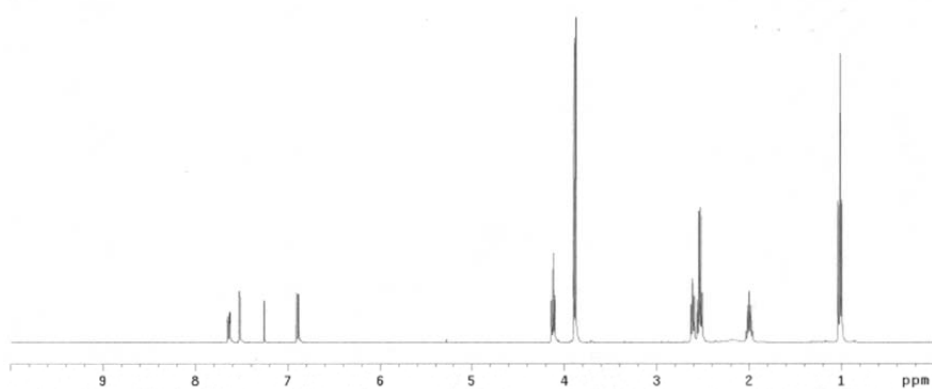
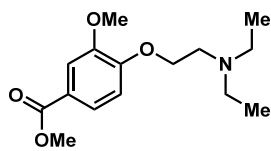


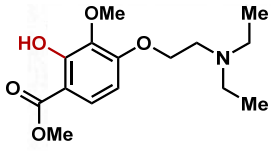




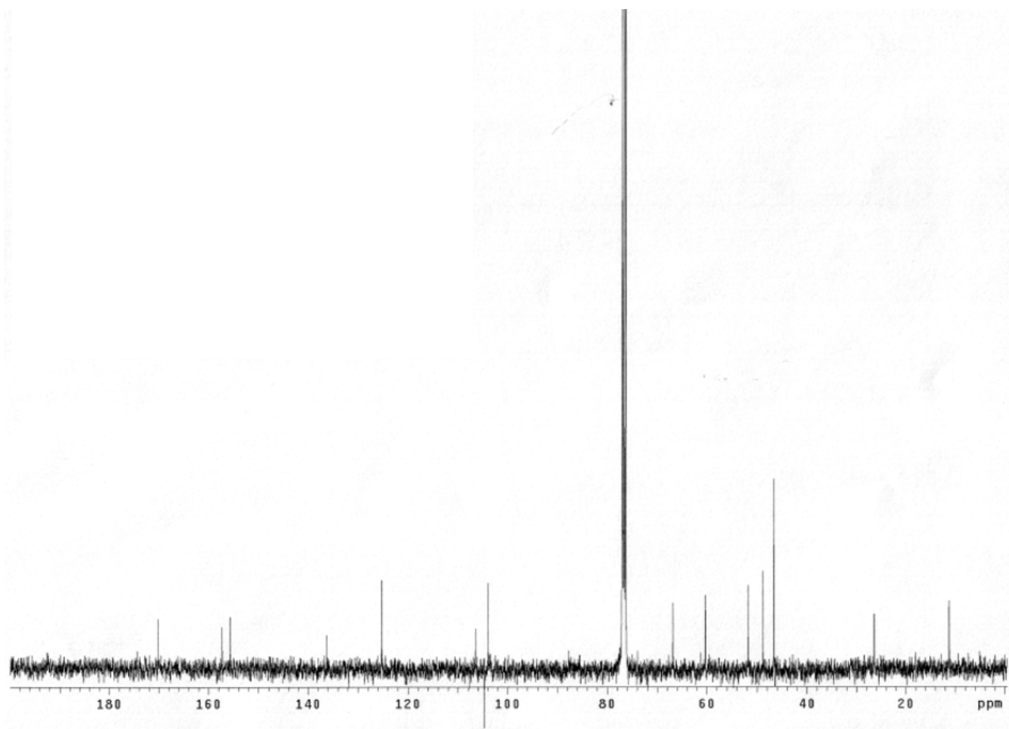
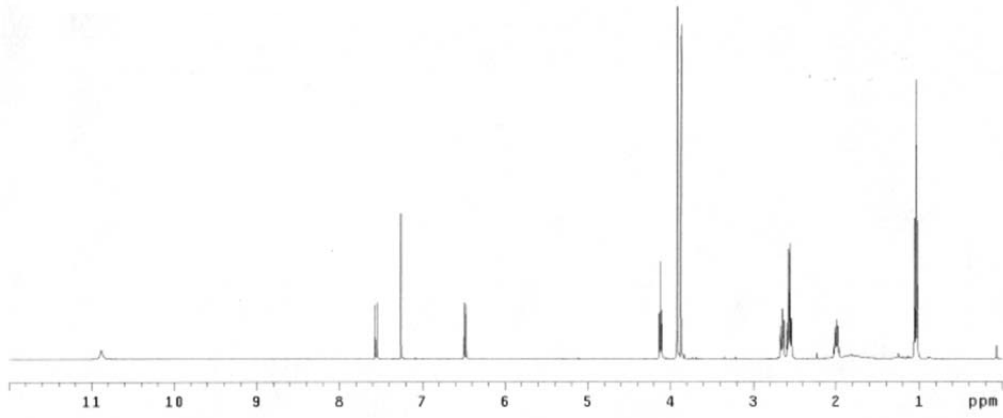




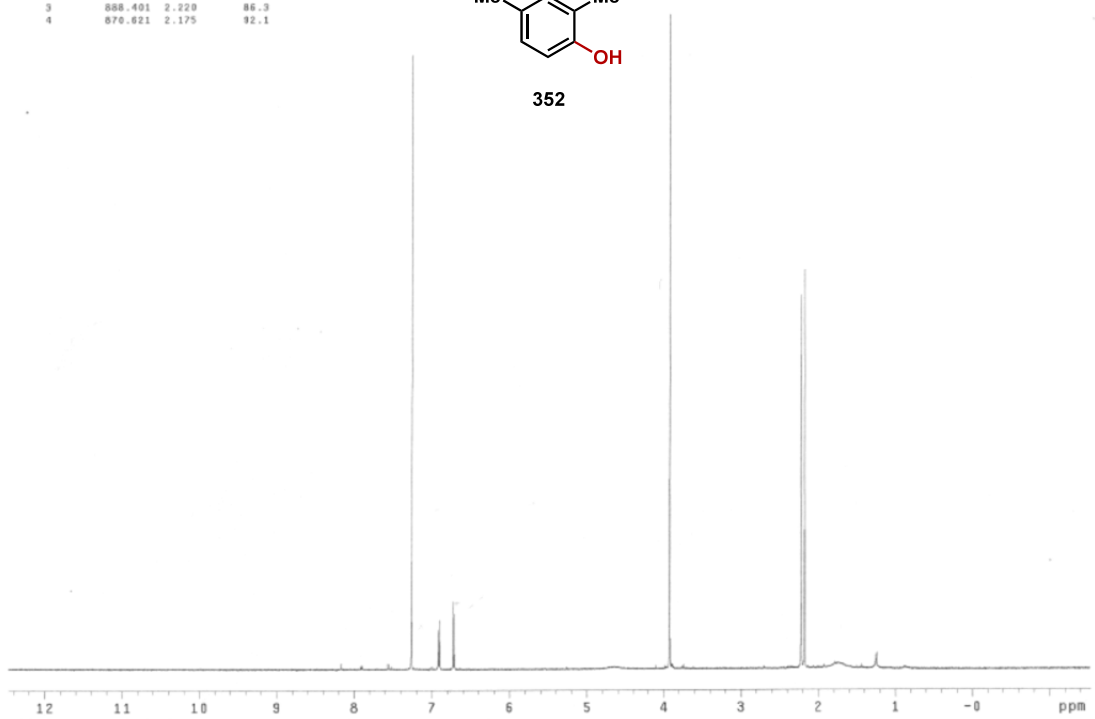
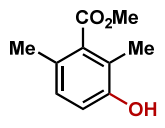




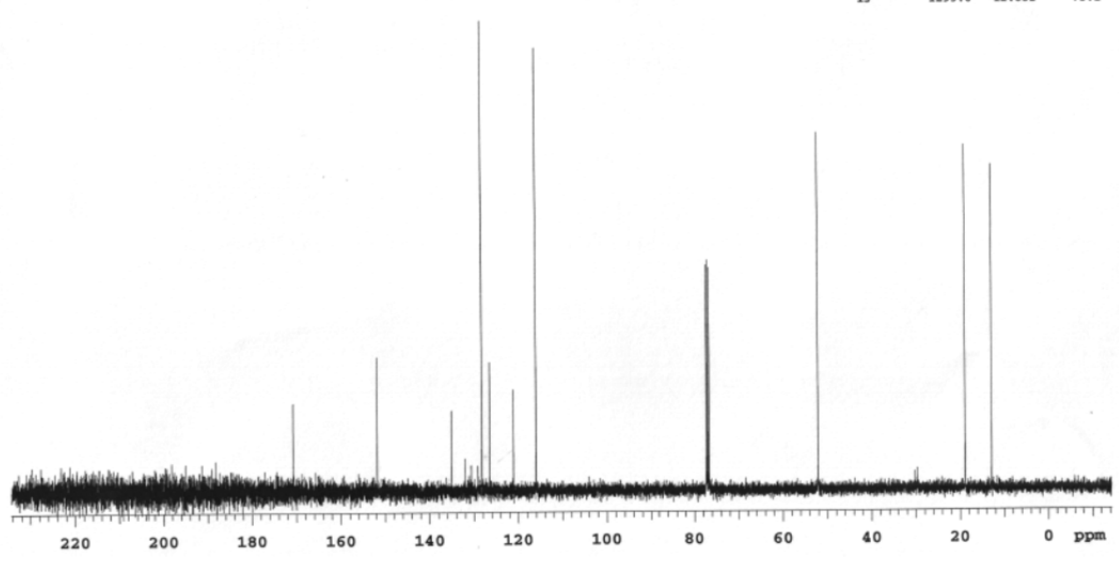
338

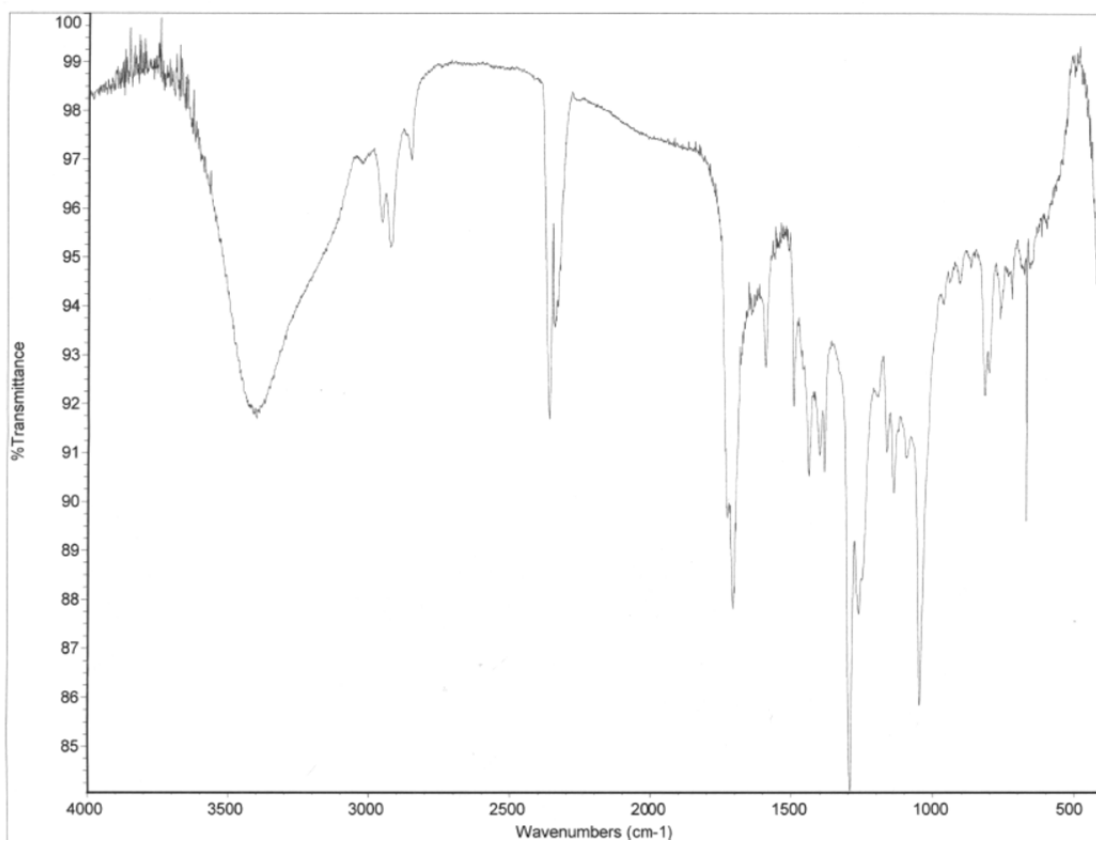


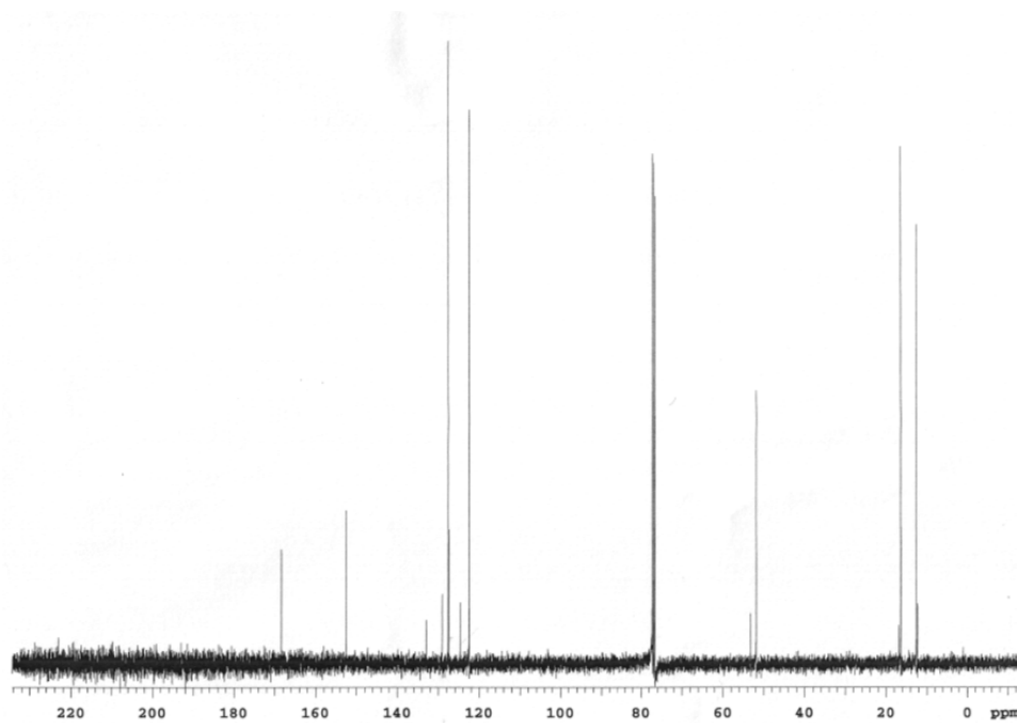
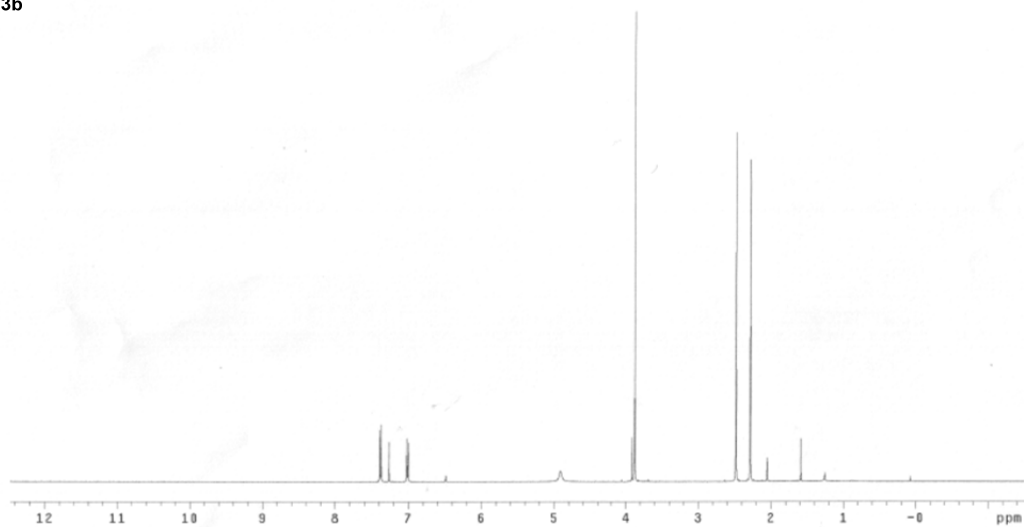
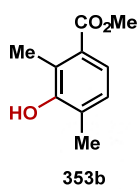
INDEX	FREQUENCY	PPM	HEIGHT
1	2905.468	7.259	141.6
2	1566.456	3.914	151.2
3	888.401	2.220	86.3
4	870.021	2.175	92.1

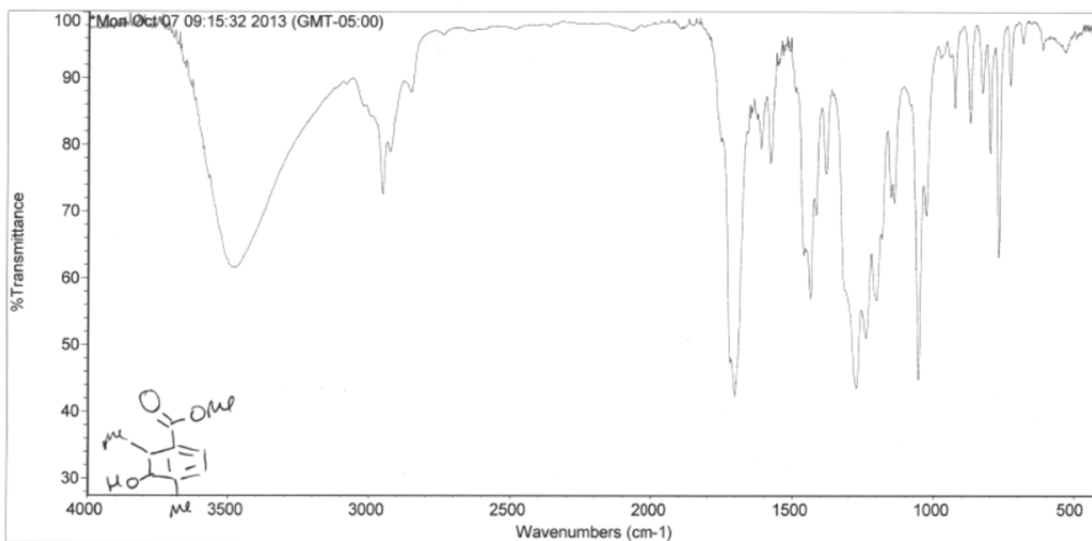


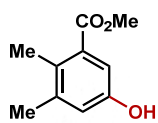
INDEX	FREQUENCY	PPM	HEIGHT
1	17179.7	170.769	19.9
2	15272.3	151.810	30.2
3	13588.5	135.072	18.2
4	12907.2	128.300	106.2
5	12726.4	126.503	28.9
6	12182.4	121.095	22.8
7	11675.8	116.060	100.0
8	7782.5	77.360	50.6
9	7750.5	77.041	51.7
10	7718.4	76.723	50.0
11	5245.0	52.136	80.6
12	1898.7	18.874	77.6
13	1293.0	12.852	73.1



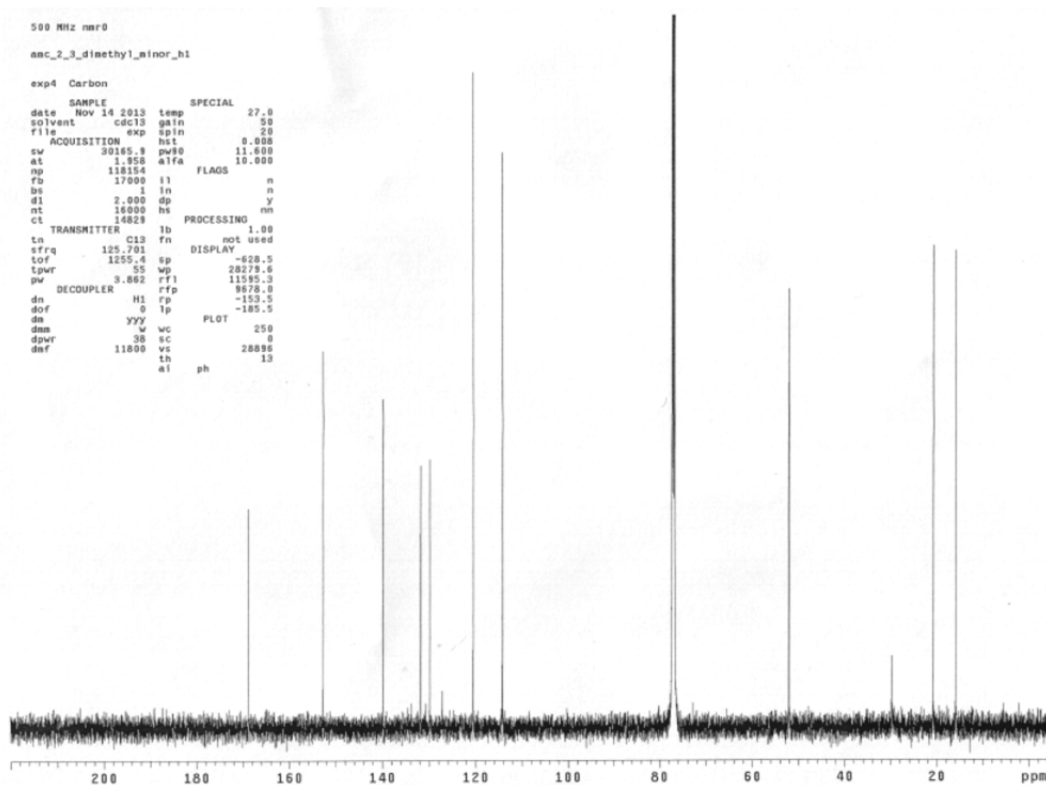
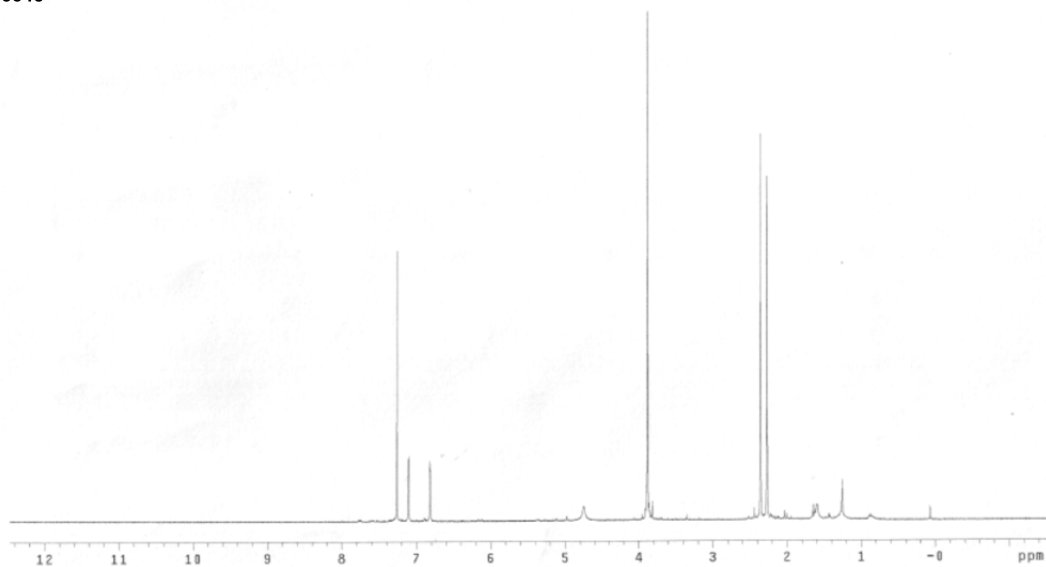


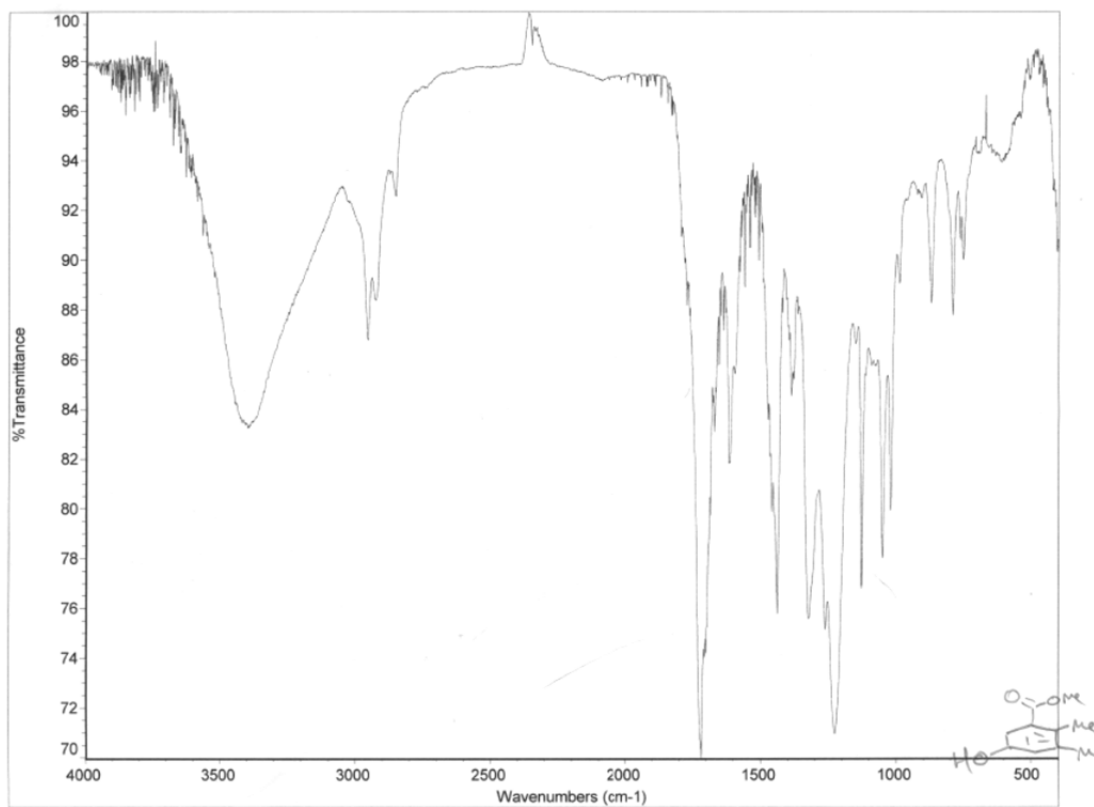






354c

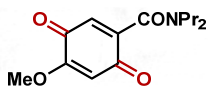




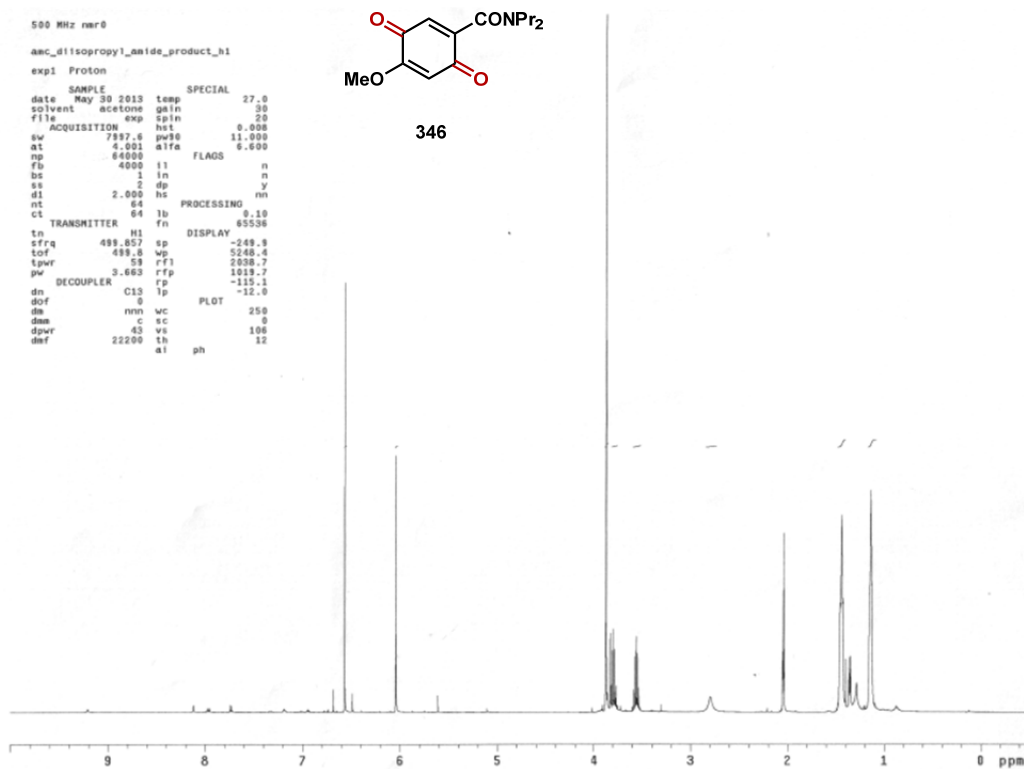
```

500 MHz nmr0
anc_diiisopropyl_amide_product_h1
exp1 Proton
SAMPLE SPECIAL
date May 30 2013 temp 27.0
solvent acetone gain 30
file exp spin 20
ACQUISITION hst 0.008
sw 7597.6 pwr0 11.000
at 4.001 d1fa 6.600
np 64000 FLAGS
fb 4000 i1 n
bs 1 in n
ss 2 dp y
d1 2.000 hs nm
nt 64 PROCESSING
ct 64 lb 0.10
fn 65536
tn H1 DISPLAY
sfrq 499.857 sp -249.9
tof 499.8 wp 5248.4
tpwr 53 rfl 2038.7
pw 3.663 rfp 1019.7
DECOUPLER C13 rp -115.1
dn 0 lp -15.0
dof 0 PLOT
dm nm wc 250
dam c sc 0
dpwr 4. ve 106
dnf 22200 lb 32
at ph

```



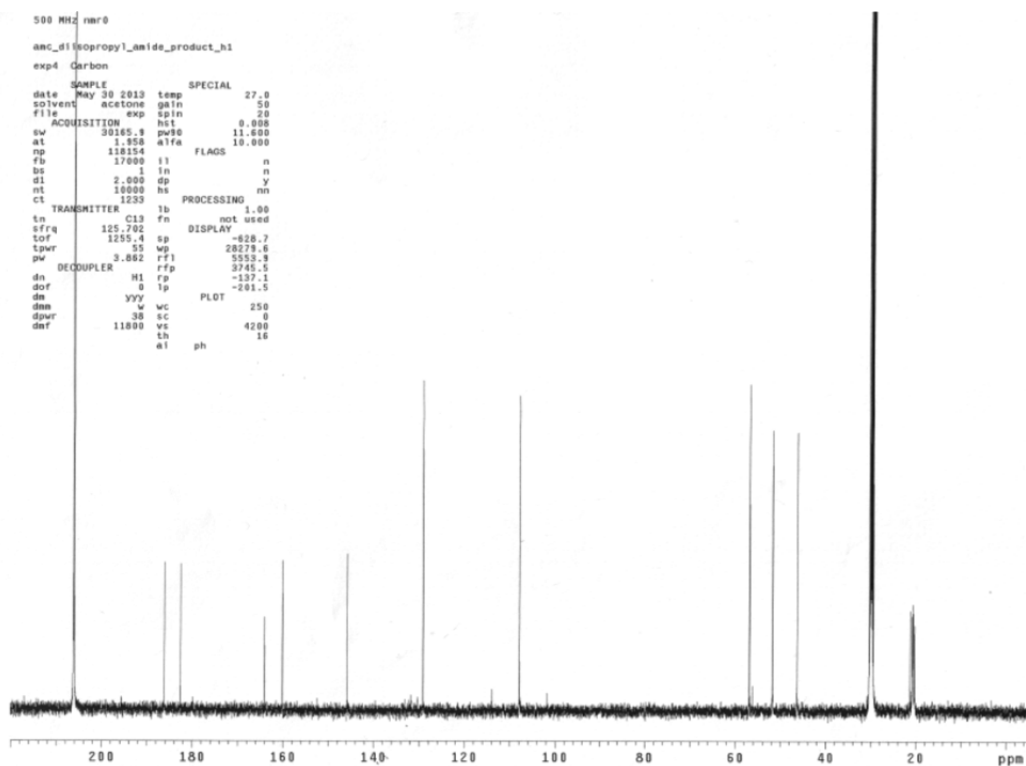
346

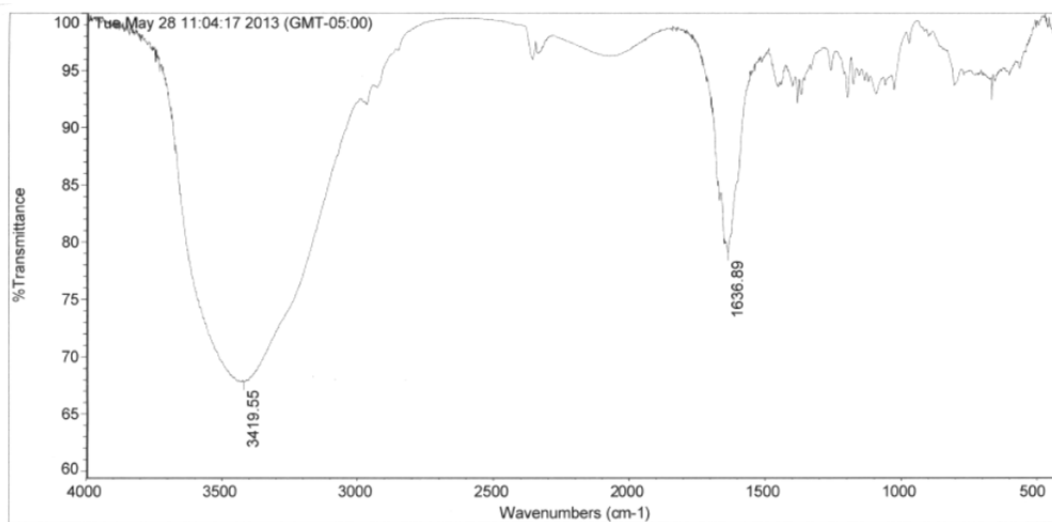


```

500 MHz nmr0
anc_diiisopropyl_amide_product_h1
exp4 Carbon
SAMPLE SPECIAL
date May 30 2013 temp 27.0
solvent acetone gain 50
file exp spin 20
ACQUISITION hst 0.008
sw 30165.9 pwr0 11.000
at 1.950 d1fa 10.000
np 118154 FLAGS
fb 17000 i1 n
bs 1 in n
ss 2 dp y
d1 2.000 hs nm
nt 16000 PROCESSING
ct 1233 lb 0.00
fn not used
tn H1 DISPLAY
sfrq 125.702 sp -628.7
tof 1255.4 wp 28279.6
tpwr 55 rfl 5553.9
pw 3.662 rfp 3745.5
DECOUPLER H1 rp -137.1
dn 3 lp -201.5
dof 3 PLOT
dm w wc 250
dam 38 sc 0
dpwr 11800 ve 4200
dnf 11800 lb 16
at ph

```



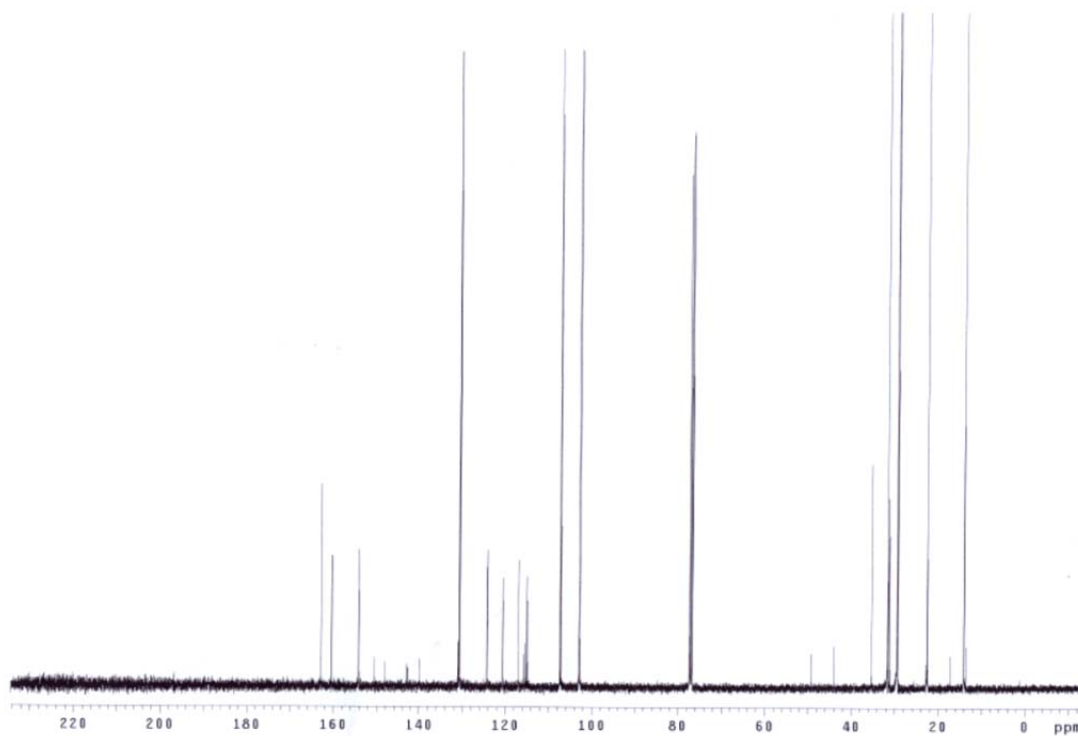
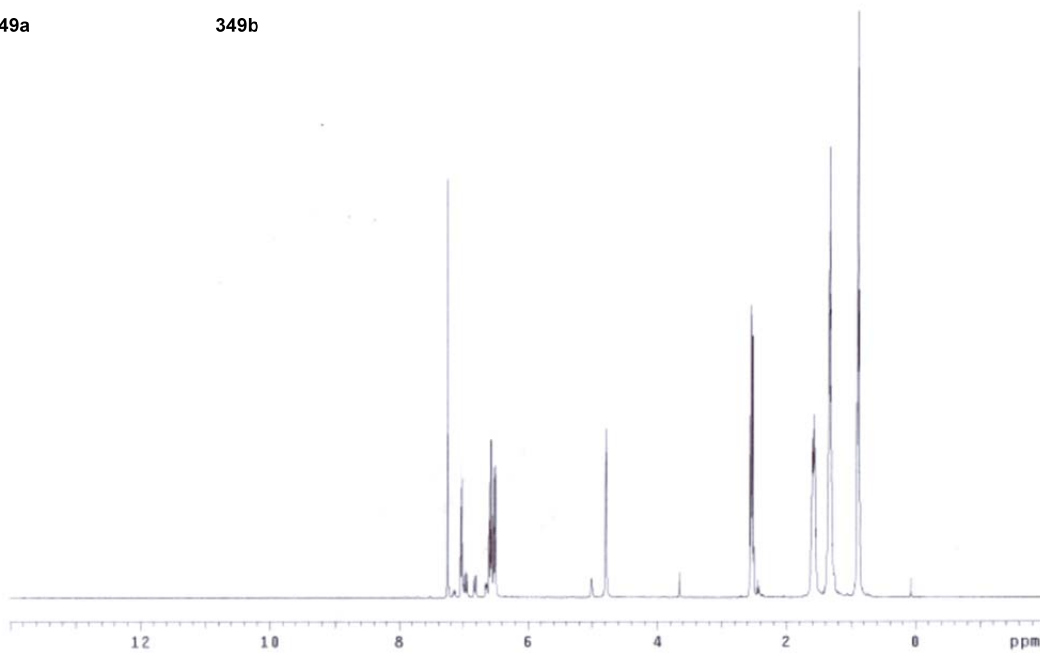
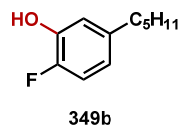
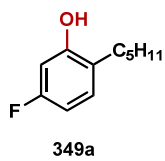


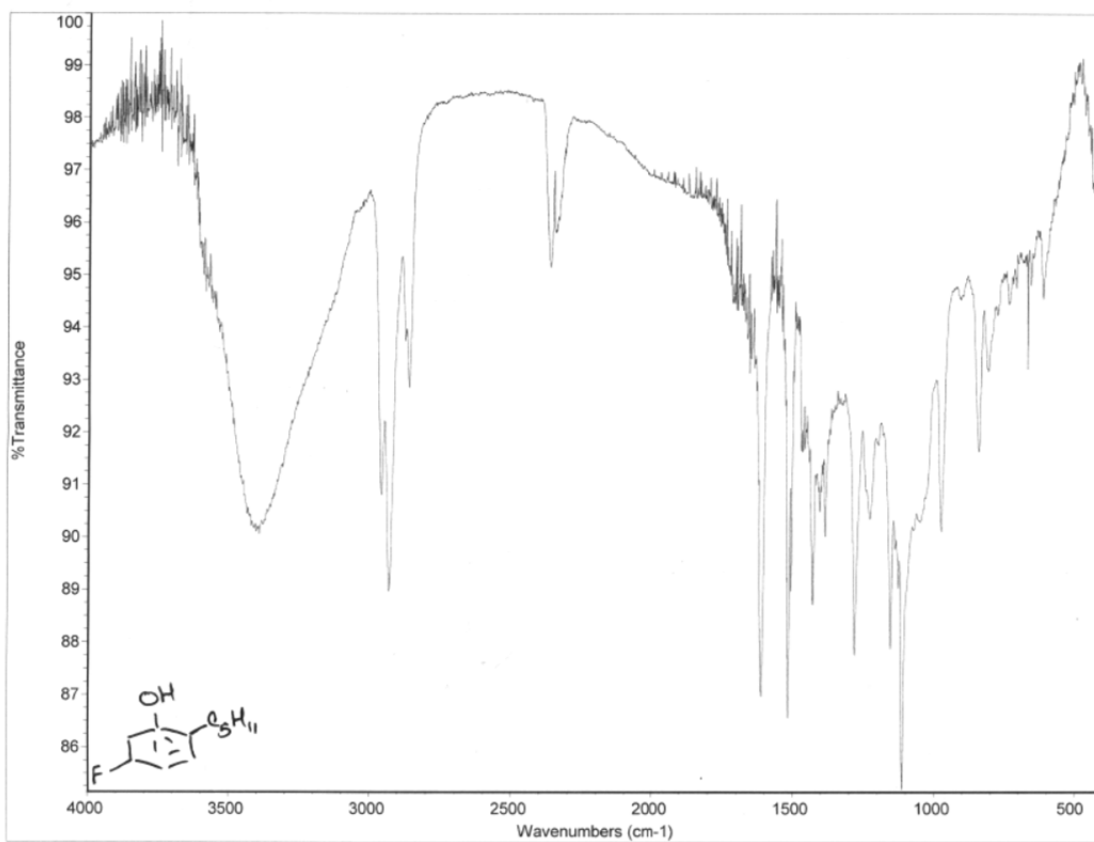
Tue May 28 11:06:08 2013 (GMT-05:00)

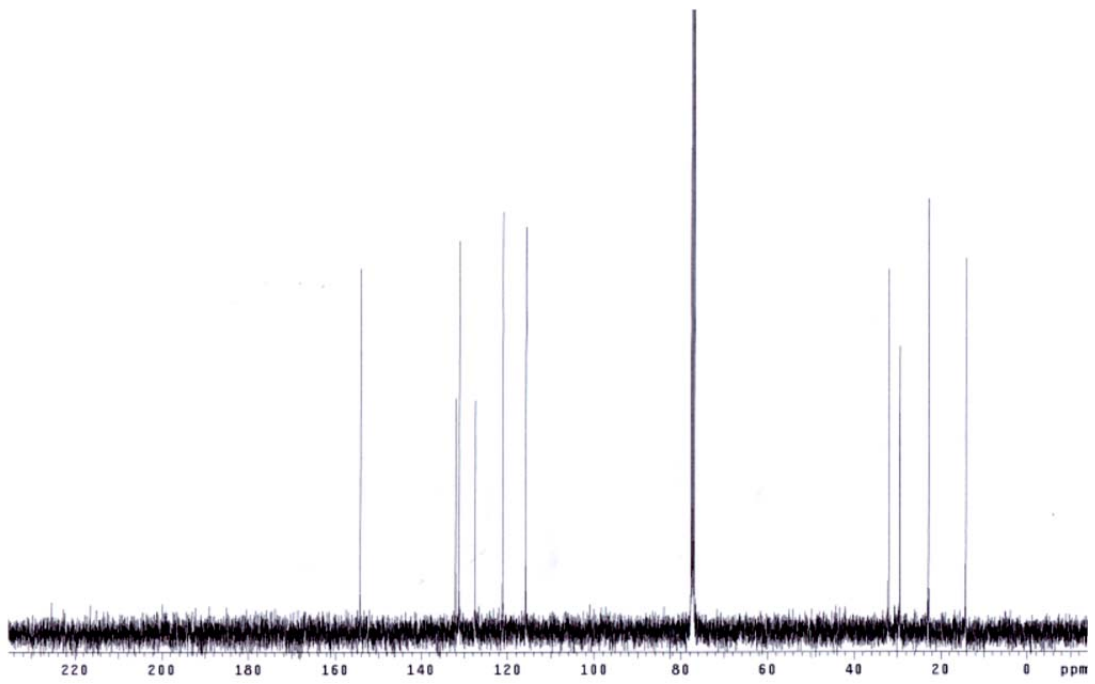
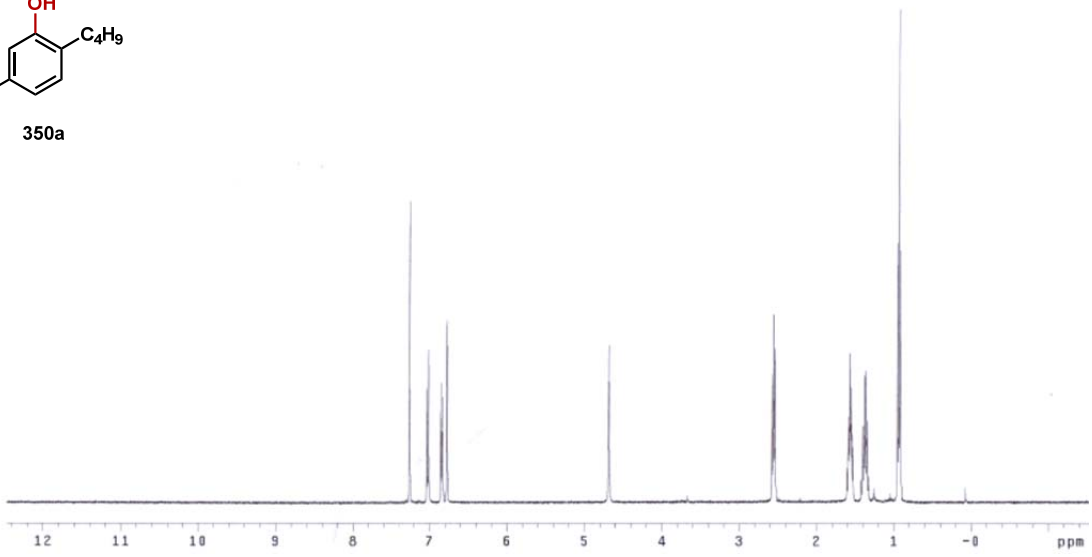
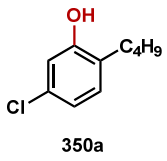
FIND PEAKS:

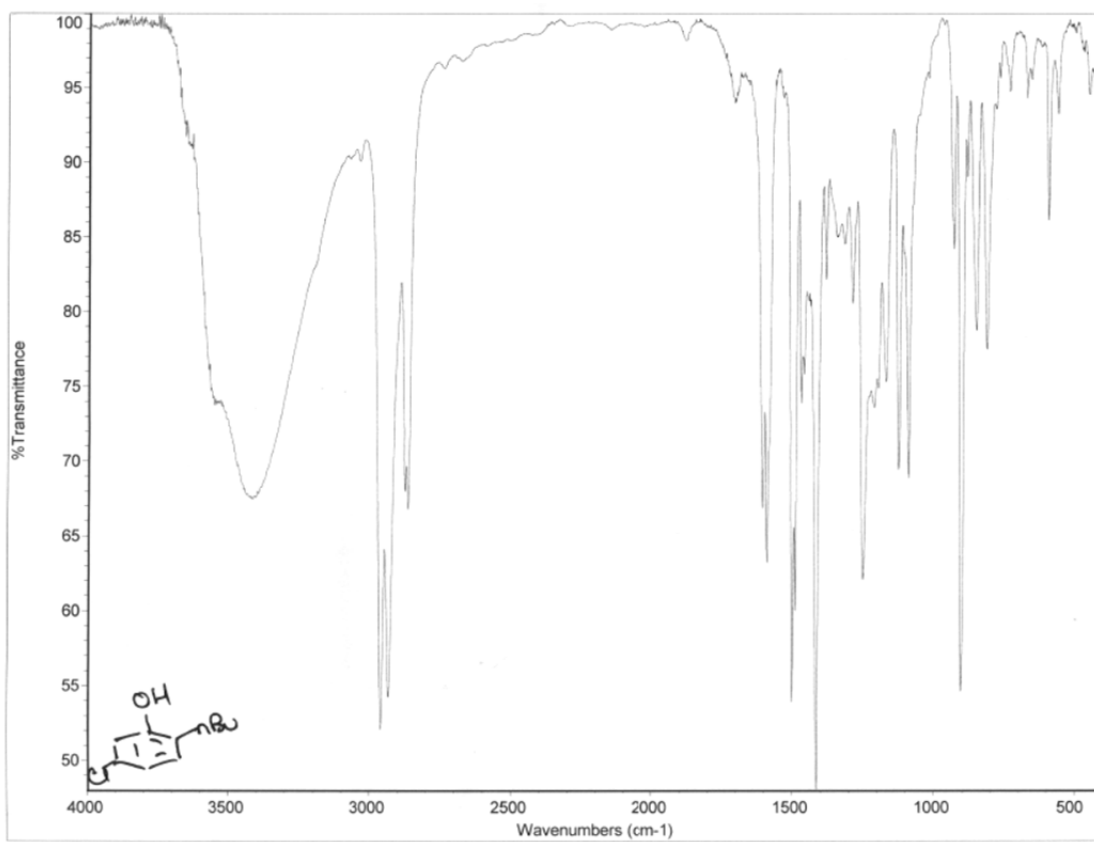
Spectrum: *Tue May 28 11:04:17 2013 (GMT-05:00)
 Region: 4000.00 400.00
 Absolute threshold: 93.557
 Sensitivity: 15
 Peak list:

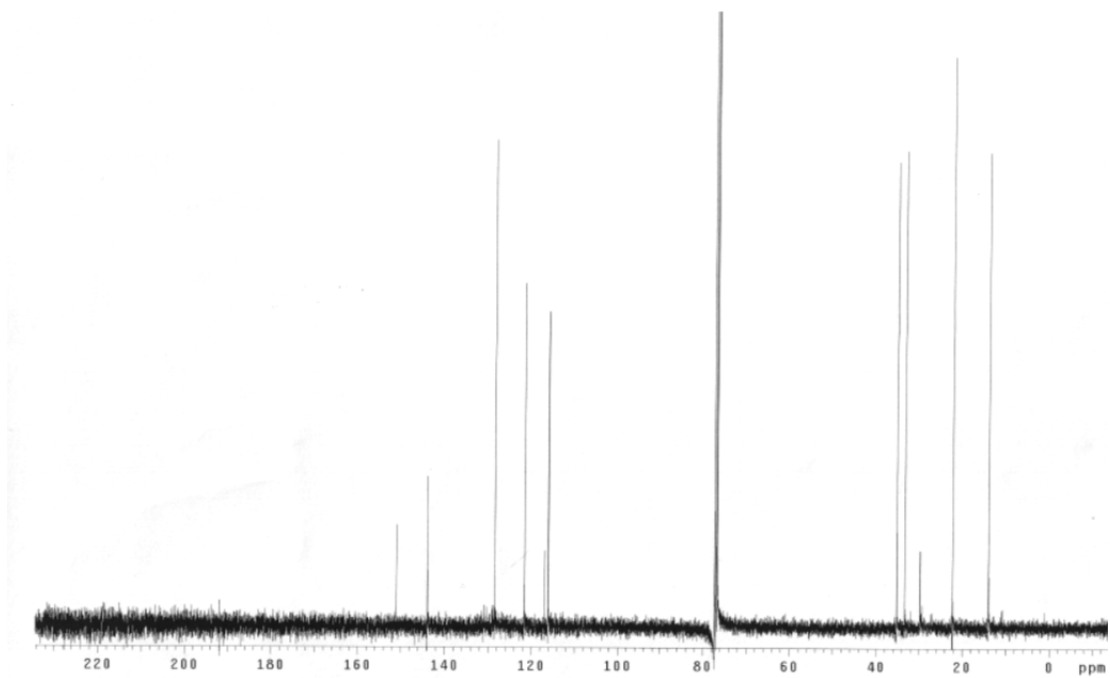
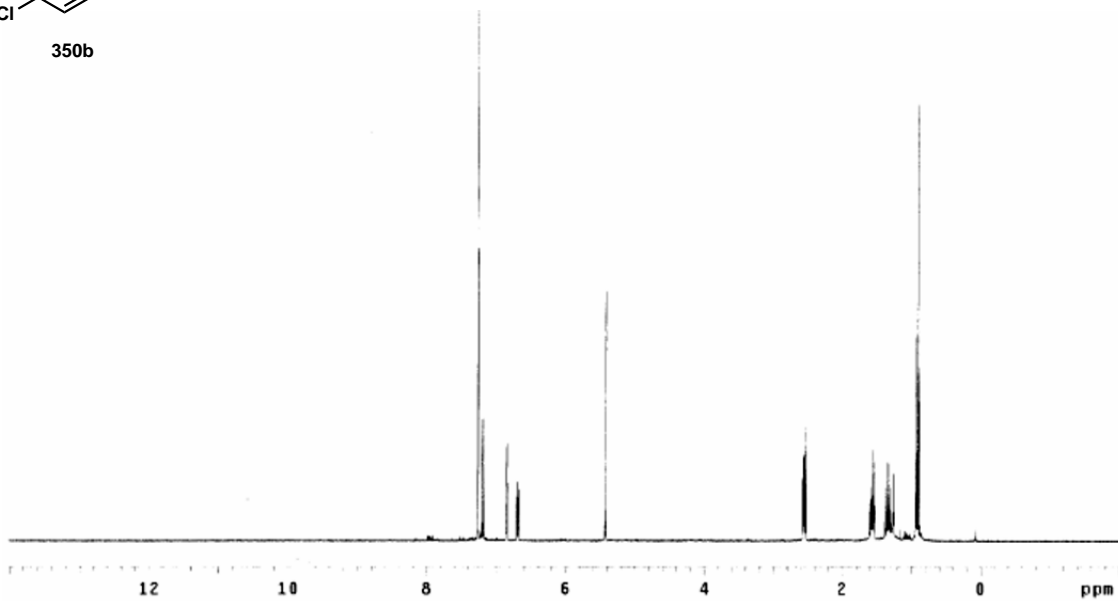
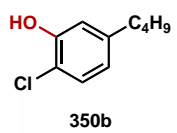
Position:	1636.89	Intensity:	79.079
Position:	3419.55	Intensity:	67.770

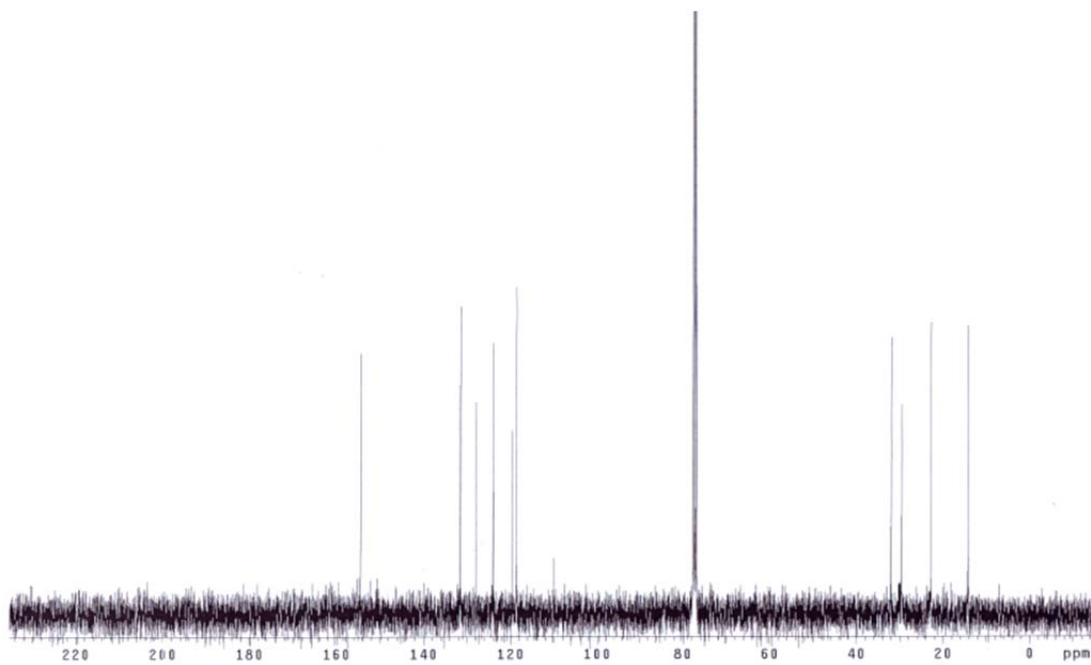
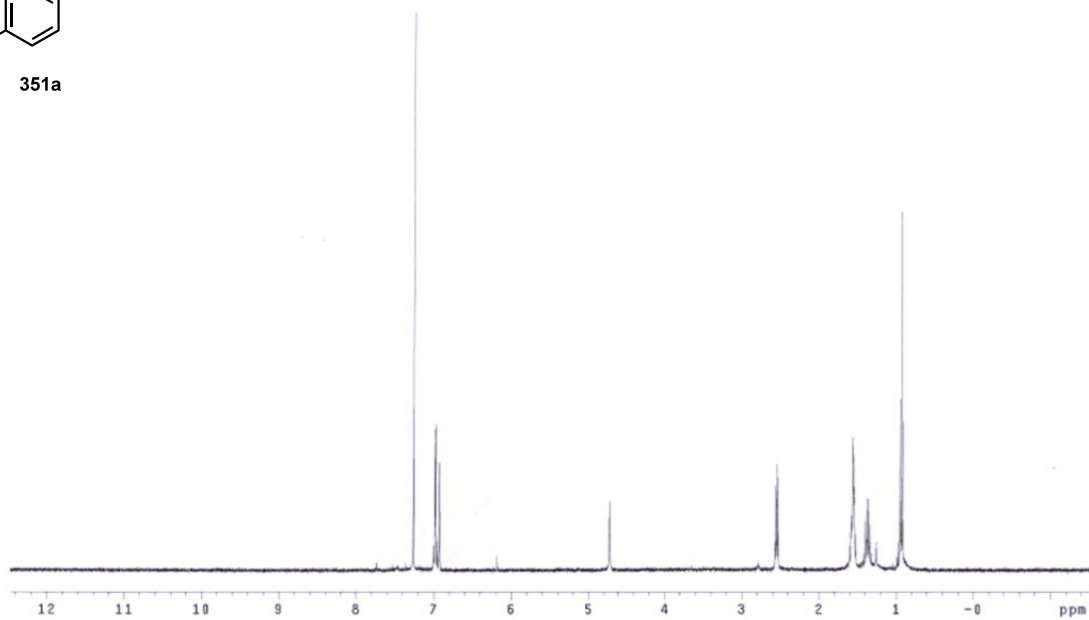
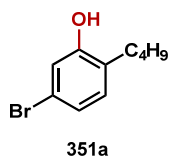


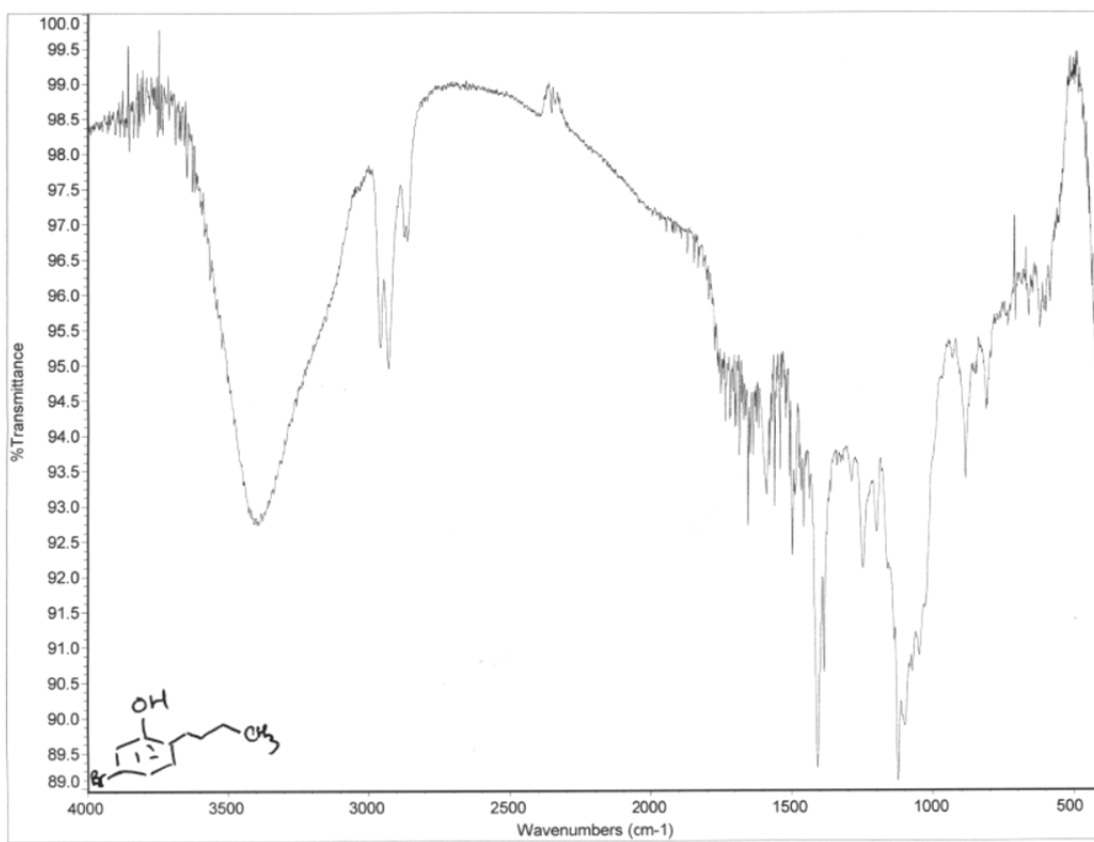


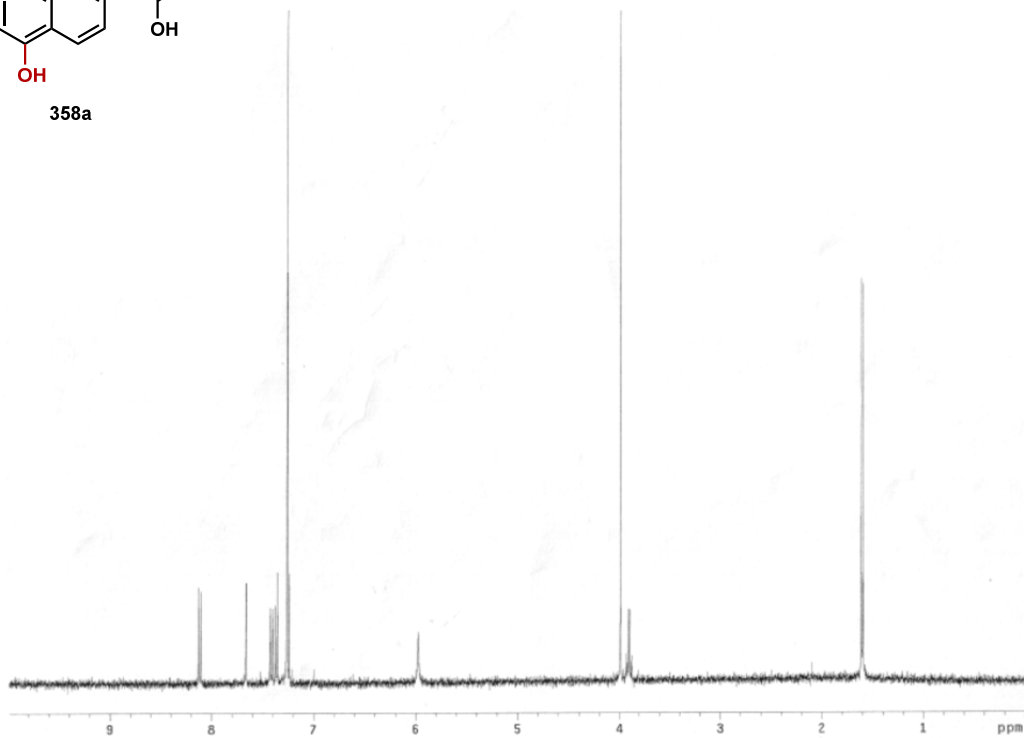
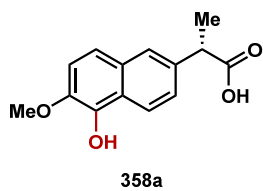




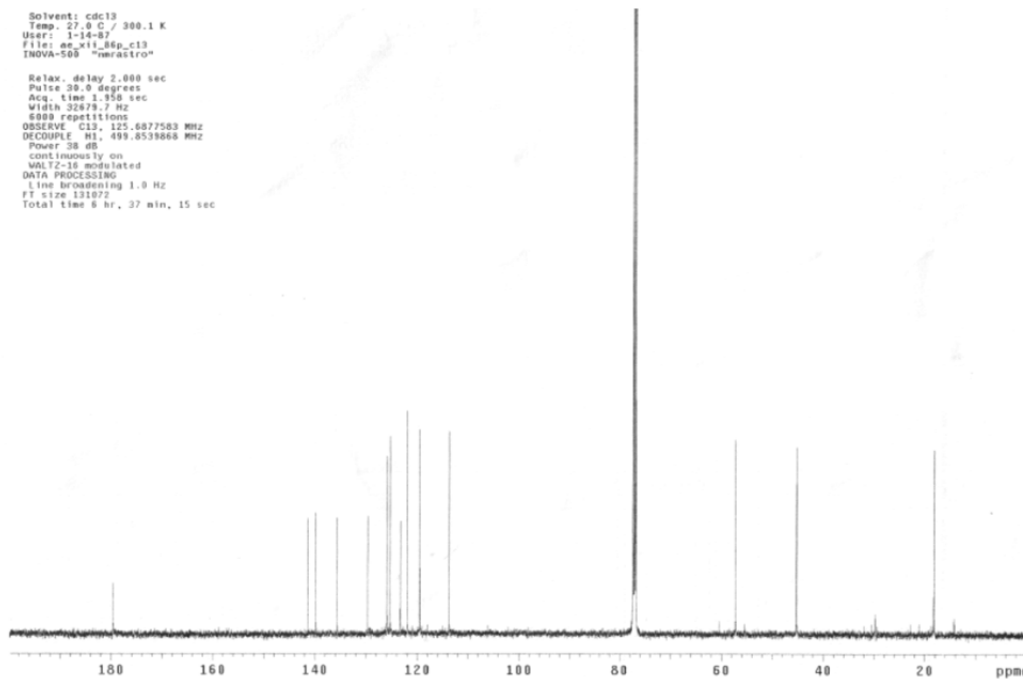


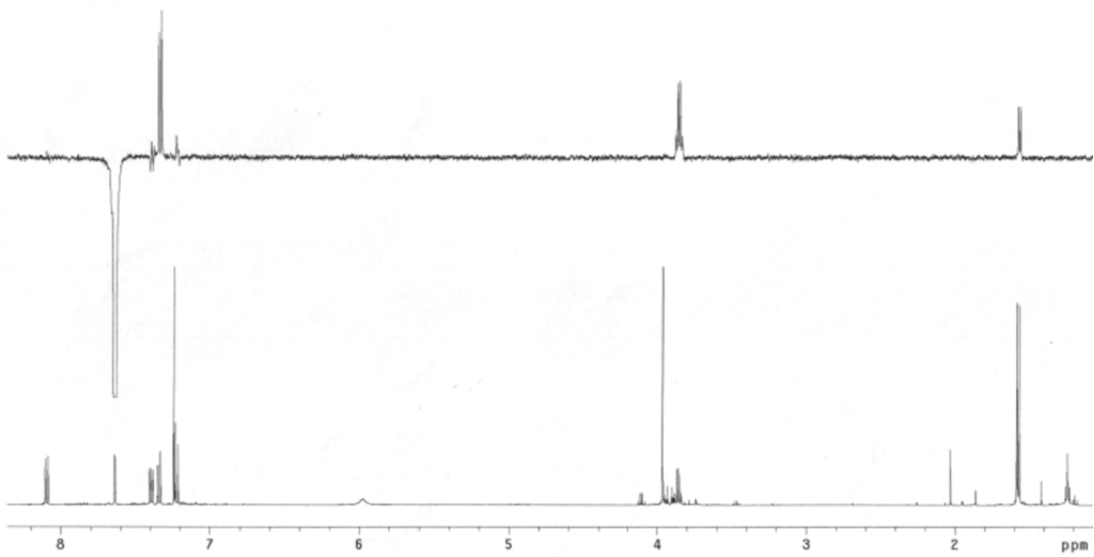
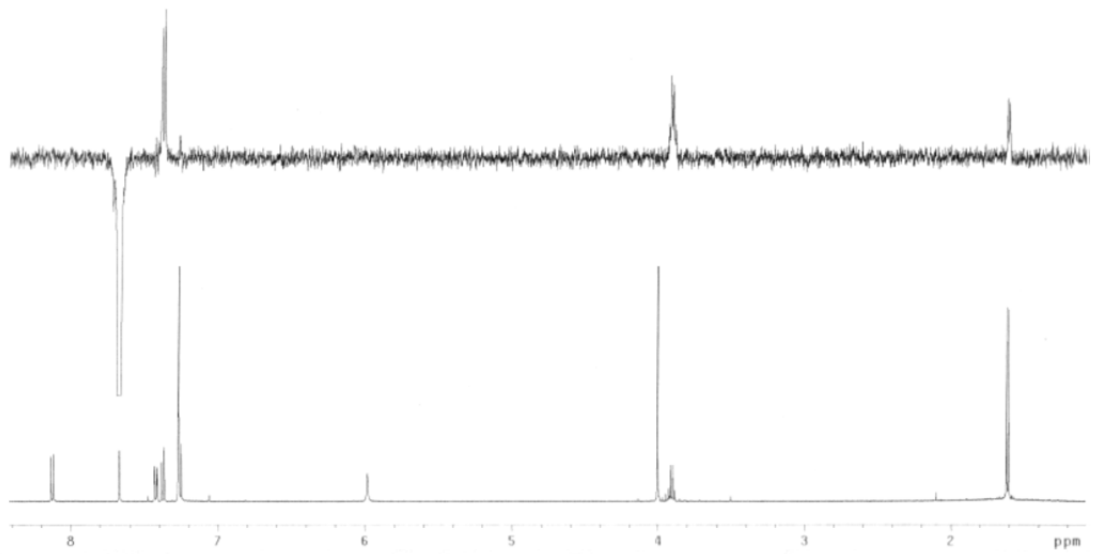


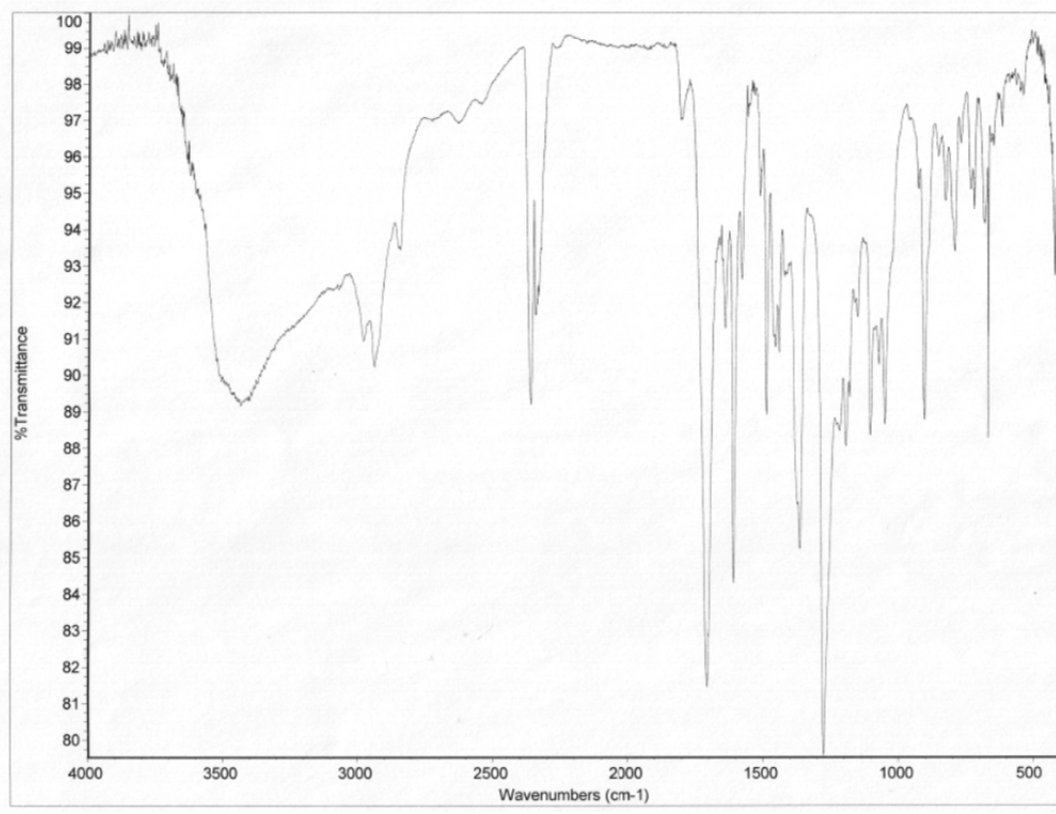
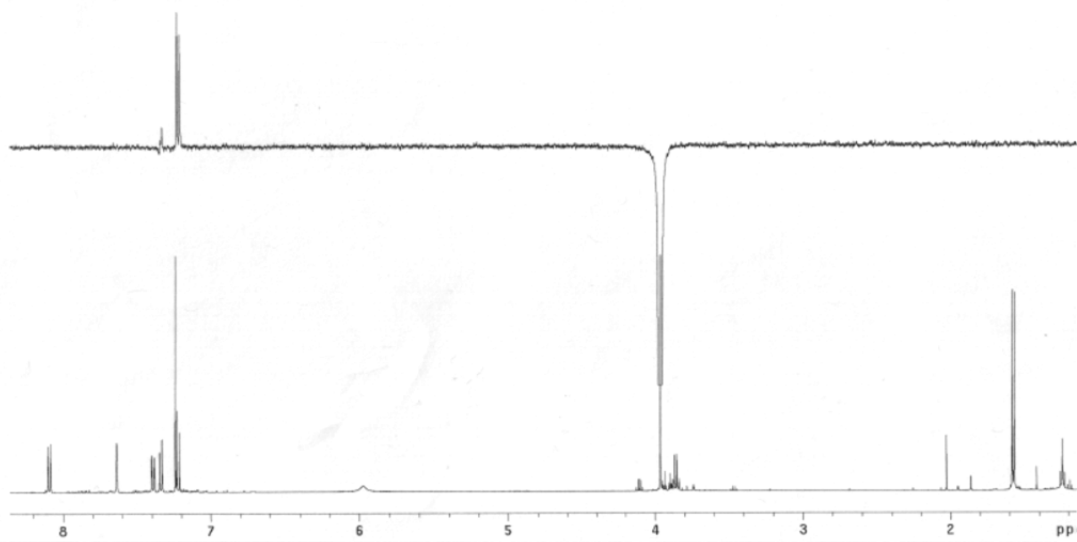


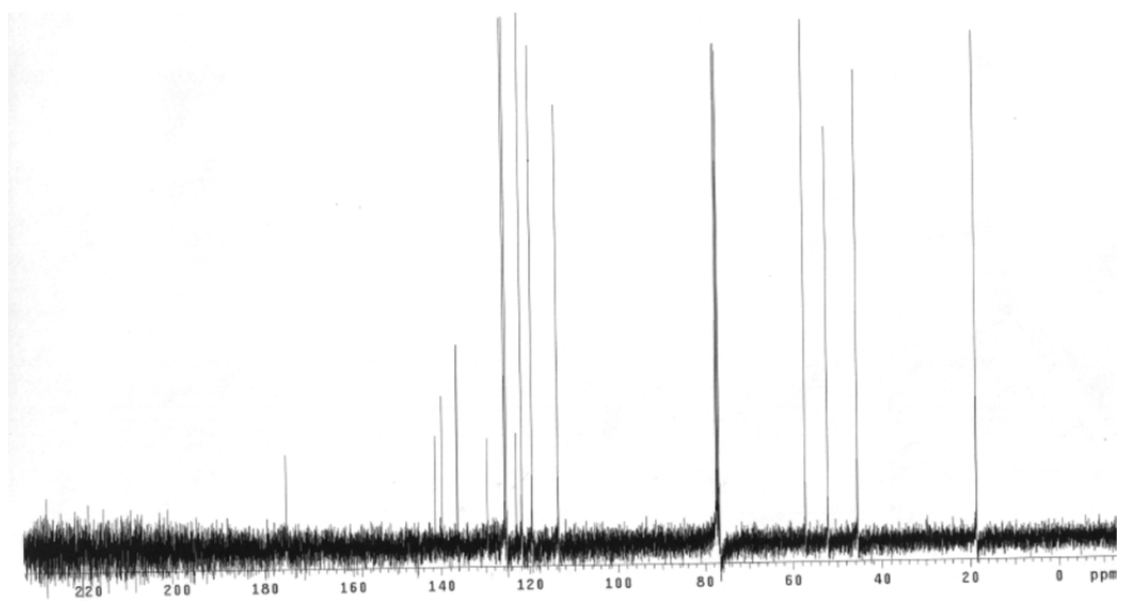
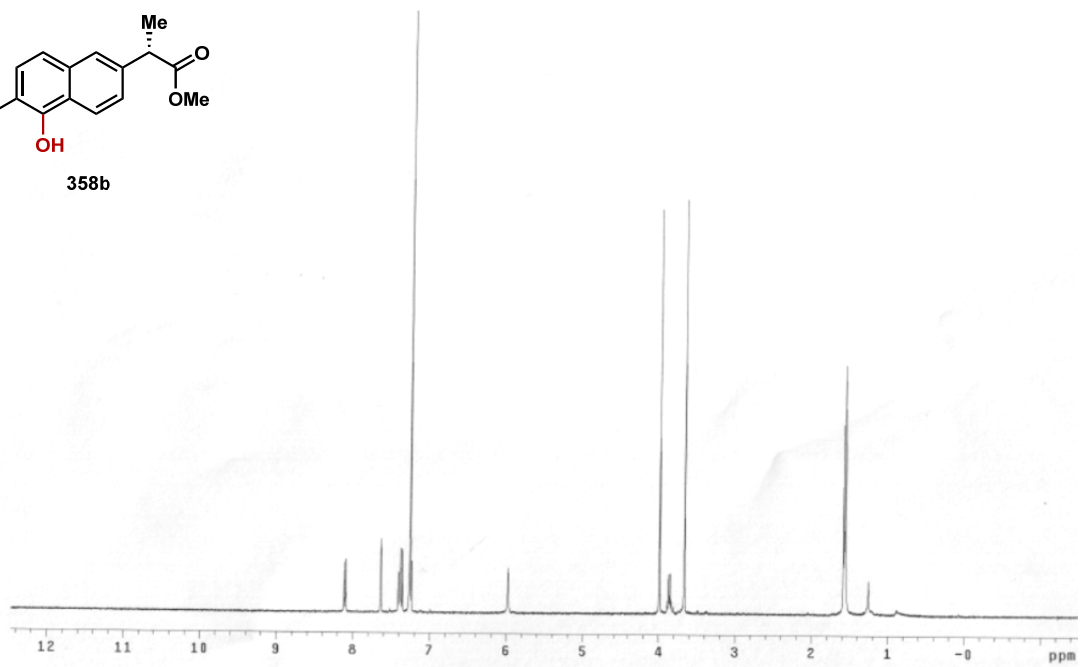
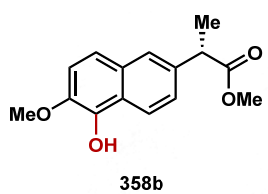


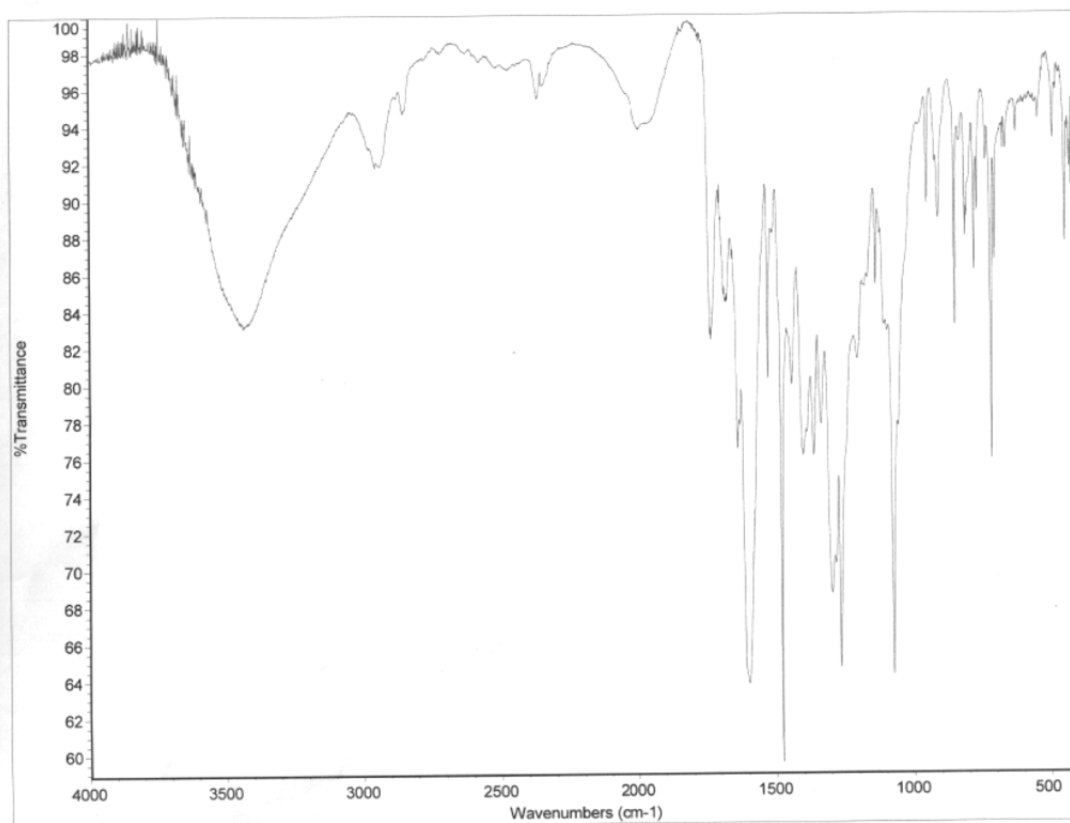
Solvent: cdcl3
 Temp: 27.0 C / 300.1 K
 User: 1-14-87
 File: ee_wi_86p_c13
 INOVA-500 "merastro"
 Relax. delay 2.000 sec
 Pulse 30.0 degrees
 Acq. time 1.350 sec
 Width 32879.7 Hz
 6000 repetitions
 OBSERVE C13, 125.687503 MHz
 DECOUPLE H1, 499.853866 MHz
 Power 38 dB
 continuous ly on
 WALTZ-16 modulated
 DATA PROCESSING
 Line broadening 1.0 Hz
 FT size 131072
 Total time 6 hr, 37 min, 15 sec

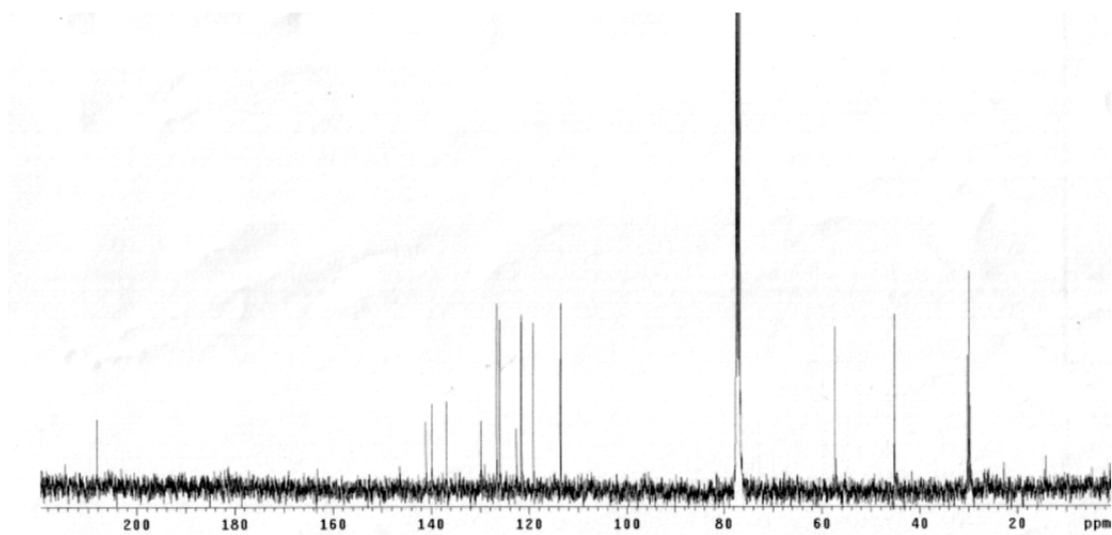
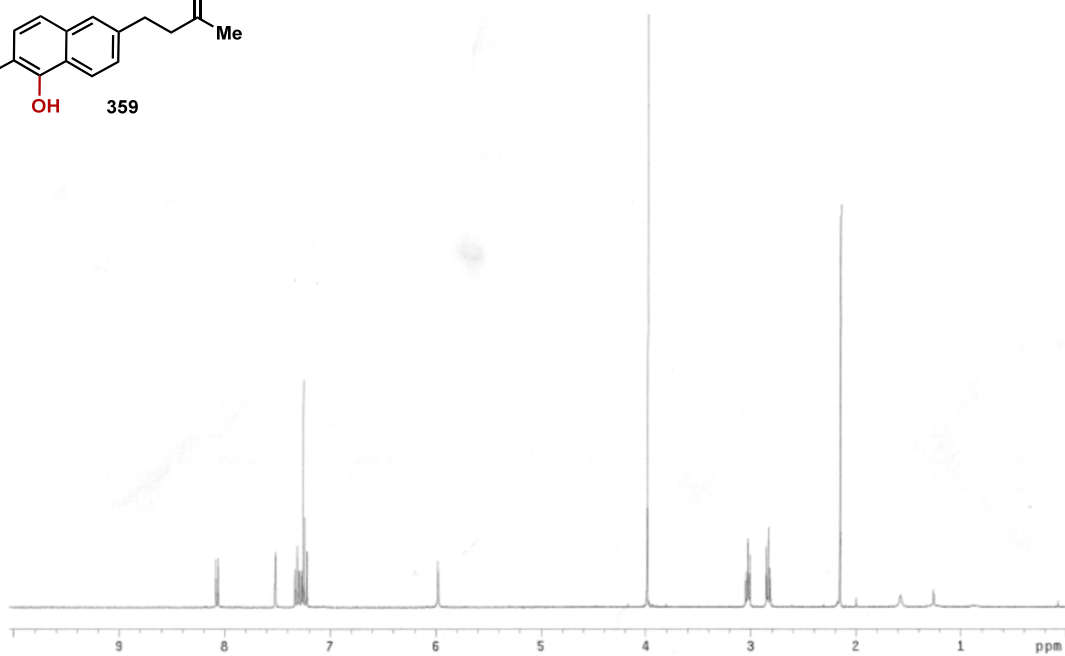
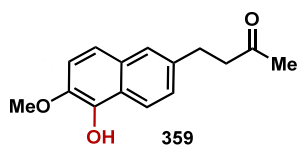


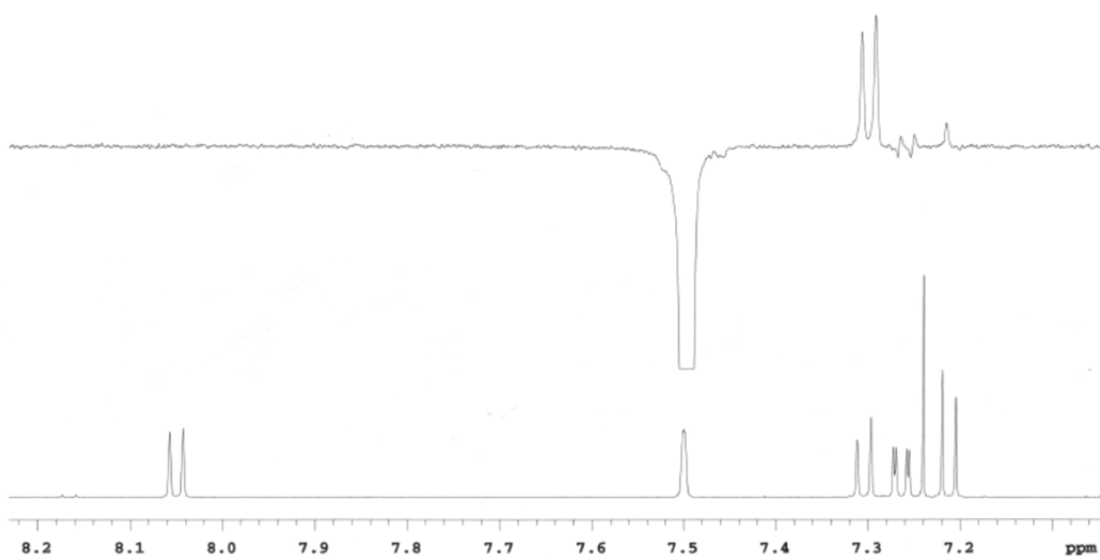
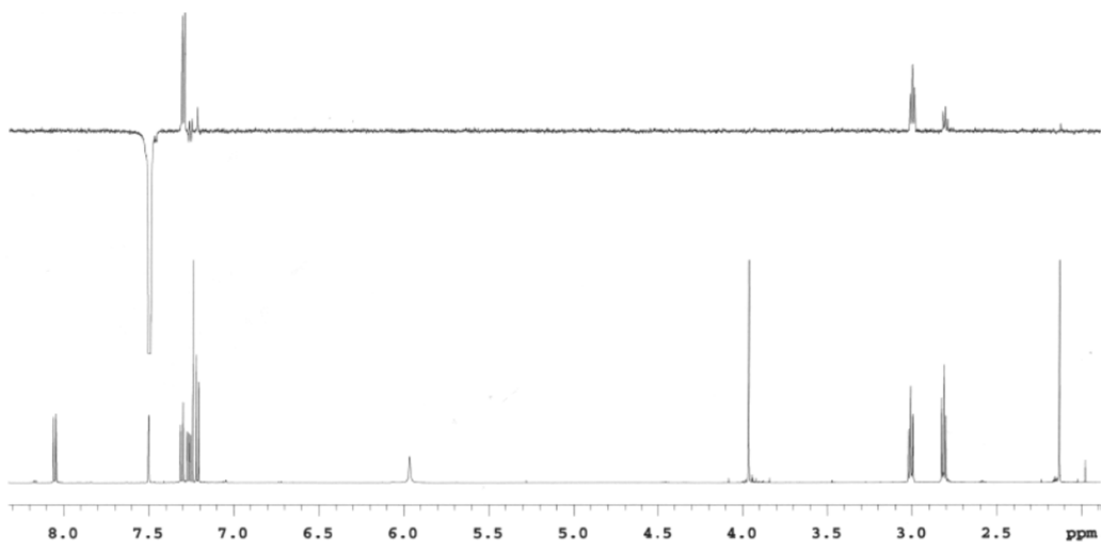


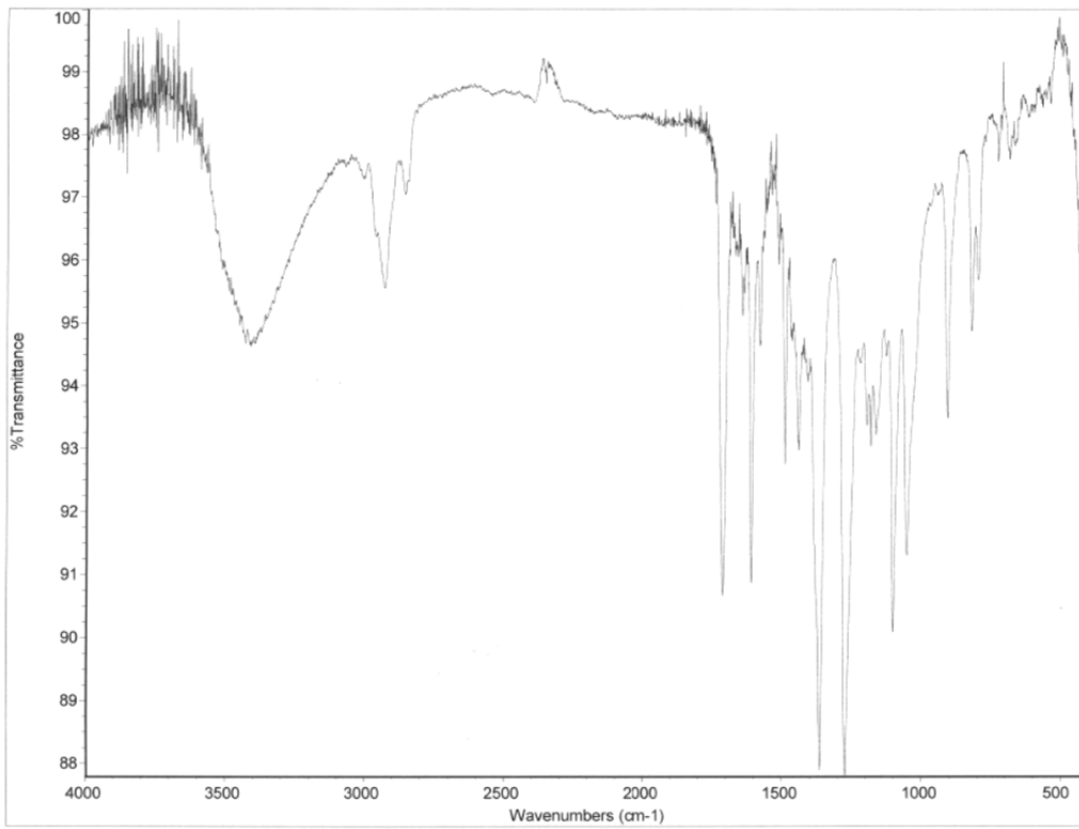


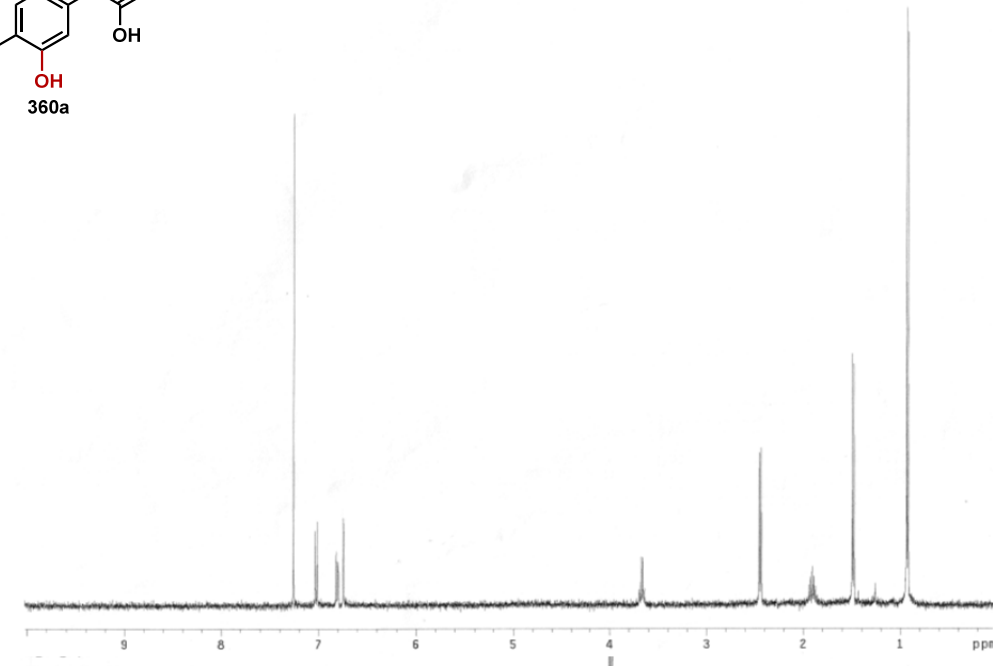
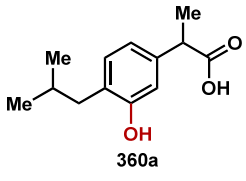




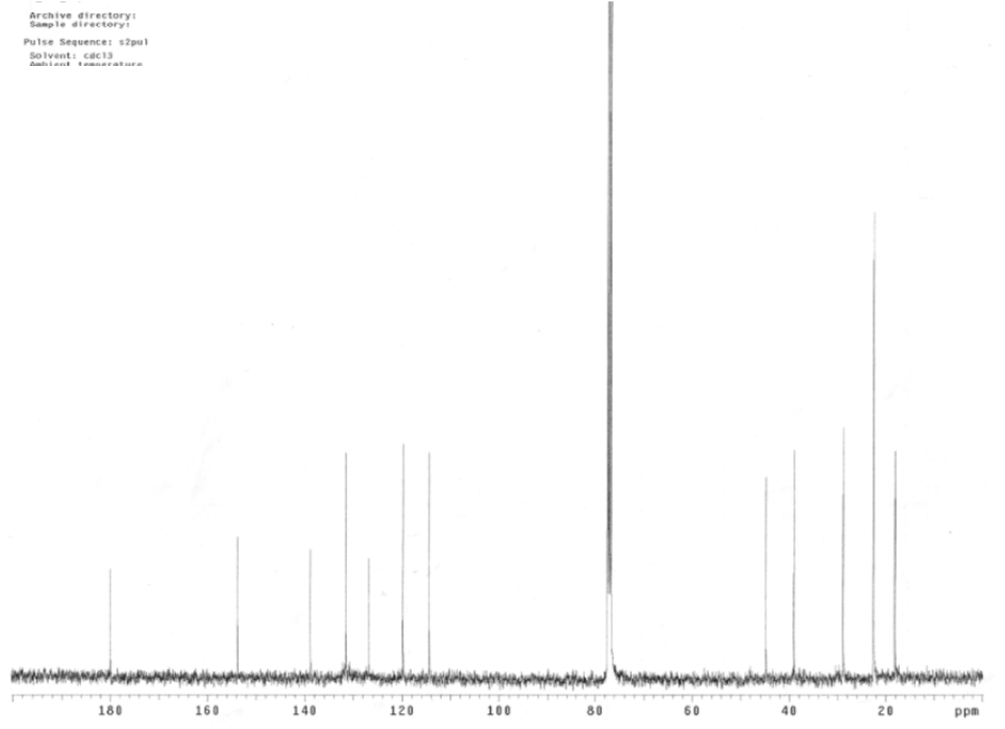


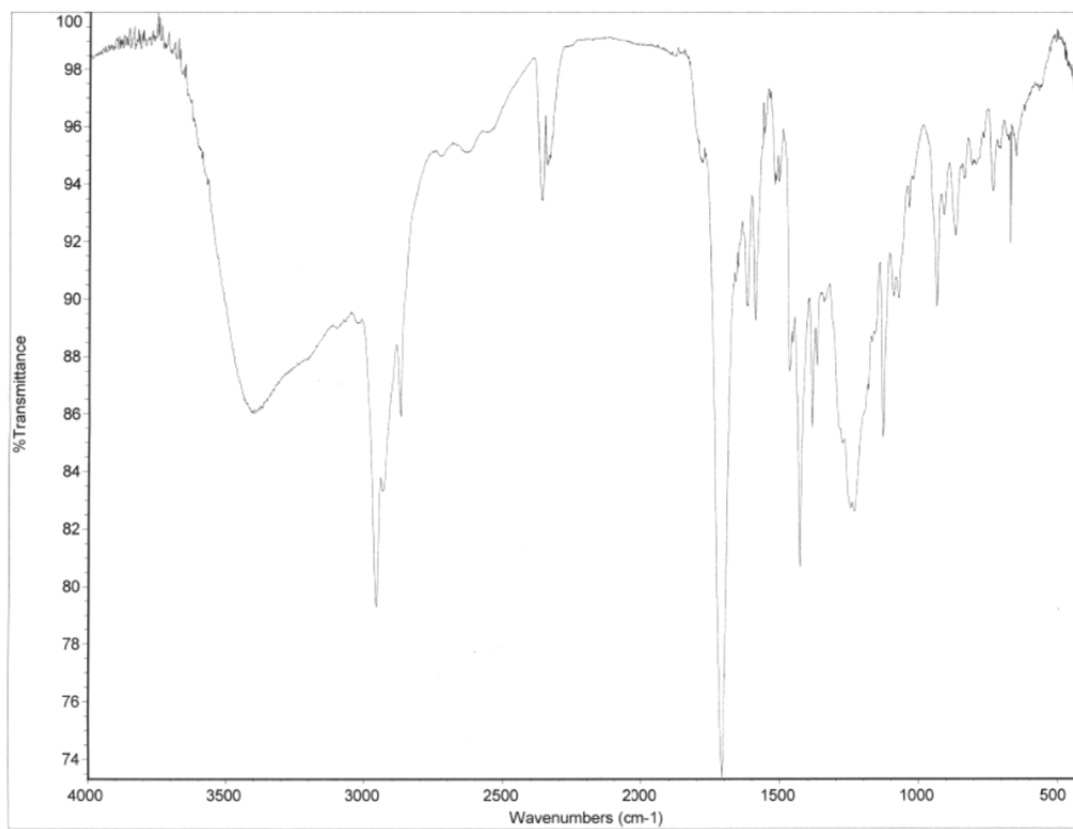






Archive directory:
Sample directory:
Pulse Sequence: s2pul
Solvent: cdcl3
Ambient temperature



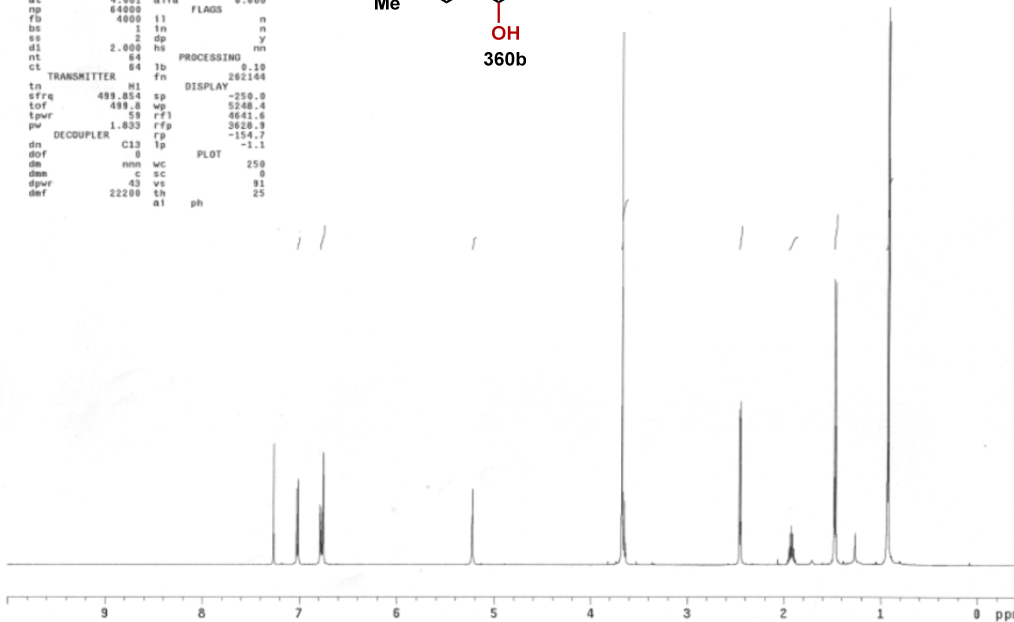
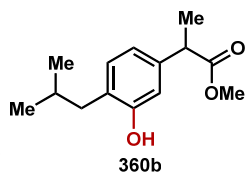


500 MHz nmr0

amc_hydroxylation_ibuprofen_major_h1

exp1 Proton

```
SAMPLE SPECIAL
date Aug 21 2013 temp 27.0
solvent cdc13 gain 20
file cdc13 spin 20
ACQUISITION hst 0.000
sv 7997.6 pwr0 11.000
at 4.001 a1fa 6.600
np 64000 FLAGS
fb 4000 i1 n
bs 1 i1 n
ss 2 dp y
d1 2.000 hs nn
nt 64 PROCESSING
ct 64 fb 0.10
TRANSMITTER H1 fn 262104
tn 499.854 sp -250.0
sfrq 498.8 wp 5248.4
tof 59 rfi 4641.6
pwr 1.833 rfp 3628.9
DECOUPLER cp -154.7
dn C13 lp -1.1
dof 0 PLOT
dm nnn wc 250
dmn c sc 0
dpr 63 vs 81
def 22200 th 25
al ph
```

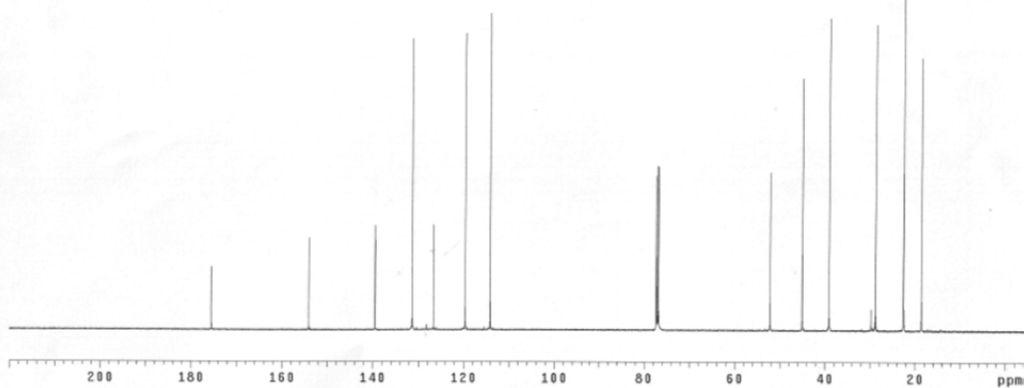


500 MHz nmr0

amc_hydroxylation_ibuprofen_major_c13

exp4 Carbon

```
SAMPLE SPECIAL
date Aug 21 2013 temp 27.0
solvent cdc13 gain 50
file cdc13 spin 20
ACQUISITION hst 0.000
sv 30165.9 pwr0 11.000
at 1.950 a1fa 10.000
np 118154 FLAGS
fb 17000 i1 n
bs 1 i1 n
d1 2.000 dp y
nt 7000 hs nn
ct 7000 PROCESSING
tn 125.701 fn 101.000
sfrq 125.4 sp -828.5
tof 55 wp 28279.6
pwr 11.600 rfi 11598.7
DECOUPLER H1 rfp 9870.0
dn yyy lp -118.6
dof 0 PLOT
dm w wc 250
dmn 30 sc 0
dpr 11800 vs 873
def al cdc ph 5
```

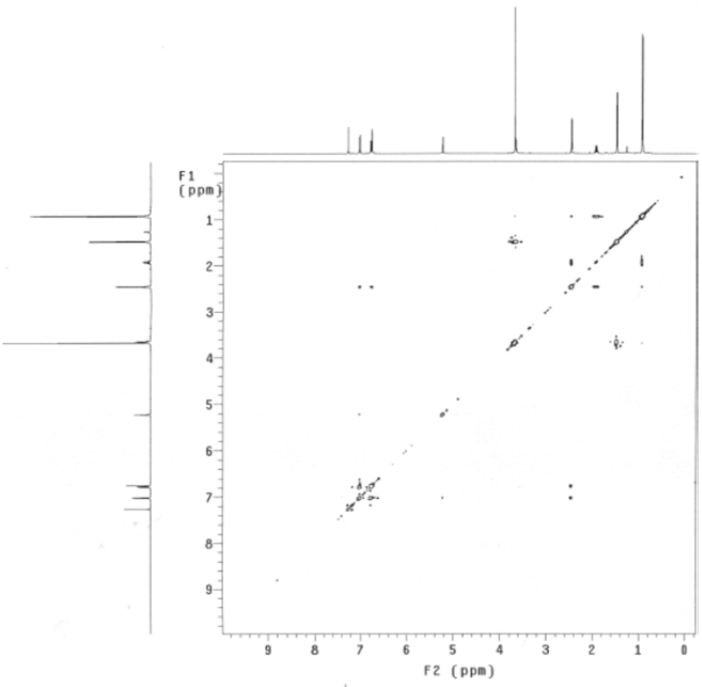


aac_hydroxylation_ibuprofen_ma_jor_gcosy
exp3 gcosy

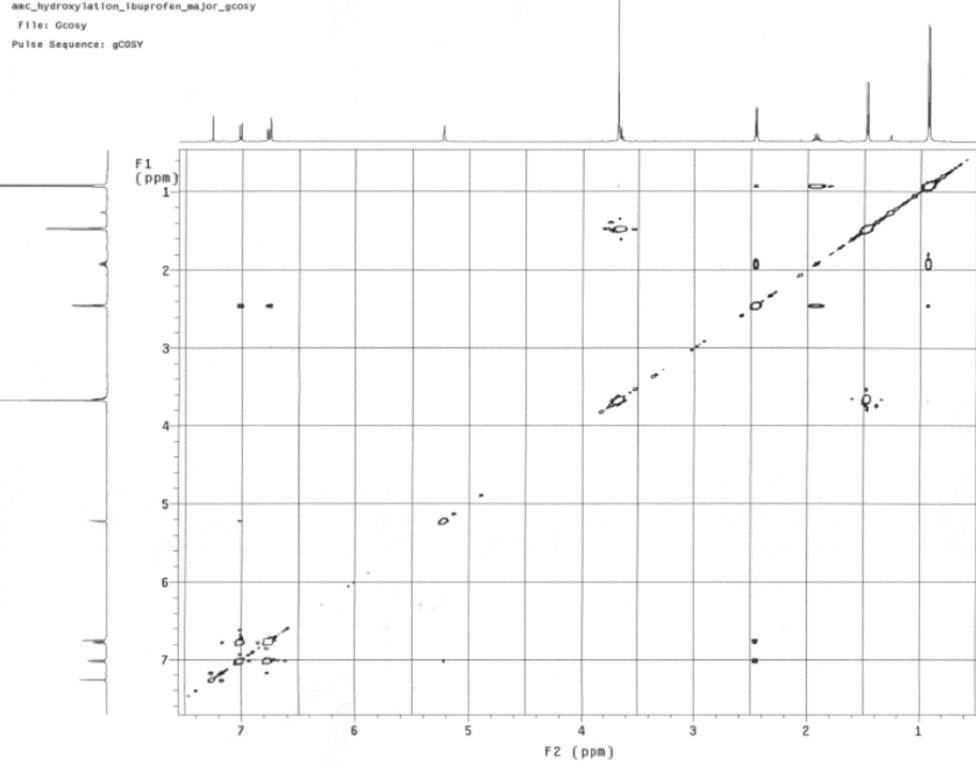
```

SAMPLE          FLAGS
date   Aug 21 2013   hs      nn
solvent cdc13      sspul    n
sample  4694       hsglv1
ACQUISITION      SPECIAL 4694
sw       510.5    temp    27.0
at       0.200    gain    30
np       2048    spin    0
fb       3000    F2 PROCESSING
ss       0       sb      -0.100
dl       2.000    sbs    not used
nt       2       fn      4096
2D ACQUISITION   F1 PROCESSING
sw1      510.5    sb1    -0.100
nl       512    sb13   not used
PRESATURATION   proc1
satmode  nnn     fn1
satdly   0       DISPLAY
satfrq   499.8    sp      -123.0
satpwr   -13     wp      5100.0
TRANSMITTER     sp1      -123.0
tn        11     wp1     5100.0
sfrq     499.854 rf1     3754.4
tof      -56.1   rfp     3628.9
tpwr     59     rf13    3754.4
pw       11.000 rfp1    3628.9
tpwr_cf  1.000
GRADIENTS      wc      116.0
gzlv11  4694    sc      10.0
g11     0.001000 wc2    116.0
g1tab   0.000500 sc2    0
DECOUPLER     vs      0
dn        C13    th      872
dm        nnn    al cdc av 2

```



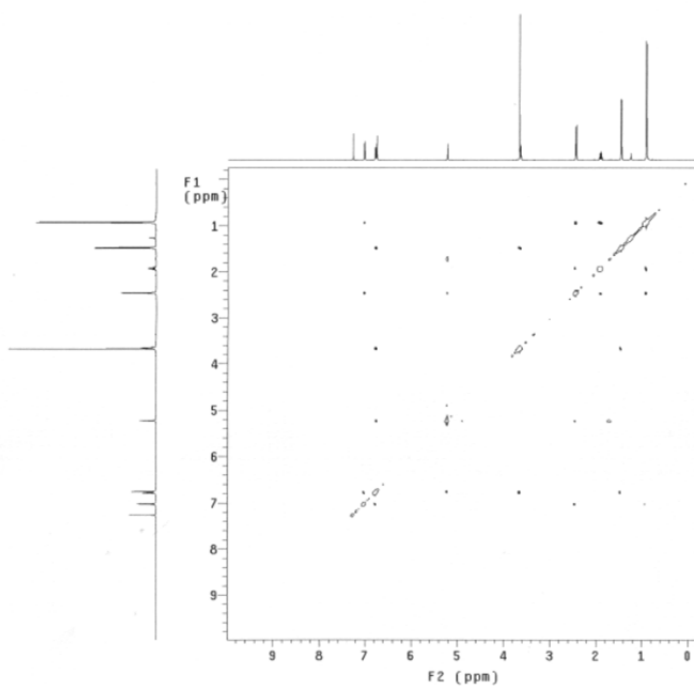
aac_hydroxylation_ibuprofen_ma_jor_gcosy
File: gcosy
Pulse Sequence: gCOSY



amc_hydroxylation_ibuprofen_major_noesy

exp8 Noesy

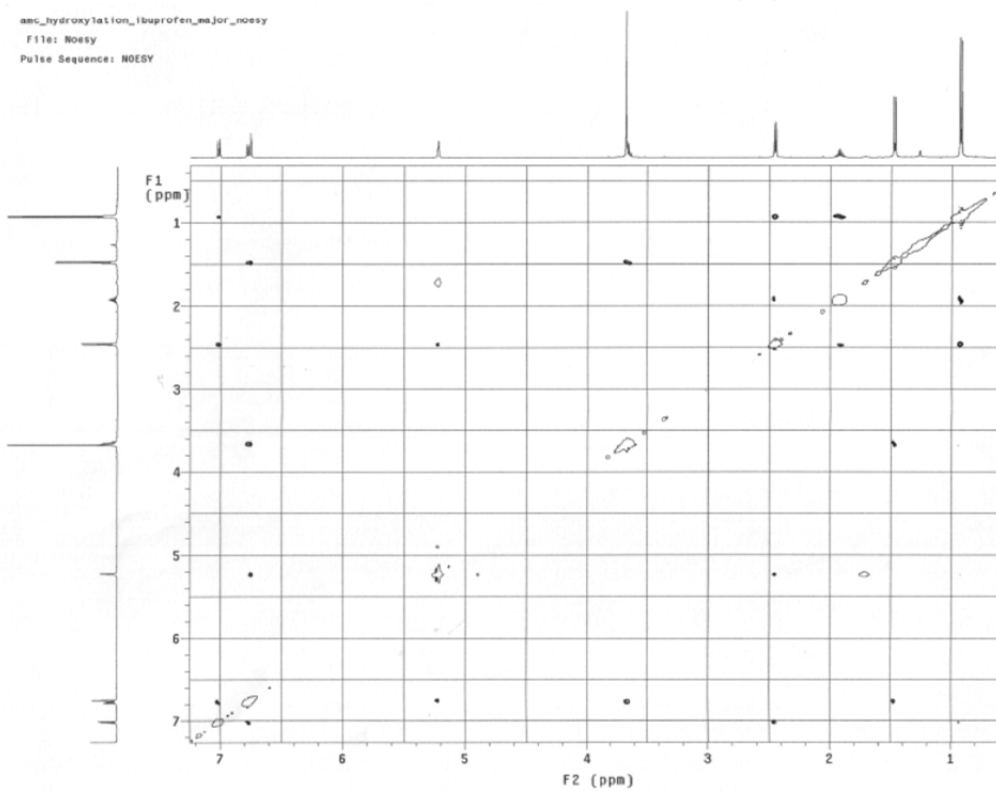
```
SAMPLE          FLAGS
date    Aug 21 2013  hs          n
solvent  cdc13          sspul    y
sample   PFGfg          y
ACQUISITION  hglvl    4694
sw       5110.5        SPECIAL  27.0
at       0.280        temp     30
np       2048        gain     0
fd       3080        spin     0
ss       32          F2 PROCESSING
d1       2.000        gf       0.093
nt       0          gfs     not used
2D ACQUISITION  fn       2048
sw1      5110.5        F1 PROCESSING
n1       256          gf1     0.046
TRANSMITTER  n1          gf1     not used
tn       499.854       f1      1p
sfrq     499.854       f1      2048
t0f      -56.1        DISPLAY
tpr      59          sp       -120.3
pw       11.000       vp       5105.5
mix      NOESY        sp1     -118.8
          0.800        wp1     5105.5
PRESATURATION  rf1     3754.2
satmode  nnn         rfp     3628.9
satpwr   -13         rf1     3752.7
satdy    0           rfp     3628.9
satfrq   499.0       PLOT
dn        DECOUPLER  wc       116.0
dm        C13        ec       10.0
          nnn        wc2     116.0
          vs         sc2     0
          vs         vs     32
          a1        cdc_ph  2
```



amc_hydroxylation_ibuprofen_major_noesy

File: Noesy

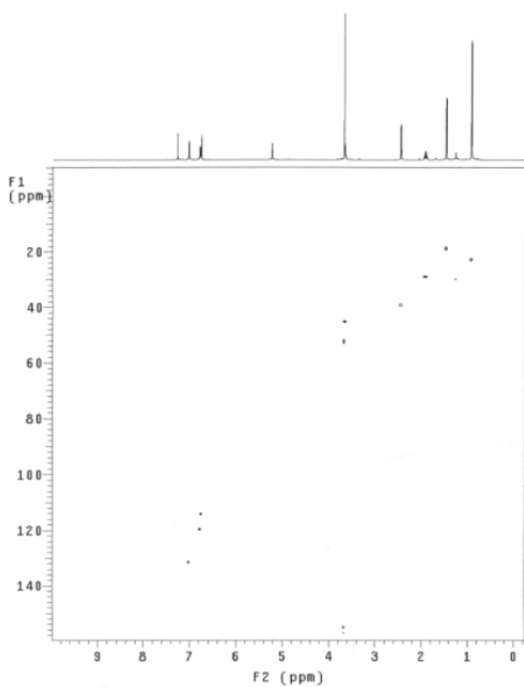
Pulse Sequence: NOESY



amc_hydroxylation_ibuprofen_major_ghsqc

exp6 Ghsqc

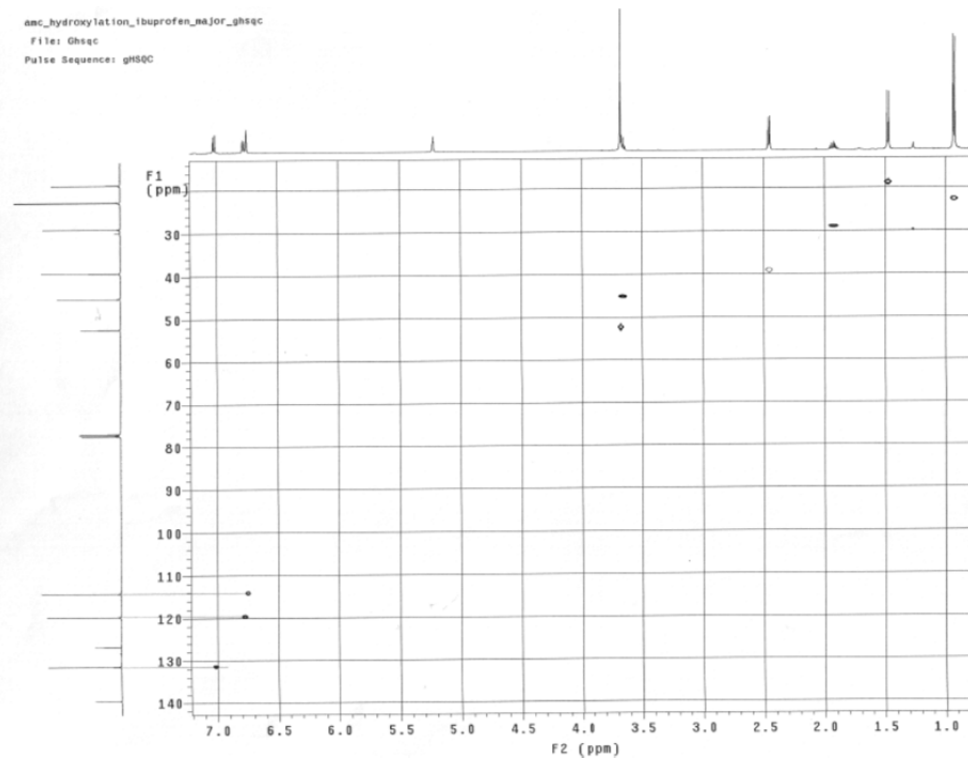
SAMPLE		FLAGS		ACQUISITION ARRAYS	
date	Aug 21 2013	hs	n	array	phase
solvent	cdcl3	ssu1	y	arraydim	S12
sample		PF0F1g	y		
ACQUISITION		hsglv1	4894	1	phase
sv	5110.5	SPECIAL		1	
at	0.199	Leap	27.0	2	2
np	2000	gain	30		
Fb	3000	epin	0		
ss	32	GRADIENTS			
st	2.000	gzlv11	4894		
nt	4	gt1	0.002000		
2D ACQUISITION		g2lv13	2347		
sv1	21367.5	gt3	0.001000		
nt	250	gstab	0.000500		
phase		arrayed F2 PROCESSING			
PRESATURATION		gf	0.092		
satwde	mmu	gfs	not used		
satdy	0	fn	4896		
satfrs	499.0	F1 PROCESSING			
satqpr	-13	gfi	0.011		
TRANSMITTER		gfs1	not used		
tn	H1	proc1	lp		
vfrq	499.854	fn1	2040		
tor	-56.1	sp	-123.1		
tpwr	53	DISPLAY			
pw	11.000	wp	5100.0		
DECOUPLER		sp1	-1270.5		
dn	C13	wp1	21346.7		
dor	-2515.2	rf1	1860.5		
de	43	rf6	1835.0		
dor	22200	rf11	7043.0		
dpr	43	rfp1	6551.6		
pwlv1	55	PLOT			
pwk	10.500	wc	116.0		
HSQC		wc	116.0		
jlwh	140.0	wc2	116.0		
multfg	y	wc2	0		
mult	z	vs	872		
		th	2		
		at	cdc ph	2	



amc_hydroxylation_ibuprofen_major_ghsqc

File: Ghsqc

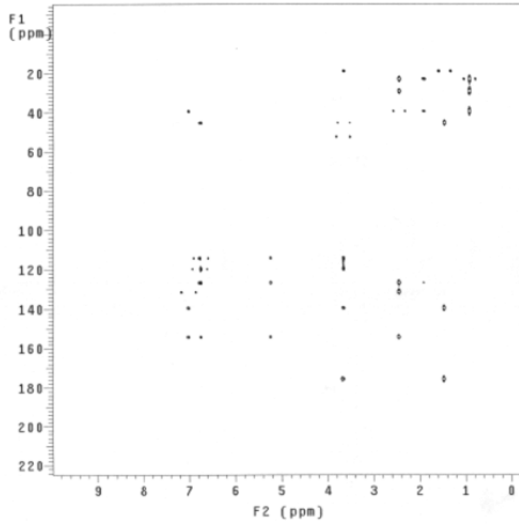
Pulse Sequence: gHSQC



amc_hydroxylation_ibuprofen_major_gmhc

exp7 gmhc

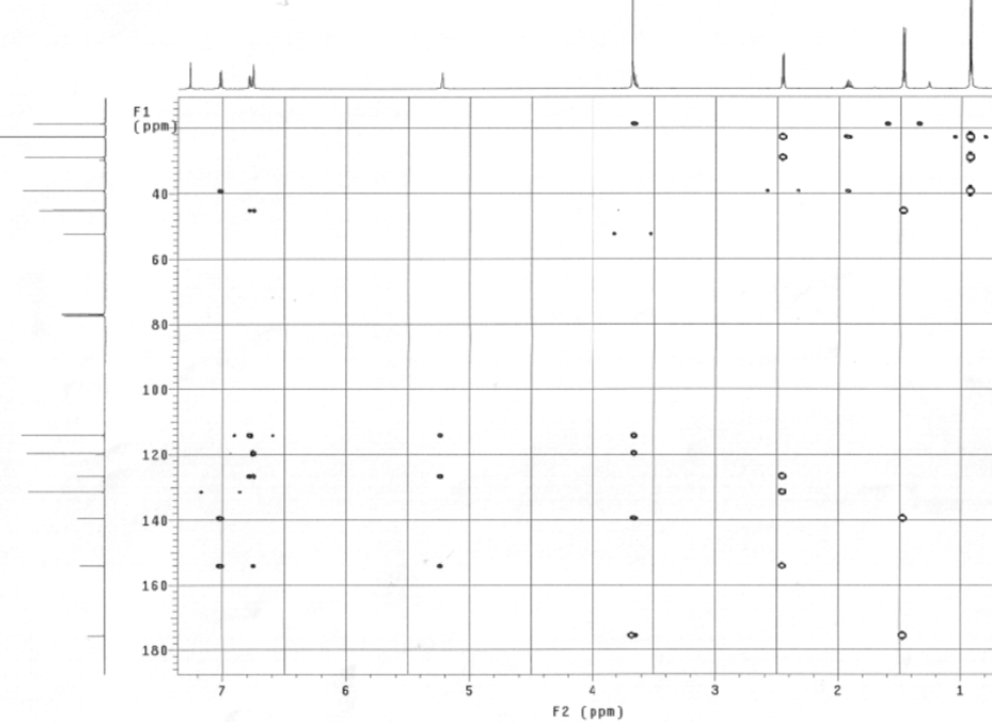
SAMPLE		FLAGS	
date	Aug 21 2013	hc	n
solvent	cdcl3	sspu1	n
sample		PF07g	y
ACQUISITION	hrglv1		4694
sw	5110.5	SPECIAL	
at	0.128	teap	27.0
ns	1300	gain	20
fb	3000	spin	0
ss	32	GRADIENTS	0
d1	2.000	g2lv11	4694
nt		gt1	0.001000
2D ACQUISITION	16	gt13	3367
sv1	30185.9	gt3	0.001000
ni	256	gntab	0.002000
phase	0	F2 PROCESSING	
PRESATURATION	sb		0.064
satmode	mn	sbs	not used
satly	0	fn	2048
satfrq	499.8	F1 PROCESSING	
satpwr	-13	sb1	0.008
TRANSMITTER		sbs1	not used
tn	h1	proc1	1p
sfrq	499.854	fn1	2048
tof	-56.1	DISPLAY	
tpr	59	sp	-120.3
pw	11.000	wp1	5105.5
DECOUPLER		wp1	-1882.8
dn	C13	wp1	30136.5
dof	1255.4	rf1	860.1
da	mn	rfp	794.8
dnr	22200	rf11	23863.5
dpr	45	rfp1	22051.1
pwlv1	55	PLOT	
pwk	10.500	wc	116.0
HMBC		sc	10.0
j1vh	140.0	wc2	116.0
j1vh	0.0	sc2	0
vs		vs	328
ls		ls	2
al	cdc	av	2



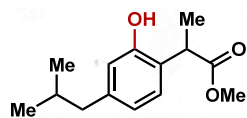
amc_hydroxylation_ibuprofen_major_gmhc

File: gmhc

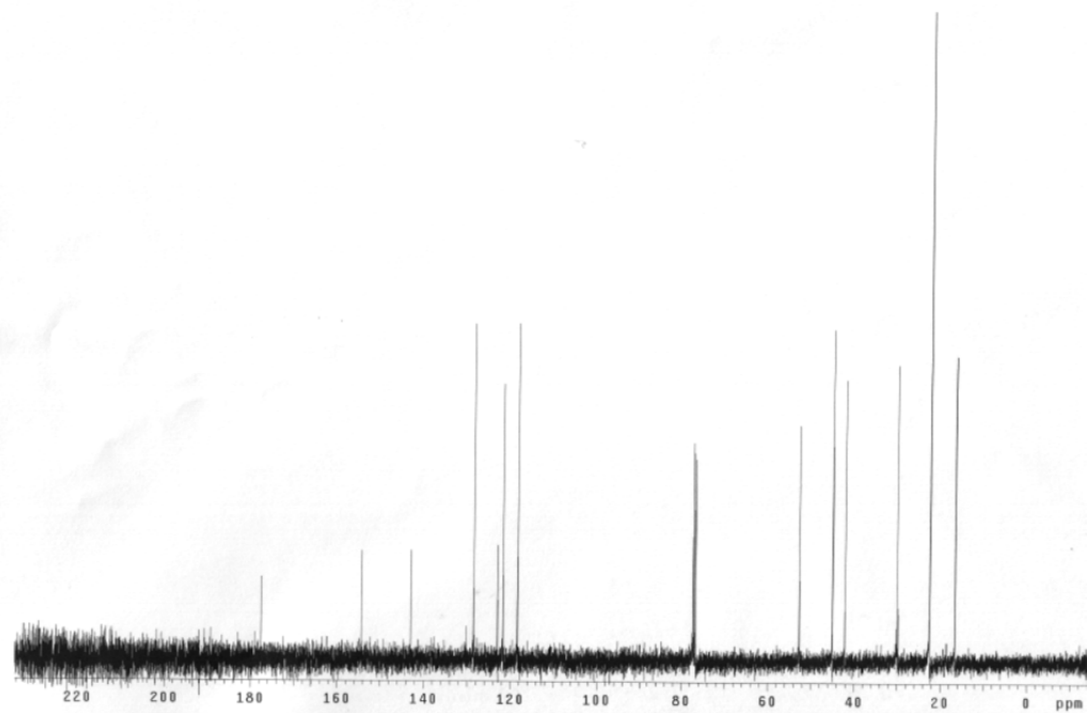
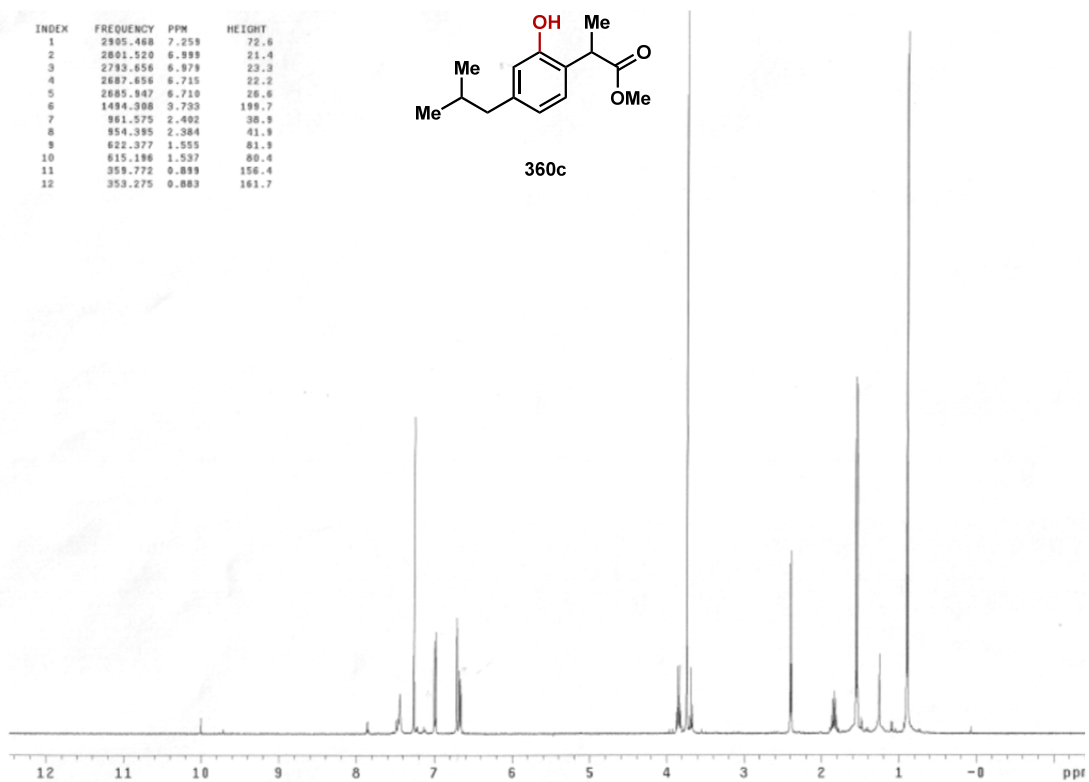
Pulse Sequence: gmhc

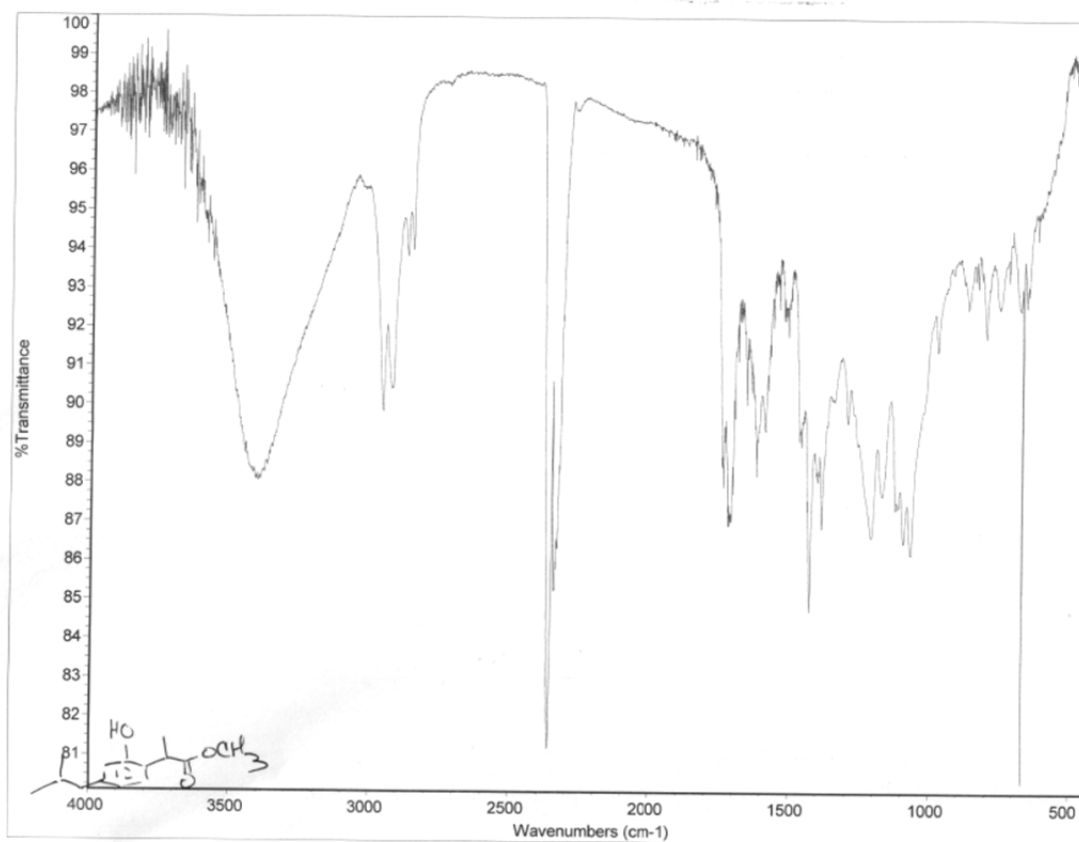


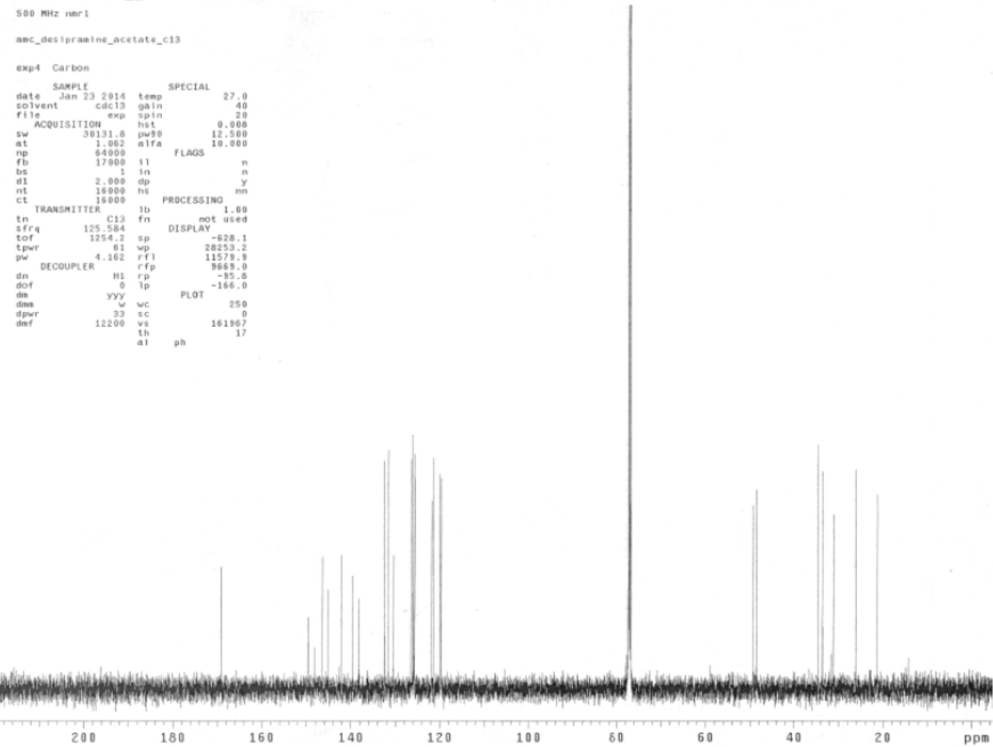
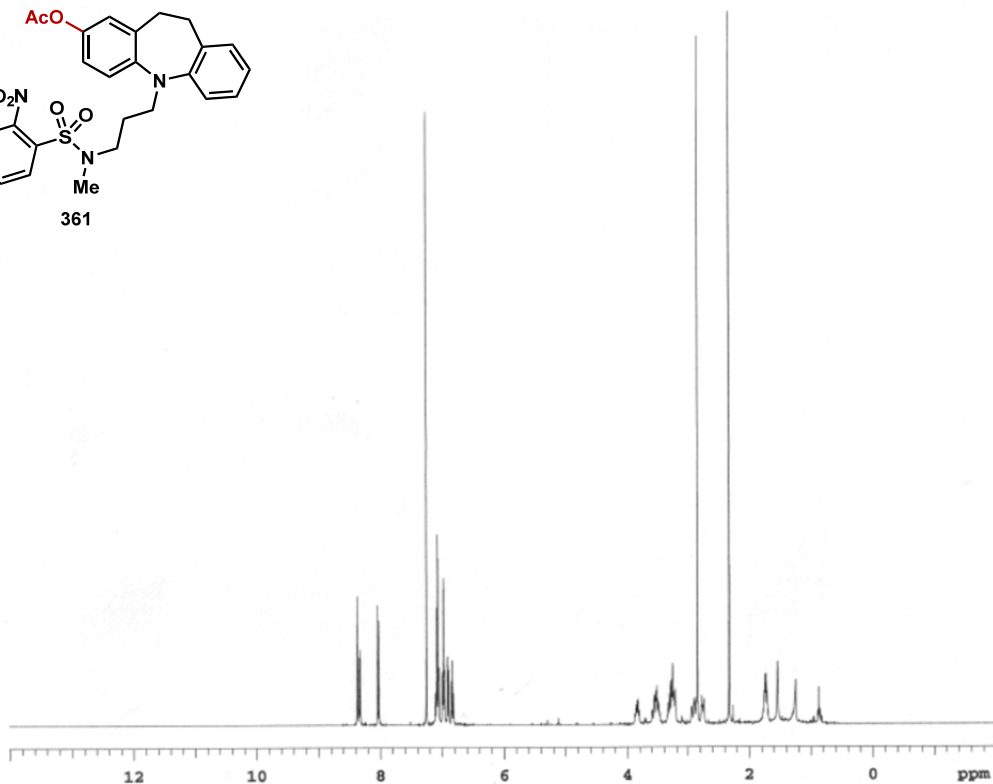
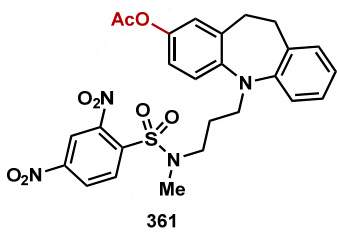
INDEX	FREQUENCY	PPM	HEIGHT
1	2305.468	7.258	72.6
2	2801.520	6.999	21.4
3	2793.656	6.979	23.3
4	2687.656	6.715	22.2
5	2685.947	6.710	26.6
6	1494.308	3.733	199.7
7	961.575	2.492	38.9
8	954.395	2.384	41.9
9	622.377	1.555	81.9
10	615.196	1.537	80.4
11	359.772	0.899	156.4
12	353.275	0.880	161.7



360c







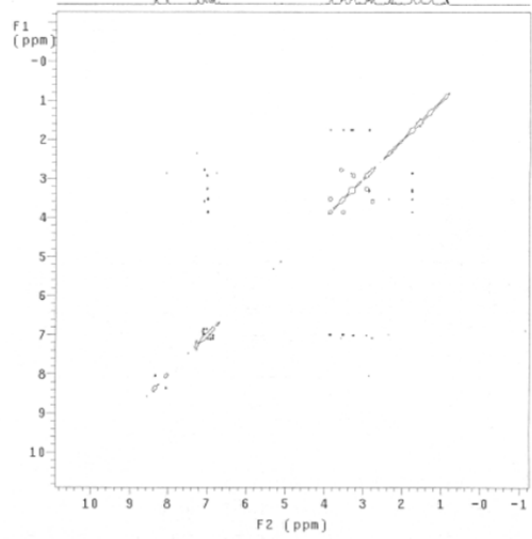
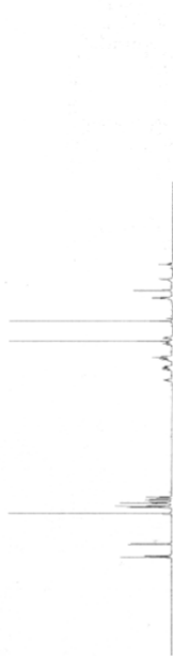
```

500 MHz nmr1
mc_desipraeine_acetate_c13
exp4 Carbon
SAMPLE SPECIAL
date Jan 23 2014 temp 27.0
solvent cdcl3 gain 40
file exp gain 20
ACQUISITION hst 0.008
sw 30131.0 pw90 12.500
at 1.862 a1fa 10.000
np 84000
fb 17900 f1 n
bs 1 1n n
st 2.800 dp y
nt 16000 hs
ct 16000
TRANSMITTER tb PROCESSING 1.00
tn C13 fn not used
f1fa 125.504 DISPLAY
tof 1254.2 sp -628.1
lpwr 61 wp -20253.2
pk 4.162 rfp 11579.9
DECOUPLER H1 rfp 9669.0
dn 0 rp -95.0
dof 0 lp -166.0
da yyy PLOT 250
dwa 33 sc 0
dpwr 12200 vs 161967
awf a1 ph 17
  
```

anc_desipramine_acetate_noesy

exp3 Noesy

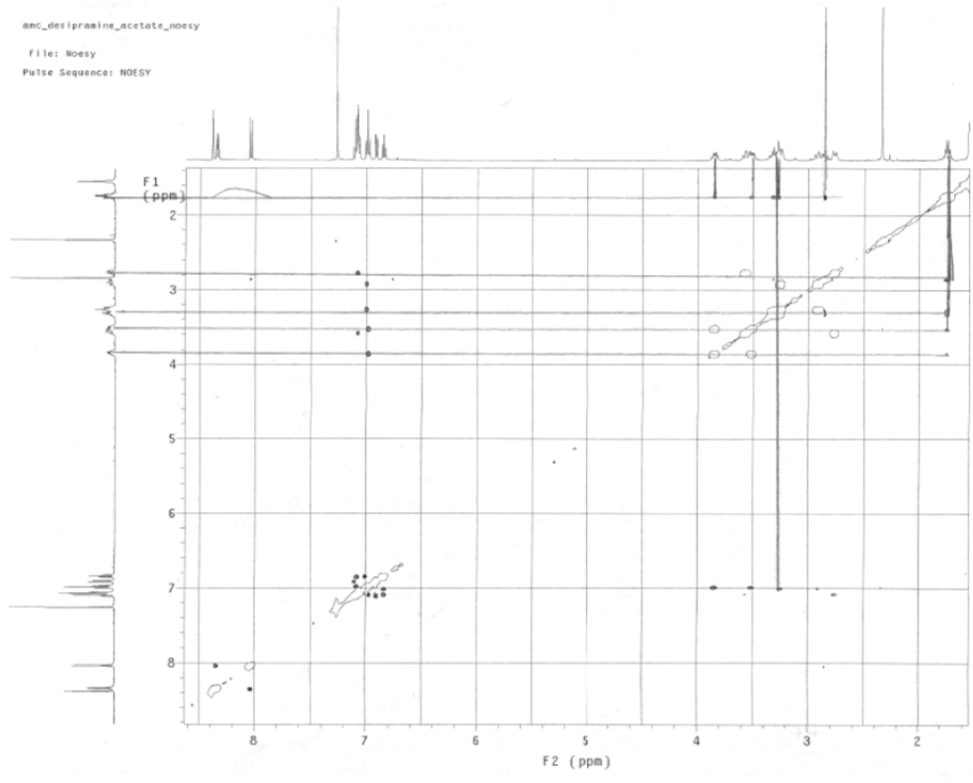
SAMPLE		FLAGS	
date	Jan 27 2014	hs	n
solvent	cdc13	sgpu1	y
sample		PFGR1g	y
ACQUISITION	hsgr1v1		9900
sw	6056.6	SPECIAL	
at	0.169	temp	27.0
np	2048	gain	60
fb	3000	spin	0
ss	0	F2 PROCESSING	
dl	2.000	gf	0.078
nt	8	gfs	not used
3D ACQUISITION	fn		2048
sw1	6056.6	F1 PROCESSING	
nt	256	gf1	not used
TRANSMITTER	gfs1		
tn	H1	proc1	ip
effa	499.390	fni	2048
tof	-31.3	DISPLAY	
tpwr	-54	sp	-627.0
pw	9.300	wc	6000.7
NOESY	0.800	wp1	-623.5
mix	0.800	wpc	6000.7
PRESATURATION	rfl		4258.5
satmode	nmn	rfp	3925.6
satpwr	-15	rfl1	4254.9
satdy	0	rfl1	3925.5
satfrg	499.0	PLOT	
DECOUPLER	wc		116.0
dn	C13	sc	10.0
ds	nmn	wc2	116.0
		sc2	0
		vs	195
		lb	2
	al	cdc	ph



anc_desipramine_acetate_noesy

File: Noesy

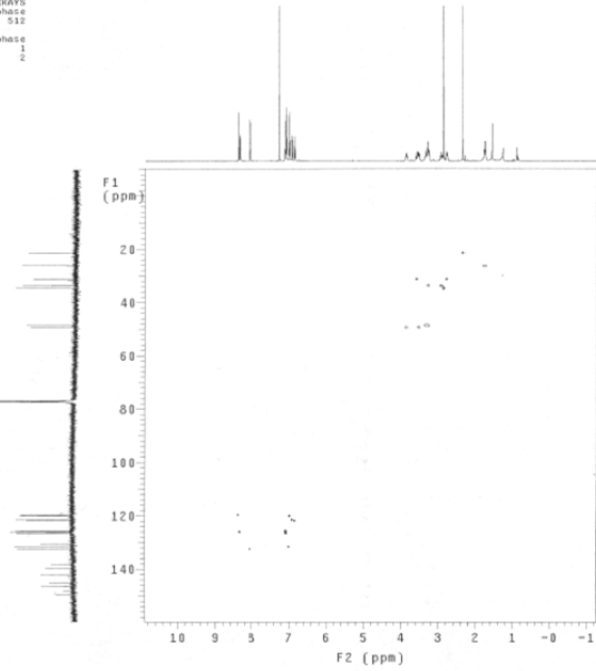
Pulse Sequence: NOESY



dec_desipramine_acetate_h1

exp6 ghsqc

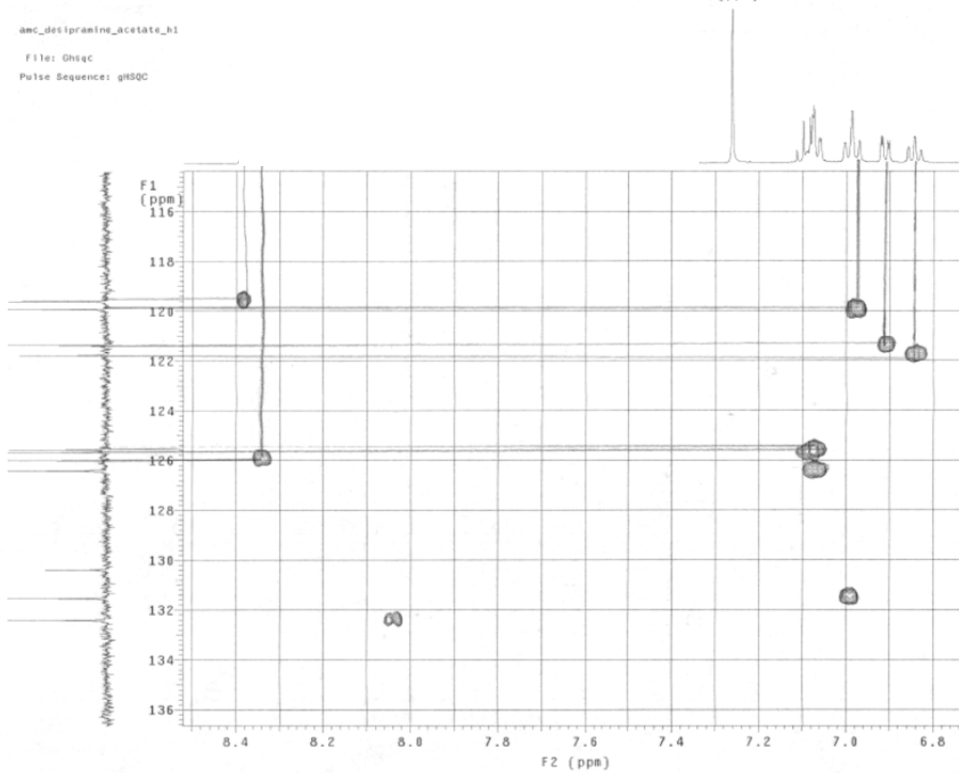
```
SAMPLE          FLAGS          ACQUISITION ARRAYS
date Jan 27 2014 hc              n array phase
solvent cdc13 sspu1             y arraydim 512
sample          PFGflg          y
ACQUISITION    hsglv1          9900 1 phase
sw 8666.6      SPECIAL 27.0 1
at 8.217      temp 27.0 2
np 2634      gain 60
fb 3000      spin 0
ss 8
d1 2.000     g2lv11 9900
nl 4         g1 0.002000
2D ACQUISITION g2lv13 4970
sw1 21394.7  g13 0.001000
nl 256      g1lab 0.000500
phase arrayed g2 PROCESSING
PRESATURATION  gf 0.100
satmode mmn  gfs not used
satcly 0   fm 4936
satfrs 499.8 f1 PROCESSING
satpar -13  gf1 0.011
TRANSMITTER H1 proc1 not used
tn 499.398  fm1 2048
strq -91.3  DISPLAY
tpr 34      sp -630.0
pw 9.300   wd 6063.6
DECOUPLER C13 sp1 -1267.1
dof -2513.0 rf1 21323.9
de vny rfp 1796.5
dmf 32258 rf11 3959.7
dpar 41    rfp1 2662.7
pwxlv1 80   PLDT
pwx 12.300 wc 116.0
HSQC 140.0  wc2 116.0
J1vb v 0
multivg z vs 018
mult 2    vs 018
at cdc ph 2
```



dec_desipramine_acetate_h1

File: ghsqc

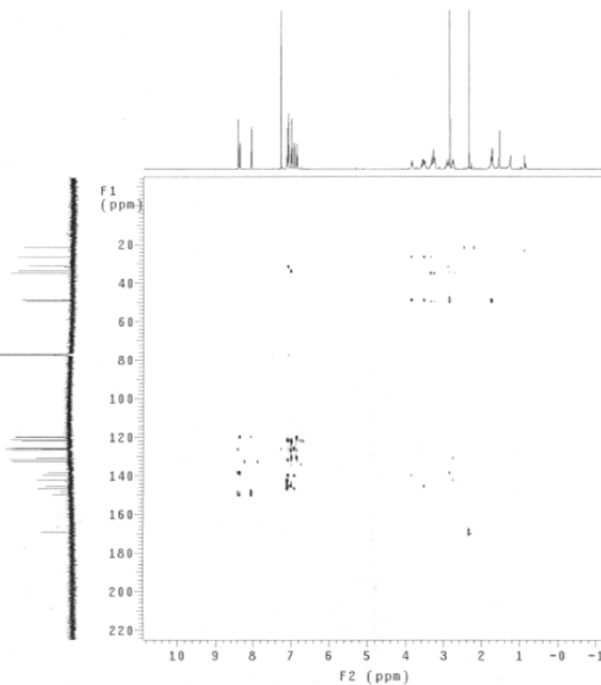
Pulse Sequence: gHSQC



amc_desipramine_acetate_gmhc

exp7 gmhc

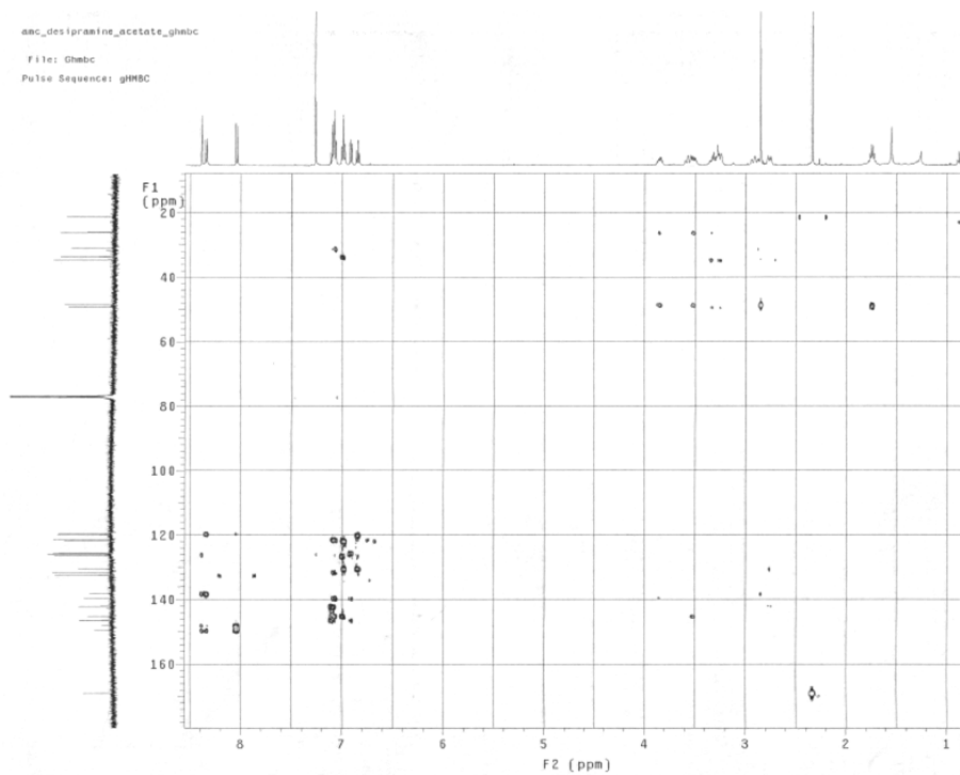
```
SAMPLE          FLAGS
date Jan 27 2014 hs n
solvent cdcl3 sspu1 n
sample PRO1g y
ACQUISITION    hsglv1 1800
cw 6086.6 SPECIAL
at 0.217 temp 27.0
rp 2624 gain 60
fo 30000 spin 0
ss 8 GRADIENTS
gt 2.000 gtlv11 0.000
nt 16 gtl1 0.001000
3D ACQUISITION gtlv13 4970
sw1 30131.8 g13 0.001000
nl 256 gtab 0.000500
phase 0 F2 PROCESSING
PRESATURATION sb 0.109
satmode mm sb5 not used
satcly 0 fs 4096
satfrq 499.8 f1 PROCESSING
SATPR -13 s01 0.408
TRANSMITTER n1 sb51 not used
in n1 pnc1 1p
sfrq 499.390 f01 4096
tdf -91.3 sp DISPLAY
LWR 34 sp -630.3
pw 9.300 wp 6963.6
DECOUPLER C13 w01 30117.1
dn 1254.2 rf1 1798.4
dm mm rfo 1195.1
dmf 32258 rf11 23112.2
dpr 41 rfp1 21118.3
pwxlv1 80 PLOT
pwx HMC 12.300 wc 116.0
j1wh 140.0 wc2 116.0
j1wh 8.0 sc2 0
ls vs 328
al cdc av 2
```

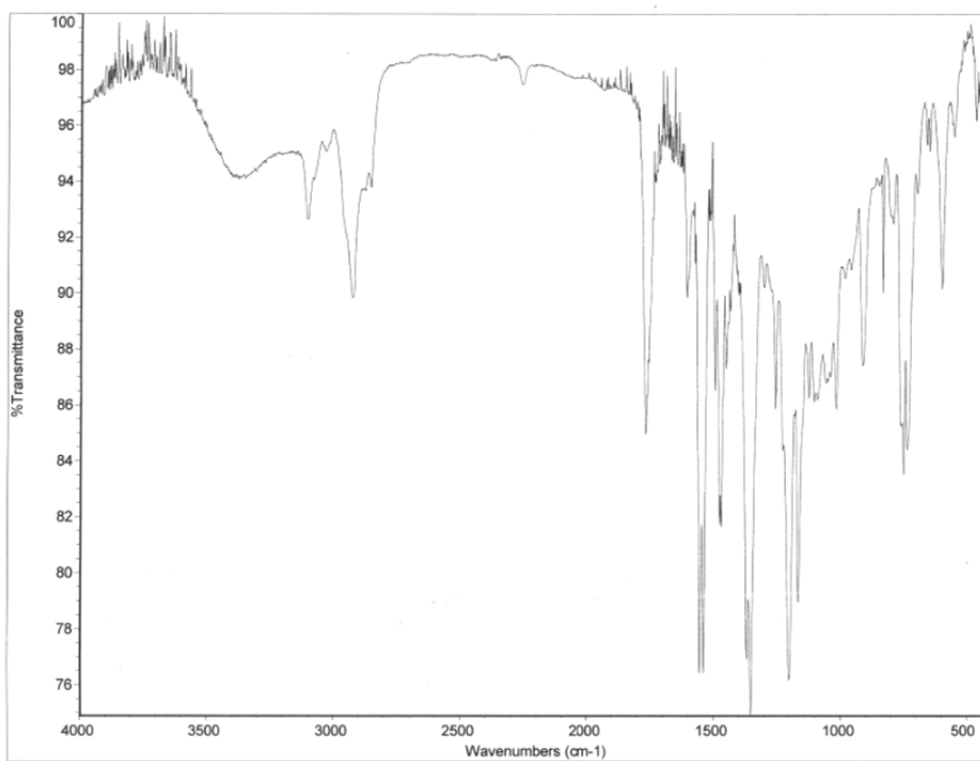


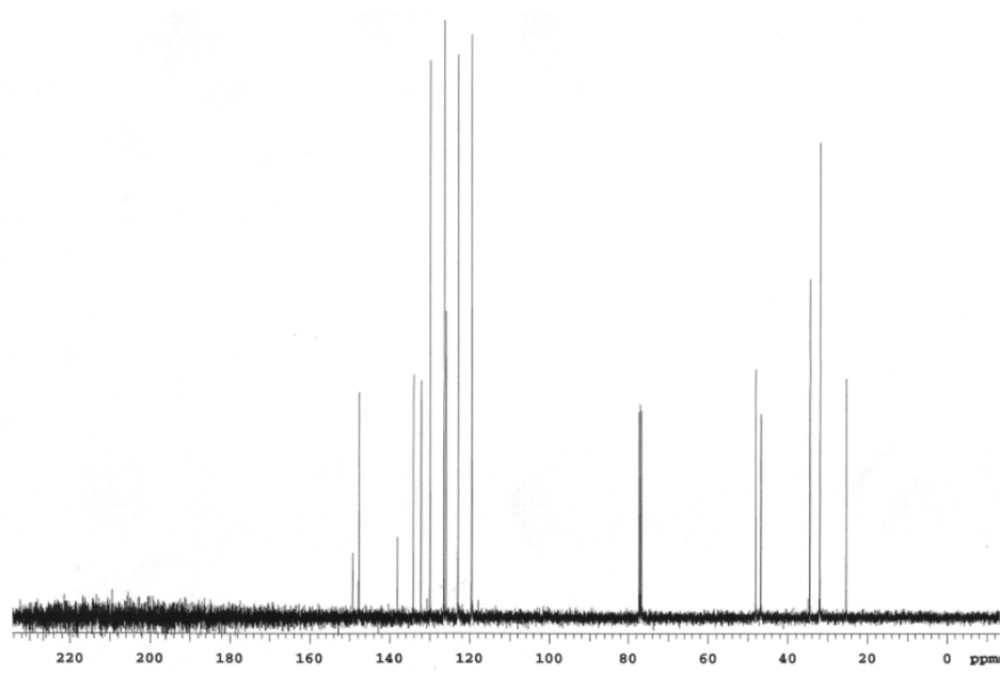
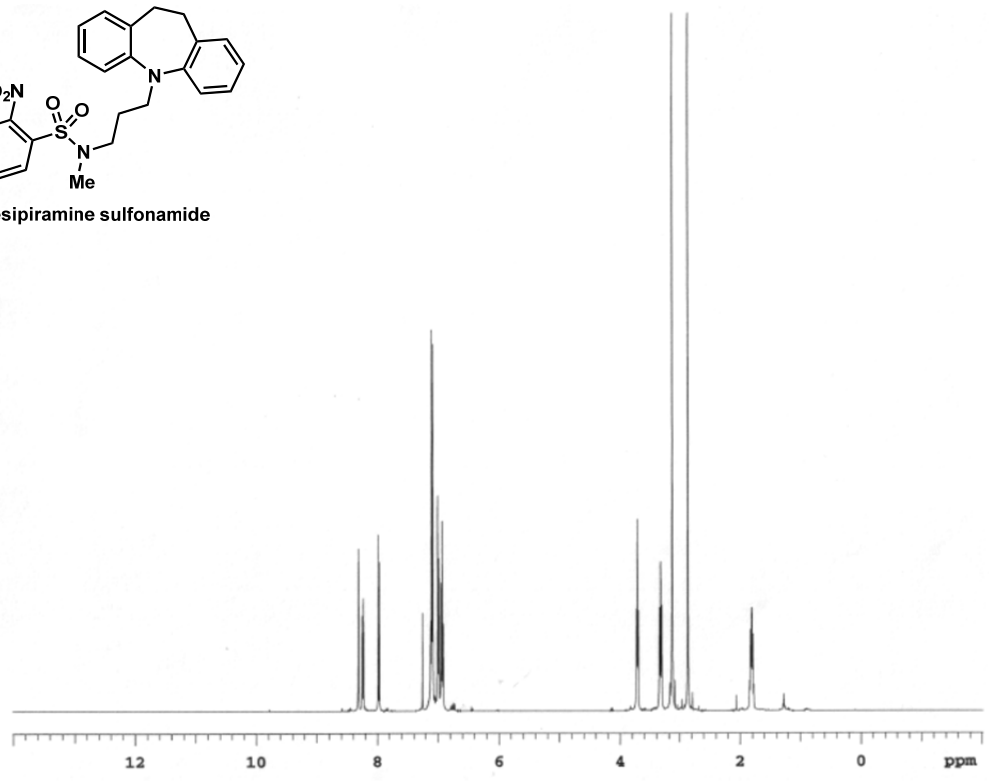
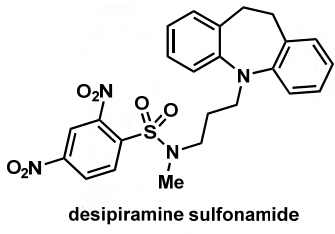
amc_desipramine_acetate_gmhc

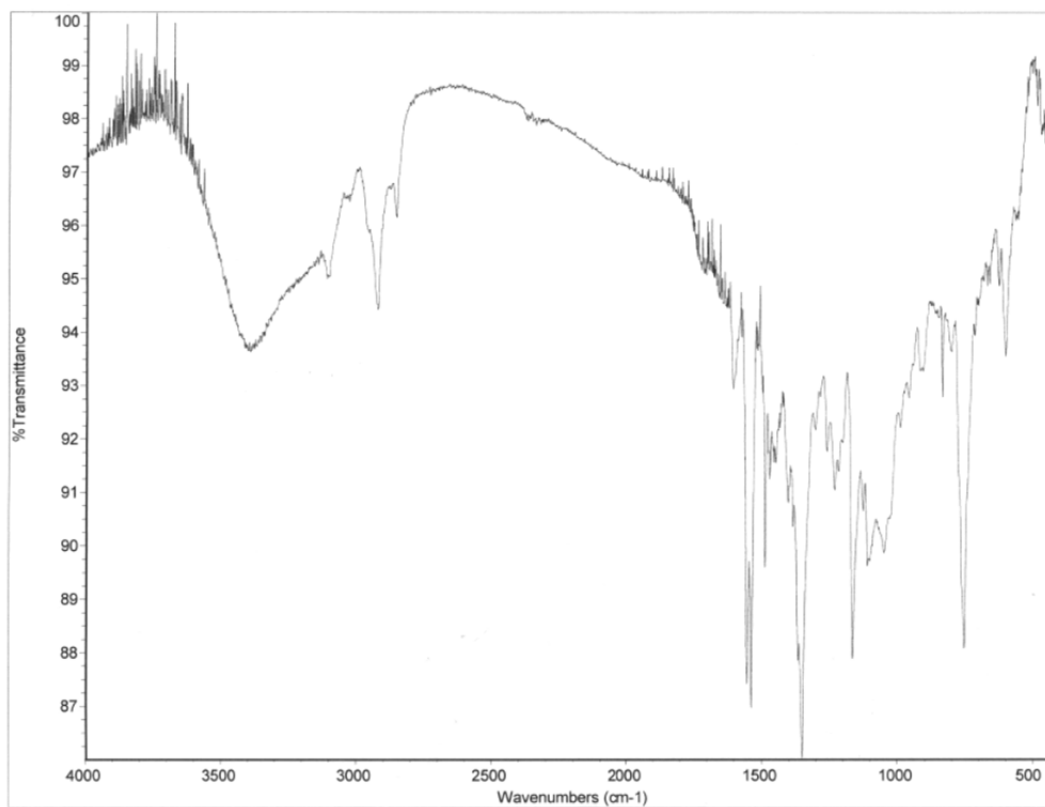
File: gmhc

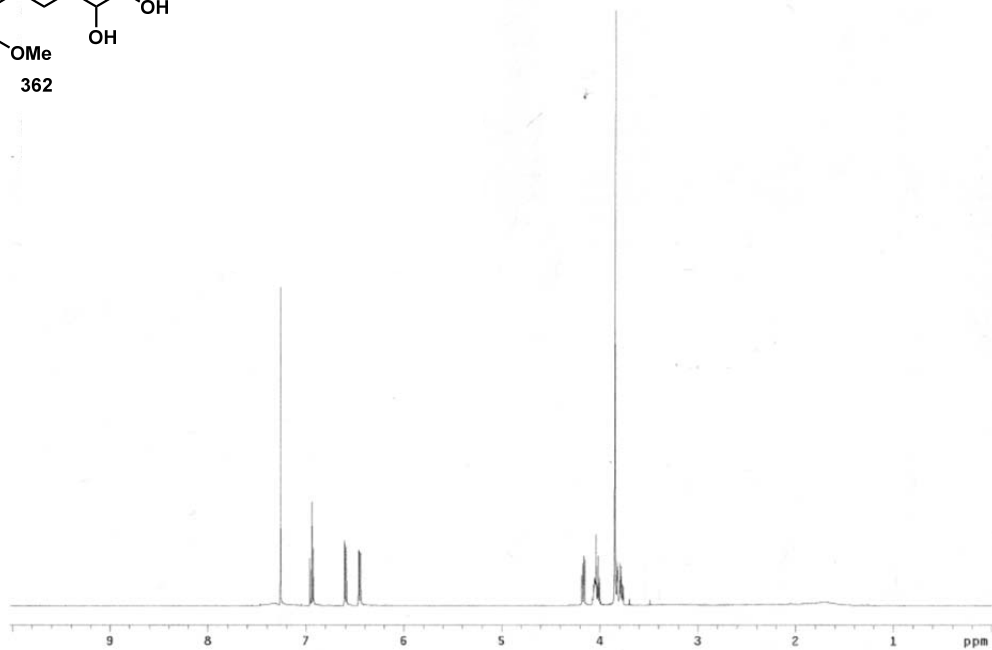
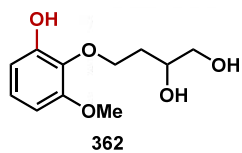
Pulse Sequence: gmhc



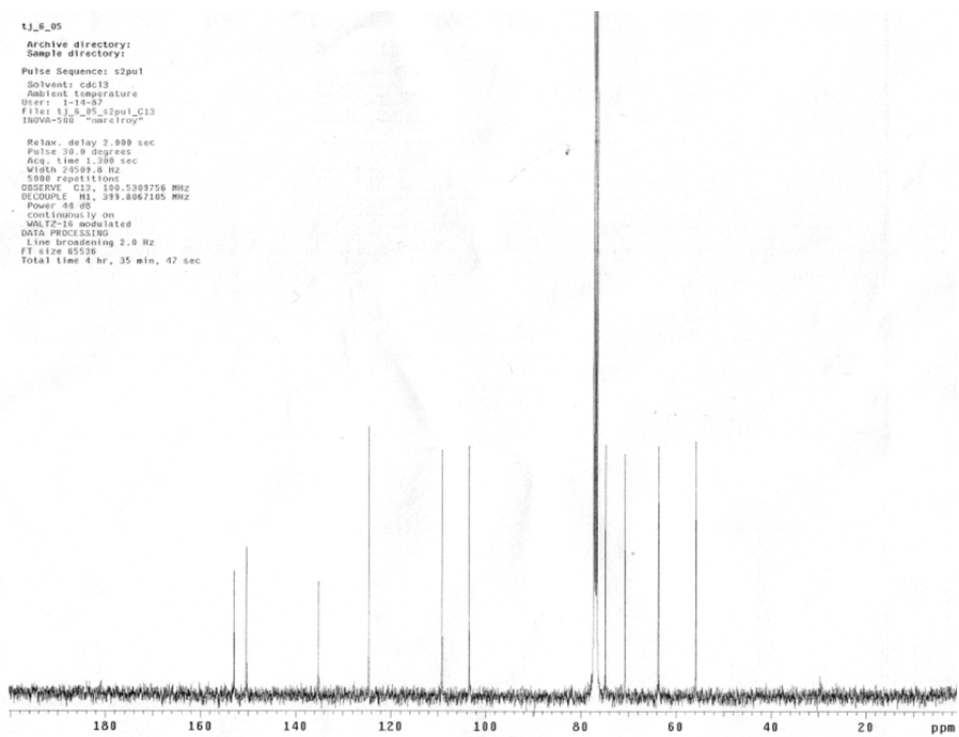




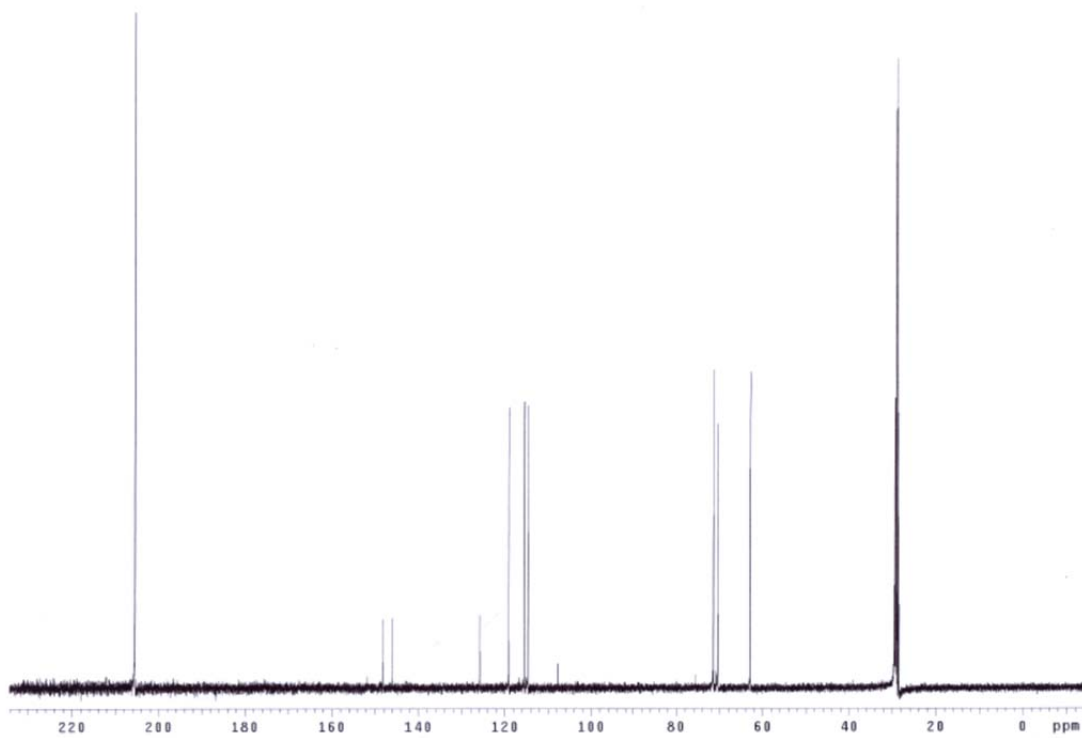
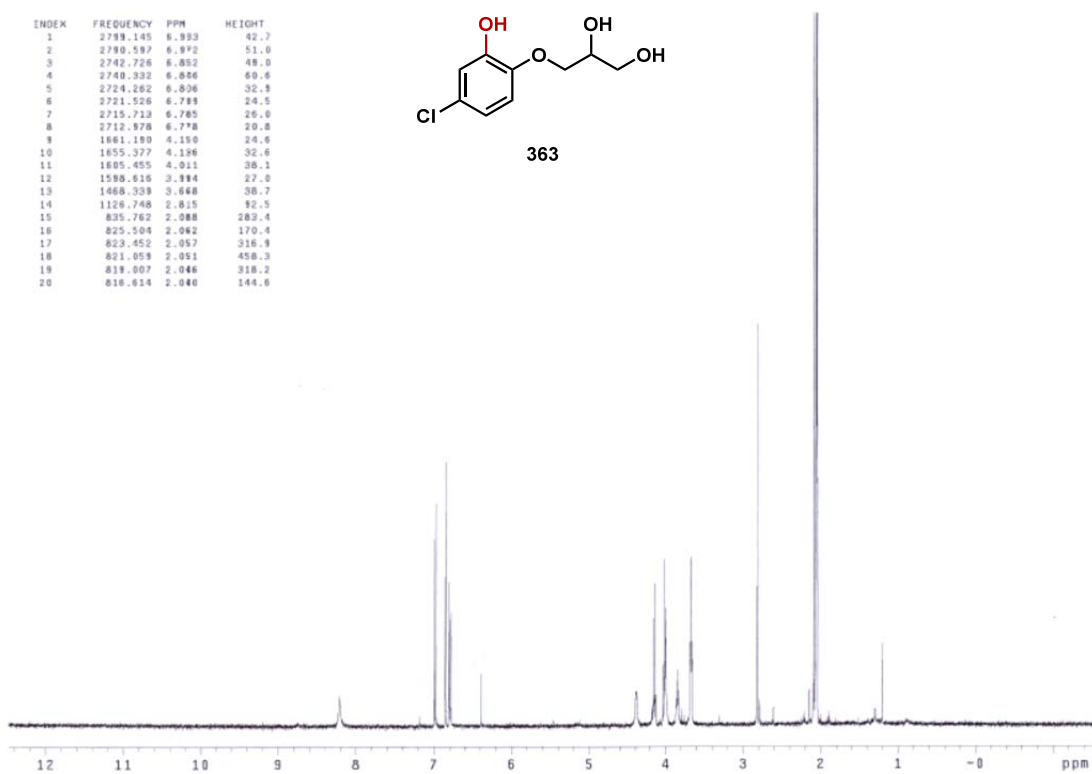
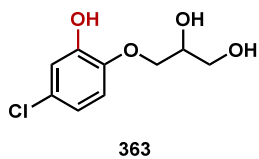


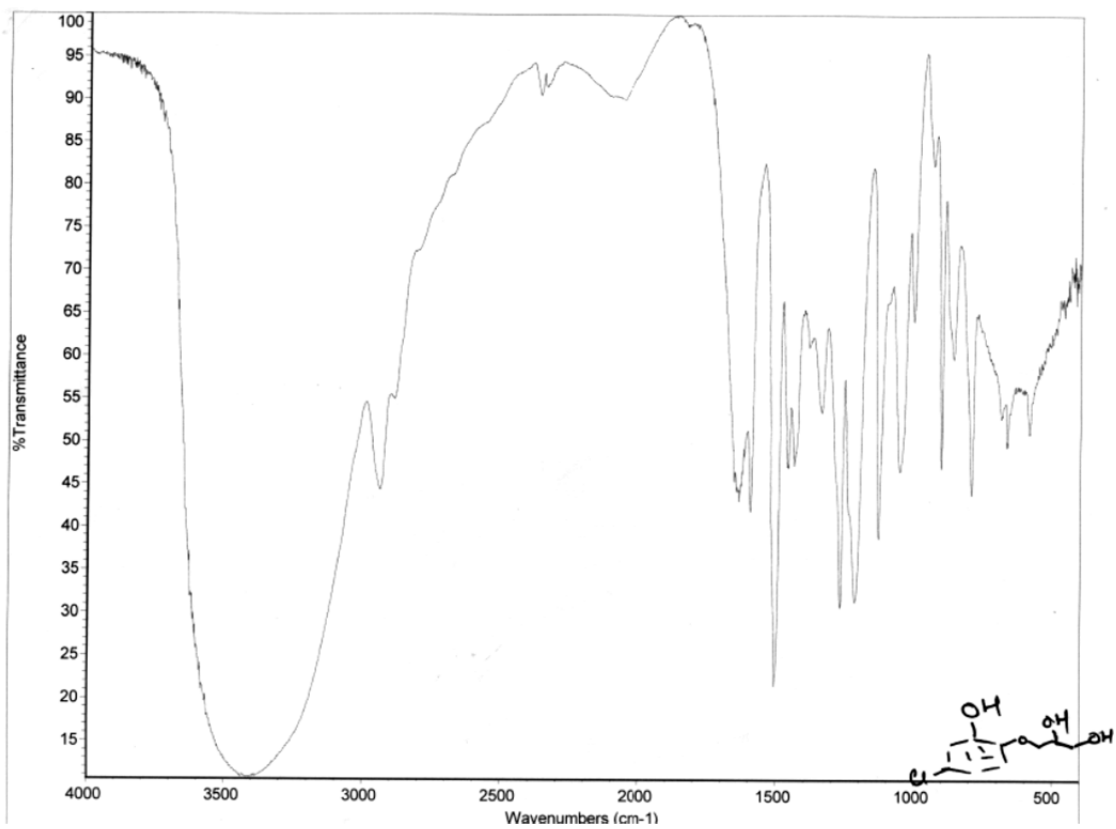


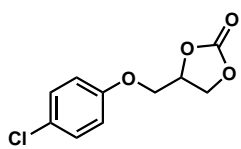
tj_6_05
 Archive directory:
 Sample directory:
 Pulse Sequence: s2pul
 Solvent: cdcl3
 Ambient temperature
 Inert: 1-14-97
 File: tj_6_05_s2pul_C13
 INOVA-500 "mercury"
 Relax. delay 2.000 sec
 Pulse 20.0 degrees
 Acq. time 1.300 sec
 Width 23500.0 Hz
 5000 repetitions
 OBSERVE C13, 100.5303756 MHz
 RECOUPLE H1, 399.8067105 MHz
 Power 48 dB
 continuously on
 WALTZ-16 modulated
 DATA PROCESSING
 Line broadening 2.0 Hz
 FT size 65536
 Total time 4 hr, 35 min, 47 sec



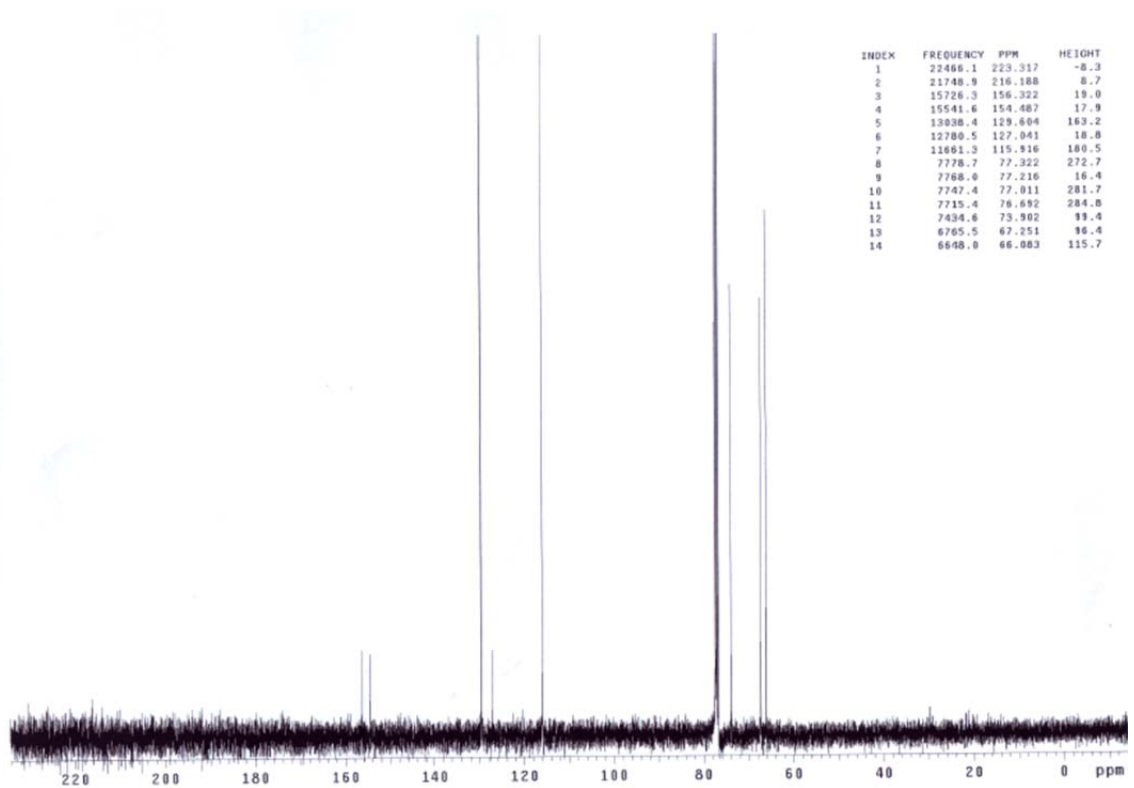
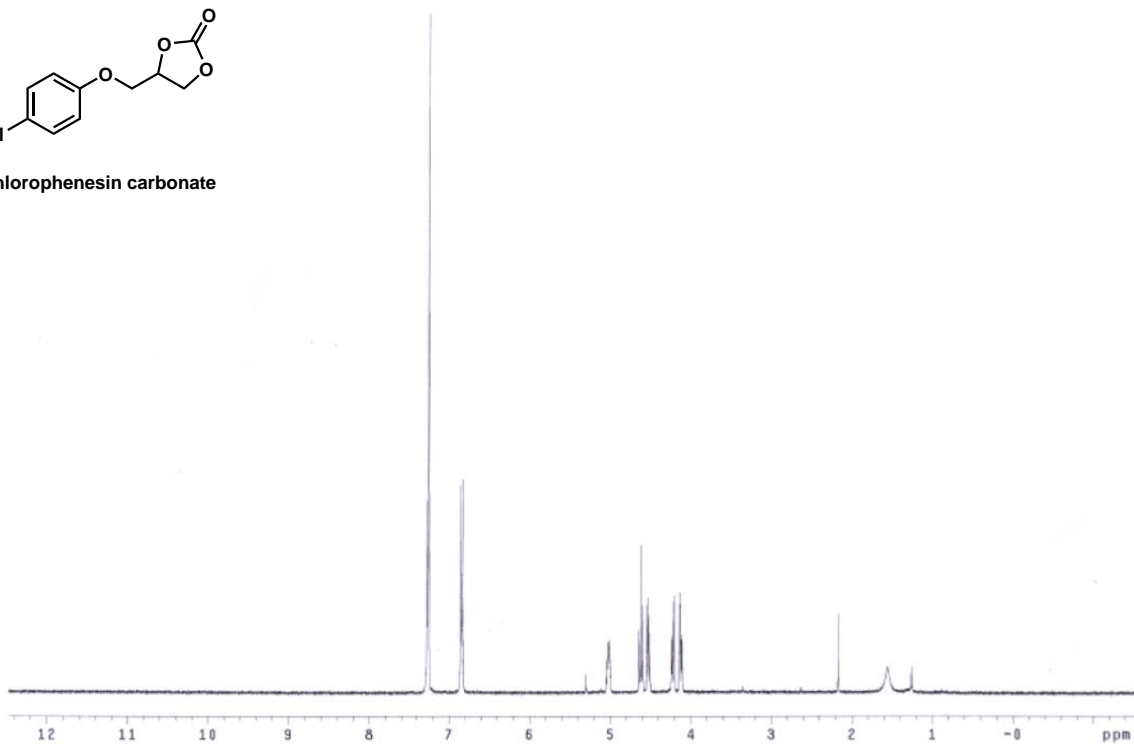
INDEX	FREQUENCY	PPM	HEIGHT
1	2789.145	6.893	42.7
2	2780.597	6.892	51.0
3	2742.726	6.852	48.0
4	2740.332	6.856	69.6
5	2724.262	6.806	32.3
6	2721.526	6.789	24.5
7	2715.713	6.785	26.0
8	2712.978	6.778	20.8
9	1881.180	4.150	24.6
10	1655.377	4.136	32.6
11	1605.455	4.011	30.1
12	1580.616	3.994	27.0
13	1486.339	3.648	36.7
14	1126.748	2.815	92.5
15	835.762	2.088	282.4
16	825.504	2.042	170.4
17	823.452	2.057	316.9
18	821.059	2.051	458.3
19	819.007	2.046	318.2
20	816.614	2.040	144.6

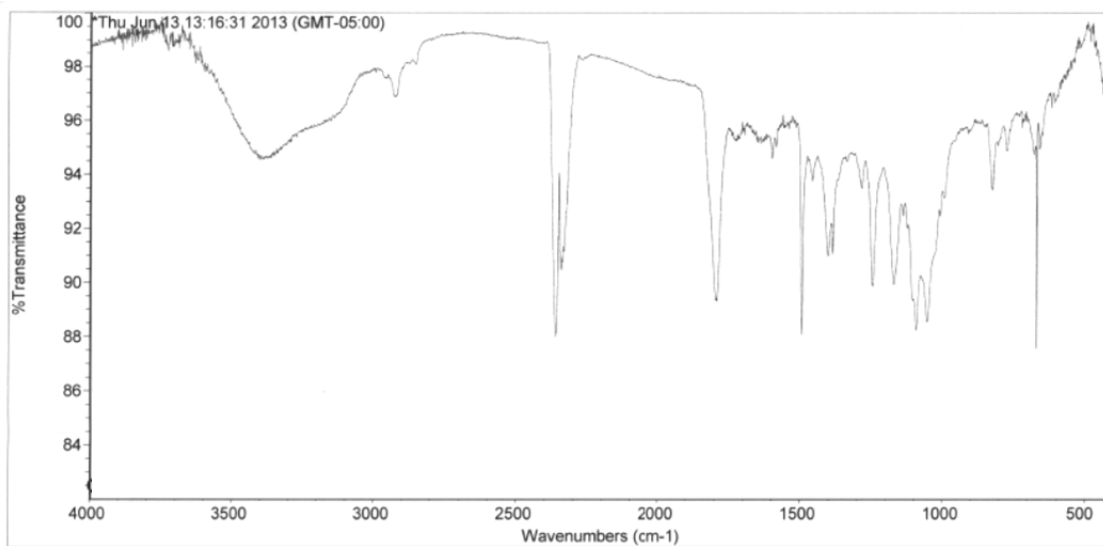






chlorophenesin carbonate





Thu Jun 13 13:18:23 2013 (GMT-05:00)

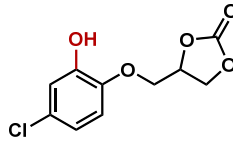
FIND PEAKS:

Spectrum: *Thu Jun 13 13:16:31 2013 (GMT-05:00)
Region: 4000.00 400.00
Absolute threshold: 82.188
Sensitivity: 50
Peak list:

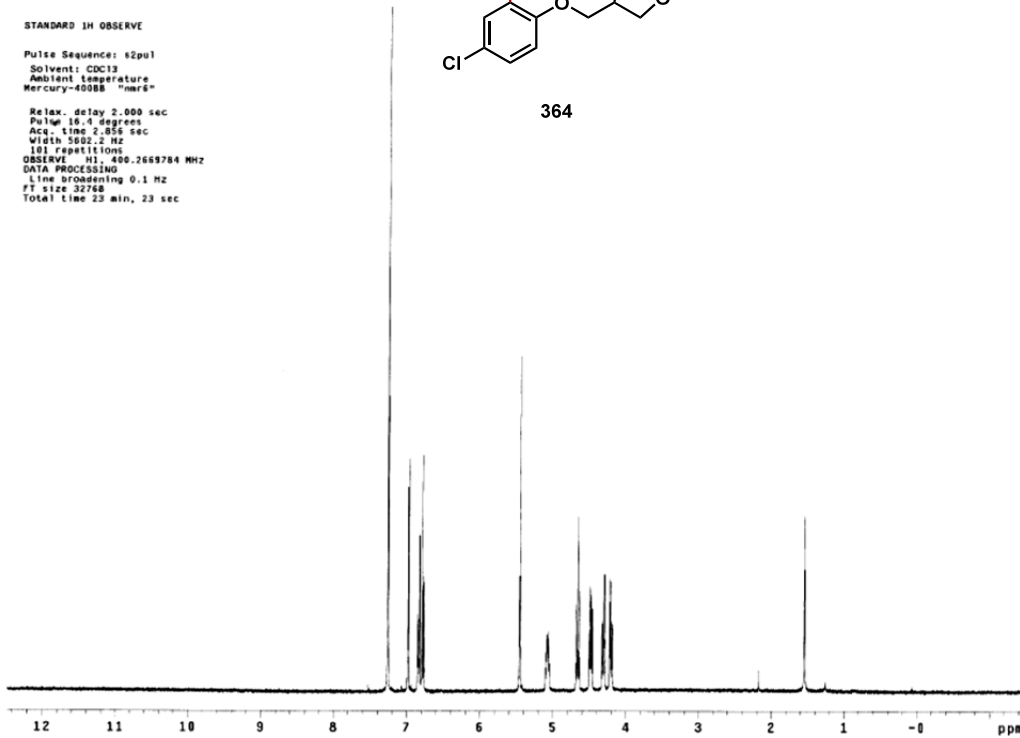
STANDARD 1H OBSERVE

Pulse Sequence: s2pul
Solvent: CDCl3
Ambient temperature
Mercury-400BB "mr6"

Relax. delay 2.000 sec
Pulse 16.0 degrees
Acq. time 2.858 sec
Width 5002.2 Hz
101 repetitions
OBSERVE H1, 400.2689784 MHz
DATA PROCESSING
Line broadening 0.1 Hz
FT size 32768
Total time 23 min, 23 sec



364



AME-Chlophenesin Hydroxylation

Sample Name:

Data Collected on:

smr02-vmsr600

Archive directory:

Sample directory:

File(s): CARBON

Pulse Sequence: CARBON (s2pul)

Solvent: acetone

Data collected on: Jun 6 2013

Temp. 25.0 C / 298.1 K

Operator: service

Relax. delay 2.000 sec

Pulse 30.0 degrees

Acq. time 2.000 sec

Width 37878.8 Hz

4000 repetitions

OBSERVE C13, 150.8078422 MHz

DECOUPLE H1, 599.7558477 MHz

Power 46 dB

continuously on

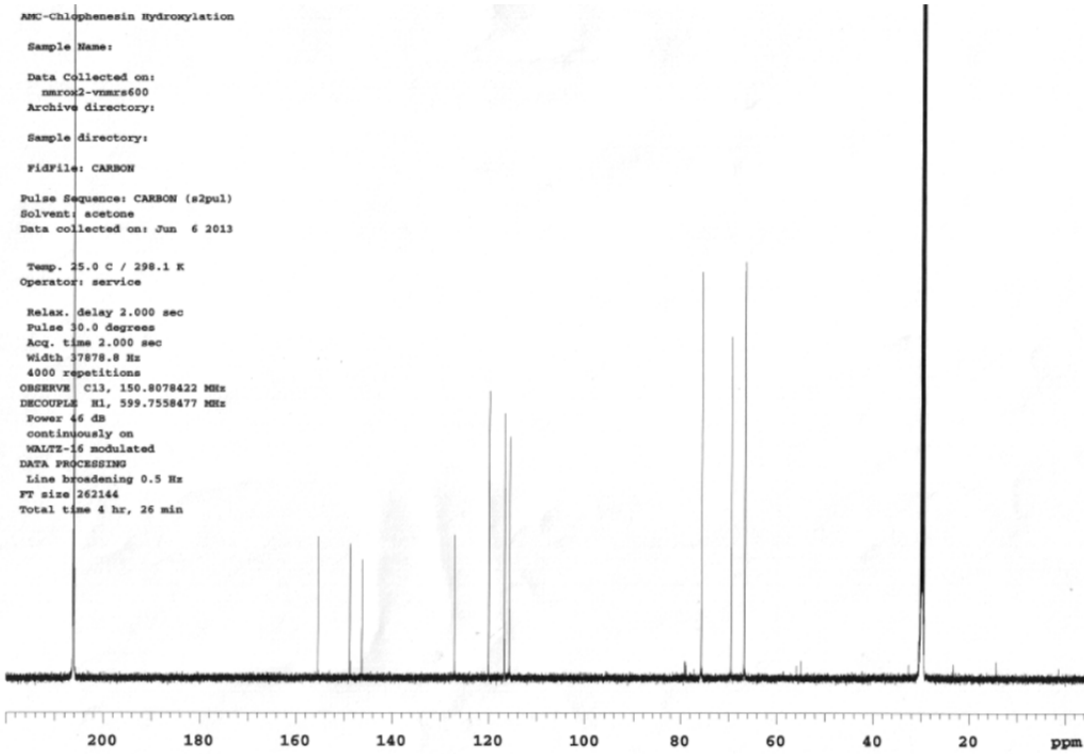
WALTZ-16 modulated

DATA PROCESSING

Line broadening 0.5 Hz

FT size 262144

Total time 4 hr, 26 min



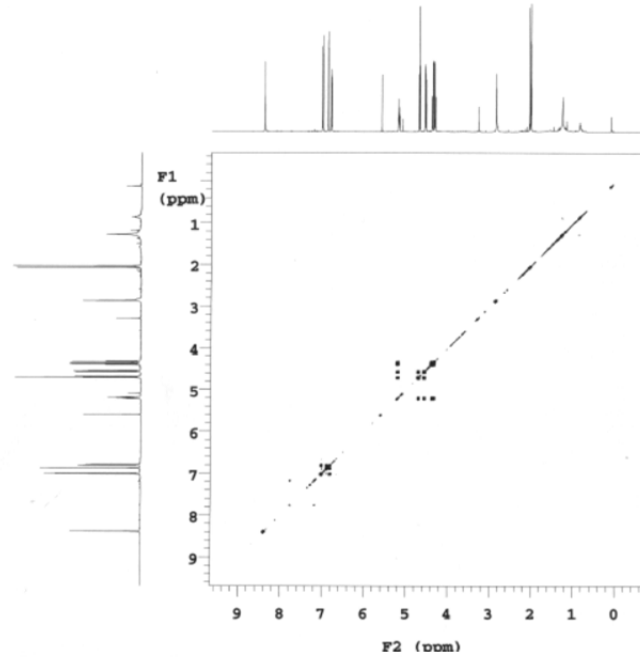
460

AMC-Chlophenesin Hydroxylation

Sample Name:
Data Collected on:
nmr02-vmr0600
Archive directory:
Sample directory:
FidFile: gCOSY
Pulse Sequence: gCOSY
Solvent: acetone
Data collected on: Jun 6 2013

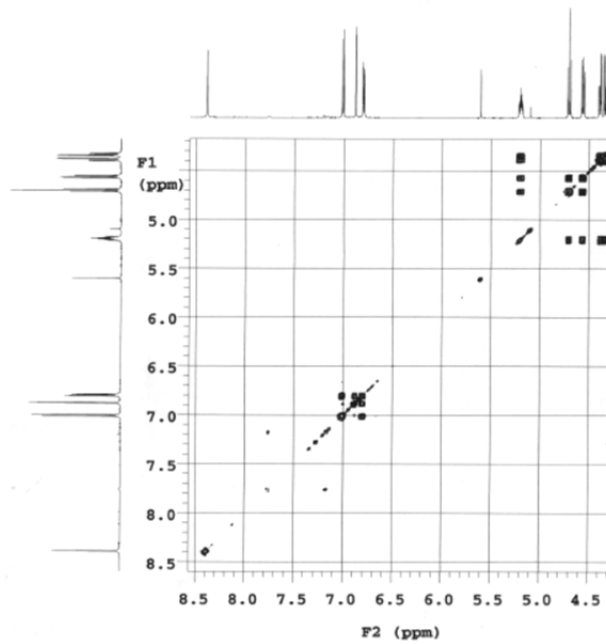
Temp. 25.0 C / 298.1 K
Operator: service

Relax. delay 2.000 sec
Acq. time 0.150 sec
Width 6218.9 Hz
2D Width 6218.9 Hz
2 repetitions
512 increments
OBSERVE F1, 599.7528489 MHz
DATA PROCESSING
Sq. sine bell 0.075 sec
F1 DATA PROCESSING
Sq. sine bell 0.082 sec
FT size 4096 x 4096
Total time 39 min



AMC-Chlophenesin Hydroxylation

Sample Name:
Data Collected on:
nmr02-vmr0600
Archive directory:
Sample directory:
FidFile: gCOSY
Pulse Sequence: gCOSY
Solvent: acetone
Data collected on: Jun 6 2013

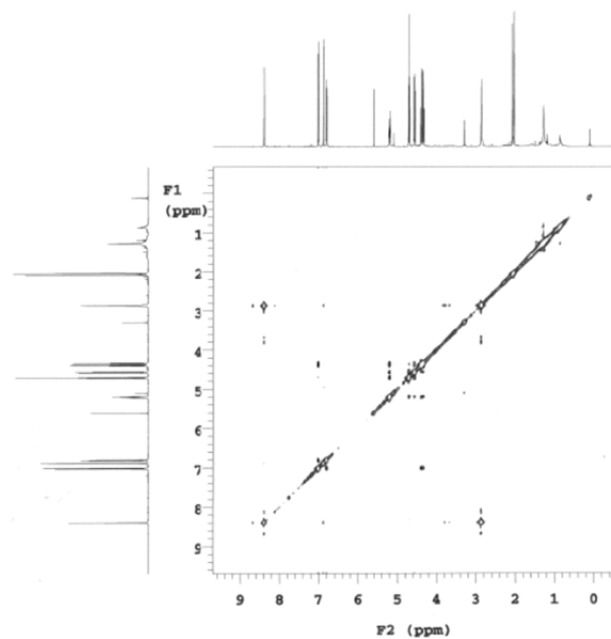


AMC-Chlophenesin Hydroxylation

Sample Name:
Data Collected on:
mmx02-vmxr600
Archive directory:
Sample directory:
Fidfile: NOESY
Pulse Sequence: NOESY
Solvent: acetone
Data collected on: Jun 6 2013

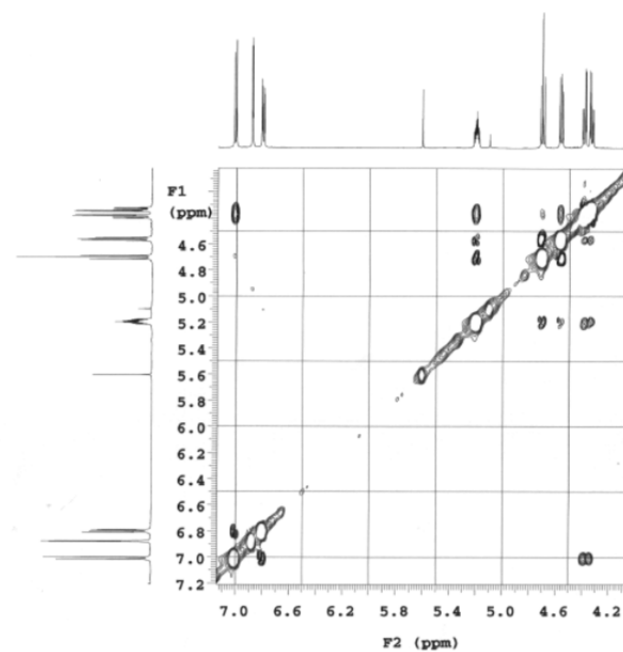
Temp. 25.0 C / 298.1 K
Operator: service

Relax. delay 2.000 sec
Acq. time 0.150 sec
Width 6218.9 Hz
3D Width 6218.9 Hz
8 repetitions
2 x 256 increments
OBSERVE H1, 599.7528489 MHz
DATA PROCESSING
Gauss apodisation 0.045 sec
F1 DATA PROCESSING
Gauss apodisation 0.018 sec
FT size 2048 x 2048
Total time 3 hr, 24 min



AMC-Chlophenesin Hydroxylation

Sample Name:
Data Collected on:
mmx02-vmxr600
Archive directory:
Sample directory:
Fidfile: NOESY
Pulse Sequence: NOESY
Solvent: acetone
Data collected on: Jun 6 2013



AMC-Chlophenesin Hydroxylation

Sample Name:

Data Collected on:
nmr02-nmrs600
Archive directory:

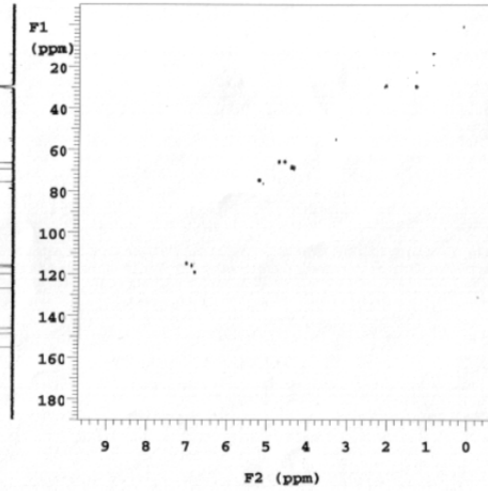
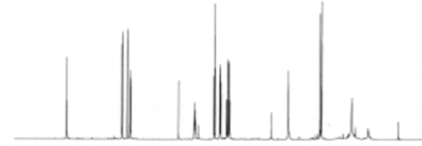
Sample directory:

Fidfile: gHSQCAD

Pulse Sequence: gHSQCAD
Solvent: acetone
Data collected on: Jun 6 2013

Temp. 25.0 C / 298.1 K
Operator: service

Relax. delay 2.000 sec
Acq. time 0.150 sec
Width 6218.9 Hz
2D Width 30165.9 Hz
4 repetitions
2 x 256 increments
OBSERVE M1, 599.7528489 MHz
DECOUPLE C13, 150.8215465 MHz
Power 37 dB
on during acquisition
off during delay
W40_DB9002 modulated
DATA PROCESSING
Gauss apodization 0.069 sec
F1 DATA PROCESSING
Resol. enhancement 0.0 Hz
Gauss apodization 0.004 sec
FT size 4096 x 2048
Total time 1 hr, 16 min



AMC-Chlophenesin Hydroxylation

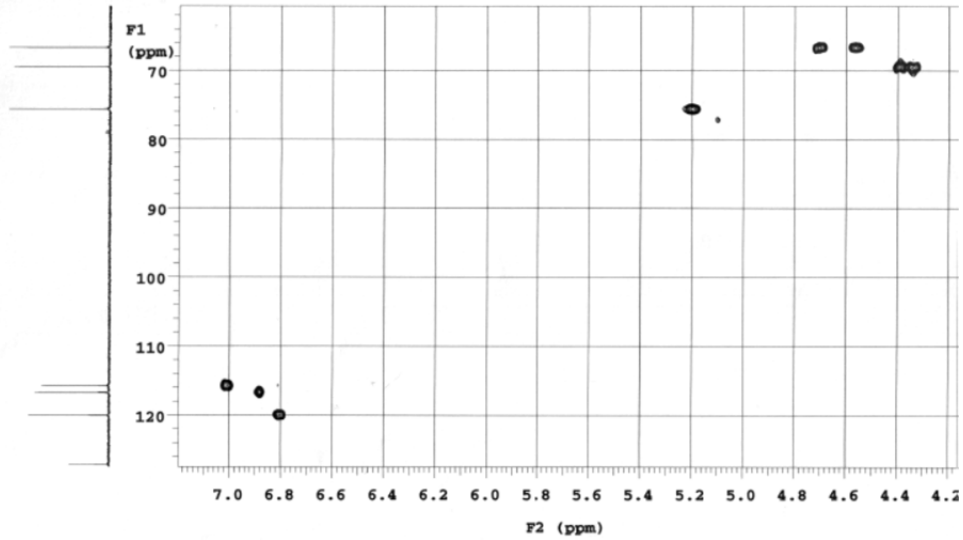
Sample Name:

Data Collected on:
nmr02-nmrs600
Archive directory:

Sample directory:

Fidfile: gHSQCAD

Pulse Sequence: gHSQCAD
Solvent: acetone
Data collected on: Jun 6 2013



AMC-Chlophenesin Hydroxylation

Sample Name:

Data Collected on:
marco2-vmars600
Archive directory:

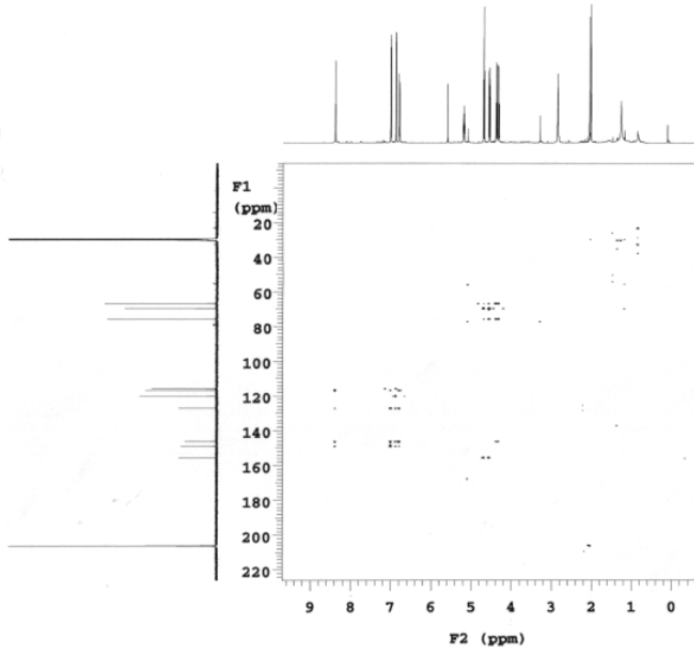
Sample directory:

FidFile: gHMCAD

Pulse Sequence: gHMCAD
Solvent: acetone
Data collected on: Jun 6 2013

Temp. 25.0 C / 298.1 K
Operator: service

Relax. delay 2.000 sec
Acq. time 0.150 sec
Width 6218.9 Hz
2D Width 36199.1 Hz
8 repetitions
2 x 512 increments
OBSERVE H1, 599.7528469 MHz
DATA PROCESSING
Sq. sine bell 0.075 sec
F1 DATA PROCESSING
Gauss apodization 0.013 sec
FT size 4096 x 4096
Total time 5 hr, 6 min



AMC-Chlophenesin Hydroxylation

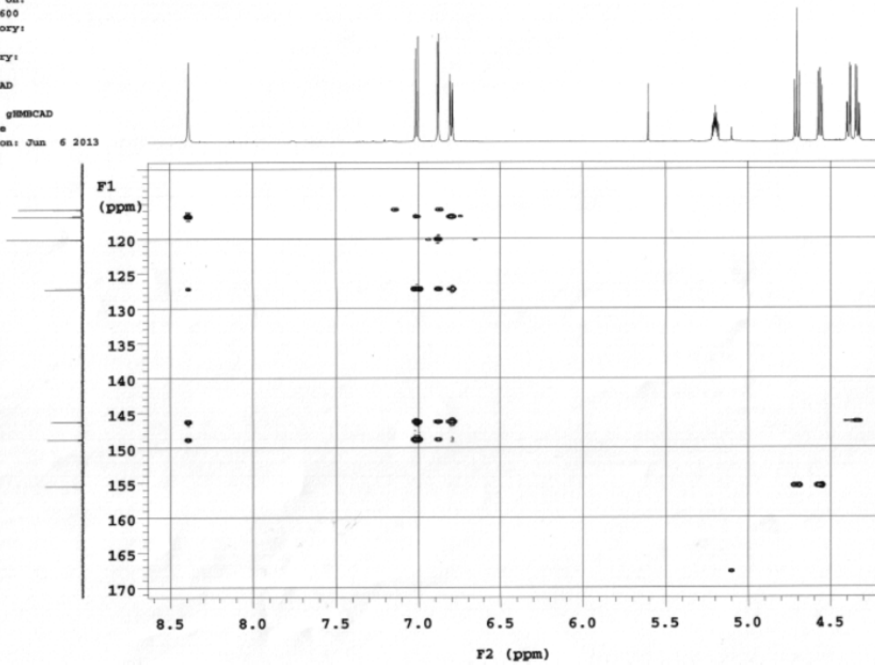
Sample Name:

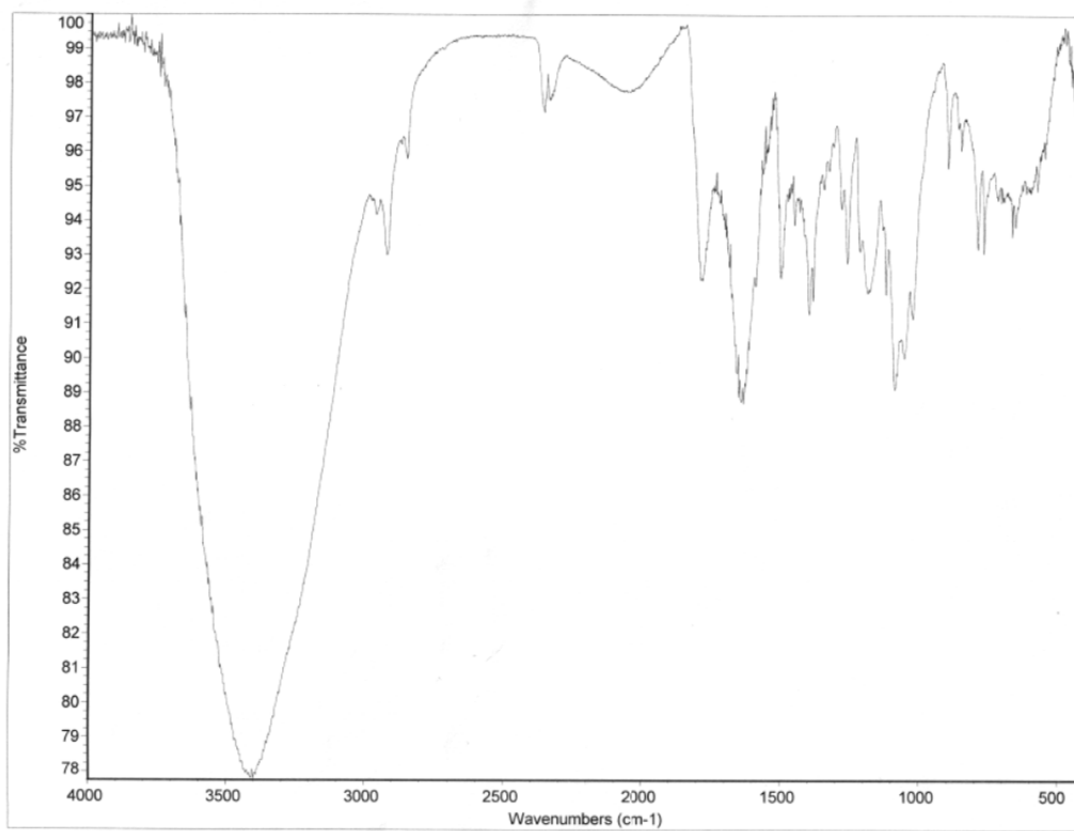
Data Collected on:
marco2-vmars600
Archive directory:

Sample directory:

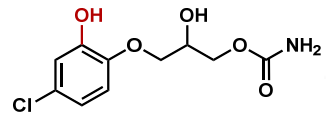
FidFile: gHMCAD

Pulse Sequence: gHMCAD
Solvent: acetone
Data collected on: Jun 6 2013

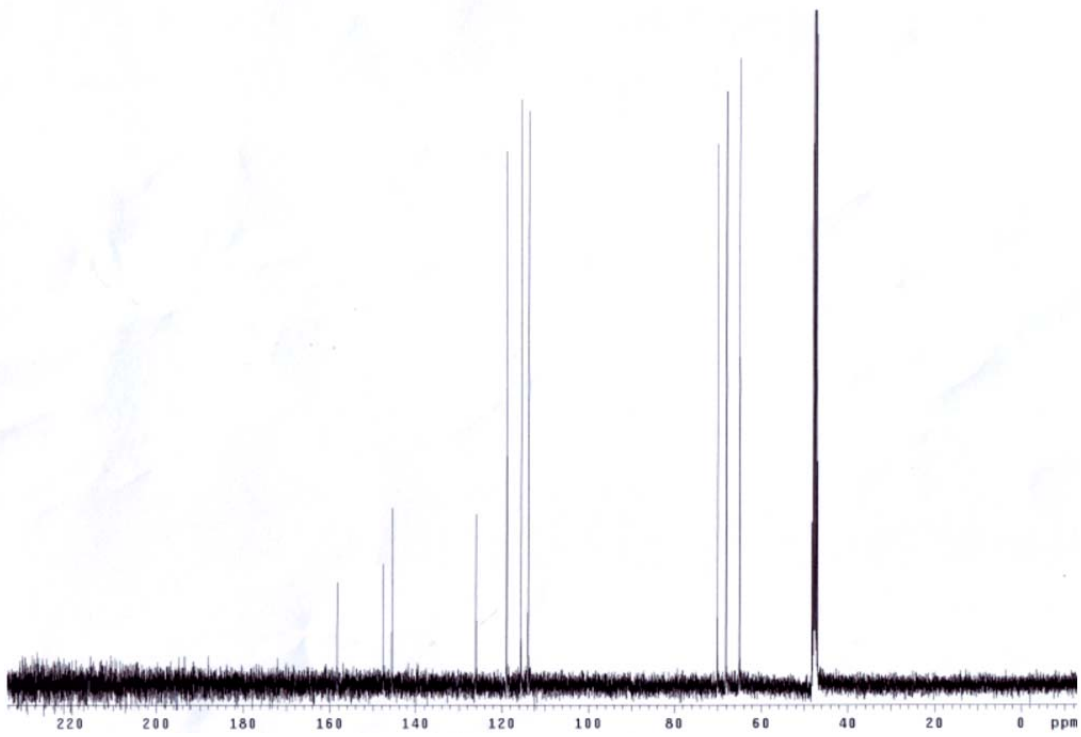
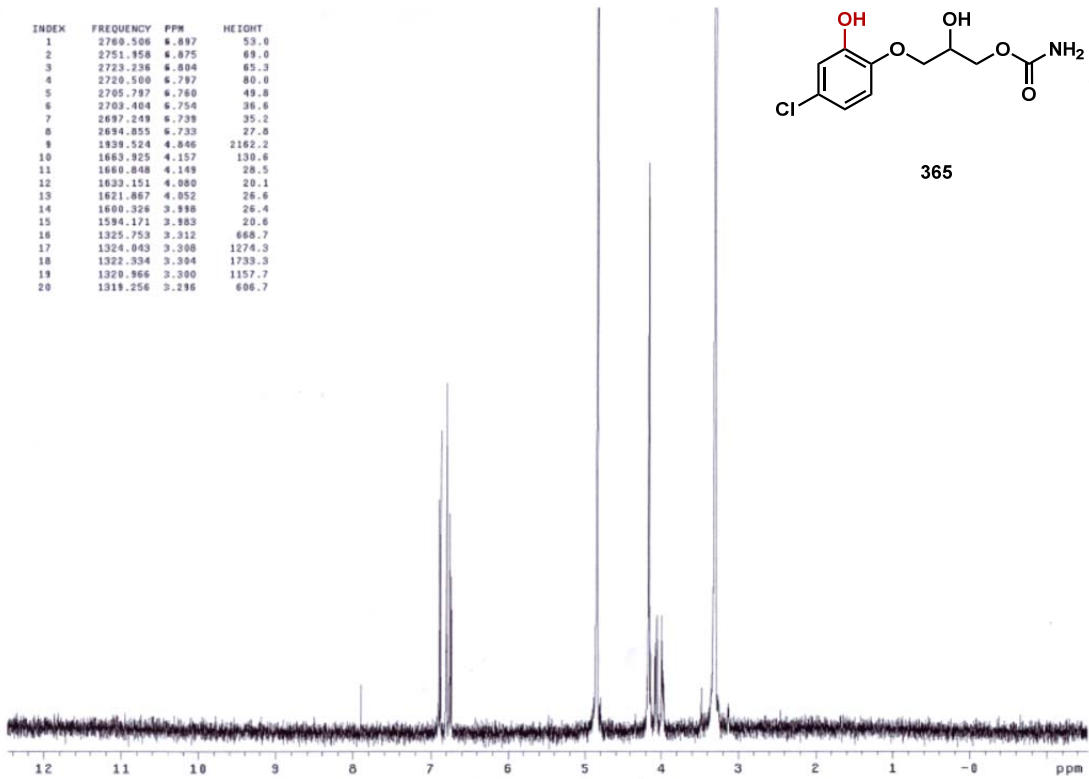


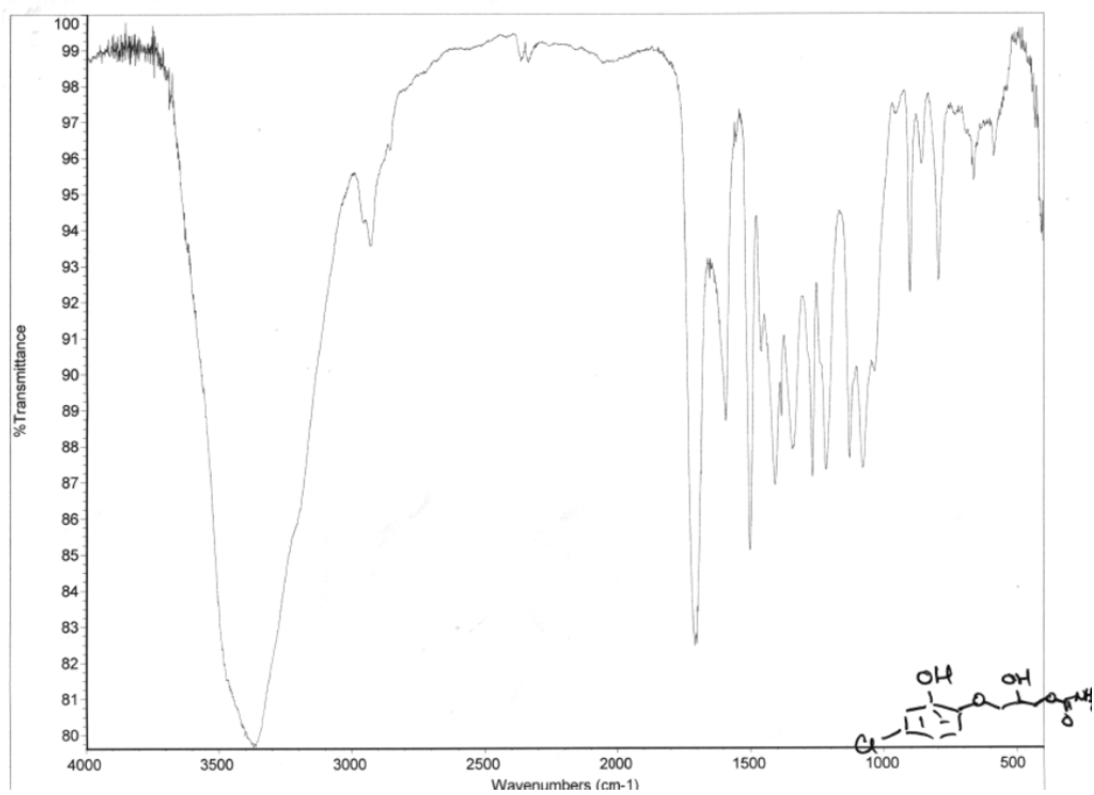


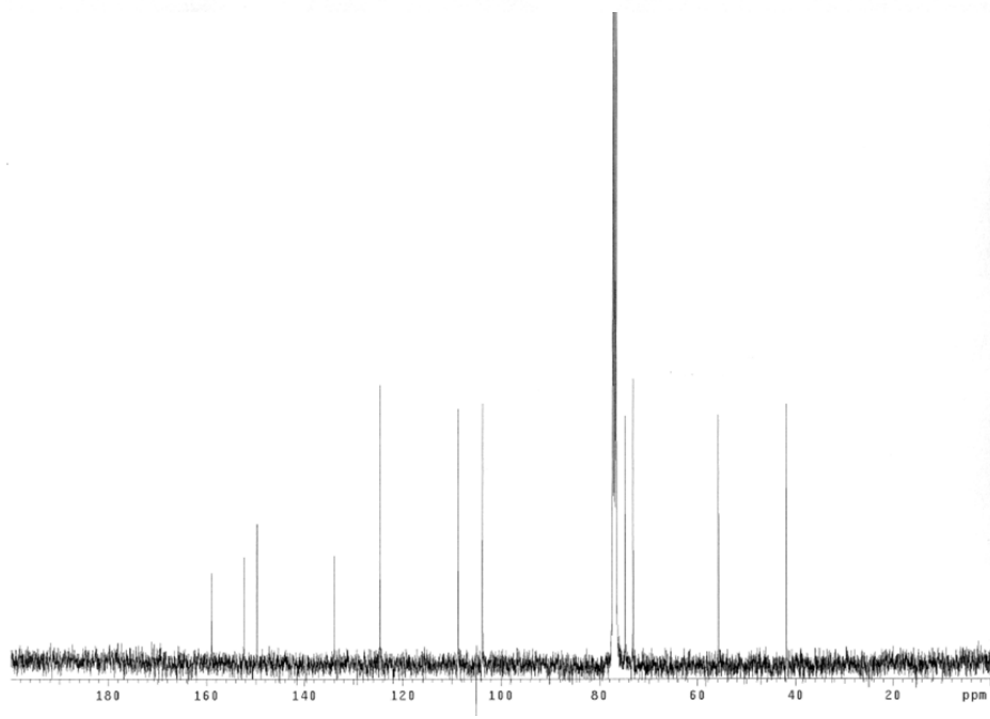
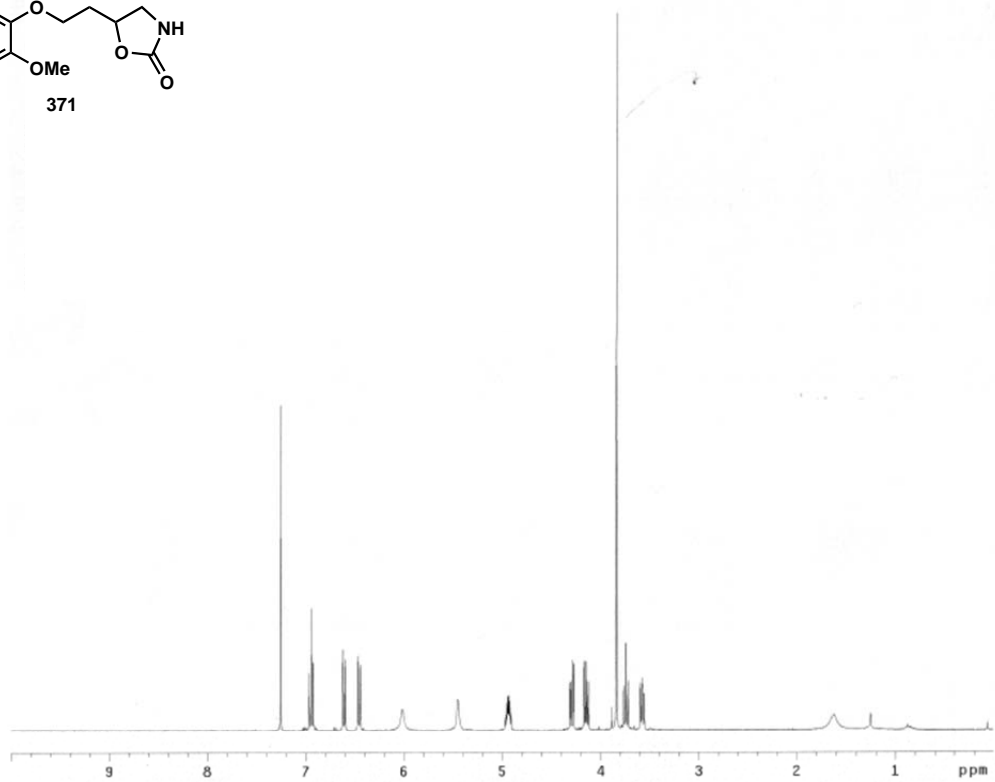
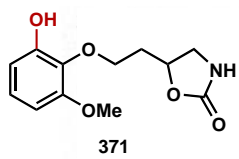
INDEX	FREQUENCY	PPM	HEIGHT
1	2769.506	4.897	53.0
2	2751.958	4.875	49.0
3	2723.236	4.804	65.3
4	2720.500	4.797	80.0
5	2705.787	4.760	49.8
6	2703.404	4.754	36.6
7	2697.249	4.739	35.2
8	2694.855	4.733	27.8
9	1839.524	4.846	2162.2
10	1663.925	4.157	130.6
11	1660.848	4.149	29.5
12	1633.151	4.080	20.1
13	1621.867	4.052	26.6
14	1600.326	3.998	26.4
15	1594.171	3.983	20.6
16	1325.753	3.312	666.7
17	1324.043	3.308	1274.3
18	1322.334	3.304	1733.3
19	1320.966	3.300	1157.7
20	1319.256	3.296	606.7

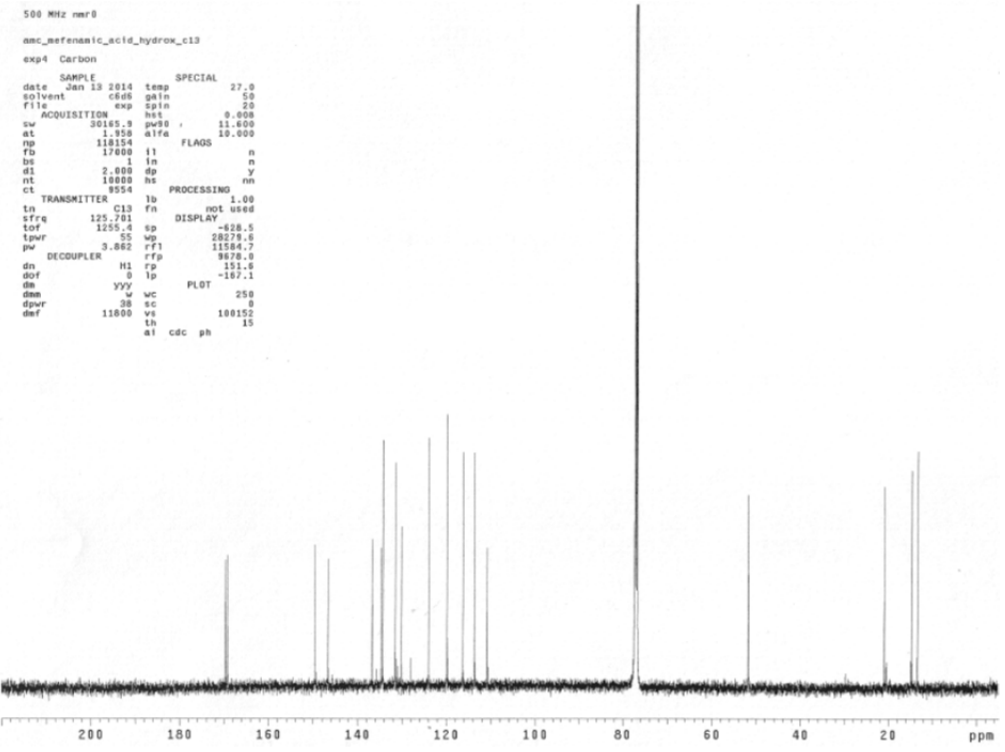
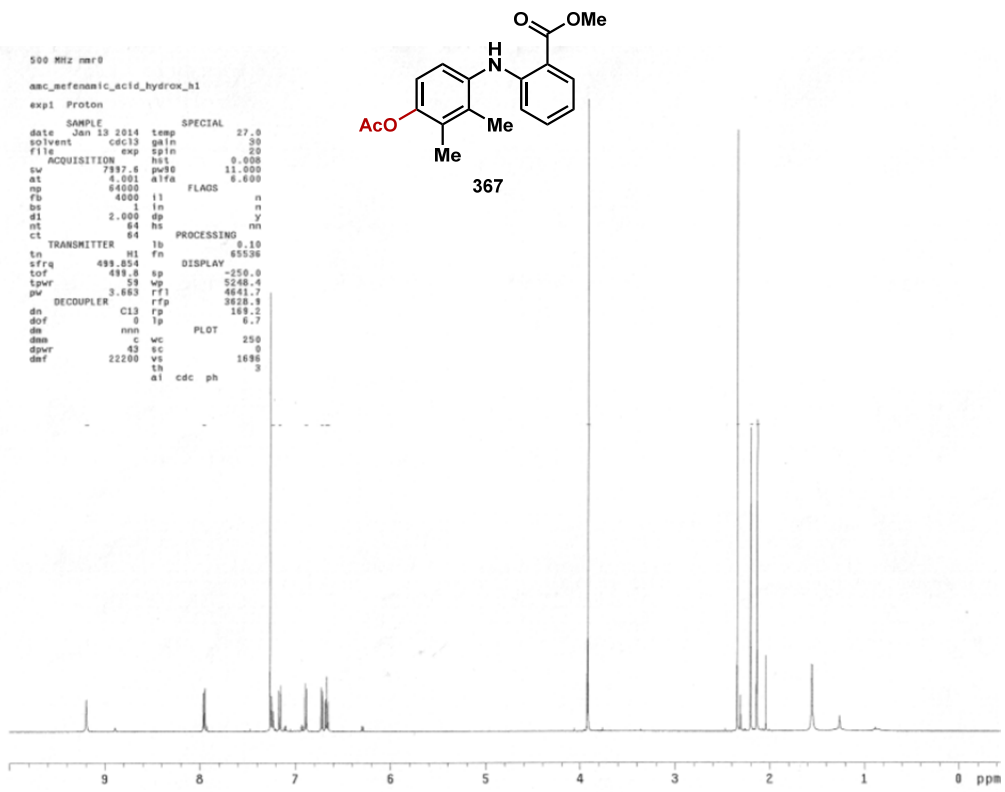


365





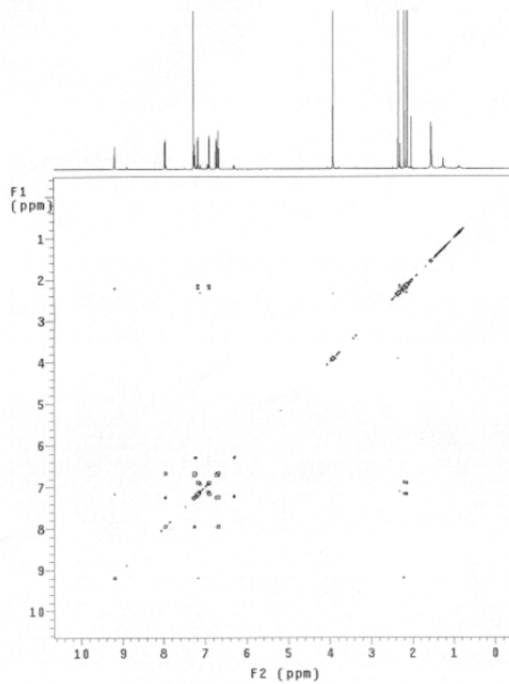




anc_mefenamic_acid_hydrox_gcasy

exp3 Gcasy

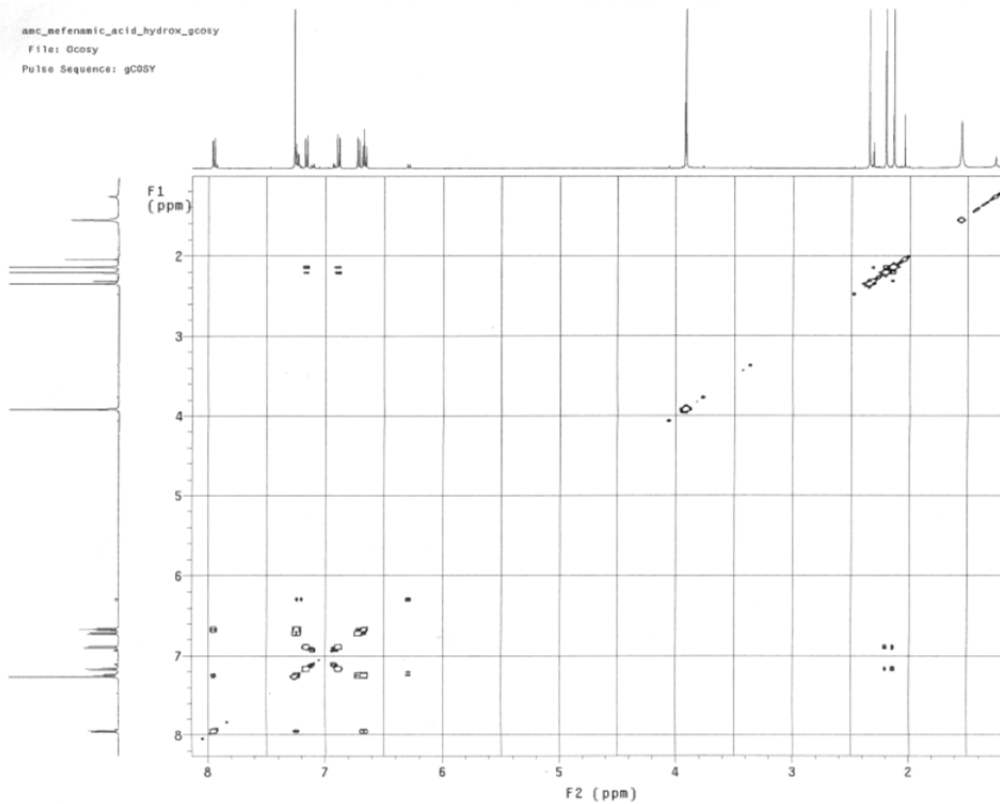
```
date Jan 13 2014 hs          FLAGS          nn
solvent cdcl3          sspol          n
sample          hglv          4694
ACQUISITION          SPECIAL          4694
sv          5555.9          temp          27.0
at          0.184          gain          30
fp          2080          spin          0
fd          3000          F2          PROCESSING          0
ss          8          sb          -0.092
d1          2.000          sbc          not used
nt          2          fn          4696
3D ACQUISITION          F1          PROCESSING          0
sw1          5555.9          sb1          -0.092
nl          512          sbf1          not used
PRESATURATION          pfocl          1p
satmode          nnn          fn1          4696
satdly          0          DISPLAY          1p
satfrq          499.8          sp          -231.1
satpwr          -13          wp          5553.2
TRANSMITTER          sp1          -231.1
tn          H1          wp1          5553.2
effq          498.854          rft          3682.7
tof          57.7          rfp          3628.9
tpwr          50          rft1          3682.8
pw          11.000          rfp1          3628.9
tpwr_cf          1.000          PLOT          116.0
GRADIENTS          wc          18.0
g2lv11          4694          sc          18.0
gt1          0.001800          wc2          116.0
g4tab          0.000500          sc2          0
DECOUPLER          vs          072
dn          C13          1h
dm          nnn          a1          cdc          av          2
```



anc_mefenamic_acid_hydrox_gcasy

File: Gcasy

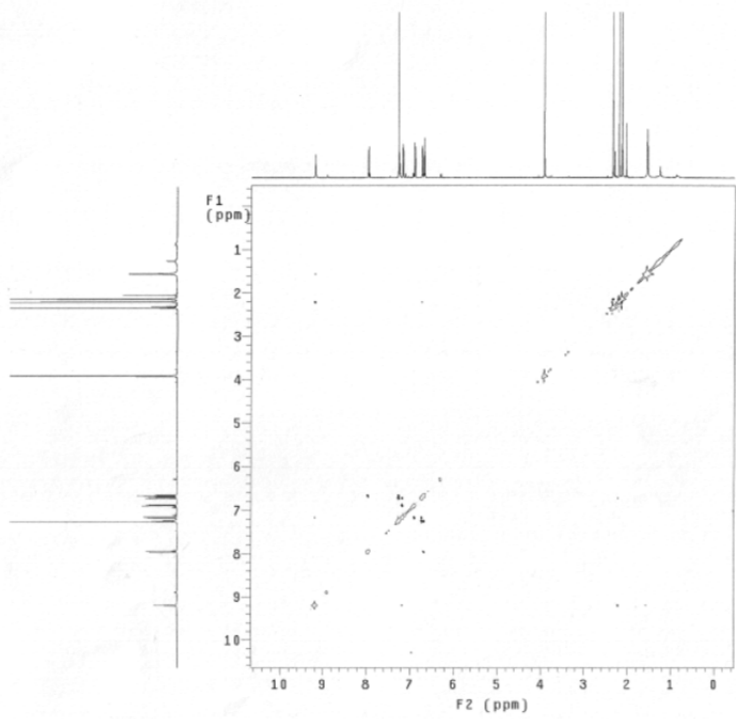
Pulse Sequence: gCOSY



amc_nefenamic_acid_hydrox_noesy

exp8 Noesy

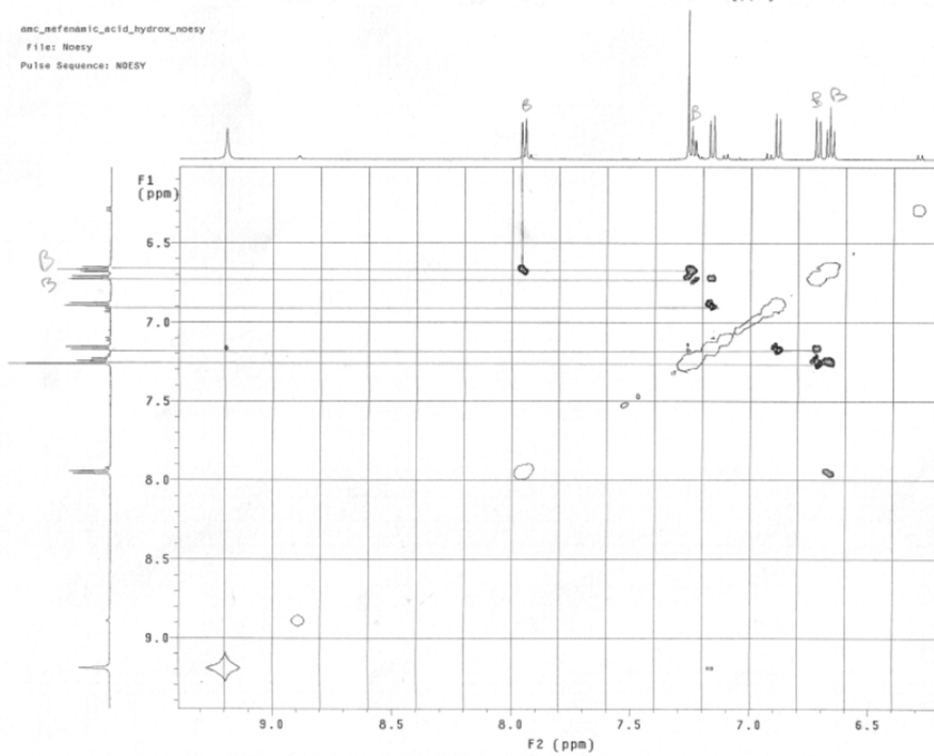
SAMPLE		FLAGS	
date	Jan 13 2014	hs	n
solvent	cdcl3	esp1	y
sample		PFO1g	y
ACQUISITION			
sv	5555.9	hsglv1	4894
at	0.184	temp	27.0
np	2048	gain	30
rb	3000	spin	0
ss	32	f2 PROCESSING	0
dt	2.000	gf	0.085
nt	16	gfs	not used
2D ACQUISITION			
sv1	5555.9	f1 PROCESSING	
nt	256	gf1	0.042
tr	TRANSMITTER	gf1	not used
ln	H1	proc1	1p
effc	499.854	fml	2048
tof	57.7	DISPLAY	
tpvr	59	sp	-228.2
pw	11.000	wp	5550.5
nk	NOESY	sp1	-228.9
mix	0.880	wp1	5550.5
PRESATURATION			
satmode	nm	rfl	4594.1
satpw	-13	rf1	4828.5
satgty	0	rfp1	4594.1
satfrq	499.8	PLOT	
DECOUPLER			
dn	C13	sc	10.0
dm	nm	uc2	116.0
		sc2	0
		vs	33390
		tn	2
		al	cdc ph



amc_nefenamic_acid_hydrox_noesy

File: Noesy

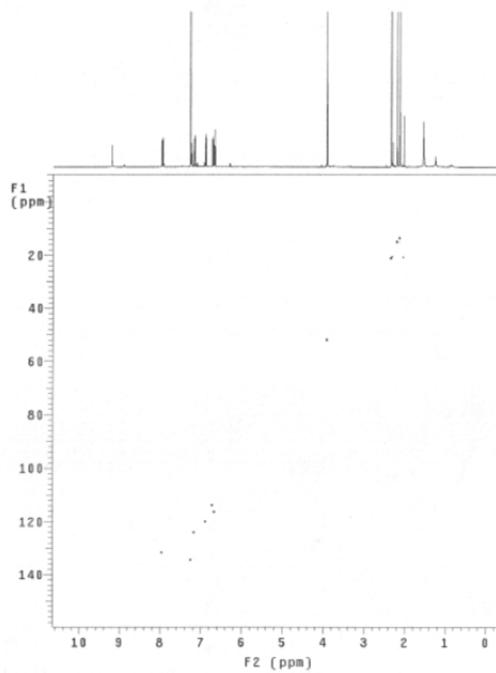
Pulse Sequence: NOESY



amc_mefenamic_acid_hydrox_ghsseq

exp6 Ghseq

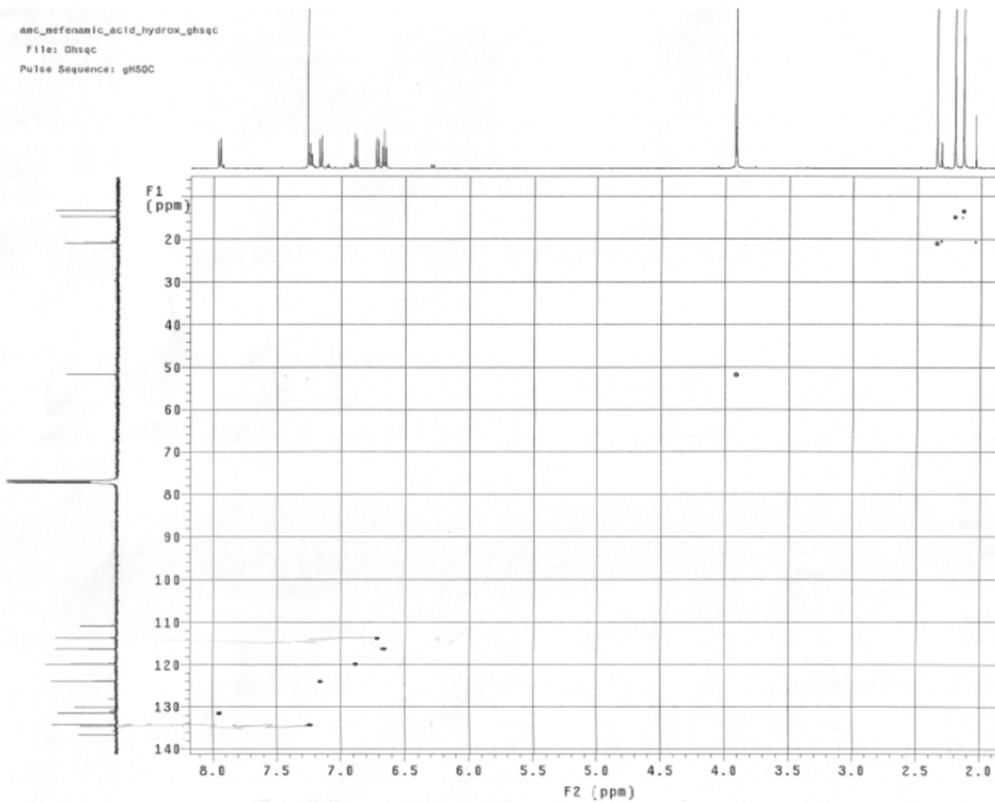
SAMPLE		FLAGS	ACQUISITION ASSAYS	
date	Jan 13 2014	hs	n array	phase
solvent	cdc13	sgpu1	y arrayelm	512
sample		PGDTg		
ACQUISITION	hsglv1	4694	1	phase
sv	5555.4	SPECIAL	27.0	2
at	0.199	temp	30	
rg	2214	gain	0	
fs	3000	spin		
ss	52	GRADIENTS	4694	
dl	2.800	g2lv1	0.002000	
nt	4	g11	2347	
2D ACQUISITION	g2lv13	0.001000		
sv1	21367.5	g13	0.001000	
nt	258	g1tab	0.000500	
phase	arrayelm	F2 PROCESSING		
PRESATURATION	gf	0.092		
satmode	nm	gfa	not used	
satdly	499.8	fn	4096	
satfrq	0	fn		
satpwr	-13	gr1	0.011	
tn	TRANSMITTER	HI	not used	
tor	57.7	groc1	16	
zfrq	499.854	fn1	2048	
tpvr	59	sp	DISPLAY	2048
pw	11.000	wp	-232.3	
DECOUPLER	C13	wp1	-1262.7	
dn	-2515.2	rf1	21346.7	
dm	nyy	rfg	2186.9	
def	22208	rf11	1853.9	
dpvr	43	rfg1	7780.5	
pwkvl	55		6495.9	
pwk	10.500	wc	PLOT	116.0
13h	HSQC	sc	10.0	
multfg	148.0	wc2	116.0	
mult	y	sc2	0	
	z	va	872	
	th		2	
	al	cdc	ph	2



amc_mefenamic_acid_hydrox_ghsseq

File: Ghseq

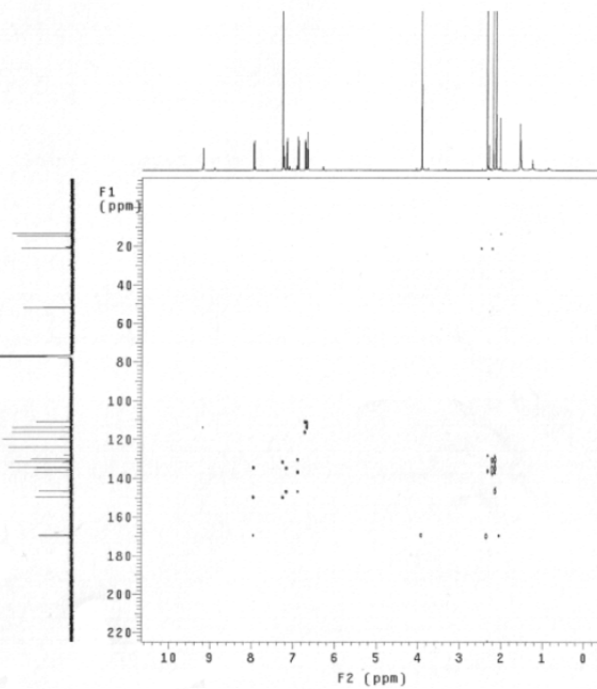
Pulse Sequence: gHSQC



anc_mefenamic_acid_hydrox_gmhc

exp7 Gmhc

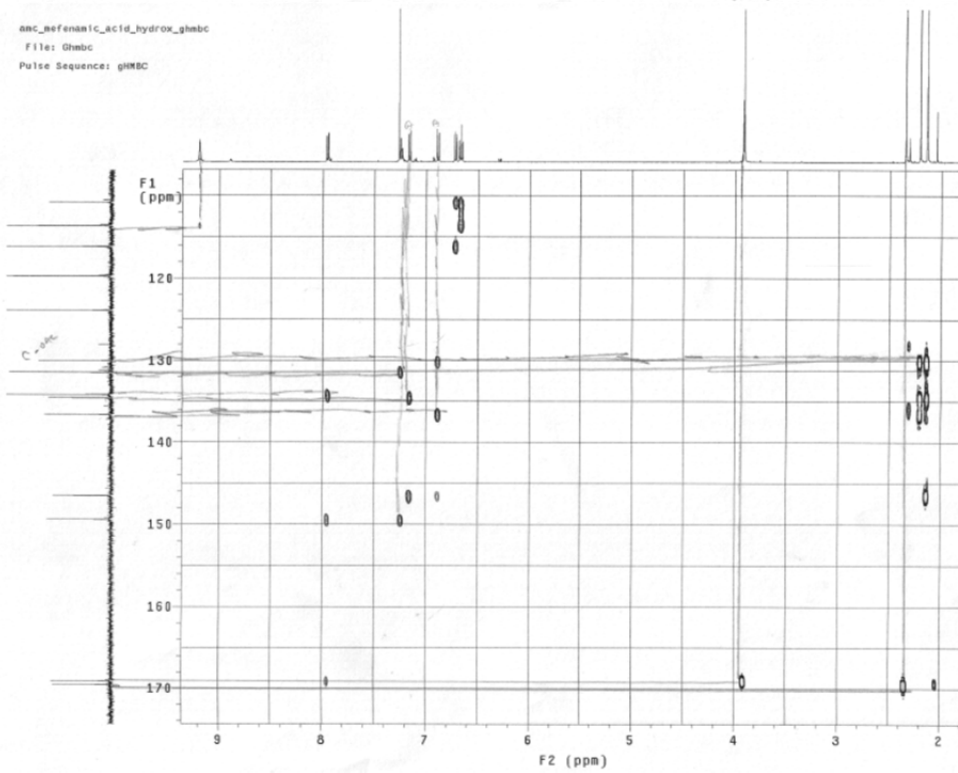
```
SAMPLE          FLAGS
date Jan 13 2014 hs          n
solvent cdc13 sspul         n
sample PEGrlg              y
ACQUISITION     hsglv1     4894
sv              5555.8     SPECIAL
at              9.128     temp 27.0
rg              1422     gain 30
fb              3000     sfn 0
ss              32     GRADIENTS
dl              2.000     g2lv11 4894
nt              18     gt1 0.001000
2D ACQUISITION  g2lv13     2247
sv1             30165.9     gt3 0.001000
nl              256     g1ab 0.000500
phase          0     F2 PROCESSING
PRESATURATION  sb          0.064
satmode       mm          sb          not used
satdly        0     fn          4098
satfrq        499.8     F1 PROCESSING
satpwr        -13     sp1          0.008
TRANSMITTER    h1          sb          not used
tn            43     g1oc1         16
sfrq          499.854     fn1         2048
tof           57.7     DISPLAY
tpr          11.000     sp          -232.3
pw           11.000     wp          5553.2
DECOUPLER      C13     wp1          -1084.5
dn            1255.4     rf1          30136.5
dof           000     rf2          2188.9
dm            22200     rf11         1353.9
dpr          43     rf21         20895.0
pwxlv1        35     PLOT
pwx           10.500     wc          116.0
HNBC          140.0     wc2         116.0
j1xh          8.0     sc2          0
j1xh          8.0     vs          328
ln            a1     cdc av          2
```

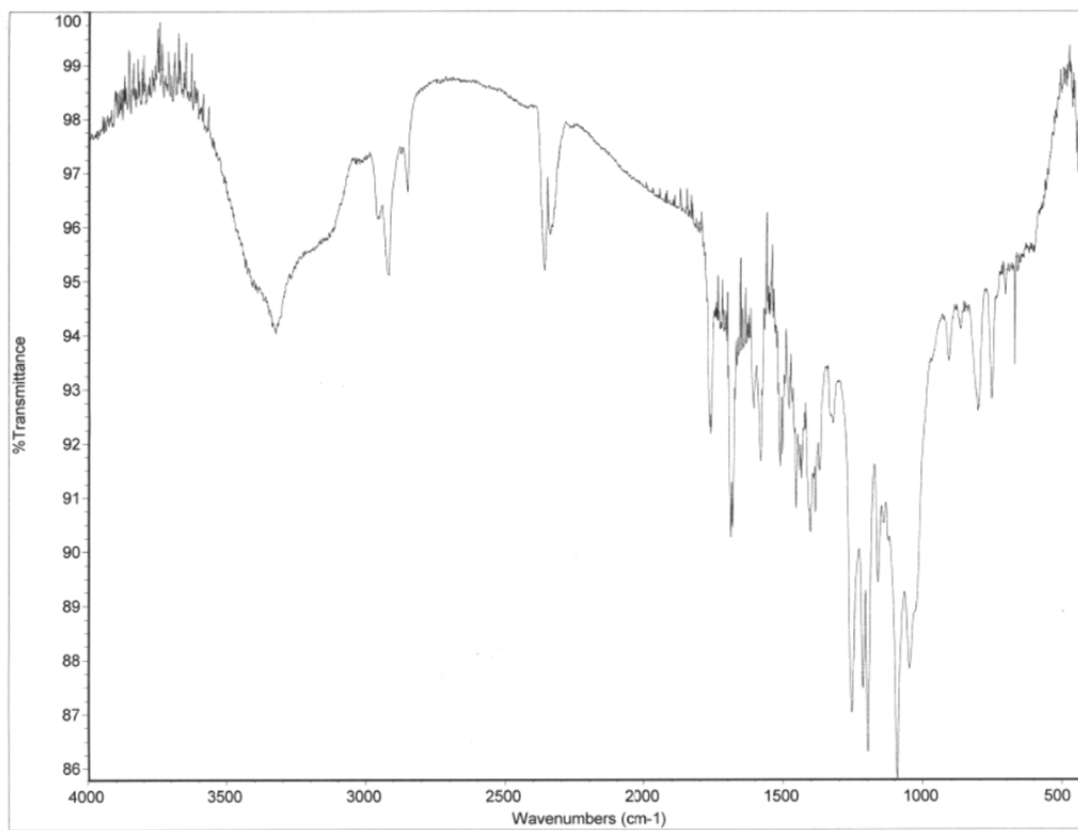


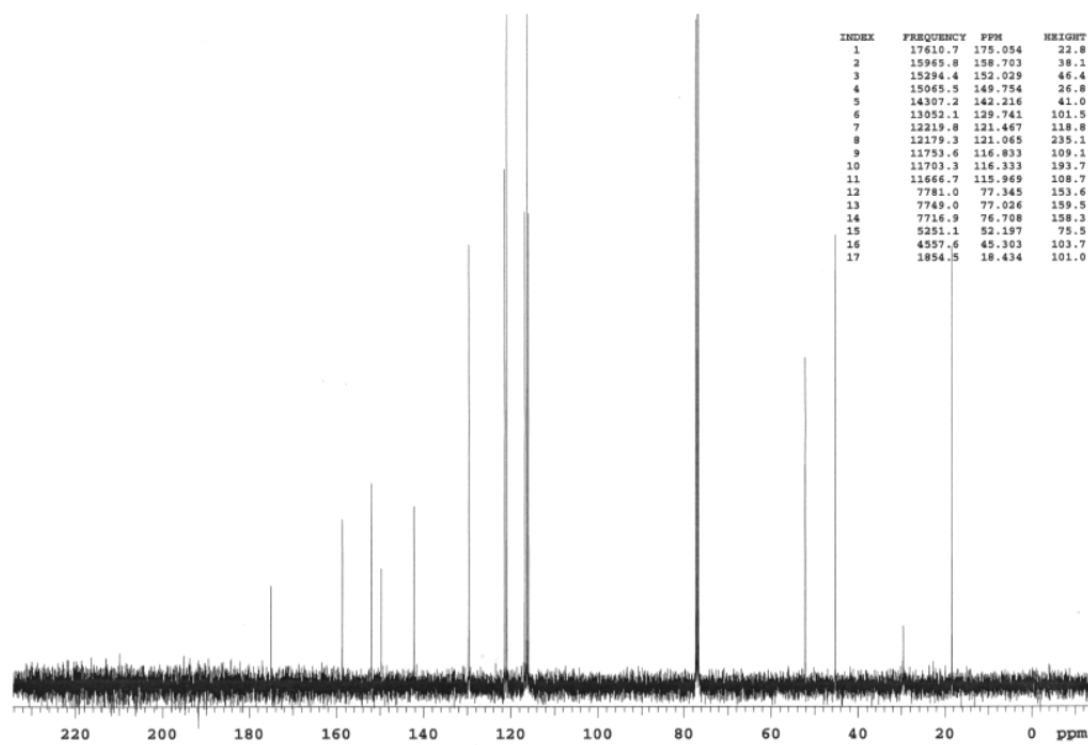
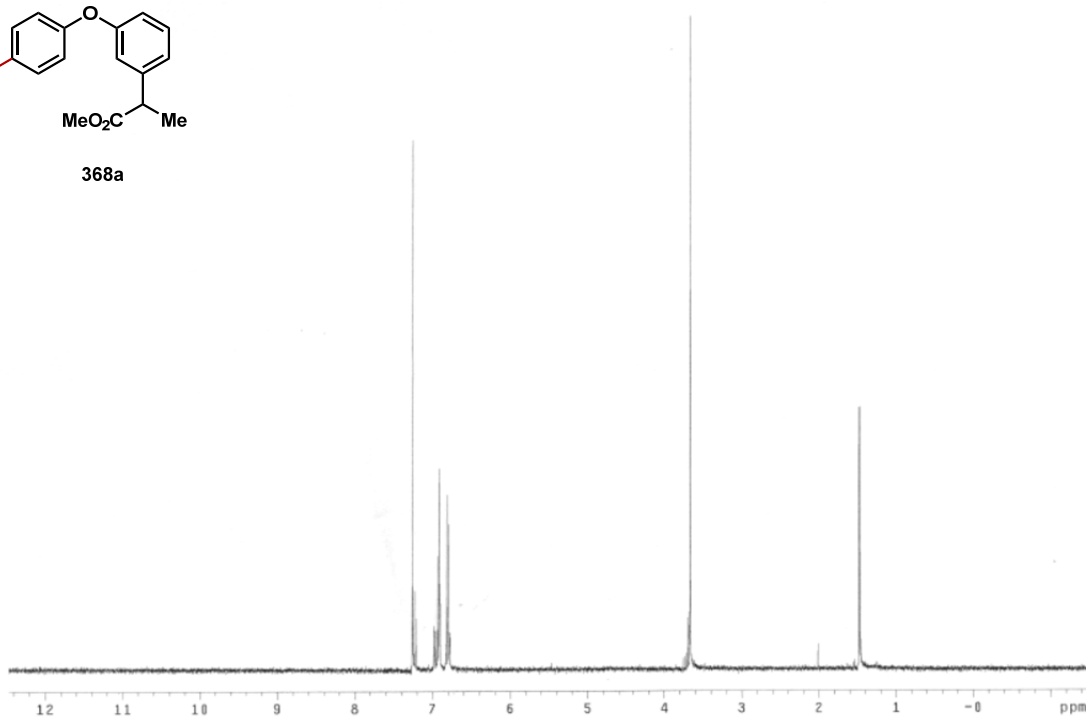
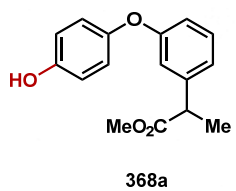
anc_mefenamic_acid_hydrox_gmhc

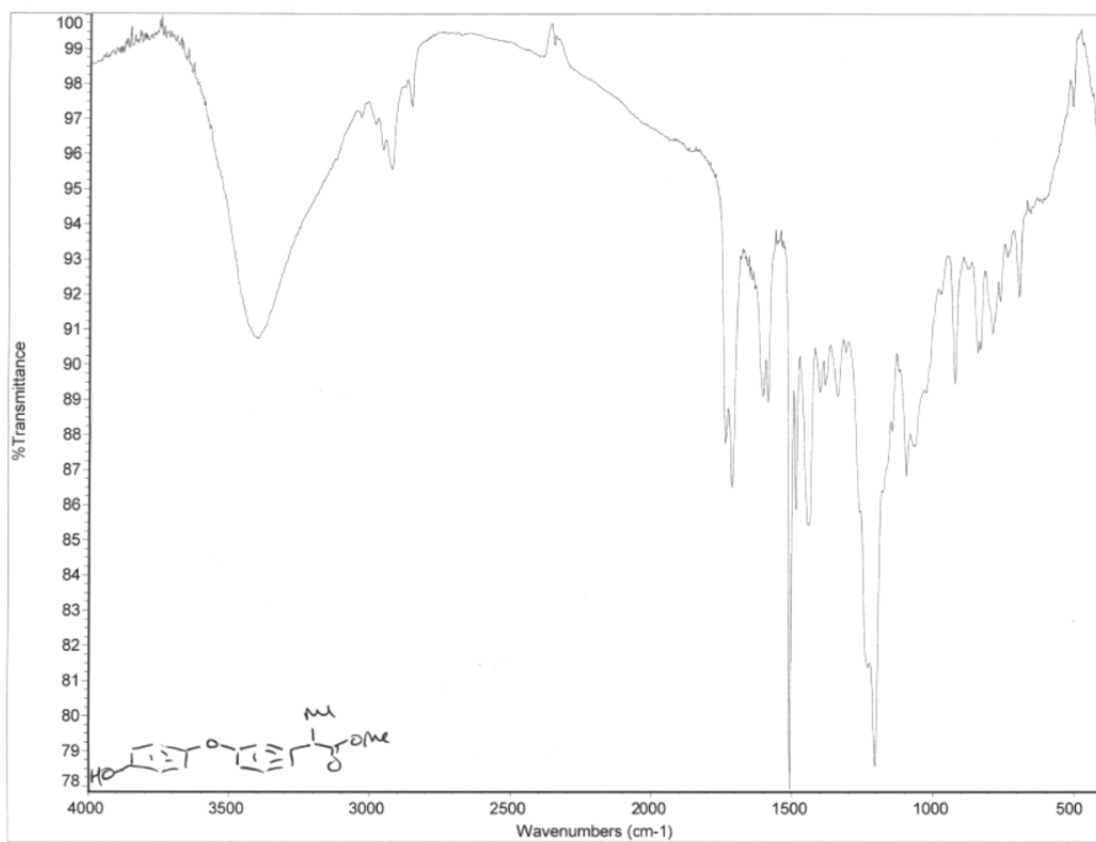
File: Gmhc

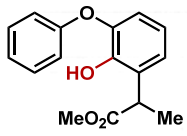
Pulse Sequence: gHNBC



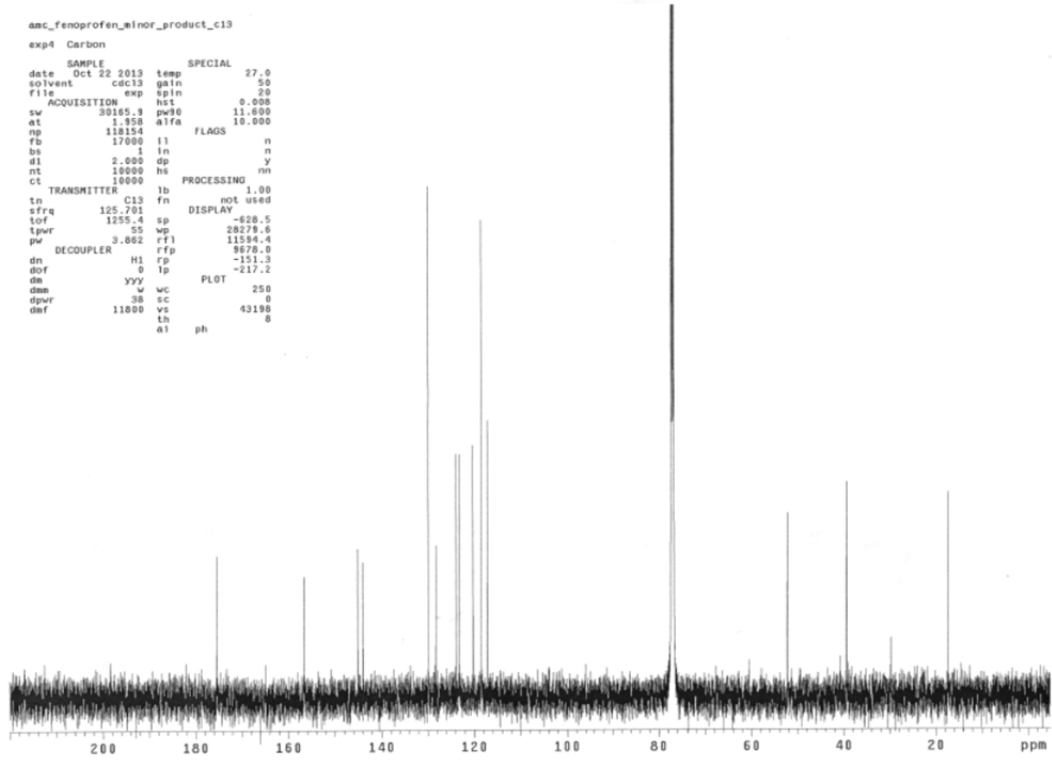
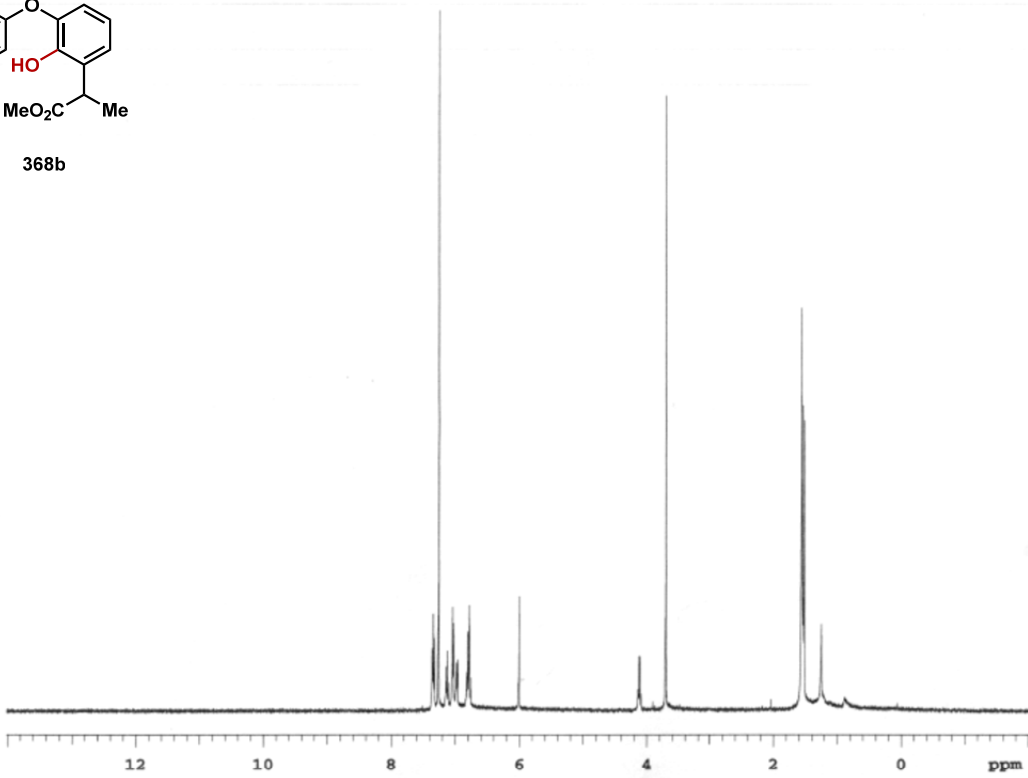








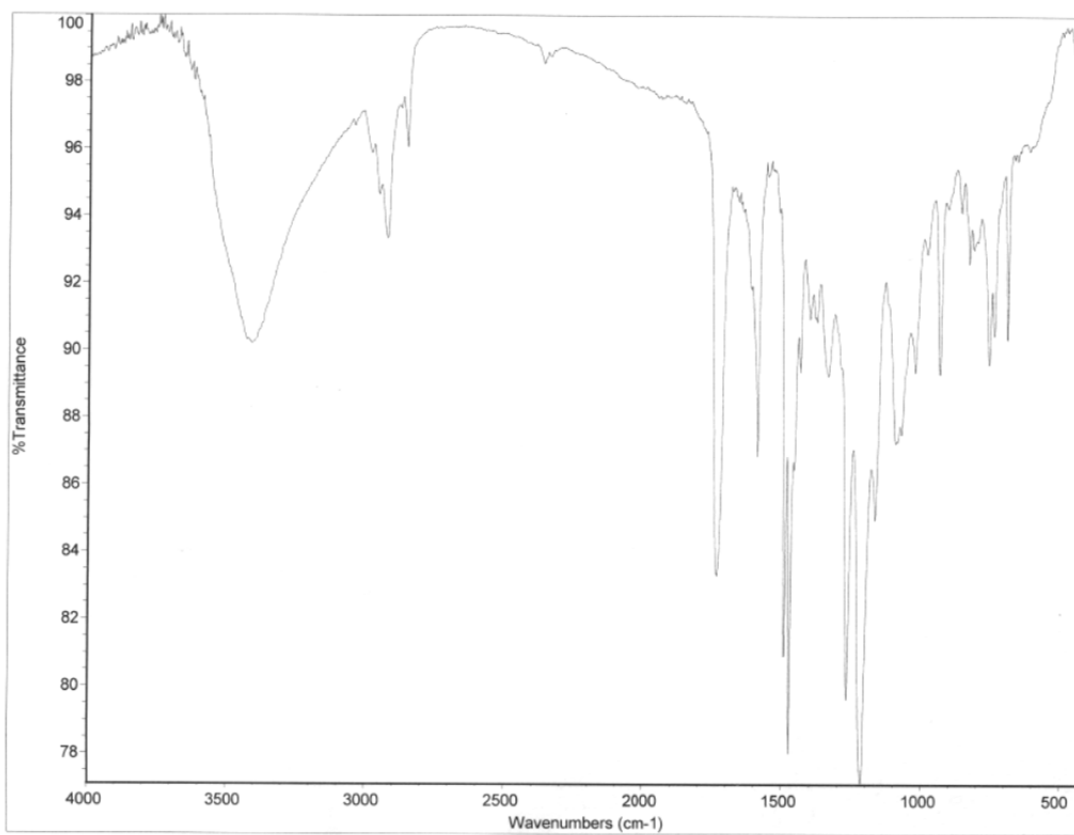
368b

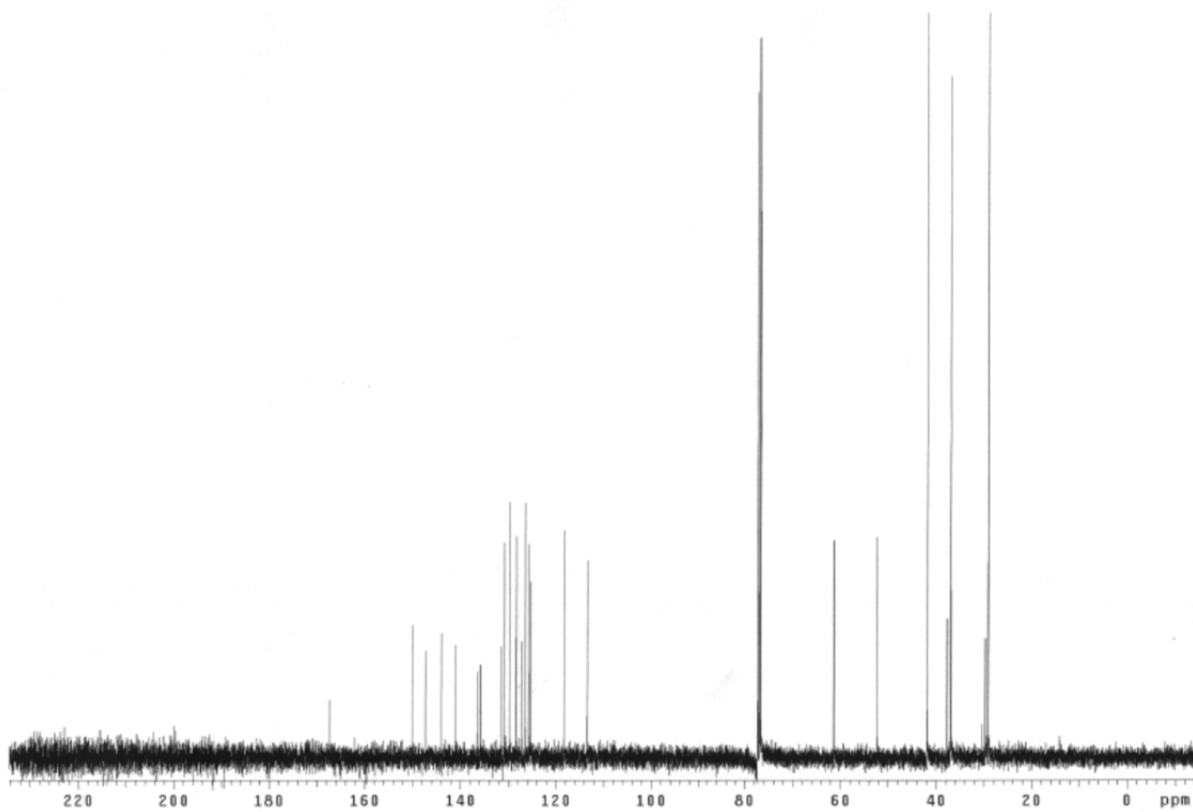
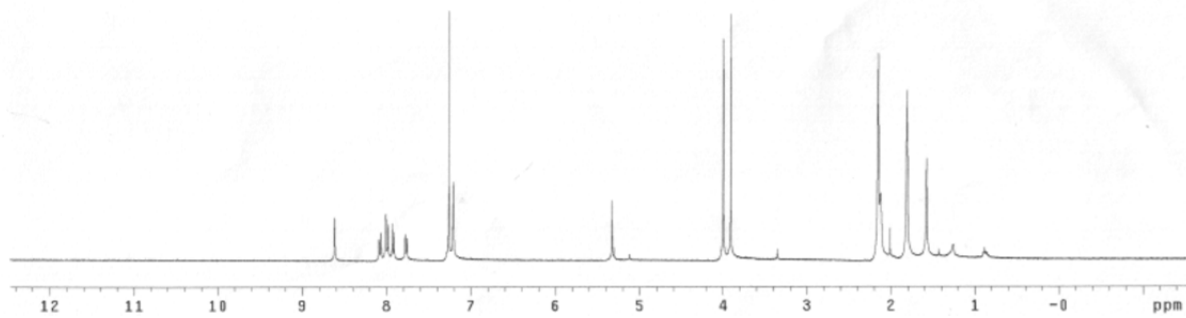
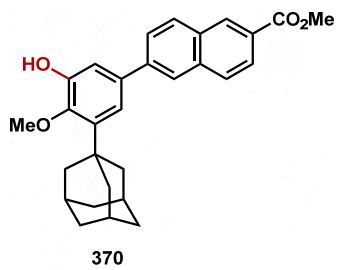


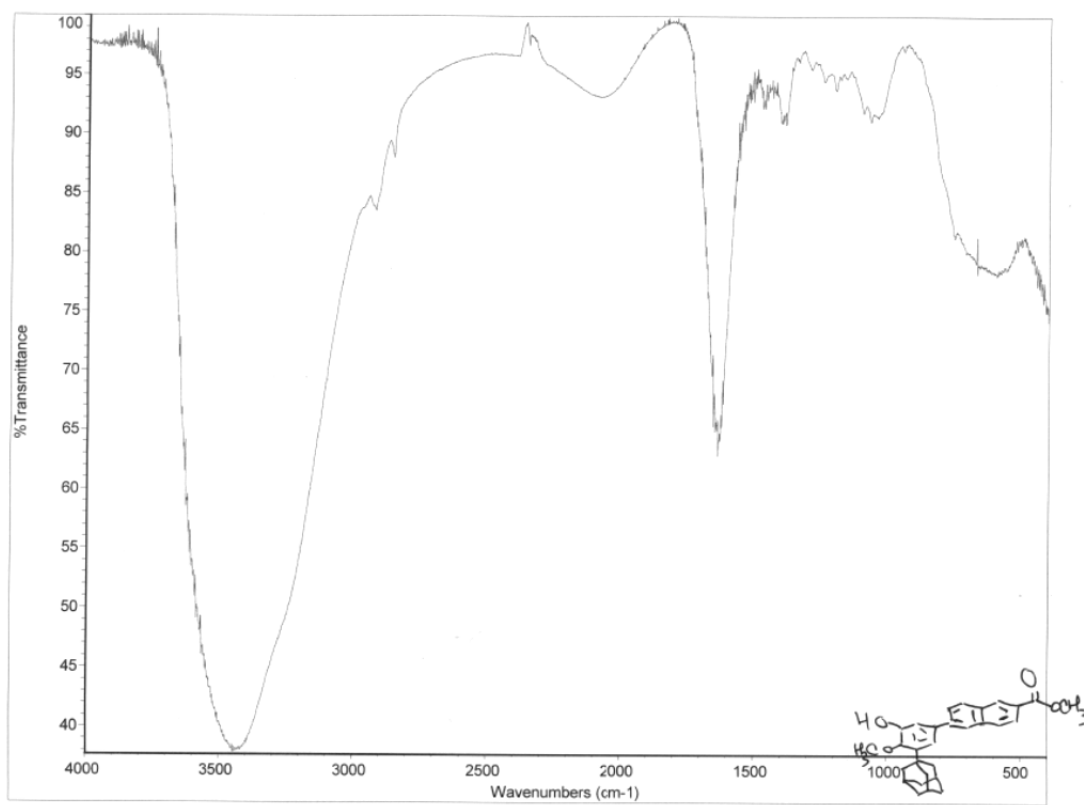
anc_fenoprofen_minor_product_c13

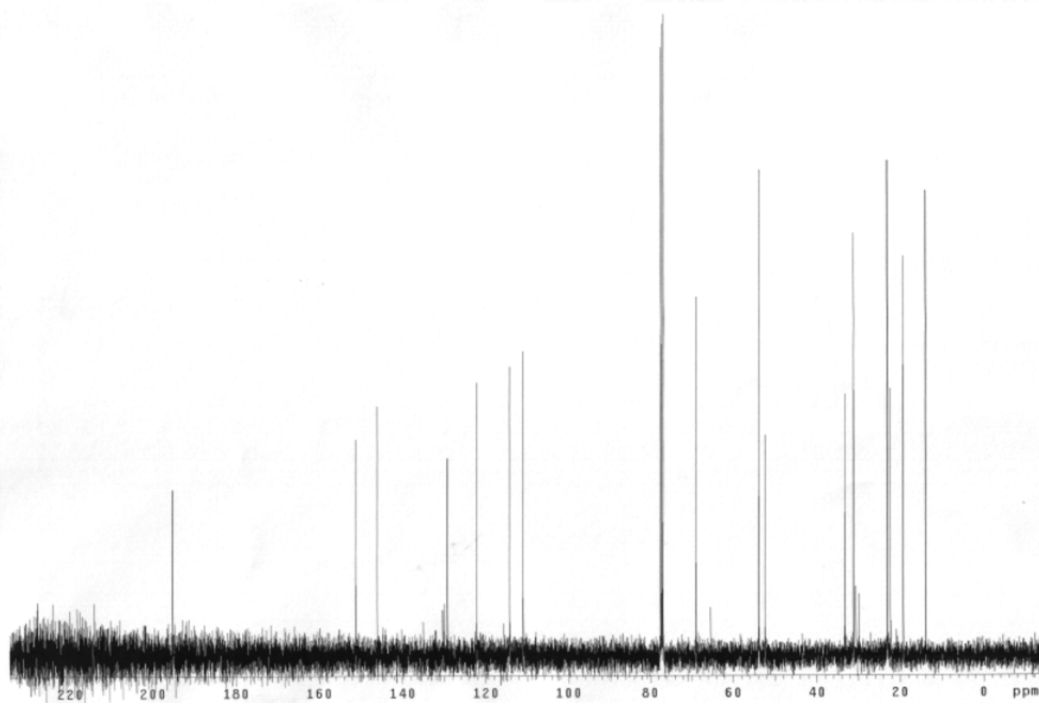
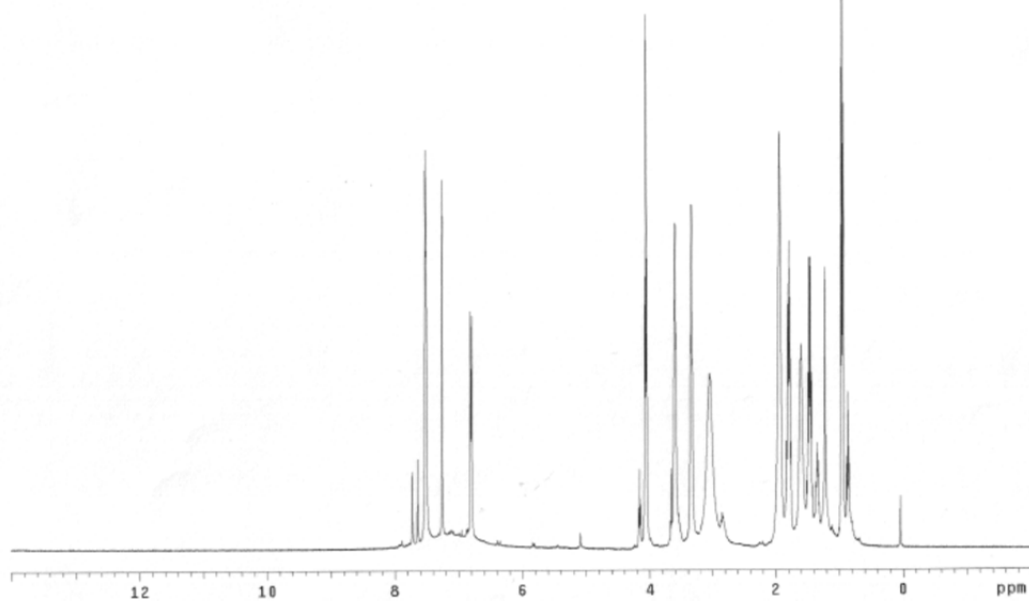
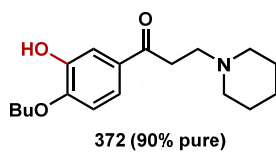
exp4 Carbon

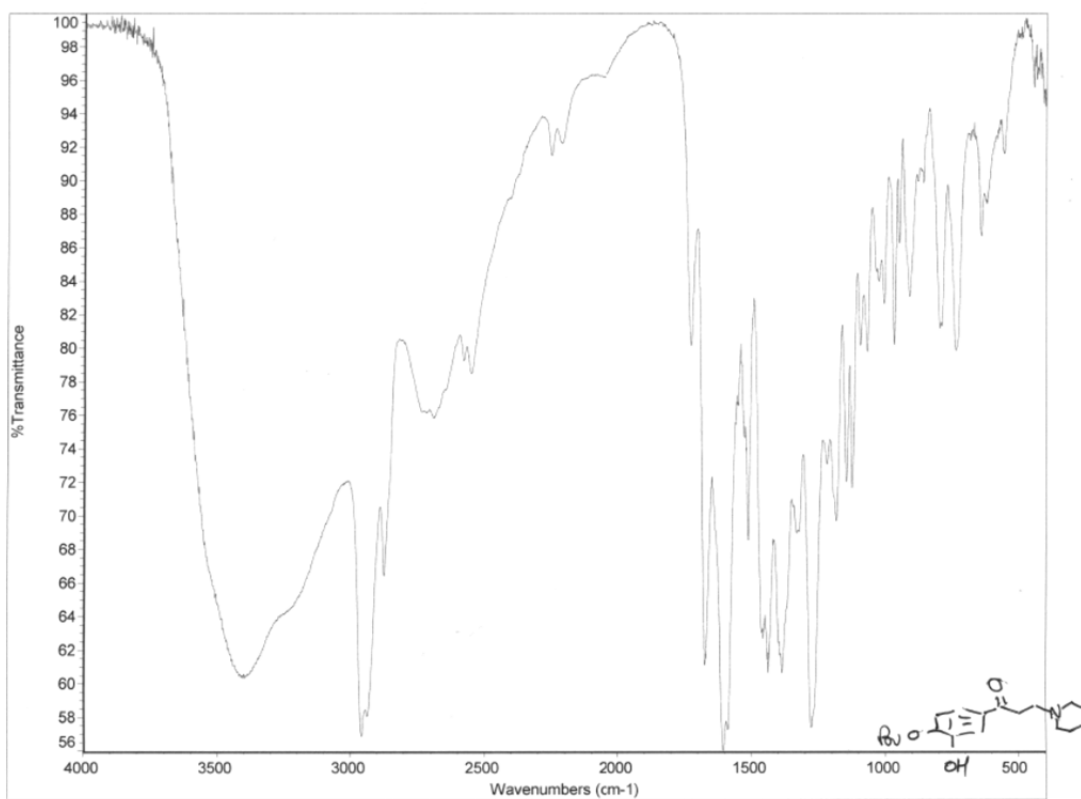
SAMPLE		SPECIAL	
date	Oct 22 2013	temp	27.0
solvent	cdcl3	gain	50
file	exp	spin	20
ACQUISITION		ST	
sw	30155.9	pw0	11.000
at	1.958	alfa	10.000
rg	118154	FLAGS	
fb	17000	l1	n
bs	1	ln	n
d1	2.000	dp	y
nt	10000	hs	nm
ct	10000	PROCESSING	
tn	C13	fb	not used
sfrq	125.701	sp	DISPLAY
tor	1255.4	wp	-628.5
tpwr	55	rfl	28278.6
pw	3.062	rfl	11594.4
DECOUPLER		rfl	9678.0
dn	H1	rp	-151.3
gof	0	lp	-217.2
da	yyy	wc	PLOT
dsm	w	sc	250
dpwr	38	vs	0
daf	11800	ts	43198
	at	ph	8



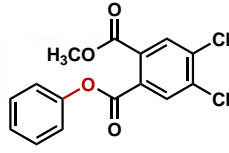




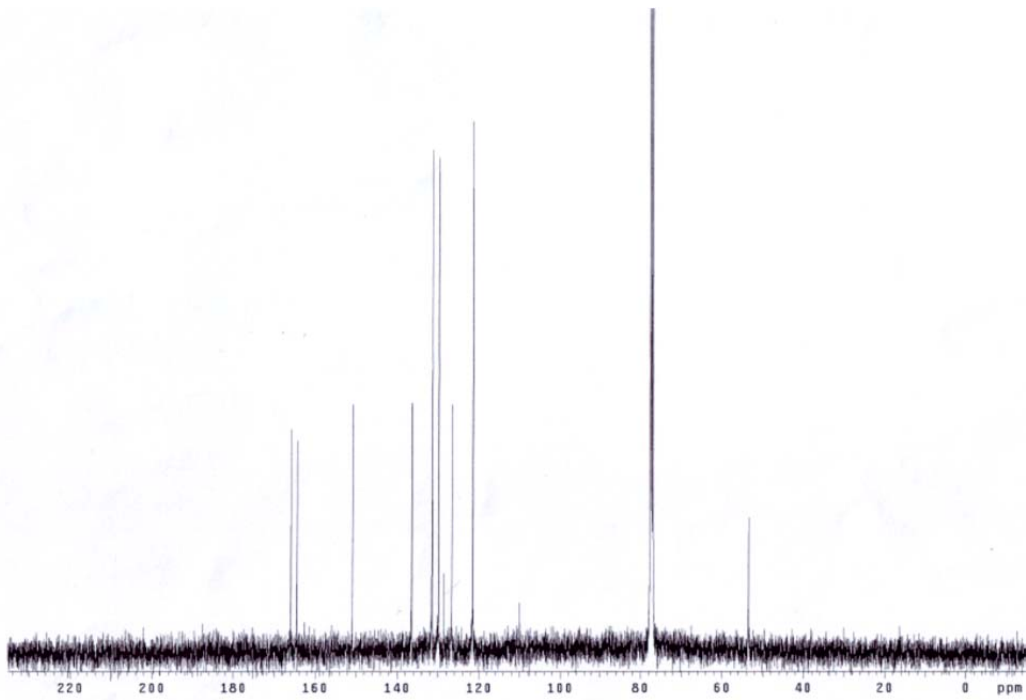
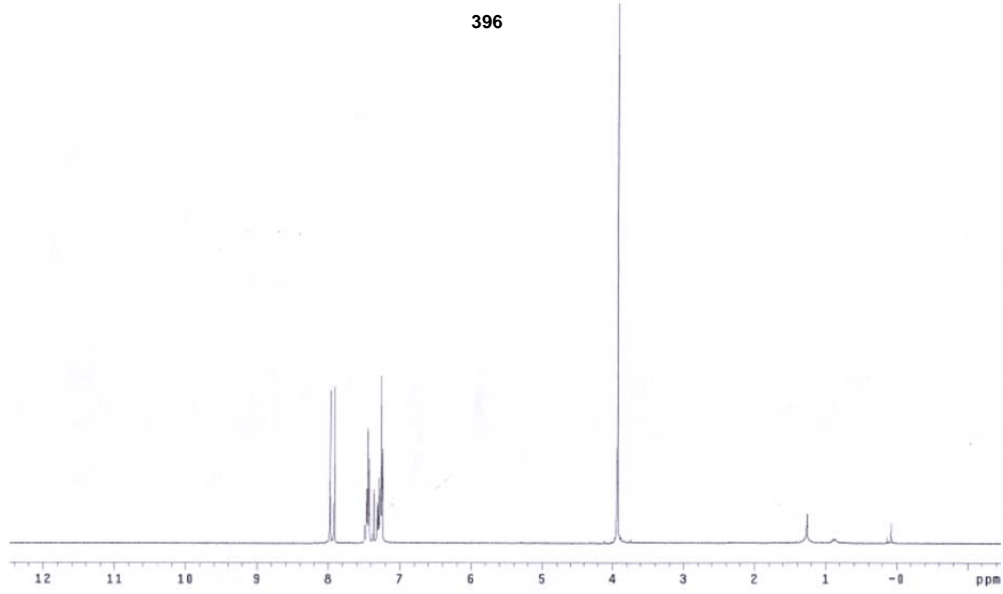


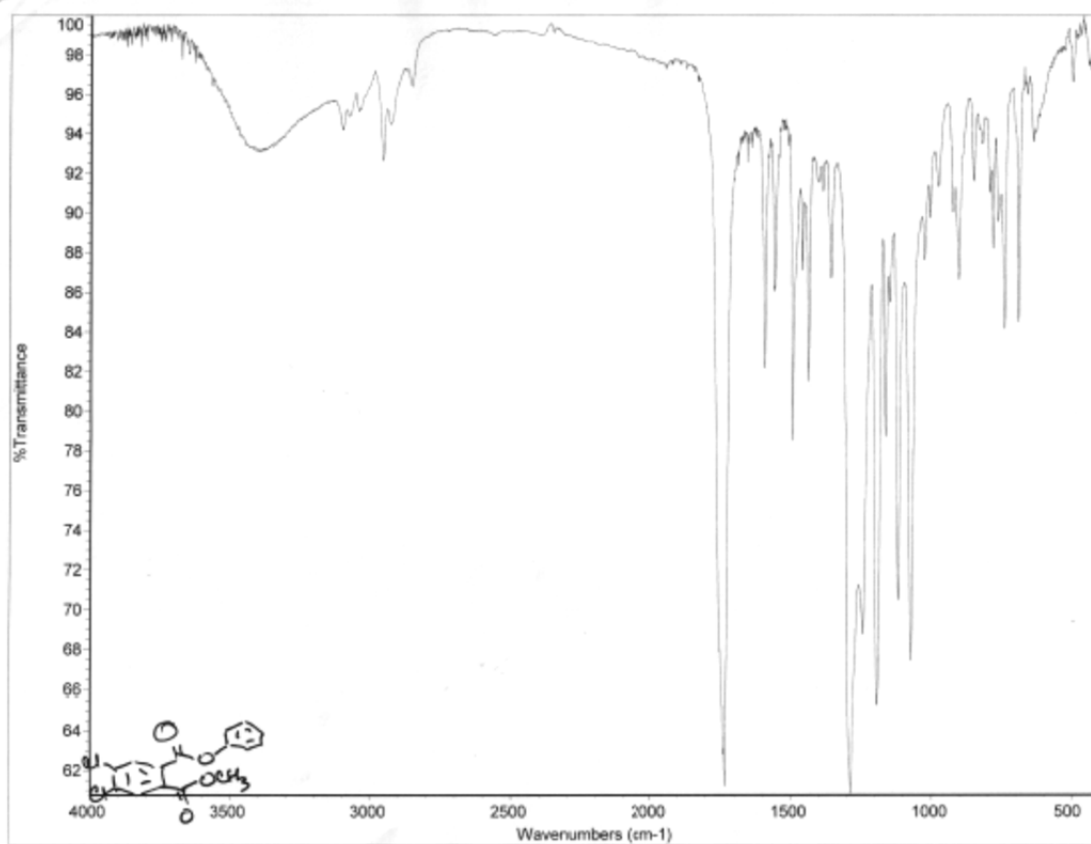


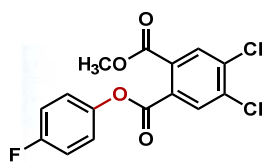
INDEX	FREQUENCY	PPM	HEIGHT
1	3190.641	7.871	30.1
2	3167.389	7.819	39.0
3	2970.399	7.442	29.7
4	2970.435	7.421	21.1
5	2905.468	7.259	41.7
6	2898.287	7.261	23.7
7	1579.991	0.925	195.2



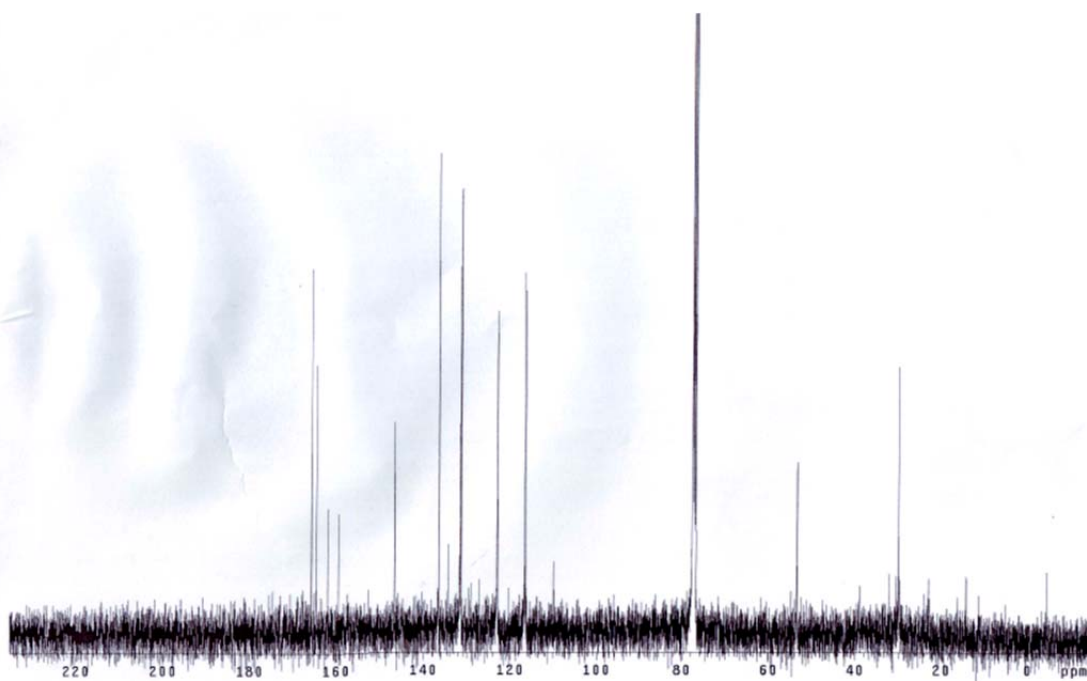
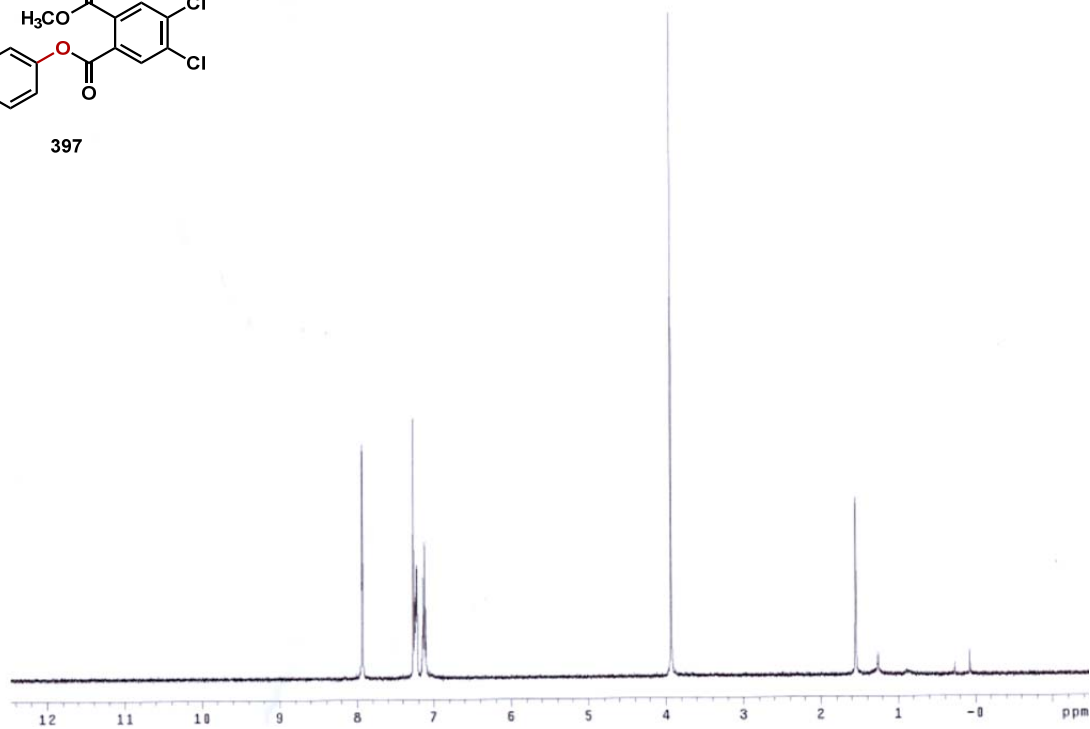
396

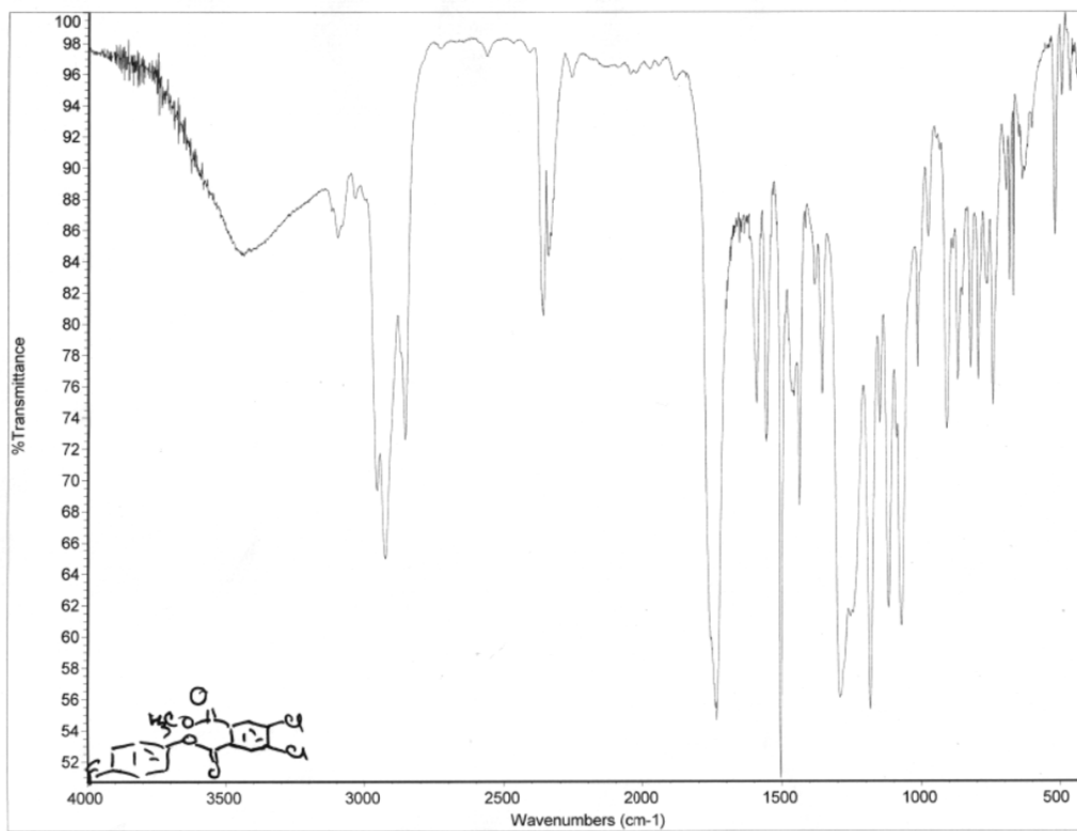


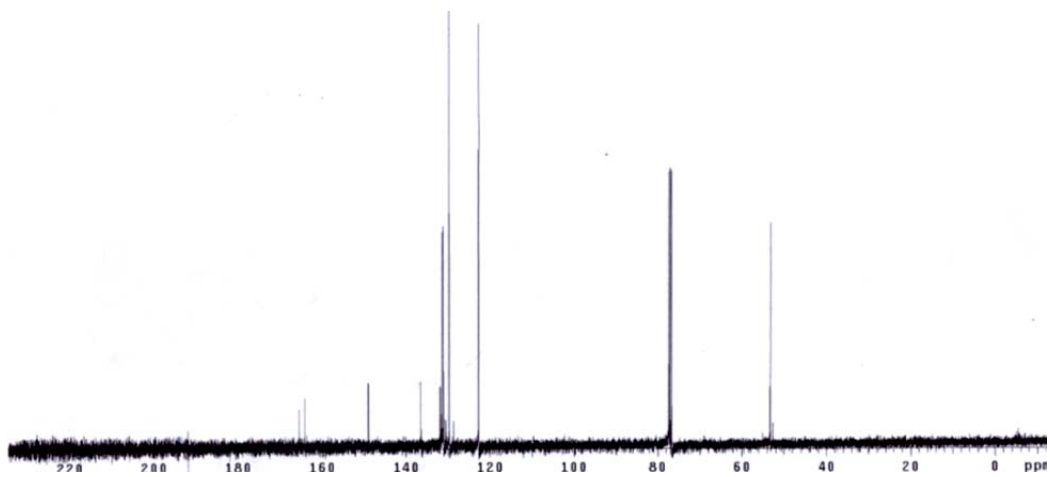
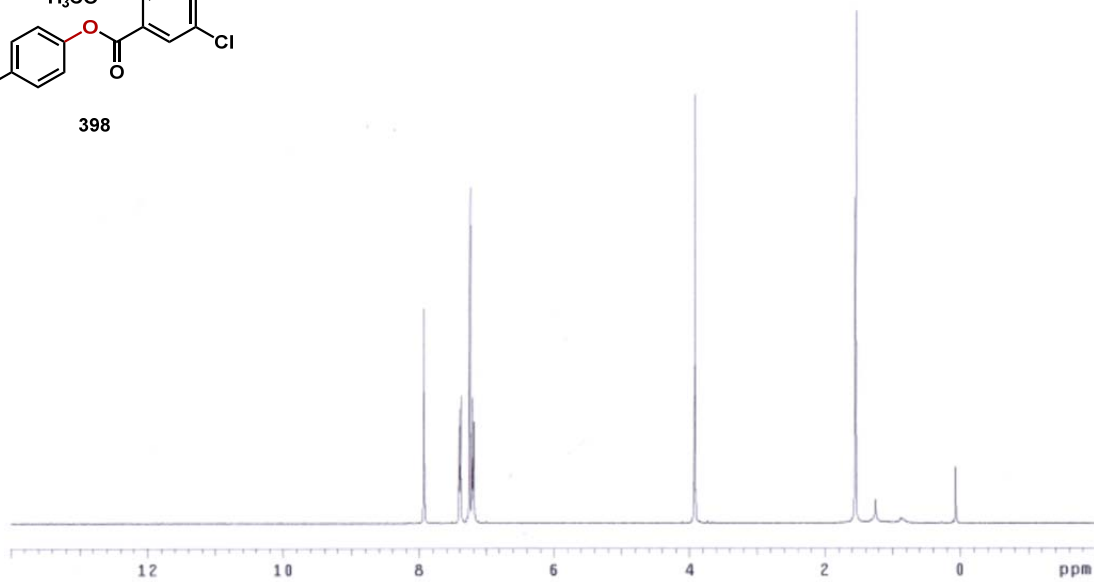
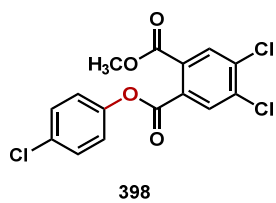


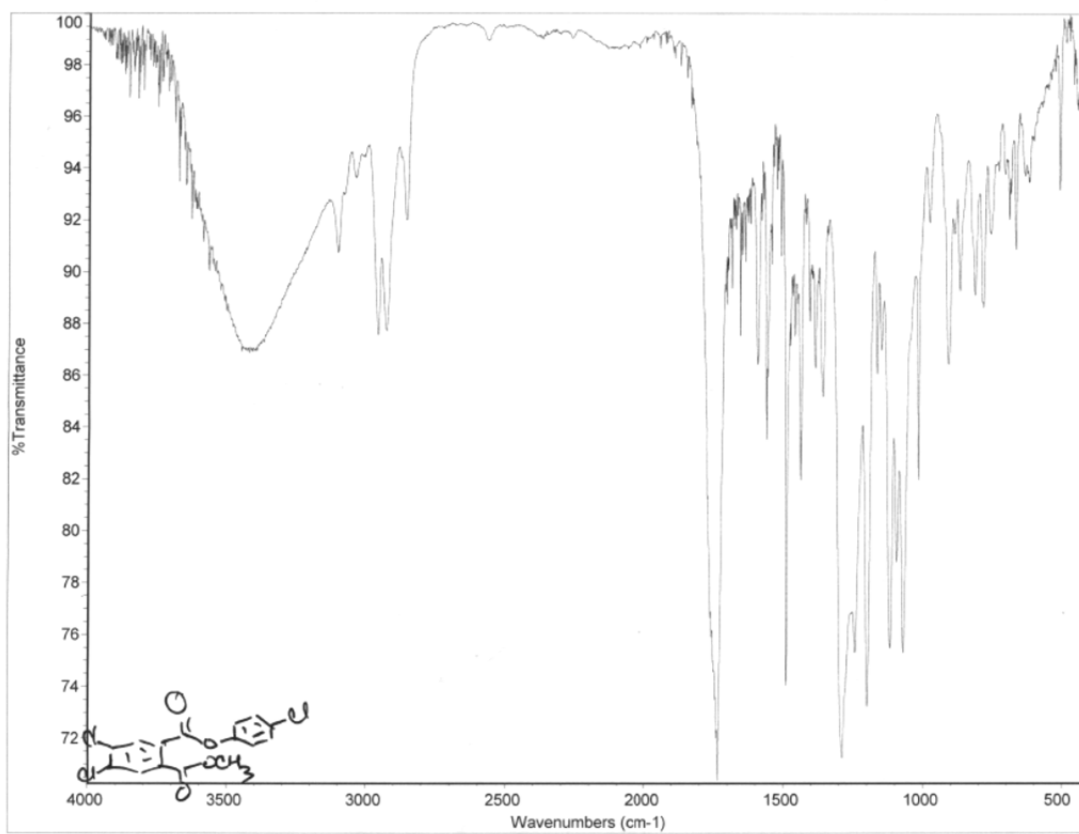


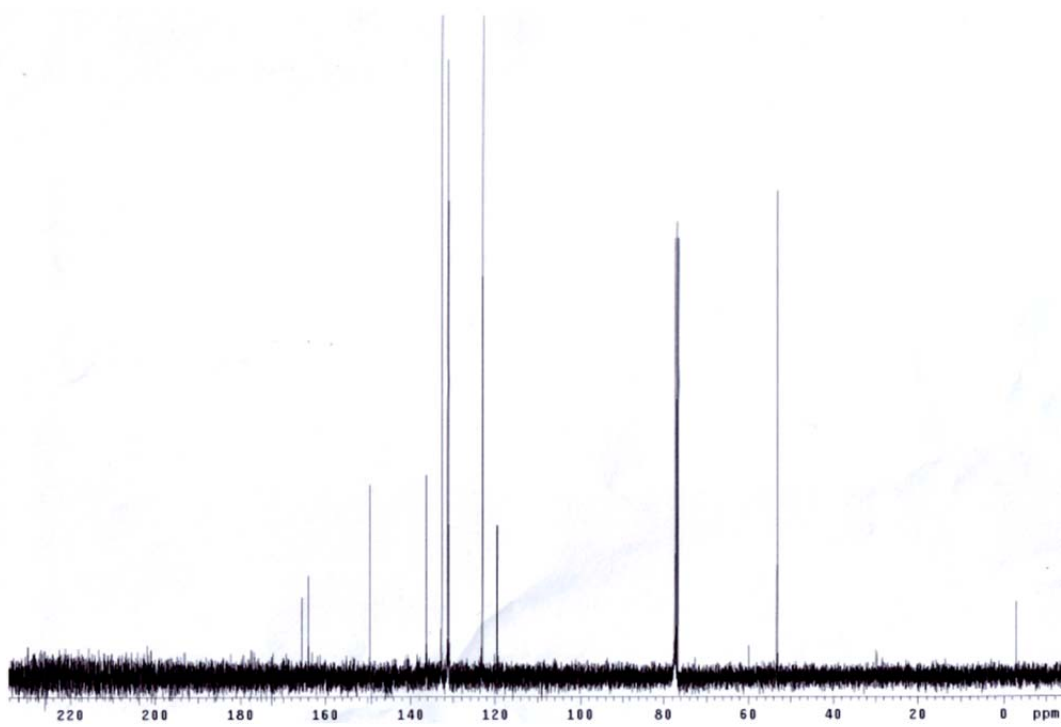
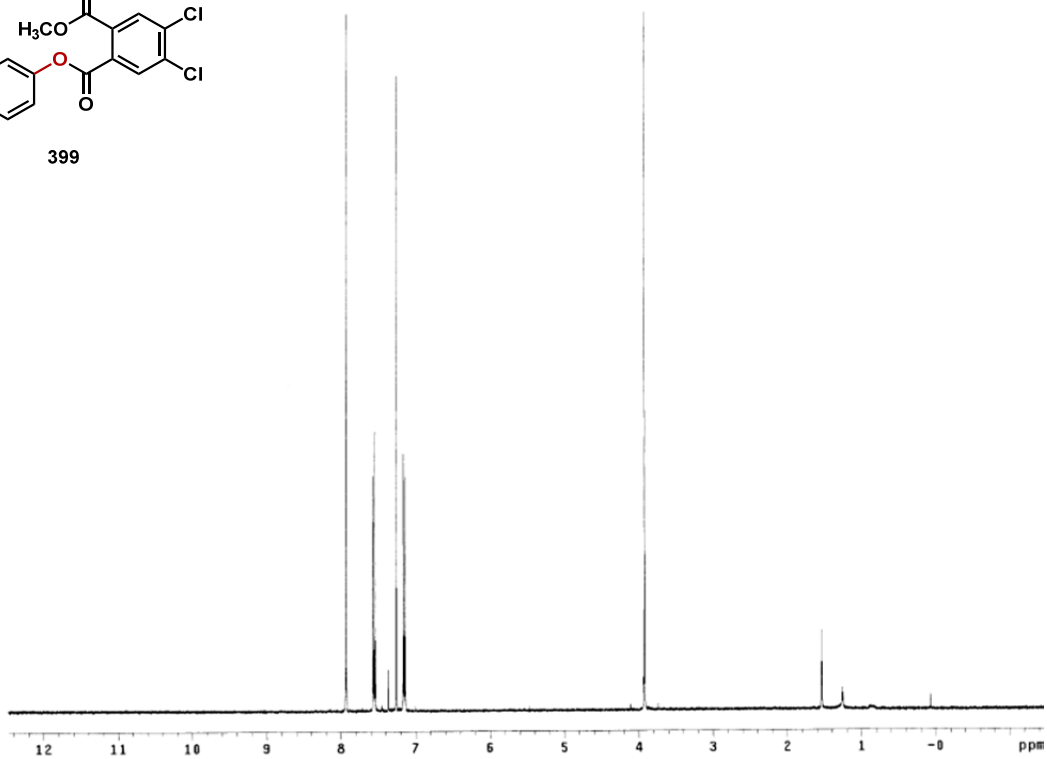
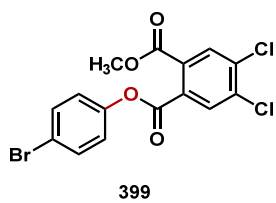
397

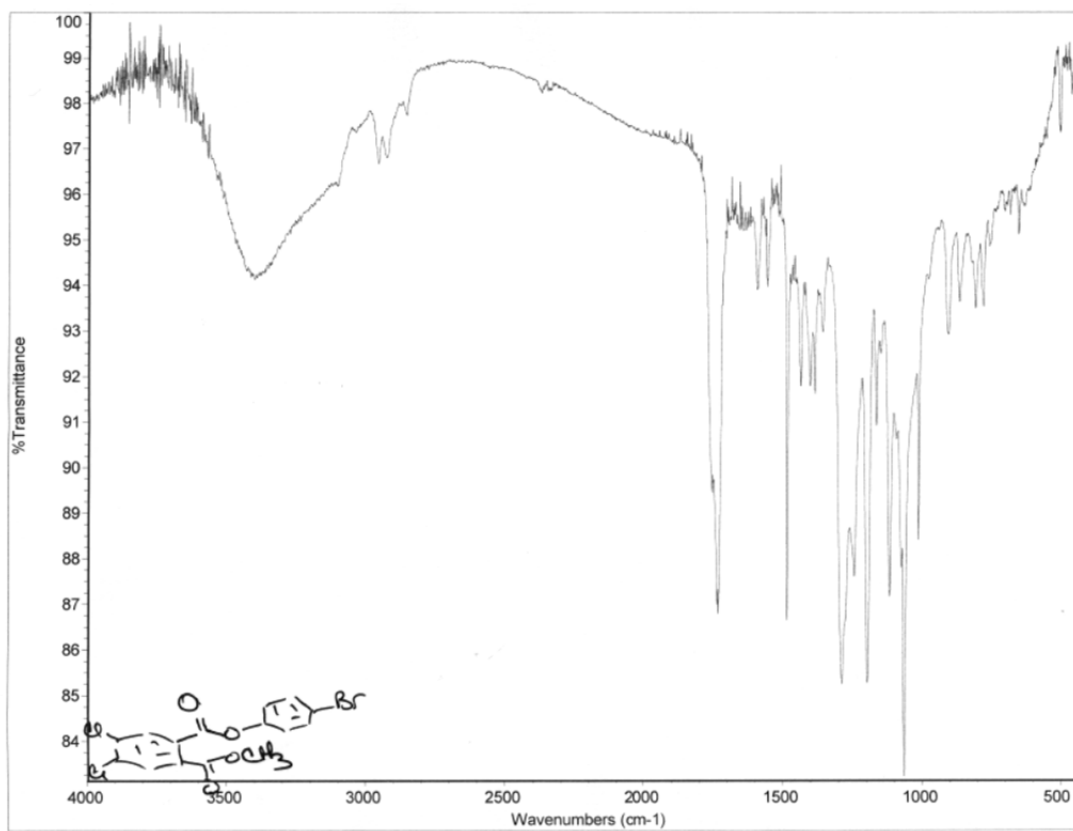








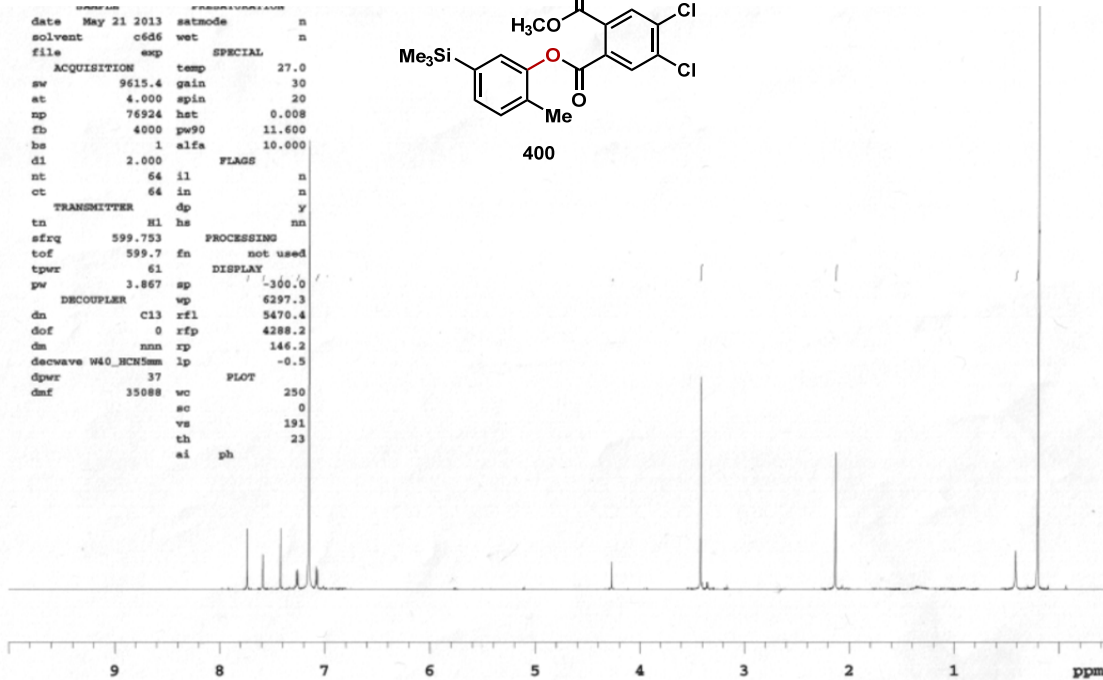
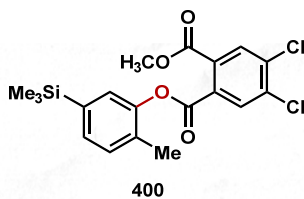




```

date May 21 2013 satmode n
solvent c6d6 wet n
file exp SPECIAL
ACQUISITION temp 27.0
sw 9615.4 gain 30
at 4.000 spin 20
np 76924 hst 0.008
fb 4000 pw90 11.600
hs 1 alfa 10.000
d1 2.000
nt 64 il FLAGS n
ct 64 in n
TRANSMITTER dp y
tn H1 hs nn
sfrq 599.753 PROCESSING
tof 599.7 fn not used
tpwr 61 DISPLAY
pw 3.867 sp -300.0
DECOUPLER wp 6297.3
dn C13 rfl 5470.4
dof 0 rfp 4288.2
dm nnn rp 146.2
decwave W40_MCH5mm lp -0.5
dpr 37 PLOT
dmf 35088 wc 250
sc 0
vs 191
th 23
ai ph

```



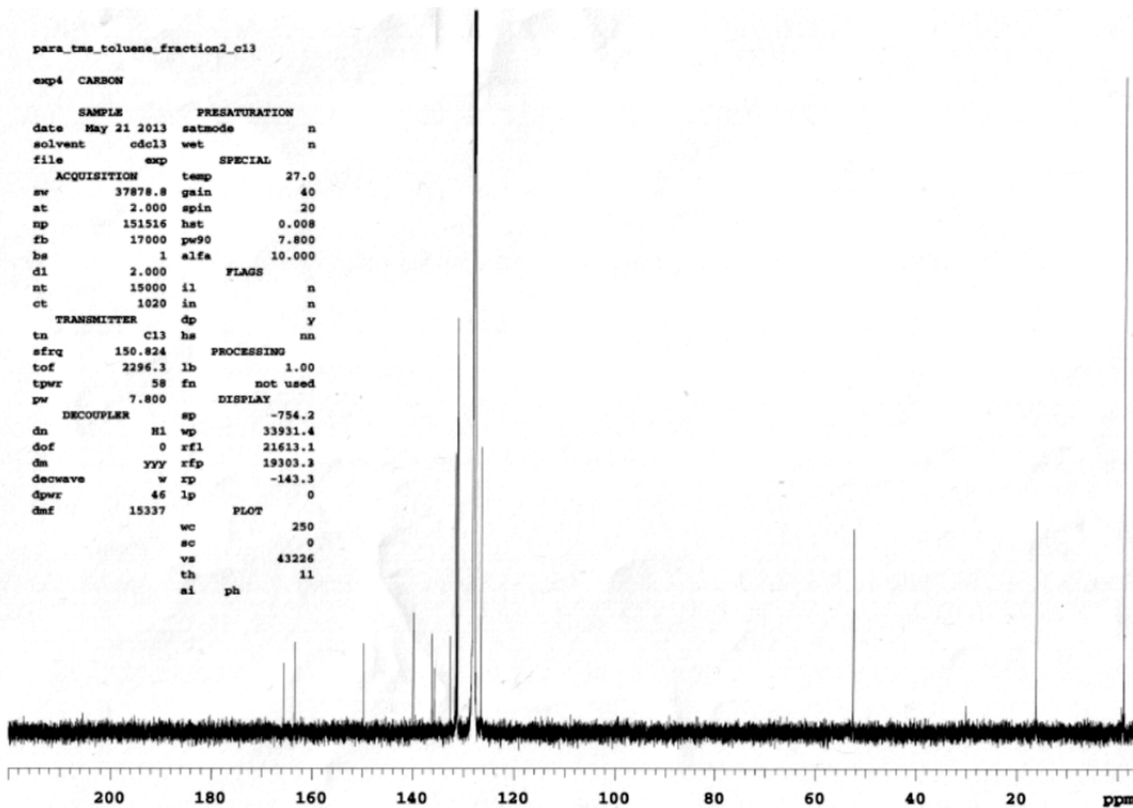
para_tms_toluene_fraction2_c13

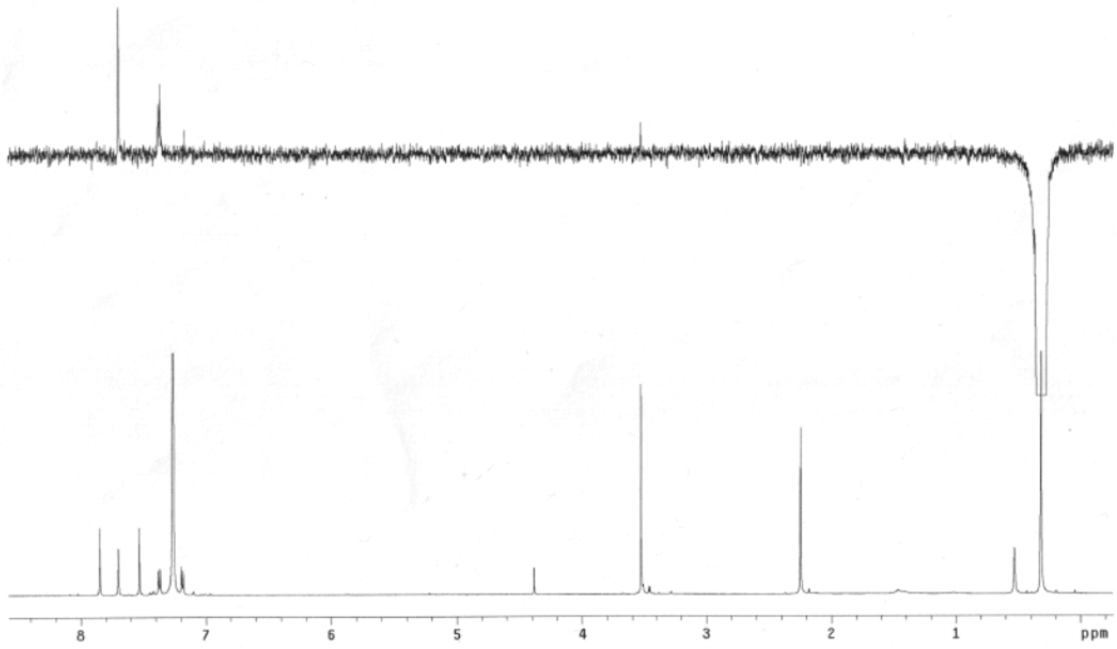
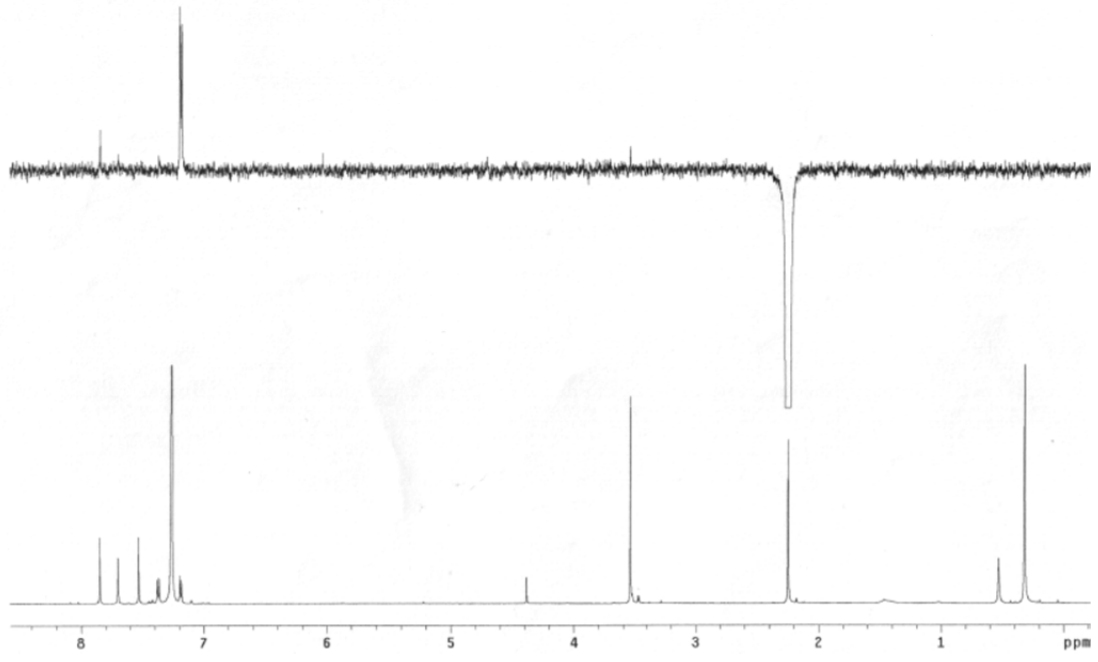
exp4 CARBON

```

SAMPLE PRESATURATION
date May 21 2013 satmode n
solvent cdcl3 wet n
file exp SPECIAL
ACQUISITION temp 27.0
sw 37878.8 gain 40
at 2.000 spin 20
np 151516 hst 0.008
fb 17000 pw90 7.800
hs 1 alfa 10.000
d1 2.000
nt 15000 il FLAGS n
ct 1020 in n
TRANSMITTER dp y
tn C13 hs nn
sfrq 150.824 PROCESSING
tof 2296.3 lb 1.00
tpwr 58 fn not used
pw 7.800 DISPLAY
DECOUPLER sp -754.2
dn H1 wp 33931.4
dof 0 rfl 21613.1
dm yyy rfp 19303.3
decwave w rp -143.3
dpr 46 lp 0
dmf 15337 PLOT
wc 250
sc 0
vs 43226
th 11
ai ph

```





para_tms_toluene_fraction2_noesy

Sample Name:

Data Collected on:

nmr02-vmr600

Archive directory:

Sample directory:

FidFile: NOESY

Pulse Sequence: NOESY

Solvent: c6d6

Data collected on: May 21 2013

Temp. 27.0 C / 300.1 K

Operator: service

Relax. delay 2.000 sec

Acq. time 0.150 sec

Width 6068.0 Hz

2D Width 6068.0 Hz

8 repetitions

2 x 256 increments

OBSERVE F1: 599.7497615 MHz

DATA PROCESSING

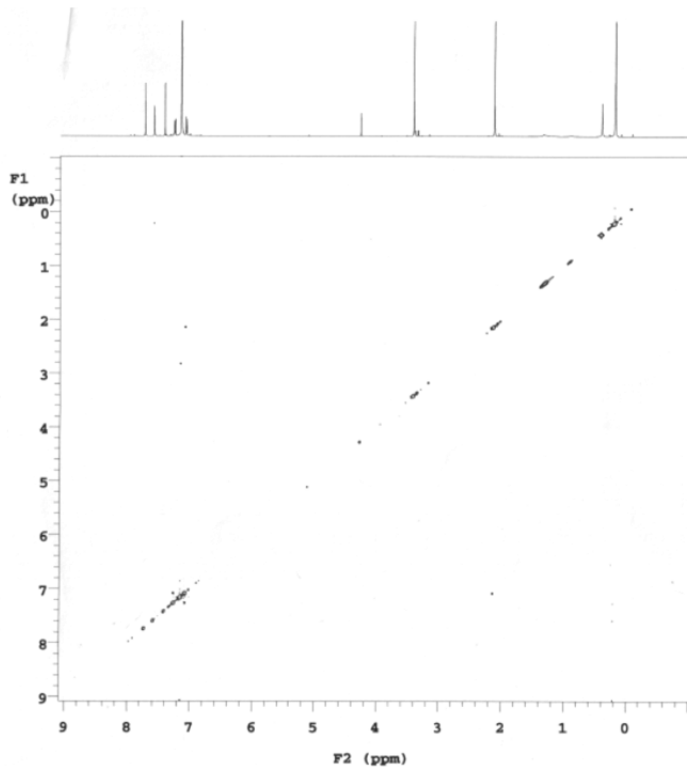
Gauss apodisation 0.069 sec

F1 DATA PROCESSING

Gauss apodisation 0.039 sec

FF size 2048 x 2048

Total time 3 hr, 24 min



para_tms_toluene_fraction2_noesy

Sample Name:

Data Collected on:

nmr02-vmr600

Archive directory:

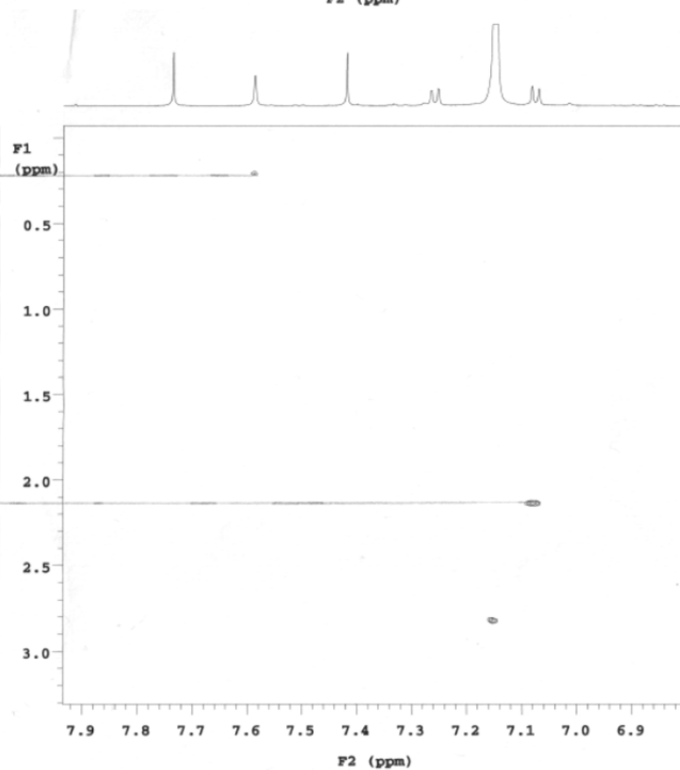
Sample directory:

FidFile: NOESY

Pulse Sequence: NOESY

Solvent: c6d6

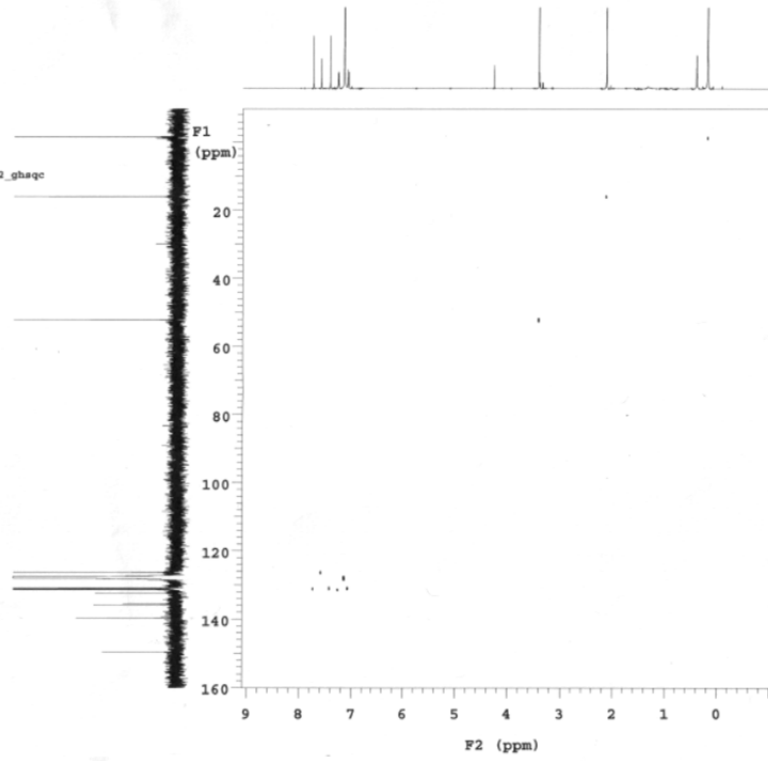
Data collected on: May 21 2013



para_tms_toluene_fraction2_ghaqc

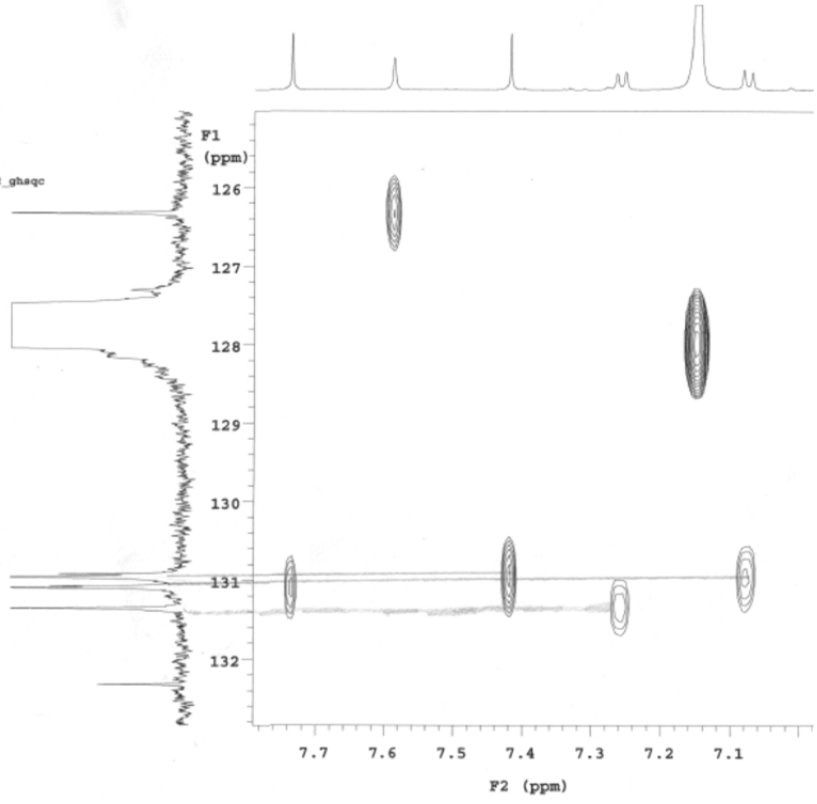
Sample Name:
Data Collected on:
nmrox2-vmrs600
Archive directory:
Sample directory:
FidFile: para_tms_toluene_fraction2_ghaqc
Pulse Sequence: ghsqc
Solvent: c6d6
Data collected on: May 21 2013
Temp. 27.0 C / 300.1 K
Operator: service

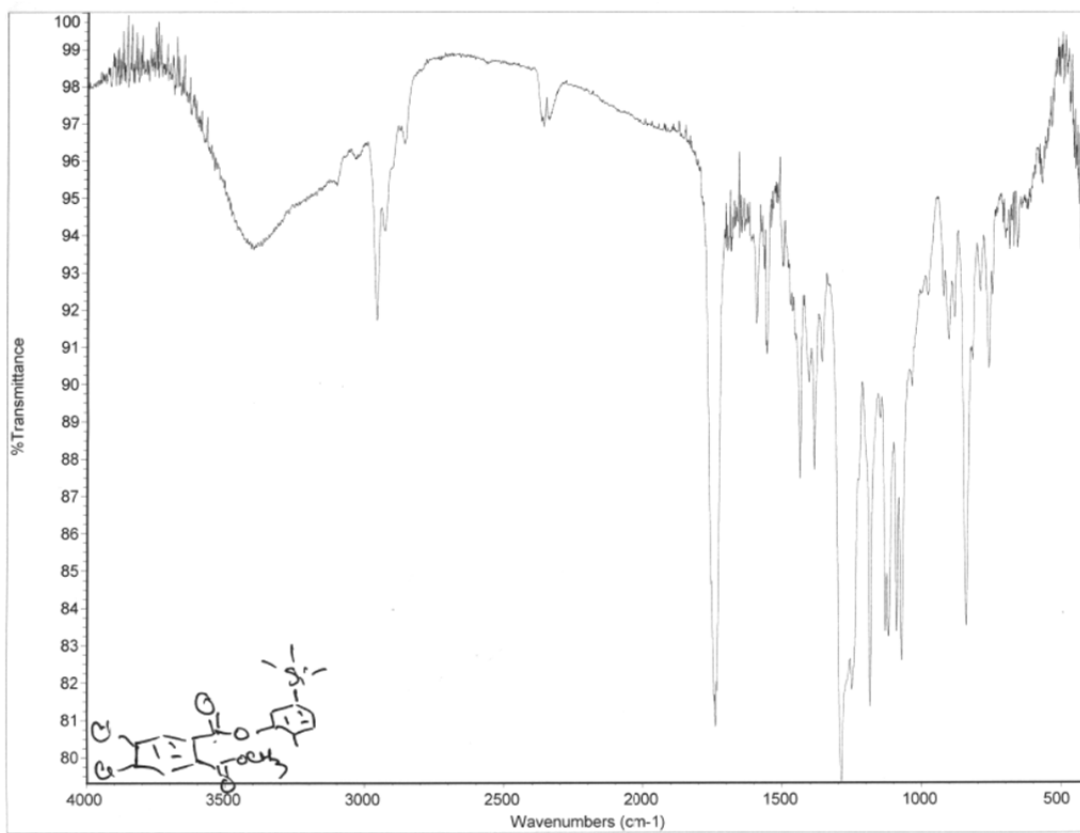
Relax. delay 2.000 sec
Acq. time 0.150 sec
Width 6069.0 Hz
2D Width 25641.0 Hz
4 repetitions
2 x 256 increments
OBSERVE H1. 599.7497621 MHz
DECOUPLE C13. 150.8185152 MHz
Power 37 dB
on during acquisition
off during delay
W40_DB9002 modulated
DATA PROCESSING
Gauss apodisation 0.069 sec
F1 DATA PROCESSING
Resol. enhancement 0.0 Hz
Gauss apodisation 0.005 sec
FT size 4096 x 2048
Total time 1 hr, 15 min

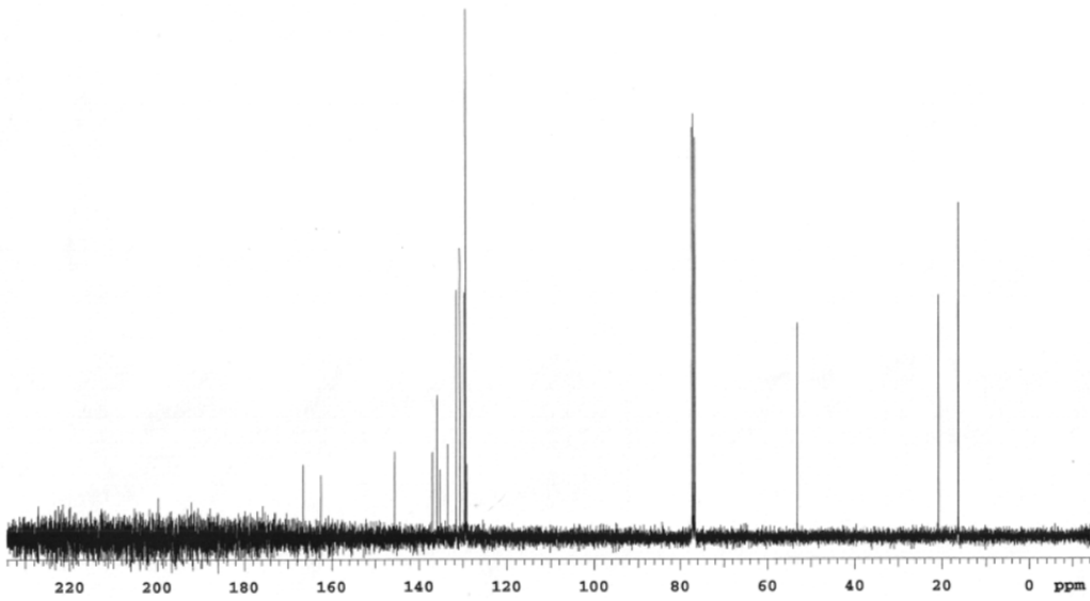
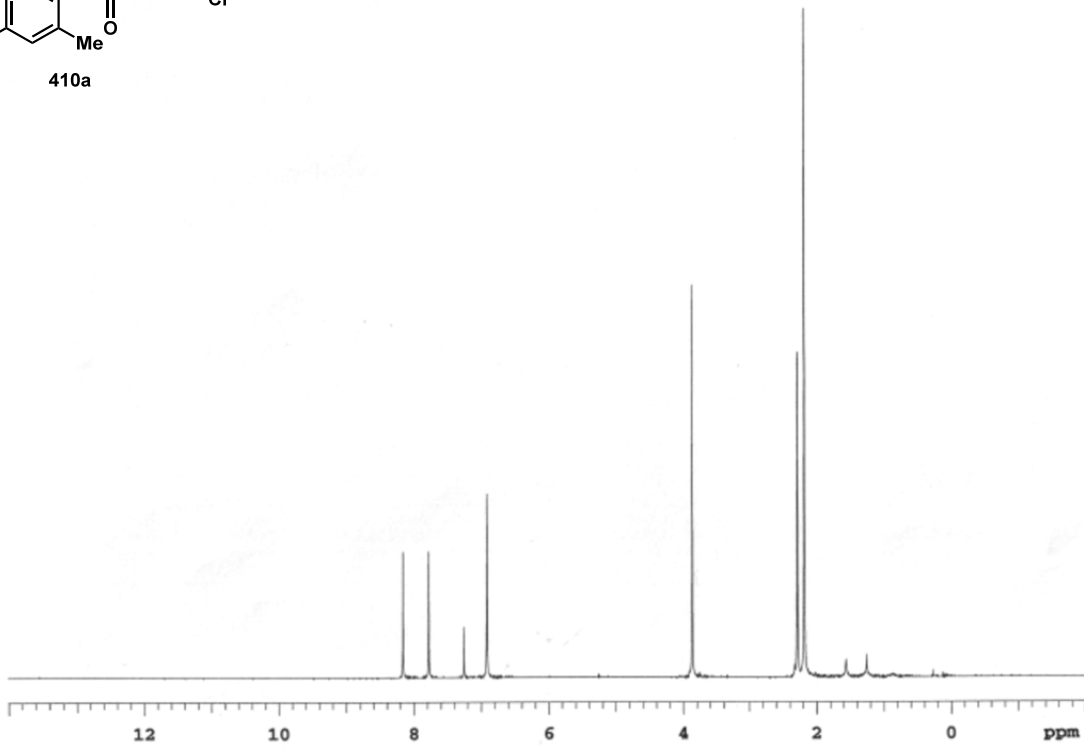
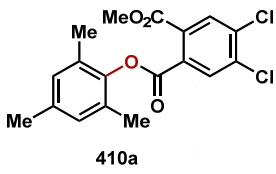


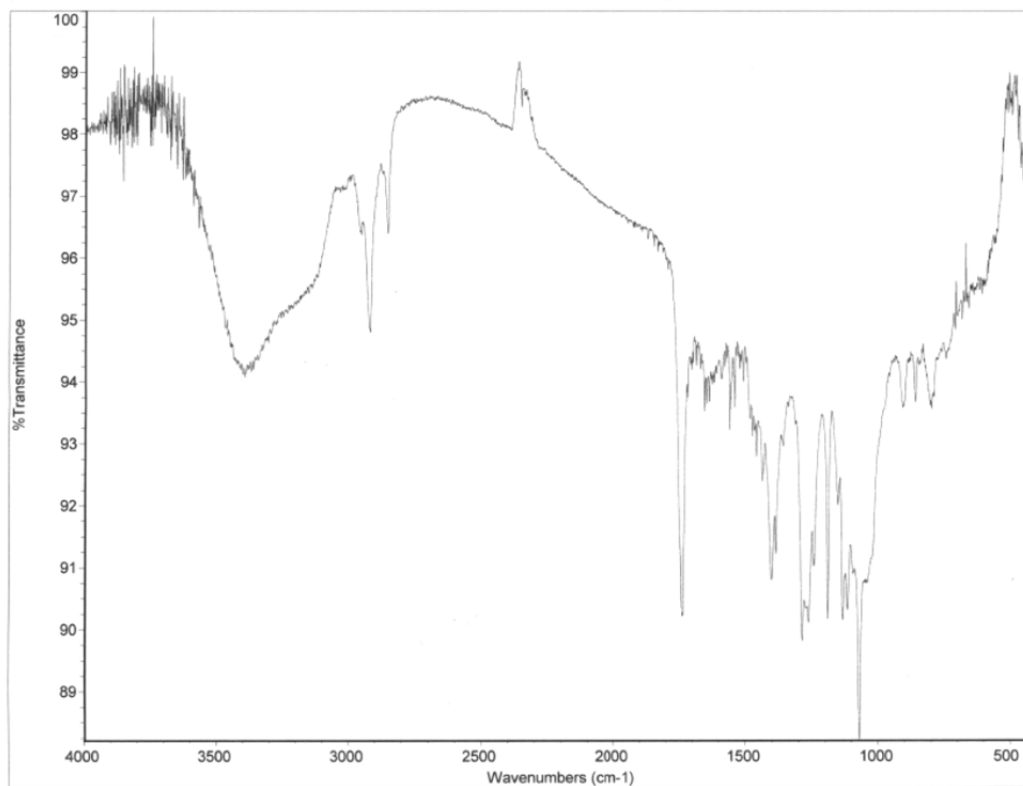
para_tms_toluene_fraction2_ghaqc

Sample Name:
Data Collected on:
nmrox2-vmrs600
Archive directory:
Sample directory:
FidFile: para_tms_toluene_fraction2_ghaqc
Pulse Sequence: ghsqc
Solvent: c6d6
Data collected on: May 21 2013









Elemental Composition Report

Single Mass Analysis (displaying only valid results)

Tolerance = 20.0 PPM / DBE: min = -1.5, max = 50.0

Selected filters: None

Monoisotopic Mass, Odd and Even Electron Ions

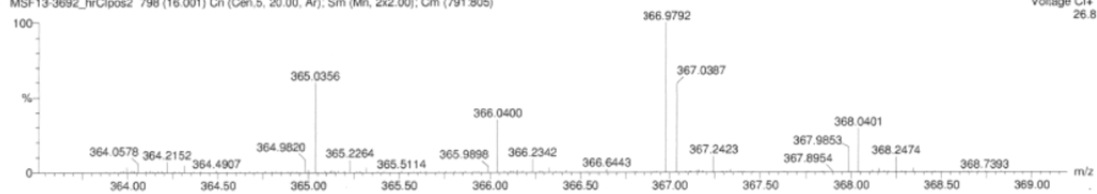
45 formula(e) evaluated with 1 results within limits (all results (up to 1000) for each mass)

Elements Used:

C: 18-18 H: 5-100 O: 4-4 SCl: 0-10 37Cl: 0-10

DCPP_Mesitylene...

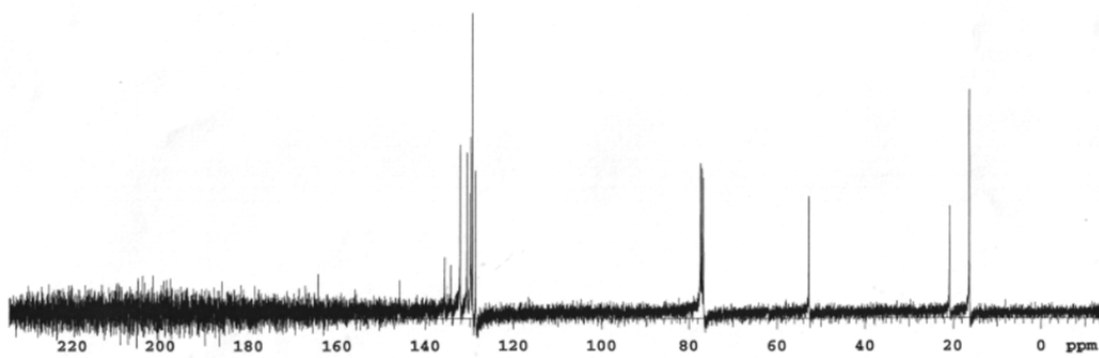
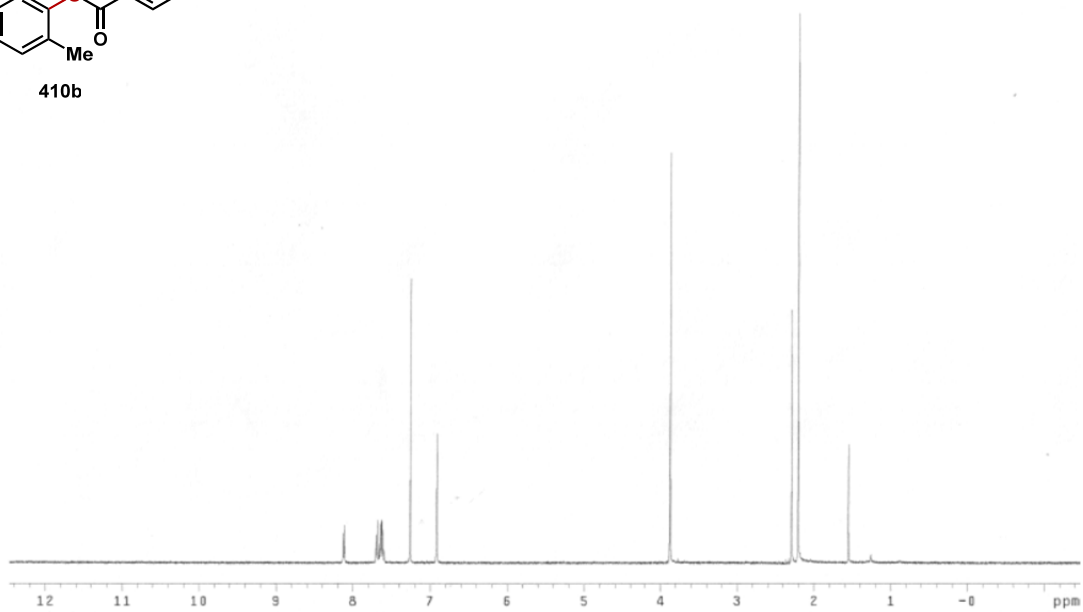
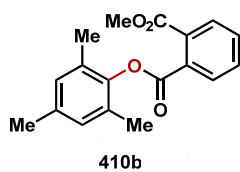
MSF13-3692_IrClpos2 798 (16.001) Cn (Cen.5, 20.00, Ar); Sm (Mn, 2x2.00); Cm (791.805)

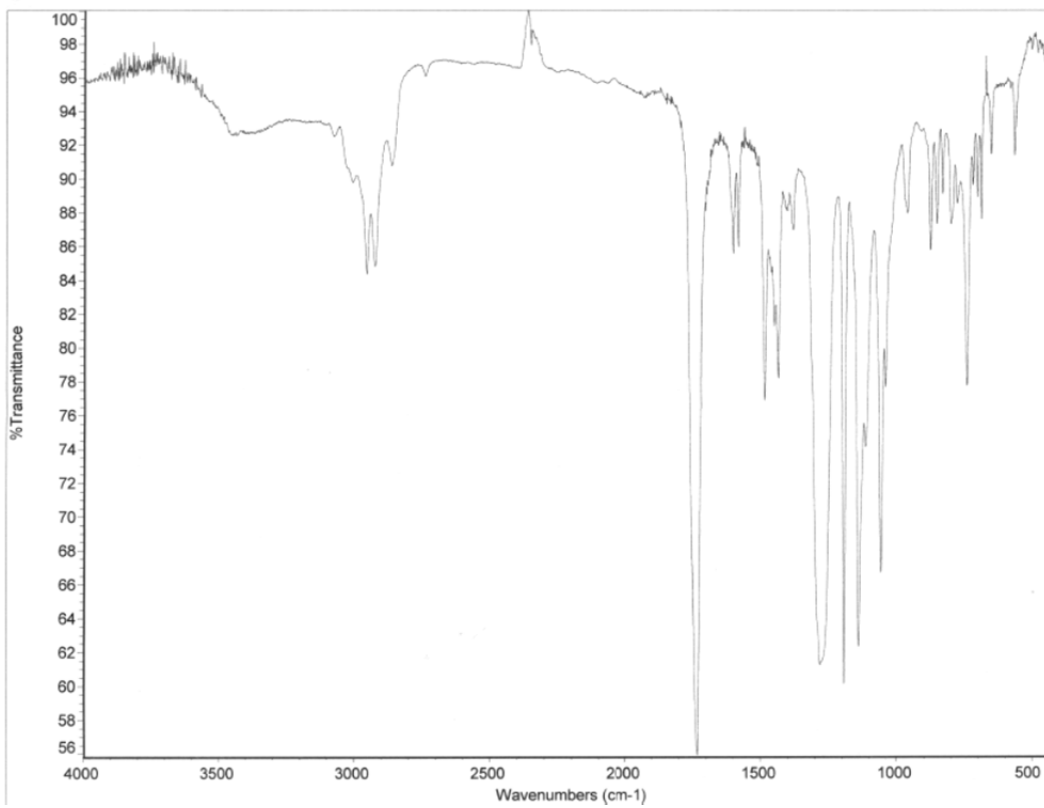


Minimum:
Maximum:

5.0 20.0 -1.5 50.0

Mass	Calc. Mass	mDa	PPM	DBE	1-FIT	Formula
365.0356	365.0347	0.9	2.5	10.5	2.2	C18 H15 O4 35Cl2





Elemental Composition Report

Multiple Mass Analysis: 6 mass(es) processed - displaying only valid results

Tolerance = 5.0 PPM / DBE: min = -1.5, max = 50.0

Selected filters: None

Monoisotopic Mass, Odd and Even Electron Ions

24 formula(e) evaluated with 2 results within limits (all results (up to 1000) for each mass)

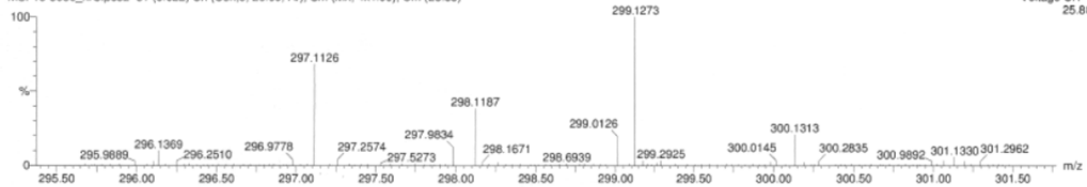
Elements Used:

C: 0-100 H: 0-100 O: 4-4

Phthaloyl...

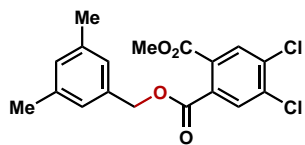
MSF13-3686_hrClpos2 31 (0.622) Cn (Cen,5, 20.00, Ar), Sm (Mn, 4x4.00), Cm (28.33)

Voltage Cl+ 25.8

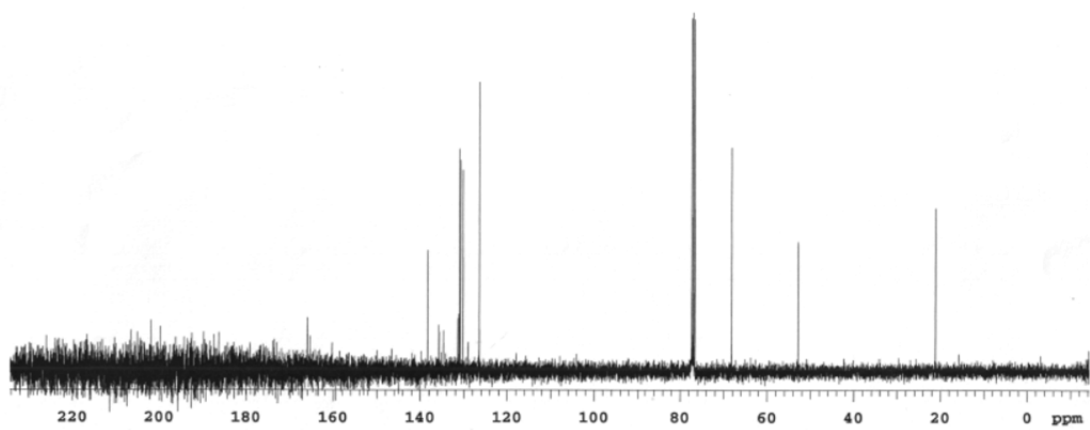
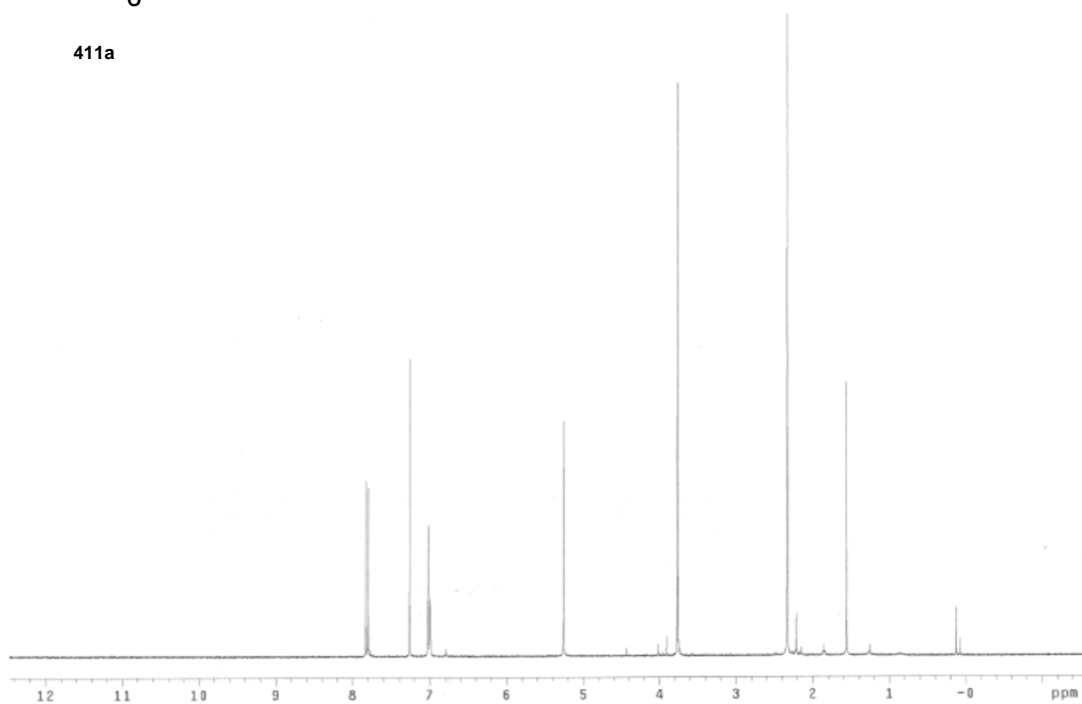


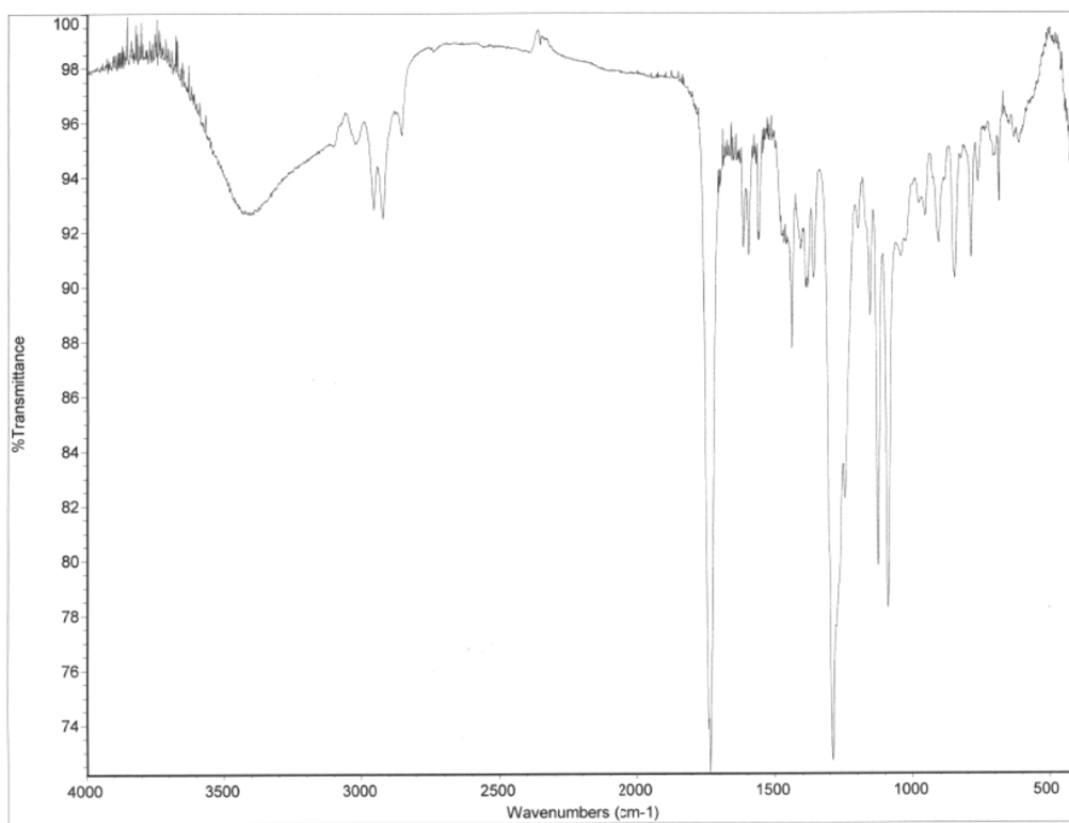
Minimum: 10.00
Maximum: 100.00

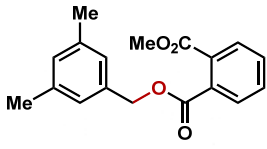
Mass	RA	Calc. Mass	mDa	PPM	DBE	i-FIT	Formula
297.1126	68.27	297.1127	-0.1	-0.3	10.5	14.3	C18 H17 O4
299.1273	100.00	299.1283	-1.0	-1.1	9.5	0.7	C18 H19 O4



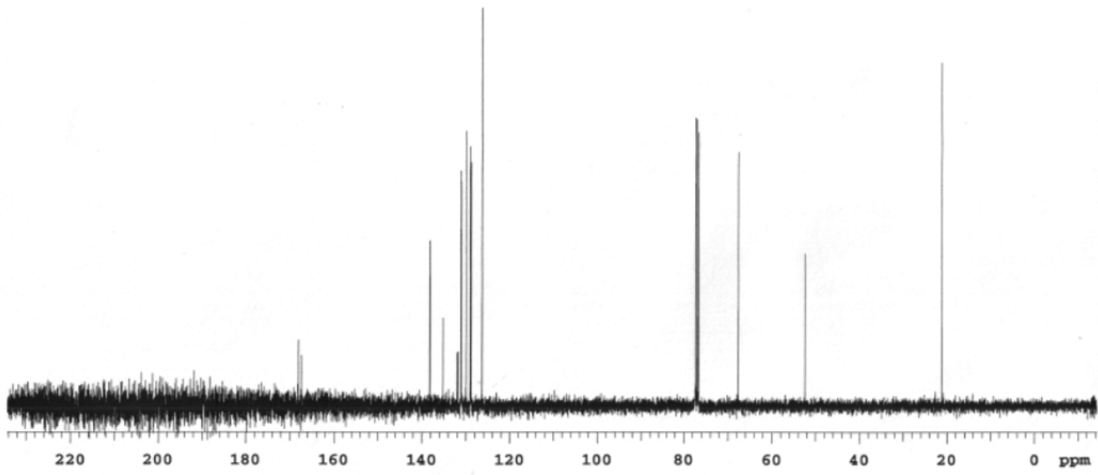
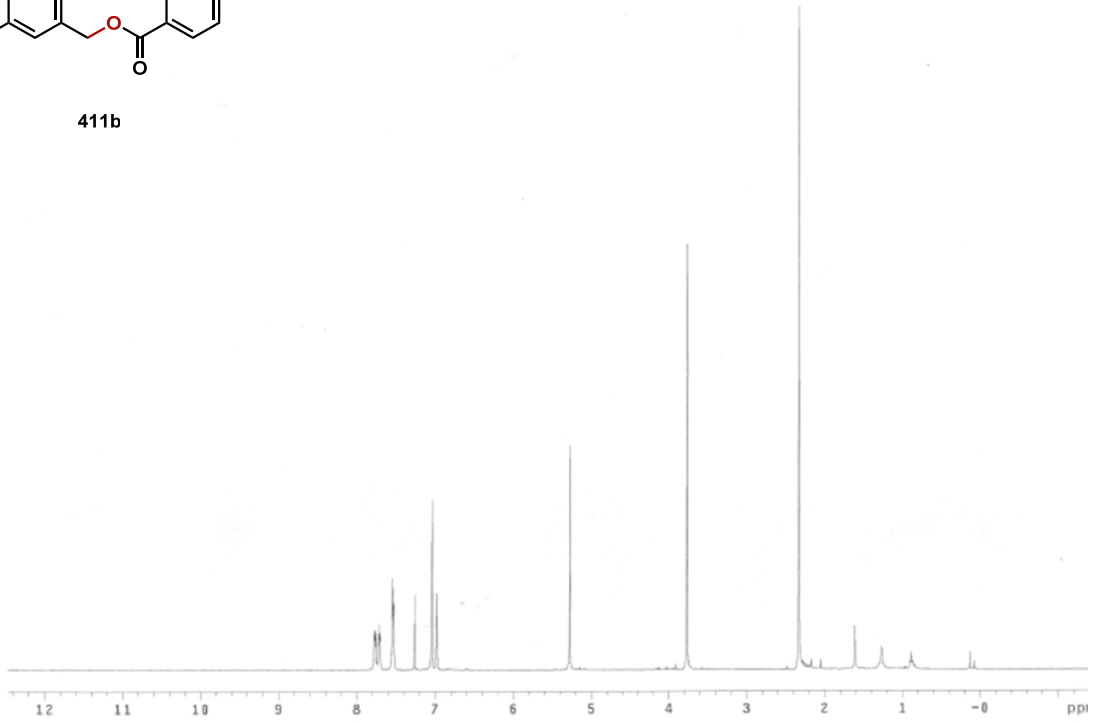
411a

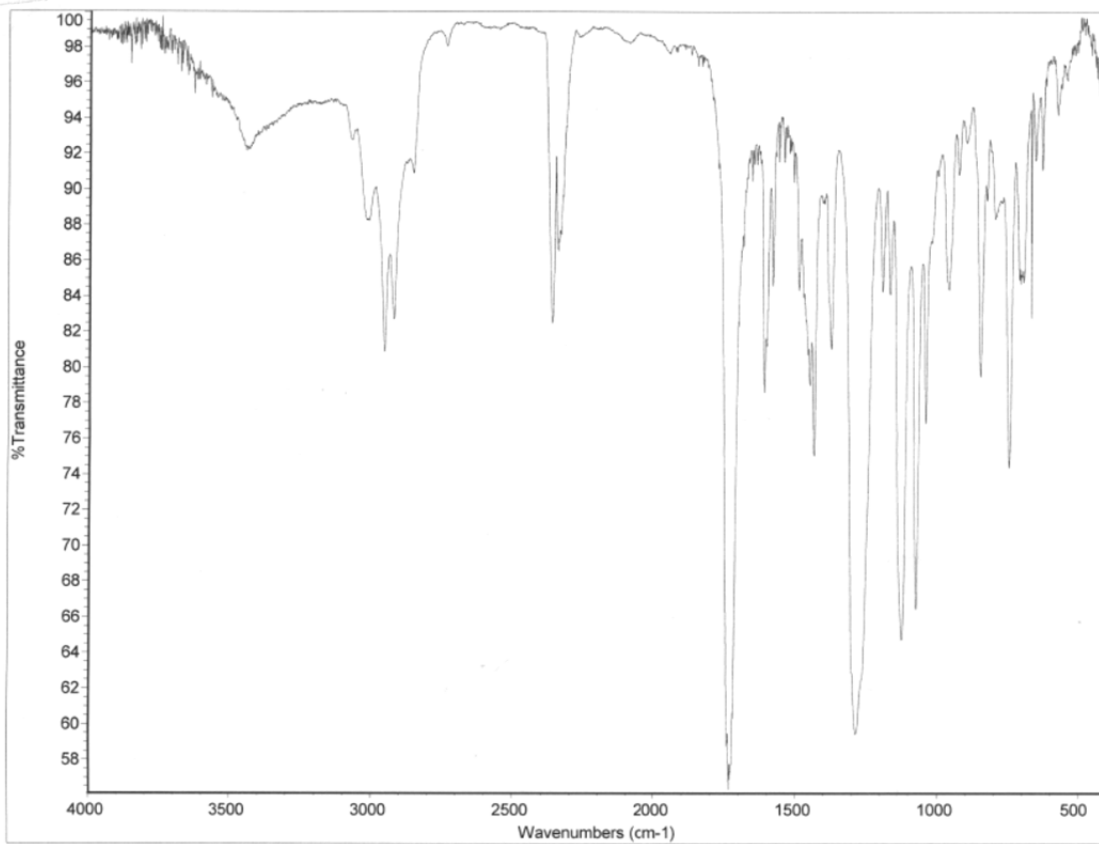


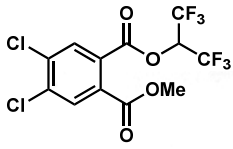




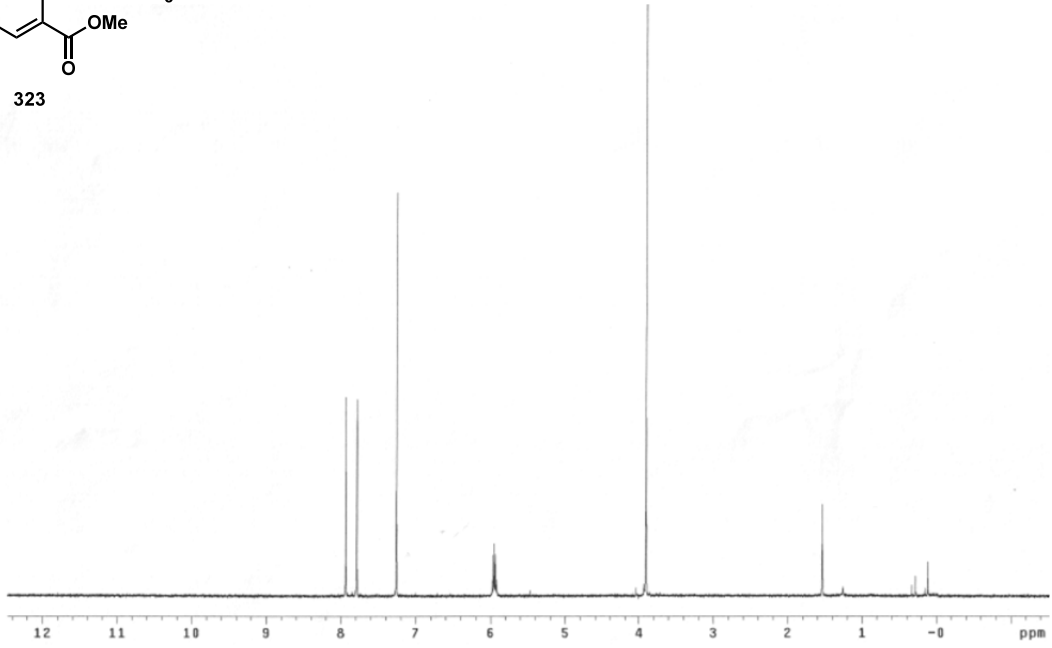
411b







323

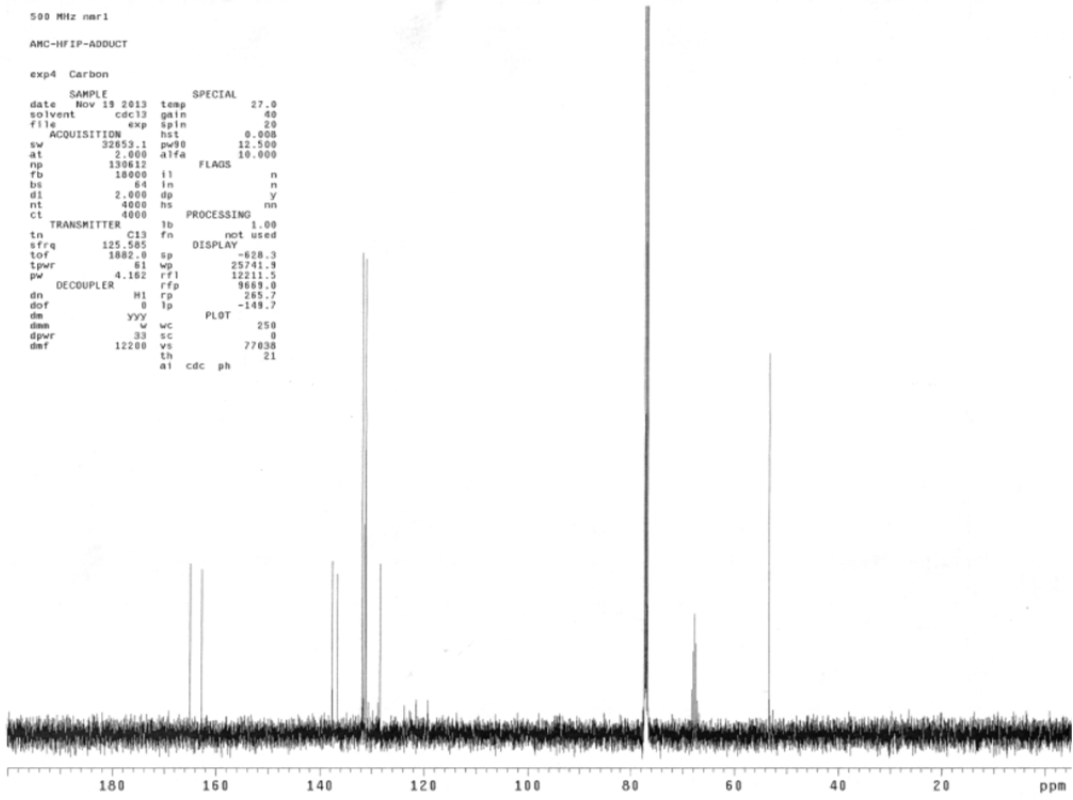


500 MHz nar1

AMC-HFIP-ADDUCT

exp4 Carbon

date	Nov 13 2013	temp	SPECIAL	27.0
solvent	cdc13	gain		40
file	exp	spin		20
ACQUISITION		hst		0.008
sw	32053.1	pw90		12.500
at	2.000	alfa		10.000
np	130612	FLAGS		
fb	18000	tl		n
bs	84	ln		n
d1	2.000	dp		y
nt	4000	hs		nn
cl	4000	PROCESSING		
tn	C13	lb		1.00
sfreq	125.505	fn		not used
tof	1882.0	sp		-828.3
tpwr	81	wp		25741.3
pw	4.162	rf1		12211.5
DECOUPLER		rfp		9685.0
dn	H1	fd		265.7
dof	0	fp		-148.7
dm	yyy	PLOT		
dsm	w	vc		250
dpwr	33	sc		0
dnr	12200	vs		77030
		th		21
		al	cdc	ph

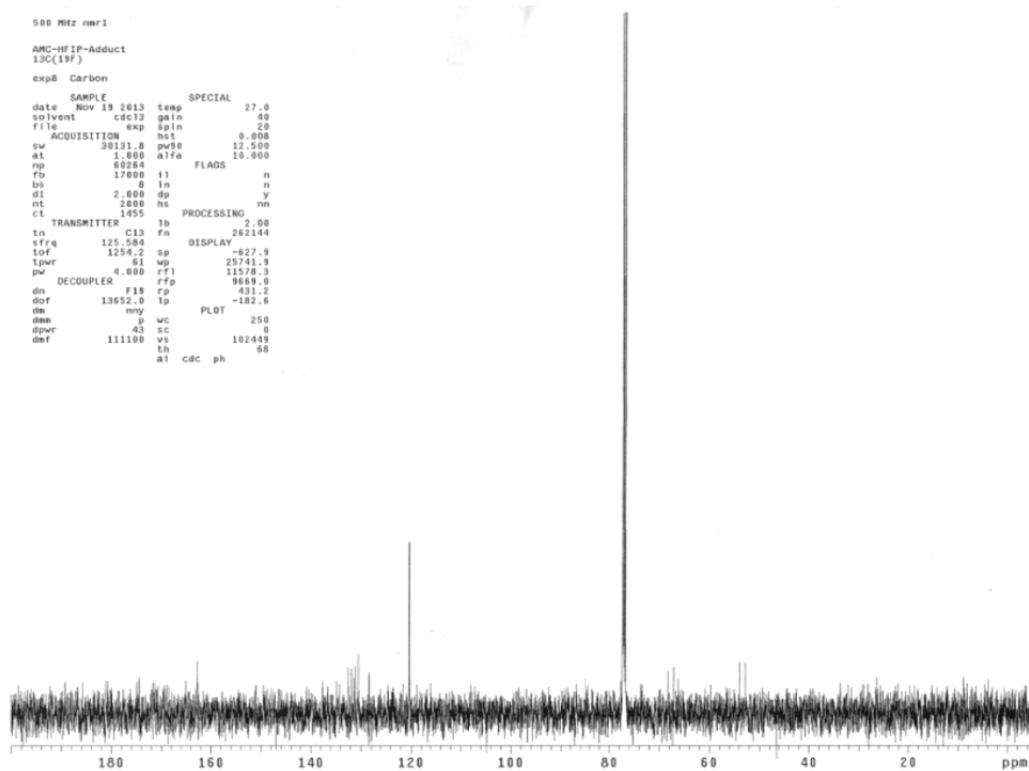


500 MHz nmr1

ANC-HFIP-Adduct
13C(19F)

exp8 Carbon

```
SAMPLE SPECIAL 27.0
date Nov 19 2013 temp 27.0
solvent cdc13 gain 40
file exp spin 20
ACQUISITION hit 0.008
sw 30131.8 pw98 12.500
at 1.000 alfa 10.000
np 49264 FLAGS n
fb 17000 i1 n
bs 8 in n
dl 2.000 dp Y
nt 2000 hs nn
ct 1455 PROCESSING Y
TRANSMITTER lb 2.00
tn C13 fn 262144
sfrq 125.286 DISPLAY
tof 1254.2 sp -627.9
tpwr 81 w9 25741.3
pw 4.000 rfp 11578.3
DECOUPLER rfp 9659.0
dn F19 rp 431.2
dof 13652.0 lp -182.6
dm mny PLOT
dss 8 wc 250
dpwr 43 sc 0
dfr 111100 vs 102488
th 88
al cdc ph
```

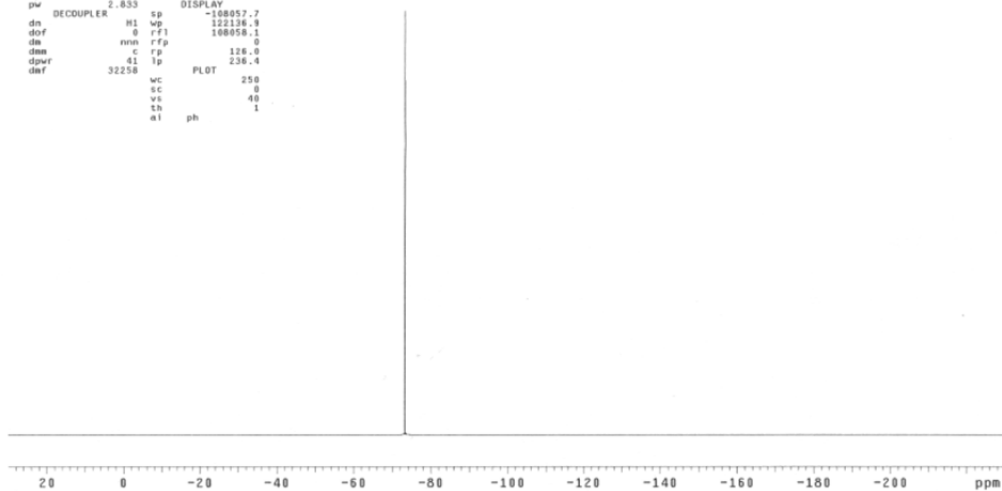


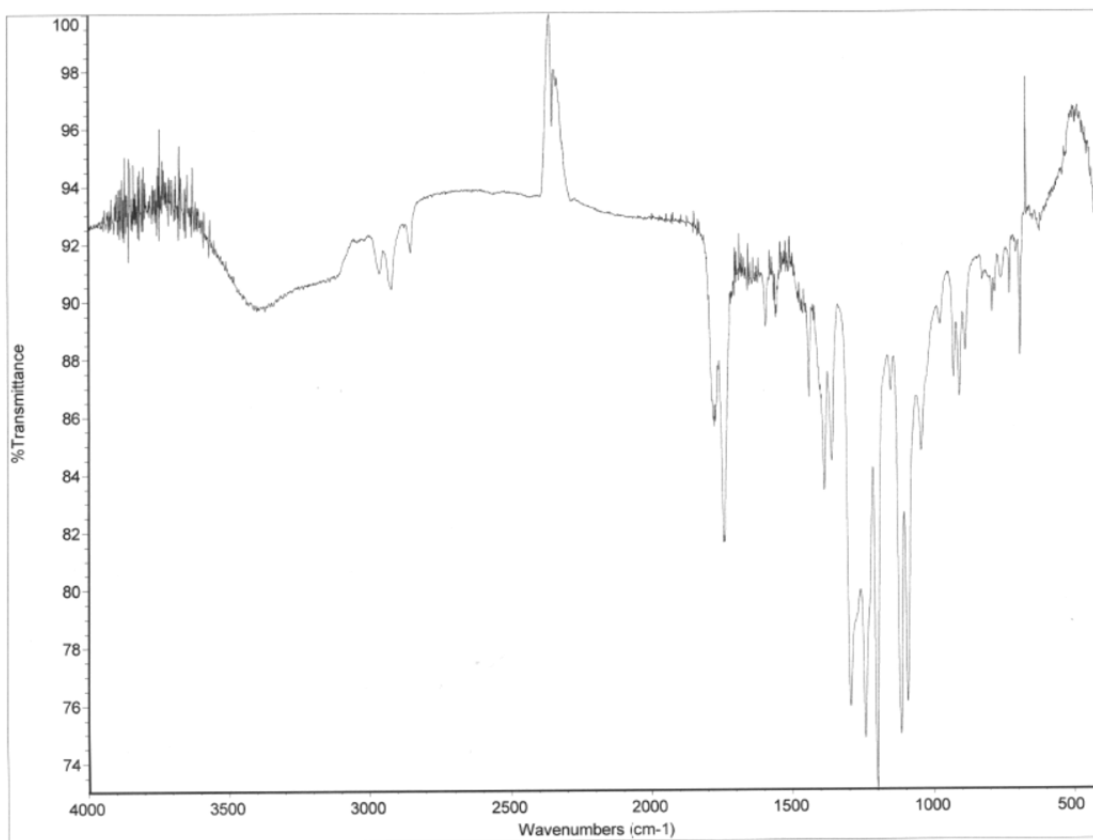
500 MHz nmr1

ANC-HFIP-ADDOUCT

exp6 Fluorine

```
SAMPLE SPECIAL 27.0
date Nov 19 2013 temp 27.0
solvent cdc13 gain 20
file exp spin 20
ACQUISITION hit 0.008
sw 122137.4 pw98 8.500
at 2.000 alfa 96.250
np 488550 FLAGS n
fb 59000 i1 n
bs 64 in n
dl 1.000 dp Y
nt 32 hs nn
ct TRANSMITTER 32 lb 0.88
tn F19 pf 0.462
sfrq 469.847 gfs not used
tof 5476.2 lctid -12
tpwr 50 fn not used
pw 2.033 DISPLAY
DECOUPLER hl sp -108057.7
dn hl wp 122136.9
dof 0 rfp 108058.1
dm nnn rfp 0
dss c rp 126.0
dpwr 41 lp 236.4
dfr 32258 PLOT
th 250
sc 0
vs 40
th 1
al ph
```





Elemental Composition Report

Multiple Mass Analysis: 4 mass(es) processed - displaying only valid results

Tolerance = 4.0 PPM / DBE: min = -1.5, max = 50.0

Selected filters: None

Monoisotopic Mass, Odd and Even Electron Ions

167 formula(e) evaluated with 4 results within limits (all results (up to 1000) for each mass)

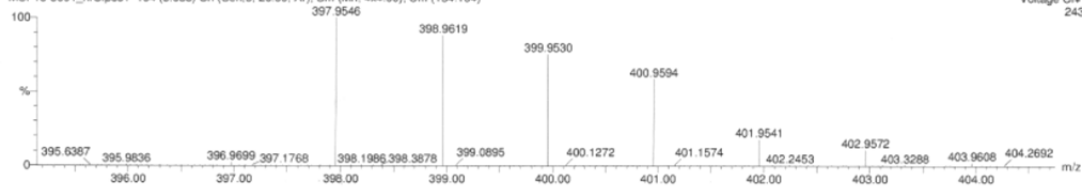
Elements Used:

C: 0-100 H: 0-100 O: 4-4 F: 6-6 ³⁵Cl: 0-10 ³⁷Cl: 0-10

DCPP_HFIP_Adduct

MSF13-3691_hrClipos1 154 (3.088) Cn (Cen.5, 20.00, Ar); Sm (Mn, 4x4.00); Cm (154-164)

Voltage Cl+ 241



Minimum: 20.00
Maximum: 100.00

Mass	RA	Calc. Mass	mDa	PPM	DBE	i-FIT	Formula
397.9546	100.00	397.9547	-0.1	-0.3	6.0	75.3	C12 H6 O4 F6 ³⁵ Cl2
398.9619	88.17	398.9626	-0.7	-1.8	5.5	64.5	C12 H ⁷ O4 F6 ³⁵ Cl2
399.9530	75.43	399.9518	1.2	3.0	6.0	48.4	C12 H6 O4 F6 ³⁵ Cl1 ³⁷ Cl1
400.9594	58.67	400.9596	-0.2	-0.5	5.5	6.2	C12 H ⁷ O4 F6 ³⁵ Cl1 ³⁷ Cl1

References

- (1) Mu, T-W.; Ong, D. S. T.; Wang, Y-J.; Balch, W. E.; Yates III, J. R.; Segatori, L.; and Kelly, J. W. *Cell* **2008**, 134, 769.
- (2) Klaic, L.; Morimoto, R. I.; and Silverman, R. B. *ACS Chemical Biology* **2012**, 7, 928.
- (3) Westerheide, S. D.; Bosman, J. D.; Mgadugha, B. N. A.; Kawahara, T. L. A.; Matsumoto, G.; Kim, S.; Gu, W.; Delvin, J. P.; Silverman, R. B.; and Morimoto, R. I. *The Journal of Biological Chemistry* **2004**, 279, 56053.
- (4) Wu, C. *Annual Review of Cell and Developmental Biology* **1995**, 11, 441.
- (5) Sarge, K. D.; Murphy, S. P.; and Morimoto, R. L. *Molecular Cellular Biology* **1993**, 13, 1392.
- (6) Holmberg, C. L.; Hietakangas, V.; Mikhailov, A.; Rantanen, J. O.; Kallio, M.; Meinander, A.; Hellman, J.; Morrice, N.; MacKintosh, C.; Morimoto, R. I.; Eriksson, J. E.; and Sistonen, L. *The EMBO Journal* **2001**, 20, 3800.
- (7) Morimoto, R. I. *Genes Development* **1998**, 12, 3788.
- (8) Lindquist, S. and Craig, E. A. *Annual Review of Genetics* **1988**, 22, 631.
- (9) Ellis, R. J. and Hartl, F. U. *Current Opinion in Structural Biology* **1999**, 9, 102.
- (10) Ellis, R. J. and Minton, A. P. *The Journal of Biological Chemistry* **2006**, 387, 485.
- (11) Minton, A. P. *Current Biology* **2006**, 16, R269.
- (12) Zhang, Y-Q. and Sarge, K. D. *The Journal of Molecular Medicine* **2007**, 85, 1421.
- (13) Muchowski, P. J.; Schagger, G.; Sittler, A.; Wanker, E. E.; Hayer-Hartle, M. K.; and Hartl, F. U. *Proceedings of the National Academy of Sciences U.S.A.* **2000**, 97, 7841.
- (14) Magrane, J. Smith, R. C.; Walsh, K.; and Querfurth, H. W. *The Journal of Neuroscience* **2004**, 24, 1700.

- (15) Auluck, P. K. and Bonini, N. M. *Nature Medicine* **2002**, 8, 1185.
- (16) Takeuchi, H.; Kobayashi, Y.; Yoshihara, T.; Niwa, J.; Doyu, M.; Ohtsuka, K.; and Sobue, G. *Brain Research* **2002**, 949, 11.
- (17) Zhang, T.; Hamza, A.; Cao, X.; Wang, B.; Yu, S.; Zhan, C-G.; and Sun, D. *Molecular Cancer Therapeutics* **2008**, 7, 162.
- (18) Peng, B.; Xu, L.; Cao, F.; Wei, T.; Yang, C.; Uzan, G.; and Zheng, D. *Molecular Cancer* **2010**, 9, 79.
- (19) Zhang, D.; Xu, L.; Cao, F.; Wei, T.; Yang, C.; Uzan, G.; and Peng, B. *Cell Stress and Chaperones* **2010**, 15, 939.
- (20) Zhang, T.; Li, Y.; Yu, Y.; Zou, P.; Jiang, Y.; Sun, D. *The Journal of Biological Chemistry* **2009**, 284, 35381.
- (21) Fukazawa, T.; Naora, Y.; Kunieda, T.; and Kubo, T. *Development* **2009**, 136, 2323.
- (22) Trott, A.; West, J. D.; Klaic, L.; Westerheide, S. D.; Silverman, R. B.; Morimoto, R. I.; and Morano, K. A. *Molecular Biology of the Cell* **2008**, 19, 1104.
- (23) Klaic, L.; Trippier, P. C.; Mishra, R. K.; Morimoto, R. I.; and Silverman, R. B. *The Journal of the American Chemical Society* **2011**, 133, 19634.
- (24) Sreeramulu, S.; Gande, S. L.; Gobel, M.; and Schwalbe, H. *Angewandte Chemie, International Edition* **2009**, 48, 5833.
- (25) Lee, J. H.; Koo, T. H.; Yoon, H.; Jung, H. S.; Jin, H. Z.; Lee, K.; Hong, Y. S.; and Lee, J. J. *Biochemical Pharmacology* **2006**, 72, 1311.
- (26) Seo, H. R.; Seo, W. D.; Pyun, B. J.; Lee, B. W.; Jin, Y. B.; Park, K. H.; Seo, E. K.; Lee, Y. J.; and Lee, Y. S. *Chemico-Biological Interactions* **2011**, 193, 34.
- (27) Gunatilaka, A. A. *Triterpenoid Quinonemethides and Related Compounds (Celastrolids)* **1996**, Vol. 67, Springer, Wien, New York.
- (28) Ham, P. J. and Whiting, D. A. *The Journal of the Chemical Society, Perkin Transactions 1*, **1972**, 330.

- (29) Wu, S.; Sun, C.; Kuiwu, W.; and Pan, Y. *The Journal of Chromatography A* **2004**, 1028, 171.
- (30) Ferreira de Santana; and Asfora, J. J. C., C. T. *Rev Inst Antibioticos (Recife)* **1971**, 11, 37.
- (31) Melo, A. M.; Jardim, M. L.; De Santana, C. F.; Lacet, Y.; Lobo Filho, J.; and De Lima e Ivan Leonicio, O. G. *Rev Inst Antibioticos (Recife)* **1974**, 14, 9.
- (32) U.S. National Institutes of Health. *United States Clinical Trials Online Registry*; National Institutes of Health: <http://clinicaltrials.gov/ct2/results?term=tripterygium+wilfordii> (accessed February 12, 2014).
- (33) Huang, F. C.; Chan, W. K.; Moriarty, K. J.; Zhang, D. C.; Chang, M. N.; He, W.; Yu, K. T.; and Zilbertstein, A. *Bioorganic & Medicinal Chemistry Letters* **1998**, 8, 1883.
- (34) Campanelli, A. R.; D'Alagni, M.; and Marini-Bettolo, G. B. *The Federation of European Biochemical Societies Letters* **1980**, 122, 256.
- (35) Kurti, L.; Chein, R-J.; and Corey, E. J. *The Journal of the American Chemical Society* **2008**, 130, 9031.
- (36) Johnson, W. S. *Angewandte Chemie, International Edition English* **1976**, 15, 9.
- (37) Yoder, R. A. and Johnston, J. N. *Chemical Reviews* **2005**, 105, 4730.
- (38) Eschenmoser, O.; Ruzicka, L.; Jeger, O.; and Arigoni, D. *Helvetica Chimica Acta* **1955**, 38, 1890.
- (39) Stadler, P. A.; Eschenmoser, A.; Schinz, H.; and Stork, G. *Helvetica Chimica Acta* **1950**, 40, 2191.
- (40) Barton, D. H. R. and de Mayo, P. *The Journal of the Chemical Society* **1957**, 150.
- (41) Barton, D. H. R.; Bockman, O. C.; and de Mayo, P. *The Journal of the Chemical Society* **1960**, 2263.
- (42) Goldsmith, D. J. *The Journal of the American Chemical Society* **1962**, 84, 3913.

- (43) van Tamelen, E. E.; Storni, A.; Hessler, E. J.; and Schwartz, M. *The Journal of the American Chemical Society* **1963**, 85, 3295.
- (44) Johnson, W. S.; Norman, J. P.; and Hooz, J. *The Journal of the American Chemical Society* **1966**, 88, 3859.
- (45) Johnson, W. S.; Kinnel, R. B. *The Journal of the American Chemical Society* **1966**, 88, 3861.
- (46) van Tamelen, E. E.; Willet, J.; Nadeau, R.; and Schwartz, M. I. *The Journal of the American Chemical Society* **1966**, 88, 5938.
- (47) Ireland, R. E.; Baldwin, S. W.; Dawson, D. J.; Dawson, M. I.; Dolfini, J. E.; Newbould, J.; Johnson, W. S.; Brown, M.; Crawford, R. J.; Hudrlik, P. F.; Rasmussen, G. H.; Schmiegel, K. K. *The Journal of the American Chemical Society* **1970**, 92, 5743.
- (48) Nagata, W. and Yoshioka, M. *Proceedings of the International Congress on Hormonal Steroids, 2nd*, **1967**, 327, 1966.
- (49) Nagata, W.; Yoshioka, M.; Narisada, M.; and Watanabe, H. *Tetrahedron Letters* **1964**, 3133.
- (50) van Tamelen, E. E.; Seiler, M. P.; and Wierenga, W. *The Journal of the American Chemical Society* **1972**, 94, 8229.
- (51) Corey, E. J. and Lee, J. *The Journal of the American Chemical Society* **1993**, 115, 8873.
- (52) Wenkert, E. and Berges, D. A. *The Journal of the American Chemical Society* **1967**, 89, 2507.
- (53) Ireland, R. E.; Dawson, M. I.; Kowalski, C. J.; Lipinski, C. A.; Marshall, D. R.; Tilley, J. W.; Bordner, J.; and Trus, B. L. *The Journal of Organic Chemistry* **1975**, 40, 973.
- (54) Johnson, W. S.; Buchanan, R. A.; Bartlett, W. R.; Tham, F. S.; and Kullnig, R. K. *The Journal of the American Chemical Society* **1993**, 115, 504.
- (55) Fish, P. V. and Johnson, W. S. *The Journal of Organic Chemistry* **1994**, 59, 2324.

- (56) Surendra, K. and Corey, E. J. *The Journal of the American Chemical Society* **2008**, 130, 8865.
- (57) Surendra, K. and Corey, E. J. *The Journal of the American Chemical Society* **2009**, 131, 13928.
- (58) (a) Corey, E. J. and Zhang, J. *Organic Letters* **2003**, 5, 3455. (b) Corey, E. J.; Noe, M. C.; and Shieh, W-C. *Tetrahedron Letters* **1993**, 34, 5995.
- (59) Ireland, R. E.; Dawson, M. I.; Welch, S. C.; Hagenbac, A.; Bordner, J.; and Trus, B. *The Journal of the American Chemical Society* **1973**, 95, 7829.
- (60) Ireland, R. E.; Evans, D. A.; Glover, D.; Rubottom, G. M.; and Young, H. *The Journal of Organic Chemistry* **1969**, 34, 3717.
- (61) Ireland, R. E. and Walba, D. M. *Tetrahedron Letters* **1976**, 14, 1071.
- (62) Marshall, J. A.; Fanta, W. I.; and Roebke, H. *The Journal of Organic Chemistry* **1966**, 31, 1016.
- (63) Ireland, R. E.; Bey, P.; Cheng, K-F.; Czarny, R. J.; Moser, J-F.; and Trust, R. I. *The Journal of Organic Chemistry* **1975**, 40, 1000.
- (64) Ireland, R. E.; McKenzie, T. C.; and Trust, R. I. *The Journal of Organic Chemistry* **1975**, 40, 1007.
- (65) Bestmann, H. J.; Ermann, P.; Ruppel, H.; and Sperling, W. *Liebigs Annalen der Chemie* **1986**, 479.
- (66) Birch, A. J. *The Journal of the Chemical Society* **1950**, 1551.
- (67) Kuenhe, M. E. and Lambert, B. F. *Organic Synthesis* **1963**, 43, 22.
- (68) Bachi, M. D.; Epstein, J. W.; Herzberg-Minly, Y.; and Loewenthal, H. J. E. *The Journal of Organic Chemistry* **1969**, 34, 126.
- (69) Hook, J. M.; Mander, L. N.; and Woolias, M. *Tetrahedron Letters* **1982**, 23, 1095.
- (70) Schultz, A. G. and Macielag, M. *The Journal of Organic Chemistry* **1986**, 51, 4983.
- (71) Shing, T. K. M.; Yeung, Y. Y.; and Su, P. L. *Organic Letters* **2006**, 8, 3149.

- (72) Cook, S. P. and Danishefsky, S. J. *Organic Letters* **2006**, 5693.
- (73) Marques-Lopez, E.; Herrera, R. P.; Marks, T.; Jacobs, W. C.; Konning, D.; de Figueiredo, R. M.; and Christmann, M. *Organic Letters* **2009**, 11, 4116.
- (74) Omura, K. and Swern, D. *Tetrahedron* **1978**, 34, 1651
- (75) Blanchette, M. A.; Choy, W.; Davis, J.T.; Essnefeld, A. P.; Masamune, S.; Roush, W. R.; and Sakai, T. *Tetrahedron Letters* **1984**, 25, 2183.
- (76) Corey, E. J. and Fuchs, P. L. *Tetrahedron Letters* **1972**, 13, 3769.
- (77) Wittig, G. and Ulrich, S. *Chemische Berichte* **1954**, 87, 1318.
- (78) Julia, M. and Paris, J-M. *Tetrahedron Letters* **1973**, 14, 4833.
- (79) Evans, D. A. and Starr, J. T. *The Journal of the American Chemical Society* **2003**, 125,13531.
- (80) Ren, F.; Hogan, P.; Anderson, A.; and Myers, A. G. *The Journal of the American Chemical Society* **2007**, 129, 5381.
- (81) Chemler, S. R.; Trauner, D.; and Danishefsky, S. J. *Angewandte Chemie, International Edition* **2001**, 40, 4544.
- (82) Miyaura, N.; Ishiyama, T.; Ishikawa, M.; and Suzuki, A. *Tetrahedron Letters* **1986**, 27, 6369.
- (83) Seyferth, D.; Marmor, R. S.; and Hilbert, P. *The Journal of Organic Chemistry* **1971**, 36, 1379.
- (84) Gilbert, J. C. and Weerasooriya, U. *The Journal of Organic Chemistry* **1982**, 47, 1837.
- (85) Corey, E. J. and Katzenellenbogen, J. A. *The Journal of the American Chemical Society* **1969**, 91, 1851.
- (86) Hall, D. G.; Chapdelaine, D.; Preville, P.; and Deslongchamps, P. *Synlett* **1994**, 661.
- (87) Evans, D. A.; Fu, G. C.; and Hoveyda, A. H. *The Journal of the American Society* **1988**, 110, 6917.

- (88) Scouten, C. G. and Brown, H. C. *The Journal of Organic Chemistry* **1973**, 38, 4092.
- (89) Luche, J. L. *The Journal of the American Chemical Society* **1978**, 100, 2226.
- (90) Wurtz, A. *Annales de Chimie et de Physique* **1855**, 44, 275.
- (91) Quintard, J. P.; Hauvett-Frey, S.; and Pereyre, M. *The Journal of Organometallic Chemistry* **1978**, 159, 147.
- (92) Still, W. C. *The Journal of the American Chemical Society* **1978**, 100, 1481.
- (93) Lipshutz, B. H. and Sengupta, S. *Organic Reactions* **1992**, 41, 135.
- (94) Lipshutz, B. H.; Crow, R.; Dimock, S. H.; Ellsworth, E. L.; Smith, R. A. J.; and Behling, J. R. *The Journal of the American Chemical Society* **1990**, 112, 4063.
- (95) Hegedus, L.; Lipshutz, B.; Nozaki, H.; Reetz, M.; Rittmeyer, P.; Smith, K.; Totter, F.; and Yamamoto, H. *Organometallics in Synthesis, A Manual*. **1994**, John Wiley & Sons Ltd. West Sussex, England.
- (96) Miyaura, N.; Yamada, K.; and Suzuki, A. *Tetrahedron Letters* **1979**, 20, 3437.
- (97) Miyaura, N. and Suzuki, A. *Chemical Communications* **1979**, 19, 866.
- (98) Corey, E. J. and Venkateswarlu, A. *The Journal of the American Chemical Society* **1972**, 94, 6190.
- (99) Corey, E. J.; Cho, H.; Rucker, C.; and Hua, D. H. *Tetrahedron Letters* **1981**, 22, 3455.
- (100) Maercker, A. and Theis, M. *Organometallic Synthesis* **1986**, 2, 378.
- (101) Maercker, A. and Girreser, U. *Angewandte Chemie* **1990**, 102, 718.
- (102) Maercker, A. and Girreser, U. *Angewandte Chemie, International Edition* **1990**, 29, 667.
- (103) Maercker, A. and Girreser, U. *Tetrahedron* **1994**, 50, 8019.
- (104) Sweeting, O. J. and Johnson, J. R. *The Journal of the American Chemical Society* **1946**, 68, 1057.

- (105) Tsuji, J.; Nagashima, H.; and Nemoto, H. *Organic Syntheses* **1990**, 7, 137.
- (106) Michel, B. W.; Camelio, A. M.; Cornell, C. N.; and Sigman, M. S. *The Journal of the American Chemical Society* **2009**, 131, 17, 6076.
- (107) Michel, B. W.; Steffens, L. D.; and Sigman, M. S. *The Journal of the American Chemical Society* **2011**, 133, 8317.
- (108) Xu, H. C.; Moeller, K. D. *The Journal of the American Chemical Society* **2008**, 130, 13542.
- (109) Xu, H. C.; Moeller, K. D. *The Journal of the American Chemical Society* **2010**, 132, 2839.
- (110) Trost, B. M. and Phan, L. T. *Tetrahedron Letters* **1993**, 4735.
- (111) Trost, B. M. and Li, Y. *The Journal of the American Chemical Society* **1996**, 118, 6625.
- (112) Wadsworth, W. J. *Organic Reactions* **1977**, 25, 74.
- (113) Harrison, G. C. and Diehl, H. *Organic Syntheses* **1955**, 3, 370.
- (114) Dess, D. B.; Martin, J. C. *The Journal of Organic Chemistry* **1983**, 48, 4155.
- (115) Snyder, S. A.; Treitler, D. S.; Brucks, A. P. *The Journal of the American Chemical Society* **2010**, 132, 14303.
- (116) Sen, S. E.; Roach, S. L.; Smith, S. M.; and Zhang, Y. Z. *Tetrahedron Letters* **1998**, 39, 3969.
- (117) Snider, B. B. and Spindell, D. K. *The Journal of Organic Chemistry* **1980**, 45, 5017.
- (118) Jung, M. E. and Halweg, K. M. *Tetrahedron Letters* **1981**, 2735.
- (119) Okauchi, T.; Kakiuchi, T.; Kitamura, N.; Utsunomiya, T.; Ichikawa, J.; and Minami, T. *The Journal of Organic Chemistry* **1997**, 62, 8419.
- (120) Fairweather, K. A. and Mander, L. N. *Organic Letters* **2006**, 8, 3395.

- (121) Burford, C.; Cooke, F.; Ehlinger, E.; and Magnus, P. D. *The Journal of the American Chemical Society* **1977**, 99, 4536.
- (122) Harirchian, B. and Magnus, P. D. *The Journal of the Chemical Society, Chemical Communications* **1977**, 15, 522.
- (123) Cooke, F. and Magnus, P. D. *The Journal of the Chemical Society, Chemical Communications* **1977**, 15, 513.
- (124) Corey, E. J. and Chaykovsky, M. *The Journal of the American Chemical Society* **1965**, 87, 1353.
- (125) Burke, S. D. and Danheiser, R. L. *Handbook of Reagents for Organic Synthesis, Oxidizing and Reducing Agents*. **1999**, "Nickel Boride" John Wiley & Sons, Ltd. West Sussex, England.
- (126) Mahoney, W. S.; Brestensky, D. M.; and Stryker, J. M. *The Journal of the American Chemical Society* **1988**, 110, 291.
- (127) Baker, B. A.; Bošković, Ž. V.; and Lipshutz, B. H. *Organic Letters* **2008**, 10, 289-292.
- (128) a) Hashimoto, N.; Aoyama, T.; and Shioiri, T. *Chemical Pharmaceutical Bulletin* **1981**, 29, 1475. b) Shioiri, T.; Aoyama, T.; Hashimoto, N. patent (Japan), JP57130925, **1982**. c) Aoyama, T.; Terasawa, S.; Sudo, K.; and Shioiri, T. *Chemical Pharmaceutical Bulletin* **1984**, 32, 3759. d) Aoyama, T. and Shioiri, T. *Tetrahedron Letters* **1990**, 31, 5507.
- (129) Strazewski, P. and Tamm, C. *Helvetica Chimica Acta* **1986**, 69, 1041.
- (130) a) Seebach, D. and Weber, T. *Helvetica Chimica Acta* **1985**, 68, 1507. b) Seebach, D.; Miller, D. D., Muller, S.; and Weber, T. *Helvetica Chimica Acta* **1985**, 68, 949. c) Seebach, D. and Weber, T. *Helvetica Chimica Acta* **1985**, 68, 155. d) Seebach, D. and Aebi, J. D. *Tetrahedron Letters* **1984**, 25, 2545. e) Seebach, D. and Aebi, J. D. *Tetrahedron Letters* **1983**, 32, 3311. f) Meyers, A. I.; Hanreich, R.; and Wanner, K. T. *The Journal of the American Chemical Society* **1985**, 107, 7776.
- (131) Li, K.; Duan, H.; Kawazoe, K.; and Takashi, Y. *Phytochemistry* **1997**, 45, 791.
- (132) Rappaport, Z. *The Chemistry of Phenols*. Wiley-Interscience: 2003; Vol. 1.

- (133) a) **Triclosan**: Coia, J. E.; Duckworth, G. J.; and Edwards, D. I. *The Journal of Hospital Infections* **2006**, 63, S1. b) Brady, L. M.; Thomson, M.; Palmer, M. A.; and Harkness, J. L. *Medical Journal of Australia* **1990**, 152, 240. c) Yazdankhah, S. P.; Scheie, A. A.; and Hoiby, E. A. *Microbial Drug Resistance* **2006**, 12, 83. **Symbicort**: d) Balanag, V. M.; Yunus, F.; Yang, P. C.; and Jorup, C. *Pulmonary Pharmacology & Therapeutics* **2006**, 19, 139. **Raloxifene**: e) Results of the Study of Tamoxifen and Raloxifene (STAR) Released: Osteoporosis Drug Raloxifene Shown to be as Effective as Tamoxifen in Preventing Invasive Breast Cancer. (Press Release) June 21, 2006. f) Vogel, V.; Constantino, J.; and Wickerman, L. *The Journal of the American Medical Association* **2006**, 295, 2727. **Loestrin 24 Fe (ethinyl estradiol)**: g) Sneader, W. *Hormone Analogues*. **2005**, Drug Discovery: A History. Hoboken, NJ: John Wiley & Sons. 188. **Asacol**: h) Kruis, W.; Schreiber, I.; Theuer, D.; Brandes, J. W.; Schutz, E.; Howaldt, S.; Krakamp, B.; Hamling, J.; Monnikes, H.; Koop, I.; Stolte, M.; Pallant, D.; and Ewald, U. *Gut* **2001**, 49, 783. i) Sandborn, W. K.; Feagan, B. G.; and Lichtenstein, G. R. *Alimentary Pharmacology & Therapeutics* **2007**, 26, 987. **Advair**: j) *Asthma Treatment and COPD: Treatment with ADVAIR*: GlaxoSmithKline. <http://www.advair.com/>. **Oxymorphone**: k) Adams, M. P. and Ahdieh, H. *Drugs in R&D* **2005**, 6, 91. **Rifaxan**: l) Dupont, H. *Clinical Infectious Diseases* **2007**, 45, S78. m) Lawrence, K. R. and Klee, J. A. *Pharmacotherapy* **2008**, 28, 1019. **Detrol LA**: n) van Kerrebroeck, P.; Kreder, K.; Jonas, U.; Zinner, N.; Wein, A. *Urology* **2001**, 57, 414. **Levothyroxine**: o) Svensson, J.; Ericsson, U. B.; and Nilsson, P. *The Journal of Clinical Endocrinology and Metabolism* **2006**, 91, 1729. **Combivent (Salbutamol)**: p) Stein, J. and Levitt, M. A. *The Journal of Academic Emergency Medicine* **2003**, 10, 31. **Zetia**: q) Garcia-Calvo, M.; Lisnock, J.; Bull, H. G.; Hawes, B. E.; Burnett, D. A.; and Braun, M. P. *Proceedings of the National Academy of Sciences, USA* **2005**, 102, 8132. **Pristiq**: r) Decher, D. C.; Beyer, C. E.; Johnston, G.; Bray, J.; Shah, S.; Abou-Gharbia, M.; and Andree, T. H. *The Journal of Pharmacology and Experimental Therapeutics* **2006**, 318, 657. **Acetaminophen**: s) *Archives of Pediatrics & Adolescent Medicine* **2004**, 158, 521. **Epinephrine**: t) Nadeau, R. A. and DeCamplain, J. *The American Heart Journal* **1979**, 98, 548. **Amoxicillin**: u) "Amoxicillin." *The American Society of Health-System Pharmacists*. Retrieved March 18, 2014.
- (134) U.S. Environment Protection Agency, 1998, Health Effects Test Guidelines, OPPTS 870.7485, Metabolism and Pharmacokinetics. (<http://www.epa.gov/epahome/research.htm>).
- (135) de Montellano, P. R. O. *Cytochrome P450: Structure, Mechanism, and Biochemistry*. Springer: 2004.

- (136) Vermerris, W. and Nicholson, R. *Phenolic Compound Biochemistry*. Springer: 2007.
- (137) a) Henderson, G. G. and Boyd, R. *The Journal of the Chemical Society, Transactions*. **1910**, 1659. b) Tyman, J. *Synthetic and Natural Phenols*. Elsevier (Amsterdam, The Netherlands and New York): 1996.
- (138) Derbyshire, D. H. and Waters, W. A. *Nature* **1950**, 165, 401.
- (139) a) McClure, J. D. and Williams, P. H. *The Journal of Organic Chemistry* **1962**, 27, 24. b) McClure, J. D. and Williams, P. H. *The Journal of Organic Chemistry* **1962**, 27, 627.
- (140) Hart, H. and Buehler, C. A. *The Journal of Organic Chemistry* **1964**, 29, 2397.
- (141) a) Kovacic, P. and Kurz, M. E. *The Journal of the American Chemical Society* **1965**, 4811. b) Kovacic, P. and Kurz, M. E. *The Journal of Organic Chemistry* **1966**, 31, 2011.
- (142) Kurz, M. E. and Kovacic, P. *The Journal of the American Chemical Society* **1967**, 89, 4960.
- (143) Kovacic, P.; Reid, C. G.; Brittain, M. J. *The Journal of Organic Chemistry* **1970**, 35, 2152.
- (144) Vesely, J. A. and Schmerling, L. *The Journal of Organic Chemistry* **1970**, 35, 4028.
- (145) Kurz, M. E.; Johnson, G. J. *The Journal of Organic Chemistry* **1971**, 36, 3184.
- (146) Snook, M. E. and Hamilton, G. A. *The Journal of the American Chemical Society* **1974**, 96, 860.
- (147) Olah, G. A. and Ohnishi, R. *The Journal of Organic Chemistry* **1978**, 43, 865.
- (148) Olah, G. A.; Fung, A. P.; and Keumi, T. *The Journal of Organic Chemistry* **1981**, 46, 4305.
- (149) Olah, G. A.; Keumi, T.; Lecoq, J. C.; Fung, A. P.; and Olah, J. A. *The Journal of Organic Chemistry* **1991**, 56, 6148.

- (150) Einhorn, J.; Luche, J. L.; and Demerseman, P. *The Journal of the Chemical Society, Chemical Communications* **1988**, 20, 1350.
- (151) Yoneyama, T. and Crabtree, R. H. *The Journal of Molecular Catalysis A: Chemical* **1996**, 108, 35.
- (152) Chen, X.; Hao, X. S.; Goodhue, C. E.; Yu, J. Q. *The Journal of the American Chemical Society* **2006**, 128, 6790.
- (153) Zhang, Y. H. and Yu, J. Q. *The Journal of the American Chemical Society* **2009**, 131, 14654.
- (154) Powers, D. C.; Xiao, D. Y.; Geibel, M. A.; and Ritter, T. *The Journal of the American Chemical Society* **2010**, 132, 14530.
- (155) Huang, C.; Ghavtadze, N.; Chattopadhyay, B.; and Gevorgyan, V. *The Journal of the American Chemical Society* **2011**, 133, 17630.
- (156) Emmert, M. H.; Cook, A. K.; Xie, Y. J.; and Sanford, M. S. *Angewandte Chemie, International Edition* **2011**, 123, 9581.
- (157) Gulevich, A. V.; Melkonyan, F. S.; Sarkar, D.; and Gevorgyan, V. *The Journal of the American Chemical Society* **2012**, 134, 5528.
- (158) Mo, F.; Trzepakowski, L. J.; and Dong, G. *Angewandte Chemie, International Edition* **2012**, 124, 13252.
- (159) Shan, G.; Yang, X.; Ma, L.; and Rao, Y. *Angewandte Chemie, International Edition* **2012**, 124, 13247.
- (160) Wang, Y.; Gulevich, A.; and Gevorgyan, V. *Chemistry: A European Journal* **2013**, 19, 15836.
- (161) Cook, A. K.; Emmert, M. H.; and Sanford, M. S. *Organic Letters* **2013**, 15, 5428.
- (162) Tamao, K.; Ishida, N.; Tanaka, T.; and Kumada, M. *Organometallics* **1983**, 2, 1694.
- (163) Fleming, I.; Henning, R.; and Plaut, H. E. *The Journal of the Chemical Society, Chemical Communications* **1984**, 29.
- (164) Fleming, I. and Sanderson, P. E. J. *Tetrahedron Letters* **1987**, 52, 4229.

- (165) Fleming, I.; Henning, R.; Parker, D. C.; Plaut, H. E.; and Sanderson, P. E. J. *The Journal of the Chemical Society, Perkin Transactions* **1995**, 1, 317.
- (166) Sunderhaus, J. D.; Lam, H.; and Dudley, G. B. *Organic Letters* **2003**, 5, 4571.
- (167) a) Hiyama, T. and Shirakawa, E. *Topics in Current Chemistry* **2002**, 219, 61. b) Denmark, S. E. and Sweis, R. F. *Chemical Pharmaceutical Bulletin* **2002**, 50, 1531. c) Denmark, S. E. and Ober, M. H. *Organic Letters* **2003**, 5, 1357. d) Denmark, S. E. and Sweis, R. F. *Accounts of Chemical Research* **2002**, 35, 835. e) Hirabayashi, K.; Ando, J.; Kawashima, J.; Nishihara, Y.; Mori, A.; and Hiyama, T. *Bulletin of the Chemical Society of Japan* **2000**, 73, 1409. f) Lickiss, P. D. *Advanced Inorganic Chemistry* **1995**, 42, 147. g) Murata, M.; Suzuki, K.; Watanabe, S.; and Masuda, Y. *The Journal of Organic Chemistry* **1997**, 62, 8569. h) Manoso, A. S. and DeShong, P. *The Journal of Organic Chemistry* **2001**, 66, 7449. i) Denmark, S. E. and Kallemeyn, J. M. *Organic Letters* **2003**, 5, 3483. j) Hartwig, J. F. *Accounts of Chemical Research* **2012**, 45, 864. k) Ishiyama, T.; Murata, M.; and Miyaura, N. *The Journal of Organic Chemistry* **1995**, 60, 7508.
- (168) a) Vollhardt, P. K. *Organic Chemistry Structure and Function*. 5th edition. New York: W. H. Freeman and Company, **2007**. b) Wade, L. G. *Organic Chemistry*. 6th edition. New Jersey: Pearson Prentice Hall, **2006**.
- (169) a) Baeyer, A. and Villiger, V. *Berichte* **1899**, 3625. b) Baeyer, A. and Villiger, V. *Berichte* **1900**, 858.
- (170) a) Greene, F. D. *The Journal of the American Chemical Society* **1956**, 78, 2246. b) Greene, F. D. *The Journal of the American Chemical Society* **1956**, 78, 2250. c) Greene, F. D. and Rees, W. W. *The Journal of the American Chemical Society* **1958**, 80, 3432. d) Greene, F. D. and Rees, W. W. *The Journal of the American Chemical Society* **1959**, 81, 1503. e) Greene, F. D. and Rees, W. W. *The Journal of the American Chemical Society* **1960**, 82, 890. f) Greene, F. D. and Rees, W. W. *The Journal of the American Chemical Society* **1960**, 82, 893.
- (171) Yuan, C.; Liang, Y.; Hernandez, T. M.; Berriochoa, A.; Houk, K. N.; and Siegel, D. *Nature* **2013**, 499, 192.
- (172) Hansch, C.; Leo, A.; and Taft, R. W. *Chemical Reviews* **1991**, 91, 165.
- (173) a) Wohl, A. *Berichte der deutschen chemischen Gesellschaft* **1919**, 52, 51. b) Ziegler, K.; Schenck, G.; Krockow, E. W.; Siebert, A.; Wenz, A.; and Weber, H. *Justus Liebig's Annalen der Chemie* **1942**, 551, 1.

- (174) Yuan, C.; Axelrod, A.; Valera, M.; Danysh, L.; Siegel, D. *Tetrahedron Letters* **2011**, 52, 2540.
- (175) Roedig, A.; Bonse, G.; Helm, R.; and Kohlhaupt, R. *Chemische Berichte* **1971**, 104, 3378.
- (176) a) “Flurbiprofen” <http://medical-dictionary.thefreedictionary.com/flurbiprofen>. Retrieved March 18, 2014. b) Risdall, P. C.; Adams, S. S.; Crampton, E. L.; and Marchant, B. *Xenobiotica* **1978**, 8, 691.
- (177) a) Bayly, C. I.; Black, W. C.; Leger, S.; Ouimet, N.; Ouellet, M.; and Percival, M. D. *Bioorganic & Medicinal Chemistry Letters* **1999**, 9, 307. b) Chen, Y.; Sun, J.; Huang, Z.; Liao, H.; Peng, S.; Lehmann, J.; and Zhang, Y. *Bioorganic & Medicinal Chemistry* **2013**, 21, 2462.
- (178) Volland, C.; Sun, H.; and Benet, L. Z. *The Journal of Chromatography B: Biomedical Sciences and Applications* **1990**, 534, 127.
- (179) a) Montville, R. and Schaffner, D. W. *The Journal of Food Protection* **2011**, 74, 1875. b) Fuls, J. L. and Rodgers, N. D. *Applied and Environmental Microbiology* **2008**, 74, 3739.
c) <http://www.fda.gov/ForConsumers/ConsumerUpdates/ucm205999.htm>. Retrieved March 18, 2014.
- (180) Rolewski, S. *The Journal of the Dermatology Nurses' Association* **2003**, 15, 447.
- (181) Kalsi, P. S. *Organic Reactions and Their Mechanisms*. **2000**, New Age International.
- (182) a) Carey, F. A. and Sundberg, R. J. *Advanced Organic Chemistry, Part A: Structure and Mechanisms*. 5th Edition. **2007**, Springer New York, New York. b) Carey, F. A. and Sundberg, R. J. *Advanced Organic Chemistry, Part B: Reactions and Synthesis*. 5th Edition. **2007**, Springer New York, New York.
- (183) Stratt, R. M. and Desjardins, S. G. *The Journal of the American Chemical Society* **1984**, 106, 256.
- (184) a) Shuklov, I. A.; Dubrovina, N. V.; and Borner, A. *Synthesis* **2007**, 2925. b) Lucarini, M.; Mugnaini, V.; Pedulli, G. F.; and Guerra, M. *The Journal of the American Chemical Society* **2003**, 125, 8318.